

# Exploration of a novel class of HO-1 inducers as potential therapeutics for inflammatory disease

**Hannah Fitzgerald**

B.A. (Mod) Molecular Medicine



A Thesis submitted to  
**Trinity College Dublin**  
for the degree of  
**Doctor of Philosophy**

**Supervisor: Prof. Aisling Dunne**

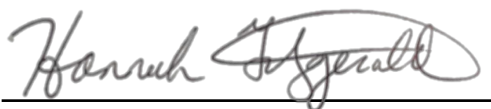
**Co-Supervisor: Prof. Jean Fletcher**

Molecular Immunology Group  
School of Biochemistry and Immunology  
Trinity College Dublin

**2022**

## Declaration of authorship

I declare that this thesis has not been submitted as an exercise for a degree at this or any other university and it is entirely my own work. I agree to deposit this thesis in the University's open access institutional repository or allow the Library to do so on my behalf, subject to Irish Copyright Legislation and Trinity College Library conditions of use and acknowledgement. I consent to the examiner retaining a copy of the thesis beyond the examining period, should they so wish (EU GDPR May 2018).

A handwritten signature in cursive script, reading "Hannah Fitzgerald", written over a horizontal line.

Hannah Fitzgerald

## Acknowledgements

Firstly, I would like to thank my supervisor, Prof. Aisling Dunne. Thank you so much for all of your support, guidance, and patience over the last 4.5 years, and for always encouraging me to push myself to do my best. I really appreciate the opportunity you gave me with this project, and I look forward to continue to work with you on our next project. I would also like to thank my co-supervisor, Prof. Jean Fletcher. I am very thankful that you were willing to help supervise me while Aisling was on maternity leave, and for all of your continued support since then. Thank you for all of your experimental input, and words of encouragement when I was struggling. I am incredibly lucky to have two brilliant supervisors who inspire me, and I really appreciate all of the time you have both invested in me during this project. It has been an honour to work with you both.

I would next like to thank all the past and present members of the Dunne lab, who have not only helped me when I needed it most, but made the lab such an enjoyable workspace. In particular I would like to thank Nicole, who was so welcoming from my first day in the lab, and patient with me as I learned everything from scratch. I can only imagine how much of a burden I was starting in your final year, but I really appreciate you as both my mentor and friend. I would also really like to thank Eva, this project would not be where it was today without your help throughout your time with us. You were an invaluable member of our lab, who I am also delighted to still have as a supportive, close friend. To the current members of the Dunne lab, Sinead and Lianne, my Mol Med gals, thank you both so much for your support and friendships. I feel so lucky to have such a tight knit lab, that is always willing to help each other no matter what, while also being such amazing friends. Thank you for always cheering me up when I need it most, I thoroughly believe we would not have gotten through this without each other. To Gearóid, our newest PhD student, I wish you the best of luck as you embark on this adventure.

I would also like to extend my thanks to the members of the Fletcher lab, Andreea, Conor and Aoife. Thank for you listening to me complain about experiments during lab meeting, and offering such helpful advice. A particular thanks to Barry for all of the help with flow

cytometry problems throughout the PhD. I would also like to thank all of the past and present members of the McLoughlin and Stevenson labs, for making lab 3.12 such an enjoyable place to work. I am very lucky to have had such fun times working with you all, and I wish you all the best for the future. I'd like to give a special thanks to Claudia for her unwavering support and friendship, I'm looking forward to visiting you in London! I'd also like to thank Emilio, for all of the amazing advice you have given me over the years, with a lot of laughs along the way. Yourself and Sinead will always be my Drag Race Huns!

I would like to thank the Health Research Board for funding this project, and all of the collaborators who were crucial to the success of this project. I would like to thank Nuno for all of your help with the FLIM experiments, I appreciate all the time you put into this work. I would like to thank Prof. Derek Nolan for invaluable Trypanosome advice, and for getting the ball rolling with this ketoacid project. I would like to thank our collaborators in UCD and St. Vincent's Hospital; Prof. Glen Doherty, Dr. Elizabeth Ryan, Dr. Jayne Doherty, and Miriam Tosetto, for providing access to IBD patient blood samples used in this project, as well as the patients themselves for donating to the project. I would also like to thank all of the staff of TBSI for all of the help and support over the years, a particular shout out to Liam Cross who I bothered on many occasions with long lists of broken equipment! I would particularly like to thank everyone in the teaching lab for your words of encouragement, on a bad day I always knew I could seek any of you out for a positive boost.

I would like to thank all of my friends for their support and friendships throughout this PhD, and in particular I would like to thank Lorna for always being my biggest cheerleader! To my family; Mam, Dad, Lucy and Grace, I could not have done this without your support, I realise I am extremely lucky to have you all. Thank you for looking after me, and encouraging me to do whatever it is I wanted to do. I would like to especially thank my Nana for always showing such enthusiastic interest in my work, and trying her best to understand what I was talking about! To Ricardo, thank you for always being there for me, I don't know what I would do without you. Thank you for supporting my interests, and trying to lighten the mood when I'm down. I look forward to what the future holds for us.

## Abstract

Autoimmune and inflammatory diseases such as rheumatoid arthritis (RA), multiple sclerosis (MS), psoriasis, and inflammatory bowel disease (IBD) are characterised by excessive and uncontrolled inflammation. Most of these diseases are incurable and their aetiology is only partially understood. Many patients become refractory to currently available treatments or show no response to these treatments from the outset. Given the increased incidence of these diseases, there is a growing need for novel anti-inflammatory therapies, with increased long-term efficacy and less adverse side effects.

It is well known that many pathogens, including parasites, suppress host immune responses to establish latency and/or maintain persistent infection. Therefore, there has been increased interest in recent years in exploiting parasite-derived products for therapeutic benefit to treat autoimmune/inflammatory conditions. The extracellular parasite and causative agent of African sleeping sickness, *Trypanosoma brucei* (*T. brucei*), has evolved a number of strategies to avoid immune detection in the host. One recently described mechanism involves the conversion of host-derived amino acids to aromatic ketoacids, which are detected at relatively high concentrations in the bloodstream of infected individuals. These ketoacids have been shown to directly suppress inflammatory responses in murine immune cells, as well as acting as potent inducers of the stress response enzyme, heme oxygenase 1 (HO-1).

Indeed, induction of HO-1 is considered a promising therapy for autoimmune and inflammatory conditions, and several studies have demonstrated that the HO reaction products, biliverdin and bilirubin, have potent anti-inflammatory, as well as antioxidant, properties. Administration of synthetic forms of these tetrapyrroles, or indeed upregulation of the inducible form of HO-1 following administration of cobalt protoporphyrin (CoPP), has been shown to alleviate inflammation in several animal models of disease. There is now a growing body of evidence supporting modulation of the HO-1 system as a treatment for gastrointestinal diseases, however, clinical implementation of HO-1 based therapies faces numerous challenges. Traditional HO-1 inducers primarily

include metalloporphyrins, which strongly upregulate HO-1 expression, but are also associated with significant toxicity concerns and, while they have shown considerable efficacy in colitis models, are unsuitable for clinical use. Therapeutic administration of linear tetrapyrroles also faces challenges, therefore there is a solid rationale to identify safer and better tolerated alternatives to currently available HO-1 inducers. The aim of this study was therefore to investigate the immunomodulatory properties of *T. brucei*-derived ketoacids in primary human immune cells and further examine their potential as HO-1 inducers and novel therapies for inflammatory diseases, with specific focus on IBD.

Results from this study demonstrate that the *T. brucei*-derived ketoacids, indole pyruvate (IP) and hydroxyphenylpyruvate (HPP), induce HO-1 expression through Nrf2 activation in human dendritic cells (DC). They also limit DC maturation, reduce the expression of co-stimulatory markers and suppress the production of pro-inflammatory cytokines, which, in turn, leads to a reduced capacity to differentiate adaptive CD4<sup>+</sup> T cells. Furthermore, the ketoacids are capable of modulating DC cellular metabolism, inhibiting glycolysis and reducing expression of the key glycolytic enzyme, hexokinase 2 (HK2), as well as modulating expression of autophagy-related proteins. Finally, it is demonstrated that *T. brucei*-derived ketoacids are capable of inhibiting proliferation and pro-inflammatory cytokine production in T cells isolated from patients with IBD. This study therefore not only provides further evidence of the immune-evasion mechanisms employed by *T. brucei*, but also supports further exploration of this new class of HO-1 inducers as potential therapeutics for the treatment of inflammatory conditions.

## Publications

**Fitzgerald, H.K.**, O'Rourke, S.A., Desmond, E., Neto, N.G.B., Monaghan, M.G., Tosetto, M., Doherty, J., Ryan, E.J., Doherty, G.A., Nolan, D.P., Fletcher, J.M., Dunne, A. (2022) The *Trypanosoma brucei*-Derived Ketoacids, Indole Pyruvate and Hydroxyphenylpyruvate, Induce HO-1 Expression and Suppress Inflammatory Responses in Human Dendritic Cells. *Antioxidants* MDPI 2022, 11(1), 164.

Campbell N.K.\* , **Fitzgerald H.K.\***, and Dunne, A. (2021) Regulation of inflammation by the antioxidant haem oxygenase 1. *Nature Reviews Immunology* Nature publishing group, 21(7), 411-425

\* Equal contribution

Campbell, N.K.\* , Williams, D.G.\* , **Fitzgerald, H.K.**, Barry, P.J., Cunningham, C.C., Nolan, D.P., Dunne, A. (2019) *Trypanosoma brucei* secreted aromatic ketoacids activate the Nrf2/HO-1 pathway and suppress pro-inflammatory responses in primary murine glia and macrophages. *Frontiers in Immunology*. Frontiers, 10:2137.

\* Equal contribution

Campbell N.K., **Fitzgerald H.K.**, Malara A., Hambly R., Sweeney C.M., Kirby B., Fletcher J.M., Dunne, A. (2018) Naturally derived Heme Oxygenase 1 inducers attenuate inflammatory responses in human dendritic cells and T cells: relevance for psoriasis treatment. *Scientific Reports* Nature Publishing Group, 8(1):10287.

Campbell N.K., **Fitzgerald H.K.**, Fletcher J.M., Dunne A. (2019) Plant-Derived Polyphenols Modulate Human Dendritic Cell Metabolism and Immune Function via AMPK-Dependent Induction of Heme Oxygenase-1. *Frontiers in Immunology* Frontiers, 10:345.

O'Rourke, S.A., Neto, N.G.B., Devilliy, E., Shanley, L.C., **Fitzgerald, H.K.**, Monaghan, M.G.\* , Dunne, A\* . (2022) Cholesterol crystals drive metabolic reprogramming and M1

macrophage polarisation in primary human macrophages. *Atherosclerosis* Elsevier, 352, 35-45.

\* Equal contribution

Neto, N.G.B., O'Rourke, S.A., Zhang, M., **Fitzgerald, H.K.**, Dunne, A., Monaghan, M.G. (2022) Non-Invasive classification of macrophage polarisation by 2P-FLIM and machine learning. *eLife* (Manuscript in revision).

## Awards

**3<sup>rd</sup> place poster presentation** September 2019 Trinity Biomedical Sciences Institute Research Symposium "*Trypanosome Brucei* secreted aromatic ketoacids activate the Nrf2/HO-1 pathway and suppress pro-inflammatory responses in primary murine and human immune cells."

**Immunotools Special Award** June 2018 "Investigating the Heme Oxygenase system as a Therapeutic intervention for Inflammatory Bowel Disease."

## Presentations

British Society for Immunology conference, December 2021, Edinburgh. **Hannah K Fitzgerald**, David G Williams, Nicole K Campbell, Paul Barry, Sinead A O'Rourke, Nuno G Neto, Michael G Monaghan, Derek P Nolan, Jean M Fletcher and Aisling Dunne. **Poster presentation** - Aromatic ketoacids represent novel therapies for autoimmune diseases through activation of the Nrf2/HO-1 pathway and suppression of pro-inflammatory responses in primary human immune cells.

Host Pathogen Communication conference, November 2021, Dublin. **Hannah K Fitzgerald**, David G Williams, Nicole K Campbell, Paul Barry, Sinead A O'Rourke, Nuno G Neto, Michael G Monaghan, Derek P Nolan, Jean M Fletcher and Aisling Dunne. **Oral presentation** -



*Trypanosoma Brucei* secreted aromatic ketoacids represent novel therapies for inflammatory diseases through suppression of pro-inflammatory responses in primary human immune cells.

European Congress of Immunology conference, September 2021, online. **Hannah K Fitzgerald**, David G Williams, Nicole K Campbell, Paul Barry, Sinead A O'Rourke, Nuno G Neto, Michael G Monaghan, Derek P Nolan and Aisling Dunne. **Oral presentation** - Aromatic ketoacids represent novel therapies for inflammatory diseases through activation of the Nrf2/HO-1 pathway and suppression of pro-inflammatory responses in primary human immune cells.

European Macrophage and Dendritic Cell conference, June 2021, online. **Hannah K Fitzgerald**, David G Williams, Nicole K Campbell, Paul Barry, Sinead A O'Rourke, Nuno G Neto, Michael G Monaghan, Derek P Nolan and Aisling Dunne. **Poster presentation** - Aromatic ketoacids, secreted by *Trypanosoma brucei*, activate the Nrf2/HO-1 pathway and suppress pro-inflammatory responses in primary human dendritic cells.

Keystone Innate Immunity eSymposia, April 2021, online. **Hannah K Fitzgerald**, David G Williams, Nicole K Campbell, Paul Barry, Sinead A O'Rourke, Nuno G Neto, Michael G Monaghan, Derek P Nolan and Aisling Dunne. **Poster presentation** - Aromatic ketoacids, secreted by *Trypanosoma brucei*, activate the Nrf2/HO-1 pathway and suppress pro-inflammatory responses in primary human dendritic cells.

Immunology Research Forum, October 2019, Dublin. **Hannah K Fitzgerald**. **Oral presentation** - The Heme Oxygenase System and Immune Modulation.

Irish Society for Immunology conference, September 2019, Dublin. **Hannah K Fitzgerald**, David G Williams, Nicole K Campbell, Paul Barry, Derek P Nolan and Aisling Dunne. **Poster presentation** - *Trypanosoma brucei* secreted aromatic ketoacids activate the Nrf2/HO-1 pathway and suppress pro-inflammatory responses in primary murine and human immune cells.

Trinity Biomedical Sciences Institute Research Symposium, September 2019, Dublin. **Hannah K Fitzgerald**, David G Williams, Nicole K Campbell, Paul Barry, Derek P Nolan and Aisling Dunne. **Poster presentation** - *Trypanosome Brucei* secreted aromatic ketoacids activate the Nrf2/HO-1 pathway and suppress pro-inflammatory responses in primary murine and human immune cells.

Irish Society for Immunology conference, August 2018, Dublin. **Hannah K. Fitzgerald**, Nicole K. Campbell, Eva Desmond, and Aisling Dunne. **Poster presentation** - AMPK-dependent induction of Heme Oxygenase modulates immune cell metabolism and function.

## Abbreviations

2-DG	2-deoxy-D-glucose
5-ALA	5-aminolevulinic acid
5-ASA	5-aminosalicylic acid
ACC	Acetyl-CoA carboxylase
ADP	Adenosine diphosphate
AHR	Aryl hydrocarbon receptor
AMP	Adenosine monophosphate
AMPK	AMP-activated protein kinase
APC	Antigen presenting cell
APS	Ammonium Persulfate
ARE	Antioxidant response element
Atg	Autophagy-related
ATP	Adenosine triphosphate
Bach1	BTB and CNC homolog 1
BMDM	Bone marrow derived macrophages
BV	Biliverdin
BVR	Biliverdin reductase
CD	Crohn's disease
CLR	C-type lectin receptors
CNS	Central nervous system
CO	Carbon monoxide
CoPP	Cobalt protoporphyrin IX
CORMs	CO releasing molecules
CPT	Carnitine palmitoyltransferase
DAMP	Danger associated molecular patterns
DC	Dendritic cell
DHA	Dihydroartemisinin
DMEM	Dulbecco's Modified Eagle's Media
DMF	Dimethyl fumarate

DMSO	Dimethyl sulfoxide
DQ-Ova	DQ-ovalbumin
DSS	Dextran Sulfate-Sodium
EAE	Experimental autoimmune encephalomyelitis
ECAR	Extracellular acidification rate
ECL	Enhanced Chemiluminescent
EDTA	Ethylenediaminetetraacetic acid
ELISA	Enzyme-linked immunosorbent assay
FAO	Fatty acid oxidation
FAS	Fatty acid synthesis
FBS	Foetal bovine serum
FCCP	Carbonyl cyanide-p trifluoromethoxyphenylhydrazone
FLIM	Fluorescence Lifetime Imaging Microscopy
FMO	Fluorescence minus one
FOXP3	Forkhead box P3
FPN1	Ferroportin 1
FSC	Forward scatter
GLUT-1	Glucose transporter 1
GM-CSF	Granulocyte-monocyte colony-stimulating factor
GSR	Glutathione Reductase
HIF1 $\alpha$	Hypoxia inducible factor 1 $\alpha$
HK2	Hexokinase-2
HO-1	Heme oxygenase-1
HPP	Hydroxyphenylpyruvate
HRP	Horseradish-peroxidase
HYCOs	Hybrid CO-releasing molecule
IBD	Inflammatory bowel disease
IBTS	Irish blood transfusion service
IFN	Interferon
IL	Interleukin
iNOS	Inducible nitric oxide synthase

IP	Indole pyruvate
KEAP1	Kelch-like ECH-associated protein 1
LPS	Lipopolysaccharide
MACS	Magnetic-Activated Cell Sorting
MAPKs	Mitogen activated protein kinases
MFI	Median fluorescent intensity
MHC	Major histocompatibility complex
MS	Multiple sclerosis
mTOR	Mammalian target of rapamycin
mTORC1	mTOR complex 1
NADH	Nicotinamide adenine dinucleotide
NADPH	Nicotinamide adenine dinucleotide phosphate
NF- $\kappa$ B	Nuclear factor $\kappa$ B
NLR	NOD-like receptors
NQO-1	NAD(P)H Quinone Oxidoreductase 1
Nrf2	Nuclear factor erythroid 2-related factor 2
OCR	Oxygen consumption rate
PAMP	Pathogen associated molecular pattern
PBMC	Peripheral blood mononuclear cells
PBS	Dulbecco's phosphate buffered saline
PCR	Polymerase chain reaction
PDH	Pyruvate dehydrogenase
PDHK	Pyruvate dehydrogenase kinase
PFA	Paraformaldehyde
PI	Propidium iodide
PI3K	Phosphatidylinositol-3 kinase
PMA	Phorbol 12-myristate 13-acetate
PP	Phenyl pyruvate
PPP	Pentose phosphate pathway
PRR	Pathogen recognition receptor
PVDF	Polyvinylidene difluoride

RA	Rheumatoid arthritis
RIR	RIG-I like receptors
ROR $\gamma$ t	Retinoid acid related orphan receptor $\gamma$ thymus
ROS	Reactive oxygen species
RPMI	Roswell Park Memorial Institute
SDS	Sodium dodecyl sulphate
SEM	Standard error of the mean
SLE	Systemic lupus erythematosus
SMAFs	Small MAF proteins
SNP	Single nucleotide polymorphism
SREBP	Sterol regulatory element binding protein
SSC	Side scatter
<i>T. brucei</i>	<i>Trypanosoma brucei</i>
TBST	Tris-Buffered Saline with Tween-20
TCA	Tricarboxylic acid
TCR	T cell receptor
TGF- $\beta$	Transforming growth factor $\beta$
Th cell	T-helper cell
TLR	Toll-like receptor
TNF	Tumour necrosis factor
Treg	Regulatory T cell
UC	Ulcerative colitis
US	Unstained
UT	Untreated
VCAM-1	Vascular cell adhesion molecule-1

# Table of contents

DECLARATION OF AUTHORSHIP .....	I
ACKNOWLEDGEMENTS .....	II
ABSTRACT .....	IV
PUBLICATIONS .....	VI
AWARDS VII	
PRESENTATIONS .....	VII
ABBREVIATIONS .....	X
TABLE OF CONTENTS .....	XIV
TABLE OF FIGURES .....	XVII
<b>CHAPTER 1: INTRODUCTION.....</b>	<b>1</b>
1.1 THE IMMUNE SYSTEM .....	2
1.1.1 Dendritic cells.....	3
1.1.2 T cells .....	5
1.2 INFLAMMATORY & AUTOIMMUNE DISEASES .....	7
1.3 IMMUNOMETABOLISM.....	9
1.3.1 Cellular respiration.....	10
1.3.2 Fatty acid metabolism .....	11
1.3.3 Metabolism and immune cells.....	12
1.3.4 Immunometabolism as a therapeutic target.....	14
1.4 AUTOPHAGY .....	16
1.4.1 Autophagy in immunity & disease .....	17
1.5 THE HEME OXYGENASE SYSTEM.....	19
1.5.1 Heme oxygenase 1.....	20
1.5.2 Beneficial role of HO-1 in disease .....	25
1.5.3 Therapeutic modulation of HO-1 .....	29
1.6 RESEARCH QUESTION.....	35
1.6.1 Specific aims .....	35
<b>CHAPTER 2: MATERIALS &amp; METHODS.....</b>	<b>36</b>
2.1 MATERIALS .....	37
2.1.1 Reagents .....	37
2.1.2 Cell culture .....	37
2.1.3 Western blotting.....	37
2.1.4 Flow cytometry .....	38
2.1.5 Polymerase chain reaction.....	39
2.1.6 Enzyme linked immunosorbent assay .....	39
2.1.7 Seahorse .....	39
2.2 METHODS .....	40
2.2.1 Cell culture .....	40
2.2.2 Cell counting .....	40
2.2.3 PBMC isolation.....	40
2.2.4 Isolation of IBD patient PBMC.....	41
2.2.5 Isolation of CD14 <sup>+</sup> and CD4 <sup>+</sup> cells.....	42
2.2.6 Culture of monocyte derived dendritic cells.....	42
2.2.7 Culture of bone marrow derived macrophages .....	43
2.2.8 SDS-PAGE and western blotting.....	43
2.2.9 Flow cytometry .....	45
2.2.10 Capture Enzyme-linked immunosorbent assay .....	47
2.2.11 Polymerase chain reaction.....	48
2.2.12 Seahorse .....	50
2.2.13 LDH assay.....	51

2.2.14 Antioxidant assay .....	52
2.2.15 Two-Photon Fluorescence Lifetime Imaging Microscopy.....	52
2.2.16 Endotoxin assay.....	53
2.2.17 Statistical analysis .....	53

### **CHAPTER 3: IMMUNOMODULATORY PROPERTIES OF T. BRUCEI-DERIVED KETOACIDS IN HUMAN DC..... 60**

3.1 INTRODUCTION .....	61
3.2 AIMS.....	63
3.3 RESULTS .....	64
3.3.1 Assessment of HPP and IP endotoxin levels.....	64
3.3.2 HPP and IP upregulate HO-1 and activate Nrf2 in BMDM.....	64
3.3.3 HPP and IP are non-toxic to primary human DC.....	65
3.3.4 HPP and IP upregulate HO-1 in primary human DC.....	65
3.3.5 HPP and IP activate Nrf2 in primary human DC.....	65
3.3.6 HPP and IP upregulate HO-1 through Nrf2 activation in primary human DC.....	66
3.3.7 HPP and IP increase the antioxidant capacity of primary human DC.....	66
3.3.8 IP, but not HPP, becomes fluorescent over time in culture media.....	67
3.3.9 IP, but not HPP, induces ROS production in primary human DC.....	67
3.3.10 HPP and IP activate the aryl hydrocarbon receptor in primary human DC.....	68
3.3.11 LPS stimulation moderately reduces ketoacid-induced HO-1 expression in human DC.....	68
3.3.12 HPP and IP reduce the production of pro-inflammatory cytokines in LPS-stimulated human DC.....	69
3.3.13 HPP, but not IP, reduces pro-IL-1 $\beta$ expression in LPS-stimulated human DC.....	69
3.3.14 HPP treatment inhibits the maturation of LPS-stimulated human DC.....	70
3.3.15 LPS stimulation upregulates glycolysis and oxidative phosphorylation in human DC.....	70
3.3.16 IP and HPP downregulate glycolysis in LPS-stimulated human DC.....	71
3.3.17 HPP favours engagement of oxidative phosphorylation over glycolysis in human DC.....	72
3.3.18 IP and HPP reduce the expression of HK2 in LPS-stimulated human DC.....	72
3.3.19 IP and HPP reduce phosphorylation of the mTOR substrate, S6, while increasing phosphorylation of AMPK in human DC.....	73
3.3.20 IP and HPP activate autophagy-related proteins in human DC.....	74
3.4 DISCUSSION .....	109

### **CHAPTER 4: IMMUNOMODULATORY PROPERTIES OF T. BRUCEI-DERIVED KETOACIDS IN HUMAN T CELLS..... 117**

4.1 INTRODUCTION .....	118
4.2 AIMS.....	119
4.3 RESULTS .....	121
4.3.1 HPP treated DC have a reduced capacity to activate allogeneic CD4 <sup>+</sup> T cells.....	121
4.3.2 Supernatants from DC treated with ketoacids reduce expression of IFN $\gamma$ in human CD4 <sup>+</sup> T cells. 122	
4.3.3 HPP and IP autofluorescence in PBMC can be resolved when replaced with fresh media after 18 hours.....	123
4.3.4 HPP, carnosol and curcumin, but not IP, significantly reduce viability of PBMC isolated from IBD patients.....	124
4.3.5 HPP, IP, carnosol and curcumin reduce proliferation of CD4 <sup>+</sup> and CD8 <sup>+</sup> T cells in PBMC isolated from IBD patients.....	125
4.3.6 HPP, IP, carnosol and curcumin reduce the secretion of cytokines from PBMC isolated from IBD patients.....	125
4.3.7 HPP, IP, carnosol and curcumin reduce cytokine expression in CD4 <sup>+</sup> and CD8 <sup>+</sup> T cells from IBD patients.....	126
4.3.8 HPP, IP, carnosol and curcumin reduce the polyfunctionality of CD4 <sup>+</sup> T cells in PBMC isolated from IBD patients.....	127
4.3.9 Ketoacid and polyphenol treatment have subtly different effects in CD4 <sup>+</sup> T cells in PBMC isolated from patients with ulcerative colitis and Crohn's disease.....	128



4.4	DISCUSSION .....	169
<b>CHAPTER 5:</b>	<b>GENERAL DISCUSSION.....</b>	<b>177</b>
5.1	GENERAL DISCUSSION .....	178
<b>REFERENCES</b>	<b>.....</b>	<b>184</b>

## Table of figures

Figure 1.1 Maturation of Dendritic Cells. ....	4
Figure 1.2 Development of helper T cell subsets. ....	6
Figure 1.3 Cellular respiration and fatty acid metabolism. ....	12
Figure 1.4 Major metabolic pathways engaged in immune cells. ....	14
Figure 1.5 The degradation of cellular products through autophagy. ....	17
Figure 1.6 Heme oxygenase and heme catabolism. ....	20
Figure 1.7 Nrf2 signalling pathway. ....	22
Figure 1.8 Chemical structures of the aromatic ketoacids indole pyruvate, phenyl pyruvate and hydroxyphenyl pyruvate, secreted by <i>T. Brucei</i> . ....	33
Figure 2.1 Monocyte purity analysed by flow cytometry. ....	55
Figure 2.2 CD4 <sup>+</sup> T cell purity analysed by flow cytometry. ....	56
Figure 2.3 Dendritic cell purity analysed by flow cytometry. ....	57
Figure 2.4 Gating strategy used to generate data shown in co-culture experiments. ....	58
Figure 2.5 Gating strategy used to generate data shown in IBD PBMC experiments. ....	59
Figure 3.1 Assessment of HPP and IP endotoxin levels. ....	75
Figure 3.2 HPP and IP upregulate HO-1 and stabilise Nrf2 in BMDM. ....	76
Figure 3.3 HPP and IP are non-toxic to primary human DC. ....	77
Figure 3.4 HPP and IP are non-toxic to primary human DC. ....	78
Figure 3.5 HPP and IP upregulate HO-1 in a concentration dependent manner in primary human DC. ....	79
Figure 3.6 HPP and IP upregulate HO-1 over time in primary human DC. ....	80
Figure 3.7 HPP and IP activate Nrf2 in human DC. ....	81
Figure 3.8 IP and HPP upregulate additional Nrf2-controlled genes in human DC. ....	82
Figure 3.9 The Nrf2 inhibitor, ML385, is non-toxic to human DC. ....	83
Figure 3.10 HPP and IP induce HO-1 through Nrf2 activation in human DC. ....	84
Figure 3.11 IP and HPP increase the antioxidant capacity of human DC. ....	85
Figure 3.12 IP, but not HPP, treatment causes autofluorescence in human DC after 24 hours. ....	86
Figure 3.13 IP, but not HPP, induces ROS production in human DC. ....	87
Figure 3.14 The increase in ROS production upon IP treatment is not due to autofluorescence. ....	88
Figure 3.15 IP and HPP upregulate CYP1A1 in human DC. ....	89
Figure 3.16 LPS stimulation moderately reduces ketoacid-induced HO-1 expression in human DC. ....	90
Figure 3.17 IP reduces the production of pro-inflammatory cytokines, and increases IL-10 production, in LPS-stimulated human DC. ....	91
Figure 3.18 HPP reduces the production of pro-inflammatory cytokines in LPS-stimulated human DC. ....	92
Figure 3.19 HPP and IP reduce pro-IL-1 $\beta$ expression in BMDM, while HPP moderately reduces pro-IL-1 $\beta$ expression in human DC. ....	93
Figure 3.20 HPP treatment reduces expression of maturation markers in LPS-stimulated human DC. ....	94
Figure 3.21 HPP treatment maintains the phagocytic capacity of LPS-stimulated human DC. ....	95

Figure 3.22 LPS stimulation increases glycolytic metabolism in time dependent manner in human DC.....	96
Figure 3.23 LPS stimulation increases respiration in time dependent manner in human DC. ....	97
Figure 3.24 LPS-stimulated human DC favour glycolysis over oxidative phosphorylation. 98	
Figure 3.25 IP and HPP treatment reduces glycolysis in LPS-stimulated human DC. ....	99
Figure 3.26 IP and HPP treatment have no effect on respiration in LPS-stimulated human DC. ....	100
Figure 3.27 IP and HPP treatment have no effect on the ECAR:OCR of LPS-stimulated human DC. ....	101
Figure 3.28 IP and HPP treated human DC primarily derive their ATP from oxidative phosphorylation. ....	102
Figure 3.29 HPP-treated human DC favour engagement of oxidative phosphorylation over glycolysis.....	103
Figure 3.30 IP and HPP treatment reduces expression of HK2 in LPS-stimulated human DC. ....	104
Figure 3.31 IP and HPP treatment moderately reduces the phosphorylation of the protein S6 in LPS-stimulated human DC. ....	105
Figure 3.32 HPP and IP phosphorylate and activate AMPK in human DC. ....	106
Figure 3.33 IP and HPP activate p62 in human DC. ....	107
Figure 3.34 IP and HPP activate LC3-II in human DC. ....	108
Figure 3.35 Model outlining the immunomodulatory effects of trypanosome-derived ketoacids and potential mechanism of action. ....	116
Figure 4.1 Ketoacid-treated LPS-stimulated DC alter the expression of ki67 in CD4 <sup>+</sup> T cells upon co-culture. ....	129
Figure 4.2 Ketoacid-treated LPS-stimulated DC alter the expression of IFN $\gamma$ in CD4 <sup>+</sup> T cells upon co-culture. ....	130
Figure 4.3 The effect of HPP- and IP-treated LPS-stimulated DC on the frequency of Tregs in CD4 <sup>+</sup> T cells upon co-culture.....	131
Figure 4.4 Ketoacid treated DC do not favour an increase in the proliferation of Tregs over non-Tregs in CD4 <sup>+</sup> T cells upon co-culture.....	132
Figure 4.5 IL-10 secretion is not altered in co-cultures of ketoacid-treated LPS-stimulated DC and CD4 <sup>+</sup> T cells.....	133
Figure 4.6 Supernatants from ketoacid treated DC induce autofluorescence in CD4 <sup>+</sup> T cells.....	134
Figure 4.7 Supernatants from ketoacid treated DC impair the viability of CD4 <sup>+</sup> T cells. ...	135
Figure 4.8 Supernatants from IP or HPP treated DC reduce the expression of IFN $\gamma$ in CD4 <sup>+</sup> T cells.....	136
Figure 4.9 IP and HPP treatment causes autofluorescence in PBMC after 4 days. ....	137
Figure 4.10 IP and HPP treatment induce less autofluorescence in PBMC when removed after 18 hours and incubated with anti-CD3 only for a further 4 days. ....	138
Figure 4.11 IP is non-toxic to <i>ex-vivo</i> stimulated PBMC from patients with IBD, while HPP, carnosol and curcumin all show significant, albeit mild, reductions in viability. ....	139
Figure 4.12 HPP, carnosol and curcumin more significantly reduce the viability of CD8 <sup>+</sup> T cells compared to CD4 <sup>+</sup> T cells, while IP has no effect on the viability of either cell type. ....	140

Figure 4.13 HPP and IP reduce proliferation of CD4 <sup>+</sup> T cells in <i>ex-vivo</i> stimulated PBMC from patients with IBD. ....	141
Figure 4.14 HPP and IP reduce proliferation of CD8 <sup>+</sup> cells in <i>ex-vivo</i> stimulated PBMC from patients with IBD. ....	142
Figure 4.15 Carnosol and curcumin reduce proliferation of CD4 <sup>+</sup> T cells in <i>ex-vivo</i> stimulated PBMC from patients with IBD. ....	143
Figure 4.16 Carnosol and curcumin reduce proliferation of CD8 <sup>+</sup> cells in <i>ex-vivo</i> stimulated PBMC from patients with IBD. ....	144
Figure 4.17 HPP inhibits secretion of cytokines from <i>ex-vivo</i> stimulated PBMC from patients with IBD. ....	145
Figure 4.18 IP inhibits secretion of cytokines from <i>ex-vivo</i> stimulated PBMC from patients with IBD. ....	146
Figure 4.19 Carnosol and curcumin inhibit secretion of cytokines from <i>ex-vivo</i> stimulated PBMC from patients with IBD. ....	147
Figure 4.20 HPP and IP reduce the frequency of IFN $\gamma$ <sup>+</sup> CD4 <sup>+</sup> T cells in <i>ex-vivo</i> stimulated PBMC from patients with IBD. ....	148
Figure 4.21 HPP and IP have no effect on the frequency of IL-17 <sup>+</sup> CD4 <sup>+</sup> T cells in <i>ex-vivo</i> stimulated PBMC from patients with IBD. ....	149
Figure 4.22 HPP, but not IP, reduces the frequency of IL-2 <sup>+</sup> CD4 <sup>+</sup> T cells in <i>ex-vivo</i> stimulated PBMC from patients with IBD. ....	150
Figure 4.23 HPP and IP have no effect on the frequency of TNF <sup>+</sup> CD4 <sup>+</sup> T cells in <i>ex-vivo</i> stimulated PBMC from patients with IBD. ....	151
Figure 4.24 Carnosol and curcumin reduce the frequency of IFN $\gamma$ <sup>+</sup> and IL-17 <sup>+</sup> CD4 <sup>+</sup> T cells in <i>ex-vivo</i> stimulated PBMC from patients with IBD. ....	152
Figure 4.25 Carnosol and curcumin reduce the frequency of IL-2 <sup>+</sup> and TNF <sup>+</sup> CD4 <sup>+</sup> T cells in <i>ex-vivo</i> stimulated PBMC from patients with IBD. ....	153
Figure 4.26 HPP and IP reduce the frequency of IFN $\gamma$ <sup>+</sup> CD8 <sup>+</sup> T cells in <i>ex-vivo</i> stimulated PBMC from patients with IBD. ....	154
Figure 4.27 HPP and IP have no effect on the frequency of IL-2 <sup>+</sup> CD8 <sup>+</sup> T cells in <i>ex-vivo</i> stimulated PBMC from patients with IBD. ....	155
Figure 4.28 HPP, but not IP, reduces the frequency of TNF <sup>+</sup> CD8 <sup>+</sup> T cells in <i>ex-vivo</i> stimulated PBMC from patients with IBD. ....	156
Figure 4.29 Carnosol and curcumin reduce the frequency of IFN $\gamma$ <sup>+</sup> , IL-2 <sup>+</sup> and TNF <sup>+</sup> CD8 <sup>+</sup> T cells in <i>ex-vivo</i> stimulated PBMC from patients with IBD. ....	157
Figure 4.30 HPP and IP reduce the frequency of IFN $\gamma$ <sup>+</sup> IL-17 <sup>+</sup> CD4 <sup>+</sup> T cells in <i>ex-vivo</i> stimulated PBMC from patients with IBD. ....	158
Figure 4.31 HPP and IP reduce the frequency of IFN $\gamma$ <sup>+</sup> TNF <sup>+</sup> CD4 <sup>+</sup> T cells in <i>ex-vivo</i> stimulated PBMC from patients with IBD. ....	159
Figure 4.32 HPP, but not IP, reduces the frequency of IL-2 <sup>+</sup> TNF <sup>+</sup> CD4 <sup>+</sup> T cells in <i>ex-vivo</i> stimulated PBMC from patients with IBD. ....	160
Figure 4.33 HPP and IP reduce the frequency of IL-2 <sup>+</sup> IFN $\gamma$ <sup>+</sup> CD4 <sup>+</sup> T cells in <i>ex-vivo</i> stimulated PBMC from patients with IBD. ....	161
Figure 4.34 Carnosol and curcumin reduce the frequency of IFN $\gamma$ <sup>+</sup> IL-17 <sup>+</sup> CD4 <sup>+</sup> T cells in <i>ex-vivo</i> stimulated PBMC from patients with IBD. ....	162
Figure 4.35 Carnosol and curcumin reduce the frequency of IFN $\gamma$ <sup>+</sup> TNF <sup>+</sup> CD4 <sup>+</sup> T cells in <i>ex-vivo</i> stimulated PBMC from patients with IBD. ....	163

Figure 4.36 Curcumin, but not carnosol, reduces the frequency of IL-2<sup>+</sup>TNF<sup>+</sup> CD4<sup>+</sup> T cells in *ex-vivo* stimulated PBMC from patients with IBD. .... 164

Figure 4.37 Carnosol and curcumin reduce the frequency of IL-2<sup>+</sup>IFN $\gamma$ <sup>+</sup> CD4<sup>+</sup> T cells in *ex-vivo* stimulated PBMC from patients with IBD. .... 165

Figure 4.38 HPP more significantly reduces IFN $\gamma$  expression in CD4<sup>+</sup> T cells in *ex-vivo* stimulated PBMC from patients with ulcerative colitis compared to Crohn's disease. ... 166

Figure 4.39 IP more significantly reduces IFN $\gamma$  expression in CD4<sup>+</sup> T cells in *ex-vivo* stimulated PBMC from patients with ulcerative colitis compared to Crohn's disease. ... 167

Figure 4.40 Carnosol and curcumin more significantly reduce TNF expression in CD4<sup>+</sup> T cells in *ex-vivo* stimulated PBMC from patients with Crohn's disease compared to ulcerative colitis..... 168

Figure 4.41 Model of immunomodulatory effects of trypanosome-derived ketoacids in human T cells..... 176

# **Chapter 1:**

## **Introduction**

## 1.1 The immune system

The mammalian immune system defends against infection or disease and is comprised of a network of many different tissues, molecules, and cells. In order to function properly, the immune system must recognise and remove pathogens from the host to ensure they do not cause excessive damage or death. It must also be capable of distinguishing between different types of pathogens, between self- and non-self, and between healthy or damaged tissue.

Vertebrates have a more complex immune system than invertebrates, which can be divided into two subsystems; the innate immune system and the adaptive immune system [1,2]. The innate immune system is the first line of defence against pathogens [3]. It is present from birth and is found in all types of plants and animals [3]. It consists of anatomical barriers, the complement system, inflammatory mediators, and leukocytes from the myeloid lineage, including phagocytic cells e.g. neutrophils, macrophages, and dendritic cells, which will be further discussed in section 1.1.1 [3]. These cells are rapidly activated upon infection and, unlike the adaptive immune system, do not carry the capacity for long-term immunological memory. However, in recent years increasing evidence has described the potential of the innate immune system to become trained and respond faster upon re-exposure to an antigen [4]. Innate immune cells express pathogen recognition receptors (PRRs), including toll-like receptors (TLRs), C-type lectin receptors (CLRs), NOD-like receptors (NLRs) and RIG-I like receptors (RLRs) [5]. These PRRs recognise pathogen-associated molecular patterns (PAMPs), for example lipopolysaccharide (LPS), which is found in the cell-wall of many strains of bacteria but not on the host's own cells [5]. Damage associated molecular patterns (DAMPs) are also recognised by PRRs [5]. These are host-derived molecules which arise as a result of cell stress, cell death, and/or tissue damage. The adaptive immune response is functional only in vertebrates and is mediated by cells of lymphoid origin, primarily T cells and B cells [1,2]. These are specialised cells which have highly variable antigen receptors, achieved through V(D)J recombination, leading to their ability to recognise and bind specific antigens [1,2]. These cells are capable of clonal expansion and possess immunological memory, a feature which provides the basis

for vaccination [1,2]. Both the innate and adaptive immune system function together to protect the host from damage and infection [6].

### *1.1.1 Dendritic cells*

Dendritic cells (DC) are mononuclear, bone-marrow-derived phagocytic cells which are a key component of the innate immune system. DC are typically considered 'professional' antigen presenting cells (APC), and act as a bridge between the innate and adaptive immune response due to their role in presenting antigen to T cells. Hence, they are critical for the induction of both a primary innate immune response, and the subsequent adaptive immune responses. There are a number of different DC subsets, with the two main subsets consisting of plasmacytoid DC and conventional DC [7]. Plasmacytoid DC are the rarer subset which typically detect viral infections via recognition of PAMPs by the endosomal TLRs, TLR7 and TLR9. In response, these cells secrete large amounts of type 1 interferons (IFN) [7]. On the other hand, conventional DC are more ubiquitous and secrete pro-inflammatory cytokines, including the interleukins (IL) IL-1, IL-23, IL-12 and IL-6, following activation of TLRs such as TLR4 and TLR2 [7]. For the purpose of this thesis, from here on 'DC' will refer to the conventional DC subset.

DC progenitors arise in the bone marrow before migrating to peripheral tissues, where the main function of these immature cells is to scavenge and capture antigen, primarily through phagocytosis. Upon antigen capture, DC undergo a number of functional and phenotypic changes as they switch from an immature to a mature state (Figure 1.1) [8]. DC must return to secondary lymphoid organs to activate naïve T cells, therefore their maturation is also linked to their migration, and is accompanied by the upregulation of the chemokine receptor, CCR7 [9]. As DC mature from a phagocytic state to an antigen presenting state, they also upregulate a number of maturation and co-stimulatory markers required for antigen presentation and T cell activation, including CD80, CD83, CD40 and CD86 [8]. This switch is also accompanied by a change in cell morphology (to better facilitate antigen presentation), and an increase in surface expression of major histocompatibility complex (MHC) molecules, upon which antigen peptides are loaded and presented to T cells on the surface of the DC [8]. Upon activation, DC also secrete many



different cytokines which play important roles in shaping the immune response, for example the secretion of certain polarising cytokines by DC can induce the differentiation of specific T cell subsets [8], which is further discussed in section 1.1.2. DC are also important for maintaining immune homeostasis and promoting T cell tolerance through the presentation of harmless or self-antigens to T cells without any accompanying activating signals, resulting in the generation of tolerance, which will be further discussed in section 1.2.

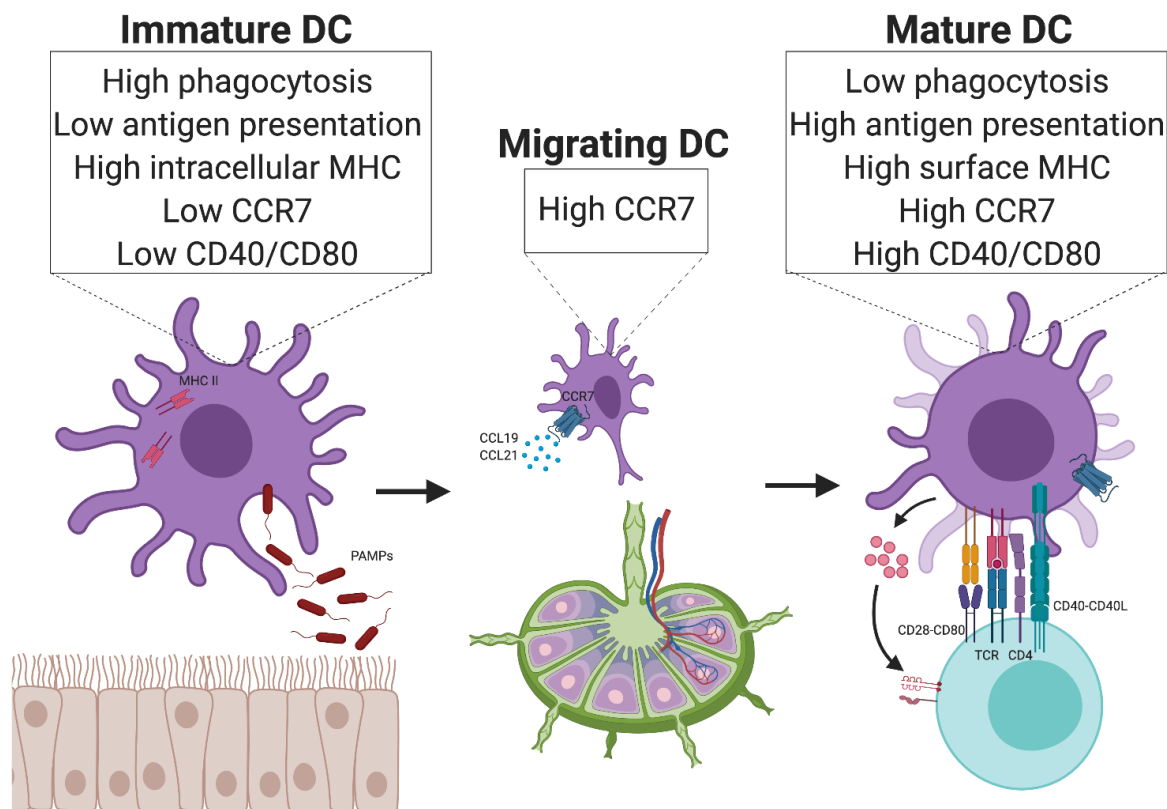


**Figure 1.1 Maturation of Dendritic Cells.**

Immature DC phagocytose PAMPs and DAMPs in the periphery. These cells have high levels of intracellular MHC molecules, as well as low surface expression of CCR7, CD40 and CD80. Upon antigen capture, and activation of DC, the cells migrate to the secondary lymphoid organs, requiring the expression of high surface levels of CCR7, to which CCL19 and CCL21 can bind. Maturation of the DC results in decreased phagocytic capacity and increased antigen presentation. This is accompanied by an increase in surface MHC expression, along with CD40 and CD80. Activated DC also release a number of cytokines. All of these factors coordinate, allowing DC to activate T cells.

### 1.1.2 T cells

T cells are important mediators of the adaptive immune response. T cells arise from bone marrow progenitors that migrate to the thymus to develop, before migration to secondary lymphoid organs, where they can be activated by APC and exported to peripheral tissue to carry out their effector functions [10]. T cells include naïve T cells, which have not yet encountered the relevant antigens for activation, and memory T cells, which have been previously activated and are important for maintaining long term immunity [10]. As mentioned, naïve T cells become activated in secondary lymphoid organs upon antigen presentation by APC. From here they migrate to the site of infection or damage to carry out their specific effector function [10]. They require three signals in order to become fully activated: binding of an antigen presented by an APC on an MHC molecule to the T cell receptor (TCR), binding of CD28 on naïve T cells to co-stimulatory molecules (e.g. CD80/86) on APC, and cytokine production by APC to instruct the T cell effector functions further [8]. For the purpose of this thesis 'T cells' will refer to cells which have an  $\alpha\beta$  T cell receptor. However, there are also 'unconventional' T cell subsets, including cells which instead have  $\gamma\delta$  T cell receptors, and have been described as acting on the border of the innate and adaptive immune response, and are reviewed in detail elsewhere [11].

CD8<sup>+</sup> T cells and CD4<sup>+</sup> T cells represent two distinct subsets of T cells. CD8<sup>+</sup> T cells are also known as cytotoxic T cells and are activated to directly kill infected cells following recognition of antigens presented on MHC class I molecules. On the other hand, CD4<sup>+</sup> T cells are also known as helper T cells and recognise antigens presented on MHC class II molecules. These cells provide help to other immune cells (e.g. B cells, macrophages, and CD8<sup>+</sup> T cells) enabling them to respond appropriately to invading pathogens. CD4<sup>+</sup> T cells can be further divided into a number of different subsets depending on the type of antigen they respond to, the transcription factors that cause their differentiation, and the cytokines they secrete (Figure 1.2). There are numerous helper T cell subsets including Th1, Th2, Th17, Th9, Th22, Tfh and regulatory T cells (Tregs) [12]. Th1 cells are generally activated in response to intracellular bacteria, Th17 cells in response to extracellular pathogens, and Th2 cells in response to extracellular parasites [12]. These cells are all generally described

as being pro-inflammatory due to the effector functions they carry out when activated. On the other hand, Treg cells are generally described as immunosuppressive, and their main role is to maintain self-tolerance and downregulate effector T cell activation. Each helper T cell subset has its own distinct cytokine profile. For example, Th1 cells secrete high levels of IFN $\gamma$ , Th17 cells secrete IL-17A and IL-17F, while Th2 cells secrete IL-4, IL-5 and IL-13 [12]. Tregs, on the other hand, secrete IL-10 along with other immunosuppressive cytokines [12]. Not surprisingly, a carefully controlled balance between different T cell subsets is important to prevent aberrant immune responses and disease, as discussed in section 1.2.

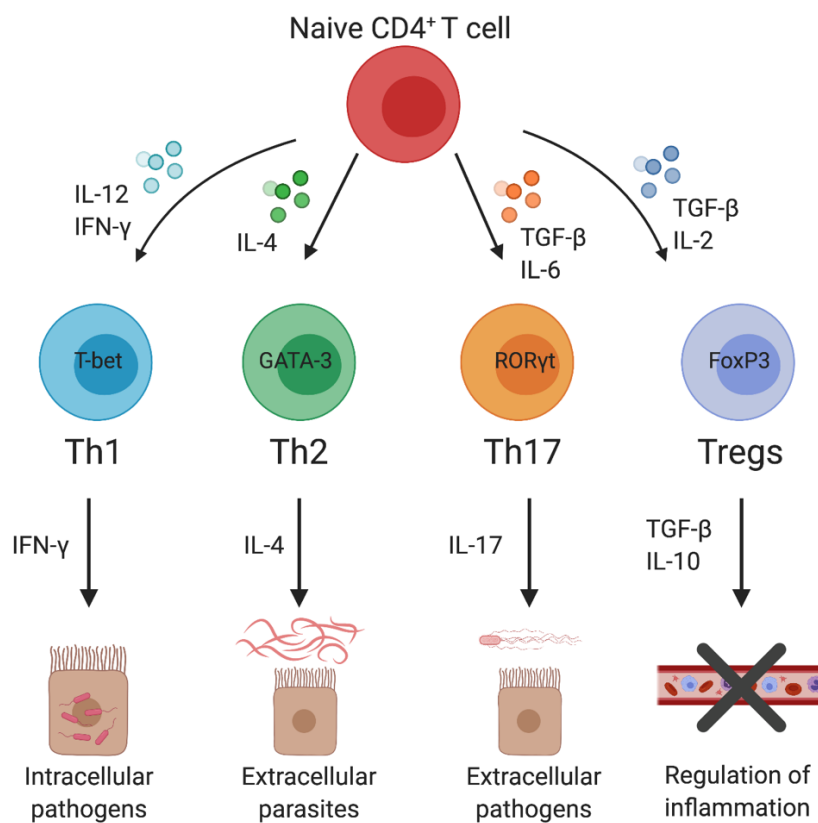


**Figure 1.2 Development of helper T cell subsets.**

Naïve CD4<sup>+</sup> T cells can differentiate into different effector subsets depending on the cytokine they are exposed to. IL-12 and IFN $\gamma$  exposure activates the transcription factor T-bet, resulting in Th1 cells, which secrete IFN $\gamma$  to fight intracellular pathogens. IL-4 exposure activates the transcription factor GATA-3, resulting in Th2 cells which secrete IL-4 to fight extracellular parasites. TGF- $\beta$  and IL-6 exposure activates the transcription factor ROR $\gamma$ t, leading to differentiation into the Th17 subset which secrete IL-17 to fight extracellular pathogens. Finally, exposure of naïve T cells to TGF- $\beta$  and IL-2 results in activation of the transcription factor FoxP3 which results in the generation of Tregs. These cells secrete TGF- $\beta$  and IL-10, and are different to the other pro-inflammatory cells listed here. Instead, they downregulate inflammation and are immunosuppressive.

## 1.2 Inflammatory & autoimmune diseases

The incidence of inflammatory and autoimmune disease is on the rise, particularly in developed countries [13]. Despite this, most of these diseases remain incurable and their aetiology is not fully understood [14]. Inflammatory diseases describe a wide number of disorders which are characterised by dysregulated inflammation. Autoimmune diseases are characterised by an abnormal immune response to self-antigens which in turn leads to excessive/uncontrolled inflammation [14]. Examples of these diseases include psoriasis, rheumatoid arthritis (RA), inflammatory bowel disease (IBD), multiple sclerosis (MS) and systemic lupus erythematosus (SLE). The initial triggering event for many of these conditions is unclear [14]. Onset does not usually occur until adulthood and despite the distinct disease pathologies seen, they all share the common hallmark features of reduced self-tolerance [14].

Self-reactive T cells are normally removed from the repertoire of T cells through a process known as negative selection which occurs in the thymus. However, in autoimmune diseases, self-reactive cells (and/or auto-antibodies) prevail in the host and cause damage due to sterile inflammation which occurs in the absence of infection [14]. As previously mentioned, DC are important mediators of tolerance and immune homeostasis. DC present in the thymus are involved in central tolerance; however, central tolerance is not sufficient to eliminate all self-reactive cells, therefore DC in the periphery are also important generators of peripheral tolerance [15–18]. In the steady state, in the absence of infection, DC will aid in the generation of peripheral tolerance. DC present self-antigens to T cells without accompanying co-stimulation. As co-stimulation is required for full T cell activation, the cells cannot be activated and instead become anergic, in which they are functionally inactivated yet still alive [19]. Tolerogenic DC will also typically secrete anti-inflammatory cytokines, for example IL-10 [20]. Both tolerogenic and mature DC are also capable of promoting Treg differentiation in the periphery, another important mechanism for limiting inflammation and damage to the host [20]. Tolerogenic DC may be exploited for therapeutic purposes to treat diseases with high levels of damaging inflammation. A number of methods have been proposed including DC treated with agents *ex vivo* which

result in the generation of tolerogenic DC, which could then be introduced into the host to dampen inflammation through the methods previously discussed [17,21,22].

Despite uncertainty surrounding the exact mechanisms underlying the initiation or pathogenesis of autoimmune diseases, it is clear that a breach in self-tolerance occurs [14]. Aberrant activation of DC can lead to the secretion of pro-inflammatory cytokines, and activation and recruitment of other inflammatory cells [23]. Th1 and Th17 cells are the most commonly implicated cells in the pathogenesis of many autoimmune diseases. As previously mentioned, both cell types are highly inflammatory and are normally involved in host defence against pathogens. IL-12 and IL-23, which share a common p40 subunit, are secreted by activated DC and are important in the differentiation of Th1 and Th17 cells, respectively [12]. Initially Th1 cells, and their secreted cytokine IFN $\gamma$ , were considered the primary pathogenic cells in autoimmune diseases, as animal models of adoptive transfer of the cells caused autoimmune diseases, while IFN $\gamma$  levels correlated with disease severity [24,25]. Mice lacking the IL-12p40 subunit were shown to resist induction of a murine model of MS, initially attributing this to the lack of induction of Th1 cells [26]. However, upon discovery of Th17 cells, and the p40 subunit being shared with IL-23, it was soon revealed that Th1 cells may not be as important in the pathogenesis as once thought. IL-17, the typical Th17 cytokine, has been found at increased levels in patients with autoimmune diseases [27]. Similarly, deficiencies or neutralisation of IL-17 or associated cytokines and cells results in resistance to these diseases [28–30]. On the other hand, as previously mentioned, Tregs are important for downregulating inflammatory immune responses and maintaining homeostasis. Therefore, any imbalance between these cell types could cause a serious issue to the host as a result of prolonged and chronic inflammation. Indeed, an increased Th17/Treg ratio has been observed in RA, IBD, MS and psoriasis patient samples [31].

Therapeutic strategies to modulate (or suppress) the immune system have and are being developed to treat autoimmune diseases. For example, tocilizumab, which targets the Th17 differentiating cytokine IL-6, has demonstrated efficacy in the treatment of RA [32–34]. Therapeutic effects were accompanied by a decrease in Th17 cell numbers and an increase in Tregs [32–34]. Secukinumab, a monoclonal antibody targeting IL-17A, exhibited

impressive therapeutic effects in psoriasis and psoriatic arthritis patients [35,36]. However, in the case of Crohn's disease (CD), administration of the antibody resulted in worsening of the disease [37] and it has been suggested that IL-17 plays a positive role in regulating normal gut homeostasis [38]. Furthermore, studies have shown that anti-IL-17 treatment lacked efficacy in RA patients [39] and while ustekinumab, which targets the shared p40 subunit of IL-12 and IL-23, demonstrated therapeutic benefit in psoriasis patients, this was not the case for MS patients [40,41]. This highlights the heterogeneity in different autoimmune diseases and the careful consideration that is required when developing disease modifying agents. Another factor to be taken into account are the many side effects associated with such treatments and, in particular, vulnerability to infections [42]. Many patients also become refractory to treatment or show no response to these treatments from the outset [42]. Therefore, there is an urgent need for novel, beneficial anti-inflammatory therapies, with increased long-term efficacy, tolerability, and less adverse side effects.

### 1.3 Immunometabolism

Every cell requires energy in order to survive and carry out normal functions. Dysregulated metabolism has long been recognised as a feature of many metabolic disorders, however more recently, metabolic reprogramming has been observed in immune cells and research in the area of 'Immunometabolism' has gained significant momentum. It has now been shown that not only do different immune cells engage different metabolic pathways, but that the activation or maturation state of the immune cell is accompanied by metabolic switches [43]. Furthermore, dysregulated immunometabolism has been recognised as a feature of many immune-mediated disorders including arthritis and psoriasis [44–46] and there is now potential to exploit metabolic reprogramming for therapeutic benefit, as discussed below.

### 1.3.1 *Cellular respiration*

Cellular respiration is the primary method cells use to generate adenosine triphosphate (ATP), the main source of energy for a cell. Cellular respiration is a multi-step, catabolic process, typically utilising glucose as an energy source to result in the generation of ATP. Glucose first passes through glycolysis, which takes place in the cytosol of the cell. This process can take place in the presence of oxygen, resulting in the generation of pyruvate, which continues through the pathways involved in respiration. Glycolysis can also occur in the absence of oxygen, resulting in the generation of lactate. This is known as anaerobic glycolysis, and the lactate produced does not proceed further in respiration. Though glycolysis is a relatively fast process, it is relatively inefficient for energy production, with a net production of only 2 ATP molecules. Despite the low energy yield obtained from glycolysis, it is still an important pathway for the generation of many intermediates which are used to produce nucleotides, fatty acids and amino acids. However, in order to yield more energy, the process of cellular respiration continues. During aerobic glycolysis, pyruvate is oxidised to acetyl-CoA which then enters the tricarboxylic acid (TCA) cycle inside the mitochondria. The acetyl-CoA is oxidised to CO<sub>2</sub> during this cycle while NAD<sup>+</sup> is reduced to NADH. This is required for the next step in respiration: oxidative phosphorylation. Oxidative phosphorylation also takes place in the mitochondria, utilising the NADH produced during the citric acid cycle to generate energy through a proton gradient set up by the electron transport chain. This energy is used to power ATP synthase, resulting in the production of large amounts of energy, yielding 32 ATP molecules. Oxygen is required for oxidative phosphorylation to take place, as the electrons passing through the electron transport chain must ultimately be transferred to oxygen to generate water and complete the chain. This process is generally slower than glycolysis, however the yield of ATP is much higher. Due to the fast production of many biosynthetic intermediates, as well as quick turnover of energy, glycolysis is generally associated with rapidly proliferating cells [43] while the slower, longer process of oxidative phosphorylation is generally utilised in cells favouring longevity [43]. Engagement of cellular respiration by cells is controlled in a number of ways, including regulation through feedback mechanisms by enzymes and products involved in this process. The mammalian target of rapamycin (mTOR), as part of

the complex mTORC1, functions as a cellular energy and nutrient sensor, and controls protein synthesis and other cellular processes including anabolic pathways, like glycolysis. Activation of mTORC1 results in the induction of a number of glycolytic genes, including glucose transporter 1 (GLUT1), which transports glucose into the cell, and hexokinase 2 (HK2), the enzyme crucial for the phosphorylation of glucose in the first step of glycolysis [47]. These glycolytic genes are activated by mTORC1 through activation of the transcription factor hypoxia-inducible factor 1 (HIF1 $\alpha$ ) [47].

### 1.3.2 *Fatty acid metabolism*

Fatty acids are the most important energy store in the body. They are essential for the formation of phospholipid bilayers for cell membranes, and also take part in cell signalling by acting as second messengers and hormones [48]. Fatty acid metabolism consists of the catabolic process of fatty acid oxidation (FAO), whereby fatty acids are broken down to release energy through  $\beta$ -oxidation, and the anabolic process of fatty acid synthesis (FAS), in which fatty acids are synthesised from acetyl-CoA, previously oxidised from pyruvate following glycolysis. FAO generates a number of intermediates, including acetyl-CoA, which can be fed into other pathways, for example the TCA cycle and oxidative phosphorylation. This can result in the generation of large amounts of energy for the cell. FAS is regulated by mTOR signalling. mTOR promotes FAS through activation of sterol regulatory element binding protein (SREBP), which activates the enzyme acetyl-CoA carboxylase (ACC). This results in the carboxylation of acetyl-CoA to malonyl Co-A. Malonyl Co-A becomes committed to FAS at this stage, and inhibits FAO through regulation of the enzyme carnitine palmitoyltransferase (CPT). This inhibition of FAO can be lifted through inhibition of FAS by 5' adenosine monophosphate-activated protein kinase (AMPK). Activation of AMPK inhibits FAS in two ways, first by directly inhibiting mTOR activation, and also through phosphorylation of ACC, resulting in its inhibition, leading to the indirect activation of FAO (Figure 1.3) [49].



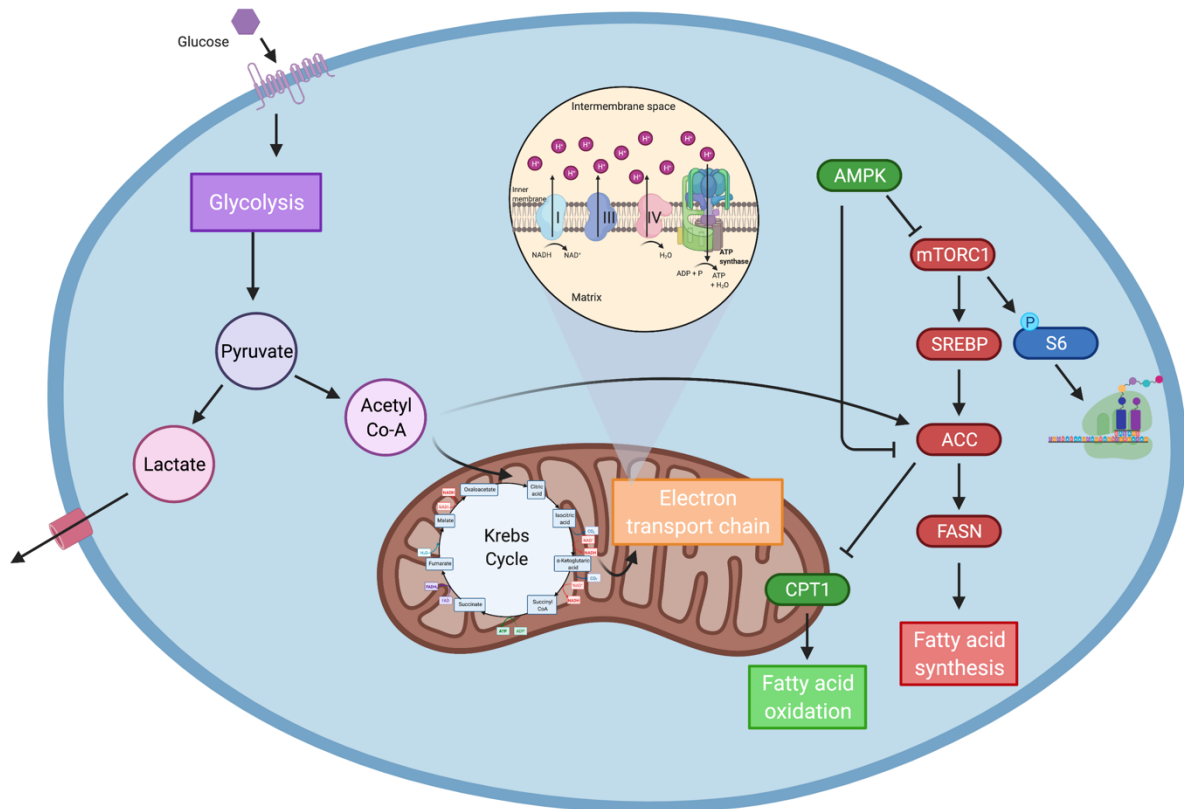


**Figure 1.3 Cellular respiration and fatty acid metabolism.**

Cells engage a range of metabolic pathways depending on their needs. Glucose is broken down by glycolysis to give pyruvate. Pyruvate can be exported from the cell as lactate under anaerobic conditions. In the presence of oxygen, pyruvate is converted to acetyl co-A which enters the Krebs cycle. NADH from the Krebs cycle passes into the electron transport chain, completing oxidative phosphorylation and generating energy through a proton gradient. Acetyl co-A can also be broken down by ACC, a crucial enzyme involved in the fatty acid synthesis pathway, which is activated by mTORC1, which also controls protein synthesis. Inhibition of this pathway by AMPK results in activation of the fatty acid oxidation pathway by lifting the inhibition placed on the enzyme CPT1.

### 1.3.3 Metabolism and immune cells

In 1956, Otto Warburg first observed that some cancer cells were increasing glycolysis, despite the presence of oxygen [50]. This phenomenon has now been observed in other cell types, particularly immune cells. As previously mentioned, rapidly proliferating cells ramp up glycolysis as a method for a quick turnover of energy, as well as utilising it to synthesise many important intermediates needed for proliferation such as nucleotides or fatty acids for new cell membranes. This increased demand for fatty acids also results in

the upregulation of FAS. This particular metabolic profile is not only seen in proliferating cells, but in other cell types with similar energy demands, including activated immune cells. For example, activated DC and macrophages alter their effector functions upon maturation, as previously outlined, and this results in altered metabolic needs [51,52]. Many effector T cell subsets, including CD8<sup>+</sup> T cells, Th1, Th2 and Th17 cells alter their metabolism in a similar manner [53]. Despite the TCA cycle and oxidative phosphorylation generally still remaining functional in these cell types, there is a shift towards glycolysis. In the case of pro-inflammatory M1 macrophages and activated DC, the TCA cycle does not appear to be intact which leads to the production of pro-inflammatory cytokines, including IL-1 $\beta$  [54–56]. This impaired TCA cycle results in the accumulation of citrate which can feed into the process of FAS. Increased FAS is crucial for the activation of M1 macrophages and DC and is elevated upon TLR stimulation in both cell types (Figure 1.4) [56,57]. On the other hand, FAO has been shown to be important in M2 macrophages, and in reducing the production of inflammatory cytokines by inflammatory macrophages (Figure 1.4) [58,59]. The balance of fatty acid metabolism is also of particular importance in T cell responses and function. Tregs exhibit increased levels of FAO and increased expression of the genes involved in this process, including CPT1A, while effector T cells downregulate FAO during activation (Figure 1.4) [60,61]. Furthermore, effector T cells, and in particular Th17 cells, exhibit increased FAS (Figure 1.4) [62]. This difference in T cell metabolism could be of particular importance for diseases in which the Th17/Treg balance is skewed, and will be discussed further in section 1.3.4.

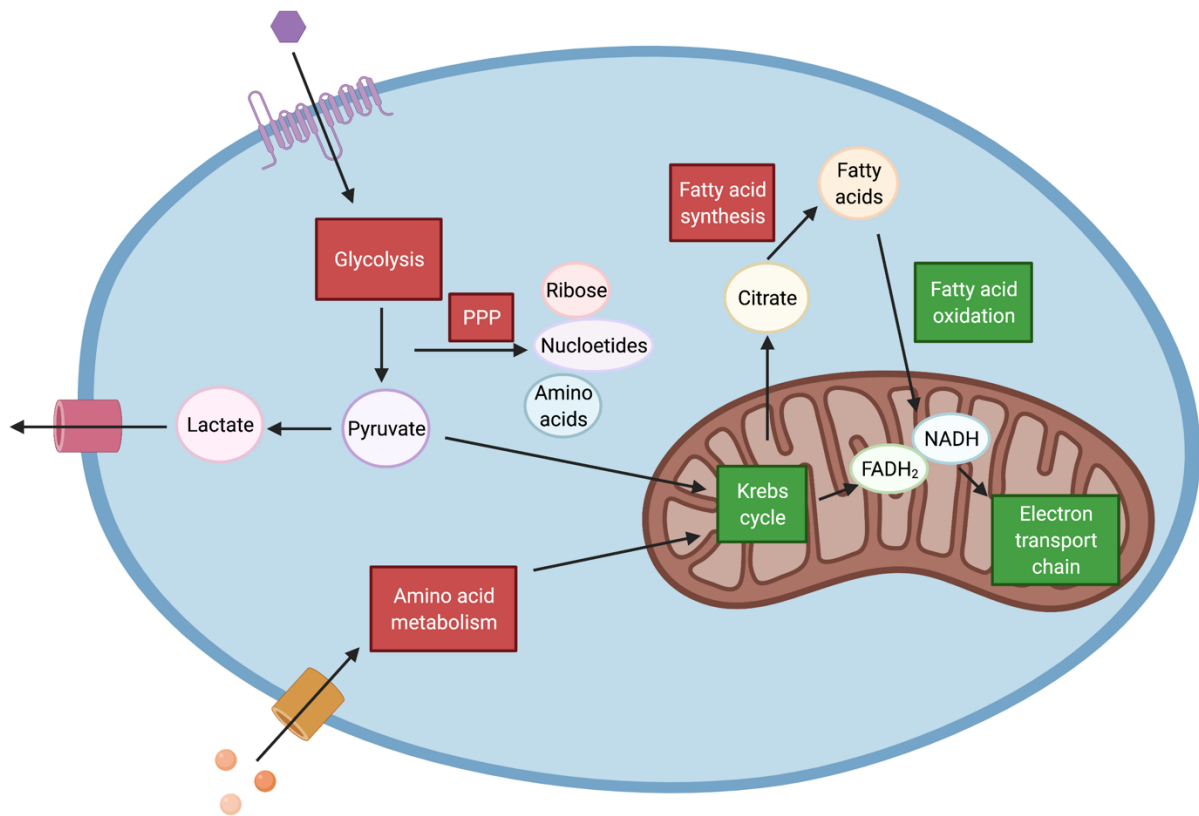


**Figure 1.4 Major metabolic pathways engaged in immune cells.**

Glycolysis converts glucose to pyruvate, which can be converted to lactate, and secreted from the cell, not progressing in any further metabolic pathways. Or pyruvate itself can enter the TCA cycle in the mitochondria, generating NADH and FADH<sub>2</sub>, feeding into the electron transport chain, completing cellular respiration, and generating ATP. Fatty acid oxidation also generates NADH and FADH<sub>2</sub> to feed into this pathway. Citrate can also be removed from the TCA cycle to feed into fatty acid synthesis. Glycolysis can feed into the pentose phosphate pathway (PPP), while amino acid metabolism also feeds into the TCA cycle. Pathways shown in red are generally associated with activated and effector immune cells, while pathways shown in green are generally associated with naive, immature, or regulatory immune cells. Figure adapted from [43].

#### 1.3.4 Immunometabolism as a therapeutic target

As discussed above, the metabolism of immune cells plays an important role in their activation status and/or effector function, therefore the manipulation of these pathways could potentially be used as a therapeutic approach to treat many diseases characterised by dysregulated inflammation. Indeed, some autoimmune diseases show specific alterations to the metabolism of the immune cells involved. For example, in SLE, T cells show persistent mitochondrial hyperpolarisation (an early step in T cell activation) as well

as ATP depletion [63]. In RA, CD4<sup>+</sup> T cells show a reduced engagement of glycolysis with an increase in the amount of glucose passed into the pentose phosphate pathway [45]. Similarly, T cells from patients with MS exhibit dampened glycolysis and mitochondrial respiration, which is restored to levels comparable to healthy subjects upon treatment with IFN- $\beta$ , a first line treatment for MS [64].

As mentioned earlier, Th17 cells (along with other effector T cell subsets) generally exhibit increased glycolysis and FAS, while Treg cells generally show increased TCA cycle, oxidative phosphorylation and FAO [53,62]. Effector T cells convert pyruvate to lactate, while Treg cells utilise the enzyme pyruvate dehydrogenase (PDH) to convert pyruvate to acetyl-CoA to continue further through the TCA cycle [61]. This is controlled by the enzyme pyruvate dehydrogenase kinase (PDHK), which inhibits PDH in effector T cells, thereby preventing them from converting pyruvate to acetyl-CoA [61]. Inhibition of PDHK overcomes this effect and could therefore be used as a potential therapy to skew the metabolic pathways engaged in T cells by enhancing processes associated with Treg cells [61]. This has shown promise in a number of animal models of disease, including experimental autoimmune encephalomyelitis (EAE) [61]. Similarly, blockade of mTOR activity in the EAE model results in increased Treg cells and an amelioration of disease progression [65]. Inhibition of ACC, a key enzyme involved in FAS downstream of mTOR, also increased Treg numbers while decreasing IL-17 and IFN $\gamma$  producing T cells in the EAE model [62]. This was accompanied by a reduction in disease pathology [62]. Inhibition of mTORC1 with rapamycin inhibits Th17 cells and promotes Tregs in patients with SLE [66]. Furthermore, metformin, a drug traditionally used to treat type II diabetes, is now showing potential as a treatment for autoimmune diseases by altering the metabolic state of immune cells. Metformin activates AMPK which in turn inhibits mTOR; this likely accounts for many of the metabolism-altering functions it carries out [67,68]. In the EAE model, metformin treatment was shown to decrease pro-inflammatory cytokines, increase Tregs numbers and slow disease progression [69]. Th17-mediated inflammation was also reduced by metformin treatment in animal models of rheumatoid arthritis and colitis, and again, effects were dependent on AMPK and mTOR signalling [70,71]. These studies indicate that drugs which alter the metabolic pathways engaged by immune cells may show therapeutic potential for autoimmune diseases.

## 1.4 Autophagy

Autophagy, derived from Greek, meaning self-eating, or devouring, is an essential, naturally occurring cellular mechanism, which allows the removal or recycling of cellular components if they are dysfunctional, no longer needed, or their breakdown is required to generate energy [72]. Autophagy is highly important for the removal of damaged organelles or misfolded proteins, and any defects in this process can result in disease or other inflammatory conditions [72,73]. There are 3 main forms of autophagy; macroautophagy, microautophagy and chaperone mediated autophagy [72]. Macroautophagy is the main autophagic pathway, in which components in the cytoplasm are targeted and engulfed by a double membrane vesicle and fused with a lysosome for degradation [72]. For the purpose of this thesis from here on 'autophagy' will refer to macroautophagy. The process of autophagy can be broken into 4 main stages: induction & initiation, elongation, maturation and lysosomal fusion [72]. Autophagy is carried out by a number of autophagy-related (Atg) genes, and initiation is under the control of the previously mentioned protein kinases mTOR and AMPK, therefore is intrinsically linked to a cell's metabolism (Figure 1.5) [72,74]. Most cells exhibit an 'autophagic flux', where autophagy is functioning at basal levels, however, the process can also be ramped up when the cell requires it [72,74]. Generally, under homeostatic conditions, mTOR inhibits autophagy through phosphorylation of the ULK kinases [74,75]. However, under conditions of stress or starvation, AMPK inhibits mTOR and activates ULK1, further activating Beclin-1, leading to the initiation of the autophagic process [74,75]. These activated complexes re-localise to the phagophore, which is the early autophagosome. The phagophore can then be elongated by a range of Atg proteins, to form the autophagosome [74,75]. This complex of Atg proteins also lipidates LC3-I, the cytosolic form, to LC3-II, which binds to the surface of the autophagosome, and further encourages its elongation (Figure 1.5) [74,75]. LC3-II bound to the autophagosome membrane allows the docking of cargos and proteins for degradation, through their binding to p62 [76]. The autophagosome fully matures and encloses, before trafficking to a lysosome and fusing, to form the autolysosome in which the contents can be degraded and recycled (Figure 1.5) [72,74].

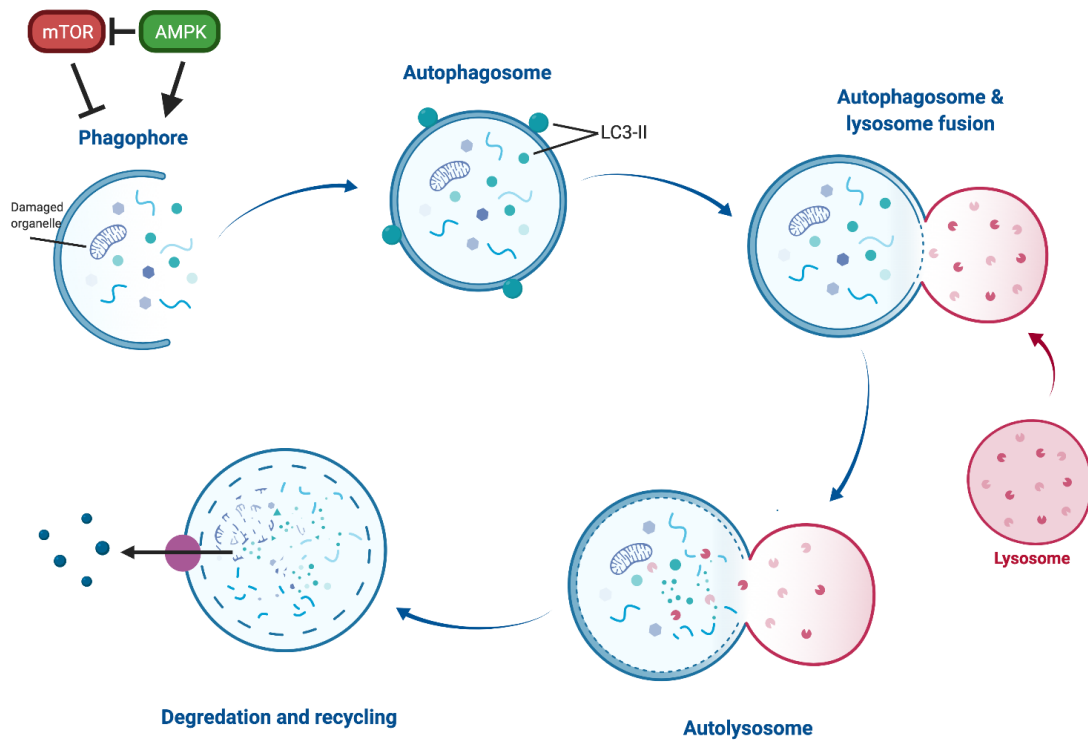


**Figure 1.5 The degradation of cellular products through autophagy.**

Autophagy is inhibited by mTOR and activated by AMPK under conditions of stress or starvation. Activation of autophagy leads to the formation of a phagophore, which can be elongated and finally fully enclose to form the autophagosome, around the proteins or organelles targeted for degradation. LC3-II is found both bound to the surface, and within, the autophagosome. The autophagosome then binds with the lysosome to form the autolysosome, resulting in the degradation and recycling of the contents.

#### 1.4.1 Autophagy in immunity & disease

Autophagy plays a number of key roles in the immune system, particularly in the innate immune response, with autophagy capable of inducing or suppressing immune responses, and vice versa [73,77]. A form of autophagy, termed xenophagy, involves the selective degradation of intracellular proteins to defend the host [73,77]. However, some pathogens, in particular mycobacterium tuberculosis, have evolved mechanisms to subvert this host defence mechanism and persist unharmed [78,79]. Autophagy is of particular importance for DC, as many of their key functions, including antigen uptake and presentation, are tightly associated with autophagy [80]. Despite some conflicting reports, generally it appears that autophagy induction results in a more tolerogenic DC phenotype, with reduced antigen presentation and maturation [80]. One of the key effects autophagy

has on the immune system is the inhibition of the inflammasome, particularly in DC and macrophages. Autophagy deficient cells have increased IL-1 $\beta$  and IL-18 production, two cytokines matured by the inflammasome, while autophagy induction has been shown to inhibit IL-1 $\beta$  production by targeting its pro form for degradation [81–83]. This inhibition of IL-1 $\beta$  production by autophagy has also been shown to regulate IL-23 production by DC and macrophages [84]. Autophagy inhibition has been shown to increase IL-23 production in these cells in a IL-1 regulated manner [84]. Furthermore these autophagy-deficient cells were capable of inducing increased secretion of pro-inflammatory cytokines by  $\gamma\delta$  T cells [84]. Given that IL-1 $\beta$  and IL-23 are highly inflammatory cytokines, important for the differentiation of Th17 cells, and the development of a number of autoimmune and inflammatory diseases, along with its other effects on the immune system, it is no surprise that defects in autophagy have been linked to a number of these diseases.

The strongest link between autophagy defects and an autoimmune disease is the relationship between a number of single nucleotide polymorphisms (SNPs) in autophagy genes and CD. Many SNPs in autophagy related genes, including ATG16L1, NOD2, IRGM, ULK1, IL-23R, and the vitamin D receptor, have all shown susceptibility to CD, however it is unclear what effects, and to what degree, they all have in the pathogenesis of the disease [85]. In 2007, the first study demonstrated a relationship between autophagy and CD, linking a SNP in the autophagy related gene ATG16L1 [86]. NOD2, a PRR, works closely with ATG16L1 to clear bacteria and maintain intestinal homeostasis [85]. It is thought that SNPs in these genes results in increased inflammasome activation, as previously discussed, and impaired xenophagy, potentially leading to dysbiosis in the gut, commonly seen in CD [87–89]. Similarly, SNPs in autophagy related genes, particularly deficiency in ATG5, have also been attributed to SLE susceptibility [90,91]. Conversely, in MS it appears that upregulated ATG5 results in intensified autophagy, leading to pathogenic inflammation [92]. It is clear that dysfunctional autophagy has a complex, interlinked relationship with immunity and inflammation, and plays a role in the development of a number of diseases. Therefore, it is a strong candidate target for the treatment of these diseases, and despite little current research underway in this field, it won't be surprising when it emerges as a therapeutic contender in the near future.

## 1.5 The Heme Oxygenase system

Heme is an iron-containing porphyrin that is a component of many biologically important proteins. These include hemoglobin and myoglobin, which are used to carry oxygen in red blood cells (RBCs) and muscle cells respectively; cytochromes, which facilitate electron transport during oxidative respiration, redox and drug metabolism; and enzymes such as catalases and heme peroxidases, which are involved in a range of critical cellular functions [93]. However, despite its ubiquitous nature within cellular proteins, free heme is highly cytotoxic and must be rapidly metabolised to avoid cell damage through oxidative stress [94,95]. Heme oxygenase enzymes catalyse the first, rate limiting, step of heme degradation, using NADPH-cytochrome p450 reductase and oxygen to generate equimolar amounts of the linear tetrapyrrole biliverdin, ferrous iron ( $\text{Fe}^{2+}$ ) and carbon monoxide (CO) [96]. Biliverdin is subsequently converted to the linear tetrapyrrole, bilirubin, by the enzyme biliverdin reductase [97,98] (Figure 1.6).



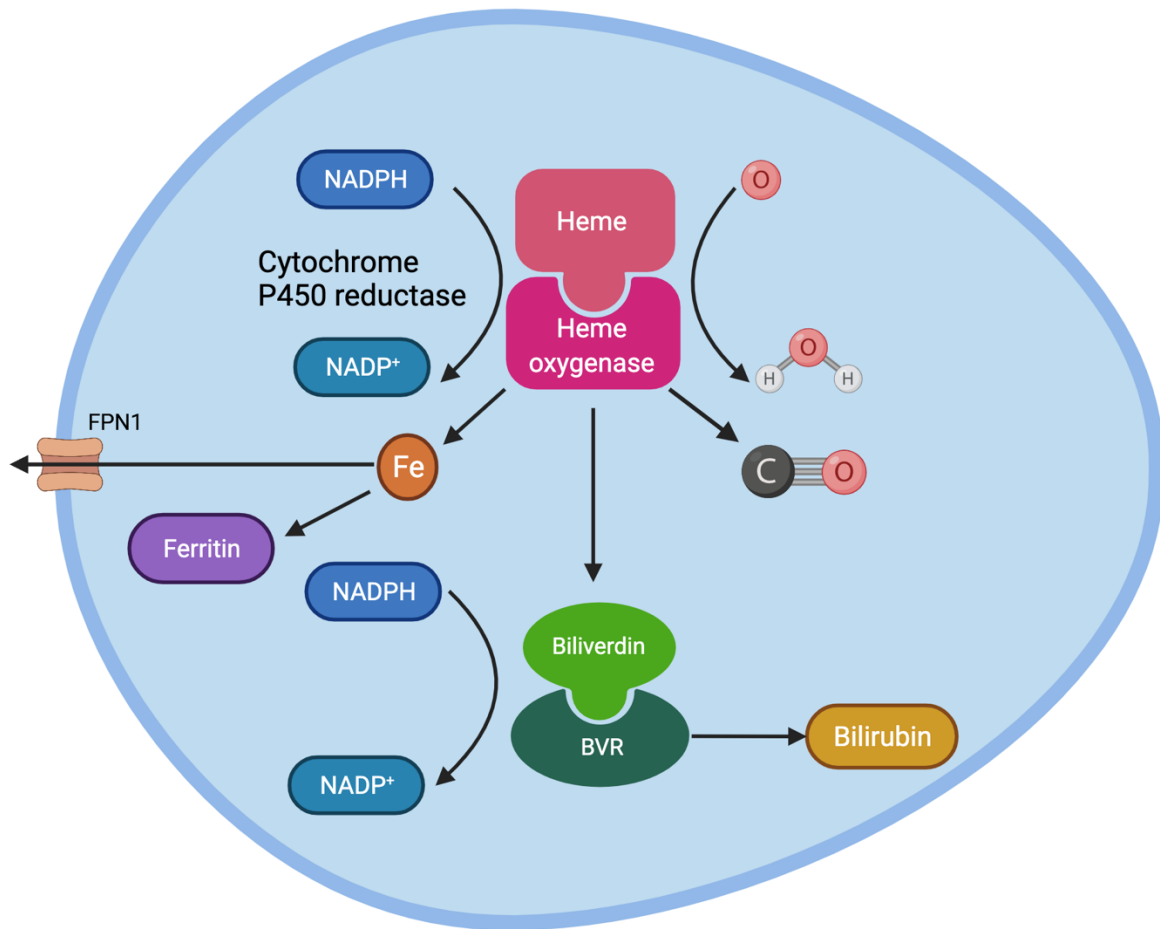


**Figure 1.6 Heme oxygenase and heme catabolism.**

Heme degradation occurs in the cytosol of the cell, where heme is catabolised by heme oxygenase (HO-1 or HO-2). This reaction requires cytochrome P450 reductase as a cofactor to metabolise NADPH and O<sub>2</sub>, leading to the production of NADP<sup>+</sup> and H<sub>2</sub>O. Breakdown of heme results in the generation of equimolar amounts of biliverdin, carbon monoxide and ferrous iron (Fe<sup>2+</sup>), which is rapidly exported from the cell via ferroportin 1 (FPN1) or sequestered into ferritin for storage. Biliverdin can be subsequently converted into bilirubin by the enzyme biliverdin reductase (BVR).

### 1.5.1 Heme oxygenase 1

Two functional isoforms of heme oxygenase exist in mammalian cells; heme oxygenase 1 (HO-1) and HO-2. HO-2 is constitutively expressed within certain tissues including the brain, testis, cardiovascular and liver, where it contributes to homeostatic iron and redox metabolism, and cellular messaging (via CO) [99–102]. In contrast, HO-1 is a stress-inducible isozyme encoded by the gene *HMOX1* in humans [103]. Under homeostatic conditions, HO-1 expression is low or absent in most cells and tissues, with some

exceptions including iron-recycling macrophages in the spleen and liver, and certain tolerogenic immune cells, which display constitutive expression of HO-1 [104]. However, HO-1 is highly upregulated by most cells in response to a vast number of stress stimuli, including various pro-oxidants and pro-inflammatory mediators [105–107]. Given its protective antioxidant and anti-inflammatory properties, understanding how HO-1 expression is controlled under different circumstances and in different cell types has been the subject of considerable research. The multi-factorial regulation of HO-1 provides important context to its functions in immune cells and in inflammatory disease, and several therapies are under investigation to target the HO-1 system.

Expression of HO-1 is largely under the control of the redox-sensitive transcription factor nuclear factor erythroid 2-related factor 2 (Nrf2), which binds to the antioxidant response element (ARE) in the promoter region of many antioxidant genes, including *HMOX1* [108]. Under steady-state conditions, Nrf2 is bound to the protein KEAP1 (Kelch-like ECH-associated protein 1) in the cytoplasm; this suppresses Nrf2 activity by facilitating the ubiquitination and subsequent degradation of Nrf2 by the proteasome [108]. However, in the presence of oxidants, reactive oxygen species (ROS), and other Nrf2 activators, cysteine residues within KEAP1 are modified resulting in the release, and consequent stabilisation, of Nrf2 [109,110]. Nrf2 can then migrate to the nucleus where it forms heterodimers with small MAF proteins (SMAFs) to bind AREs and promote expression of antioxidant genes (Figure 1.7) [108]. BACH1, a transcriptional repressor and heme sensor, also forms heterodimers with SMAFs and regulates HO-1 expression by competing with Nrf2 for the ARE binding site on the *HMOX1* promoter [111]. Binding of free heme to BACH1 causes it to dissociate from the ARE, after which it is exported from the nucleus, ubiquitinated and degraded, allowing *HMOX1* transcription to occur [112,113]. Together, Nrf2, KEAP1 and BACH1 comprise an intricate feedback system, which enables cells to respond to oxidative stress and increased levels of cytotoxic heme through upregulation of HO-1. However, it is important to note that other genes involved in antioxidant and anti-inflammatory responses that are independent of HO-1 are also regulated by Nrf2 and heme (via both BACH1-dependent and BACH1-independent mechanisms) [114–116]. Therefore, care must be taken when interpreting the role of HO-1 in situations where the presence or activity of these transcriptional regulators is altered.

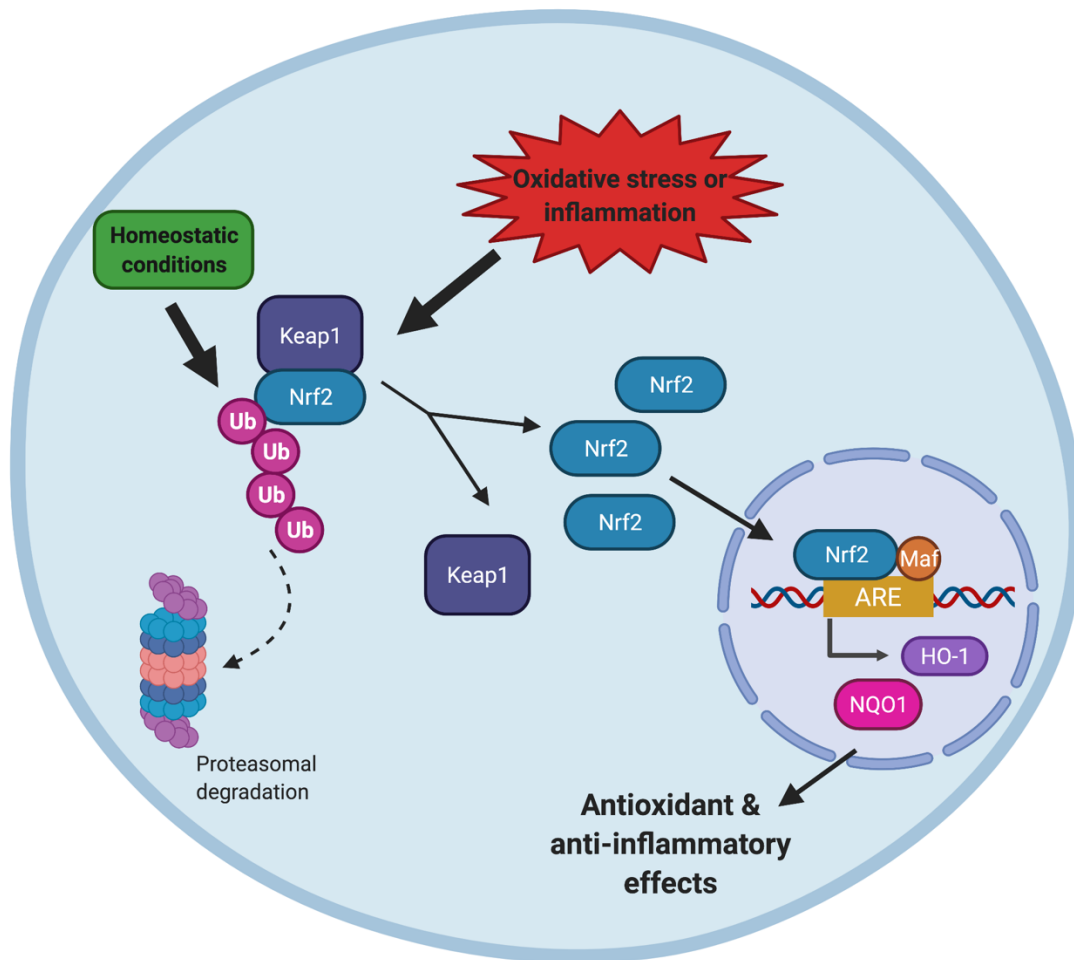


**Figure 1.7 Nrf2 signalling pathway.**

Nrf2 is bound to KEAP1 in the cytosol, where it is targeted for ubiquitination and degradation under homeostatic conditions. Under conditions of oxidative stress or inflammation it is released from KEAP1, where it can translocate to the nucleus and bind to the ARE in complex with Maf proteins, promoting the transcription of antioxidant genes, including HO-1 and NQO1.

Although Nrf2 and BACH1 are the primary regulators of HO-1, other transcription factors have also been described to modulate HO-1 expression, such as HIF-1 $\alpha$  and various SMAD dimers [108,117,118]. With particular relevance to immune cells, binding sites for the pro-inflammatory transcription factors NF- $\kappa$ B and AP-1 have been identified within the *HMOX1* promoter [119]. Furthermore, some instances of HO-1 upregulation *in vitro* have been shown to be dependent on, or correlated with, NF- $\kappa$ B or AP-1 expression (reviewed in Ref. [120]). HO-1 may therefore be upregulated during inflammation to protect against potential deleterious effects of ROS and pro-inflammatory cytokines, and to provide negative feedback during induction of inflammatory responses. In addition to direct regulation by transcription factors, emerging evidence suggests a role for epigenetic

regulation of HO-1 expression [121–123], as well as post-transcriptional regulation by alternative-splicing and miRNAs [124,125]: while poorly understood at present, these indirect regulatory mechanisms represent interesting avenues to explore when considering targeting HO-1 expression.

While there appear to be multiple transcriptional regulators of HO-1 expression, many HO-1 inducers do not interact with transcription factors directly, but instead activate them via intermediate signalling pathways. Protein kinase pathways associated with responses to cellular stress have been implicated in the regulation of HO-1 expression. For example, the mitogen activated protein kinases (MAPKs) ERK, JNK, and p38 have all been reported to regulate HO-1 expression in different cell types and conditions; however, p38 appears to be the most common MAPK involved in HO-1 upregulation [120]. The phosphatidylinositol-3 kinase (PI3K)–AKT pathway can also regulate HO-1 expression in response to cytokines and prostaglandins as well as some alternative HO-1 inducers [126–128]. For example, the upregulation of HO-1 by the cytokine IL-10 is thought to be achieved via activation of PI3K and STAT3 [129,130]. Finally, the cellular energy sensor AMPK has recently been identified as a modulator of HO-1 expression, and is responsible for the upregulation of HO-1 by many metabolic regulators and HO-1 inducers [131–134]. The mechanism by which AMPK upregulates HO-1 appears to involve cross-talk between AMPK, its downstream effectors, and Nrf2 [132,133,135–137]. In summary, induction of HO-1 is a general adaptive mechanism by cells to protect against damage under stress conditions, and HO-1 upregulation can be achieved through activation of multiple different regulatory mechanisms. While this adaption is most clearly indicated during oxidative stress, it has also evolved as a component of metabolic and immune signalling, with particular relevance for immunomodulation of certain immune cells.

The HO-1 system also has important anti-inflammatory properties [130,138,139]. These are exemplified by the rare HO-1 deficiencies seen in humans and by HO-1-deficient animal models, which in addition to showing increased sensitivity to oxidative stress, are characterised by high levels of chronic inflammation [140–142]. Two rare cases of HO-deficient humans exhibited systemic inflammation with leukocytosis, as well as increased levels of C-reactive protein and IL-6 [141,143]. LPS stimulation of splenocytes from HO-1

knockout mice resulted in increased secretion of IL-1, IL-6 and TNF, compared to cells from wild type mice [142]. Similarly, increased levels of IFN $\gamma$ , IL-6 and IL-12 were secreted from HO-1<sup>-/-</sup> splenocytes upon stimulation with anti-CD3/CD28 [142]. HO-1 knockout mice were also more vulnerable upon challenge with LPS compared to wild type mice [140]. The anti-inflammatory properties of HO-1 have been attributed to the HO-1 reaction products, CO and the linear tetrapyrroles, biliverdin and bilirubin. CO binds strongly to hemoglobin and reduces its ability to carry oxygen, therefore it is regarded as highly toxic. However, this only occurs at high concentrations, while at low concentrations its functions as both a cellular messenger and an anti-inflammatory agent. CO treatment has been shown to inhibit pro-inflammatory cytokine production in LPS-stimulated murine macrophages, while at the same time, increasing anti-inflammatory IL-10 production [144–146]. CO has also been shown to inhibit DC maturation and antigen presentation to T cells [147–149]. *In vivo* studies (e.g. EAE and colitis models) have also examined the effects of CO administration and, in each case, therapeutic levels of CO improved disease outcomes [150–153]. Indeed, CO itself has been shown to induce HO expression, as have CO releasing molecules (CORMs), such as tricarbonyldichlororuthenium (II) dimer, and tricarbonylchloro(glycinato)ruthenium (II) [154–157].

Similar to CO, bilirubin is toxic at high concentrations and must undergo glucuronidation by the enzyme glucuronyltransferase prior to excretion as accumulation can otherwise lead to jaundice (a delay in expression of glucuronyltransferase is often seen in pre-mature infants [158]). Non-toxic concentrations of bilirubin are reported to have many anti-inflammatory properties. It has been shown to inhibit inducible nitric oxide synthase (iNOS) expression and TNF production in LPS-treated rats, as well as in LPS-stimulated RAW 264.7 murine macrophages [159,160]. In the DSS-colitis model, bilirubin administration was shown to suppress vascular cell adhesion molecule-1 (VCAM-1)-dependent cell signalling which resulted in reduced migration of leukocytes to their target tissue and a subsequent reduction in inflammation of the colon [161]. Similarly, biliverdin administration has been reported to ameliorate chronic inflammation observed in HO-2 knockout mice [162,163]. Biliverdin has also been shown to reduce pro-inflammatory cytokine production, including IL-1, IL-6 and TNF, in a number of murine studies [164,165].

### *1.5.2 Beneficial role of HO-1 in disease*

Given the anti-inflammatory properties of the HO-1 system, induction of the enzyme is considered a promising therapy for a number of autoimmune and inflammatory diseases. Evidence supporting the therapeutic potential of HO-1 has come from numerous disease models, some of which will be discussed in the following sections.

#### *1.5.2.1 Inflammatory bowel disease*

IBD is a term used to describe two conditions: Ulcerative Colitis (UC) and Crohn's disease (CD). It affects approximately 2.2 million individuals in Europe and approximately 20,000 people in Ireland [166]. Both UC and CD are characterised by chronic relapsing inflammation of the gastrointestinal tract. Patients with IBD also have increased risk of developing colorectal cancer when compared to the general population and are pre-disposed to other inflammatory diseases such as psoriasis [167]. The exact cause of IBD is unknown, however there are many risk factors which contribute to the development of this condition, including host genetics, the environment and gut microbiota [168]. As the main aetiology of the disease is dysregulated/overactive immune responses, patients are treated largely with anti-inflammatories including 5-aminosalicylic acid (5-ASA), corticosteroids, methotrexate and anti-TNF therapies [169]. However, many patients are/become refractory to these treatments and will require surgery in their lifetime [169]. Therefore, similar to many other autoimmune diseases, there is a need for new anti-inflammatory therapies with better efficacy, tolerability, and fewer side-effects.

Under homeostatic conditions, HO-1 is weakly expressed in the gastrointestinal tract. However, increased HO-1 expression has been observed in both inflammatory cells and intestinal epithelial cells from patients with IBD [170,171]. In murine models of colitis, increased levels of HO-1 have been observed in inflamed colonic tissue, particularly in endothelial cells, macrophages, and neutrophils, and it has been proposed that these cells may increase HO-1 expression to control inflammation and oxidative stress [172–174]. In support of this hypothesis, inhibition of HO activity results in increased damage to the

colon in the TNBS-colitis model [173], and elevated levels of pro-inflammatory cytokines in the DSS-colitis model [174]. Furthermore, administration of low concentrations of CO alleviates colitis symptoms in mouse models through upregulation of HO-1 expression [152,153]. Bilirubin has also been reported to attenuate symptoms of colitis in multiple models, through limiting leukocyte trafficking and pro-inflammatory cytokine production, and promoting IL-10 signalling [161,175,176]. HO-1 induction via hemin in the DSS-colitis model was correlated with an inhibition of Th17 cell responses, and promotion of Treg cell numbers and function [177]. Hemin administration has also recently been reported to attenuate colitis symptoms by reducing the number of pro-inflammatory myeloid-derived cells, such as M1 macrophages, and increasing anti-inflammatory M2 macrophages in colon tissue [178]. Furthermore, administration of the HO-1 inducer cobalt protoporphyrin IX (CoPP) prior to initiation of DSS-colitis has been reported to reduce apoptosis of colonic epithelial cells and decrease colonic inflammation [171]. Interestingly 5-ASA, an anti-inflammatory drug used as a first-line treatment for IBD, may attribute its mechanism of action, in part, to upregulation of HO-1 [179,180]. Together, this evidence provides a strong basis for HO-1 induction as a potential therapy for IBD; however, further clinical investigation is necessary.

#### 1.5.2.2 *Psoriasis*

Psoriasis is an autoimmune, inflammatory disease, which is characterised by areas of inflamed, scaly skin at any location across the body. Patients with psoriasis have increased risk of other inflammatory diseases, including psoriatic arthritis and IBD [181,182]. The exact cause of psoriasis is unknown; however, like IBD, there is a strong genetic component [183,184]. The psoriatic lesions which appear on the skin are due to aberrant proliferation of keratinocytes which occurs in response to inflammatory factors secreted by immune cells, including DC, macrophages, and T cells. There is no cure for psoriasis and instead treatments are focused on controlling disease symptoms. They include topical creams, or, similar to IBD, medications to suppress overactive immune responses [185,186].

The skin is constantly exposed to environmental stressors such as UV radiation, requiring it to have access to a robust suite of antioxidant and anti-inflammatory mediators,

including both HO-1 and HO-2, to protect itself from cellular damage [187]. In psoriasis, HO-1 appears to play a central role in the protection of skin from chronic inflammation: upregulation of HO-1 has been observed in psoriatic plaques, and increased levels of HO-1 have been detected in the patient sera compared to controls [188,189]. Furthermore, upregulation of HO-1 has been demonstrated to inhibit skin inflammation and keratinocyte proliferation in preclinical models of psoriasis. In two different rodent models, upregulation of HO-1 via CoPP was associated with improvements in skin lesions and reduced inflammation; Listopad *et al.* reported a decrease in T cell-mediated skin inflammation which was accompanied by increased HO-1 activity in APC, while Ma *et al.* observed a reduction in TNF and an increase in IL-10 expression, which were reversible with HO-1 inhibition [190,191]. Similarly, topical application of hemin in the imiquimod-induced psoriasis model resulted in increased expression of HO-1 and a concomitant decrease in the severity of psoriatic lesions, attributed to negative regulation of STAT3 signalling by HO-1 [192]. Interestingly, induction of HO-1 is also associated with existing treatments for psoriasis. For example, phototherapy involving exposure to UVA radiation upregulates HO-1 expression in skin [187,193]. Dimethyl fumarate (DMF), an immunosuppressant used to treat both psoriasis and MS, has also been reported to act in part through HO-1 induction [194–198]. Whether HO-1 activity is required for the efficacy of these therapies remains unclear, however, these studies provide further support for the modulation of HO-1 expression as a potential treatment for psoriasis.

### 1.5.2.3 Multiple Sclerosis

MS is an autoimmune disease in which the myelin sheaths surrounding neurons in the central nervous system (CNS) become damaged and destroyed. This damage results in altered communication along these nerves, which can lead to impaired coordination and muscle weakness [199]. MS is usually characterised as relapsing-remitting MS which may, or may not, lead to secondary progressive MS. Similar to most autoimmune diseases, the initial trigger(s) is not known; however, evidence would suggest that the disease is linked to a combination of genetic and environmental factors [199]. Treatments include IFN- $\beta$ , immunomodulators including DMF and fingolimod, and a number of biologics, such as



natalizumab [200]. However, many patients become refractory to these treatments and/or suffer undesirable side effects which can make patient compliance unpredictable [200].

HO-1 and its products have been shown to have protective effects in MS and its mouse model, EAE [201,202]. HO-1 expression is reduced in the peripheral blood mononuclear cells (PBMCs) of patients with MS compared to controls, and is further downregulated in patients experiencing disease relapse compared to those with stable disease or receiving corticosteroid treatment [203]. Furthermore, HO-1 upregulation has been observed in glial cells within MS plaques, likely as a local response to neuroinflammation [204]. In an EAE model, HO-1-deficient mice presented with a more severe disease phenotype when compared to wild-type mice, and induction of HO-1 resulted in reduced disease scores and a reduction in inflammatory T cell infiltration into the CNS [202]. Induction of HO-1 during EAE has also been reported to reduce production of pro-inflammatory cytokines and to increase production of IL-10 [205]. Furthermore, CO has been demonstrated to improve disease outcomes in EAE, while biliverdin reductase and bilirubin suppressed EAE onset and progression [202,206–208]. While research in this area is still in early stages, these studies indicate that therapies modulating the HO-1 system may be beneficial as a novel treatment strategy for MS.

#### *1.5.2.4 Organ transplantation*

Oxidative damage and ischaemic stress are of major concern during organ transplantation, as they can negatively impact on the health and survival of grafted tissue [209]. Furthermore, ongoing suppression of the host immune response is necessary to prevent graft rejection [210]. HO-1 and its products are all under investigation as protective agents during transplantation, due to their recognised antioxidant and anti-inflammatory properties. Biliverdin administration has been found to be particularly efficacious against ischaemia–reperfusion injury (IRI) in animal models of small bowel [211], liver [212], lung [213] and heart transplant [214]. Furthermore, CO administration during models of organ transplantation has been shown to limit IRI to donor organs and suppress graft rejection (reviewed in [215]). Dual treatment with both biliverdin and CO displayed increased efficacy compared to either treatment alone in animal models of lung transplant [216], or

heart and kidney transplant [217]. Furthermore, HO-1 induction displayed protection during transplantation of pancreatic islets for treatment of type 1 diabetes, improving the survival, function and number of effectively transplanted islets [218,219]. As well as providing graft protection during transplant, Nrf2 activation and/or HO-1 induction have been reported to increase long-term host survival rates in a murine model of graft versus host disease [220], and attenuate chronic rejection following transplantation [221–223]. Furthermore, a *HMOX1* polymorphism resulting in higher HO-1 expression results in better survival rates for patients undergoing bone marrow transplants [224].

In summary, HO-1 and its products have been demonstrated to protect against harmful inflammation in numerous preclinical disease models. This compelling evidence supports HO-1 as a viable therapeutic target for the treatment of chronic inflammation. However, clinical implementation of this treatment strategy faces further challenges, discussed in the next section.

### 1.5.3 *Therapeutic modulation of HO-1*

Despite the body of evidence supporting modulation of the HO-1 system as a treatment for diseases characterised by damaging inflammation or oxidative stress, clinical implementation of HO-1 based therapies faces numerous challenges [225,226]. Therefore, there is a great need to identify safer and better tolerated alternatives to currently available sources of HO-1 inducers and reaction products. Some of the most promising candidates are highlighted in the following sections.

#### 1.5.3.1 *Phytochemicals*

Many plant-derived compounds (phytochemicals) are commonly used as dietary and health supplements, and have been extensively studied as antioxidant and anti-inflammatory agents [227]. Some examples include resveratrol, quercetin, carnosol and curcumin. Due to their natural occurrence and regular consumption, indicating low toxicity, many are being explored as potential disease-modifying drugs, and a number have been

reported to upregulate HO-1 [127,228–231]. Despite the considerable number of preclinical studies which support the use of phytochemicals as anti-inflammatories and alternative HO-1 inducers, much of this research is limited in its applicability to human disease. For example, many phytochemicals have poor oral bioavailability, and/or are digested and metabolised into different conjugates prior to reaching systemic circulation [232]. Moreover, they are frequently studied at supra-physiological concentrations far in excess of those achievable by dietary consumption [232,233]. It is therefore clear that consideration of bioavailability, route of administration, and effective dosages, as well as further human studies, are necessary before phytochemical HO-1 inducers can be translated to the clinic.

#### *1.5.3.2 Existing drugs*

Certain existing drugs used to treat inflammation have been reported to activate Nrf2 and/or upregulate HO-1. As previously mentioned, DMF, a drug licensed for treatment of psoriasis and MS, may partially attribute its efficacy to activation of Nrf2 and induction of HO-1 [194–198]. DMF treatment has also shown promise in a colitis model, in which it attenuated disease symptoms and reduced pro-inflammatory markers through Nrf2 activation [234]. Similarly, 5-ASA, the aforementioned first-line therapy for IBD, may also count HO-1 upregulation as part of its mechanism of action [179,180]. Administration of 5-ASA in the TNBS-model increased colonic heme oxygenase activity and HO-1 expression, and reduced colonic inflammation, while inhibition of HO-1 abolished its anti-colitic effect [179]. Interestingly, 5-ASA and its prodrug sulfasalazine only activated Nrf2 and HO-1 when gut inflammation was present, which was attributed to the oxidation requirement of the drug [180]. 5-aminolevulinic acid (5-ALA) is a heme precursor typically used in the diagnosis and treatment of cancer, and a recent study reported that HO-1 induction may partially contribute to its therapeutic mechanism [235]. Nrf2 activation and HO-1 upregulation by 5-ALA has also shown therapeutic potential for prolonging graft survival and treatment of RA [236,237]. Interestingly, in a murine model of IBD, dihydroartemisinin (DHA), a drug typically used to treat malaria, ameliorated disease symptoms by decreasing the number

of inflammatory CD4<sup>+</sup> T cells through HO-1 induction [238]. These drugs could therefore be suitable for use as HO-1 inducers due to their existing regulatory approval and safety data.

### *1.5.3.3 Carbon monoxide-based therapies*

CO releasing molecules (CORMs) are CO-carrier compounds designed to deliver controlled-release of CO to target tissues, as an alternative to CO gas inhalation. Interestingly, two CORM candidates, CORM-A1 and CORM3, have been reported to upregulate HO-1 and provide protection in various models of inflammation [239–242]. This method of CO administration may therefore allow for safer therapeutic use of CO, particularly as CORMs do not alter levels of CO-bound hemoglobin, overcoming the risk of CO poisoning associated with gas inhalation [243]. However, further research is required before progressing the use of CORMs to clinical settings, particularly regarding the toxicity associated with the backbone carrier moiety of these compounds, which typically contains a heavy metal, as well as determining a safe dose that will produce an effective concentration in specific tissues [244]. Hybrid CO-releasing molecules (HYCOs) are an interesting class of novel CO-based therapies, synthesised by conjugation of a CORM with an Nrf2-inducing factor, for example CORM-401 combined with analogues of DMF. These compounds have the dual benefit of releasing CO for initial, rapid action, followed by longer-lasting protection produced by activation of Nrf2 [245,246]. Examples of these compounds have been confirmed to activate Nrf2 and upregulate HO-1 in different cells and tissues, and to reduce inflammation in LPS-challenged mice and in models of psoriasis and MS [245,246]. However, similar to their parent compounds, HYCOs face challenges regarding their toxicity due to the presence of metals in their structures.

### *1.5.3.4 Novel inducers*

Recently, there has been interest in identifying novel HO-1 inducers that may show potential as anti-inflammatory therapies. Itaconate, an endogenous metabolite, has been reported to activate Nrf2 through modification of cysteine residues on KEAP1, inducing downstream HO-1 expression and reducing inflammation in both murine and human

immune cells [247]. Itaconate also ameliorated disease severity in a murine model of psoriasis, and limited pro-inflammatory cytokine production via Nrf2 activation in samples from patients with SLE [248,249]. Another novel Nrf2 activator, KI-696, has shown therapeutic potential for chronic obstructive pulmonary disease (COPD). This compound specifically inhibits the KEAP1–Nrf2 interaction, leading to activation of Nrf2 and upregulation of Nrf2-regulated genes, including HO-1 [250]. KI-696 has shown therapeutic potential to treat COPD by reducing the number of inflammatory cells in the bronchoalveolar lavage fluid of ozone-exposed mice, used as a model of respiratory disease, as well as increasing the phagocytic capacity of lung macrophages in patients with COPD [251]. Finally, aromatic ketoacids secreted by the parasite *Trypanosoma brucei* have recently been reported to induce HO-1 via Nrf2 activation and are discussed in further detail below.

#### 1.5.3.5 *Trypanosome-derived ketoacids*

Infection of the mammalian vasculature and central nervous system (CNS) with the extracellular protozoan parasite *Trypanosoma brucei* (*T. brucei*) can lead to fatal human sleeping sickness, also known as African trypanosomiasis. Like most parasites, trypanosomes are continuously challenged by the host-immune system, however, they have evolved very effective evasion strategies in order to maintain infection and prolong the host's survival [252]. An infection with *T. brucei* is accompanied by the excretion of high levels of ketoacids into the host's bloodstream [253,254], a phenomenon that was, until recently, largely unexplained. The ketoacids are derived from the conversion of aromatic amino acids (tryptophan, tyrosine, and phenylalanine) to indole pyruvate (IP), hydroxyphenylpyruvate (HPP), and phenyl pyruvate (PP) (Figure 1.8), through the action of a cytoplasmic aspartate aminotransferase (TbcASAT), which is expressed by the parasite.

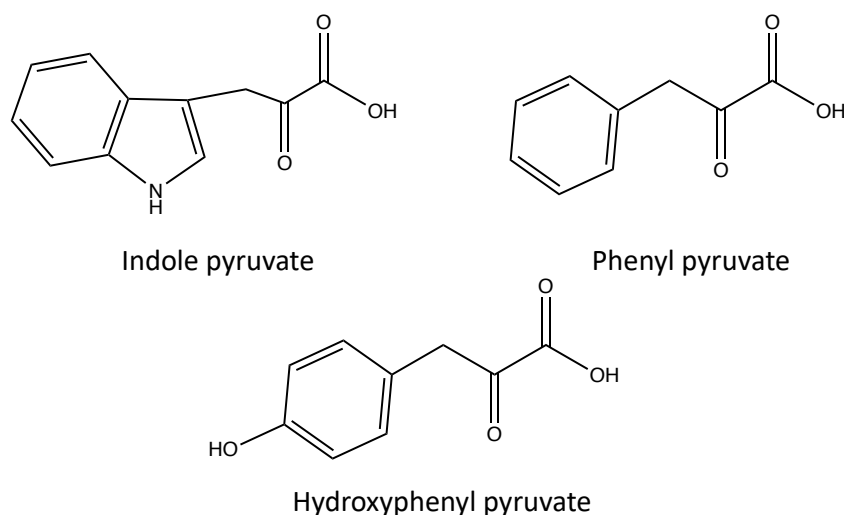


**Figure 1.8 Chemical structures of the aromatic ketoacids indole pyruvate, phenyl pyruvate and hydroxyphenyl pyruvate, secreted by *T. Brucei*.**

In recent years, it has been demonstrated that these molecules have potent immunomodulatory properties, which likely contribute to the suppression of host immune responses, but that may also be exploited for potential therapeutic benefit [255–259]. For example, our laboratory has demonstrated IP and HPP are potent inducers of HO-1 in murine glia and macrophages [256]. This occurs in a Nrf2 dependent manner and leads to a reduction in LPS-induced pro-inflammatory cytokines and innate immune cell maturation. In addition to HO-1 induction, *T. brucei*-derived ketoacids are also capable of inhibiting HIF-1 $\alpha$ -induced pro-IL-1 $\beta$  expression, as well as prostaglandin production, an effect which was shown to be dependent on the activation of the aryl hydrocarbon receptor (AHR) [255,259]. The immunomodulatory effects of IP and HPP have also been confirmed in animal models of disease. In a murine model of skin damage caused by exposure to ultraviolet B radiation, administration of IP resulted in a reduction in damage lesions and expression of the pro-inflammatory cytokines, IL-1 $\beta$  and IL-6 [257]. Furthermore, IP administration reduced disease severity in the DSS colitis model, and this was accompanied by a decrease in the expression of pro-inflammatory cytokines IL-12, TNF, IFN $\gamma$ , and IL-1 $\beta$ , and an increase in the expression of the anti-inflammatory cytokine IL-10 [258]. A reduction in Th1 cells, as well as a reduced capacity for DC to activate T cells, was also observed [258].

### 1.5.3.6 Limitations of HO-1 based therapies

Despite the large amount of evidence presented in support of HO-1 as a promising candidate to treat inflammatory diseases, there remain many limitations to its application that need to be overcome. The majority of studies examining the role of HO-1 in disease have used metalloporphyrins, Hmox1<sup>-/-</sup> animals, or gene silencing to modify HO-1 expression and determine HO-1-specific efficacy. However, these methodologies are not suitable for use in humans, making the findings of these studies difficult to translate to the clinic. These methods can also produce off-target effects, for example, metalloporphyrins can inhibit other important signalling molecules, and simultaneously increase HO-1 expression while inhibiting its enzymatic activity [225,226]. Some HO-1 inducers may not appear to attribute their immunomodulatory effects to HO-1, however these associations can be difficult to test experimentally; for example, the weak enzymatic inhibitors available for HO-1 may be overwhelmed by particularly strong inducers, while use of Hmox1<sup>-/-</sup> mice is often limited by breeding difficulties associated with this particular strain [226]. Many studies have therefore turned to Nrf2 inhibitors or knockout mice as an alternative, but it is then difficult to parse HO-1-specific effects given the wide range of antioxidant and cytoprotective genes regulated by Nrf2. Finally, as mentioned earlier, many HO-1-based therapeutics under investigation have associated toxicity or bioavailability concerns, while HO-1 induction itself can prove detrimental in situations where inflammation is beneficial, potentially putting patients at increased risk of infection or cancer [260–262]. All of these factors must be considered for successful translation of potential HO-1-based therapeutics to the clinic.

## 1.6 Research question

Research in recent years has provided ample evidence supporting HO-1 induction as a potential therapy to treat autoimmune and inflammatory conditions. However, as mentioned above, there are many limitations surrounding the use of currently available HO-1 inducers. Therefore, there is a solid rationale to identify novel HO-1 inducers which may be of beneficial use in the clinic, either alone or in combination with existing therapeutics. Given their immunosuppressive properties, aromatic ketoacids such as those produced during *T.brucei* infection represent a promising class of such compounds. However, to date, they have been studied primarily in murine immune cells, with very little evidence to support their mechanism of action in human immune cells. Therefore, the goal of this study is to investigate the immunomodulatory properties of the *T. brucei*-derived ketoacids, IP and HPP, in primary human immune cells and to further examine their potential as a therapy for autoimmune/inflammatory disease.

### 1.6.1 *Specific aims*

- To characterise the immunomodulatory role of trypanosome-derived ketoacids in primary human DC.
- To investigate the effects of trypanosome-derived ketoacids on the metabolic profile of primary human DC.
- To assess T cell responses upon co-culture with trypanosome-derived ketoacid-treated DC.
- To explore the therapeutic potential of trypanosome-derived ketoacids in PBMC isolated from patients with IBD.



# **Chapter 2:**

## **Materials & Methods**

## 2.1 Materials

### 2.1.1 Reagents

4-hydroxyphenylpyruvic acid (HPP) and indole-3-pyruvic acid (IP) were purchased from Merck and dissolved in RPMI to a final concentration of 2 mM before use. Ultrapure lipopolysaccharide (LPS) from *E. Coli* O111:B4 was purchased from Enzo Life Sciences (Bruxelles, Belgium). Carnosol (from *Rosemarinus officinalis*) and curcumin (from *Curcuma longa*) were purchased from Merck and dissolved in DMSO, also purchased from Merck. Human monoclonal anti-CD3 antibody and anti-CD28 antibody were purchased from Invitrogen. The Antioxidant assay kit was purchased from Merck. The CyQUANT™ LDH Cytotoxicity Assay Kit was purchased from Invitrogen. ML385 and VPS34-IN1 were purchased from Merck.

### 2.1.2 Cell culture

Complete RPMI, complete DMEM or complete IMDM were prepared by supplementing with 10% foetal bovine serum (FBS), 2 mM L-glutamine, 100 U/mL penicillin, and 100 µg/mL streptomycin, which were all purchased from Merck. The concentration of glucose in the RPMI was 11 mM, and the concentration of glucose in both the DMEM and IMDM was 25 mM. Lymphoprep is manufactured by Axis-Shield poC. GM-CSF and IL-4 were purchased from Miltenyi Biotec. The MagniSort Human CD14 Positive Selection kit and MagniSort Human CD4 T cell Positive Selection kit were purchased from Thermo Fisher Scientific. Dulbecco's phosphate buffered saline (PBS) was also purchased from Merck. The HEK-Blue™ hTLR4 assay system was purchased from InvivoGen.

### 2.1.3 Western blotting

The protease inhibitor cocktail was purchased from Roche and Phosphatase inhibitor cocktail 3 was purchased from Merck. The western blot antibodies for Nrf2, pro-IL-1β, HK2, p-AMPK, t-AMPK, pS6, p62 and LC3 were all purchased from Cell Signalling Technology, while the antibody for HO-1 was purchased from Enzo Life Sciences, and the β-actin antibody and secondary anti-rabbit were purchased from Merck. All chemicals used for

western blotting buffers and solutions listed in Table 2.1 were purchased from Sigma-Aldrich. Acrylamide was purchased from Fisher scientific. SeeBlue Plus2 Pre-Stained Protein Standard was purchased from Invitrogen. Immobilin polyvinylidene difluoride (PVDF) membrane and Enhanced Chemiluminescent (ECL) Horseradish-Peroxidase (HRP) Substrate were purchased from Merck.

**Table 2.1 Buffers for Western blotting**

Buffer	Reagents
1 M Tris-HCL (pH 6.8)	121.4 g Tris, 1 L dH <sub>2</sub> O, pH using HCL.
1.5 M Tris-HCL (pH 8.8)	181.71 g Tris, 1 L dH <sub>2</sub> O, pH using HCL.
10% SDS	10 g SDS, 100 ml dH <sub>2</sub> O.
10% Ammonium Persulfate (APS)	100 mg APS, 10 ml dH <sub>2</sub> O
10X Running Buffer (pH8.3)	30.3 g Tris, 144 g Glycine, 10 g SDS, 1 L dH <sub>2</sub> O. Dilute 1:10 in dH <sub>2</sub> O to use at 1X concentration.
10X Transfer Buffer (pH ~8)	30 g Tris, 144 g Glycine, 1 L dH <sub>2</sub> O. Dilute 1:10 in dH <sub>2</sub> O to use at 1X concentration.
10X Tris-Buffered Saline with Tween-20 (TBST) (pH 7.6)	24.2 g Tris, 88 g NaCl, 10 ml Tween-20, 990 ml dH <sub>2</sub> O. Dilute 1:10 in dH <sub>2</sub> O to use at 1X concentration.

#### 2.1.4 Flow cytometry

The Fixable Viability Dye, and Annexin V & PI staining kit were all purchased from eBioscience. The DQ-Ovalbumin, FIX & PERM™ Cell Permeabilization Kit, CellROX™ green, Fixable Viability Dye eFluor506 and Anti-mouse Ig CompBeads were purchased from Invitrogen. The Zombie NIR™ Fixable Viability kit was purchased from BioLegend. Phorbol 12-myristate 13-acetate (PMA), ionomycin, and brefeldin A were purchased from Merck. Fluorochrome-conjugated antibodies were purchased as listed below in Table 2.2.

**Table 2.2 Fluorochrome-conjugated antibodies**

Specificity	Fluorochrome	Clone	Supplier
CD14	FITC	HCD14	Biolegend
CD209	PE-Cy7	9E9A8	Biolegend
CD40	efluor 450	5C3	Invitrogen
CD80	FITC	2D10	Biolegend
CD86	APC	IT2.2	Biolegend
CD83	PE	HB15e	Biolegend
CD3	PE-Cy5.5	SK7	Invitrogen
CD8	AF700	RPA-T8	BD biosciences
CD4	PE-CF594	L200	BD biosciences
Ki67	AF488	B56	BD biosciences

	PE-Cy7	B56	BD biosciences
IFN $\gamma$	APC	B27	BD biosciences
IL-17	PE	eBio64DEC17	Invitrogen
TNF	PerCP-Cy5.5	MAb11	Invitrogen
IL-2	PE-CF594	5344.111	BD biosciences
FOXP3	PE	236A/E7	Invitrogen
CD127	BV711	AO19D5	Biologend
CD25	PE-Cy7	BC96	Invitrogen

### 2.1.5 Polymerase chain reaction

High-Pure RNA Isolation Kits were purchased from Roche. The High-Capacity cDNA reverse transcription kit was purchased from Applied Biosystems and the iTaq Universal SYBR Green mastermix from Bio-Rad. Forward and reverse primers for NQO1, GSR, CYP1A1 and  $\beta$ -actin were purchased from Merck. The primer sequences are detailed in Table 2.3.

**Table 2.3 Primer sequences.**

Table containing the forward and reverse primer sequences for NQO1, GSR, and  $\beta$ -actin.

Gene	Forward Primer	Reverse Primer
NQO1	5' TGAAGAAGAAAGGATGGGAG 3'	5' TTTACCTGTGATGTCCTTTC 3'
GSR	5' GACCTATTCAACGAGCTTTAC 3'	5' CAACCACCTTTTCTTCCTTG 3'
CYP1A1	5' CATTAAACATCGTCTTGGACC 3'	5' TCTTGGATCTTCTCTGTACC 3'
$\beta$ -actin	5' GGACTTCGAGCAAGAGATGG 3'	5' AGCACTGTGTTGGCGTACAG 3'

### 2.1.6 Enzyme linked immunosorbent assay

Human IL-10, IL-23, IL-12p70, IL-6, TNF, IL-17 and IFN $\gamma$  uncoated ELISA kits were purchased from Invitrogen.

### 2.1.7 Seahorse

The Complete XF assay medium was purchased from Agilent. The Corning™ Cell-Tak Cell and Tissue Adhesive was purchased from Fisher Scientific. Oligomycin was purchased from Cayman Chemicals and carbonyl cyanide-p trifluoromethoxyphenylhydrazone (FCCP) from Santa Cruz biotechnology. Rotenone, antimycin A, and 2-deoxy-D-glucose (2-DG) were all purchased from Merck.

## 2.2 Methods

### 2.2.1 Cell culture

Cells were cultured at 37°C with an atmosphere of 95% humidity and 5% CO<sub>2</sub>. RPMI, IMDM and DMEM medium were supplemented with 10% FBS, 2mM L-Glutamine, 100 U/ml penicillin and 100 µg/ml streptomycin.

### 2.2.2 Cell counting

Cells in media were diluted in trypan blue and 10 µl was loaded onto a haemocytometer, a Hycor Galsstic slide, and viewed under a light microscope. Cell viability was assessed by dye exclusion. The total number of viable cells was calculated using the formula:

$$\text{Number of cells/ml} = \text{Average number of cells counted} \times 10^4 \times \text{dilution factor}$$

### 2.2.3 PBMC isolation

The Irish Blood Transfusion Service (IBTS) at St. James's Hospital in Dublin supplied leukocyte-enriched buffy coats for these studies, from donors who provided informed written consent. Ethical approval was obtained from the research ethics committee of the School of Biochemistry and Immunology at Trinity College Dublin, and all experiments were carried out in accordance with the Declaration of Helsinki. Buffy coats were diluted 1:2 with sterile PBS and centrifuged at 1250 g for 10 minutes at room temperature with the brake off. The buffy coat layer was carefully removed, diluted in sterile PBS, and 25 ml was layered over 17.5 ml Lymphoprep. PBMC were isolated by density gradient centrifugation at 800 g at room temperature for 20 minutes with the brake off. The PBMC layer was carefully removed using a Pasteur pipette, washed in sterile PBS and centrifuged at 650 g for 10 minutes. The cells were washed again in sterile PBS and centrifuged at 300 g for 10 minutes. The PBMC were then resuspended and cultured in RPMI.

#### 2.2.4 Isolation of IBD patient PBMC

This study received ethical approval from St Vincent's University Hospital Ethics and Medical Research Committee to take blood samples from consenting patients ( $N = 14$ ) attending a specialist outpatient clinic for inflammatory bowel disease (IBD). Table 2.4 outlines a number of parameters regarding the patient's data, including gender (male or female), IBD condition (ulcerative colitis (UC) or Crohn's disease (CD)), and the extent of the disease. PBMC were isolated as above and cryopreserved at  $-80^{\circ}\text{C}$ . PBMC were thawed and treated with either IP or HPP (250–1000  $\mu\text{M}$ ) or carnosol or curcumin (5  $\mu\text{M}$ ) for 6 hours prior to stimulation with anti-CD3 (1  $\mu\text{g}/\text{mL}$ ) for 12 hours. The media was then removed and replaced with fresh media to circumvent issues that occur as the compounds become fluorescent after incubations over long periods of time, and cells were maintained in the presence of anti-CD3 for a further four days. The supernatants were then removed for analysis of cytokines by ELISA and PBMC were restimulated in complete IMDM medium in the presence of 50 ng/mL PMA, 500 ng/mL ionomycin, and 5  $\mu\text{g}/\text{mL}$  brefeldin A for 4 hours. Cells were then stained for extracellular and intracellular markers as outlined below, and analysed using flow cytometry. All antibodies used in this experiment were carefully chosen to avoid channels which still had some fluorescence issues, despite the steps taken to overcome this. Gating strategy shown in Figure 2.5.

**Table 2.4 Patient data**

A table outlining data regarding the patient's gender (male or female), IBD condition (ulcerative colitis (UC) or Crohn's disease (CD)), and the extent of the disease.

Patient sample number	Male/Female	UC/CD	Extent of disease
1	Female	CD	Crohn's colitis, perianal
2	Male	CD	Crohn's colitis, perianal
3	Male	UC	Proctitis
4	Male	CD	Ileitis
5	Male	CD	Crohn's colitis, perianal
6	Female	UC	Pancolitis
7	Female	CD	Crohn's colitis, perianal
8	Female	UC	Proctitis
9	Male	CD	Ileitis, perianal
10	Female	CD	Ileo-colitis
11	Female	UC	Left-sided colitis
12	Female	UC	Proctosigmoiditis
13	Male	UC	N/A
14	Male	UC	Pancolitis

### *2.2.5 Isolation of CD14<sup>+</sup> and CD4<sup>+</sup> cells*

CD14<sup>+</sup> monocytes and CD4<sup>+</sup> T cells were isolated from PBMC using magnetic activated sorting using the Magnisort Human CD14 positive selection kit or the Magnisort Human CD4 T cell Positive Selection kit. PBMC were washed in MACS buffer (PBS containing 2% FBS and 2mM EDTA) and pelleted by centrifugation at 300 g for 5 minutes. The pellet was resuspended in MACS buffer at  $1 \times 10^8$  cells/ml in a 12 x 75 mm 5 ml tube and incubated with anti-CD14 biotin (10  $\mu$ l per 100  $\mu$ l cells) for 10 minutes at room temperature. Cells were then washed in 4 ml MACS buffer and pelleted by centrifugation at 300 g for 5 minutes. Supernatant was discarded; cells were re-suspended in their original volume of MACS buffer and incubated with MagniSort positive selection beads (15  $\mu$ l per 100 $\mu$ l cells) for 10 minutes at room temperature. The volume was then adjusted to 2.5 ml and the tube placed inside the magnetic field of a Magneto cell sorter for 5 minutes. The negative fraction was then poured off by inverting the tube while held inside Magneto, and the remaining cells were re-suspended in 2.5 ml MACS buffer. This step was repeated two times and then the positive fraction containing the CD14<sup>+</sup> monocytes was re-suspended in RPMI and counted. The purity of the sorted cells was assessed by flow cytometry and was routinely > 85% (Figure 2.1). For the CD4<sup>+</sup> T cell isolation, the negative fraction from the CD14 sort was collected, counted, and the above protocol was followed using anti-CD4 biotin instead. The purity of the sorted cells was assessed by flow cytometry and was routinely > 90% (Figure 2.2).

### *2.2.6 Culture of monocyte derived dendritic cells*

CD14<sup>+</sup> monocytes isolated from human PBMC as above were then cultured at  $1 \times 10^6$  cells/mL in RPMI and supplemented with GM-CSF (50 ng/mL) and IL-4 (40 ng/mL) to generate monocyte-derived DC. On day three of culture, half of the media was replaced with fresh media supplemented with cytokines at the same starting concentration. On day six, non-adherent and loosely adherent cells were gently removed for use. The purity of CD14<sup>lo</sup>DC-SIGN<sup>+</sup> DC was confirmed by flow cytometry and was routinely >95% (Figure 2.3). DC were cultured at  $1 \times 10^6$  cells/mL for all further assays.

### *2.2.7 Culture of bone marrow derived macrophages*

Primary bone marrow derived macrophages (BMDM) were obtained from the hind legs of adult C57BL/6 mice. Bone marrow from the tibiae and femurs were flushed out with DMEM using a 27 Gauge needle and broken up by trituration using a 19 Gauge needle. The cell suspension was centrifuged at 300 g for 5 minutes. The cell pellet was re-suspended in 2 ml of filter sterilised ammonium chloride solution at 37°C for 2 minutes to lyse red blood cells. 8 ml of DMEM was added to stop cell lysis and the cell solution was centrifuged at 300 g for 5 minutes. Cells were seeded in 10 ml petri dishes at  $1 \times 10^6$  cells/ml in DMEM containing 20% L929 medium containing M-CSF. The cultures were incubated at 37°C in 5% CO<sub>2</sub> humidified atmosphere. 1 ml of L929 medium containing M-CSF was added on day 3. Cells were harvested on day 6 by replacing the medium on the cells with 5 ml of DMEM and scraping using a cell scraper. The cell suspension was then centrifuged at 300 g for 5 minutes and the pellet was re-suspended in DMEM. Cells were plated in 24-well plates at  $1 \times 10^6$  cells/ml in DMEM containing 10% L929 medium containing M-CSF.

### *2.2.8 SDS-PAGE and western blotting*

#### *2.2.8.1 Sample preparation*

Cell lysates were prepared by removing cell supernatants and washing cells in PBS prior to addition of lysis buffer. Different lysis protocols were used depending on the protein of interest. RIPA buffer (Tris 50 mM; NaCl 150 mM; SDS 0.1%; Na.Deoxycholate 0.5%; Triton X 100) was used to lyse samples for detecting HO-1 expression. For detection of Nrf2, pro-IL-1 $\beta$ , HK2, AMPK, and pS6 expression, cells were lysed in 1x Laemmli loading buffer. For detection of p62 and LC3, cells were lysed in 1x Laemmli loading buffer and sonicated for 30 seconds. All samples were lysed in the presence of a protease inhibitor cocktail and phosphatase inhibitor cocktail set on ice for 30 minutes. The samples were then centrifuged at 16,000 g for 5 minutes to pellet debris, and the lysates were transferred to new microcentrifuge tubes. Samples were boiled at 100°C for 5 minutes, and either used immediately or stored at -20°C until use.



### 2.2.8.2 SDS-PAGE

Samples were prepared by the addition of 5x Laemmli buffer (containing 20%  $\beta$ -mercaptoethanol) in a ratio of 1:4 (if not already lysed in 1x Laemmli buffer) prior to boiling at 100°C for 5 minutes. Depending on the size of the target protein, either 8%, 10%, 12% or 16% polyacrylamide gels were used (see Table 2.5 for composition of gels). Samples and a pre-stained protein standard were loaded into the gel. Electrophoresis was carried out at 120 volts (V) for 90-120 minutes.

**Table 2.5 Composition of SDS-Polyacrylamide Gel.**

	<b>8% Resolving Gel</b>	<b>10% Resolving Gel</b>	<b>12% Resolving Gel</b>	<b>16% Resolving Gel</b>	<b>Stacking Gel</b>
<b>30% Acrylamide</b>	4 ml	5 ml	6 ml	8 ml	0.67 ml
<b>H<sub>2</sub>O</b>	6.9 ml	5.9 ml	4.9 ml	2.9 ml	2.7 ml
<b>1.5 M Tris-HCl</b>	3.8 ml	3.8 ml	3.8 ml	3.8 ml	-
<b>1 M Tris-HCl</b>	-	-	-	-	0.5 ml
<b>10% SDS</b>	0.15 ml	0.15 ml	0.15 ml	0.15 ml	40 $\mu$ l
<b>10% APS</b>	0.15 ml	0.15 ml	0.15 ml	0.15 ml	40 $\mu$ l
<b>Temed</b>	6 $\mu$ l	6 $\mu$ l	6 $\mu$ l	6 $\mu$ l	6 $\mu$ l

### 2.2.8.3 Transfer of proteins onto PVDF membrane

The resolved proteins were transferred onto a PVDF membrane. A wet transfer sandwich was prepared in the following order: sponge, filter paper, gel, PVDF membrane, filter paper, sponge. PVDF membrane was first activated by submersion in methanol. All other components of the transfer sandwich were first submerged in transfer buffer. The transfer sandwich was placed into the transfer system with the gel on the cathode side and the membrane on the anode side. After ensuring that there were no air bubbles in the system, the proteins were transferred at 200 milliamperes (mA) for 90-120 minutes depending on the size of the protein.

### 2.2.8.4 Immunodetection of proteins

Following the transfer, the membrane was incubated in blocking buffer, 5% (w/v) milk in 1 x Tris buffered saline (TBST), under agitation for 1 hour at room temperature. The membrane was incubated in primary antibody (see Table 2.6 for dilutions) with agitation,

overnight at 4°C. The membrane was washed 5 times for 5 minutes each with 1x TBST prior to incubation in secondary antibody (See Table 2.6 for dilutions) for 2 hours at room temperature. The membrane was washed a further 5 times for 5 minutes each and then developed with freshly prepared ECL using Chemi-Luminescent gel documentation system. The membranes were subsequently re-probed with a loading control,  $\beta$ -actin, in order to normalise the protein of interest to the loading control for densitometric analysis.

**Table 2.6 Dilutions for western blot antibodies.**

Primary antibody	Dilution	Secondary antibody	Dilution
Anti-HO-1	1:1000	Anti-Rabbit	1:2000
Anti-phospho-AMPK	1:1000	Anti-Rabbit	1:2000
Anti-total-AMPK	1:1000	Anti-Rabbit	1:2000
Anti-phospho-S6	1:2000	Anti-Rabbit	1:2000
Anti-Nrf2	1:1000	Anti-Rabbit	1:2000
Anti-pro-IL-1 $\beta$	1:1000	Anti-Mouse	1:2000
Anti-HK2	1:1000	Anti-Rabbit	1:2000
Anti-p62	1:1000	Anti-Rabbit	1:2000
Anti-LC3	1:1000	Anti-Rabbit	1:2000
Anti- $\beta$ -actin- peroxidase	1:50,000	-	-

## 2.2.9 Flow cytometry

### 2.2.9.1 Extracellular staining

For staining of cells with fluorochrome-conjugated antibodies against extracellular markers, cells were harvested and washed in PBS. Cells were first stained with a viability dye which binds to dead cells by incubating them in 50  $\mu$ l Fixable Viability Dye (diluted 1:1000) or Zombie NIR<sup>TM</sup> Fixable Viability kit (diluted 1:500) in PBS for 15 minutes at room temperature, protected from light. Cells were then washed in PBS and centrifuged at 300 g for 5 minutes. The supernatant was discarded and cells were incubated in 50  $\mu$ l PBS containing fluorochrome-conjugated antibodies for 15 minutes at room temperature protected from light. Following extracellular staining, cells were washed in PBS, centrifuged at 300 g and fixed with 50  $\mu$ l Fix & Perm solution A for 15 minutes at room temperature, protected from light. Cells were washed in PBS, centrifuged as before and resuspended in PBS for acquisition.

#### *2.2.9.2 Intracellular staining*

Cells were restimulated in media in the presence of 50 ng/mL PMA, 500 ng/mL ionomycin, and 5 µg/mL brefeldin A for 4 hours. Cells were stained with live/dead viability dye and surface markers as above. Cells were fixed with 50 µl Fix & Perm solution A for 15 minutes at room temperature, protected from light. Cells were washed and stained for intracellular markers in 50 µl Fix & Perm solution B (permeabilisation buffer) for 15 minutes at room temperature in the dark. Cells were washed in PBS, and resuspended in PBS for acquisition.

#### *2.2.9.3 Intranuclear staining*

For staining of intranuclear markers, cells were stained with live/dead viability dye and surface markers as above. Cells were resuspended in 200 µl FOXP3 fixation buffer for 15 minutes at room temperature, protected from light. Cells were then washed with 1 ml 1x FOXP3 permeabilisation buffer and centrifuged at 300 g for 5 minutes. Cells were then stained with intranuclear fluorescently labelled antibodies in 50 µl permeabilisation buffer and incubated for 30 minutes at room temperature in the dark. Cells were washed again in permeabilisation buffer and centrifuged at 300 g for 5 minutes. Cells were then resuspended in PBS and analysed by flow cytometry.

#### *2.2.9.4 Annexin V & PI staining*

For assessment of apoptosis and necrosis, cells were stained with fluorochrome-conjugated anti-Annexin V and PI. Cells were washed in 1x Annexin V binding buffer and pelleted by centrifugation at 300 g for 5 minutes. Supernatant was discarded and cells were incubated in 50 µl 1x binding buffer containing 2.5 µl fluorochrome-conjugated anti-Annexin V and 5 µl PI for 15 minutes at room temperature, protected from light. 400 µl of 1x binding buffer was added to the cells, and they were immediately acquired.

#### *2.2.9.5 DQ-Ovalbumin*

For assessment of phagocytosis or antigen uptake, cells were incubated with fresh media containing DQ-Ova (500 ng/ml) for 20 minutes at 37°C, before transferring to 4 °C for a further 10 minutes incubation to stop the uptake of the model antigen. Cells were then

washed in PBS, centrifuged at 300 g for 5 minutes, resuspended in PBS and acquired immediately. Unstained cells (cells given fresh media containing no DQ-Ova) were used as a gating control for DQ-Ova positive cells.

#### *2.2.9.6 CellRox*

For assessment of cellular ROS, cells were incubated with fresh media containing CellRox green (5  $\mu$ M) for 30 minutes at 37°C. Cells were washed in PBS, centrifuged at 300 g for 5 minutes, and fixed with 4% PFA for 15 minutes. Cells were washed in PBS, centrifuged at 300 g for 5 minutes, and resuspended in PBS before acquiring.

#### *2.2.9.7 Acquisition, compensation and analysis*

Where flow cytometry experiments contained more than one fluorochrome, single-stained controls were prepared for each fluorochrome using compbeads in order to calculate spectral compensation. Samples were acquired on a BD FACSCanto II or a BD LSRFortessa flow cytometer. All flow cytometry data analysis was performed using FlowJo v10 software.

#### *2.2.10 Capture Enzyme-linked immunosorbent assay*

The concentrations of cytokines present in the supernatants from cell cultures were measured by Enzyme-Linked Immunosorbent Assay (ELISA) using Invitrogen uncoated ELISA kits for IL-6, IL-12p70, IL-23, IL-10, TNF, IL-17 and IFN $\gamma$ . 75  $\mu$ l of capture antibody diluted in coating buffer (1:250 dilution) was applied to high-binding 96-well plates. Plates were incubated overnight at 4°C, capture antibody was removed and non-specific binding sites were blocked with 1x assay diluent for 1 hour at room temperature. After blocking, plates were washed four times in PBS-tween solution (PBS, 0.0005% Tween-20), dried and 75  $\mu$ l of supernatant samples were loaded into wells in triplicates either neat or diluted with 1x assay diluent. A standard curve of serially diluted recombinant cytokine standard was also loaded onto the plates in triplicate. Blank wells, containing assay diluents only, were included on each plate to allow the subtraction of background from each sample. Samples were incubated overnight at 4°C. The following day the plates were again washed four times, prior to the addition of 75  $\mu$ l of biotinylated detection antibody diluted in 1x assay diluent (1:250 dilution) to each well, and incubated for 2 hours at room temperature.

Plates were washed four times and 75 µl of horseradish-peroxidase (HRP) conjugated to streptavidin diluted in 1x assay diluent (1:250 dilution) was applied to wells for 30 minutes in the dark. Wells were thoroughly washed and the substrate, TMB, was added as required by manufacturer. The enzyme-mediated colour reaction was protected from light while developing and stopped with the addition of 1M H<sub>2</sub>SO<sub>4</sub>. The optical density of the colour was determined by measuring the absorbance at 450 nm using a microtiter plate reader. A standard curve was generated using the serially diluted protein standards and used to determine the concentration of cytokine in the supernatant.

### *2.2.11 Polymerase chain reaction*

#### *2.2.11.1 RNA isolation*

Supernatants were removed and cells were washed once with PBS before the addition of 400µl of lysis/binding buffer and 200 µl of PBS per well. The lysates were transferred to a High Pure Filter Tube that was inserted into a collection tube. Samples were centrifuged at 8,000 g for 15 seconds (Spectrafuge 24 D). The flowthrough liquid was discarded and 90 µl of DNase incubation buffer with 10 µl DNase I was added to each Filter Tube and incubated for 15 minutes at room temperature. 500 µl of Wash Buffer I was then added to the Filter Tubes which were centrifuged at 8,000 g for 15 seconds. The flow-through liquid was discarded and 500 µl of Wash Buffer II was added to the Filter Tubes which were centrifuged again at 8,000 g for 15 seconds. The flow-through liquid was discarded and a further 200 µl of Wash Buffer II was added to Filter Tubes and centrifuged at 13,000 g for 2 minutes. The flow-through liquid was discarded and samples were centrifuged at 13,000 g for a further 1 minute. The collection tubes were discarded and the Filter Tubes were placed into sterile, RNase-free 1.5 ml microcentrifuge tubes. 50 µl of Elution Buffer was added to the filter tubes and centrifuged at 8,000 x g for 1 minute. The concentration of eluted RNA in each sample was determined using a NanoDrop 2000c UV-Vis Spectrophotometer and then equalised by the addition of Elution Buffer, where necessary.

### 2.2.11.2 cDNA synthesis

cDNA synthesis was then carried out using the High capacity cDNA reverse transcription kit (Applied Biosystems). A 2X Reverse Transcription (RT) master mix was prepared with the components in Table 2.7.

**Table 2.7 Components and volumes required for the 2X RT Master Mix.**

Component	Volume added (per sample)
10X RT Buffer	2 $\mu$ l
25X dNTP Mix (100mM)	0.8 $\mu$ l
10X RT Random Primers	2 $\mu$ l
Multiscribe Reverse Transcriptase	1 $\mu$ l

14.2  $\mu$ l of RNA (250 ng) and 5.8  $\mu$ l of the 2X RT master mix were added to RNase-free PCR tubes and the reverse transcription (see Table 2.8) was performed using the Mini Amp Thermal Cycler.

**Table 2.8 cDNA Reverse Transcription Reaction.**

	Step 1	Step 2	Step 3	Step 4
Temperature ( $^{\circ}$ C)	23	37	85	4
Time (Minutes)	10	120	5	Indefinitely

### 2.2.11.3 Real time Polymerase Chain Reaction

Real time Polymerase Chain Reaction (PCR) was carried out using the iTaq Universal SYBR Green Supermix and oligonucleotide primers. Reactions were made up, as detailed in Table 2.9, into a 96-well PCR microplate. The PCR reaction is detailed in Table 2.10.

**Table 2.9 Components and volumes required for iTaq Universal SYBR Green reaction.**

Component	Volume added (per sample)
Forward Primer (Target gene or EC)	0.5 $\mu$ l
Reverse Primer (Target gene or EC)	0.5 $\mu$ l
Sigma H <sub>2</sub> O (RNase/DNase free)	4 $\mu$ l
Syber MM.	4 $\mu$ l
Diluted cDNA sample.	1 $\mu$ l
<b>Total Volume</b>	<b>10 <math>\mu</math>l</b>

**Table 2.10 Thermal cycling parameters for iTaq Universal SYBR Green real-time PCR.**

	Step 1	Step 2	Step 3	Step 4	Step 5	Step 6
Temperature ( $^{\circ}$ C)	95	95	60	Plate Read	72	Go to Step 2
Time (Seconds)	10 (mins)	15	30	-	30	x 40

The real-time PCR reactions (detailed in Table 2.9 and Table 2.10) were performed using the BioRad CFX Touch Real-Time PCR detection system. For each sample, mRNA concentration was normalised using the crossing threshold of the housekeeping gene  $\beta$ -actin. Gene expression, relative to untreated samples, was determined using the  $2^{-\Delta\Delta C_t}$  algorithm.

### *2.2.12 Seahorse*

The Seahorse cartridge plate, consisting of the sensors for O<sub>2</sub> and pH, was hydrated by the addition of 200  $\mu$ l XF calibrant fluid per well, and incubated in a non-CO<sub>2</sub> incubator at 37°C for a minimum of 8 hours prior to use. DC were cultured with LPS and ketoacids as appropriate in a tissue culture plate as normal, and the cell culture medium was then replaced with complete XF assay medium (pH of 7.4, supplemented with 10 mM glucose, 1 mM sodium pyruvate, 2 mM L-glutamine). DC were then transferred to a Seahorse cell culture 96-well microplate at a density of  $2 \times 10^5$  cells/well, which had been previously coated with Corning™ Cell-Tak Cell and Tissue Adhesive in order to adhere the DC to the plate. This plate was then incubated in a non-CO<sub>2</sub> incubator for 30 minutes. Blank wells were prepared containing XF assay medium only (no cells) to subtract the background oxygen consumption rate (OCR), extracellular acidification rate (ECAR) and proton efflux rate (PER) during analysis. The inhibitors used during the Seahorse assay; Oligomycin (1 mM), FCCP (1 mM), rotenone (500 nM), antimycin A (500 nM), and 2-DG (25 mM), were prepared in XF assay medium. Inhibitors were loaded into the appropriate injection ports on the hydrated cartridge plate and incubated for 10 minutes in a non-CO<sub>2</sub> incubator at 37 °C. The cartridge was loaded into the machine and the machine was calibrated. The cell plate was subsequently placed into the machine. Oligomycin, FCCP, rotenone and antimycin A, and 2-DG were sequentially injected while the OCR, ECAR and PER readings were simultaneously measured. Wave software (Agilent Technologies, California, USA) was used to analyse the results. The rates of basal glycolysis, max glycolysis, glycolytic reserve, basal respiration, max respiration, respiratory reserve and ATP production rate were calculated as detailed in the manufacturer's protocol and as outlined in Table 2.11.

**Table 2.11 Seahorse calculations.**

Table outlining the calculations used to determine the measurements for the Seahorse assay.

Rate	Calculation
Basal glycolysis	Average ECAR values prior to oligomycin treatment – non-glycolytic ECAR
Max glycolysis	Average ECAR values after oligomycin and before FCCP
Glycolytic reserve	Max glycolysis – basal glycolysis
Basal respiration	Average OCR values prior to oligomycin treatment – non-mitochondrial OCR
Max respiration	Average OCR values after FCCP & before Rotenone/antimycin A treatment
Respiratory reserve	Max respiration – basal respiration
Mitochondrial ATP production rate	$OCR_{ATP} * 2 * P/O$ ratio
Glycolytic ATP production rate	PER - mitoPER
Total cellular ATP production rate	GlycoATP production rate + MitoATP production rate

### 2.2.13 LDH assay

The CyQUANT™ LDH Cytotoxicity Assay Kit was used to detect lactate dehydrogenase (LDH) present in the media during culture, as this can be used as an indicator of cellular cytotoxicity. After treatment was complete, 50 µl of supernatant was removed and placed in a new 96 well plate. 50 µl of reaction mixture was added and left at room temperature for 30 minutes in the dark. 50 µl of stop solution was then added. The absorbances of the samples were read at 490 nM and 680 nM. The data was analysed by subtracting the background absorbances, read at 680 nM, from the absorbances read at 490 nM. LDH present in the media can catalyse the conversion of lactate to pyruvate via NAD<sup>+</sup> reduction to NADH. NADH is subsequently oxidised by diaphorase which leads to the reduction of a tetrazolium salt (INT) to a red formazan product that can be measured spectrophotometrically at 490 nm, giving a directly proportional readout of cytotoxicity. The percentage cytotoxicity was calculated as following:

$$\begin{aligned} & \% \text{ cytotoxicity} \\ & = \left( \frac{\text{Compound treated LDH activity} - \text{Spontaneous LDH activity}}{\text{Maximum LDH activity} - \text{Spontaneous LDH activity}} \right) \times 100 \end{aligned}$$



Compound treated LDH activity represents the samples with the treatment of interest. Spontaneous LDH activity represents untreated control samples. Maximum LDH activity represents positive control samples treated with Triton X-100 for 1 hour.

#### *2.2.14 Antioxidant assay*

DC were lysed by sonication in ice-cold PBS and centrifuged at 14,000 rpm for 10 minutes to pellet any debris. The total antioxidant capacity of the cells was analysed using an Antioxidant assay kit according to the manufacturer's protocol. The assay measures the reduction of  $\text{Cu}^{2+}$  by an antioxidant to  $\text{Cu}^+$ , which can subsequently form a coloured complex with a dye reagent in the kit. The absorbances of the samples were read at 570 nm and compared to the absorbances of a range of known concentrations of Trolox standards. The data is displayed as the total antioxidant capacity of the cells expressed as an equivalent concentration of Trolox ( $\mu\text{M}$ ).

#### *2.2.15 Two-Photon Fluorescence Lifetime Imaging Microscopy*

Two-photon excited NAD(P)H- Fluorescence Lifetime Imaging Microscopy (FLIM) was used to measure the levels of free and protein-bound NADH within cells, and was performed on a custom multiphoton system. A titanium:sapphire laser (Chameleon, Coherent®) was used for multiphoton excitation. A water-immersion 25x objective (Olympus, 1.05NA) was utilised on an upright (Olympus BX61WI) laser scanning microscope. Two-photon excitation of nicotinamide adenine dinucleotide phosphate (NAD(P)H) fluorescence was performed with 760 nm excitation wavelength. A 455/90 nm bandpass filter was used to isolate NAD(P)H fluorescence signal. 512x512 pixel images were acquired with a pixel dwell time of 3.81  $\mu\text{s}$  and 30-second collection time. A PicoHarp 300 TCSPC system operating in the time-tagged mode coupled with a PMA hybrid detector (PicoQuant GmbH, Germany) was used for fluorescence decay measurements yielding 256 time bins per pixel. At least three images for each model were acquired. Afterwards, regions of interest (ROI) were selected, and the NAD(P)H fluorescence decay was analysed.

For the NAD(P)H fluorescence decay analysis, an overall decay curve was generated by the contribution of all pixels in the ROI area. Afterwards, it was fitted with a double exponential decay curve (Equation (1)):

$$I(t) = \alpha_1 e^{-\frac{t}{\tau_1}} + \alpha_2 e^{-\frac{t}{\tau_2}} + c \quad (1)$$

$I(t)$  represents the fluorescence intensity at time ( $t$ ) after laser excitation.  $\alpha_1$  and  $\alpha_2$  represent the fraction of the overall signal comprised of a short and long lifetime component, respectively.  $\tau_1$  and  $\tau_2$  are the long and short lifetime components, respectively.  $c$  corresponds to background light.  $\chi^2$  is calculated to evaluate the goodness of multi-exponential fit to the raw fluorescence decay data—the lowest  $\chi^2$  values were considered in this study.

For NAD(P)H, a two-component fit was used to differentiate between the free ( $\tau_1$ ) and protein-bound ( $\tau_2$ ) NAD(P)H. The average lifetime ( $\tau_{avg}$ ) of NAD(P)H for each pixel is calculated by a weighted average of both the free and bound lifetime contributions (Equation (2)):

$$\tau_{avg} = \frac{(\alpha_1 \times \tau_1) + (\alpha_2 \times \tau_2)}{(\alpha_1 + \alpha_2)} \quad (2)$$

### 2.2.16 Endotoxin assay

The HEK-Blue™ hTLR4 assay system was used to test IP and HPP for LPS contamination. HEK-blue cells ( $5 \times 10^5$  cells/mL) expressing TLR4 were stimulated with LPS (0.1–100 ng/mL; positive control), or HPP or IP (both 1000  $\mu$ M) for 24 hours. The expression of secreted alkaline phosphatase (SEAP) which is under the control of NF- $\kappa$ B and AP-1 was tested by incubating cell supernatants with HEK-blue detection medium for 30 minutes at 37 °C and absorbance was read at 650 nm.

### 2.2.17 Statistical analysis

Prism 9 software (GraphPad Software Inc., California, USA) was used to perform the statistical analysis on all datasets. A repeated measures one-way ANOVA, with either

Dunnett's or Šídák's post hoc test, as appropriate, was used for analysis of three or more datasets. A Paired Student's t-test was used for the analysis of only two datasets. The analysis of datasets with more than one variable were performed using a two-way ANOVA with Šídák's multiple comparisons post hoc test. Asterisks are used in the figures to denote  $p$  values  $< 0.05$ , which were considered significant.

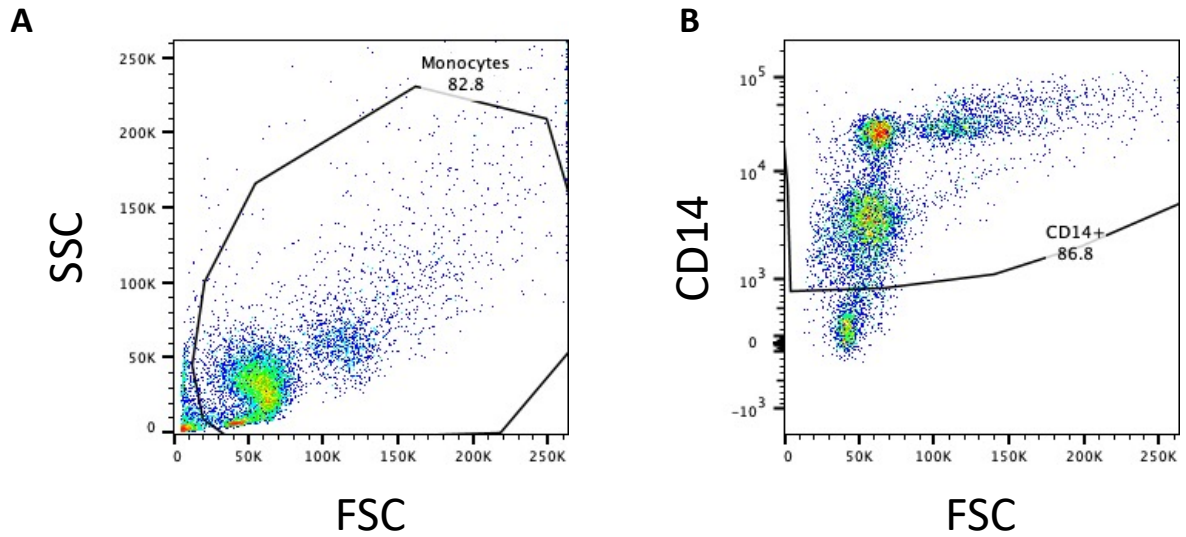


**Figure 2.1 Monocyte purity analysed by flow cytometry.**

The expression of CD14 on purified monocytes was analysed by flow cytometry. **(A)** Dead cells and cellular debris were excluded using forward scatter (FSC) and side scatter (SSC).

**(B)** Monocyte purity was then determined by gating on CD14<sup>+</sup> cells.

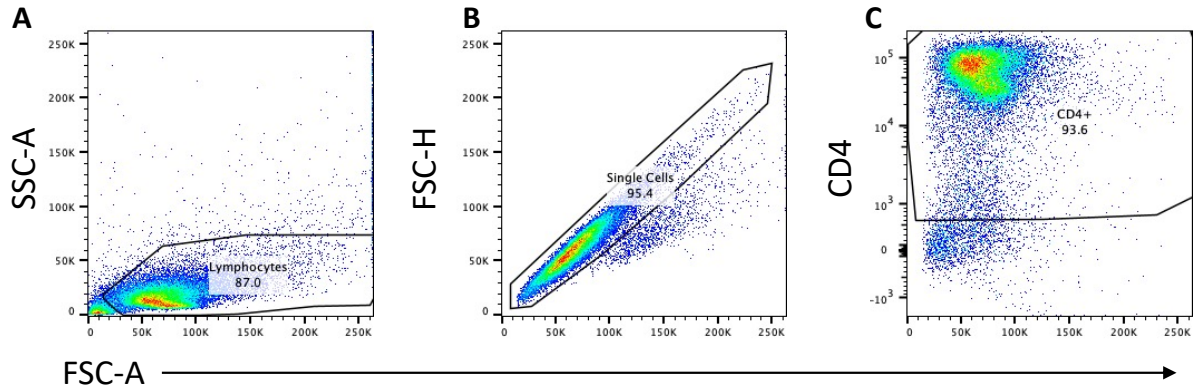


**Figure 2.2 CD4<sup>+</sup> T cell purity analysed by flow cytometry.**

The expression of CD4 on purified T cells was analysed by flow cytometry. **(A)** Dead cells and cellular debris were excluded using forward scatter (FSC) and side scatter (SSC). **(B)** Single cells were gated on using FSC-A and FSC-H to exclude doublets. **(C)** T cell purity was then determined by gating on CD4<sup>+</sup> cells.

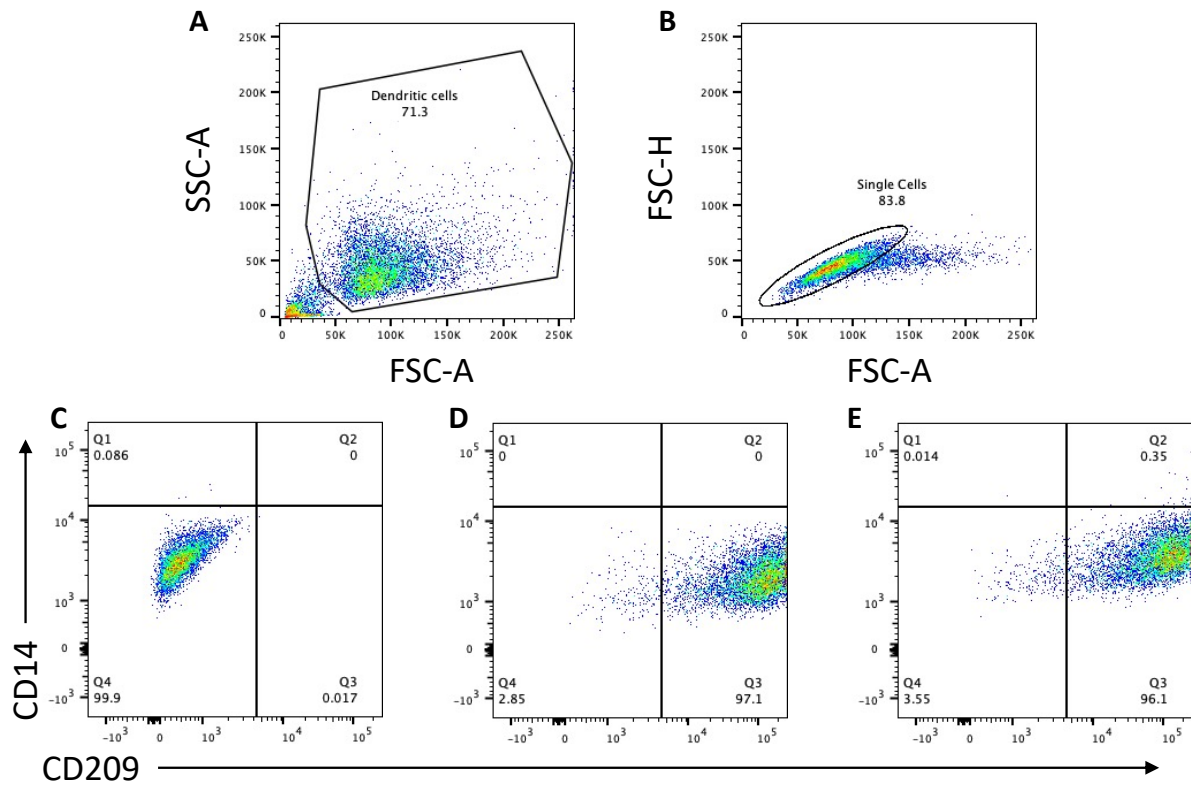


**Figure 2.3 Dendritic cell purity analysed by flow cytometry.**

(A) Dead cells and cellular debris were excluded using FSC and SSC. (B) Single cells were gated on using FSC-A and FSC-H to exclude doublets. Fluorescence minus one (FMO) controls for (C) CD29 and (D) CD14 were used to gate on the double stained sample (E) to determine DC purity. DC were defined as CD14<sup>-</sup>CD29<sup>+</sup>.

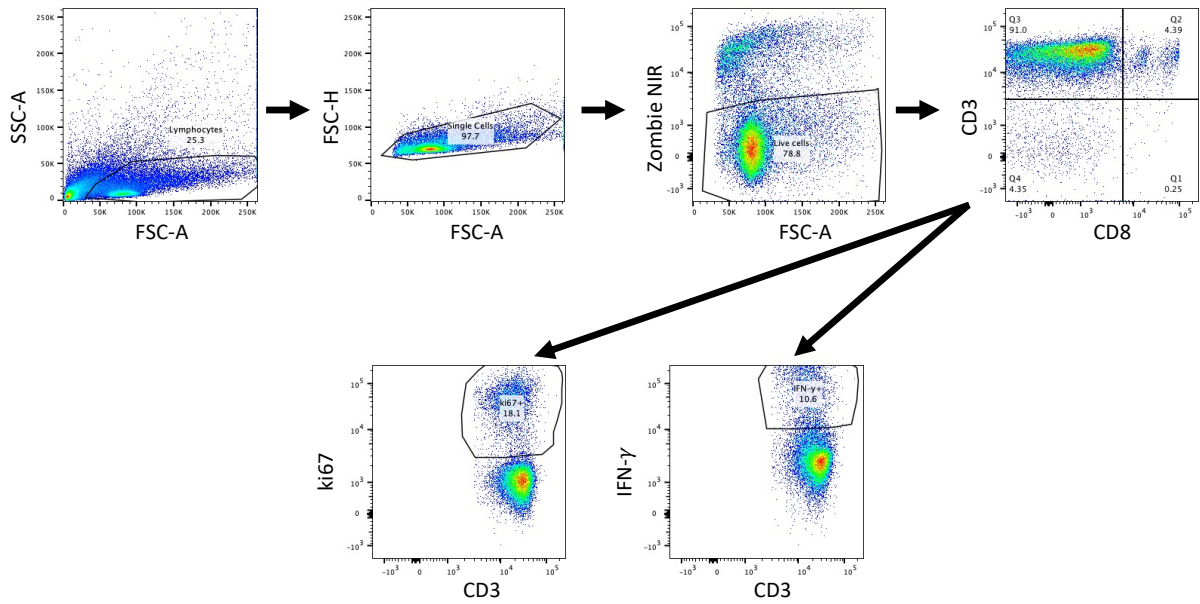


**Figure 2.4 Gating strategy used to generate data shown in co-culture experiments.**

To assess proliferation and cytokine production in T cells co-cultured with DC, lymphocytes were gated on based on forward and side scatter and doublets were excluded. Viable single cells were then gated on by excluding cells which had taken up the viability dye. The CD4 T cell population was approximated by gating on CD3<sup>+</sup>CD8<sup>-</sup> cells (Q1), as CD4 is often downregulated during restimulation with PMA and ionomycin. Representative dot plots for IFN $\gamma$  and ki67 expression in the CD3<sup>+</sup>CD8<sup>-</sup> population are shown. Cytokine gates were set using unstimulated PBMC incubated in the presence of brefeldin A.

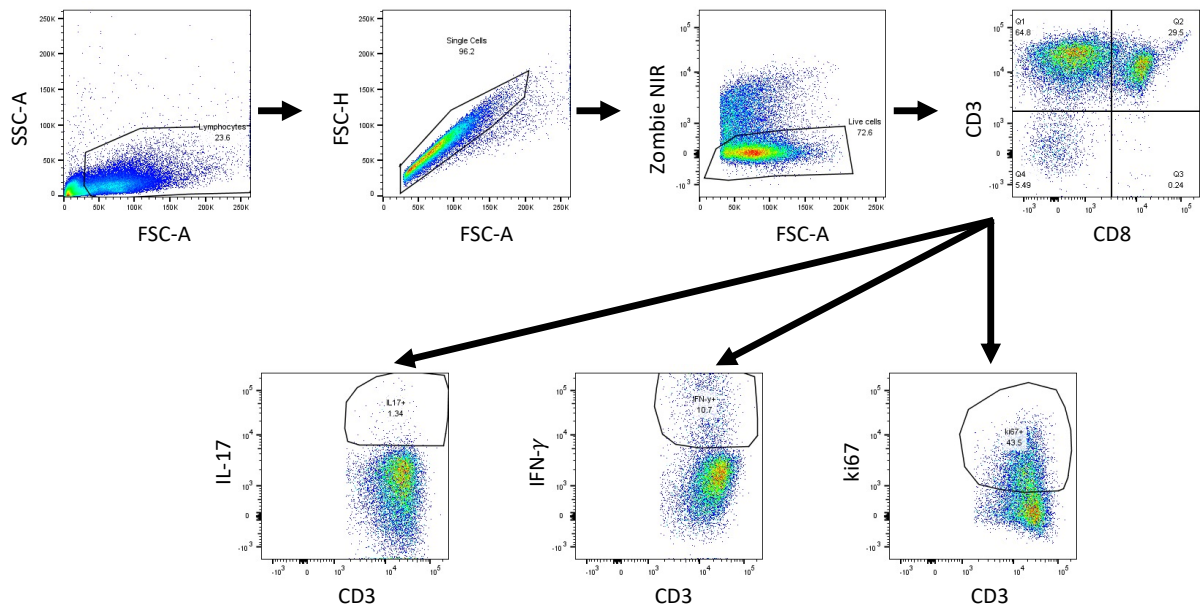


**Figure 2.5 Gating strategy used to generate data shown in IBD PBMC experiments.**

To assess proliferation and cytokine production in *ex-vivo* stimulated PBMC from patients with inflammatory bowel disease, lymphocytes were first gated on based on forward and side scatter and doublets were excluded. Viable cells were then gated on by excluding cells which had taken up the viability dye. The CD4 T cell population was approximated by gating on CD3<sup>+</sup>CD8<sup>-</sup> cells (Q1), as CD4 is often downregulated during restimulation with PMA and ionomycin. Representative dot plots for IFN $\gamma$  and ki67 expression in the CD3<sup>+</sup>CD8<sup>-</sup> population are shown. Cytokine gates were set using unstimulated PBMC incubated in the presence of brefeldin A.



**Chapter 3:**  
**Immunomodulatory properties of *T. brucei*-  
derived ketoacids in human DC**

### 3.1 Introduction

Infection with the parasite *T. brucei* is accompanied by the production of large amounts of aromatic ketoacids [253,254]. Recent studies have demonstrated that these molecules suppress host immune responses [255,256] which likely serves to benefit the parasite by prolonging infection, proliferation, and, ultimately, survival in the host. While the secretome of *T. brucei* has been shown to reduce the secretion of IL-12, IL-10, IL-6, and TNF in both murine and human DC [263,264], the ketoacids, IP and HPP, have been shown to directly ameliorate inflammatory cytokine production in murine macrophages and glia [255,256]. This is further supported by studies demonstrating their therapeutic efficacy in murine models of disease [255,257,258]. Given the key role played by DC in shaping both innate and adaptive immune cell responses, it was of interest to determine if these effects translate to this vital immune cell population, which not only serves to present antigens during infection, but also plays a key role in determining pathogenic T cell responses during disease.

Unlike macrophages, which typically upregulate HO-1 in response to pro-inflammatory signals and cellular stress, HO-1 is constitutively expressed by immature DC both *in vitro* and *in vivo*, and is downregulated upon DC maturation [265,266]. Inhibition of HO-1 in DC reduces their phagocytic capacity, enhances their expression of co-stimulatory molecules, and increases their production of pro-inflammatory cytokines such as IL-12 and IL-23. This in turn results in polarisation of T cells towards inflammatory subsets e.g. Th1 and Th17 cells [191,265–269]. Conversely, HO-1 induction promotes tolerogenic DC by inhibiting pro-inflammatory functions and maintaining DC in an immature-like state, with a consequential reduction in effector T cell responses. This is often accompanied by an increase in regulatory T cell responses [265,266,268–270]. These observations are supported by multiple *in vivo* models of inflammatory or autoimmune disease, where upregulation of HO-1 in DC was responsible for the suppression of pro-inflammatory T cells, promotion of Treg cell differentiation, and amelioration of harmful inflammation [202,271–273]. Hence, the HO-1 system is of particular importance in DC, and given the central immunoregulatory role played by these cells in the generation of both innate and

adaptive immune responses, they represent an attractive target for the development of novel anti-inflammatory therapies.

In terms of new therapeutics, components of metabolic pathways are currently being explored since it was discovered that, not only do different immune cells engage different metabolic pathways, but that the activation/maturation state of immune cells is accompanied by metabolic switches. Generally it appears that when DC are activated, they ramp up glycolysis, which is a requirement for many of their effector functions, including upregulation of co-stimulatory markers and cytokine production [43,51,274]. When glycolysis is blocked, these processes are impaired, leading to an inability to activate T cells [43,51,274]. mTOR plays a central role in enhancing glycolysis and is activated in DC following inactivation of the mTOR inhibitor, AMPK [51,274]. Emerging evidence suggests that cross-talk between the HO-1 system and cellular metabolism may contribute to the regulation of immune cells by HO-1, while metabolic signalling has also been described to regulate HO-1 expression [104]. Many of the effects of HO-1 on cellular and systemic metabolism have been attributed to the activity of its reaction products [275]. For example, CO has been described to inhibit glycolysis and promote mitochondrial metabolism [275], and numerous similarities between the activities of CO and the anti-diabetic drug, metformin, have been observed in metabolic disease [276]. Meanwhile, Gilbert syndrome, which is characterised by hyper-bilirubinaemia, is believed to be protective against metabolic syndrome, diabetes and obesity [277,278]. Increased activation of AMPK has been reported in anti-inflammatory immune cells such as Tregs, alternatively activated/M2-like macrophages and tolerogenic DC [279–281], and signalling through AMPK can activate Nrf2 to upregulate HO-1 in multiple cell types [131–136]. In addition to controlling metabolic pathways, AMPK also plays a major role in the activation of autophagy, which is of particular importance in DC. For example, activation of autophagy results in a more tolerogenic DC phenotype [80]. Autophagy is also intrinsically linked to HO-1 induction via the autophagy-related protein, p62 [282–284]. Specifically, Nrf2 is activated upon release from KEAP1, which can occur when p62 sequesters KEAP1, targeting it for degradation and allowing Nrf2 to translocate to the nucleus [282–284].

In summary, DC are key cells which bridge the innate and adaptive immune system, and the expression of HO-1 in these cells promotes a more tolerogenic phenotype. Furthermore, the autophagy pathway and metabolic reprogramming play important roles in controlling the phenotype of human DC, and there is evidence to suggest that these pathways are inherently linked to HO-1 signalling. Ketoacids have been shown to induce HO-1 in murine macrophages and glia [256], however their effects on human DC, metabolic reprogramming, and autophagy have not yet been explored. Experiments were therefore designed to gain more insight into the mechanism of action of these novel HO-1 inducers which have potential therapeutic applications.

### 3.2 Aims

- To characterise the immunomodulatory properties of *T. brucei*-derived ketoacids in primary human DC.
- To investigate the effects of *T. brucei*-derived ketoacids on HO-1/Nrf2 signalling in primary human DC.
- To explore the effect of *T. brucei*-derived ketoacids on metabolic reprogramming and autophagy-related proteins in primary human DC.

## 3.3 Results

### 3.3.1 Assessment of HPP and IP endotoxin levels.

Given that DC are highly sensitive to LPS, it was imperative to carry out an endotoxin detection assay prior to conducting experiments in order to ensure that the prepared solutions of ketoacids were free from contaminating LPS. To test this, HEK-Blue™ hTLR4 reporter cells were incubated with HPP or IP (both 1000 µM) for 24 hours, or stimulated with increasing concentrations of LPS as a positive control. The concentration of ketoacids used in this study is based on the concentrations of ketoacids detected in the blood close to the peak of parasitaemia during trypanosomiasis, and has been used for *in vitro* assays in previously published studies [255,256,259,285]. The HEK-Blue™ hTLR4 cells have been engineered such that expression of secreted alkaline phosphatase (SEAP) is under control of the NF-κB and AP-1 promoters and indicates TLR4 activation. As expected, robust secretion of SEAP was observed following stimulation with LPS; however, neither HPP nor IP increased the production of SEAP from these cells (Figure 3.1). These results confirm that the prepared ketoacids were not contaminated with endotoxin and were suitable for use in follow-up experiments.

### 3.3.2 HPP and IP upregulate HO-1 and activate Nrf2 in BMDM.

It has recently been reported that *T. brucei*-derived ketoacids exhibit immunomodulatory effects in murine immune cells [255,257–259], while upregulation of the anti-inflammatory enzyme, HO-1, has been demonstrated in certain parasitic infections [286–288]. It was therefore hypothesised that the ketoacids may be upregulating HO-1 as a means of dampening host immune responses. In order to investigate this, BMDM were treated with IP, HPP and PP (all 1000 µM) for 24 hours and HO-1 expression was assessed by western blotting. Both IP and HPP were found to strongly upregulate HO-1 expression while PP had no effect (Figure 3.2A). It was next investigated if IP and HPP can activate the HO-1 transcriptional regulator, Nrf2. BMDM were treated with either IP or HPP (250-1000 µM) for 6 hours, and in both cases, an increase in Nrf2 expression was observed. This was particularly evident at the higher concentrations examined (Figure 3.2 B and C).

### *3.3.3 HPP and IP are non-toxic to primary human DC.*

Having confirmed that IP and HPP induced HO-1 in murine cells, it was of interest to investigate the potential anti-inflammatory effects of these compounds in human immune cells. Prior to conducting detailed experiments, viability assays were carried out to ensure the ketoacids are non-toxic in primary human immune cells at the proposed study doses. DC were treated with two concentrations (500  $\mu$ M and 1000  $\mu$ M) of HPP and IP for 24 hours. Cell viability was assessed by Annexin V/PI staining and LDH secretion. Both HPP and IP were found to be non-toxic to human DC, having no effect on cell viability at the concentrations tested (Figure 3.3 & Figure 3.4).

### *3.3.4 HPP and IP upregulate HO-1 in primary human DC.*

Having confirmed that IP and HPP are non-toxic in primary human DC, western blotting was carried out to determine if the ketoacids upregulate HO-1 at the protein level. Expression of the enzyme was examined at a range of IP and HPP concentrations (250–1000  $\mu$ M) and at different time-points (3, 6, and 24 hours). Immature DC constitutively expressed HO-1 in line with previous reports [266,269,289], however, treatment with either HPP or IP resulted in a trend towards increased expression of HO-1 at all concentrations tested with significance observed at 1000  $\mu$ M in each case (Figure 3.5). At this concentration, significant upregulation of HO-1 occurred within 3 hours of HPP treatment, while significant induction of HO-1 occurred following 24 hours treatment with IP (Figure 3.6).

### *3.3.5 HPP and IP activate Nrf2 in primary human DC.*

As outlined above, HPP and IP activate Nrf2 in murine immune cells, and this is the likely mechanism through which they upregulate HO-1. It was therefore of interest to investigate if the ketoacids have a similar mechanism of action in human DC. To test this, DC were treated with HPP or IP (both 1000  $\mu$ M) for 6 and 24 hours, and Nrf2 protein expression was measured by western blot. An increase in Nrf2 protein was observed in HPP-treated DC at 6 hours (Figure 3.7B), while IP-treated DC showed increased Nrf2 protein expression (and therefore accumulation) at 24 hours (Figure 3.7D). HPP and IP (1000  $\mu$ M) were also found

to upregulate mRNA expression of the additional Nrf2-regulated genes, NQO1 and GSR, further confirming their ability to activate this transcription factor (Figure 3.8).

### *3.3.6 HPP and IP upregulate HO-1 through Nrf2 activation in primary human DC.*

In order to confirm that the ketoacids are inducing HO-1 via Nrf2 activation, DC were treated with IP and HPP in the presence and absence of the Nrf2 inhibitor, ML385. DC were first treated with ML385 alone at the recommended dose (10  $\mu$ M) for 24 hours to ensure it is non-toxic at this concentration. Cell viability was assessed using FixVia efluor506 and it was confirmed that ML385 is non-toxic to DC under these conditions (Figure 3.9). DC were then pre-treated with ML385 for 1 hour prior to treatment with IP or HPP (both 1000  $\mu$ M) for 24 hours. HO-1 expression was examined by western blot and as before, IP and HPP treatment significantly upregulated HO-1 expression. However, pre-treatment with ML385 resulted in a significant decrease in the expression of HO-1 with both IP and HPP treatments, when compared to ketoacid treatment alone (Figure 3.10). These results confirm that ketoacid-induced HO-1 expression is regulated by Nrf2 in human DC.

### *3.3.7 HPP and IP increase the antioxidant capacity of primary human DC.*

Given that IP and HPP can induce the expression of antioxidant proteins, it was of interest to determine if the ketoacids can themselves function as antioxidants. To test this, the Antioxidant Assay Kit (Merck) was used to assess the antioxidant capacity of DC following treatment with HPP or IP. DC were treated for 1 hour with either HPP or IP (both 1000  $\mu$ M), or the known HO-1 inducers, carnosol or curcumin (both 10  $\mu$ M), and the antioxidant capacity of the cells was measured and expressed as equivalent Trolox concentrations. Both HPP and IP increased the total antioxidant capacity of DC after 1 hour of incubation with either compound (Figure 3.11). The ketoacids also appear to be more potent antioxidants than the established HO-1 inducers, carnosol and curcumin (Figure 3.11). Given that observed effects occurred within 1 hour of ketoacid treatment, these results indicate that IP and HPP may function themselves as antioxidants at early time-points, in addition to acting as inducers of Nrf-2-dependent genes.

### *3.3.8 IP, but not HPP, becomes fluorescent over time in culture media.*

During this study, it was noted that IP undergoes a colour change over time when incubated with/without cells in RPMI. It is likely that this is a result of IP converting to another form over time in aqueous solution, or switching between its keto and enol states [290,291]. It was therefore necessary to determine if IP becomes fluorescent over time as this would potentially effect fluorescence-based analysis including flow cytometry. In order to assess the endogenous fluorescence of IP, DC were cultured with IP (or HPP as a control) for 24 hours and left unstained, before examining by flow cytometry. The fluorescence of the samples were analysed in all 8 channels of the FACS Canto, and displayed as overlaid histograms to examine relevant fluorescence between samples (Figure 3.12). Unstained samples containing IP, but not HPP, exhibited increased fluorescence compared to untreated controls in all channels of the FACS Canto, with the highest fluorescence seen at the highest concentration examined i.e. 1000  $\mu$ M (Figure 3.12). This indicates IP becomes fluorescent over time, a finding that was taken into account when conducting further fluorescent based assays.

### *3.3.9 IP, but not HPP, induces ROS production in primary human DC.*

Antioxidant genes can be upregulated in cells in response to the production of potentially harmful ROS in the cell. Having demonstrated that both IP and HPP upregulate HO-1 and Nrf2 in human DC, it was of interest to determine if the ketoacids themselves can induce ROS production. To test this, DC were treated with IP or HPP (both 1000  $\mu$ M) over 24 hours and stained with CellRox, which becomes fluorescent upon oxidation by ROS. HPP treatment had no significant effect on the production of cellular ROS (Figure 3.13B), however, IP treatment significantly induced ROS production at 12 and 24 hours (Figure 3.13A). In order to confirm that the observed increase in ROS production is not an artefact of endogenous IP fluorescence, unstained controls were analysed alongside CellRox-stained samples. At all time-points tested, the CellRox-stained samples exhibited a higher fluorescence than unstained samples (Figure 3.14) which peaked at 12 hours and then began to decline. This indicates that the increase in fluorescence seen upon IP treatment is due to actual ROS production rather than IP autofluorescence.



### *3.3.10 HPP and IP activate the aryl hydrocarbon receptor in primary human DC.*

A study by Aoki *et al* which examined the therapeutic potential of HPP and IP in a colitis mouse model attributed their effects to activation of the AHR [258]. Furthermore, it was recently demonstrated that IP is capable of inhibiting prostaglandin production in an AHR dependent manner [259]. Experiments were therefore carried out to determine if IP and HPP are also capable of activating the AHR in human DC. CYP1A1 expression is upregulated by the AHR and its expression can be used as a readout of AHR activation. DC were treated with either IP or HPP (both 1000  $\mu$ M) for 6 or 24 hours, and expression of CYP1A1 was examined by qPCR. IP significantly increased CYP1A1 mRNA expression after 6 hours, while HPP treatment resulted in a trend towards increased mRNA expression ( $p = 0.05$ ) (Figure 3.15A). No significant upregulation was observed at the 24 hour time-point, despite IP treatment resulting in a mean relative CYP1A1 mRNA expression of over 3000 fold higher than untreated control cells (Figure 3.15B). While further analysis is required, these results indicate that IP (and possibly HPP) can activate the AHR in human DC.

### *3.3.11 LPS stimulation moderately reduces ketoacid-induced HO-1 expression in human DC.*

Immature DC constitutively express HO-1, and this is downregulated upon DC maturation [265,266]. As cells were to be stimulated/activated with LPS in subsequent experiments, it was necessary to ensure that HO-1 expression can still be induced by the ketoacids under these circumstances. To test this, DC were pre-treated with HPP or IP (both 1000  $\mu$ M) for 6 hours prior to stimulation with LPS (100 ng/ml) for 24 hours. As before, ketoacid treatment upregulated HO-1 expression, and while LPS stimulation resulted in reduced expression of HO-1 by the ketoacids, this was not significantly different when compared to ketoacid treatment alone (Figure 3.16).

### *3.3.12 HPP and IP reduce the production of pro-inflammatory cytokines in LPS-stimulated human DC.*

Our laboratory has recently demonstrated that HPP and IP are capable of reducing the production of pro-inflammatory cytokines in murine glia and macrophages [256]. Experiments were therefore carried out to determine if the ketoacids have immune modulating activity in human DC. To test this, DC were treated with either HPP or IP (500 and 1000  $\mu$ M) for 6 hours prior to stimulation with LPS (100 ng/ml) for 24 hours. Cytokine concentrations were measured in cell supernatants by ELISA. Both HPP and IP treatment dose-dependently reduced production of the pro-inflammatory cytokines TNF, IL-6, IL-12p70, and IL-23, and this effect was most potent at the 1000  $\mu$ M concentration (Figure 3.17 and 3.18). As well as driving the production of pro-inflammatory cytokines, LPS treatment over time is usually accompanied by production of the anti-inflammatory cytokine IL-10 as a means of regulating inflammatory responses. Interestingly, IP treatment resulted in a significant enhancement of IL-10, while HPP treatment showed a similar, albeit non-significant, trend (Figure 3.17E and 3.18E). These results suggest that both IP and HPP are capable of reducing the production of pro-inflammatory cytokines in LPS-stimulated DC, whilst also promoting a more anti-inflammatory phenotype.

### *3.3.13 HPP, but not IP, reduces pro-IL-1 $\beta$ expression in LPS-stimulated human DC.*

It has previously been reported that IP inhibits expression of the pro-inflammatory cytokine, pro-IL-1 $\beta$ , in murine BMDM via inhibition of the transcriptional regulator HIF-1 $\alpha$  [255]. To validate these findings, BMDM were treated with IP, HPP or PP (all 1000  $\mu$ M) for 30 minutes, prior to stimulation with LPS (100 ng/ml) for 24 hours, and pro-IL-1 $\beta$  expression was examined by western blotting. As expected, stimulation with LPS alone resulted in robust pro-IL-1 $\beta$  expression, however pre-treatment with either IP or HPP attenuated this effect. Conversely, pre-treatment with PP had no effect on LPS-induced pro-IL-1 $\beta$  (Figure 3.19B). This was next investigated in human DC. Cells were treated with either HPP or IP (both 1000  $\mu$ M) for 6 hours prior to stimulation with LPS (100 ng/ml) for 24 hours. Interestingly, cells pre-treated with HPP, but not IP, prior to stimulation with LPS showed a trend towards reduced expression of pro-IL-1 $\beta$  by western blot ( $p = 0.08$ ) (Figure

3.19D). The results indicate that the ketoacids may exert cell type or species-specific effects.

#### *3.3.14 HPP treatment inhibits the maturation of LPS-stimulated human DC.*

As mentioned previously, HO-1 induction maintains DC in a more immature phenotype [292]. In order to determine if the ketoacids impact DC maturation, human DC were treated with HPP (1000  $\mu$ M) for 6 hours prior to stimulation with LPS (100 ng/ml) for 24 hours. Surface expression of maturation and co-stimulatory markers (CD40, CD80, CD83 and CD86) were measured by flow cytometry. Due to the fluorescent nature of IP it was unsuitable for this flow cytometric analysis and hence was not included in these experiments. As expected, the expression of co-stimulatory markers was increased in LPS-stimulated DC. The average Median Fluorescent Intensity (MFI) of these cells was set to 100% and used as a control for comparison to the HPP-treated cells. There was a significant decrease in MFI at both HPP concentrations when compared to the LPS-stimulated control (Figure 3.20). Immature DC also have increased phagocytic capacity when compared to mature DC, as their main role is scavenging for antigen [8]. Therefore, it was hypothesised that the ketoacid-treated DC would have increased phagocytic capacity compared to stimulated, mature DC. To test this, DC were treated as above, and the phagocytic capacity of the cells was measured upon incubation with FITC-conjugated DQ-Ovalbumin (DQ-Ova; 500 ng/mL). Uptake of this model antigen was assessed by flow cytometry. Compared to untreated cells, the ability of LPS-treated DC to phagocytose DQ-OVA was significantly impaired, signifying a heightened maturation status, however, pre-incubation with HPP prior to LPS treatment attenuated this effect and maintained the DC in an immature state (Figure 3.21).

#### *3.3.15 LPS stimulation upregulates glycolysis and oxidative phosphorylation in human DC.*

Metabolic reprogramming has been observed in immune cells and numerous recent studies have demonstrated that their activation/maturation is accompanied by a metabolic switch favouring glycolysis over oxidative phosphorylation [43]. LPS itself is known to induce metabolic reprogramming in DC by enhancing their use of the glycolytic pathway

[134]. Prior to examining the effects of HO-1 on LPS-induced metabolic changes, DC were stimulated over time with LPS to determine the optimal time-point for experimental analysis. DC were stimulated with LPS (100 ng/ml) for 6, 12 or 24 hours and analysed in a Seahorse XFe96 analyser following the addition of oligomycin (1 mM); an inhibitor of mitochondrial complex V, FCCP (1 mM); a mitochondrial uncoupler, rotenone (500 nM) and antimycin A (500 nM); which are inhibitors of the mitochondrial complexes I & III, respectively, and 2-DG (25 mM); an inhibitor of glycolysis. The metabolic activity of the cells was then determined by measuring the ECAR, which is a measure of glycolysis, and the OCR, which is a measure of oxidative phosphorylation. LPS stimulation resulted in a trend towards an increase in basal and max glycolysis at 6 and 12 hours, with a return to baseline at 24 hours (Figure 3.22 B and C). There was no observed change in the glycolytic reserve at either 6 or 12 hours, while there was a trend towards a reduction below baseline levels after 24 hours (Figure 3.22D). There was also a trend towards an increase in the basal respiration, max respiration and respiratory reserve at 6 and 12 hours (Figure 3.23). At all time-points tested, there was a trend towards an increase in the ECAR:OCR ratio when compared to untreated control, with the greatest increase seen after 12 hours LPS stimulation (Figure 3.24). Based on these results, the 12 hour time-point was chosen for subsequent studies examining LPS-induced changes in the metabolic profile of these cells.

### *3.3.16 IP and HPP downregulate glycolysis in LPS-stimulated human DC.*

In order to determine if *T. brucei*-derived ketoacids have an effect on LPS-induced metabolic reprogramming, DC were pre-treated with IP or HPP (both 1000  $\mu$ M) for 6 hours prior to stimulation with LPS (100 ng/ml) for 12 hours. These cells were then analysed in a Seahorse XFe96 analyser following the addition of oligomycin, FCCP, rotenone and antimycin A, and 2-DG, as before. ECAR and OCR measurements were then taken over time. IP- and HPP-treated DC showed no change in basal glycolysis when compared to LPS stimulation alone (Figure 3.25B). LPS-treated cells showed a trend towards increased max glycolysis ( $p = 0.06$ ), and this was significantly decreased in the presence of either HPP or IP (Figure 3.25C). Both IP and HPP were also capable of significantly decreasing the glycolytic reserve in LPS-stimulated cells (Figure 3.25D). There were no significant changes in the basal respiration (Figure 3.26B), max respiration (Figure 3.26C), and respiratory

reserve (Figure 3.26D) in IP- or HPP-treated DC when compared to LPS stimulation alone, suggesting that they have no impact on oxidative phosphorylation. Similarly IP and HPP treatment had no effect on the ECAR:OCR ratio compared to LPS stimulation alone (Figure 3.27). Interestingly, DC treated with IP or HPP derive their ATP primarily from oxidative phosphorylation (Figure 3.28). Furthermore, IP treated DC show a trend towards a reduction in the percentage of ATP derived from glycolysis when compared to the LPS stimulation alone (Figure 3.28).

### *3.3.17 HPP favours engagement of oxidative phosphorylation over glycolysis in human DC.*

The effects of HPP treatment on the metabolism of DC was further investigated using Fluorescence lifetime imaging microscopy (FLIM), which measures the intracellular levels of bound and free NADH (IP was excluded from this analysis due to autofluorescence issues). Bound NADH, which is associated with oxidative phosphorylation, or free NADH, which is associated with glycolysis, can be distinguished based on their distinct lifetimes upon fluorescence excitation. The ratio of bound to free NADH can be used to measure whether a cell is favouring the engagement of glycolysis (characterised by a decrease in the ratio due to increased free NADH) or oxidative phosphorylation (characterised by an increase in the ratio due to increased bound NADH). DC were treated with HPP (1000  $\mu$ M) for 6 hours prior to stimulation with LPS (100 ng/ml) for 12 hours, and analysed by FLIM. Similar to the Seahorse results reported above, LPS-stimulated DC ramped up glycolysis, as represented by a decrease in the  $\tau$  average (see section 2.2.15 for detailed explanation regarding calculation of this value) compared to untreated DC (Figure 3.29). In contrast, cells pre-treated with HPP exhibited a significant increase in the  $\tau$  average compared to the LPS-stimulated controls, indicating they are favouring oxidative phosphorylation to generate their energy (Figure 3.29).

### *3.3.18 IP and HPP reduce the expression of HK2 in LPS-stimulated human DC.*

Given the results indicating that the ketoacids may be downregulating glycolysis and favouring oxidative phosphorylation in human DC, it was of interest to determine what factors may be contributing to this shift in the metabolic profile in the cells. HK2 is the rate

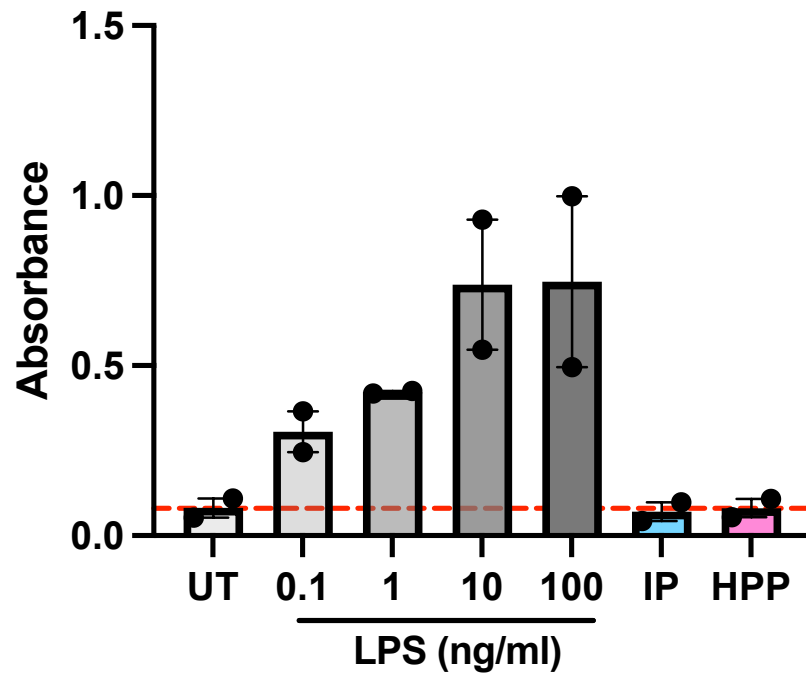
limiting enzyme in the glycolytic pathway and is known to be upregulated by LPS. Expression of this enzyme was therefore assessed in LPS-stimulated cells in the presence and absence of the ketoacids. DC were treated with IP or HPP (both 1000  $\mu$ M) for 6 hours prior to stimulation with LPS (100 ng/ml) for 12 hours. As expected, LPS stimulation induced the upregulation of HK2 in DC (Figure 3.30). However, there was significantly reduced expression of the enzyme in IP-treated DC, and a trend towards reduced expression (albeit not significant) in HPP-treated DC when compared to LPS-stimulation alone ( $p = 0.09$ ) (Figure 3.30). This indicates that the ketoacids (in particular IP) can block upregulation of this enzyme in LPS-stimulated DC, and this in turn can impact on the cell's ability to utilise glycolysis.

### *3.3.19 IP and HPP reduce phosphorylation of the mTOR substrate, S6, while increasing phosphorylation of AMPK in human DC.*

mTOR, the major promoter of anabolic metabolism, is activated in response to LPS stimulation [55,293,294]. S6 is a protein which is phosphorylated by mTOR and is commonly used as a readout for mTOR activation. In order to determine if the ketoacids have any impact on mTOR activation, DC were pre-treated with IP or HPP (both 1000  $\mu$ M) for 15 minutes prior to stimulation with LPS (100 ng/ml) for 1 hour, and phosphorylation of S6 was examined by western blot. IP and HPP treatment showed a trend towards a reduction in the phosphorylation of S6 compared to LPS stimulation alone (Figure 3.31). mTOR can be inhibited by AMPK, the cellular energy sensor and master regulator of catabolic metabolism. In order to determine if the ketoacids have any impact on AMPK activation, DC were treated with IP or HPP (both 1000  $\mu$ M) for 15 minutes and phosphorylation (and therefore activation) of AMPK was assessed by western blotting. IP treatment resulted in a significant increase in AMPK phosphorylation while HPP treatment also trended towards an increase, which was approaching significance with a  $p$  value of 0.06 (Figure 3.32). This indicates the ketoacids are activating AMPK, which may be responsible for the inhibition of mTOR, and may also contribute to the subsequent modulation of DC metabolism.

### *3.3.20 IP and HPP activate autophagy-related proteins in human DC.*

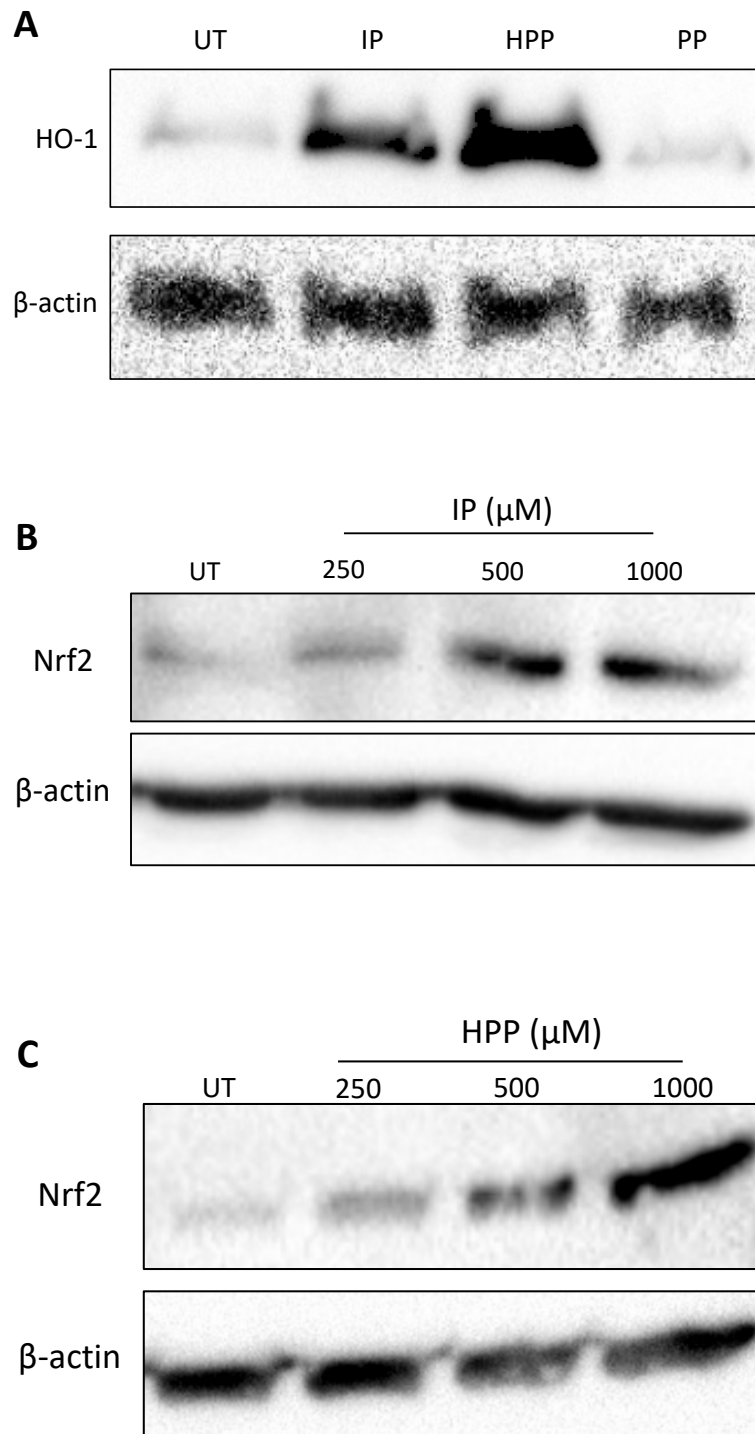
AMPK is not only important for cellular metabolism, but is also a key protein controlling autophagy in cells. Indeed, activation of AMPK is one of the initiating steps in the autophagy pathway [74,75]. As the ketoacids are capable of activating AMPK, it was of interest to investigate if they had any effect on other autophagy-related proteins in DC. To examine this, DC were treated with IP or HPP (both 1000  $\mu$ M) for 6, 12 or 24 hours and expression of the autophagy-related proteins, p62 and LC3, were examined by western blotting. IP treatment upregulated both p62 and LC3-II expression over time (LC3-I is converted to LC3-II during autophagy), and this was most potent after 24 hours (Figure 3.33D & 3.34D). HPP treatment significantly increased p62 expression after 6 hours and significantly increased LC3-II expression after 24 hours (Figure 3.33B & 3.34D). These results indicate both ketoacids are activating autophagy-related proteins in human DC. This may also have implications for Nrf2 activation given that p62 can sequester the Nrf2 inhibitor, KEAP1.



**Figure 3.1 Assessment of HPP and IP endotoxin levels.**

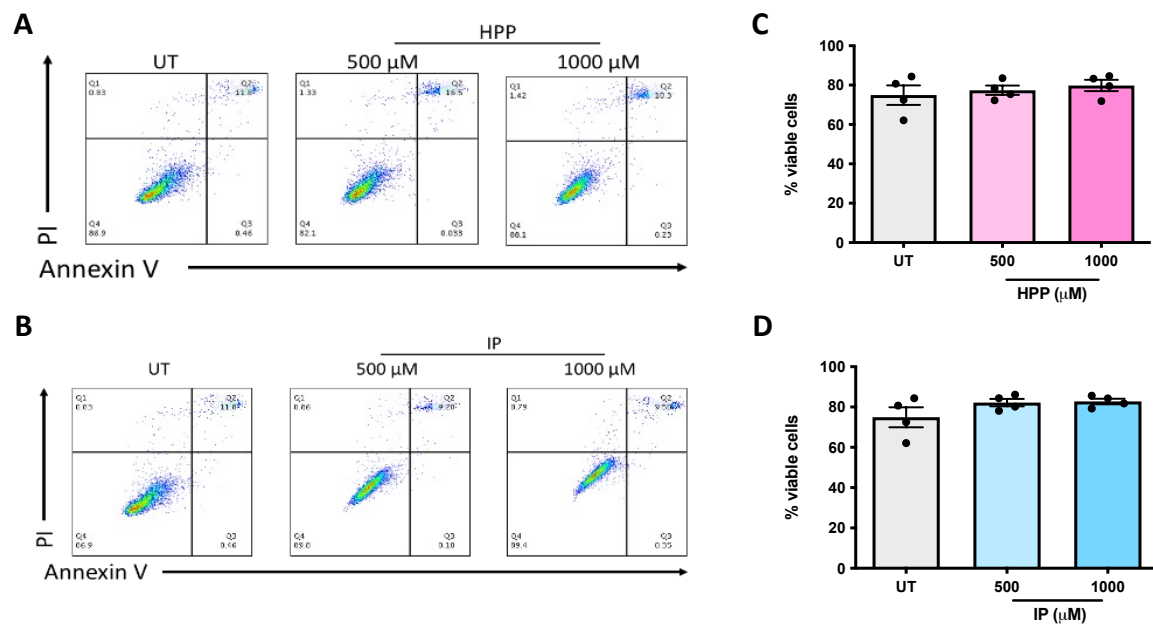
HEK-blue cells expressing TLR4 were left untreated (UT), stimulated with LPS (0.1–100 ng/ml; positive control), or incubated with HPP or IP (both 1000  $\mu$ M) for 24 hours. The expression of SEAP which is under the control of NF- $\kappa$ B and AP-1 was tested by incubating cell supernatants with HEK-blue detection medium for 30 minutes at 37  $^{\circ}$ C and absorbance was read at 650 nm. Pooled data showing the mean ( $\pm$  SEM) absorbance readings from two independent experiments.





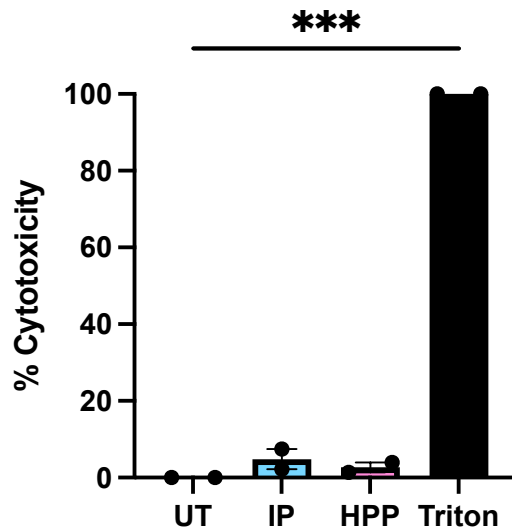
**Figure 3.2 HPP and IP upregulate HO-1 and stabilise Nrf2 in BMDM.**

**(A)** BMDM were left untreated (UT) or incubated with IP, HPP or PP (1000  $\mu$ M) for 24 hours. HO-1 expression was detected by western blot. BMDM were left UT or incubated with **(B)** IP or **(C)** HPP (250-1000  $\mu$ M) for 24 hours. Nrf2 expression was detected by western blot. Blots are representative of 2 individual experiments.



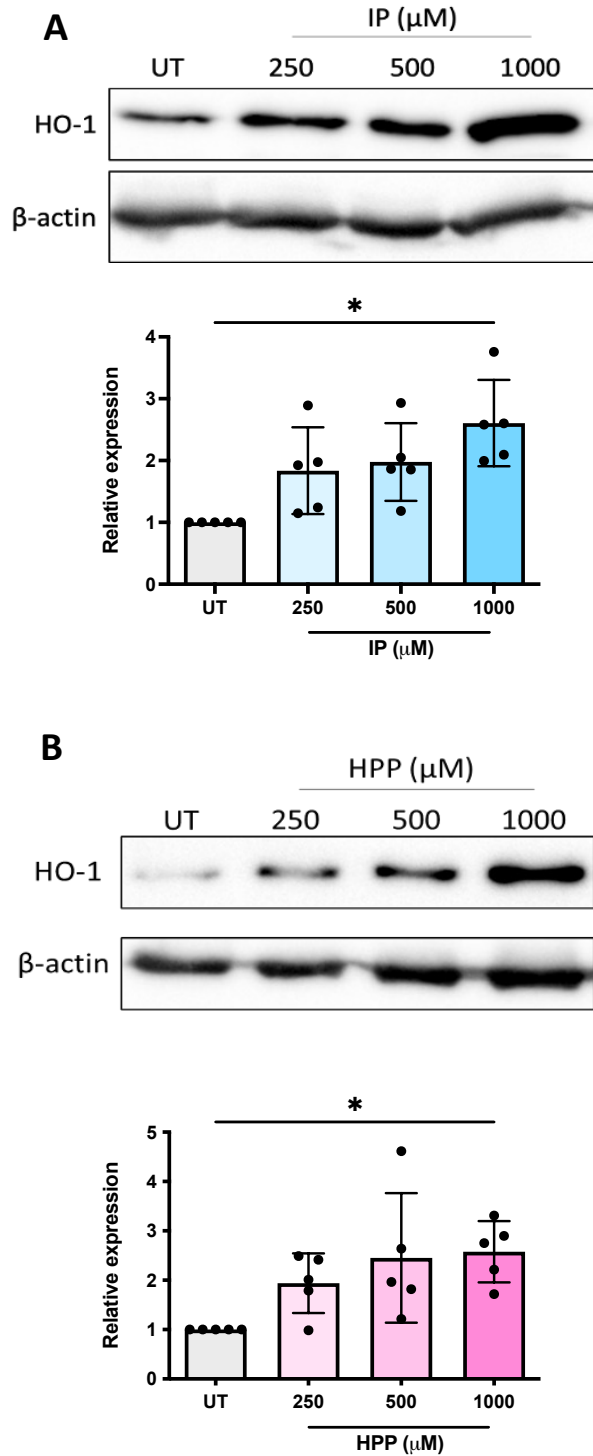
**Figure 3.3 HPP and IP are non-toxic to primary human DC.**

Primary human DC were left untreated (UT) or incubated with **(A & C)** HPP or **(B & D)** IP (both 500-1000  $\mu$ M) for 24 hours. Cells were stained for Annexin V and PI uptake, as indicators of apoptosis/necrosis, and analysed by flow cytometry. Debris was excluded by gating, and viable cells were defined as Annexin V<sup>-</sup> PI<sup>-</sup> (non-apoptotic/necrotic cells). **(A & B)** Dot plots depicting Annexin V and PI expression from one representative experiment. **(C & D)** Pooled data showing the mean ( $\pm$  SEM) of Annexin V<sup>-</sup> PI<sup>-</sup> cells as a percentage from 4 healthy donors.



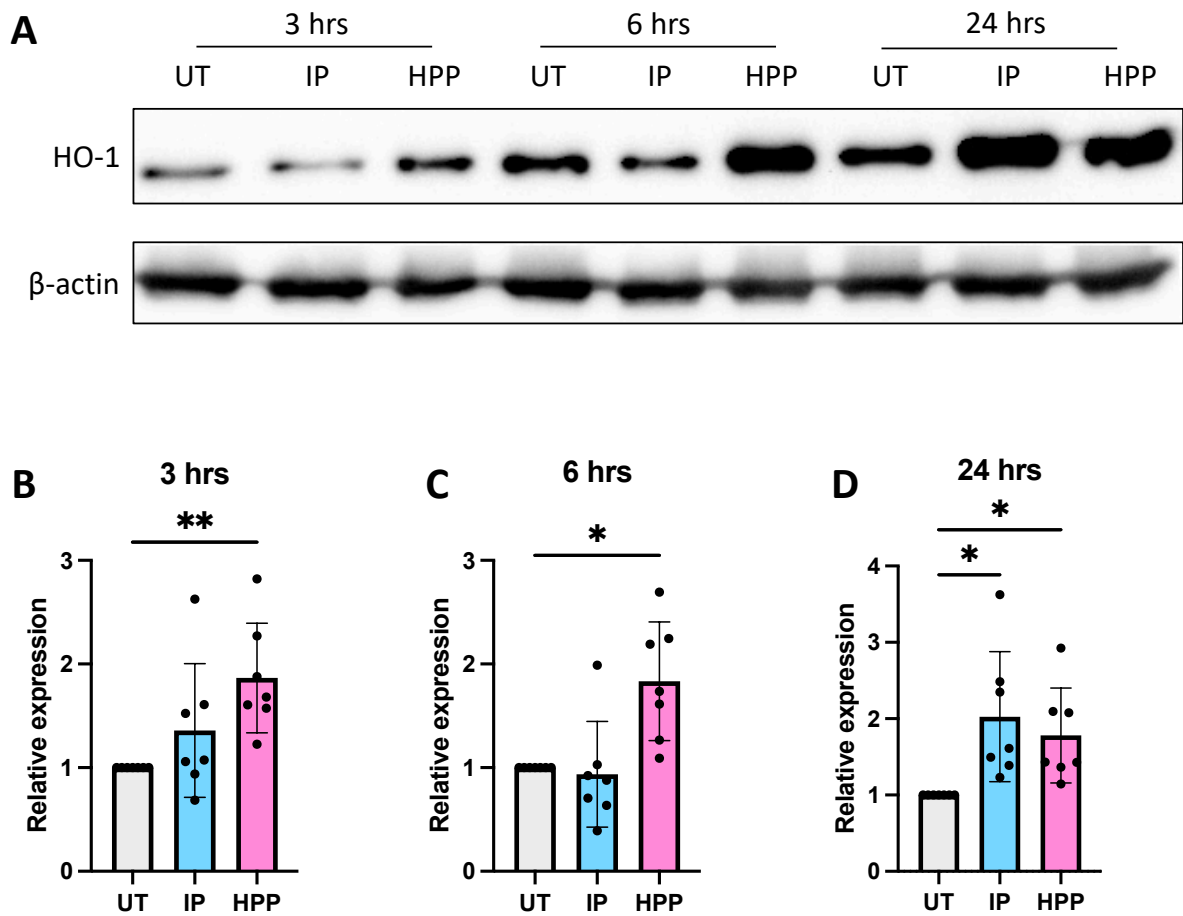
**Figure 3.4 HPP and IP are non-toxic to primary human DC.**

Primary human DC were left untreated (UT) or incubated with HPP or IP (1000  $\mu$ M) for 24 hours, or Triton X-100 for 1 hour. Supernatants were removed and analysed for LDH expression. Pooled data showing the mean ( $\pm$  SEM) % cytotoxicity from 2 healthy donors. Repeated measures one-way ANOVA, with Dunnett's multiple comparisons post hoc test, was used to determine statistical significance by comparing means of treatment groups against the mean of the control group (\*\*\*)  $p < 0.001$ ).



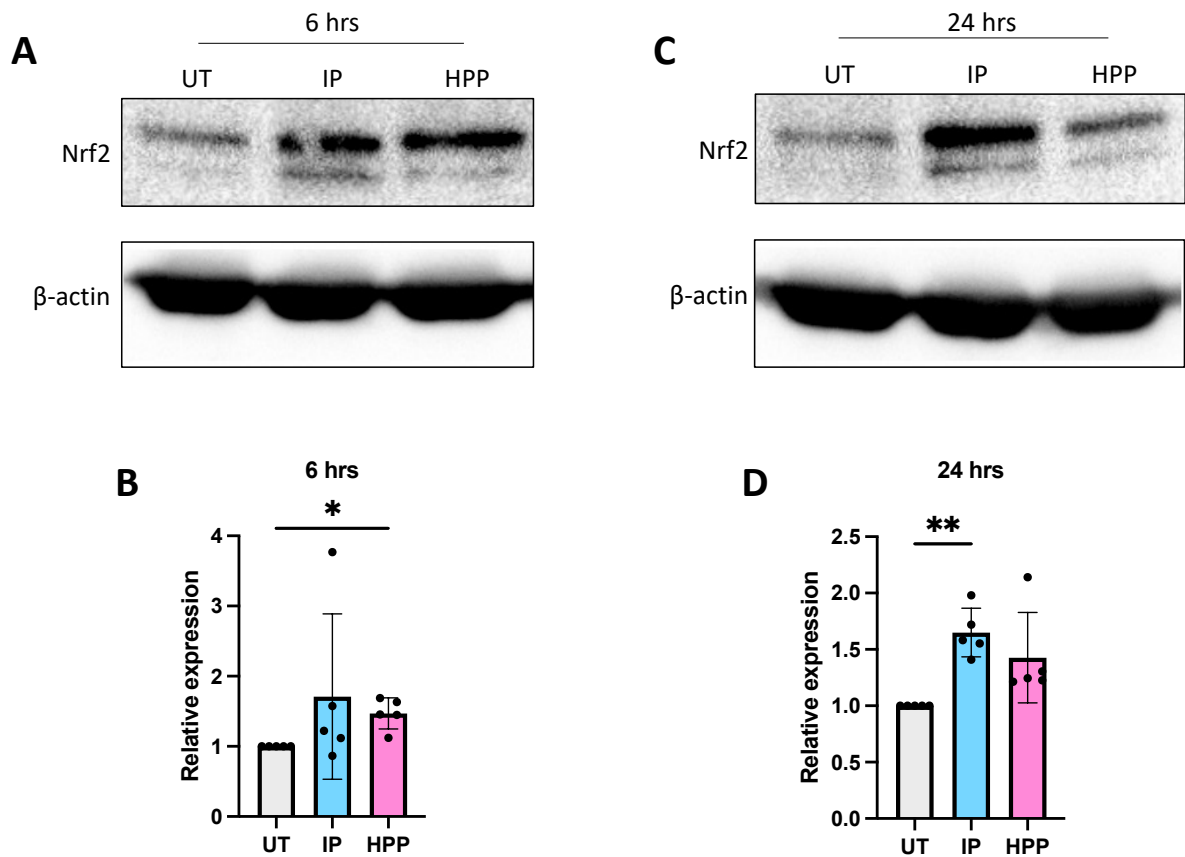
**Figure 3.5 HPP and IP upregulate HO-1 in a concentration dependent manner in primary human DC.**

Primary human DC were left untreated (UT) or incubated with **(A)** IP or **(B)** HPP (250-1000  $\mu\text{M}$ ) for 24 hours. HO-1 expression was detected by western blot. Densitometry results shown are mean  $\pm$  SEM of the relative expression of HO-1:  $\beta$ -actin from 5 healthy donors. Repeated measures one-way ANOVA, with Dunnett's multiple comparisons post hoc test, was used to determine statistical significance by comparing means of treatment groups against the mean of the control group (\* $p < 0.05$ ). ImageLab (Bio-Rad) software was used to perform densitometric analysis.



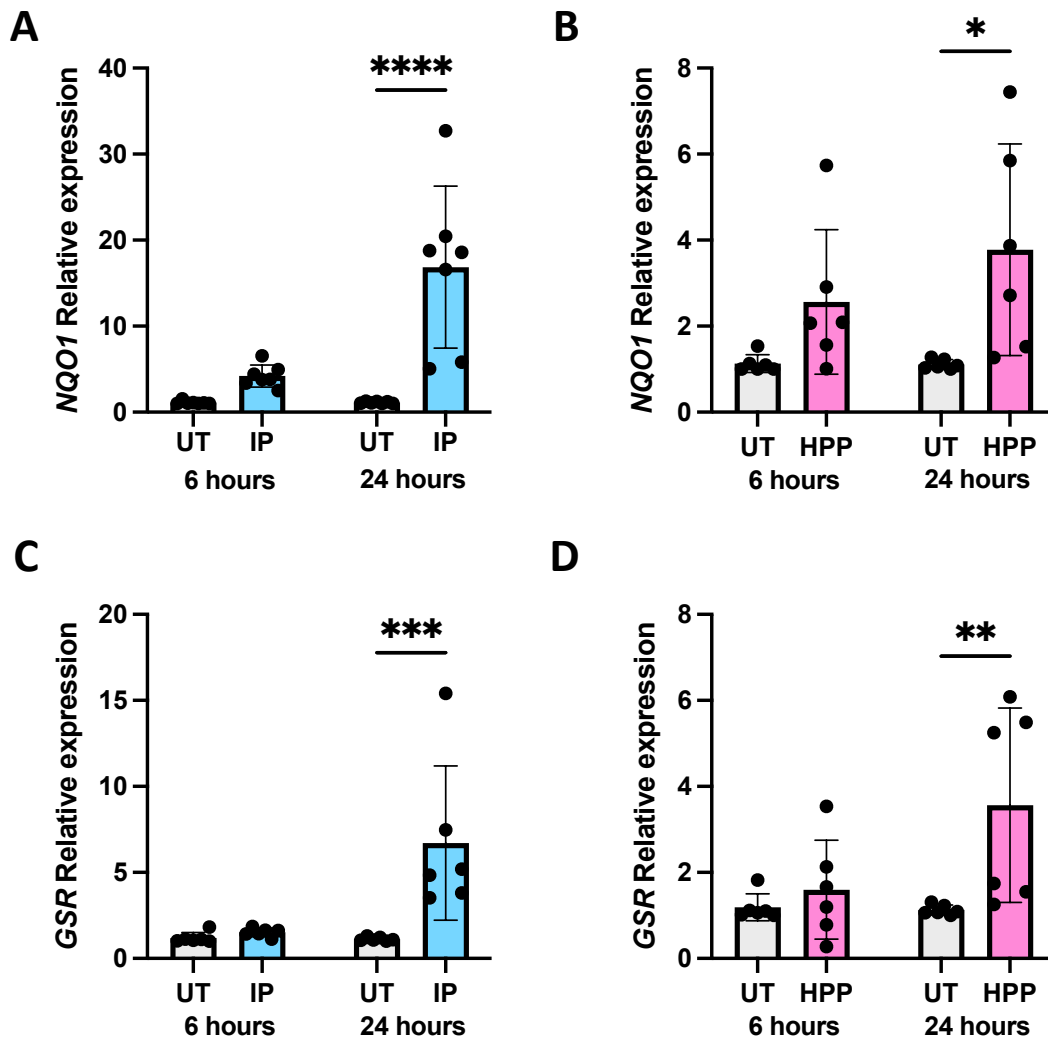
**Figure 3.6 HPP and IP upregulate HO-1 over time in primary human DC.**

Primary human DC were left untreated (UT) or incubated with HPP or IP at 1000  $\mu$ M for 3, 6 or 24 hours. **(A)** HO-1 expression was detected by western blot. **(B, C & D)** Densitometry results shown are mean  $\pm$  SEM of the relative expression of HO-1:  $\beta$ -actin from 7 healthy donors. Repeated measures one-way ANOVA, with Dunnett's multiple comparisons post hoc test, was used to determine statistical significance by comparing means of treatment groups against the mean of the control group (\*\*  $p < 0.01$ , \*  $p < 0.05$ ). ImageLab (Bio-Rad) software was used to perform densitometric analysis.

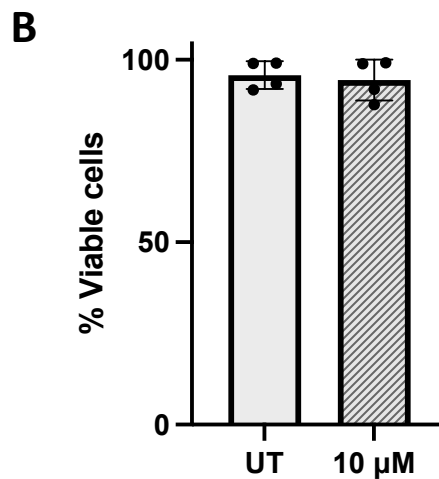
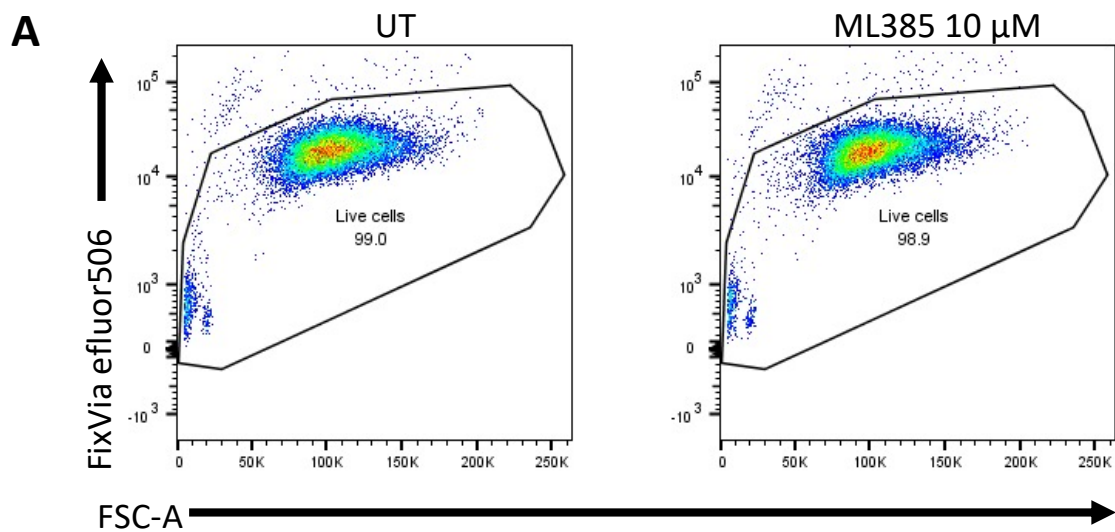


**Figure 3.7 HPP and IP activate Nrf2 in human DC.**

Primary human DC were left untreated (UT) or incubated with HPP or IP at 1000  $\mu$ M for 6 (**A & B**) or 24 hours (**C & D**). Nrf2 expression was measured by western blot. Densitometry results shown are mean  $\pm$  SEM of the relative expression of Nrf2:  $\beta$ -actin from 5 healthy donors. Repeated measures one-way ANOVA, with Dunnett's multiple comparisons post hoc test, was used to determine statistical significance by comparing means of treatment groups against the mean of the control group (\*\*  $p < 0.01$ , \*  $p < 0.05$ ). ImageLab (Bio-Rad) software was used to perform densitometric analysis.



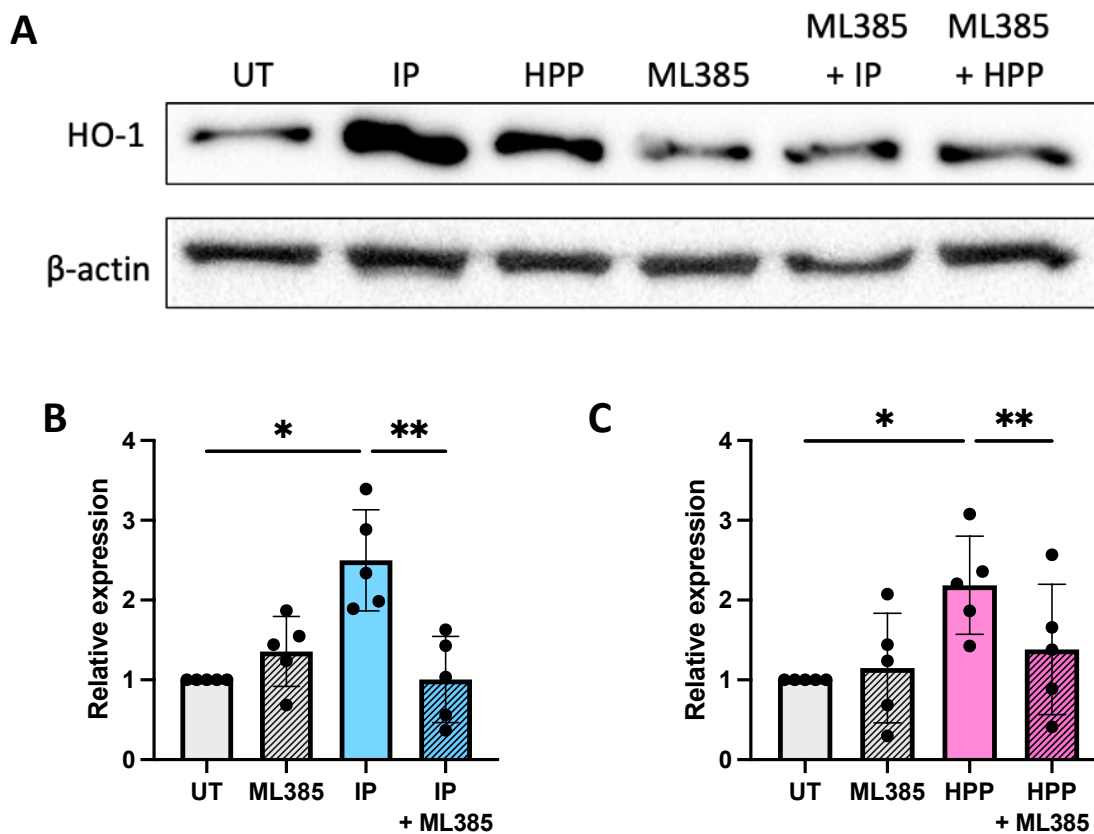
**Figure 3.8 IP and HPP upregulate additional Nrf2-controlled genes in human DC.** Primary human DC were left untreated (UT) or incubated with IP (A & C) or HPP (B & D) at 1000  $\mu$ M for 6 or 24 hours. mRNA expression of the Nrf2-dependent genes NQO-1 (A & B) and GSR (C & D) were measured by RT-PCR. Results show mean ( $\pm$ SEM) for 6 healthy donors. Two-way ANOVA, with Šídák's multiple comparisons post hoc test, was used to determine statistical significance (\*\*\*\*  $p < 0.0001$ , \*\*\*  $p < 0.001$ , \*\*  $p < 0.01$ , \*  $p < 0.05$ ).



**Figure 3.9 The Nrf2 inhibitor, ML385, is non-toxic to human DC.**

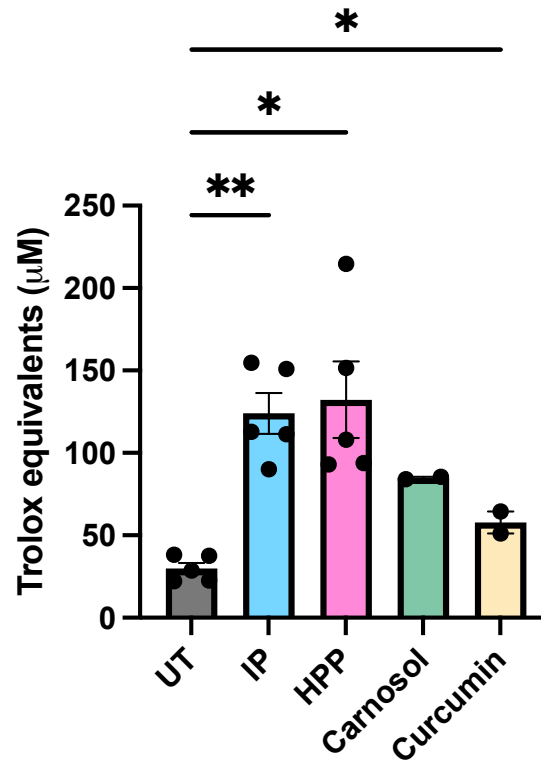
Primary human DC were left untreated (UT) or incubated with ML385 (10  $\mu$ M) for 24 hours. Cells were stained for viability using FixVia efluor506. Debris was excluded by gating, and viable cells were defined as FixVia efluor506<sup>-</sup>. **(A)** Dot plots depicting FixVia efluor506 expression from one representative experiment. **(B)** Pooled data showing the mean ( $\pm$  SEM) of viable cells as a percentage from 4 healthy donors.





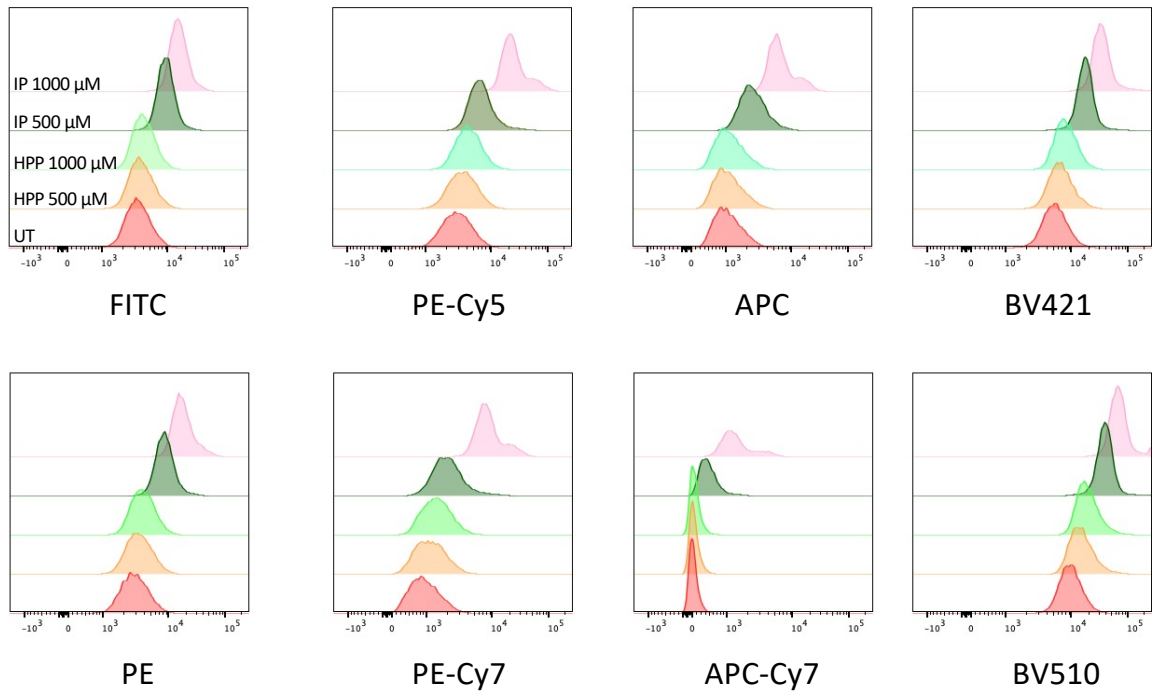
**Figure 3.10 HPP and IP induce HO-1 through Nrf2 activation in human DC.**

Primary human DC were pre-treated either with or without the Nrf2 inhibitor ML385 (10  $\mu$ M) for 1 hour, prior to incubation with **(B)** IP or **(C)** HPP at 1000  $\mu$ M for 24 hours. **(A)** HO-1 expression was measured by western blot. **(B & C)** Densitometry results shown are mean  $\pm$  SEM of the relative expression of HO-1:  $\beta$ -actin from 5 healthy donors. Repeated measures one-way ANOVA, with Šídák's multiple comparisons post hoc test, was used to determine statistical significance by comparing means of pre-selected pairs (\*\*  $p < 0.01$ , \* $p < 0.05$ ).



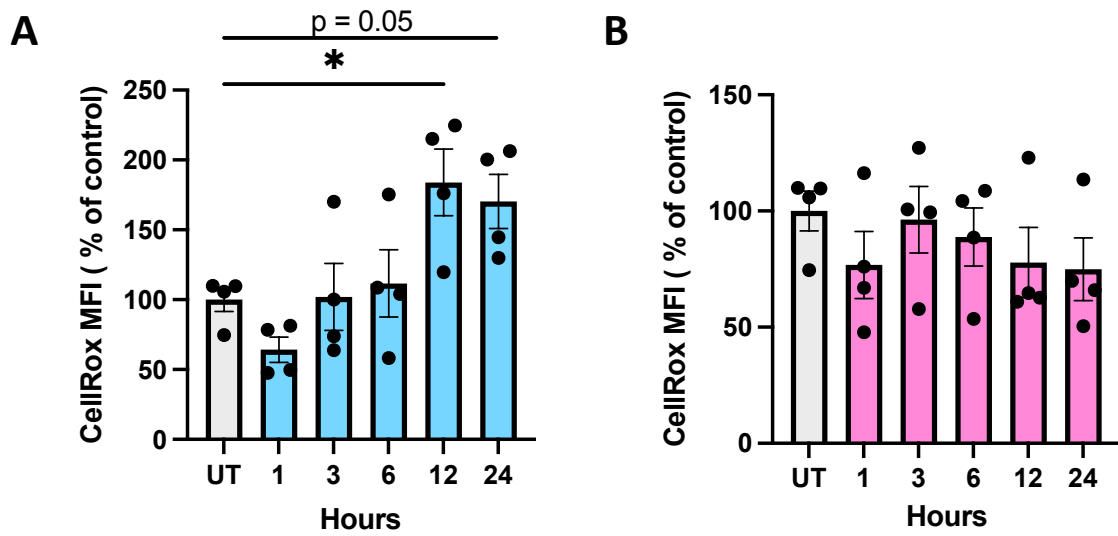
**Figure 3.11 IP and HPP increase the antioxidant capacity of human DC.**

Primary human DC were left untreated (UT) or incubated with HPP or IP (both 1000 µM), or carnosol or curcumin (both 10 µM) for 1 hour. Total antioxidant capacity of the cells was determined and expressed as equivalent concentration of Trolox (µM). Pooled data showing the mean (± SEM) from 5 healthy donors. Repeated measures one-way ANOVA, with Dunnett's multiple comparisons post hoc test, was used to determine statistical significance by comparing means of treatment groups against the mean of the control group (\*\* p < 0.01, \*p < 0.05).



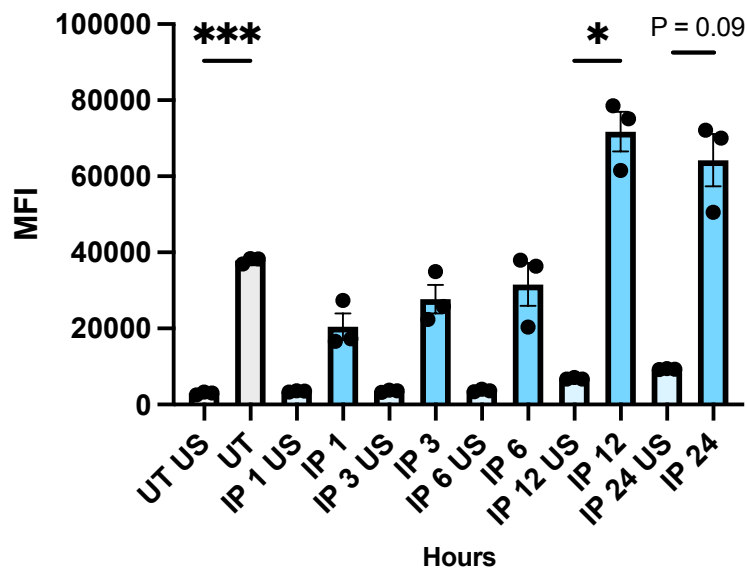
**Figure 3.12 IP, but not HPP, treatment causes autofluorescence in human DC after 24 hours.**

Primary human DC were left untreated (UT) or incubated with HPP or IP (1000  $\mu\text{M}$ ) for 24 hours. Samples were analysed on all channels of a BD FACS Canto II without staining. Histograms showing fluorescence of samples compared to untreated control.



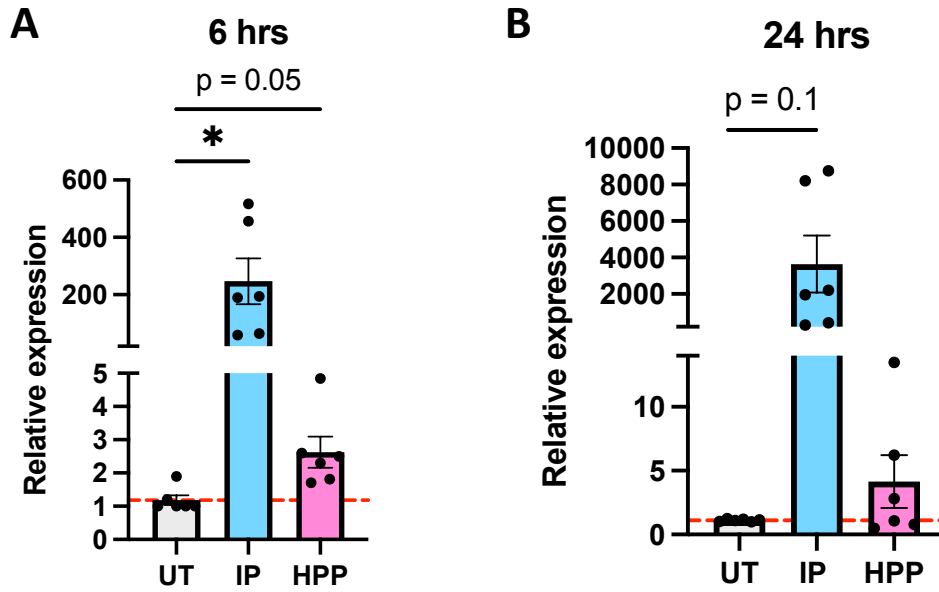
**Figure 3.13 IP, but not HPP, induces ROS production in human DC.**

Primary human DC were left untreated (UT) or incubated with **(A)** IP or **(B)** HPP (both 1000  $\mu$ M) for 1, 3, 6, 12 or 24 hours. Cells were stained with CellRox to examine ROS production and analysed by flow cytometry. Pooled data showing the mean ( $\pm$  SEM) MFI expressed as a percentage of control, from 4 healthy donors. Repeated measures one-way ANOVA, with Dunnett's multiple comparisons post hoc test, was used to determine statistical significance by comparing means of treatment groups against the mean of the control group (\* $p < 0.05$ ).



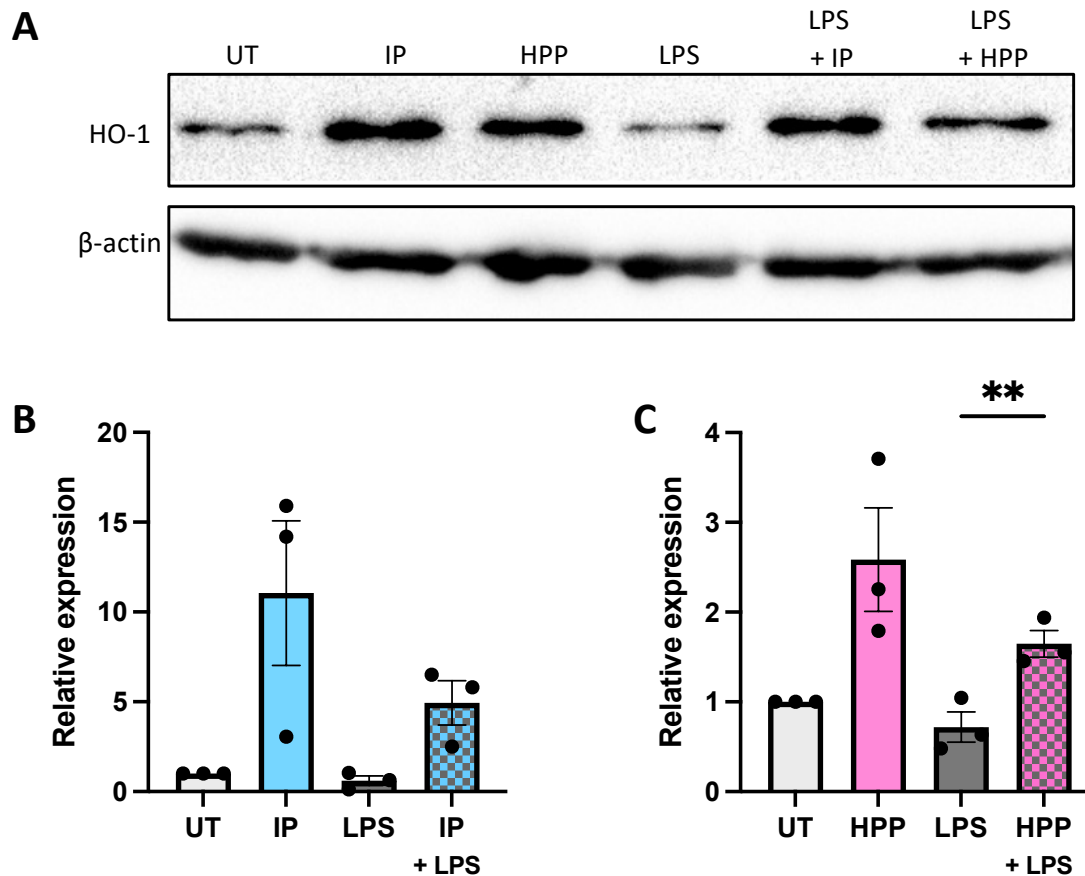
**Figure 3.14 The increase in ROS production upon IP treatment is not due to autofluorescence.**

Primary human DC were left untreated (UT) or incubated with IP (1000  $\mu$ M) for 1, 3, 6, 12 or 24 hours. Cells were either stained with CellRox or left unstained, and analysed by flow cytometry. Pooled data showing the mean ( $\pm$  SEM) MFI from 3 healthy donors. Repeated measures one-way ANOVA, with Šídák's multiple comparisons post hoc test, was used to determine statistical significance by comparing means of pre-selected pairs (\*\*\*)  $p < 0.001$ , \* $p < 0.05$ ).



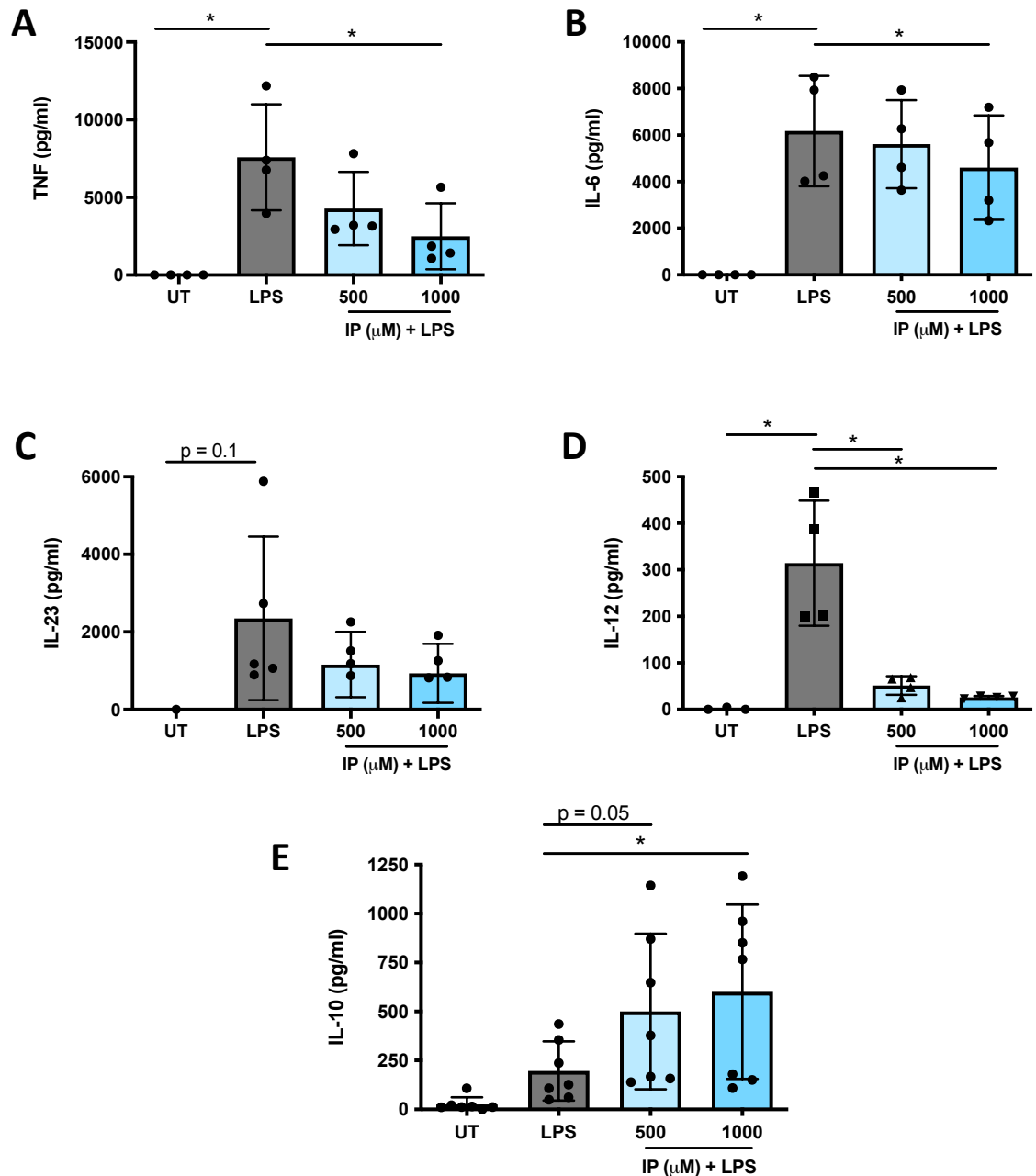
**Figure 3.15 IP and HPP upregulate CYP1A1 in human DC.**

Primary human DC were left untreated (UT) or incubated with IP or HPP at 1000  $\mu$ M for **(A)** 6 or **(B)** 24 hours. mRNA expression of CYP1A1 was measured by RT-PCR. Results show mean ( $\pm$ SEM) for 6 healthy donors. Repeated measures one-way ANOVA, with Dunnett's multiple comparisons post hoc test, was used to determine statistical significance by comparing means of treatment groups against the mean of the control group (\* $p < 0.05$ ).



**Figure 3.16 LPS stimulation moderately reduces ketoacid-induced HO-1 expression in human DC.**

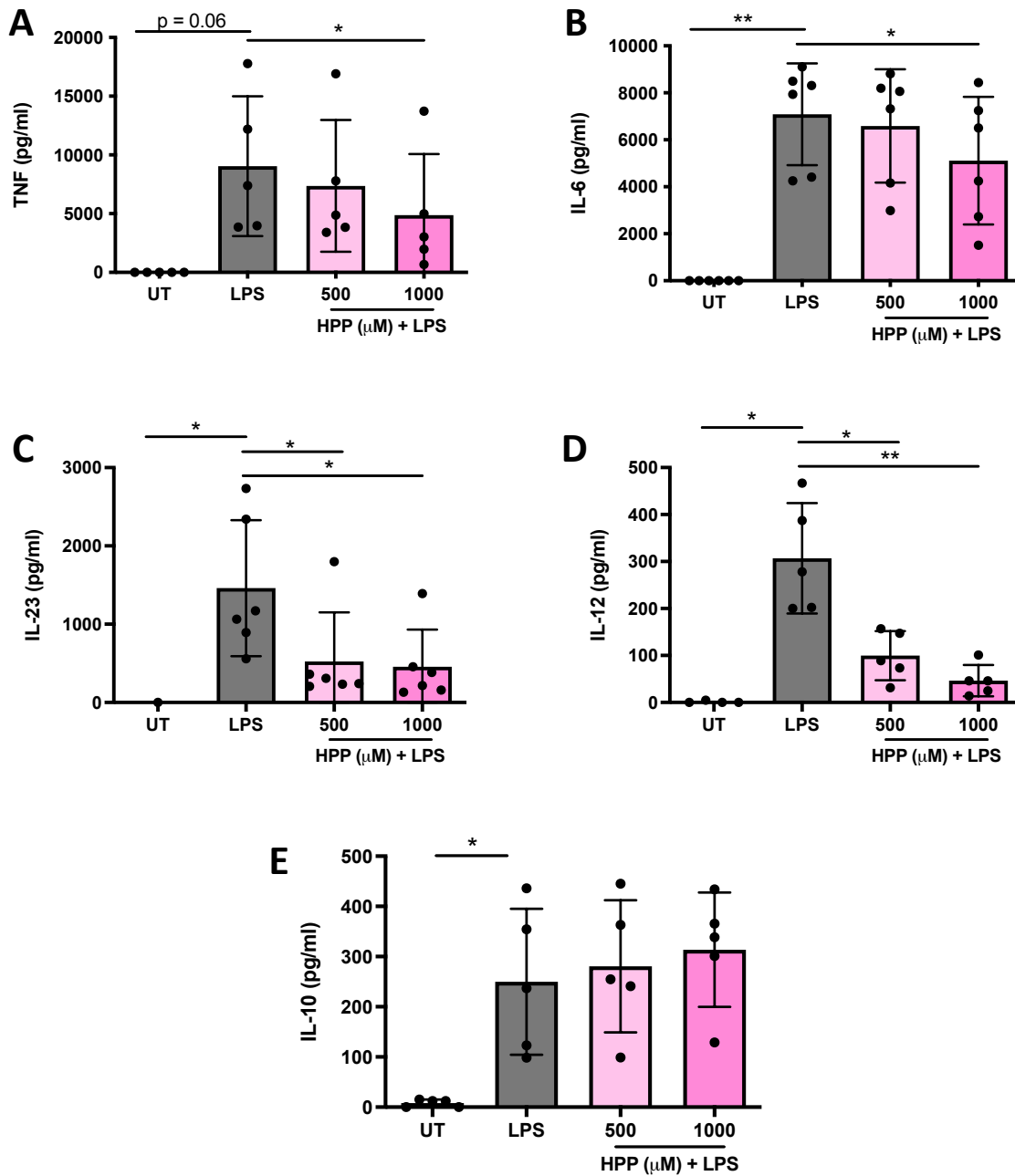
Primary human DC were left untreated (UT) or incubated with IP (1000  $\mu$ M) for 6 hours prior to stimulation with LPS (100 ng/ml) for 24 hours. **(A)** HO-1 expression was detected by western blot. **(B & C)** Densitometry results shown are mean  $\pm$  SEM of the relative expression of HO-1:  $\beta$ -actin from 5 healthy donors. ImageLab (Bio-Rad) software was used to perform densitometric analysis. Repeated measures one-way ANOVA, with Šídák's multiple comparisons post hoc test, was used to determine statistical significance by comparing means of pre-selected pairs (\*\*  $p < 0.01$ ).



**Figure 3.17 IP reduces the production of pro-inflammatory cytokines, and increases IL-10 production, in LPS-stimulated human DC.**

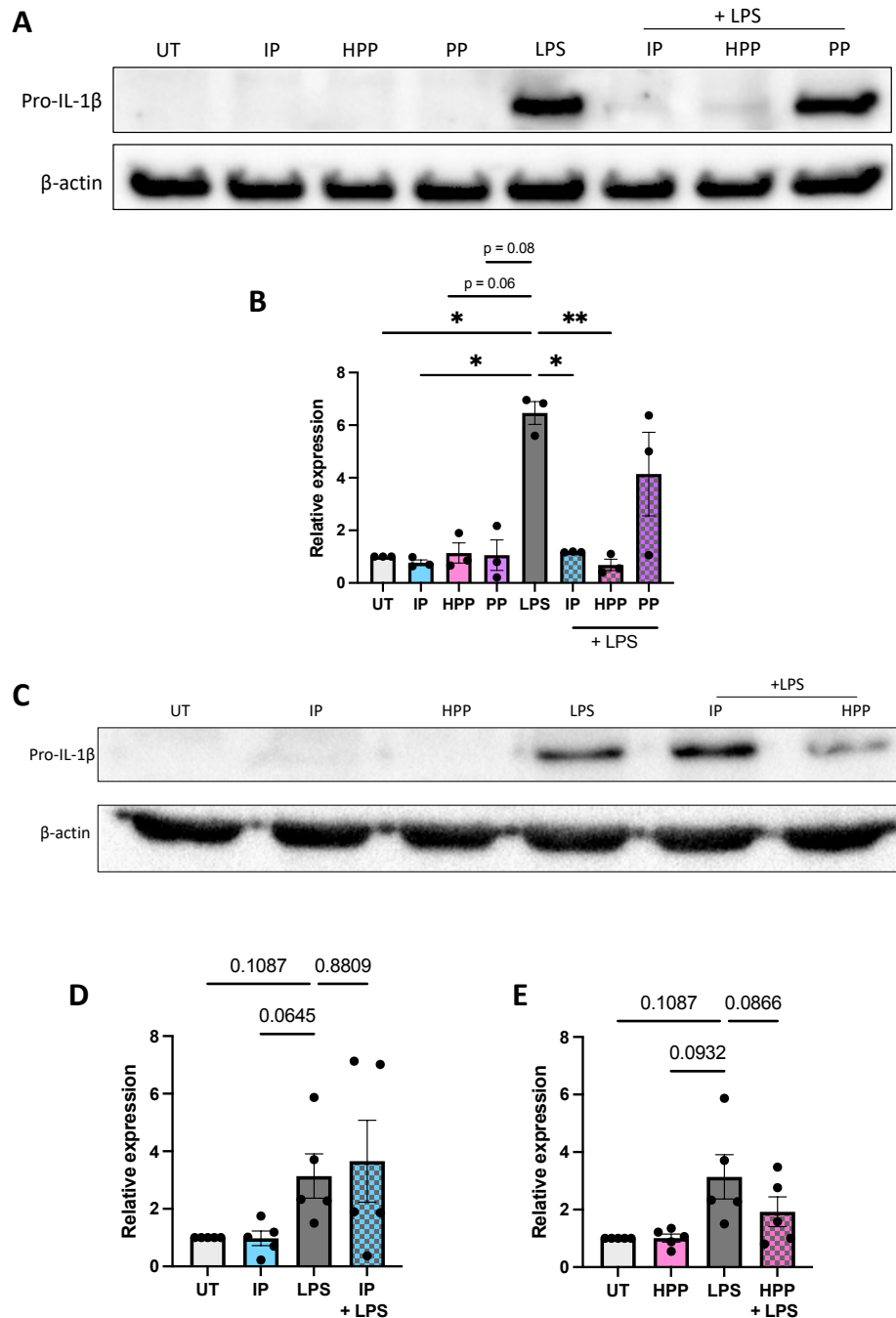
Primary human DC were left untreated (UT) or incubated with IP (500-1000  $\mu$ M) for 6 hours prior to stimulation with LPS (100 ng/ml) for 24 hours. Cell supernatants were assessed for (A) TNF, (B) IL-6, (C) IL-23, (D) IL-12p70, and (E) IL-10 secretion by ELISA. Pooled data depicts mean ( $\pm$ SEM) cytokine concentrations for 4-7 healthy donors (means of three technical replicates per donor). Repeated measures one-way ANOVA, with Dunnett's multiple comparisons post hoc test, was used to determine statistical significance, by comparing means of treatment groups against the mean of the control group (\* $p$  < 0.05).





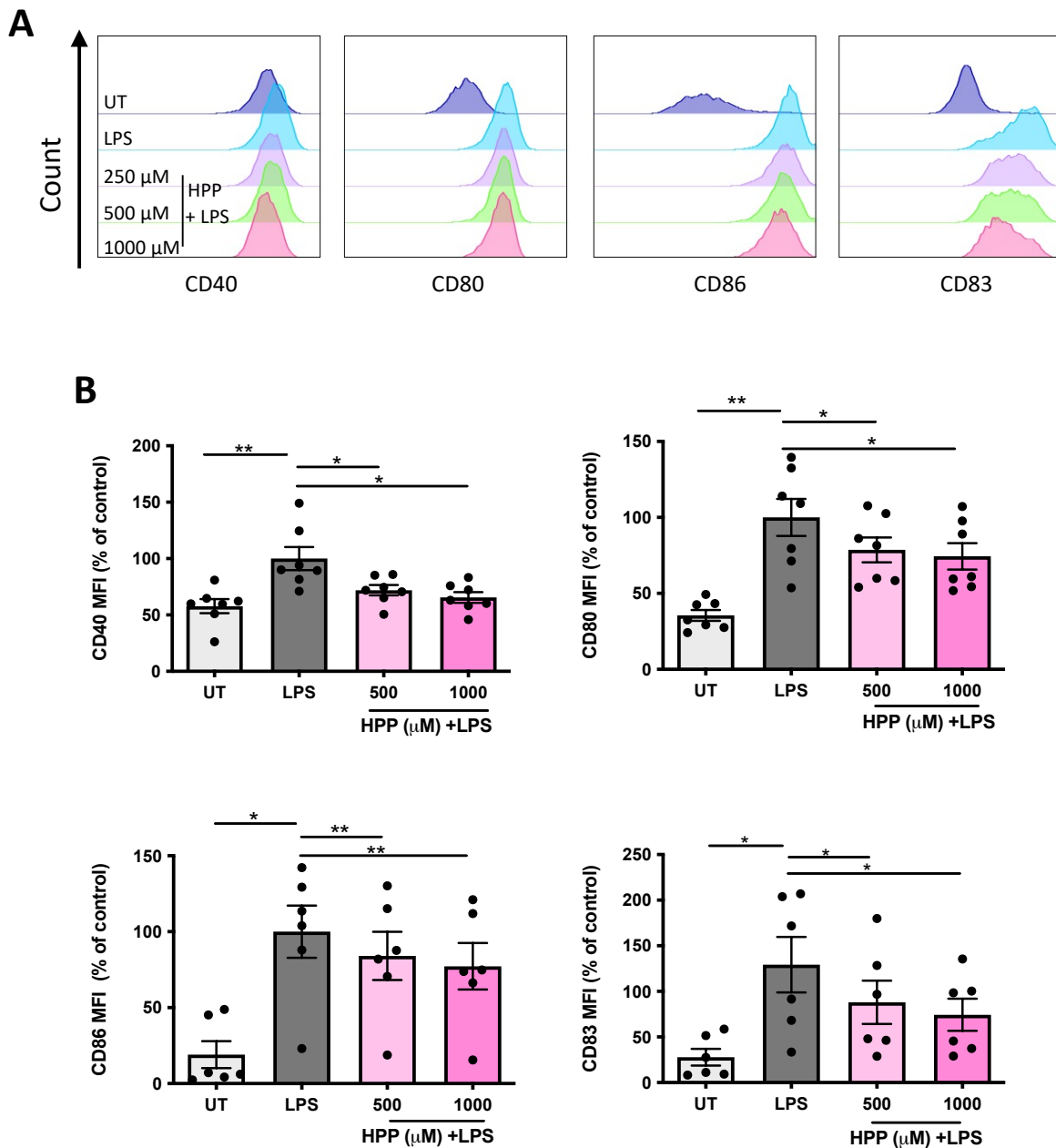
**Figure 3.18 HPP reduces the production of pro-inflammatory cytokines in LPS-stimulated human DC.**

Primary human DC were left untreated (UT) or incubated with HPP (500-1000  $\mu$ M) for 6 hours prior to stimulation with LPS (100 ng/ml) for 24 hours. Cell supernatants were assessed for (A) TNF, (B) IL-6, (C) IL-23, (D) IL-12p70, and (E) IL-10 secretion by ELISA. Pooled data depicts mean ( $\pm$ SEM) cytokine concentrations for 5-6 healthy donors (means of three technical replicates per donor). Repeated measures one-way ANOVA, with Dunnett's multiple comparisons post hoc test, was used to determine statistical significance, by comparing means of treatment groups against the mean of the control group (\*\*  $p < 0.01$ , \*  $p < 0.05$ ).



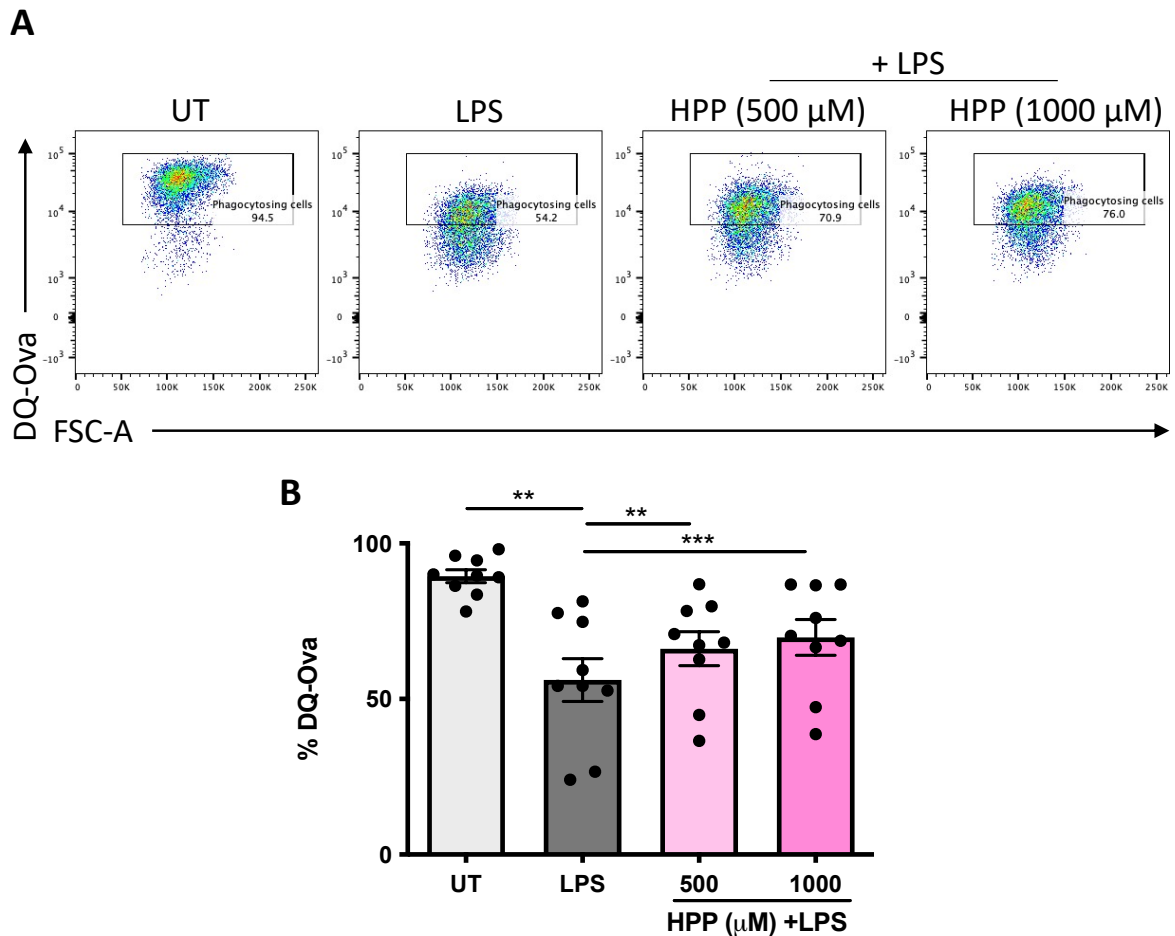
**Figure 3.19 HPP and IP reduce pro-IL-1 $\beta$  expression in BMDM, while HPP moderately reduces pro-IL-1 $\beta$  expression in human DC.**

**(A)** BMDM left untreated (UT) or incubated with IP, HPP or PP (1000  $\mu$ M) for 30 minutes prior to stimulation with LPS for 24 hours. **(C)** Primary human DC were left UT or incubated with IP or HPP (1000  $\mu$ M) for 6 hours prior to stimulation with LPS (100 ng/ml) for 24 hours. **(A & C)** Pro-IL-1 $\beta$  expression was measured by western blot. **(B)** Densitometry results shown are mean  $\pm$  SEM of the relative expression of HO-1:  $\beta$ -actin from 3 individual experiments. **(C & D)** Densitometry results shown are mean  $\pm$  SEM of the relative expression of HO-1:  $\beta$ -actin from 5 healthy DC donors. Repeated measures one-way ANOVA, with Dunnett's multiple comparisons post hoc test, was used to determined statistical significance, by comparing means of treatment groups against the mean of the control group (\*\*  $p < 0.01$ , \*  $p < 0.05$ ).



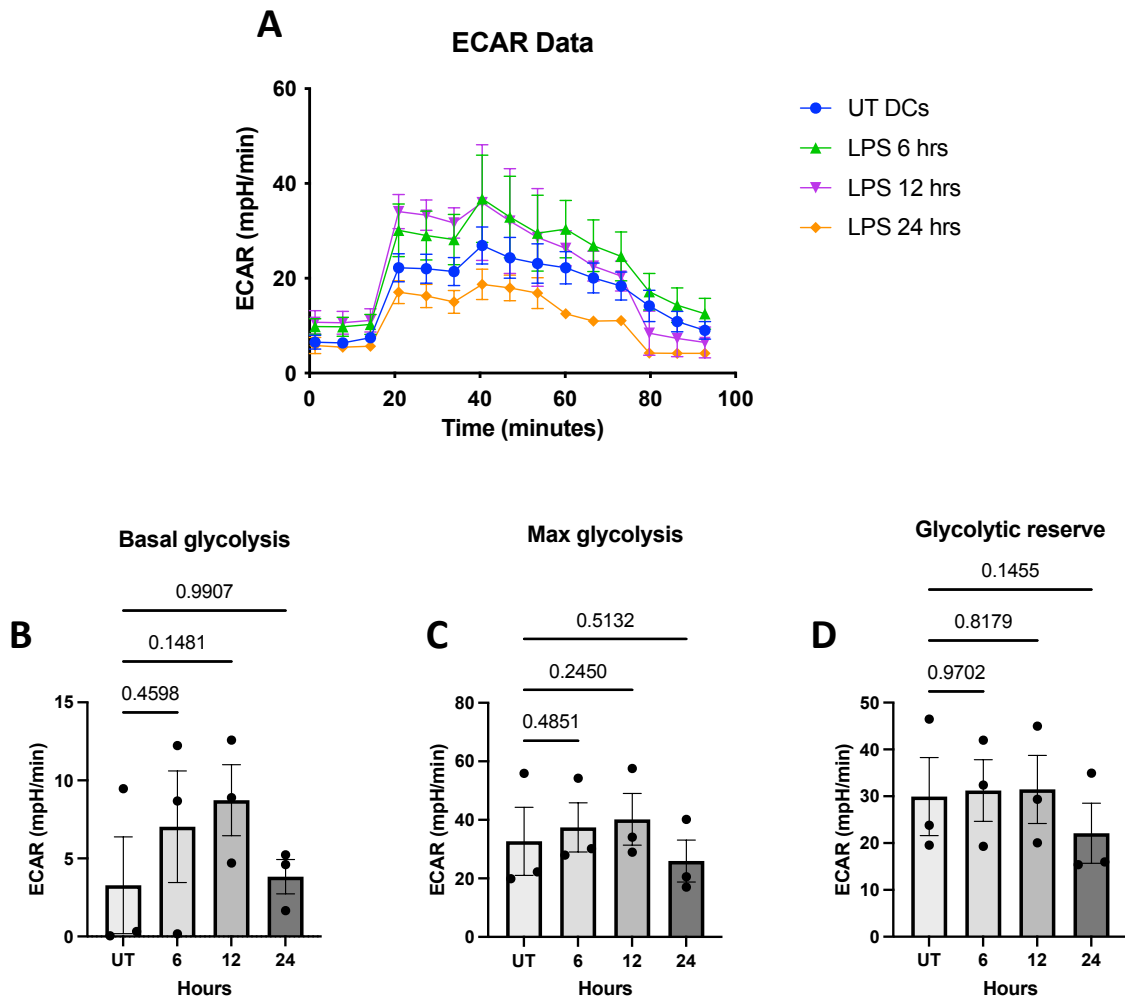
**Figure 3.20 HPP treatment reduces expression of maturation markers in LPS-stimulated human DC.**

Primary human DC were left untreated (UT) or incubated with HPP (500-1000  $\mu$ M) for 6 hours prior to stimulation with LPS (100 ng/ml) for 24 hours. Cells were stained for CD40, CD80, CD86 and CD83 and analysed by flow cytometry. **(A)** Histograms showing the expression of maturation markers for HPP-treated LPS-stimulated DC compared to unstimulated cells or LPS stimulation alone from one representative experiment. **(B)** Pooled data showing the mean ( $\pm$  SEM) MFI for each marker expressed as percentage of control (LPS stimulation alone), from 6-7 healthy donors. Repeated measures one-way ANOVA, with Dunnett's multiple comparisons post hoc test, was used to determine statistical significance by comparing means of treatment groups against the mean of the control group (\*\*  $p < 0.01$ , \*  $p < 0.05$ ).



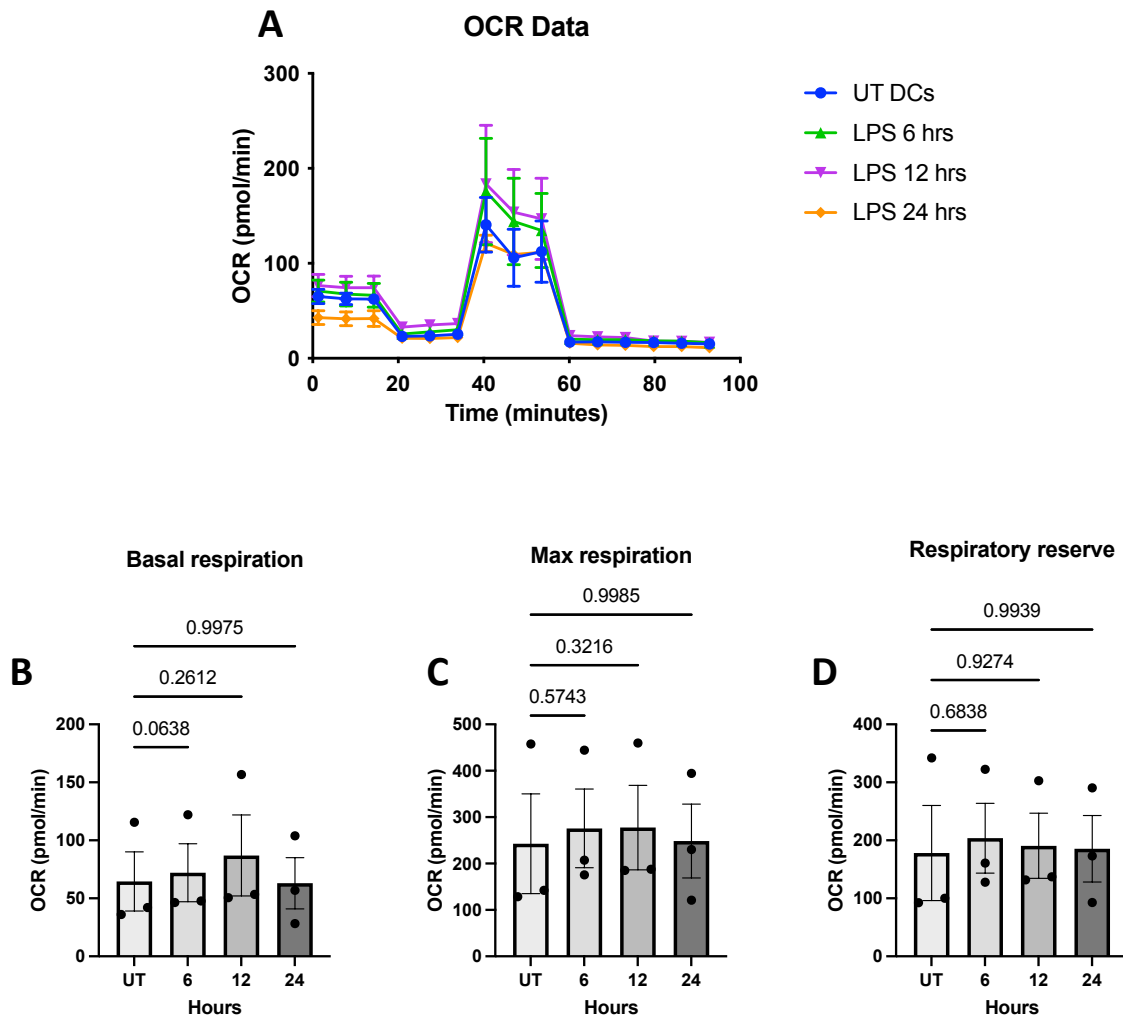
**Figure 3.21 HPP treatment maintains the phagocytic capacity of LPS-stimulated human DC.**

Primary human DC were left untreated (UT) or incubated with HPP (500-1000  $\mu\text{M}$ ) for 6 hours prior to stimulation with LPS (100 ng/ml) for 24 hours. DC were incubated with FITC conjugated DQ-Ovalbumin (DQ-Ova; 500 ng/ml) for 20 minutes and were immediately acquired by flow cytometry. **(A)** Dot plots depicting DQ-Ova uptake from one representative experiment. **(B)** Pooled data showing the mean ( $\pm$  SEM) DQ-Ova uptake as a percentage of total cells from 9 healthy donors. Repeated measures one-way ANOVA, with Dunnett's multiple comparisons post hoc test, was used to determine statistical significance by comparing means of treatment groups against the mean of the control group (\*\* $p < 0.01$ , \*\*\* $p < 0.001$ , \* $p < 0.05$ ).



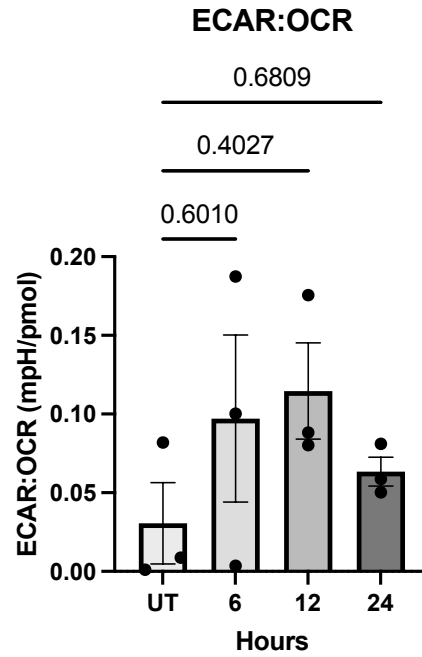
**Figure 3.22 LPS stimulation increases glycolytic metabolism in time dependent manner in human DC.**

Primary human DC were stimulated with LPS (100 ng/ml) for 6, 12 or 24 hours. The extracellular acidification rate (ECAR) was measured using a Seahorse XFe96 analyser before and after the injections of oligomycin (1 mM), FCCP (1 mM), antimycin A (500 nM), and rotenone (500 nM), and 2-DG (25 mM). Bioenergetic profiles from one representative experiment depicting (A) ECAR measurements over time. Pooled data (n = 3) depicts the calculated mean ( $\pm$  SEM) of (B) basal glycolytic rate, (C) max glycolytic rate and (D) glycolytic reserve for each treatment group. Repeated measures one-way ANOVA, with Dunnett's multiple comparisons post hoc test, was used to determine statistical significance by comparing means of treatment groups against the mean of the control group. P values are shown on the graphs.

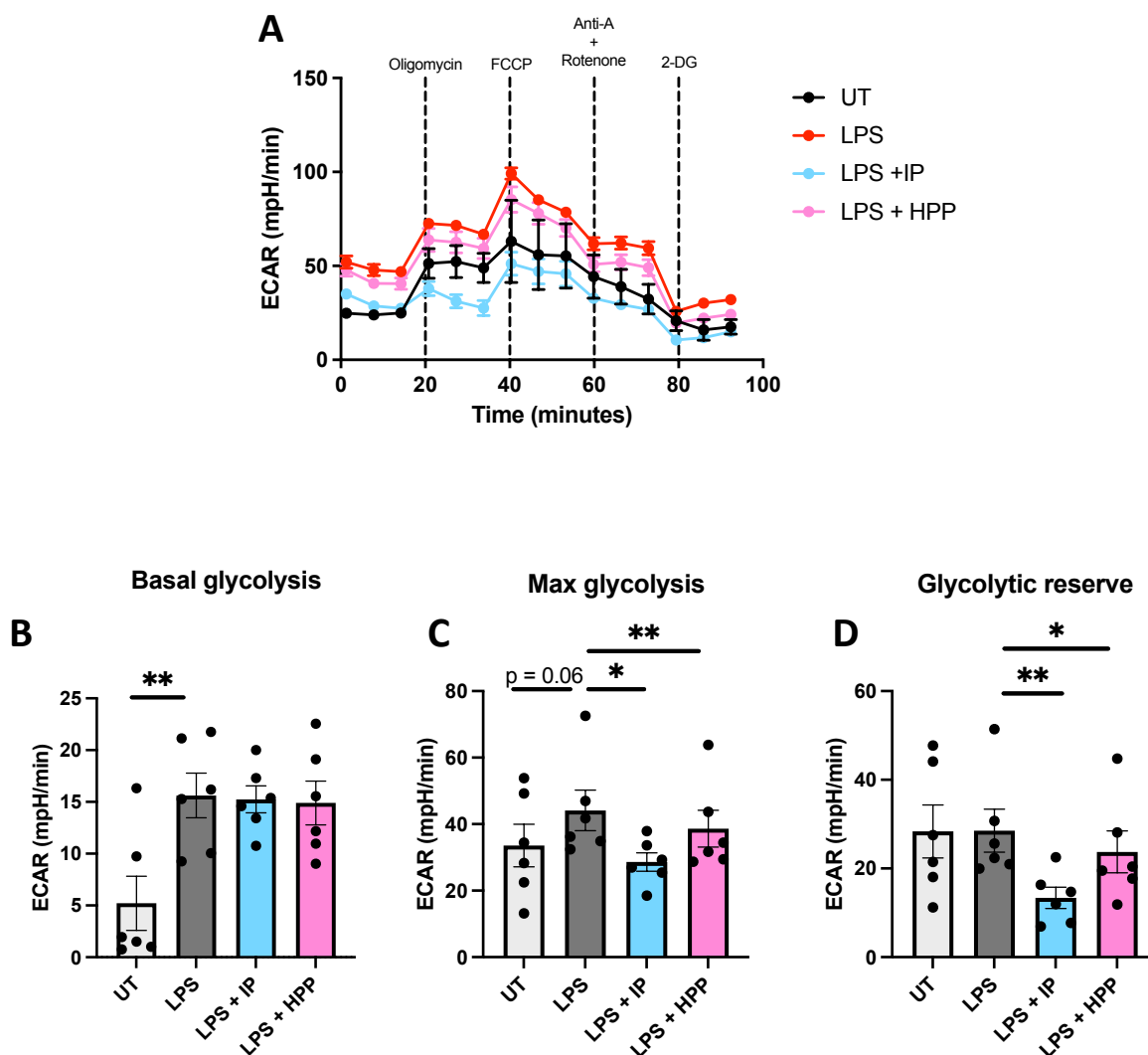


**Figure 3.23 LPS stimulation increases respiration in time dependent manner in human DC.**

Primary human DC were stimulated with LPS (100 ng/ml) for 6, 12 or 24 hours. The oxygen consumption rate (OCR) was measured using a Seahorse XFe96 analyser before and after the injections of oligomycin (1 mM), FCCP (1 mM), antimycin A (500 nM), and rotenone (500 nM), and 2-DG (25 mM). Bioenergetic profiles from one representative experiment depicting **(A)** OCR measurements over time. Pooled data (n = 3) depicts the calculated mean ( $\pm$  SEM) of **(B)** basal respiratory rate, **(C)** max respiratory rate, and **(D)** respiratory reserve for each treatment group. Repeated measures one-way ANOVA, with Dunnett's multiple comparisons post hoc test, was used to determine statistical significance by comparing means of treatment groups against the mean of the control group. P values are shown on the graphs.



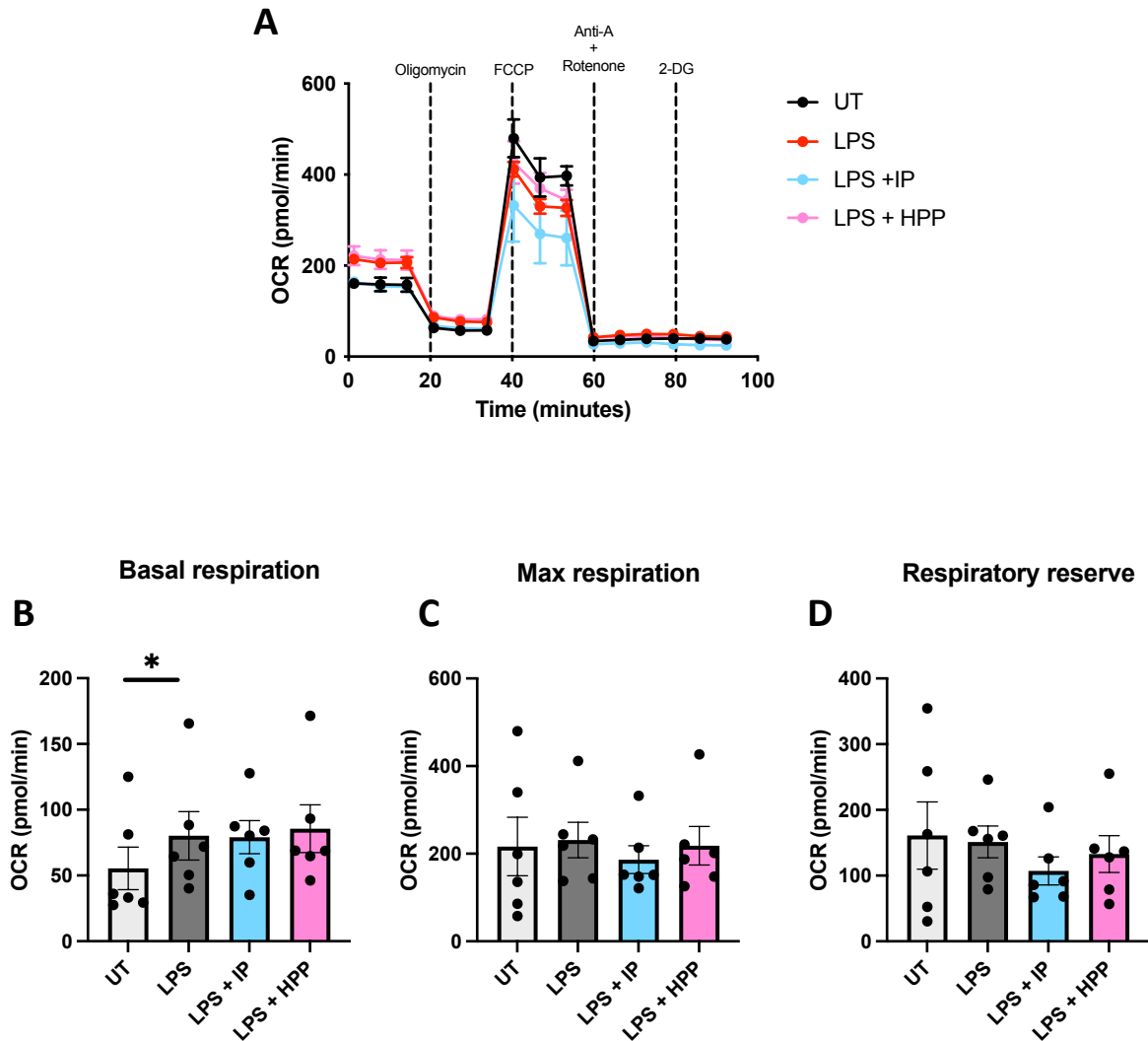
**Figure 3.24 LPS-stimulated human DC favour glycolysis over oxidative phosphorylation.** Primary human DC were stimulated with LPS (100 ng/ml) for 6, 12 or 24 hours. The basal extracellular acidification rate (ECAR) and basal oxygen consumption rate (OCR) were measured using a Seahorse XFe96 analyser. Pooled data (n = 3) depicts the calculated mean ( $\pm$  SEM) of ECAR:OCR for each treatment group. Repeated measures one-way ANOVA, with Dunnett's multiple comparisons post hoc test, was used to determine statistical significance by comparing means of treatment groups against the mean of the control group. P values are shown on the graphs.



**Figure 3.25 IP and HPP treatment reduces glycolysis in LPS-stimulated human DC.**

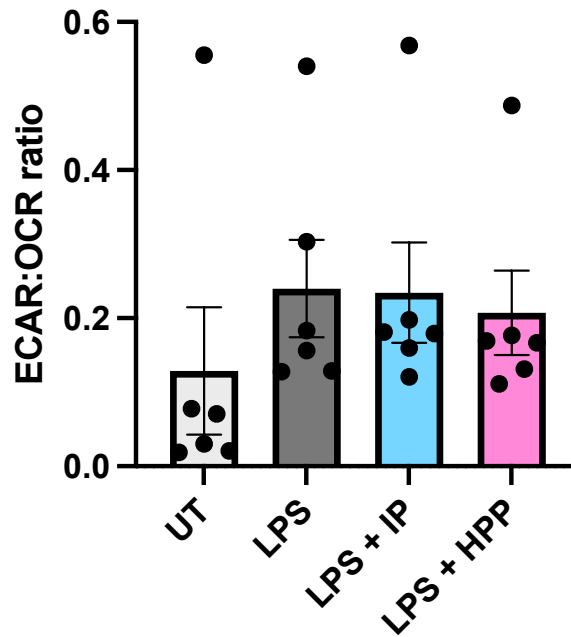
Primary human DC were pre-treated with either HPP or IP at 1000  $\mu$ M for 6 hours before stimulation with LPS (100 ng/ml) for 12 hours. The extracellular acidification rate (ECAR) was measured using a Seahorse XFe96 analyser before and after the injections of oligomycin (1 mM), FCCP (1 mM), antimycin A (500 nM), and rotenone (500 nM), and 2-DG (25 mM). Bioenergetic profiles from one representative experiment depicting (A) ECAR measurements over time. Pooled data (n = 6) depicts the calculated mean ( $\pm$  SEM) of (B) basal glycolytic rate, (C) max glycolytic rate and (D) glycolytic reserve for each treatment group. Repeated measures one-way ANOVA, with Dunnett's multiple comparisons post hoc test, was used to determine statistical significance by comparing means of treatment groups against the mean of the control group (\*\* p < 0.01, \* p < 0.05).





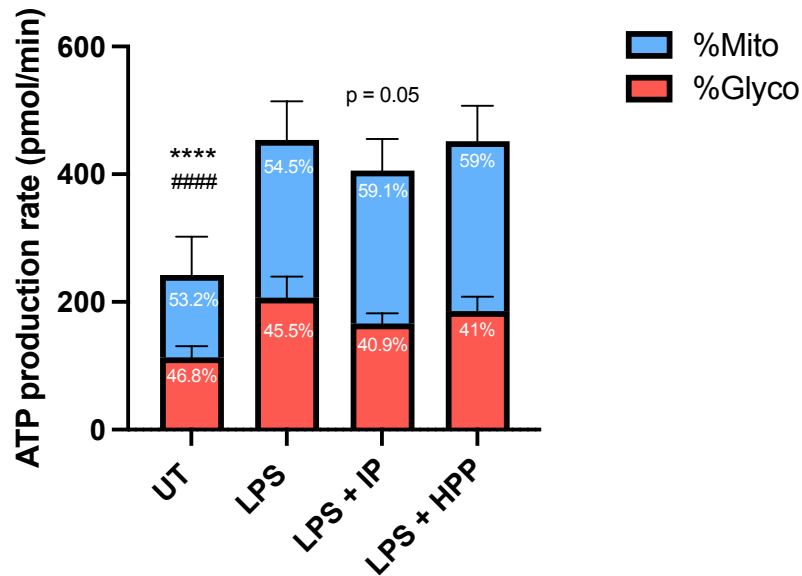
**Figure 3.26 IP and HPP treatment have no effect on respiration in LPS-stimulated human DC.**

Primary human DC were pre-treated with either HPP or IP at 1000  $\mu$ M for 6 hours before stimulation with LPS (100 ng/ml) for 12 hours. The oxygen consumption rate (OCR) was measured using a Seahorse XFe96 analyser before and after the injections of oligomycin (1 mM), FCCP (1 mM), antimycin A (500 nM), and rotenone (500 nM), and 2-DG (25 mM). Bioenergetic profiles from one representative experiment depicting **(A)** OCR measurements over time. Pooled data (n = 6) depicts the calculated mean ( $\pm$  SEM) of **(B)** basal respiratory rate, **(C)** max respiratory rate, and **(D)** respiratory reserve for each treatment group. Repeated measures one-way ANOVA, with Dunnett's multiple comparisons post hoc test, was used to determine statistical significance by comparing means of treatment groups against the mean of the control group (\*p < 0.05).



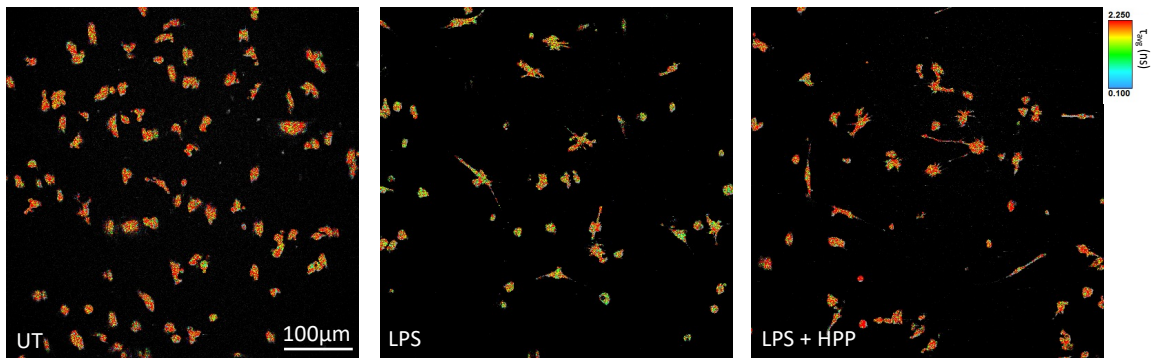
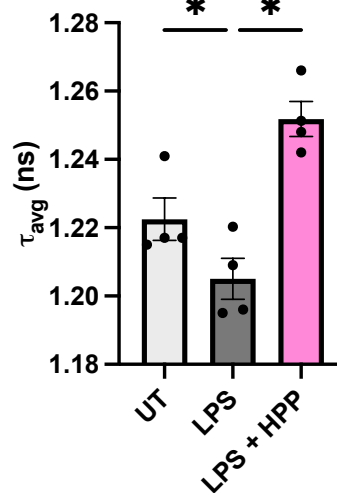
**Figure 3.27 IP and HPP treatment have no effect on the ECAR:OCR of LPS-stimulated human DC.**

Primary human DC were pre-treated with either HPP or IP at 1000  $\mu$ M for 6 hours before stimulation with LPS (100 ng/ml) for 12 hours. The basal extracellular acidification rate (ECAR) and basal oxygen consumption rate (OCR) were measured using a Seahorse XFe96 analyser. Pooled data (n = 6) depicts the calculated mean ( $\pm$  SEM) of ECAR:OCR for each treatment group.



**Figure 3.28 IP and HPP treated human DC primarily derive their ATP from oxidative phosphorylation.**

Primary human DC were pre-treated with either HPP or IP at 1000  $\mu$ M for 6 hours before stimulation with LPS (100 ng/ml) for 12 hours. The extracellular acidification rate (ECAR), oxygen consumption rate (OCR), and proton efflux rate (PER) were measured using a Seahorse XFe96 analyser before and after the injections of oligomycin (1 mM), FCCP (1 mM), antimycin A (500 nM), and rotenone (500 nM), and 2-DG (25 mM). Pooled data (n = 6) depicts the calculated mean ( $\pm$  SEM) of the ATP production rate, and the average percentages attributed to ATP derived from glycolysis or ATP derived from mitochondria. Two-way ANOVA, with Šídák's multiple comparisons post hoc test, was used to determine statistical significance. (\*\*\*\* p < 0.0001: denotes differences for %Glyco ATP compared to control, ##### p < 0.0001: denotes differences for %Mito ATP compared to control. P = 0.05 denotes differences for %Glyco ATP compared to control).

**A****B**

**Figure 3.29 HPP-treated human DC favour engagement of oxidative phosphorylation over glycolysis.**

Primary human DC were pre-treated with HPP at 1000  $\mu\text{M}$  for 6 hours before stimulation with LPS (100 ng/ml) for 12 hours. **(A)** FLIM images of DC measuring intracellular NADH. **(B)** Pooled data ( $n = 4$ ) depicts the mean ( $\pm$  SEM) of the ratio of bound:free NADH, represented by the  $\tau$  average. Repeated measures one-way ANOVA, with Dunnett's multiple comparisons post hoc test, was used to determine statistical significance by comparing means of treatment groups against the mean of the control group (\* $p < 0.05$ ).

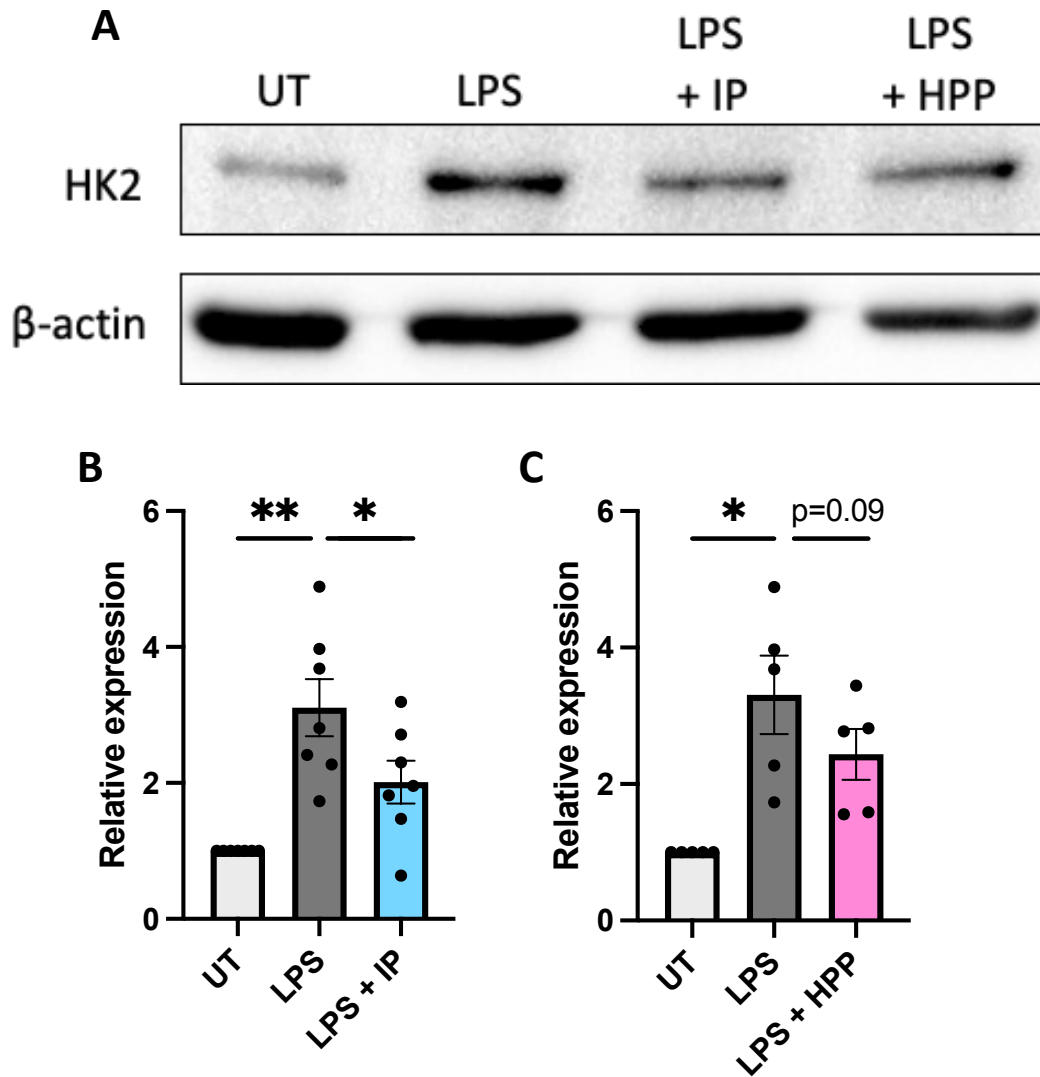


**Figure 3.30 IP and HPP treatment reduces expression of HK2 in LPS-stimulated human DC.**

Primary human DC were pre-treated with either **(B)** IP or **(C)** HPP at 1000  $\mu$ M for 6 hours before stimulation with LPS (100 ng/ml) for 12 hours. **(A)** HK2 expression was measured by western blot. **(B & C)** Densitometry results shown are mean  $\pm$  SEM of the relative expression of HK2:  $\beta$ -actin from 5-7 healthy donors. Repeated measures one-way ANOVA, with Dunnett's multiple comparisons post hoc test, was used to determine statistical significance by comparing means of treatment groups against the mean of the control group (\*\*  $p < 0.01$ , \* $p < 0.05$ ). ImageLab (Bio-Rad) software was used to perform densitometric analysis.

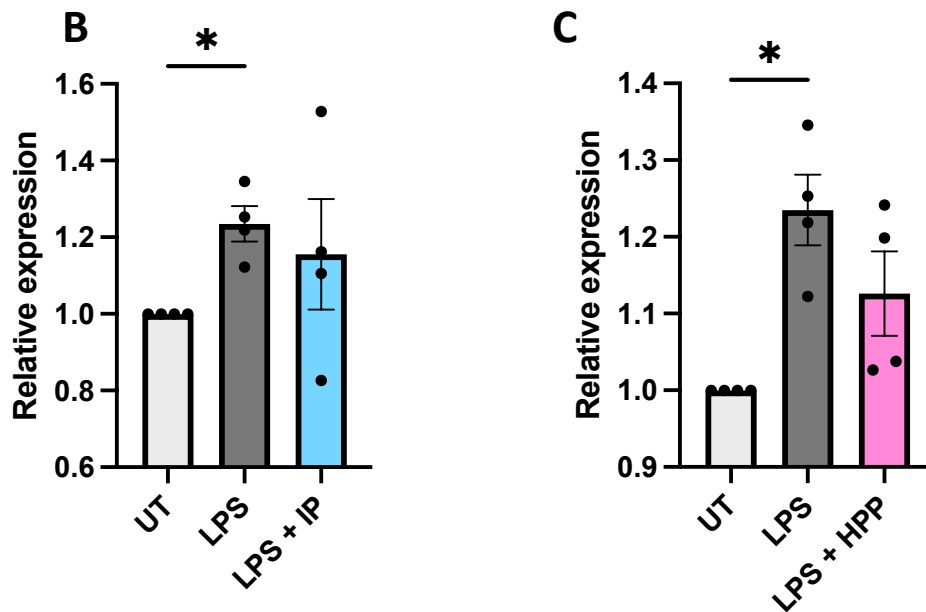
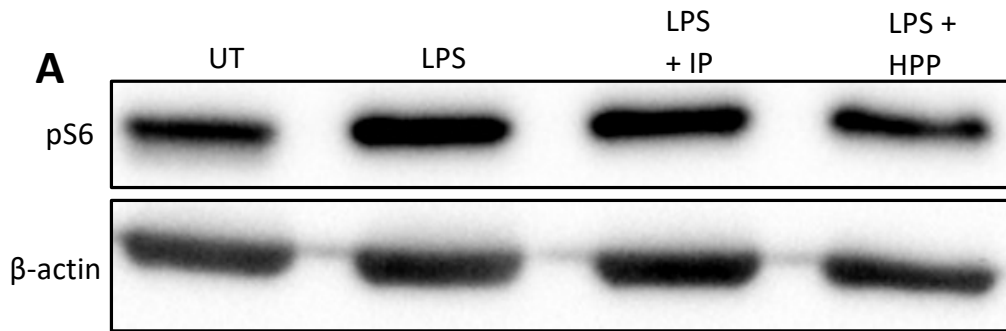


**Figure 3.31 IP and HPP treatment moderately reduces the phosphorylation of the protein S6 in LPS-stimulated human DC.**

Primary human DC were pre-treated with either (B) IP or (C) HPP at 1000  $\mu$ M for 15 minutes before stimulation with LPS (100 ng/ml) for 1 hour. (A) Phosphorylation of S6 was measured by western blot. (B & C) Densitometry results shown are mean  $\pm$  SEM of the relative expression of pS6:  $\beta$ -actin from 4 healthy donors. Repeated measures one-way ANOVA, with Dunnett's multiple comparisons post hoc test, was used to determine statistical significance by comparing means of treatment groups against the mean of the control group (\* $p$  < 0.05). ImageLab (Bio-Rad) software was used to perform densitometric analysis.

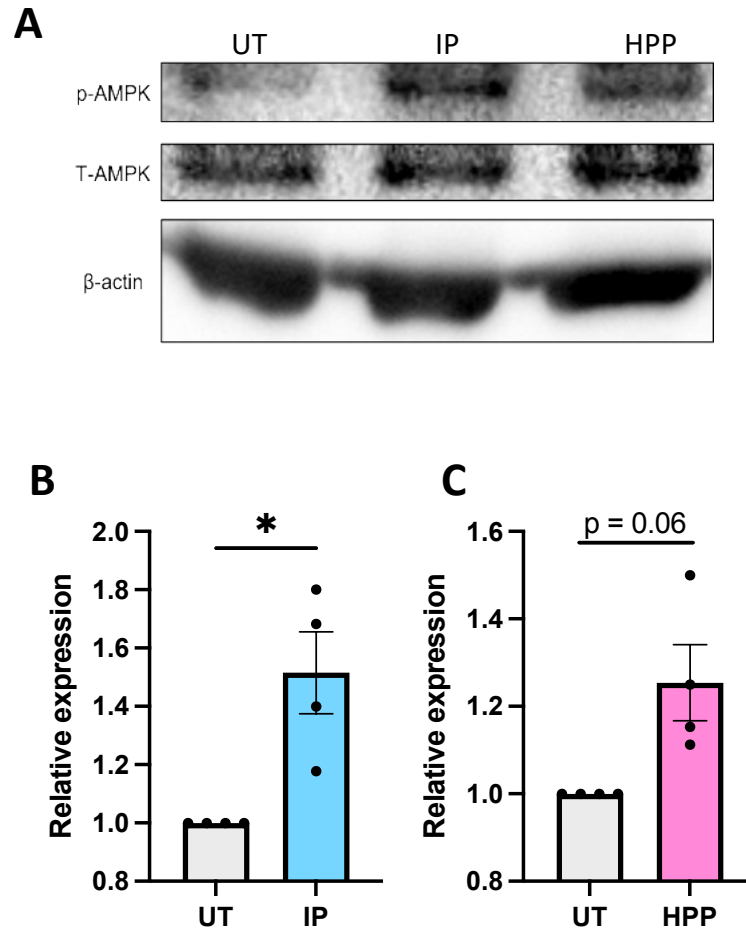


**Figure 3.32 HPP and IP phosphorylate and activate AMPK in human DC.**

Primary human DC were left untreated (UT) or incubated with IP or HPP at 1000  $\mu$ M for 15 minutes. **(A)** Phosphorylation of AMPK was measured by western blot. **(B & C)** Densitometry results shown are mean  $\pm$  SEM of the relative expression of p-AMPK:  $\beta$ -actin from 4 healthy donors. A paired T test was used to determined statistical significance. (\* $p < 0.05$ ). ImageLab (Bio-Rad) software was used to perform densitometric analysis.

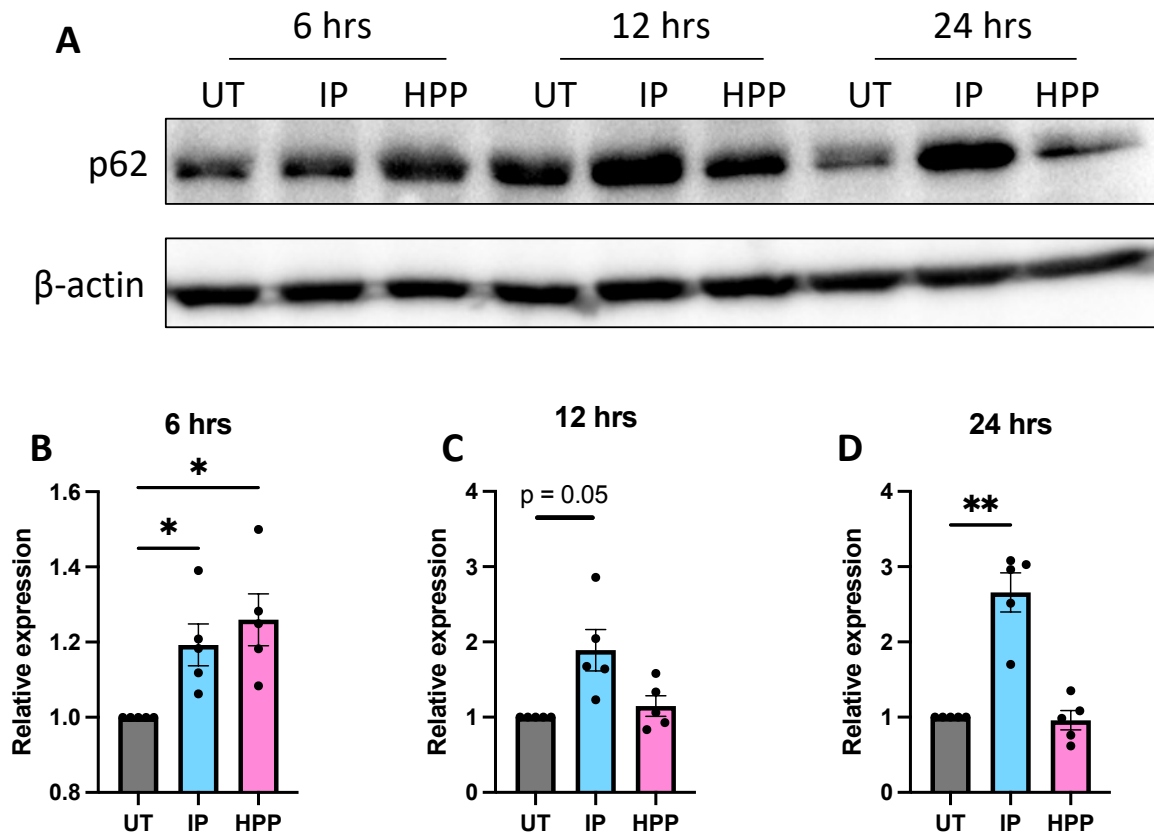


**Figure 3.33 IP and HPP activate p62 in human DC.**

Primary human DC were left untreated (UT) or incubated with IP or HPP at 1000  $\mu$ M for (B) 6, (C) 12 or (D) 24 hours. (A) Expression of p62 was measured by western blot. (B, C & D) Densitometry results shown are mean  $\pm$  SEM of the relative expression of p62:  $\beta$ -actin from 5 healthy donors. Repeated measures one-way ANOVA, with Dunnett's multiple comparisons post hoc test, was used to determine statistical significance by comparing means of treatment groups against the mean of the control group (\*\*  $p < 0.01$ , \* $p < 0.05$ ). ImageLab (Bio-Rad) software was used to perform densitometric analysis.



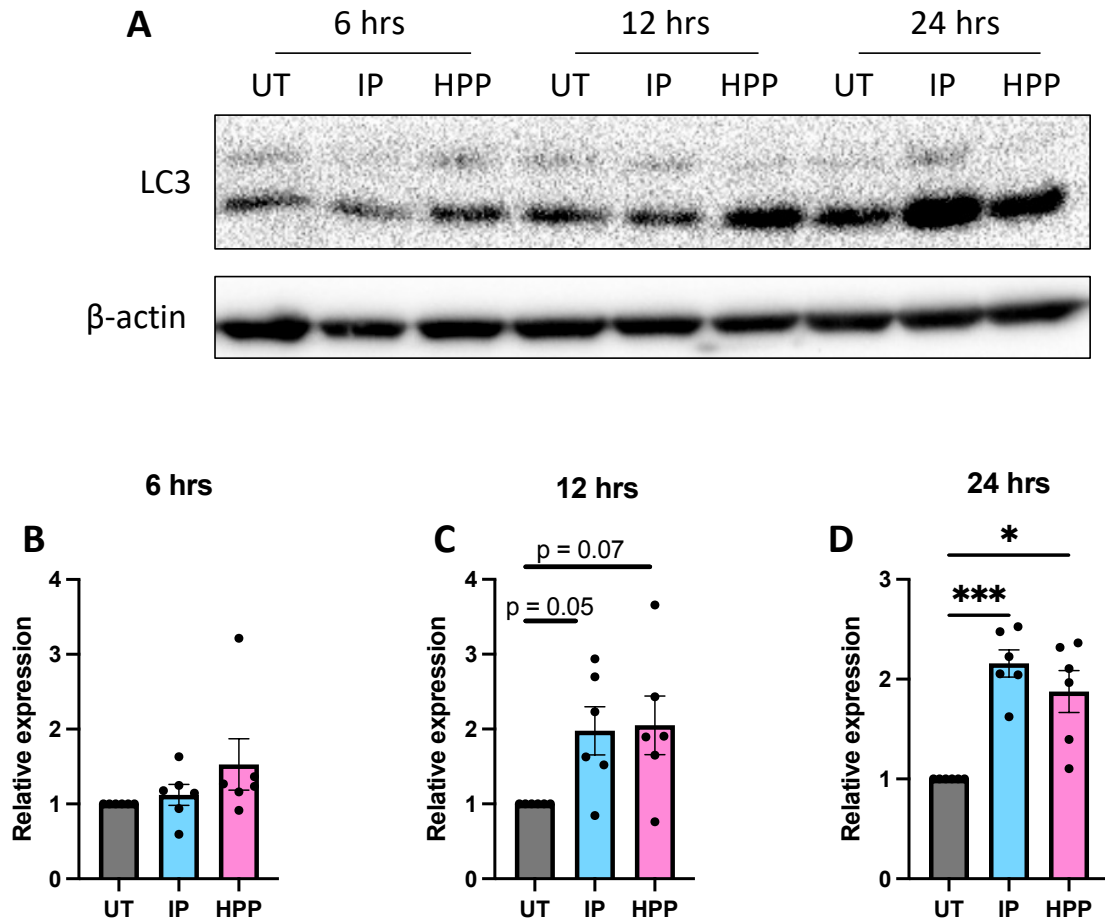


**Figure 3.34 IP and HPP activate LC3-II in human DC.**

Primary human DC were left untreated (UT) or incubated with IP or HPP at 1000  $\mu$ M for **(B)** 6, **(C)** 12 or **(D)** 24 hours. **(A)** Expression of LC3 was measured by western blot. **(B, C & D)** Densitometry results shown are mean  $\pm$  SEM of the relative expression of LC3 II:  $\beta$ -actin from 6 healthy donors. Repeated measures one-way ANOVA, with Dunnett's multiple comparisons post hoc test, was used to determine statistical significance by comparing means of treatment groups against the mean of the control group (\*\*\*)  $p < 0.001$ , \* $p < 0.05$ ). ImageLab (Bio-Rad) software was used to perform densitometric analysis.

### 3.4 Discussion

Despite many advances in the field of study of autoimmune/inflammatory disease, there is still an urgent need for novel anti-inflammatory therapies, with increased long-term efficacy, tolerability, and less adverse side effects. It is well known that many pathogens, including parasites, suppress host immune responses to establish latency and/or maintain persistent infection [295–300], and there has been increased interest in recent years in exploiting parasite-derived products for therapeutic benefit [301–304]. Like most pathogens, the parasite *T. brucei*, which causes sleeping sickness, has evolved numerous strategies to evade the host immune response [252,305,306] and recent studies have identified aromatic ketoacids secreted by trypanosomes as mediators of some of these effects [255,256,259]. This study was carried out to assess the effect of ketoacids in human immune cells in order to gain further insight into their therapeutic potential.

HO-1 induction has been observed in other parasitic infections such as *Leishmania Chagasi*, *Fasciola hepatica* and *Plasmodium* infection, and it was hypothesised that ketoacids produced during *T. brucei* infection may induce HO-1 as a means of dampening host immune responses [286–288]. Indeed, results from our laboratory demonstrated that the secretome of *T. brucei* causes a potent upregulation of HO-1 in murine immune cells and this effect is inhibited when the enzyme responsible for ketoacid production is deleted [256]. Early experiments in this chapter confirmed that IP and HPP can activate Nrf2 and induce HO-1 in BMDM, however the main focus of this chapter was human DC, which are key antigen presenting cells and, as discussed previously, HO-1 is of particular importance in DC, where it promotes a more tolerogenic phenotype [265,266,269]. Results demonstrate that IP and HPP are capable of inducing HO-1 (in addition to NQO-1 and GSR) in primary human DC in both a time and concentration dependent manner. Furthermore, the expression of HO-1 was found to be, at least partially, dependent on the transcription factor, Nrf2.

It was of interest to determine how the ketoacids may be activating the Nrf2/HO-1 pathway. Given that Nrf2 is activated during oxidative stress, experiments were carried out

to determine if the ketoacids alter the redox state of DC. Carnosol and curcumin are phytochemicals which are well established antioxidants and inducers of HO-1 [196,269,307,308]. Both of these compounds were confirmed to increase the total antioxidant capacity of DC after 1 hour. The ketoacids were also found to increase the antioxidant capacity of DC, and did so to a greater extent, indicating that they may themselves function as antioxidants at early time-points. Antioxidants such as resveratrol and quercetin (also HO-1 inducers), inactivate free radicals through the donation of hydrogen atoms in a process known as hydrogen atom transfer (HAT) [309,310]. This results in the delocalisation of unpaired electrons on the free radicals, therefore increasing their stability [309,310]. This method of action is common in antioxidants containing hydroxyl groups, and may explain at least how HPP, which contains a hydroxyl group, functions as an antioxidant.

In addition to assessing the antioxidant capacity of the ketoacids, it was important to determine if the ketoacids can drive cellular ROS, as this can also lead to Nrf2 activation. Specifically, Nrf2 is activated by oxidative stress when cysteine residues on KEAP1 are modified by free radicals, releasing Nrf2 and allowing it to translocate to the nucleus to induce expression of antioxidant genes [109,110,311]. Interestingly, IP and HPP may differ in their mechanism of activation of Nrf2, as IP, but not HPP, significantly increased ROS production in DC. Further experiments are therefore required to determine if IP alters thiol groups on KEAP1. Of note, the anti-inflammatory metabolite, itaconate, activates Nrf2 through alkylation of cysteine residues on KEAP1 [312]. Mass spectrometry to assess cysteine alkylation will also be of benefit to gain further insight into the mechanism of Nrf2 activation by these ketoacids.

Another potential pathway to Nrf2 activation may occur via the AHR as IP was also found to potently induce expression of CYP1A1 in human DC. CYP1A1 expression is under control of the AHR, which functions as a transcription factor to control expression of the cytochrome P450 family of enzymes. Ligands for the AHR include tryptophan and its derivatives, which are primarily indole compounds [313]. This likely explains why IP is capable of activating the AHR. Indeed, it was recently demonstrated that IP is capable of inhibiting prostaglandin production in murine macrophages, an effect that is dependent

on the activation of the AHR [259]. Furthermore, the therapeutic potential of IP in a murine model of colitis was attributed to its ability to activate this transcription factor [258]. Interestingly, activation of the AHR is intrinsically linked to heme metabolism and redox signalling. Biliverdin and bilirubin are ligands for the AHR, while cytochrome P450 enzymes require heme as a cofactor. Furthermore, the AHR can directly activate Nrf2, or can do so indirectly via the generation of ROS by CYP1A1 [96,313–315]. It is therefore possible that the activation of Nrf2 by IP may be due to IP itself inducing ROS or via CYP1A1-induced ROS production. Finally, AHR activation is important for maintaining DC in a more tolerogenic state, and for increasing the differentiation of anti-inflammatory T cells [313]. While further study is required, it is possible that the immunomodulatory properties of the ketoacids outlined below involve synergistic signalling by both the AHR and Nrf2/HO-1.

The secretome of *T.brucei* has been shown to reduce the secretion of IL-12, IL-10, IL-6 and TNF in both murine and human DC [263,264]. Furthermore, studies from our laboratory have demonstrated that IP and HPP are capable of reducing pro-inflammatory cytokines in murine immune cells [255,256]. In this study, both IP and HPP were shown to significantly reduce the secretion of a number of pro-inflammatory cytokines, including TNF, IL-6, IL-12 and IL-23 in LPS-stimulated human DC. Some species specific differences may occur as the ketoacids had no effect on TNF secretion in murine glia, and were incapable of inhibiting TNF or IL-6 secretion in murine BMDM [255,256]. These results indicate that the suppression of cytokines by DC may be of particular importance in dampening the host immune response during *T.brucei* infection. Furthermore, IP treatment significantly increased the secretion of the anti-inflammatory cytokine IL-10, while HPP treatment also trended towards an increase in production of this cytokine. Previous studies have described an important link between IL-10 expression and HO-1 induction, with HO-1 identified as a downstream effector of IL-10 [129,130,266]. HO-1 expression was upregulated in macrophages upon administration of IL-10 both *in vitro* and *in vivo*, while inhibition of HO-1 suppressed the protective effects of IL-10 in LPS-stimulated macrophages and in an *in vivo* murine model of LPS-induced septic shock [130]. While it is very clear that Nrf2 is involved in the induction of HO-1 by the ketoacids, it is also possible that ketoacid-induced IL-10 may be contributing to the upregulation of HO-1 in human DC. Future studies, for example, using IL-10 deficient cells or IL-10 blocking antibodies, are

required to confirm if this is indeed the case. Interestingly, both IP and HPP were capable of reducing pro-IL-1 $\beta$  expression in murine BMDM, however while HPP reduced expression of this protein in human DC, IP had no effect. IL-1 $\beta$  is regulated through a number of signalling pathways, for example by HIF-1 $\alpha$  and NF- $\kappa$ B, therefore future studies investigating the effect of ketoacid treatment on these regulators will provide further insight into these differences.

When DC undergo maturation, they switch from being a phagocytosing cell scavenging for antigen, to a cell prepared for antigen presentation [8]. This results in increased expression of maturation and co-stimulatory markers, and decreased phagocytic capabilities [8]. The secretome of *T.brucei* has been shown to reduce a number of maturation and co-stimulatory markers in both murine and human DC [263,264], therefore it was of interest to investigate if the ketoacids are exerting a similar effect. Results demonstrate that HPP-treatment of LPS-stimulated DC results in reduced expression of maturation and co-stimulatory markers, and an increased capacity for antigen uptake, as assessed using DQ-Ova as a model antigen. This impact on DC phenotype may be a direct result of the HO-1 upregulated by the ketoacids, as HO-1 induction promotes tolerogenic DC [265,266,268–270]. It was not possible to study these effects using IP given its intrinsic autofluorescence and further studies using alternative readouts are required to fully explore the impact of this ketoacid on DC maturation.

A switch in the metabolic profile of DC is also an important characteristic as these cells change from immature phagocytosing cells, to activated, mature cells. The majority of studies investigating DC metabolism have been carried out in murine cells, and have demonstrated that the cells upregulate glycolysis while simultaneously downregulating oxidative phosphorylation [56,316–318]. On the other hand, human DC stimulated with LPS appear to upregulate both glycolysis and oxidative phosphorylation temporally [134,319]. The results in this chapter support previous findings that LPS stimulation increases both glycolysis and oxidative phosphorylation in a time-dependent manner [134,319], with a general return to baseline by 24 hours. Despite the increase in both pathways, the stimulated cells favour glycolysis, as demonstrated by an increase in the ECAR:OCR ratio. This increase in glycolytic metabolism is important to rapidly generate

sufficient energy and building blocks required to fight infection [43]. However, this phenomenon is also a feature of pathogenic immune cells, and a significant effort is underway to determine if controlling/preventing dysregulated metabolic reprogramming can serve to ameliorate detrimental immune cell activation during disease. Therefore, there is increased interest in therapies which modulate metabolic reprogramming as part of their mechanism of action. As both ketoacids investigated were capable of maintaining DC in a more immature, tolerogenic state, it was hypothesised they may be exerting some effects on the metabolic pathways engaged by the cells. Both IP and HPP decreased the max glycolysis and glycolytic reserve of DC, and had no significant effect on their respiration. These results indicate that the ketoacids can downregulate glycolysis in stimulated DC. This is in line with previous work demonstrating that IP downregulates glycolysis in LPS-stimulated BMDM [255]. Interestingly HPP had no effect on the glycolytic state of LPS-stimulated BMDM [255], however, it did inhibit glycolysis in LPS-stimulated RAW 264.7 macrophages [320], albeit at a higher concentration than used in this study. Despite not observing an increase in engagement of oxidative phosphorylation when conducting Seahorse experiments, FLIM analysis demonstrated that HPP-treated cells favour the engagement of oxidative phosphorylation over glycolysis. As before, it was not possible to examine IP using this technique due to autofluorescence issues. In order to ascertain what may be causing the reduction in glycolysis in ketoacid-treated cells, the expression of hexokinase 2 (the rate-limiting enzyme in glycolysis) was examined. IP and HPP were capable of reducing, but not completely abrogating, the expression of HK2. This low level of HK2 may allow for normal glycolytic function under basal conditions, however, upon incubation with oligomycin and the associated change in ATP:ADP ratio, the cells are unable to increase their glycolytic function further. This would however allow for a decrease in the max glycolysis and glycolytic reserve. These results are in line with the notion that metabolism is intricately linked with immune cell activation, and that downmodulation of glycolysis in immune cells promotes a more tolerogenic phenotype.

AMPK, a key cellular energy sensor, and mTOR, a master regulator of cellular growth and nutrient sensing, appear to play opposing roles in the metabolism of immune cells. mTOR functions as part of the mTORC1 complex and is required for protein synthesis, which is important for cellular growth and proliferation [321,322]. Generally, increased levels of

mTORC1 are associated with increased anabolic pathways including glycolysis and FAS, which are in turn important for antigen presentation and proliferation of activated immune cells [322]. On the other hand, AMPK is activated when ATP becomes limited in the cell and is associated with the induction of autophagy [323] and upregulation of catabolic pathways, including FAO [43,49]. Activation of AMPK results in inhibition of mTORC1 and is also associated with suppression of inflammatory responses. For example, AMPK activation has been shown to attenuate pro-inflammatory cytokine production and DC maturation [279,317]. In this study, IP and HPP treatment were shown to inhibit mTOR and activate AMPK in human DC (as assessed by decreased phosphorylation of S6 and increased phosphorylation of AMPK). Interestingly, activation of AMPK has also been linked to Nrf2 activation and induction of HO-1 in many cell types, including human DC [131–136]. Therefore, the activation of AMPK by ketoacids may also contribute to the upregulation of HO-1 in this cell type. However, further work is required to confirm this, for example through the use of the AMPK inhibitors. Indeed, attempts were made to assess this using Compound C (an AMPK inhibitor), however toxicity issues prevented any meaningful analysis (data not shown).

As well as controlling metabolic pathways, mTOR and AMPK are also important for controlling activation of autophagy. Autophagy is an important cellular process required for removal or recycling of cellular components if they are dysfunctional, no longer needed, or their breakdown is required to generate energy. Autophagy is a complex process which can be initiated by activation of AMPK and inhibition of mTOR, however it is continuously occurring at basal levels in a cell in a cyclical fashion. Given the observed increase in AMPK activation by the ketoacids, it was important to assess additional autophagy-related proteins. Both IP and HPP increased levels of p62 and LC3-II in DC, indicating potential activation of the autophagy pathway. Interestingly, autophagy activation has been shown to inhibit IL-1 $\beta$  production by targeting its pro form for degradation [81–83], therefore activation of autophagy-related proteins may contribute to the observed inhibition of pro-IL-1 $\beta$  in DC by HPP. Autophagy activation has also been linked to induction of a more tolerogenic DC phenotype [80]. Notably, p62 also plays a crucial role in the activation of Nrf2 [282–284]. Nrf2 is activated upon release from KEAP1, which can occur when p62 sequesters KEAP1, targeting it for degradation and allowing Nrf2 to translocate to the

nucleus [282–284]. Therefore, the activation of p62 by both ketoacids, but in particular IP, may be responsible for the subsequent activation of Nrf2, and therefore HO-1 induction, by these ketoacids.

In conclusion, the results presented in this chapter demonstrate that not only do *T.brucei*-secreted aromatic ketoacids serve as mediators of immune evasion in human DC, but may also represent potential anti-inflammatory therapies for the treatment of autoimmune/inflammatory diseases. These compounds are capable of suppressing pro-inflammatory DC responses, through the induction of HO-1, increased secretion of IL-10 and decreased DC maturation and glycolysis. They do so via activation of the transcription factor Nrf2, and a number of potential, and possibly parallel, pathways leading to its activation are outlined in the model below (Figure 3.35). While further research is required, these ketoacids represent exciting novel HO-1 inducers with intriguing therapeutic potential.



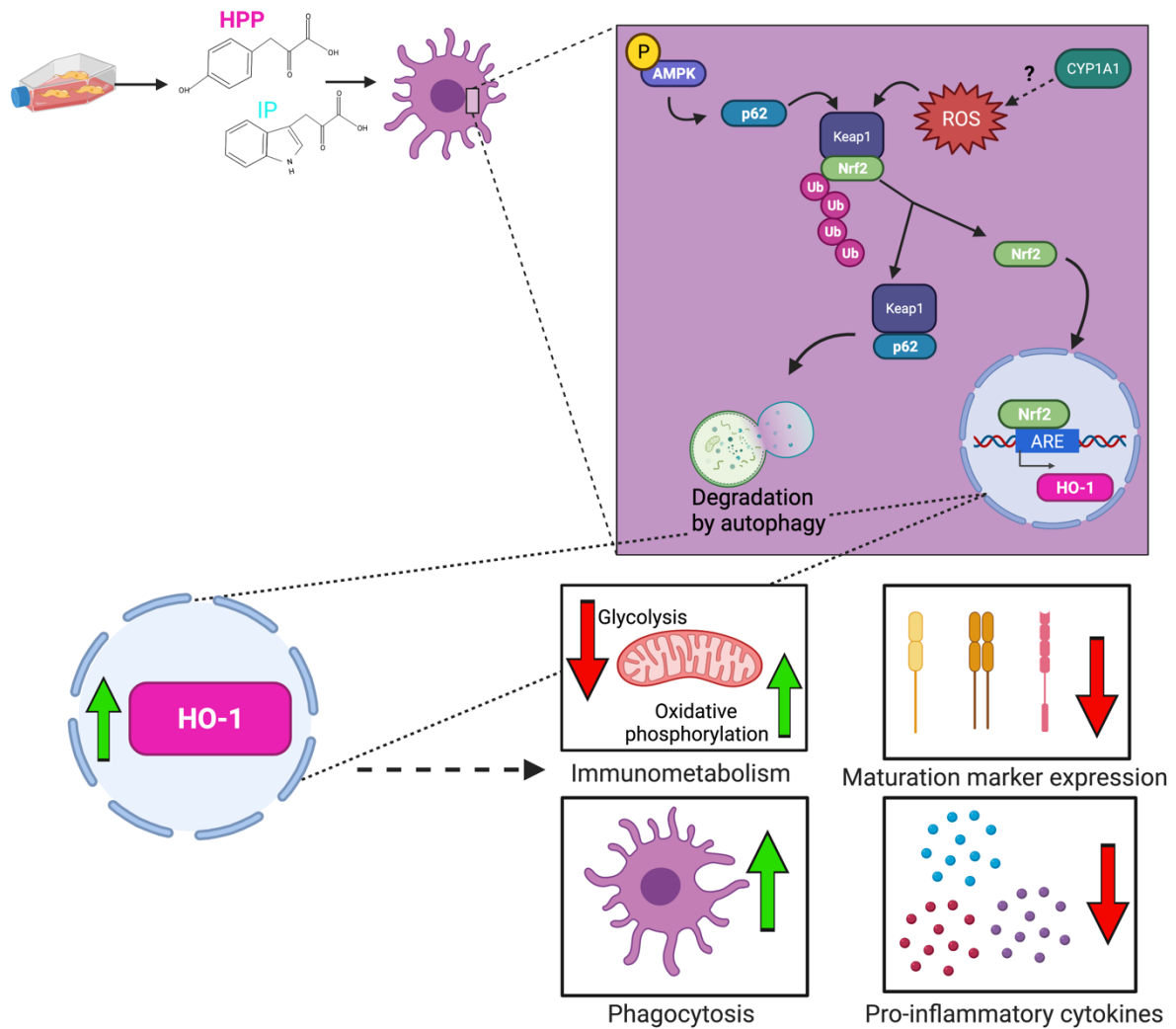


**Figure 3.35 Model outlining the immunomodulatory effects of trypanosome-derived ketoacids and potential mechanism of action.**

Culturing of human DC with IP or HPP leads to phosphorylation of AMPK and potential activation of the autophagy pathway. IP and HPP also activate CYP1A1, which potentially leads to generation of ROS. p62 and ROS activate Nrf2, leading to induction of antioxidant genes including HO-1. HO-1 may or may not be (dashed arrow) directly responsible for the immunomodulatory effects of the ketoacids in DC, including inhibition of glycolysis and activation of oxidative phosphorylation, inhibition of maturation marker expression, enhanced phagocytosis and inhibition of pro-inflammatory cytokine production.

**Chapter 4:**  
**Immunomodulatory properties of *T. brucei*-  
derived ketoacids in human T cells**

## 4.1 Introduction

T cells, in particular Th1 and Th17 cells, are commonly implicated in the pathogenesis of many autoimmune and inflammatory diseases. On the other hand, Tregs are important for downregulating inflammatory immune responses and maintaining homeostasis. Therefore, an imbalance between these cell types favouring Th1/Th17 cells can lead to prolonged and chronic inflammation. Several therapies targeting pathogenic T cells have been, or are being, developed, and include a number of biologics targeting specific T cell subsets and/or their cytokines. For example, ustekinumab, a monoclonal antibody targeting the p40 subunit of IL-12 and IL-23, indirectly inhibits Th1 and Th17 cells, and provides therapeutic benefit in some psoriasis patients, although it is less efficacious in MS patients [40,41]. The monoclonal antibody guselkumab, which targets IL-23, has demonstrated efficacy for the treatment of psoriasis and psoriatic arthritis [324,325]. Secukinumab, a monoclonal antibody which targets IL-17A, has been shown to improve symptoms in patients with psoriasis and psoriatic arthritis [35,36], while adalimumab, an anti-TNF agent, has been shown to induce remission in patients with IBD, RA and psoriasis [326–328]. Abatacept, an immune checkpoint inhibitor, which functions by binding to CD80 and CD86 on APC, preventing the activation of T cells through these co-stimulatory markers, has also demonstrated therapeutic efficacy in RA patients [329]. Therefore, there is solid rationale to support the use of anti-inflammatory therapies that target both DC and T cells, in order to limit inappropriate inflammation induced by these cell types.

IBD is an umbrella term used to describe two conditions; UC and CD. Both conditions are characterised by chronic relapsing inflammation of the gastrointestinal tract, but despite their similarities, they differ in disease phenotype. For example, the inflammation observed in UC is localised to the colon, while CD can affect any part of the GI tract [168,330]. The type of inflammation also differs between these conditions; CD presents with areas of patchy, discontinuous, transmural inflammation, whereas UC typically presents with continuous, superficial inflammation, beginning in the rectum and extending proximally through the colon [168,330]. Unsurprisingly, there is strong evidence to support the involvement of the immune system in the pathogenesis of IBD, with high levels of pro-

inflammatory cytokines (including IL-6, IL-23, IL-12 and TNF) and Th1/Th17 cells observed in the gut of affected individuals [331]. Uncontrolled activation of mucosal APC, T cells, and innate lymphoid cells leads to the production of pro-inflammatory cytokines that can promote persistent and chronic inflammation in the gastrointestinal tract. Classically, CD is described as a Th1 type immune response characterised by the secretion of APC-derived IL-12 and TNF, and Th1 cell derived IFN $\gamma$  [331]. In contrast, UC is viewed similar to an atypical Th2 type immune response which generates high levels of IL-5, IL-4, and IL-13 [331]. In addition, several studies have implicated the Th17 associated cytokines (i.e. IL-23, IL-22, and IL-6,) as well as IL-17 itself in the pathogenesis of both diseases [331–333]. The genetic risk factors associated with IBD are also directly linked to the immune system. For example, polymorphisms have been identified in genes linked to the IL-23/Th17 pathway as well as NOD2 and IL-10 signalling [85,168]

Trypanosome-derived ketoacids have not been extensively studied in adaptive immune cells, however an important study from Aoki *et al.* recently demonstrated that the aromatic ketoacid, IP, reduced disease severity in the acute murine colitis model and this was accompanied by a decrease in the expression of pro-inflammatory cytokines IL-12, IFN $\gamma$ , TNF and IL-1 $\beta$ . Furthermore, a reduction in Th1 cells was observed and there was a reduced capacity for DC to activate T cells. IP was also found to increase the frequency of Tregs and increase expression of anti-inflammatory cytokine, IL-10 [258]. This suggests that aromatic ketoacids may have therapeutic potential for the treatment of conditions such as IBD. There is however limited research supporting this, with no evidence to date assessing their effect on human T cells responses. Therefore, the main aim of this chapter is to investigate the effects of ketoacids on T cells from healthy donors, as well as PBMC from individuals with IBD.

## 4.2 Aims

- To assess the effects of ketoacid-treated DC on the activation and proliferation of CD4<sup>+</sup> T cells.

- To determine if ketoacid-treated DC can skew CD4<sup>+</sup> T cells to a less inflammatory phenotype by increasing Tregs or inhibiting pro-inflammatory cytokines.
- To investigate ketoacid treatment as a potential therapeutic for IBD using *ex vivo* stimulated PBMC from patients with IBD.

## 4.3 Results

### *4.3.1 HPP treated DC have a reduced capacity to activate allogeneic CD4<sup>+</sup> T cells.*

Mature DC are typically responsible for the activation of naïve T cells, and can skew them to a more pro-inflammatory phenotype, which is desired in cases of infection, but can be detrimental in cases of autoimmune disease [23]. In addition to antigen presentation and cytokine production, the expression of maturation and co-stimulatory markers on DC is required for the full activation of T cells. As demonstrated in chapter 3, along with reducing the secretion of pro-inflammatory cytokines, HPP treatment reduced the maturation of LPS-stimulated DC, and while it was not possible to assess IP in these experiments, it may also have a similar effect. In order to determine if the reduced DC activation status that occurs in the presence of HPP (and possibly IP) has an impact on T cell activation, DC were treated with HPP or IP (both 1000  $\mu$ M) for 6 hours prior to stimulation with LPS (100 ng/ml) for 24 hours. The cells were then incubated with allogeneic CD4<sup>+</sup> T cells at a ratio of 10:1 (CD4<sup>+</sup> T cells:DC) for five days. This model assessed the ability of DC to drive T cell activation and differentiation of naïve T cells, since the allo-specific T cells present should all be naïve rather than memory T cells. The supernatants were removed for cytokine analysis by ELISA and cells were stimulated with PMA, ionomycin and brefeldin A for 4 hours. Expression of ki67, as a measure of cell proliferation, was assessed by flow cytometry in CD3<sup>+</sup>CD8<sup>-</sup> cells. As expected, LPS-stimulated DC increased the proliferation of T cells upon co-culture (Figure 4.1). However, T cells co-cultured with LPS-stimulated DC that had been pre-treated with HPP, showed a trend towards reduced ki67 expression when compared to T cells co-cultured with LPS-stimulated DC alone (Figure 4.1B). Interestingly, IP-treated, LPS-stimulated DC actually enhanced the proliferation of co-cultured T cells (Figure 4.1C). IFN $\gamma$  expression was also examined, and as expected, LPS-stimulated DC increased the expression of this cytokine in CD4<sup>+</sup> T cells, while HPP treatment resulted in a trend towards reduced IFN $\gamma$  expression in co-cultured CD4<sup>+</sup> T cells (Figure 4.2B). In contrast, and in align with the proliferation results highlighted above, IP pre-treatment of LPS-stimulated DC resulted in a trend towards increased expression of IFN $\gamma$  in CD4<sup>+</sup> T cells (Figure 4.2C).

It was next examined if ketoacid treatment of DC has any effect on the induction of Tregs. In this case, Tregs are denoted as CD4<sup>+</sup>FoxP3<sup>+</sup>CD127<sup>lo</sup>CD25<sup>+</sup>. Results demonstrated that there was an increase in the percentage of Tregs when CD4<sup>+</sup> T cells were co-cultured with LPS-stimulated DC (Figure 4.3). In contrast, HPP-treatment of LPS-stimulated DC resulted in a trend towards reduced expression of Treg-associated markers in co-cultured CD4<sup>+</sup> T cells, while IP treatment appeared to have no effect (Figure 4.3 C and D). Given that IP was found to increase T cell proliferation, it was hypothesised that the increase observed may be accounted for by the Treg population. However, comparison of ki67 expression in Treg versus non-Treg cells confirmed that this was not the case (Figure 4.4). Secretion of the anti-inflammatory cytokine, IL-10, was also examined in the supernatants from co-culture experiments. Interestingly, T cells co-cultured with LPS-stimulated DC pre-treated with HPP, exhibited a trend towards enhanced production of IL-10, when compared to T cells co-cultured with LPS-stimulated DC alone,  $p = 0.1$  (Figure 4.5A). However, this effect was not reflected in co-culture experiments using IP-treated DC (Figure 4.5B). These results indicate that the ketoacids differ in their ability to modulate allogeneic T cells responses.

#### *4.3.2 Supernatants from DC treated with ketoacids reduce expression of IFN $\gamma$ in human CD4<sup>+</sup> T cells.*

DC secrete many cytokines which play an important role in activating T cells and polarising them to specific effector cell subsets. For example, IL-12 is an important Th1 polarising cytokine, while IL-6 exposure can promote Th17 differentiation [12]. As outlined in chapter 3, IP and HPP treatment of human DC inhibits the production of certain pro-inflammatory cytokines. Experiments were therefore carried out to determine if the supernatants from ketoacid-treated DC had an impact on CD4<sup>+</sup> T cell phenotype. To test this, DC were pre-treated with IP or HPP (both 500  $\mu$ M) for 6 hours and then stimulated with LPS (100 ng/ml) for 24 hours. Supernatants were removed, diluted 1:2 with fresh media, and added to purified human CD4<sup>+</sup> T cells for 4 days in the presence of anti-CD3 (1  $\mu$ g/mL) and anti-CD28 (2  $\mu$ g/mL), before analysing by flow cytometry. Unstained samples were run initially to check if there was any endogenous autofluorescence of the ketoacids, as they were still present in the supernatants. Importantly, no fluorescence was detected in the unstained

IP or HPP treated samples when analysed in the channel used to assess viability (LD Near IR) or the APC channel (used to stain for IFN $\gamma$  expression) (Figure 4.6 A and B). However, fluorescence was detected in all other channels, particularly in the case of the IP-treated samples, and more in-depth analysis of proliferation, along with the expression of other cytokines (TNF, IL-2 and IL-17), was not possible (Figure 4.6). Furthermore, the viability of the T cells was quite low in the presence of the DC supernatants, regardless of treatment (Figure 4.7). It was however, possible to examine IFN $\gamma$  expression in the live cell population. As expected CD4<sup>+</sup> T cells cultured with supernatants from LPS-stimulated DC exhibited increased IFN $\gamma$  expression when compared to CD4<sup>+</sup> T cells cultured with supernatants from the untreated control (Figure 4.8). On the other hand, CD4<sup>+</sup> T cells treated with supernatants from DC pre-treated with either IP or HPP prior to LPS stimulation, exhibited a trend towards reduced expression of IFN $\gamma$  (Figure 4.8). These results were similar to the effects shown in the co-culture model with HPP-treated cells, however in this case IP treatment also yielded a similar result. It should however be noted that the ketoacids may be having an additional direct effect on the T cells given their presence in the cell supernatants.

#### *4.3.3 HPP and IP autofluorescence in PBMC can be resolved when replaced with fresh media after 18 hours.*

Prior to conducting any experiments assessing the direct effect of the ketoacids in PBMC from patient samples, it was important to develop a protocol to allow for analysis of these samples by flow cytometry (given the issues outlined above regarding ketoacid autofluorescence). T cell responses are normally assessed in PBMC following 4 days of culture with anti-CD3 in the presence/absence of the given treatment. As expected, when PBMC were treated with IP and HPP (both 500-1000  $\mu$ M) for 6 hours prior to stimulation with anti-CD3 (1  $\mu$ g/mL) for 4 days, the unstained samples exhibited high levels of autofluorescence in most channels on the LSRFortessa flow cytometer (Figure 4.9). This experimental set up was therefore not suitable for meaningful analysis and modification of the protocol was required. After careful optimisation, it was determined that the following protocol was sufficient to allow for flow cytometry based analysis in certain channels of the LSRFortessa flow cytometer. PBMC were pre-treated with IP and HPP for 6



hours, prior to stimulation with anti-CD3 (1 µg/mL) for 12 hours. The media, containing the ketoacids was then removed, and replaced with fresh media, and the cells were stimulated with anti-CD3 for a further 4 days (Figure 4.10). However, some channels still detected autofluorescence, particularly the BV channels, therefore going forward with this experimental set up, antibodies had to be carefully chosen to avoid these channels.

#### *4.3.4 HPP, carnosol and curcumin, but not IP, significantly reduce viability of PBMC isolated from IBD patients.*

It has previously been reported that IP has powerful immune suppressive effects in a murine experimental colitis model [258]. In order to determine if these results translate to a more clinical setting, the potential immunomodulatory properties of the ketoacids were examined in PBMC isolated from patients with IBD. Furthermore, the known polyphenolic inducers of HO-1, carnosol and curcumin, were included as controls given their previously reported anti-inflammatory activity [269,307,308,334–336]. PBMC were incubated with IP, HPP, (both 250–1000 µM), carnosol or curcumin (both 5 µM) for 6 hours, prior to stimulation with anti-CD3 (1 µg/mL) for 12 hours. The media, containing the ketoacids or polyphenols, was then removed, and replaced with fresh media, and the cells were stimulated with anti-CD3 (1 µg/mL) for a further 4 days. Viability was examined by flow cytometry. IP treatment had no effect on the viability of PBMC at any concentration tested, however, HPP, carnosol or curcumin treatment resulted in reduced PBMC viability, particularly at the higher concentrations (Figure 4.11). In order to further investigate if these treatments were reducing the viability of a specific T cell subset, cells were first gated for CD3 and CD8 expression, and viability was examined within the CD3<sup>+</sup>CD8<sup>+</sup> (CD8 T cell) subset and the CD3<sup>+</sup>CD8<sup>-</sup> subset (assumed to be CD4<sup>+</sup> T cells for the purpose of these experiments). CD8<sup>+</sup> T cells stimulated with anti-CD3 alone had reduced viability when compared to their CD4<sup>+</sup> counterparts (Figure 4.12). IP treatment exerted no effect on the viability of either T cell subset (Figure 4.12A). HPP, carnosol and curcumin treatment significantly reduced the viability of both CD4<sup>+</sup> and CD8<sup>+</sup> T cell subsets, however, these reductions appeared to be more pronounced in the CD8<sup>+</sup> subset, and showed greater statistical significance (Figure 4.12, HPP 1000 µM: p value = 0.0002 for CD4<sup>+</sup> cells vs. p value < 0.0001 for CD8<sup>+</sup> cells, carnosol: p value = 0.0026 for CD4<sup>+</sup> cells vs. p value = 0.0007 for

CD8<sup>+</sup> cells, curcumin: p value = 0.0120 for CD4<sup>+</sup> cells vs. p value = 0.0068 for CD8<sup>+</sup> cells). Any further examination of these samples by flow cytometry was gated within the live cell population to ensure that any changes seen were not due to dead cells skewing the data.

#### *4.3.5 HPP, IP, carnosol and curcumin reduce proliferation of CD4<sup>+</sup> and CD8<sup>+</sup> T cells in PBMC isolated from IBD patients.*

In order to investigate if the ketoacids have any effect on the proliferation of T cells from patients with IBD, PBMC were isolated from IBD patient samples and treated with IP or HPP (both 250–1000 µM), or carnosol or curcumin (both 5 µM) for 6 hours, prior to stimulation with anti-CD3 (1 µg/mL) for 12 hours. The media, containing the treatments was then removed, and replaced with fresh media, and the cells were stimulated with anti-CD3 (1 µg/mL) for a further 4 days. Expression of the proliferation marker, ki67, was assessed by flow cytometry in CD3<sup>+</sup>CD8<sup>-</sup> (CD4<sup>+</sup> T cells) and CD3<sup>+</sup>CD8<sup>+</sup> cells (CD8<sup>+</sup> T cells). IP and HPP significantly reduced the expression of ki67 in both CD4<sup>+</sup> and CD8<sup>+</sup> T cells (Figure 4.13 and 4.14), as did carnosol and curcumin (Figure 4.15 and 4.16). These results indicate that the ketoacids and polyphenols reduce the proliferation of T cells, which could otherwise contribute to the pathogenesis of IBD.

#### *4.3.6 HPP, IP, carnosol and curcumin reduce the secretion of cytokines from PBMC isolated from IBD patients.*

It was next investigated if the ketoacids have any effect on the secretion of cytokines from PBMC isolated from IBD patients. PBMC were treated with IP or HPP (both 250-1000 µM) or carnosol or curcumin (both 5 µM) for 6 hours, stimulated with anti-CD3 (1 µg/mL) for 12 hours, prior to replacement of the media, and stimulation with anti-CD3 (1 µg/mL) for a further 4 days. Supernatants were removed and analysed for secretion of cytokines by ELISA. HPP dose dependently reduced the secretion of IL-10, IFN $\gamma$  and IL-17 from PBMC, with the strongest reductions seen at the highest concentration tested (Figure 4.17). Similarly IP dose dependently reduced the secretion of all cytokines examined, however, more potent and significant effects were seen at all concentrations examined (Figure 4.18). Carnosol and curcumin also significantly reduced the secretion of all cytokines examined and appeared to be more potent than the ketoacids (Figure 4.19).

#### *4.3.7 HPP, IP, carnosol and curcumin reduce cytokine expression in CD4<sup>+</sup> and CD8<sup>+</sup> T cells from IBD patients.*

The effect of the ketoacids on cytokine expression in specific T cell subtypes was next investigated in PBMC isolated from IBD patients. CD4<sup>+</sup> T cells are the primary T cell subtype known to have a pathogenic role in IBD. However, CD8<sup>+</sup> T cells have recently been implicated as additional drivers of inflammation in this disease [337]. Therefore cytokine expression was examined in both CD4<sup>+</sup> and CD8<sup>+</sup> T cells. As before, PBMC from IBD patients were isolated and treated with IP or HPP (both 250–1000  $\mu$ M), or carnosol or curcumin (both 5  $\mu$ M) for 6 hours, prior to stimulation with anti-CD3 (1  $\mu$ g/mL) for 12 hours. The media was replaced with fresh media, and the cells were stimulated with anti-CD3 (1  $\mu$ g/mL) for a further 4 days. Expression of the cytokines IFN $\gamma$ , IL-17, IL-2 and TNF was measured by flow cytometry in CD3<sup>+</sup>CD8<sup>-</sup> (CD4 T cells) and CD3<sup>+</sup>CD8<sup>+</sup> cells (CD8 T cells). IP and HPP significantly reduced IFN $\gamma$  expression in CD4<sup>+</sup> T cells at the highest dose tested (Figure 4.20). Interestingly, there was no reduction in the levels of intracellular IL-17 in CD4<sup>+</sup> T cells upon treatment with either ketoacid (Figure 4.21). The highest concentration of HPP examined caused a significant reduction in IL-2 expression, while IP treatment had no effect on this cytokine at any concentration tested in CD4<sup>+</sup> T cells (Figure 4.22). Furthermore, neither ketoacid had an effect on the levels of intracellular TNF in CD4<sup>+</sup> T cells (Figure 4.23). Carnosol and curcumin also significantly reduced the expression of all cytokines tested in CD4<sup>+</sup> T cells (Figure 4.24 and 4.25). IP treatment significantly reduced IFN $\gamma$  expression but had no effect on IL-2 or TNF expression in CD8<sup>+</sup> T cells (Figure 4.26-4.28) and while HPP treatment had no effect on IL-2 expression, it did significantly reduce IFN $\gamma$  and TNF expression at the lowest concentration examined in CD8<sup>+</sup> T cells (Figure 4.26-4.28). Both carnosol and curcumin were also capable of significantly reducing the expression of all cytokines examined in CD8<sup>+</sup> T cells (Figure 4.29). These results demonstrate that the ketoacids and polyphenols have immunomodulatory properties in both CD4<sup>+</sup> and CD8<sup>+</sup> T cells from patients with IBD and appear to exhibit some differences in their anti-inflammatory activity.

#### *4.3.8 HPP, IP, carnosol and curcumin reduce the polyfunctionality of CD4<sup>+</sup> T cells in PBMC isolated from IBD patients.*

Not surprisingly, pro-inflammatory T cells can produce multiple different cytokines at once, and these so-called polyfunctional T cells have been shown to be more pathogenic in autoimmune conditions such as RA [338]. Therefore, it was of interest to further explore the effects of ketoacid treatment on the polyfunctionality of T cells. As before, PBMC were isolated from IBD patients, treated with IP or HPP (both 250-1000  $\mu$ M) or carnosol or curcumin (both 5  $\mu$ M) for 6 hours, stimulated with anti-CD3 (1  $\mu$ g/mL) for 12 hours, prior to replacement of the media, and stimulation with anti-CD3 (1  $\mu$ g/mL) for a further 4 days. CD3<sup>+</sup>CD8<sup>-</sup> cells (CD4 T cells) expressing IFN $\gamma$ <sup>+</sup>IL-17<sup>+</sup>, IFN $\gamma$ <sup>+</sup>TNF<sup>+</sup>, IL-2<sup>+</sup>TNF<sup>+</sup>, and IL-2<sup>+</sup>IFN $\gamma$ <sup>+</sup> were examined by flow cytometry. Anti-CD3 stimulation resulted in very low percentages of IFN $\gamma$ <sup>+</sup>IL-17<sup>+</sup> cells, however, IP-treatment significantly reduced the percentage of these double positive cells at the top concentration examined (Figure 4.30B). HPP treatment also trended towards a reduction in these cells at the 1000  $\mu$ M concentration ( $p = 0.08$ ) (Figure 4.30C). Both IP and HPP were capable of significantly reducing the frequency of IFN $\gamma$ <sup>+</sup>TNF<sup>+</sup> double positive cells (Figure 4.31). Similar to the effect seen in section 4.3.7, where HPP but not IP was capable of reducing IL-2 expression, the top concentration of HPP significantly reduced the frequency of IL-2<sup>+</sup>TNF<sup>+</sup> double positive cells, while IP had no effect at any concentration examined (Figure 4.32). Both IP and HPP significantly reduced the percentage of IL-2<sup>+</sup>IFN $\gamma$ <sup>+</sup> double positive cells (Figure 4.33), while carnosol and curcumin treatment significantly reduced the frequency of IFN $\gamma$ <sup>+</sup>IL-17<sup>+</sup> (Figure 4.34), IFN $\gamma$ <sup>+</sup>TNF<sup>+</sup> (figure 4.35), and IL-2<sup>+</sup>IFN $\gamma$ <sup>+</sup> cells (Figure 4.37) compared to anti-CD3 stimulation alone. Curcumin treatment also resulted in a trend towards a reduction in IL-2<sup>+</sup>TNF<sup>+</sup> double positive cells ( $p = 0.05$ ), while carnosol treatment had no effect on these cells (Figure 4.36). Overall, these results indicate that the ketoacids and polyphenols can reduce pro-inflammatory polyfunctional T cells in PBMC from IBD patients.

#### *4.3.9 Ketoacid and polyphenol treatment have subtly different effects in CD4<sup>+</sup> T cells in PBMC isolated from patients with ulcerative colitis and Crohn's disease.*

As mentioned previously, IBD can be classified as either CD or UC. In order to gain further insight into whether the ketoacids represent a potential treatment for these diseases, data was stratified further into two groups; whether the patients had either CD or UC, and analysis was carried out on the data for each of these disease subsets. Data generated from the CD4<sup>+</sup> T cells was the main focus in this analysis. It was determined that HPP treatment has a more pronounced effect on proliferation and cytokine expression (in particular IFN $\gamma$  and TNF) in CD4<sup>+</sup> T cells isolated from patients with UC, compared to patients with CD (Figure 4.38). On the other hand, IP reduced the proliferation of CD4<sup>+</sup> T cells from patients with CD when compared to patients with UC (Figure 4.39). Treatment with this ketoacid did, however, dose dependently reduce IFN $\gamma$  expression in CD4<sup>+</sup> T cells from patients with both conditions, with a significant decrease at all concentrations tested in T cells from UC patients (Figure 4.39). Carnosol and curcumin treatment decreased proliferation and expression of IFN $\gamma$ , IL-17 and IL-2 at similar rates between CD and UC patients (Figure 4.40) and, while the polyphenols significantly reduced expression of TNF in patients with CD, this was not the case in PBMC from patients with UC (Figure 4.40). These results indicate that despite the similarities between these diseases, there still may subtle differences that need to be considered when considering appropriate therapies.

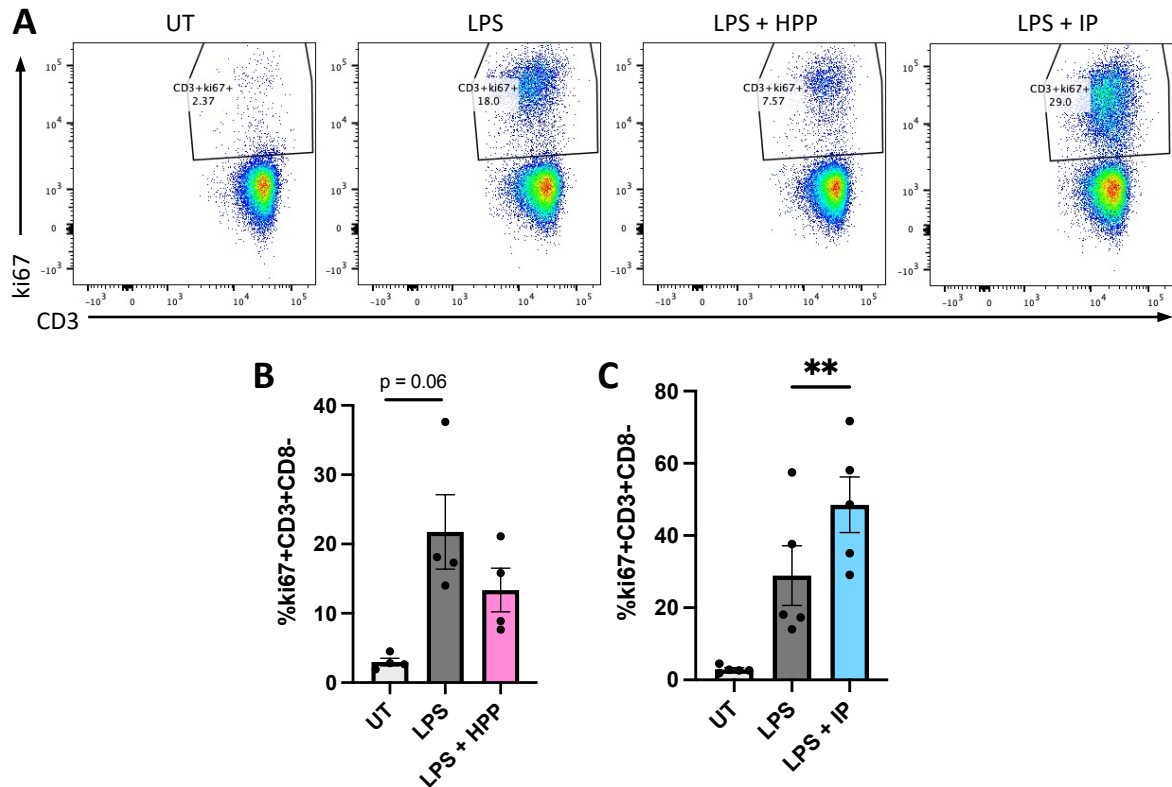


**Figure 4.1 Ketoacid-treated LPS-stimulated DC alter the expression of ki67 in CD4<sup>+</sup> T cells upon co-culture.**

Primary human DC were left untreated (UT) or pre-treated with HPP or IP (1000  $\mu$ M) for 6 hours prior to the addition of LPS (100 ng/ml) for a further 24 hours. The RPMI was replaced on these DC before subsequently culturing them with purified CD4<sup>+</sup> T cells for 5 days. **(A)** Dot plots depicting ki67 expression (as a measure of proliferation) from one representative experiment. **(B & C)** Pooled data showing the mean ( $\pm$  SEM) of ki67<sup>+</sup> as a percentage of CD3<sup>+</sup> CD8<sup>-</sup> cells from 4-5 healthy donors. Repeated measures one-way ANOVA, with Dunnett's multiple comparisons post hoc test, was used to determine statistical significance by comparing means of treatment groups against the mean of the control group (\*\*  $p < 0.01$ ).

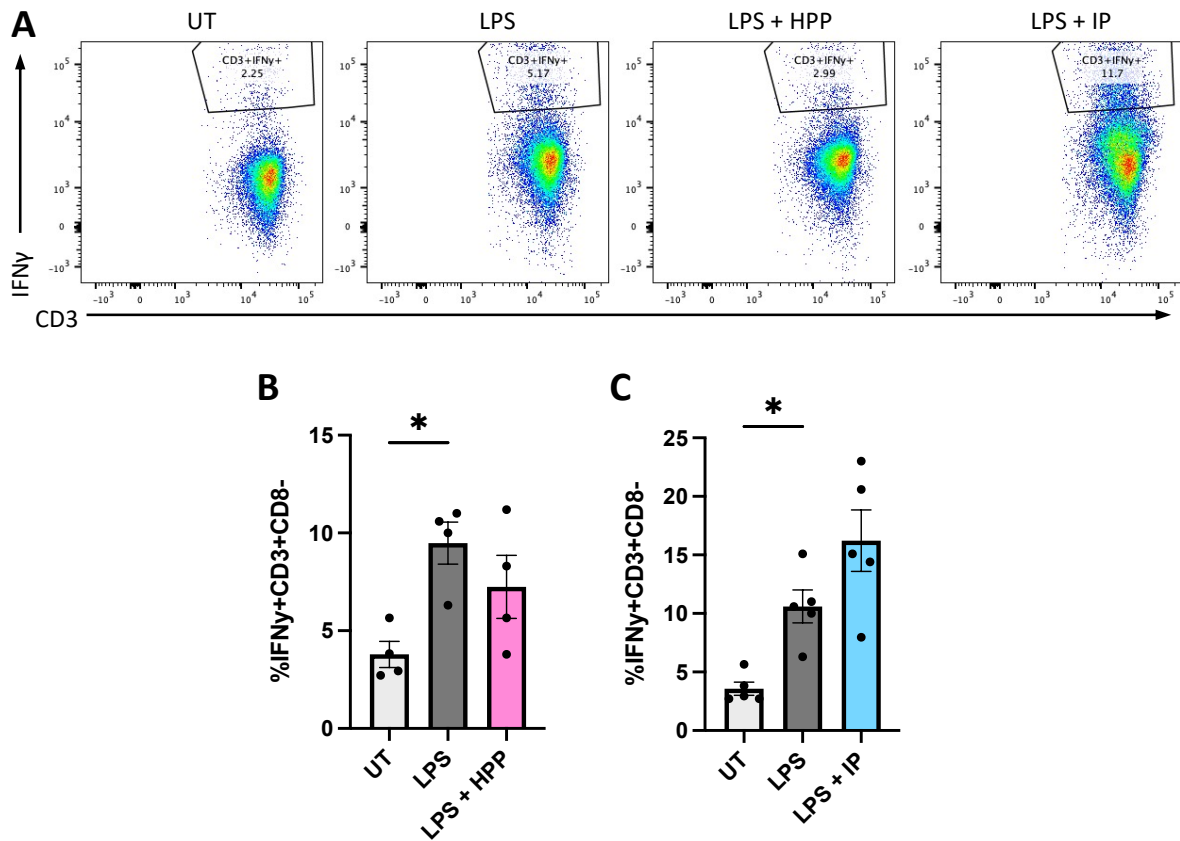


**Figure 4.2 Ketoacid-treated LPS-stimulated DC alter the expression of IFN $\gamma$  in CD4 $^+$  T cells upon co-culture.**

Primary human DC were left untreated (UT) or pre-treated with HPP or IP (1000  $\mu$ M) for 6 hours prior to the addition of LPS (100 ng/ml) for a further 24 hours. The RPMI was replaced on these DC before subsequently culturing them with purified CD4 $^+$  T cells for 5 days. **(A)** Dot plots depicting IFN $\gamma$  expression from one representative experiment. **(B & C)** Pooled data showing the mean ( $\pm$  SEM) of IFN $\gamma$  $^+$  as a percentage of CD3 $^+$  CD8 $^-$  cells from 4-5 healthy donors. Repeated measures one-way ANOVA, with Dunnett's multiple comparisons post hoc test, was used to determine statistical significance by comparing means of treatment groups against the mean of the control group (\*  $p < 0.05$ ).

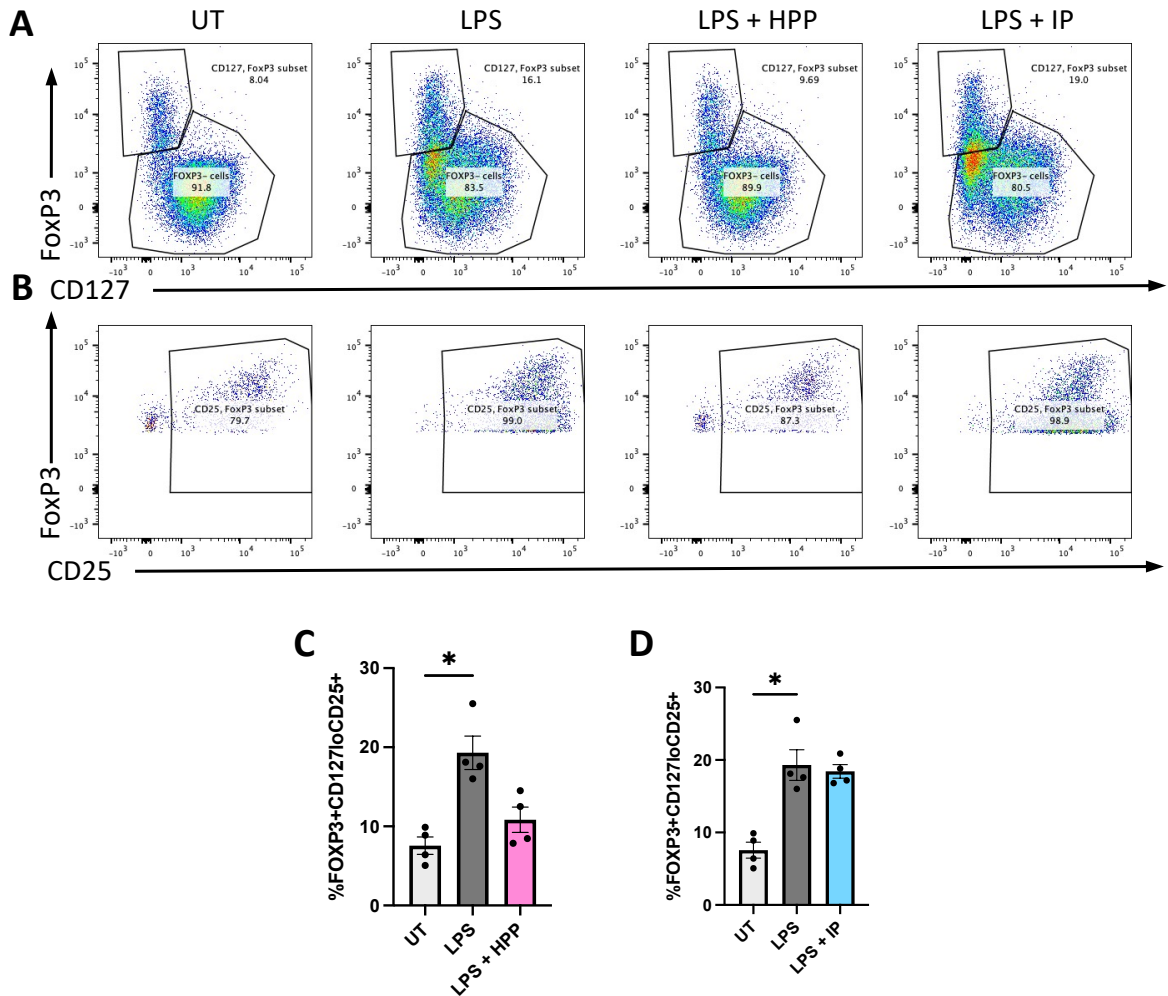


**Figure 4.3 The effect of HPP- and IP-treated LPS-stimulated DC on the frequency of Tregs in CD4<sup>+</sup> T cells upon co-culture.**

Primary human DC were left untreated (UT) or pre-treated with HPP or IP (1000  $\mu$ M) for 6 hours prior to the addition of LPS (100 ng/ml) for a further 24 hours. The RPMI was replaced on these DC before subsequently culturing them with purified CD4<sup>+</sup> T cells for 5 days. **(A)** Dot plots depicting FoxP3 and CD127 expression from one representative experiment, FoxP3<sup>+</sup>CD127<sup>lo</sup> cells were selected. **(B)** Dot plots depicting FoxP3 and CD25 expression from one representative experiment, FoxP3<sup>+</sup>CD25<sup>+</sup> cells were selected. **(C & D)** Pooled data showing the mean ( $\pm$  SEM) of FOXP3<sup>+</sup>CD127<sup>lo</sup>CD25<sup>+</sup> cells as a percentage of CD4<sup>+</sup> cells from 4 healthy donors. Repeated measures one-way ANOVA, with Dunnett's multiple comparisons post hoc test, was used to determine statistical significance by comparing means of treatment groups against the mean of the control group (\*  $p < 0.05$ ).



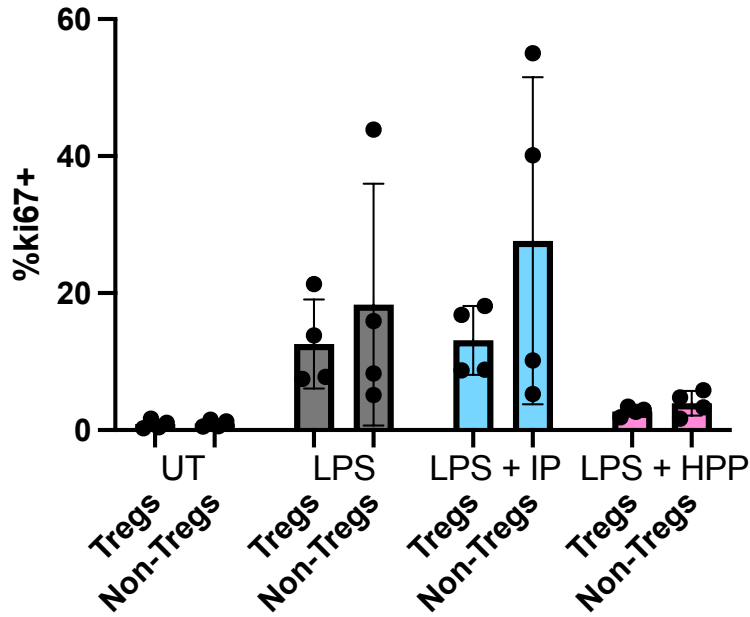


**Figure 4.4 Ketoacid treated DC do not favour an increase in the proliferation of Tregs over non-Tregs in CD4<sup>+</sup> T cells upon co-culture.**

Primary human DC were left untreated (UT) or pre-treated with HPP or IP (1000  $\mu$ M) for 6 hours prior to the addition of LPS (100 ng/ml) for a further 24 hours. The RPMI was replaced on these DC before subsequently culturing them with purified CD4<sup>+</sup> T cells for 5 days. Pooled data showing the mean ( $\pm$  SEM) of ki67<sup>+</sup> cells as a percentage of CD4<sup>+</sup> cells from 4 healthy donors for Tregs (FOXP3<sup>+</sup>CD127<sup>lo</sup>CD25<sup>+</sup>) vs. non-Tregs (FOXP3<sup>-</sup>).

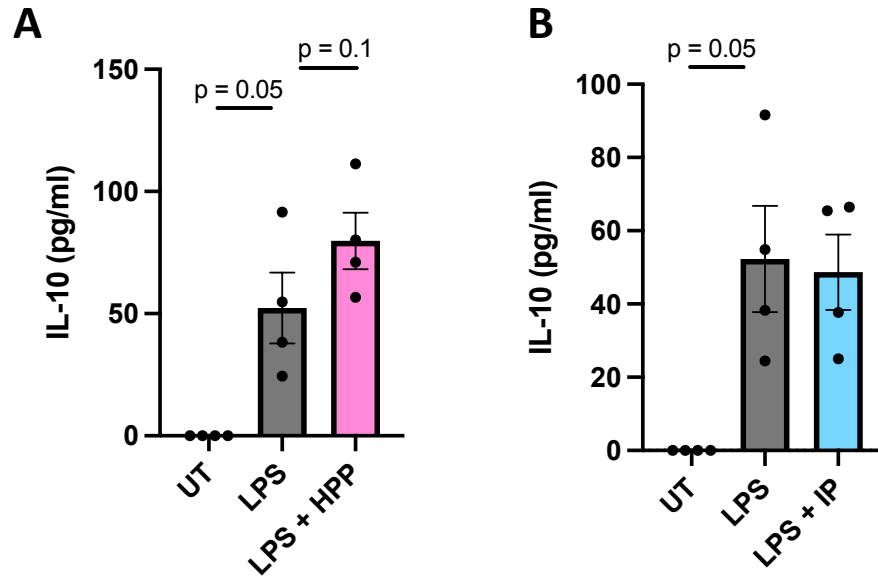


**Figure 4.5 IL-10 secretion is not altered in co-cultures of ketoacid-treated LPS-stimulated DC and CD4<sup>+</sup> T cells.**

Primary human DC were left untreated (UT) or pre-treated with **(A)** HPP or **(B)** IP (1000  $\mu$ M) for 6 hours prior to the addition of LPS (100 ng/ml) for a further 24 hours. The RPMI was replaced on these DC before subsequently culturing them with purified CD4<sup>+</sup> T cells for 5 days. Cell supernatants were assessed for IL-10 secretion by ELISA. Pooled data depicts mean ( $\pm$ SEM) cytokine concentrations for 4 healthy donors (means of three technical replicates per donor). Repeated measures one-way ANOVA, with Dunnett's multiple comparisons post hoc test, was used to determine statistical significance by comparing means of treatment groups against the mean of the control group.

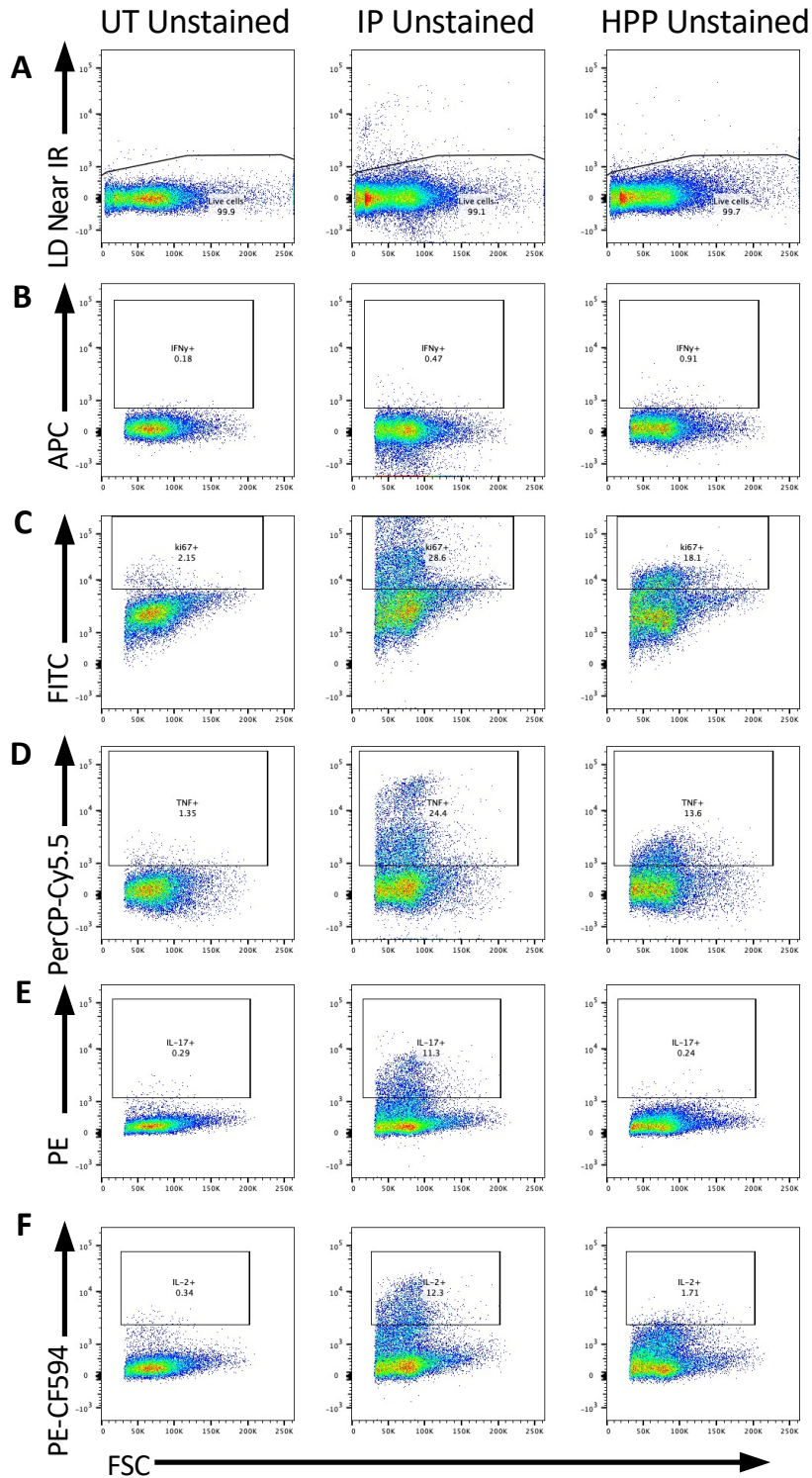


**Figure 4.6 Supernatants from ketoacid treated DC induce autofluorescence in CD4<sup>+</sup> T cells.**

Primary human DC were left untreated (UT) or incubated with IP or HPP (both 500  $\mu$ M) for 6 hours prior to stimulation with LPS (100 ng/ml) for 24 hours. Supernatants were removed and added to purified CD4<sup>+</sup> T cells at a 1:2 ratio in the presence of anti-CD3 (1  $\mu$ g/mL) and anti-CD28 (2  $\mu$ g/mL) for 4 days. Samples were analysed on a BD LSRFortessa without staining, looking at autofluorescence in the channels required for the markers in the experiment: **(A)** LD Near IR, **(B)** APC, **(C)** FITC, **(D)** PerCP-Cy5.5, **(E)** PE, and **(F)** PE-CF594.

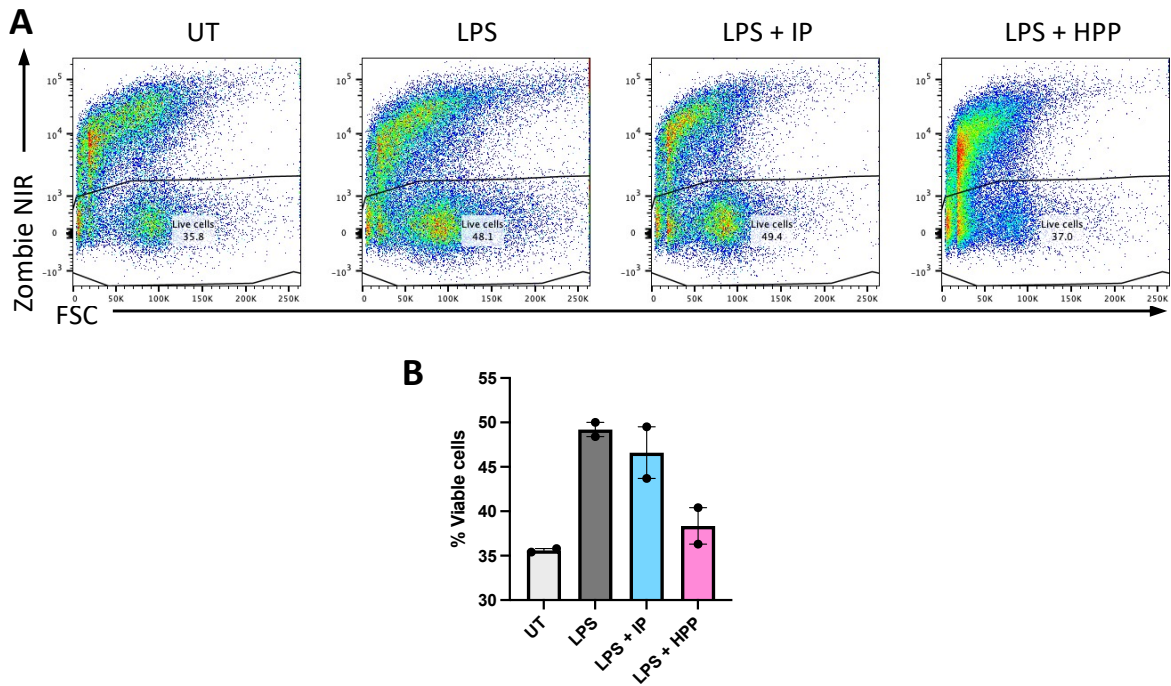


**Figure 4.7 Supernatants from ketoacid treated DC impair the viability of CD4<sup>+</sup> T cells.**

Primary human DC were left untreated (UT) or pre-treated with IP or HPP (both 500  $\mu$ M) for 6 hours prior to the addition of LPS (100 ng/ml) for a further 24 hours. Supernatants were removed from the DC and added to purified CD4<sup>+</sup> T cells at a 1:2 ratio in the presence of anti-CD3 (1  $\mu$ g/ml) and anti-CD28 (2  $\mu$ g/ml) for 4 days. Cells were stained for viability using Zombie NIR<sup>TM</sup> Fixable Viability kit. Debris was excluded by gating, and viable cells were defined as Zombie NIR<sup>-</sup>. **(A)** Dot plots depicting Zombie NIR expression from one representative experiment. **(B)** Pooled data showing the mean ( $\pm$  SEM) of viable cells as a percentage from 2 healthy controls.

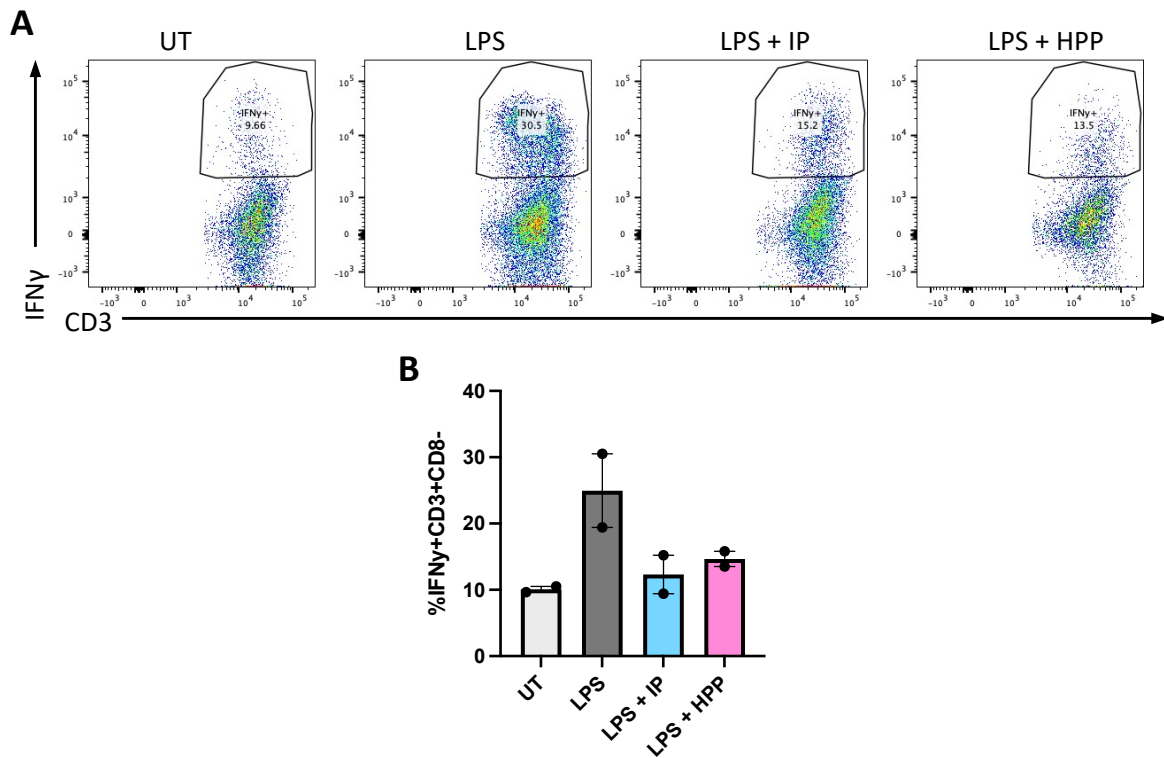


**Figure 4.8 Supernatants from IP or HPP treated DC reduce the expression of IFN $\gamma$  in CD4 $^+$  T cells.**

Primary human DC were left untreated (UT) or pre-treated with IP or HPP (both 500  $\mu$ M) for 6 hours prior to the addition of LPS (100 ng/ml) for a further 24 hours. Supernatants were removed from the DC and added to purified CD4 $^+$  T cells at a 1:2 ratio in the presence of anti-CD3 (1  $\mu$ g/ml) and anti-CD28 (2  $\mu$ g/ml) for 4 days. **(A)** Dot plots depicting IFN $\gamma$  expression from one representative experiment. **(B)** Pooled data showing the mean ( $\pm$  SEM) of IFN $\gamma^+$  as a percentage of CD3 $^+$  CD8 $^-$  cells from 2 healthy donors.

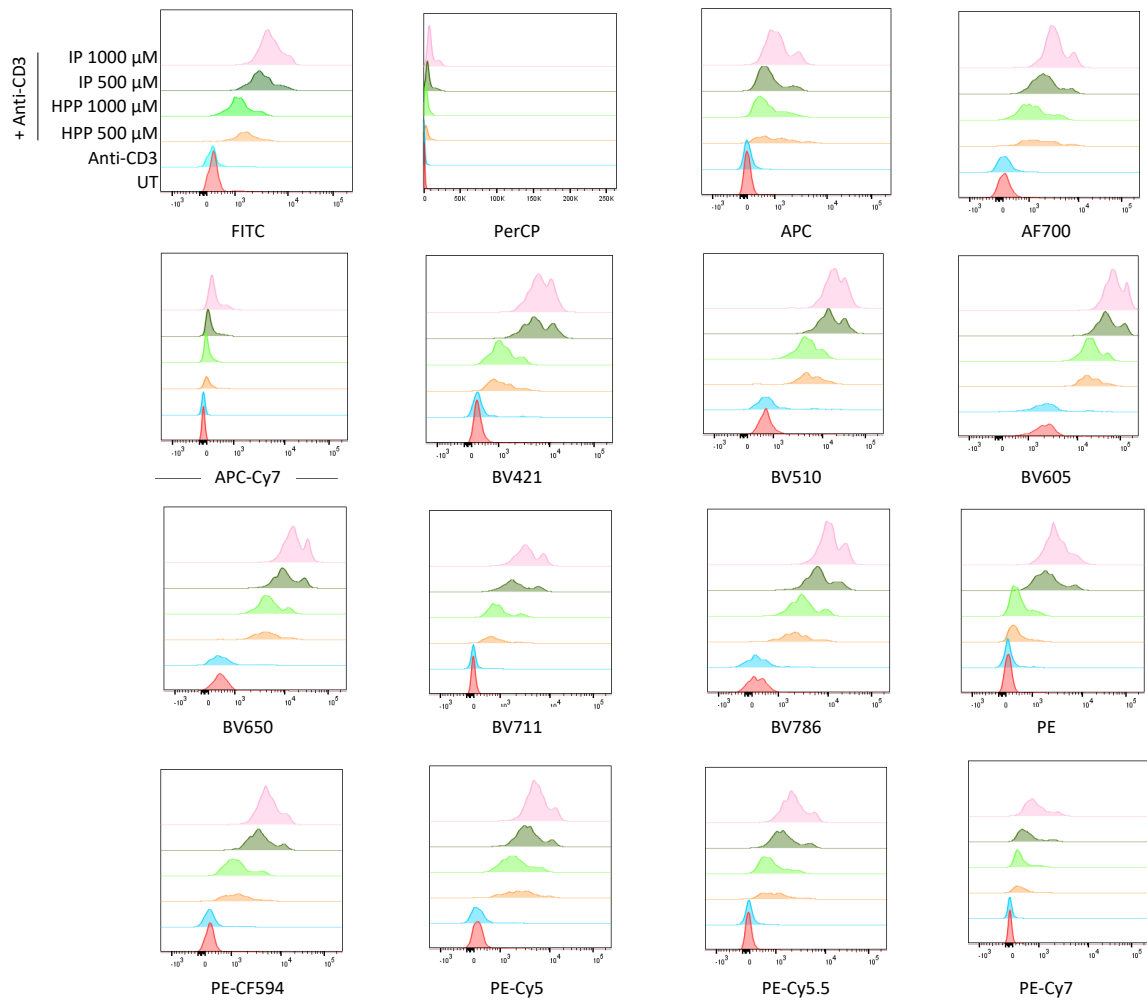


**Figure 4.9 IP and HPP treatment causes autofluorescence in PBMC after 4 days.** PBMC were left untreated (UT) or incubated with HPP or IP (500 - 1000  $\mu$ M) for 6 hours prior to stimulation with anti-CD3 (1  $\mu$ g/mL) for 4 days, in the presence of ketoacids. Samples were analysed on all channels of a BD LSRFortessa without staining. Histograms showing fluorescence of samples compared to UT control and cells stimulated with anti-CD3 only.

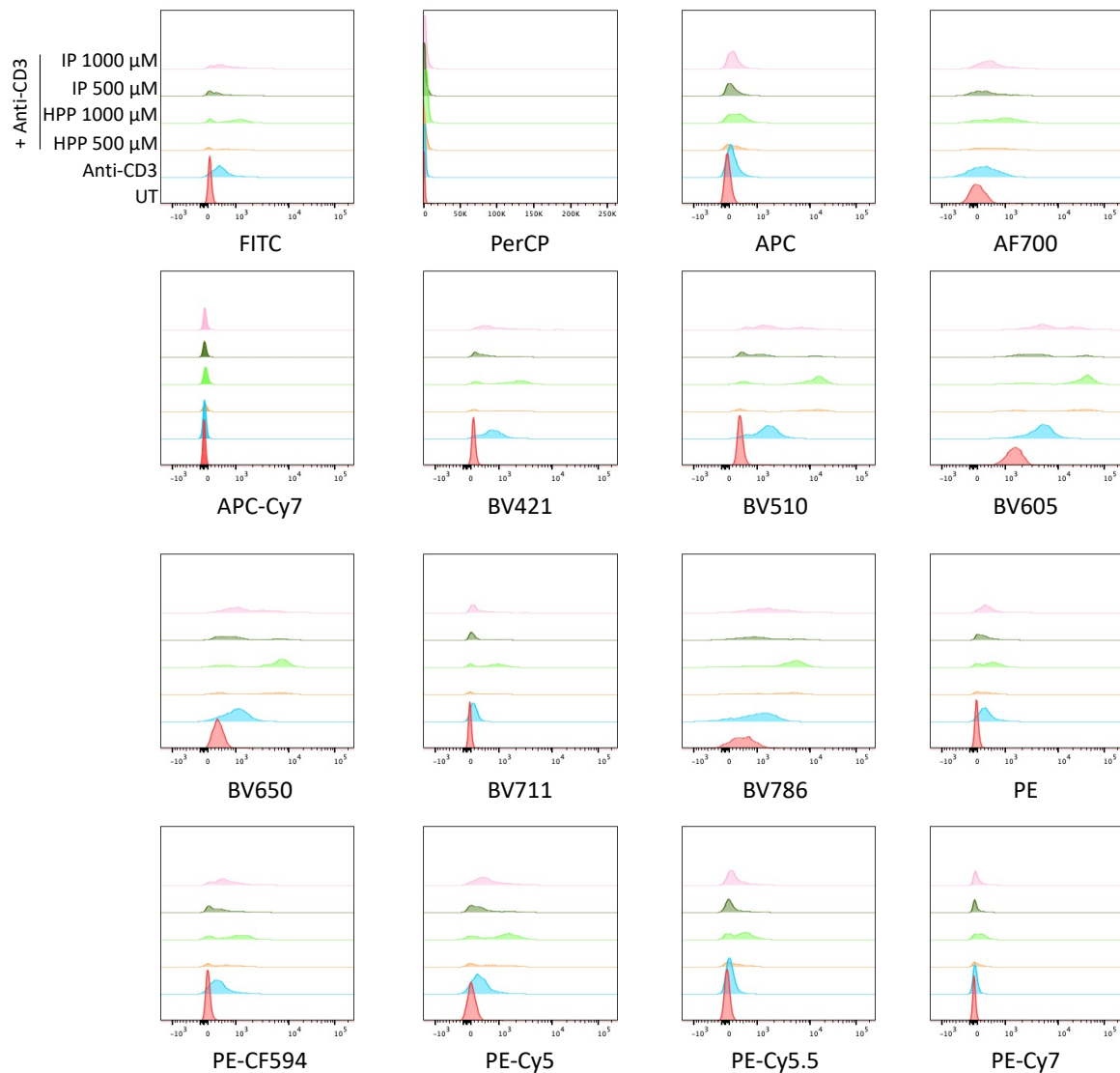


**Figure 4.10 IP and HPP treatment induce less autofluorescence in PBMC when removed after 18 hours and incubated with anti-CD3 only for a further 4 days.**

PBMC were left untreated (UT) or incubated with HPP or IP (500 - 1000  $\mu\text{M}$ ) for 6 hours prior to stimulation with anti-CD3 (1  $\mu\text{g}/\text{mL}$ ) for 12 hours. The media was replaced with fresh media, and cells were incubated for a further 4 days with anti-CD3 (1  $\mu\text{g}/\text{mL}$ ) stimulation, without ketoacids. Samples were analysed on all channels of a BD LSRFortessa without staining. Histograms showing fluorescence of samples compared to UT control and cells stimulated with anti-CD3 only.

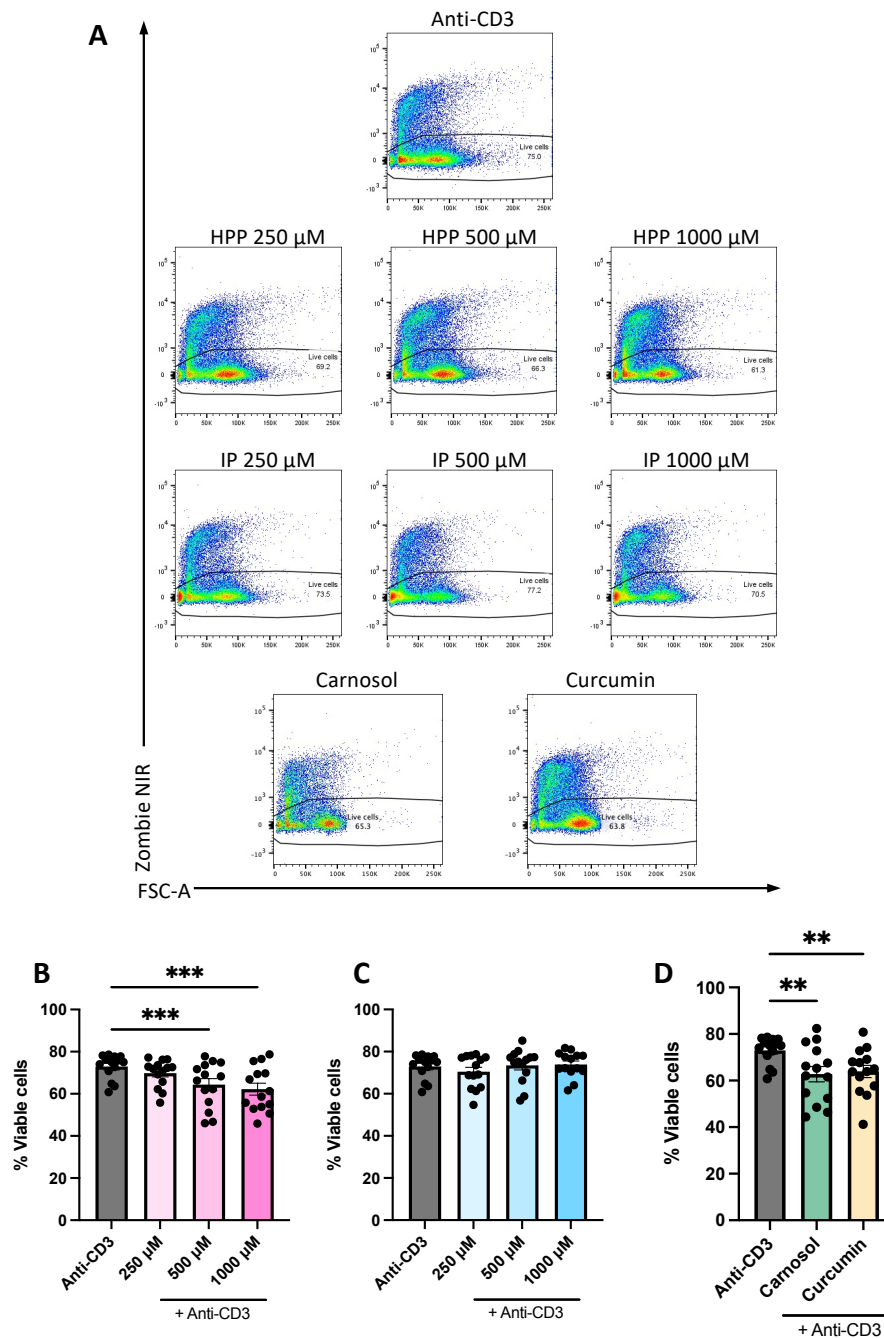


**Figure 4.11 IP is non-toxic to *ex-vivo* stimulated PBMC from patients with IBD, while HPP, carnosol and curcumin all show significant, albeit mild, reductions in viability.** PBMC isolated from IBD patients were treated with **(B)** HPP or **(C)** IP (both 250  $\mu$ M – 1000  $\mu$ M), or **(D)** carnosol or curcumin (both 5  $\mu$ M) for 6 hours prior to stimulation with anti-CD3 (1  $\mu$ g/mL) for 12 hours. The media was replaced with fresh media, and incubated for a further 4 days with anti-CD3 (1  $\mu$ g/mL) stimulation, without ketoacids, carnosol or curcumin. Cells were stained for viability using Zombie NIR™ Fixable Viability kit. Debris was excluded by gating, and viable cells were defined as Zombie NIR<sup>-</sup>. **(A)** Dot plots depicting Zombie NIR expression from one representative experiment. **(B, C & D)** Pooled data showing the mean ( $\pm$  SEM) of viable cells as a percentage from 14 IBD patients. Repeated measures one-way ANOVA, with Dunnett's multiple comparisons post hoc test, was used to determine statistical significance by comparing means of treatment groups against the mean of the control group (\*\*\*)  $p < 0.001$ , \*\*  $p < 0.01$ ).



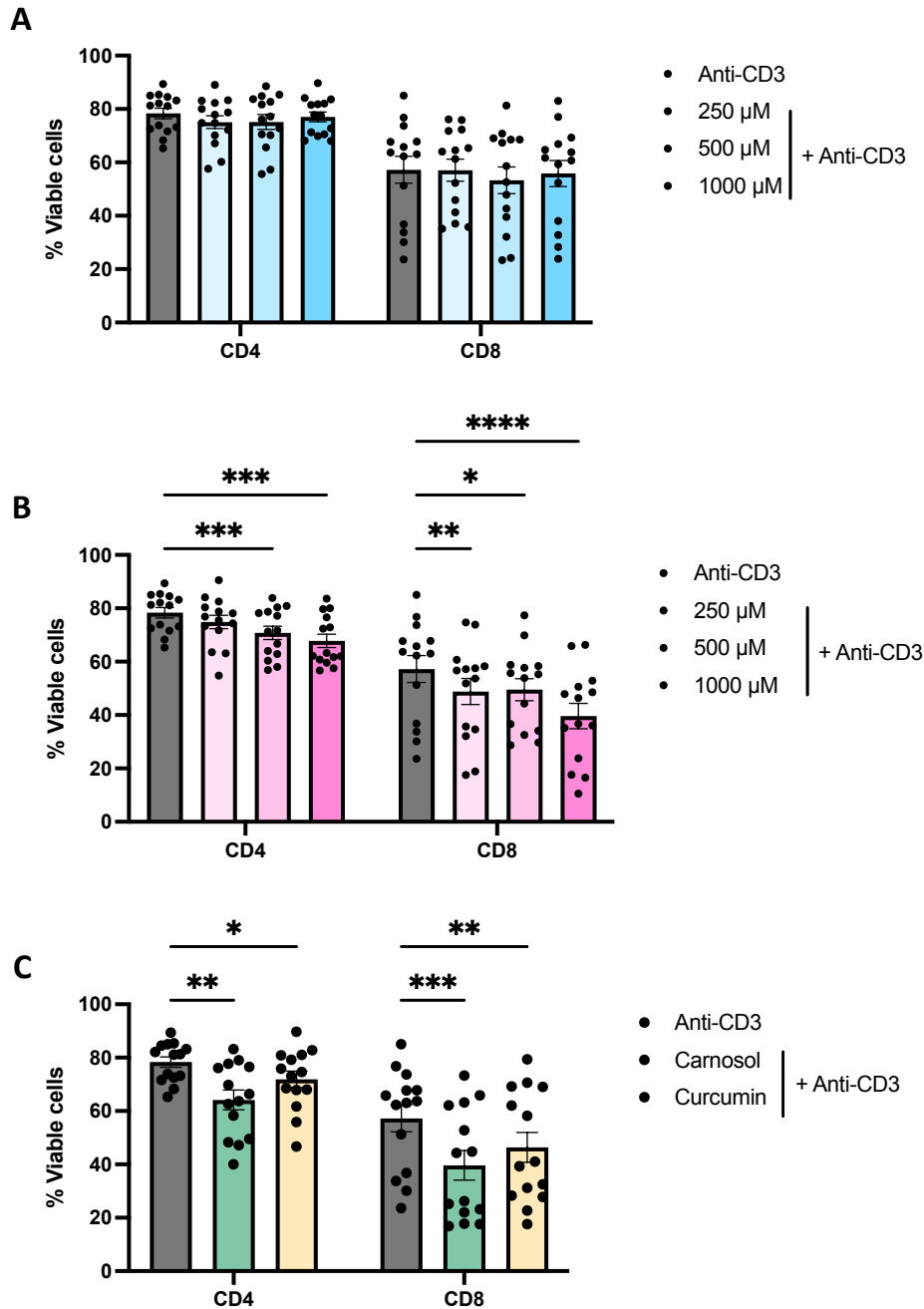


**Figure 4.12 HPP, carnosol and curcumin more significantly reduce the viability of CD8<sup>+</sup> T cells compared to CD4<sup>+</sup> T cells, while IP has no effect on the viability of either cell type.** PBMC isolated from IBD patients were treated with **(A)** HPP or **(B)** IP (both 250  $\mu$ M – 1000  $\mu$ M), or **(C)** carnosol or curcumin (both 5  $\mu$ M) for 6 hours prior to stimulation with anti-CD3 (1  $\mu$ g/mL) for 12 hours. The media was replaced with fresh media, and incubated for a further 4 days with anti-CD3 (1  $\mu$ g/mL) stimulation, without ketoacids, carnosol or curcumin. Cells were stained for viability using Zombie NIR™ Fixable Viability kit. Cells were initially gated for CD3 and CD8 expression, and viable cells were defined as Zombie NIR<sup>-</sup>. **(A, B & C)** Pooled data showing the mean ( $\pm$  SEM) of viable cells as a percentage from 14 IBD patients. Two-way ANOVA, with Šídák's multiple comparisons post hoc test, was used to determine statistical significance by comparing means of treatment groups against the mean of the control group within each cell subtype (\*\*\*\*  $p < 0.0001$ , \*\*\*  $p < 0.001$ , \*\*  $p < 0.01$ , \*  $p < 0.05$ ).

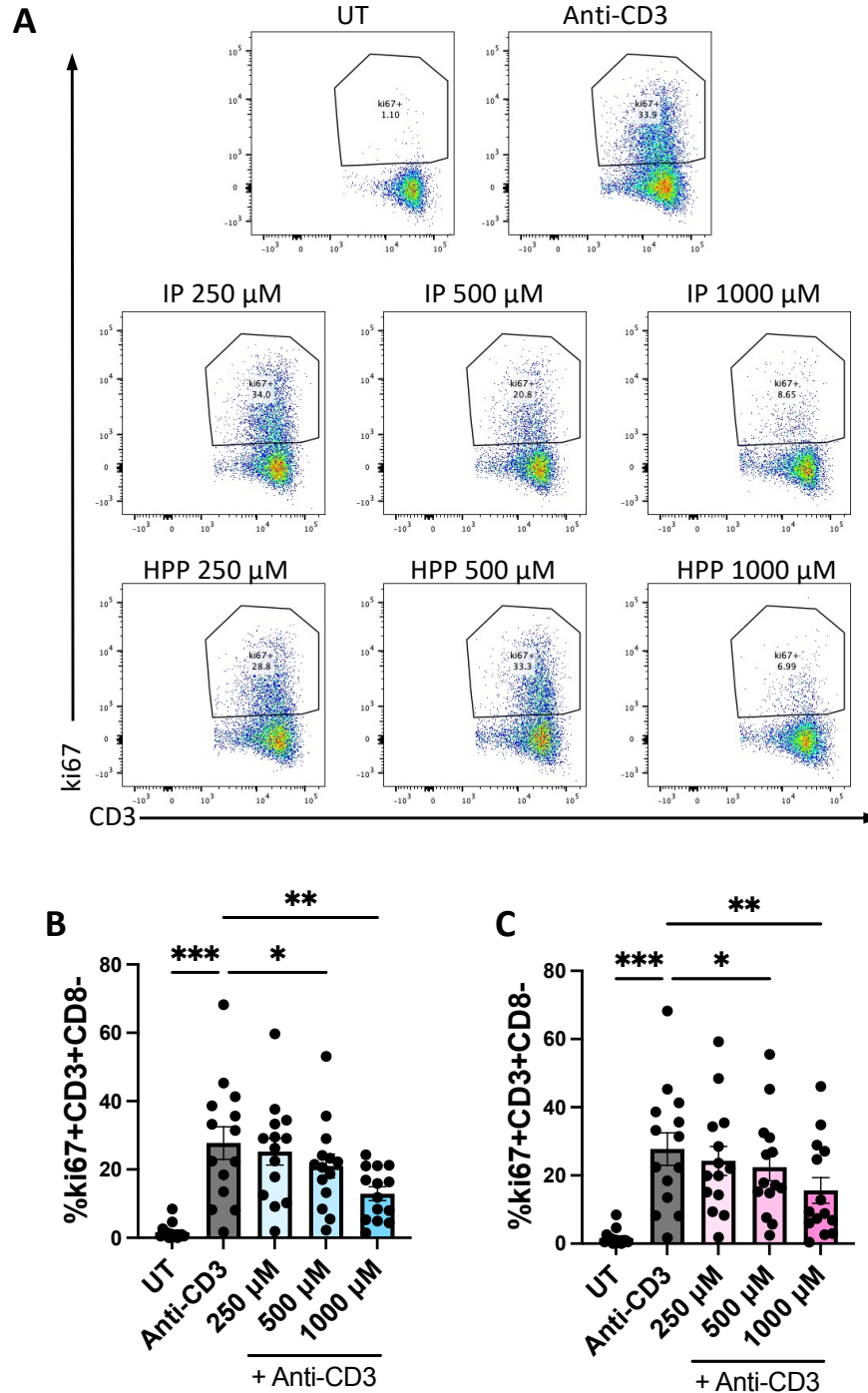


**Figure 4.13 HPP and IP reduce proliferation of CD4<sup>+</sup> T cells in *ex-vivo* stimulated PBMC from patients with IBD.**

PBMC isolated from IBD patients were treated with **(B)** IP or **(C)** HPP (250  $\mu$ M – 1000  $\mu$ M) for 6 hours prior to stimulation with anti-CD3 (1  $\mu$ g/mL) for 12 hours. After 18 hours culture media was replaced with fresh media and cells were incubated for a further 4 days with anti-CD3 (1  $\mu$ g/mL) stimulation, without ketoacids. **(A)** Dot plots depicting ki67 expression (as a measure of proliferation) by CD3<sup>+</sup>CD8<sup>-</sup> cells from one representative experiment. **(B & C)** Pooled data (n = 14) depicting the mean  $\pm$  SEM of ki67<sup>+</sup> in CD3<sup>+</sup>CD8<sup>-</sup> T cells. Repeated measures one-way ANOVA, with Dunnett's multiple comparisons post hoc test, was used to determine statistical significance by comparing means of treatment groups against the mean of the control group (\*\*\*) p < 0.001, \*\* p < 0.01, \* p < 0.05).

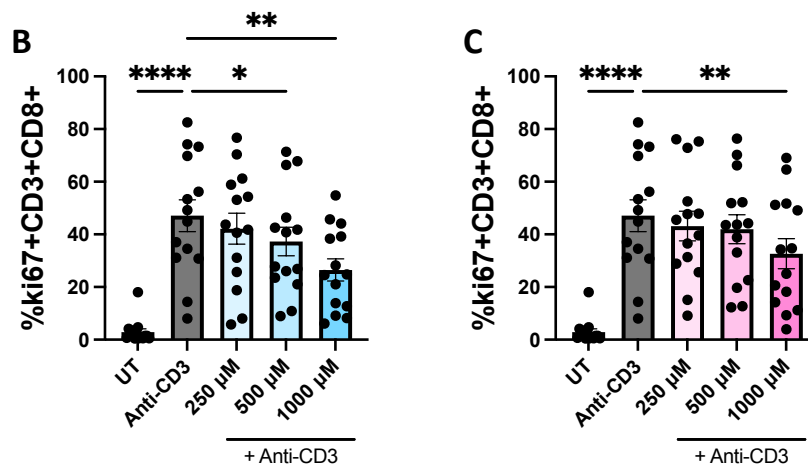
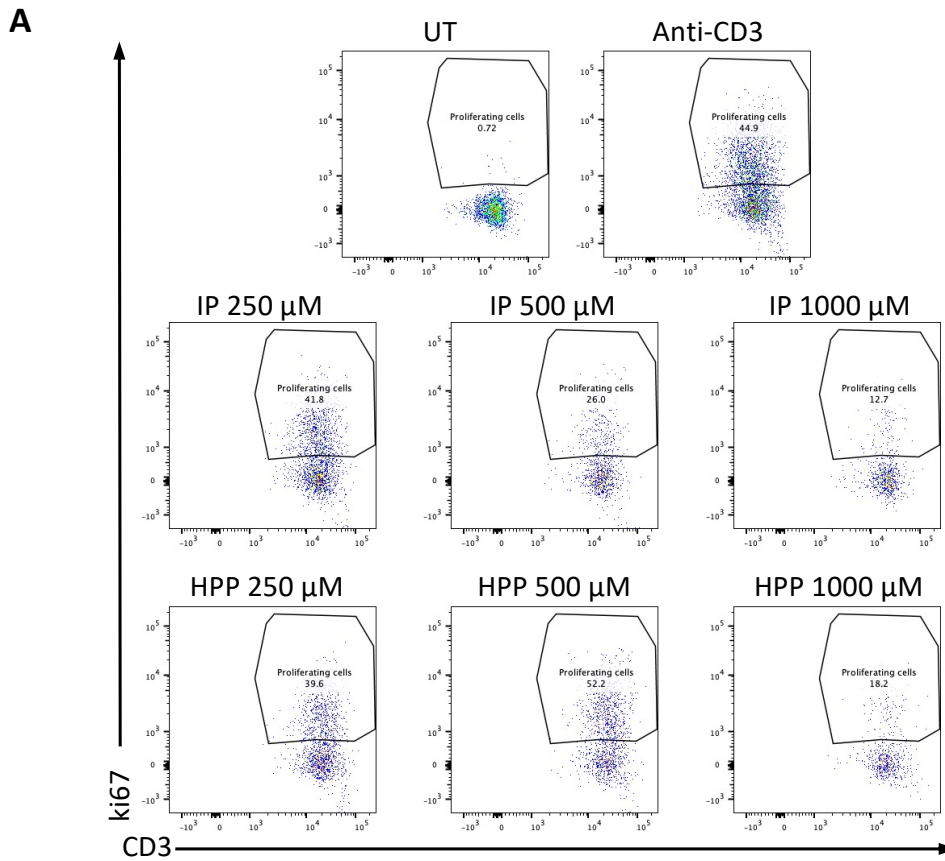


**Figure 4.14 HPP and IP reduce proliferation of CD8<sup>+</sup> cells in *ex-vivo* stimulated PBMC from patients with IBD.**

PBMC isolated from IBD patients were treated with **(B)** IP or **(C)** HPP (250  $\mu$ M – 1000  $\mu$ M) for 6 hours prior to stimulation with anti-CD3 (1  $\mu$ g/mL) for 12 hours. After 18 hours culture media was replaced with fresh media and cells were incubated for a further 4 days with anti-CD3 (1  $\mu$ g/mL) stimulation, without ketoacids. **(A)** Dot plots depicting ki67 expression (as a measure of proliferation) by CD3<sup>+</sup>CD8<sup>+</sup> cells from one representative experiment. **(B & C)** Pooled data (n = 14) depicting the mean  $\pm$  SEM of ki67<sup>+</sup> in CD3<sup>+</sup>CD8<sup>+</sup> T cells. Repeated measures one-way ANOVA, with Dunnett's multiple comparisons post hoc test, was used to determine statistical significance by comparing means of treatment groups against the mean of the control group (\*\*\*\* p < 0.0001, \*\* p < 0.01, \* p < 0.05).

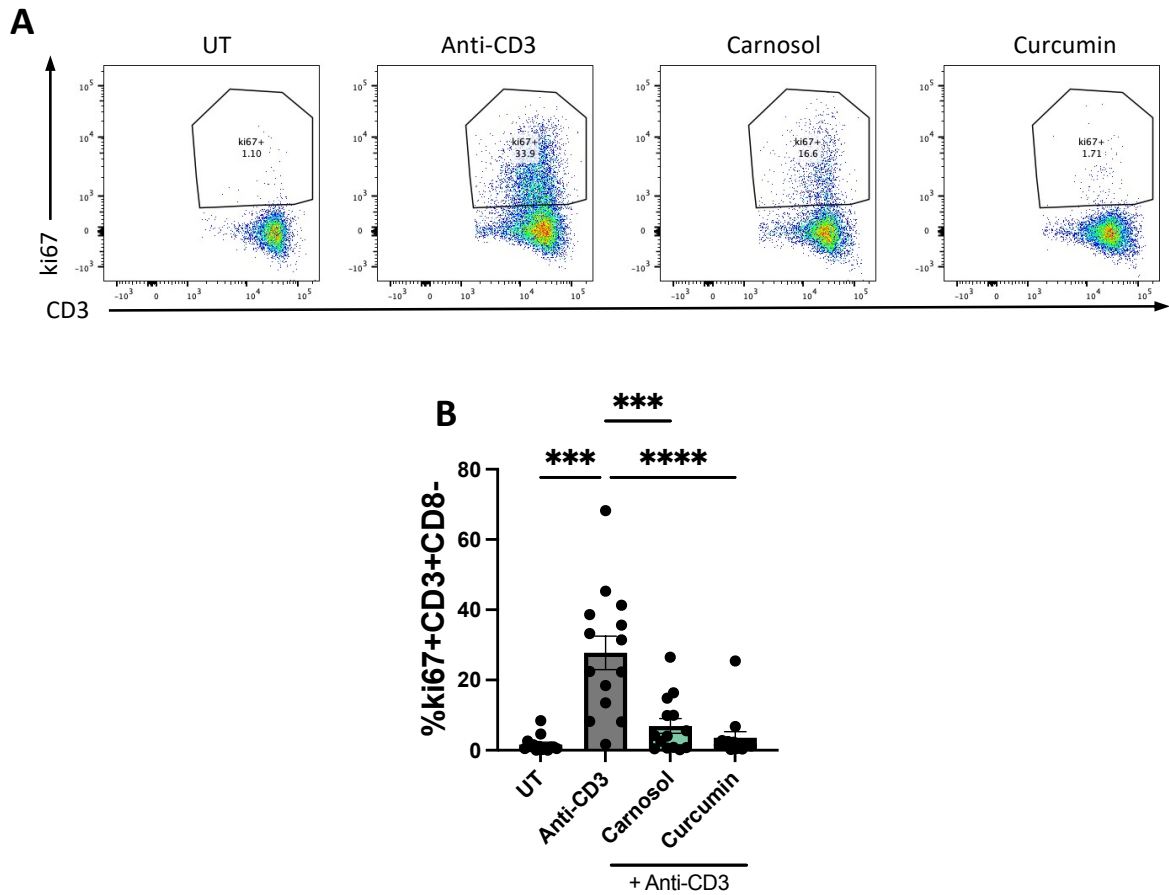


**Figure 4.15 Carnosol and curcumin reduce proliferation of CD4<sup>+</sup> T cells in *ex-vivo* stimulated PBMC from patients with IBD.**

PBMC isolated from IBD patients were treated with carnosol or curcumin (5  $\mu$ M) for 6 hours prior to stimulation with anti-CD3 (1  $\mu$ g/mL) for 12 hours. After 18 hours culture media was replaced with fresh media and cells were incubated for a further 4 days with anti-CD (1  $\mu$ g/mL) 3 stimulation, without carnosol or curcumin. **(A)** Dot plots depicting ki67 expression (as a measure of proliferation) by CD3<sup>+</sup>CD8<sup>-</sup> cells from one representative experiment. **(B)** Pooled data (n = 14) depicting the mean  $\pm$  SEM of ki67<sup>+</sup> in CD3<sup>+</sup>CD8<sup>-</sup> T cells. Repeated measures one-way ANOVA, with Dunnett's multiple comparisons post hoc test, was used to determine statistical significance by comparing means of treatment groups against the mean of the control group (\*\*\*) p < 0.001).

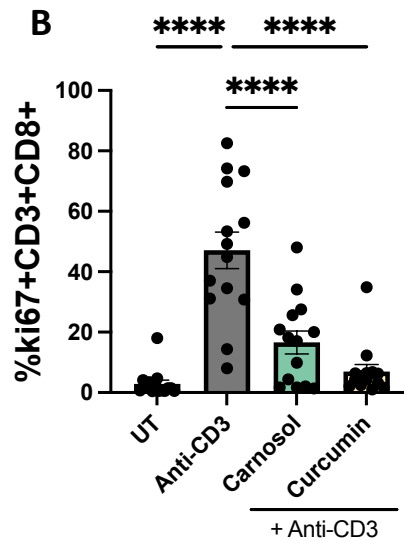
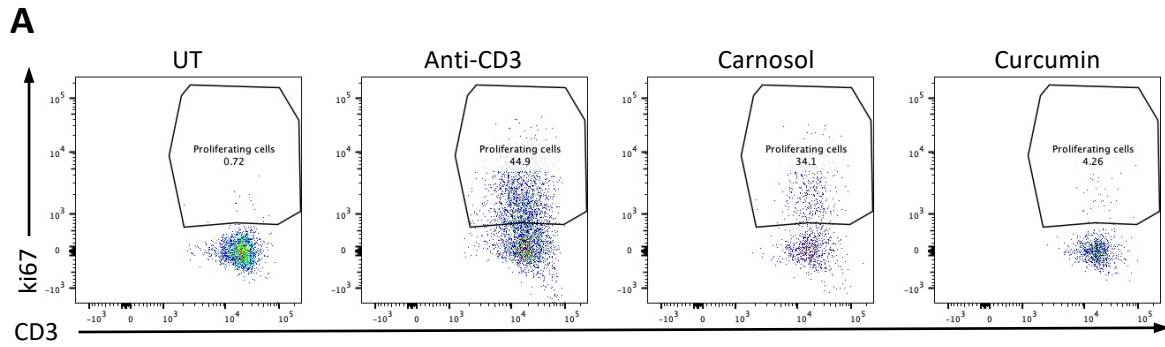


**Figure 4.16 Carnosol and curcumin reduce proliferation of CD8<sup>+</sup> cells in *ex-vivo* stimulated PBMC from patients with IBD.**

PBMC isolated from IBD patients were treated with carnosol or curcumin (5  $\mu$ M) for 6 hours prior to stimulation with anti-CD3 (1  $\mu$ g/mL) for 12 hours. After 18 hours culture media was replaced with fresh media and cells were incubated for a further 4 days with anti-CD3 (1  $\mu$ g/mL) stimulation, without ketoacids. **(A)** Dot plots depicting ki67 expression (as a measure of proliferation) by CD3<sup>+</sup>CD8<sup>+</sup> cells from one representative experiment. **(B)** Pooled data (n = 14) depicting the mean  $\pm$  SEM of ki67<sup>+</sup> in CD3<sup>+</sup>CD8<sup>+</sup> T cells. Repeated measures one-way ANOVA, with Dunnett's multiple comparisons post hoc test, was used to determine statistical significance by comparing means of treatment groups against the mean of the control group (\*\*\*\* p < 0.0001).

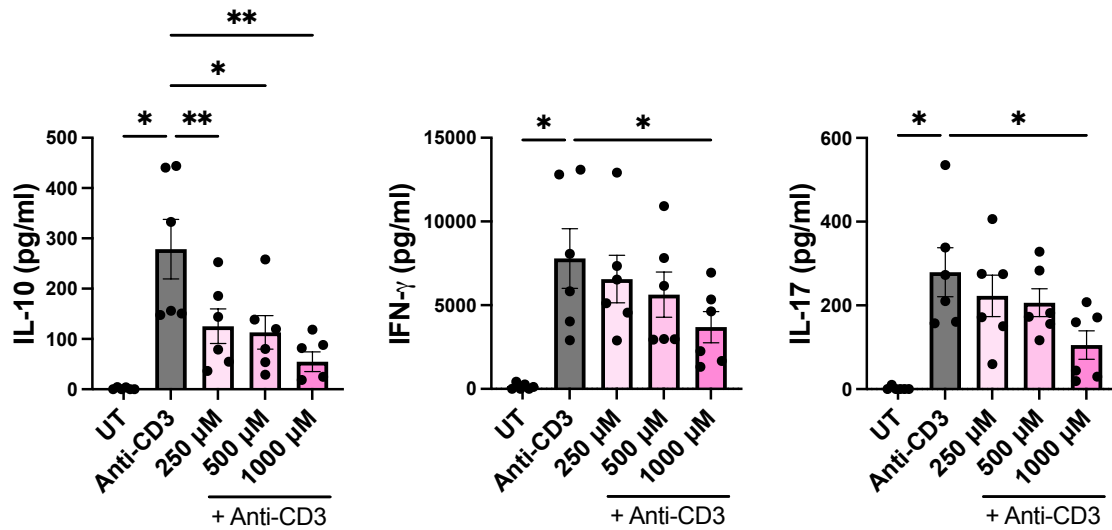


**Figure 4.17 HPP inhibits secretion of cytokines from *ex-vivo* stimulated PBMC from patients with IBD.**

PBMC isolated from IBD patients were treated with HPP (250  $\mu$ M – 1000  $\mu$ M) for 6 hours prior to stimulation with anti-CD3 (1  $\mu$ g/mL) for 12 hours. After 18 hours culture media was replaced with fresh media and cells were incubated for a further 4 days with anti-CD3 (1  $\mu$ g/mL) stimulation, without HPP. Cell supernatants were assessed for concentrations of (A) IL-10, (B) IFN $\gamma$  and (C) IL-17 by ELISA. Pooled data depicts mean ( $\pm$ SEM) cytokine concentrations for 6 IBD patients (means of three technical replicates per donor). Repeated measures one-way ANOVA, with Dunnett's multiple comparisons post hoc test, was used to determine statistical significance by comparing means of treatment groups against the mean of the control group (\*\* p < 0.01, \*p < 0.05).

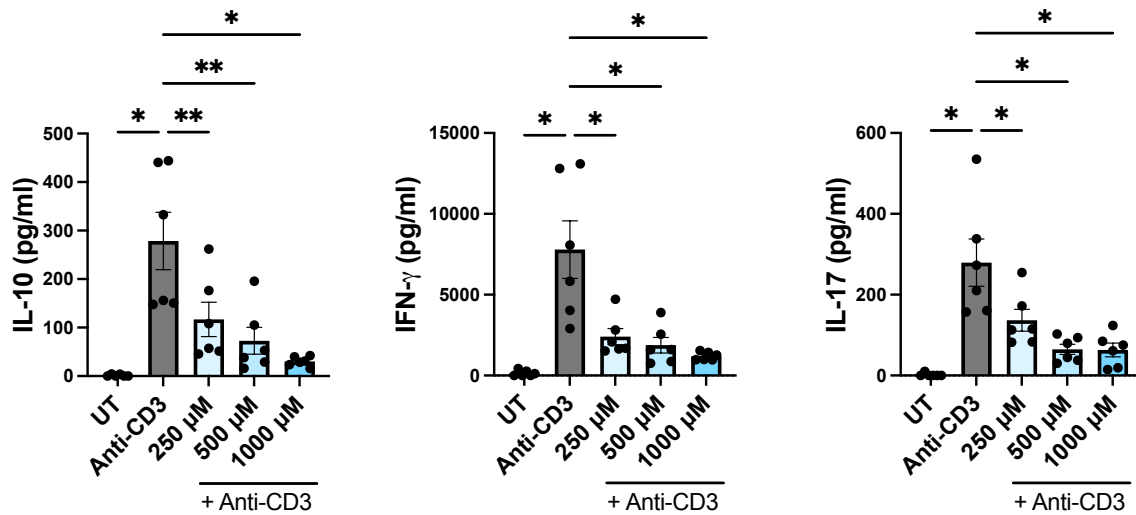


**Figure 4.18 IP inhibits secretion of cytokines from *ex-vivo* stimulated PBMC from patients with IBD.**

PBMC isolated from IBD patients were treated with IP (250  $\mu$ M – 1000  $\mu$ M) for 6 hours prior to stimulation with anti-CD3 (1  $\mu$ g/mL) for 12 hours. After 18 hours culture media was replaced with fresh media and cells were incubated for a further 4 days with anti-CD3 (1  $\mu$ g/mL) stimulation, without IP. Cell supernatants were assessed for concentrations of (A) IL-10, (B) IFN $\gamma$  and (C) IL-17 by ELISA. Pooled data depicts mean ( $\pm$ SEM) cytokine concentrations for 6 IBD patients (means of three technical replicates per donor). Repeated measures one-way ANOVA, with Dunnett's multiple comparisons post hoc test, was used to determine statistical significance by comparing means of treatment groups against the mean of the control group (\*\* p < 0.01, \*p < 0.05).

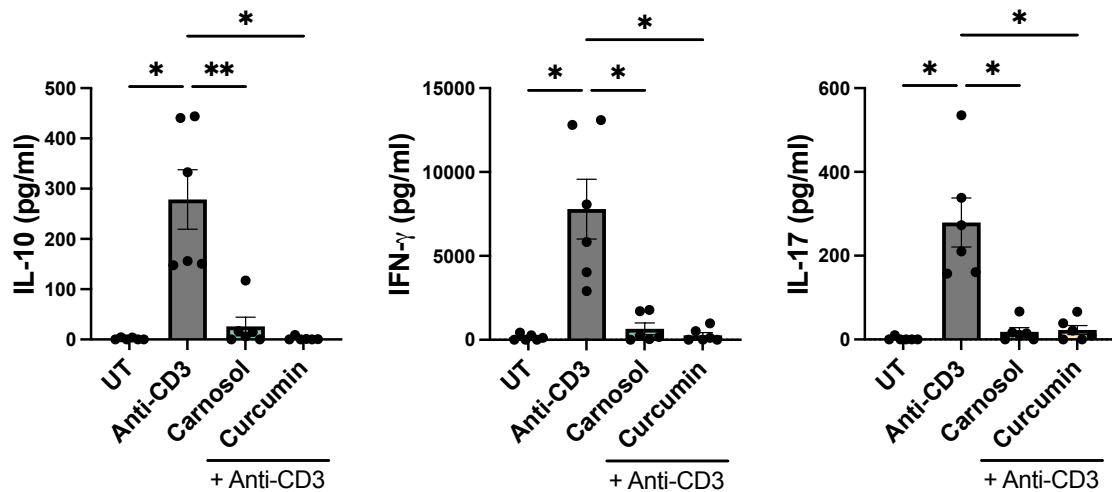


**Figure 4.19 Carnosol and curcumin inhibit secretion of cytokines from *ex-vivo* stimulated PBMC from patients with IBD.**

PBMC isolated from IBD patients were treated with carnosol or curcumin (5  $\mu$ M) for 6 hours prior to stimulation with anti-CD3 (1  $\mu$ g/mL) for 12 hours. After 18 hours culture media was replaced with fresh media and cells were incubated for a further 4 days with anti-CD3 (1  $\mu$ g/mL) stimulation, without carnosol or curcumin. Cell supernatants were assessed for concentrations of (A) IL-10, (B) IFN $\gamma$  and (C) IL-17 by ELISA. Pooled data depicts mean ( $\pm$ SEM) cytokine concentrations for 6 IBD patients (means of three technical replicates per donor). Repeated measures one-way ANOVA, with Dunnett's multiple comparisons post hoc test, was used to determine statistical significance by comparing means of treatment groups against the mean of the control group (\*\* p < 0.01, \*p < 0.05).



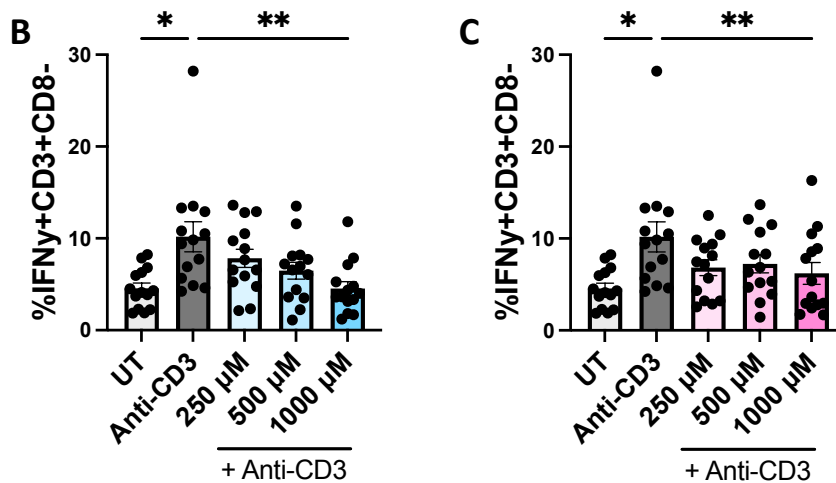
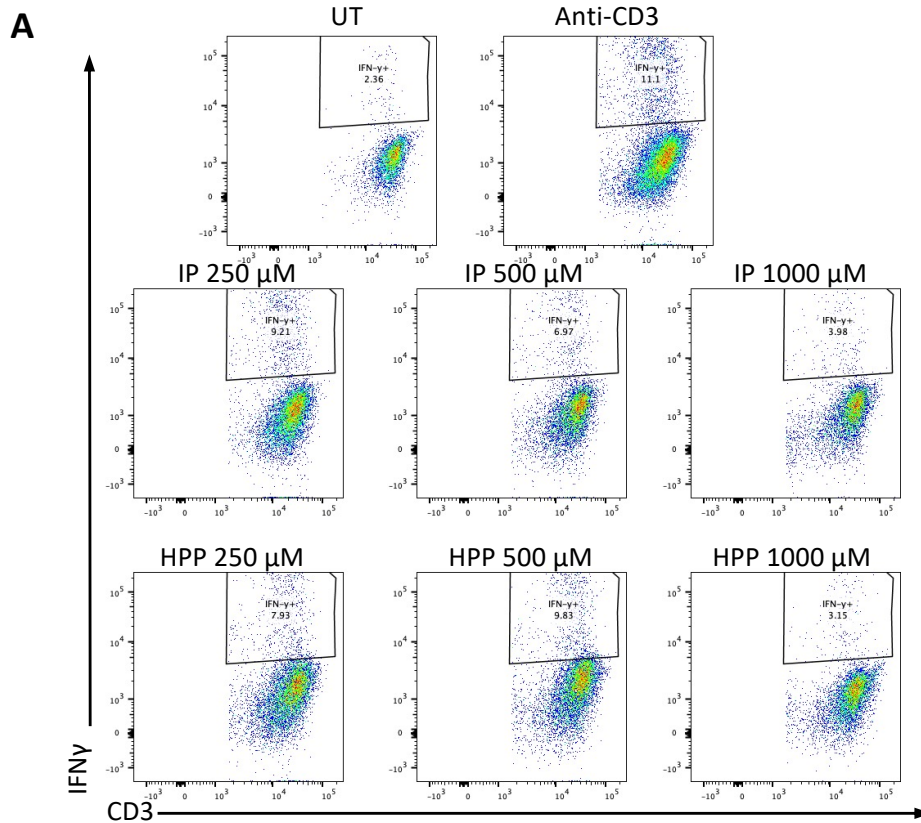


**Figure 4.20 HPP and IP reduce the frequency of IFN $\gamma$ <sup>+</sup> CD4<sup>+</sup> T cells in *ex-vivo* stimulated PBMC from patients with IBD.**

PBMC isolated from IBD patients were treated with **(B)** IP or **(C)** HPP (250  $\mu$ M – 1000  $\mu$ M) for 6 hours prior to stimulation with anti-CD3 (1  $\mu$ g/mL) for 12 hours. After 18 hours culture media was replaced with fresh media and cells were incubated for a further 4 days with anti-CD3 (1  $\mu$ g/mL) stimulation, without ketoacids. **(A)** Dot plots depicting IFN $\gamma$  expression by CD3<sup>+</sup>CD8<sup>-</sup> cells from one representative experiment. **(B & C)** Pooled data (n = 14) depicting the mean  $\pm$  SEM of IFN $\gamma$ <sup>+</sup> in CD3<sup>+</sup>CD8<sup>-</sup> T cells. Repeated measures one-way ANOVA, with Dunnett's multiple comparisons post hoc test, was used to determine statistical significance by comparing means of treatment groups against the mean of the control group (\*\* p < 0.01, \*p < 0.05).

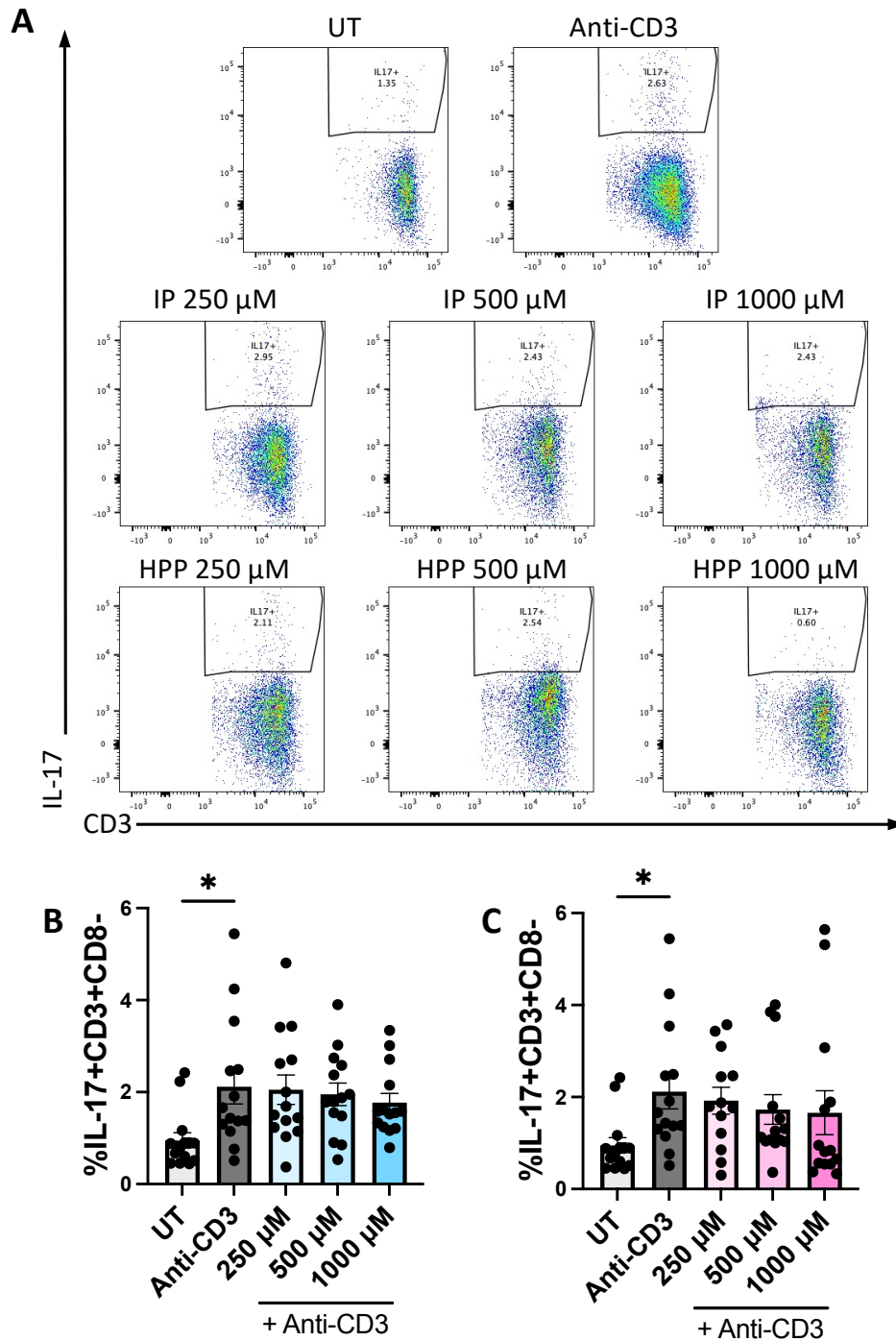


**Figure 4.21 HPP and IP have no effect on the frequency of IL-17<sup>+</sup> CD4<sup>+</sup> T cells in *ex-vivo* stimulated PBMC from patients with IBD.**

PBMC isolated from IBD patients were treated with **(B)** IP or **(C)** HPP (250 μM – 1000 μM) for 6 hours prior to stimulation with anti-CD3 (1 μg/mL) for 12 hours. After 18 hours culture media was replaced with fresh media and cells were incubated for a further 4 days with anti-CD3 (1 μg/mL) stimulation, without ketoacids. **(A)** Dot plots depicting IL-17 expression by CD3<sup>+</sup>CD8<sup>-</sup> cells from one representative experiment. **(B & C)** Pooled data (n = 14) depicting the mean ± SEM of IL-17<sup>+</sup> in CD3<sup>+</sup>CD8<sup>-</sup> T cells. Repeated measures one-way ANOVA, with Dunnett's multiple comparisons post hoc test, was used to determine statistical significance by comparing means of treatment groups against the mean of the control group (\*p < 0.05).

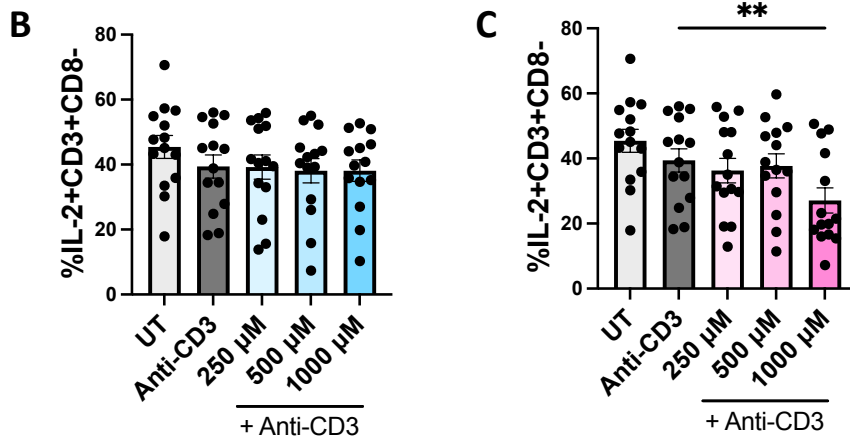
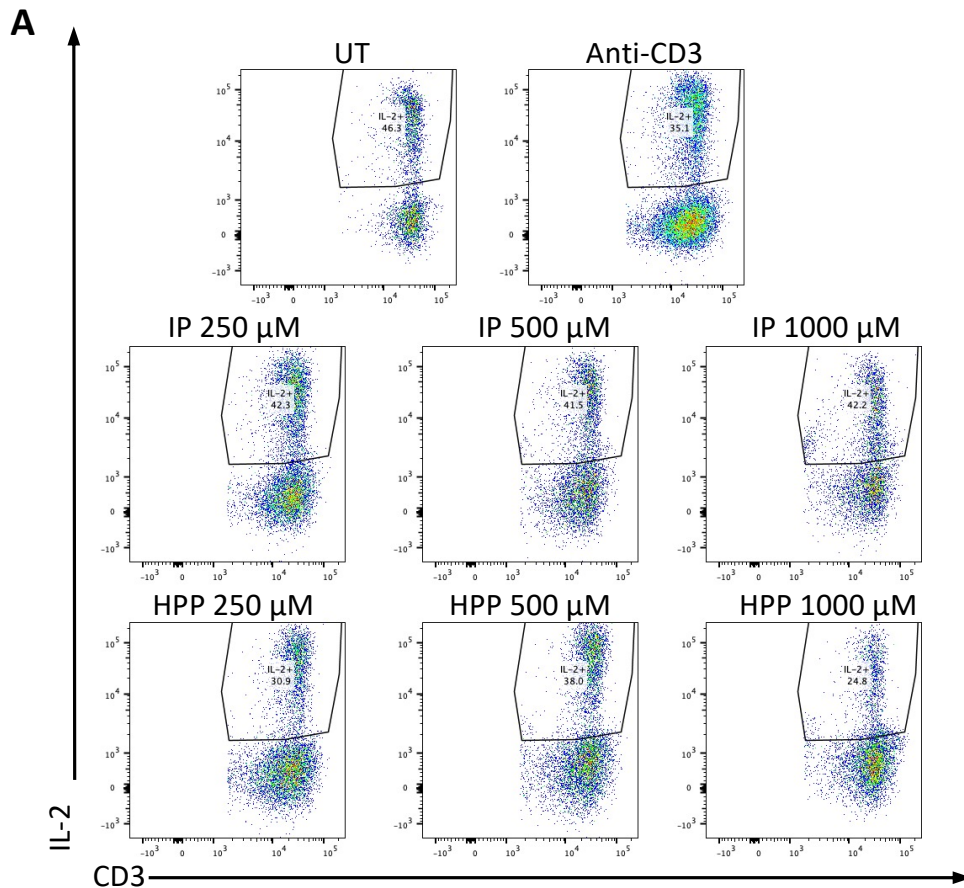


**Figure 4.22 HPP, but not IP, reduces the frequency of IL-2<sup>+</sup> CD4<sup>+</sup> T cells in *ex-vivo* stimulated PBMC from patients with IBD.**

PBMC isolated from IBD patients were treated with **(B)** IP or **(C)** HPP (250  $\mu$ M – 1000  $\mu$ M) for 6 hours prior to stimulation with anti-CD3 (1  $\mu$ g/mL) for 12 hours. After 18 hours culture media was replaced with fresh media and cells were incubated for a further 4 days with anti-CD3 (1  $\mu$ g/mL) stimulation, without ketoacids. **(A)** Dot plots depicting IL-2 expression by CD3<sup>+</sup>CD8<sup>-</sup> cells from one representative experiment. **(B & C)** Pooled data (n = 14) depicting the mean  $\pm$  SEM of IL-2<sup>+</sup> in CD3<sup>+</sup>CD8<sup>-</sup> T cells. Repeated measures one-way ANOVA, with Dunnett's multiple comparisons post hoc test, was used to determine statistical significance by comparing means of treatment groups against the mean of the control group (\*\* p < 0.01).

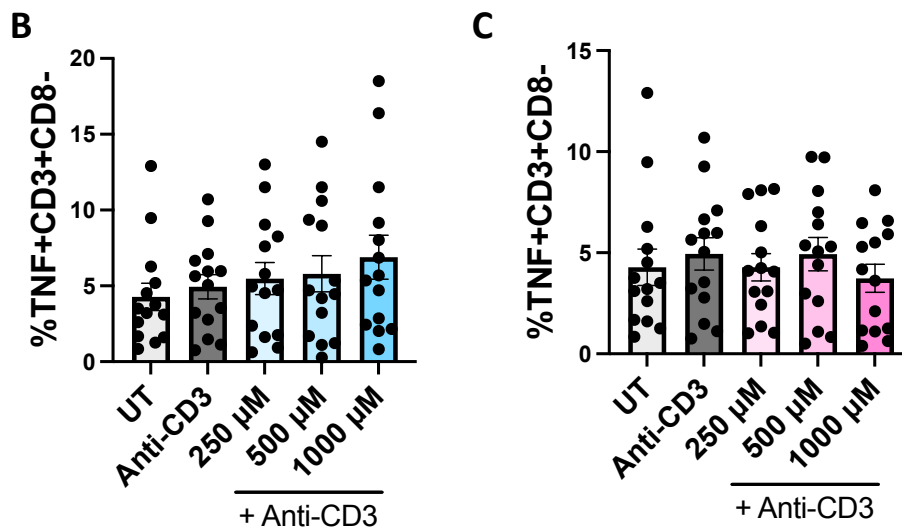
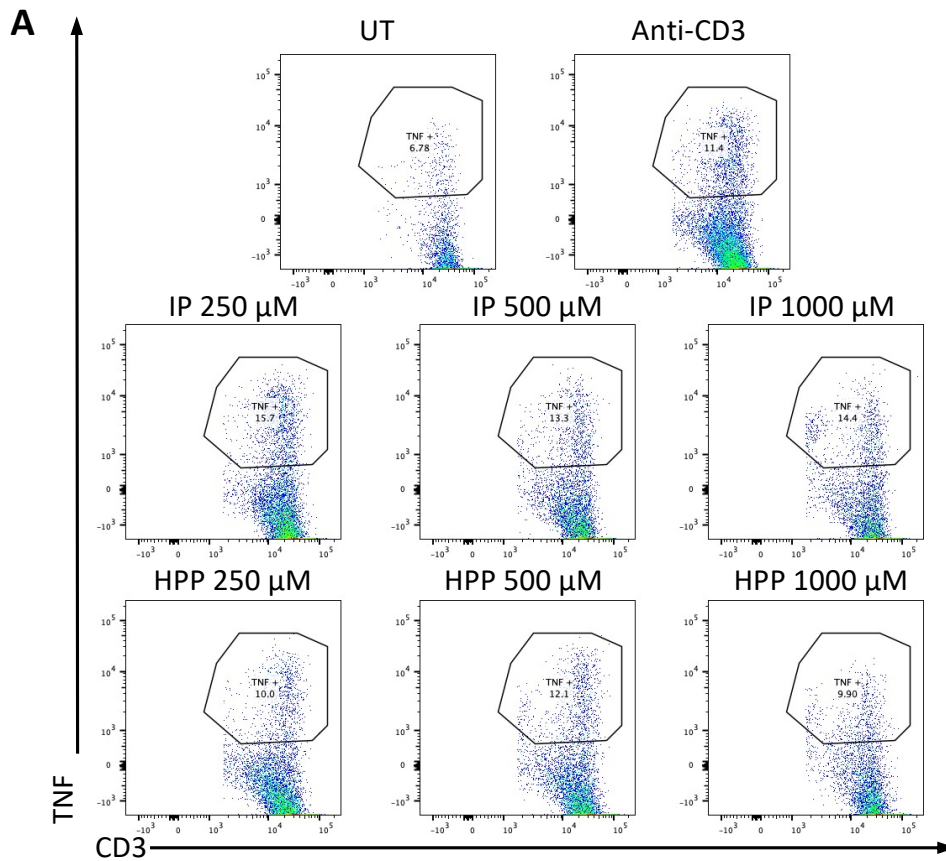


**Figure 4.23** HPP and IP have no effect on the frequency of TNF<sup>+</sup> CD4<sup>+</sup> T cells in *ex-vivo* stimulated PBMC from patients with IBD.

PBMC isolated from IBD patients were treated with **(B)** IP or **(C)** HPP (250  $\mu$ M – 1000  $\mu$ M) for 6 hours prior to stimulation with anti-CD3 (1  $\mu$ g/mL) for 12 hours. After 18 hours culture media was replaced with fresh media and cells were incubated for a further 4 days with anti-CD3 (1  $\mu$ g/mL) stimulation, without ketoacids. **(A)** Dot plots depicting TNF expression by CD3<sup>+</sup>CD8<sup>-</sup> cells from one representative experiment. **(B & C)** Pooled data (n = 14) depicting the mean  $\pm$  SEM of TNF<sup>+</sup> in CD3<sup>+</sup>CD8<sup>-</sup> T cells.

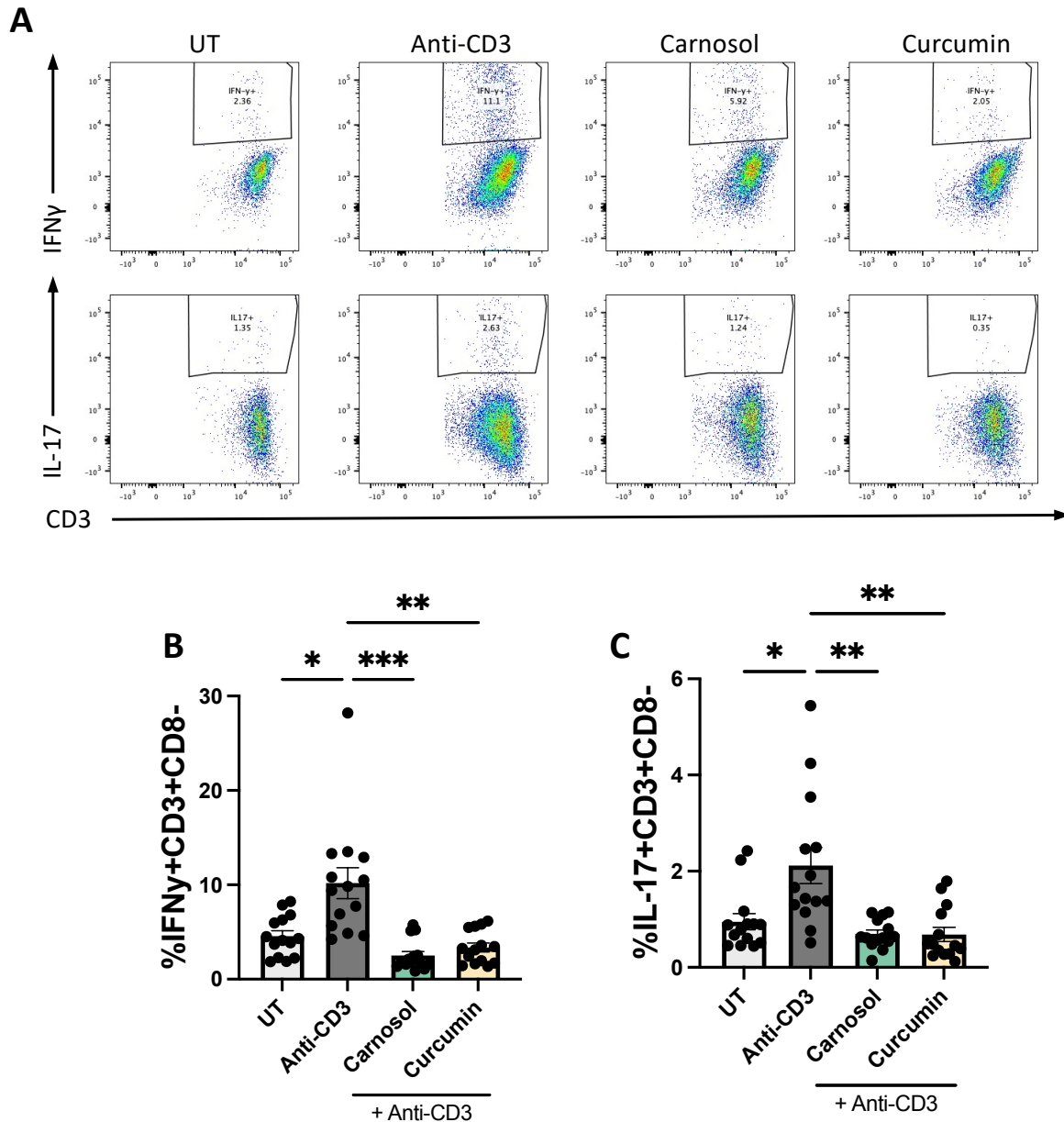


**Figure 4.24 Carnosol and curcumin reduce the frequency of IFN $\gamma$ <sup>+</sup> and IL-17<sup>+</sup> CD4<sup>+</sup> T cells in *ex-vivo* stimulated PBMC from patients with IBD.**

PBMC isolated from IBD patients were treated with carnosol or curcumin (5  $\mu$ M) for 6 hours prior to stimulation with anti-CD3 (1  $\mu$ g/mL) for 12 hours. After 18 hours culture media was replaced with fresh media and cells were incubated for a further 4 days with anti-CD3 (1  $\mu$ g/mL) stimulation, without carnosol or curcumin. **(A)** Dot plots depicting IFN $\gamma$  and IL-17 expression by CD3<sup>+</sup>CD8<sup>-</sup> cells from one representative experiment. **(B & C)** Pooled data (n = 14) depicting the mean  $\pm$  SEM of **(B)** IFN $\gamma$ <sup>+</sup> and **(C)** IL-17<sup>+</sup> in CD3<sup>+</sup>CD8<sup>-</sup> T cells. Repeated measures one-way ANOVA, with Dunnett's multiple comparisons post hoc test, was used to determine statistical significance by comparing means of treatment groups against the mean of the control group (\*\*\*)  $p < 0.001$ , \*\*  $p < 0.01$ , \*  $p < 0.05$ ).

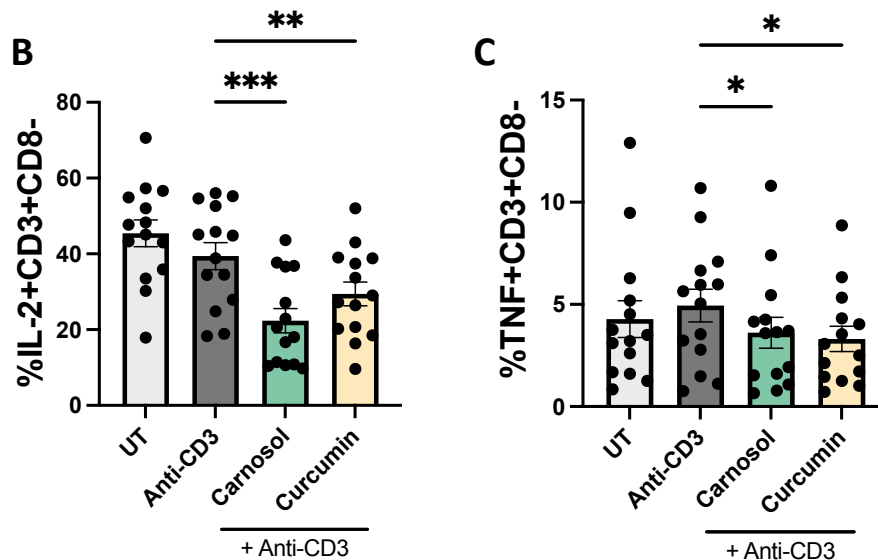
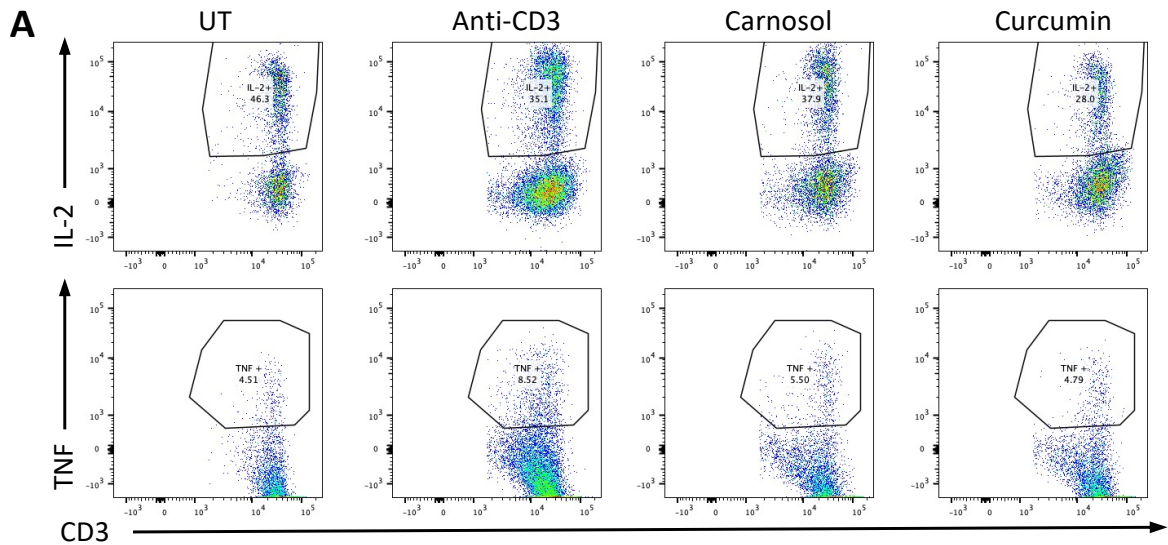


**Figure 4.25 Carnosol and curcumin reduce the frequency of IL-2<sup>+</sup> and TNF<sup>+</sup> CD4<sup>+</sup> T cells in *ex-vivo* stimulated PBMC from patients with IBD.**

PBMC isolated from IBD patients were treated with carnosol or curcumin (5  $\mu$ M) for 6 hours prior to stimulation with anti-CD3 (1  $\mu$ g/mL) for 12 hours. After 18 hours culture media was replaced with fresh media and cells were incubated for a further 4 days with anti-CD3 (1  $\mu$ g/mL) stimulation, without carnosol or curcumin. **(A)** Dot plots depicting IL-2 and TNF expression by CD3<sup>+</sup>CD8<sup>-</sup> cells from one representative experiment. **(B & C)** Pooled data (n = 14) depicting the mean  $\pm$  SEM of **(B)** IL-2<sup>+</sup> and **(C)** TNF<sup>+</sup> in CD3<sup>+</sup>CD8<sup>-</sup> T cells. Repeated measures one-way ANOVA, with Dunnett's multiple comparisons post hoc test, was used to determine statistical significance by comparing means of treatment groups against the mean of the control group (\*\*\*)  $p < 0.001$ , \*\*  $p < 0.01$ , \*  $p < 0.05$ ).

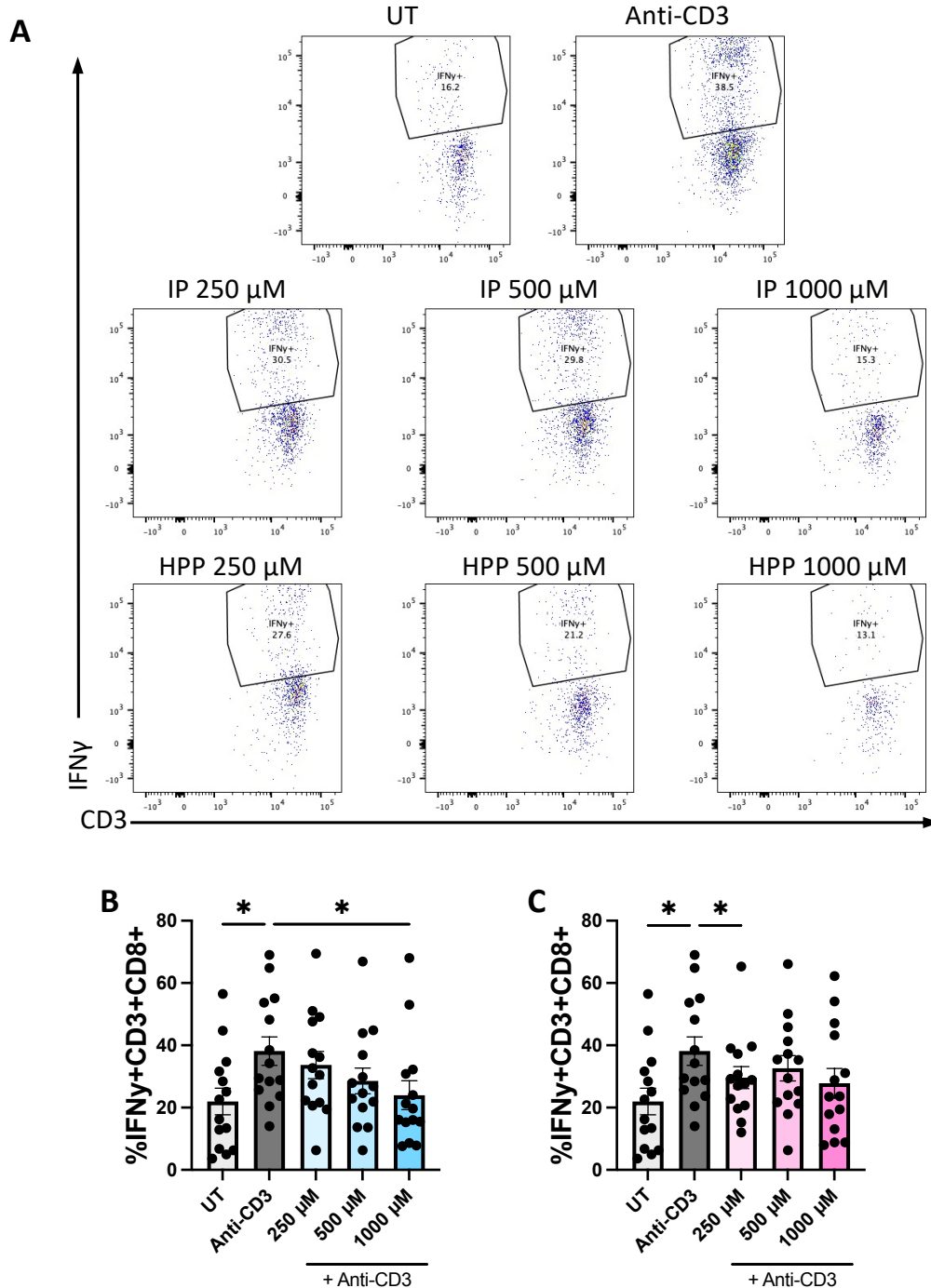


**Figure 4.26 HPP and IP reduce the frequency of IFN $\gamma$ <sup>+</sup> CD8<sup>+</sup> T cells in *ex-vivo* stimulated PBMC from patients with IBD.**

PBMC isolated from IBD patients were treated with **(B)** IP or **(C)** HPP (250  $\mu$ M – 1000  $\mu$ M) for 6 hours prior to stimulation with anti-CD3 (1  $\mu$ g/mL) for 12 hours. After 18 hours culture media was replaced with fresh media and cells were incubated for a further 4 days with anti-CD3 (1  $\mu$ g/mL) stimulation, without ketoacids. **(A)** Dot plots depicting IFN $\gamma$  expression by CD3<sup>+</sup>CD8<sup>+</sup> cells from one representative experiment. **(B & C)** Pooled data (n = 14) depicting the mean  $\pm$  SEM of IFN $\gamma$ <sup>+</sup> in CD3<sup>+</sup>CD8<sup>+</sup> T cells. Repeated measures one-way ANOVA, with Dunnett's multiple comparisons post hoc test, was used to determine statistical significance by comparing means of treatment groups against the mean of the control group (\*p < 0.05).

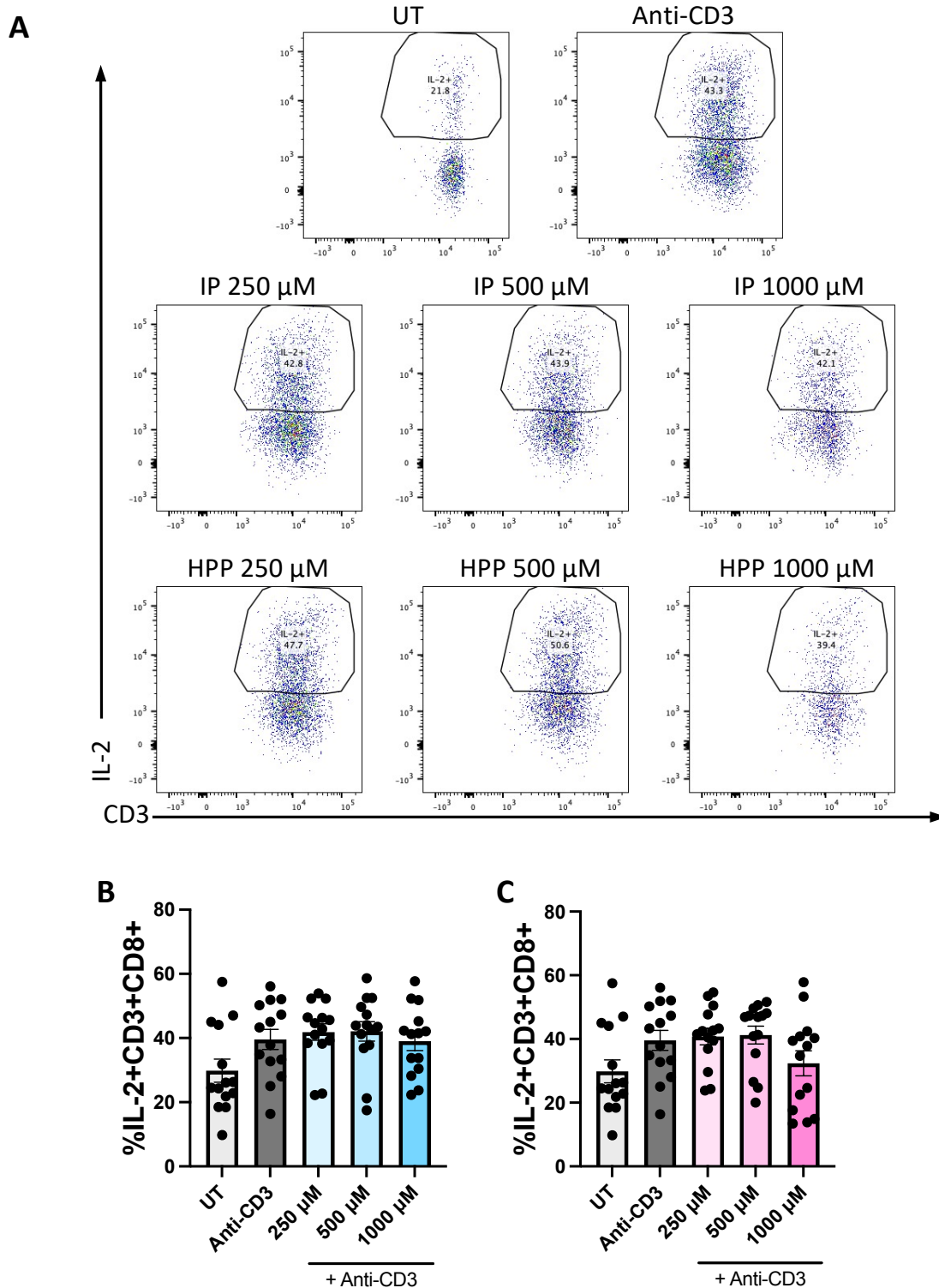


**Figure 4.27 HPP and IP have no effect on the frequency of IL-2<sup>+</sup> CD8<sup>+</sup> T cells in *ex-vivo* stimulated PBMC from patients with IBD.**

PBMC isolated from IBD patients were treated with **(B)** IP or **(C)** HPP (250  $\mu$ M – 1000  $\mu$ M) for 6 hours prior to stimulation with anti-CD3 (1  $\mu$ g/mL) for 12 hours. After 18 hours culture media was replaced with fresh media and cells were incubated for a further 4 days with anti-CD3 (1  $\mu$ g/mL) stimulation, without ketoacids. **(A)** Dot plots depicting IL-2 expression by CD3<sup>+</sup>CD8<sup>+</sup> cells from one representative experiment. **(B & C)** Pooled data (n = 14) depicting the mean  $\pm$  SEM of IL-2<sup>+</sup> in CD3<sup>+</sup>CD8<sup>+</sup> T cells.



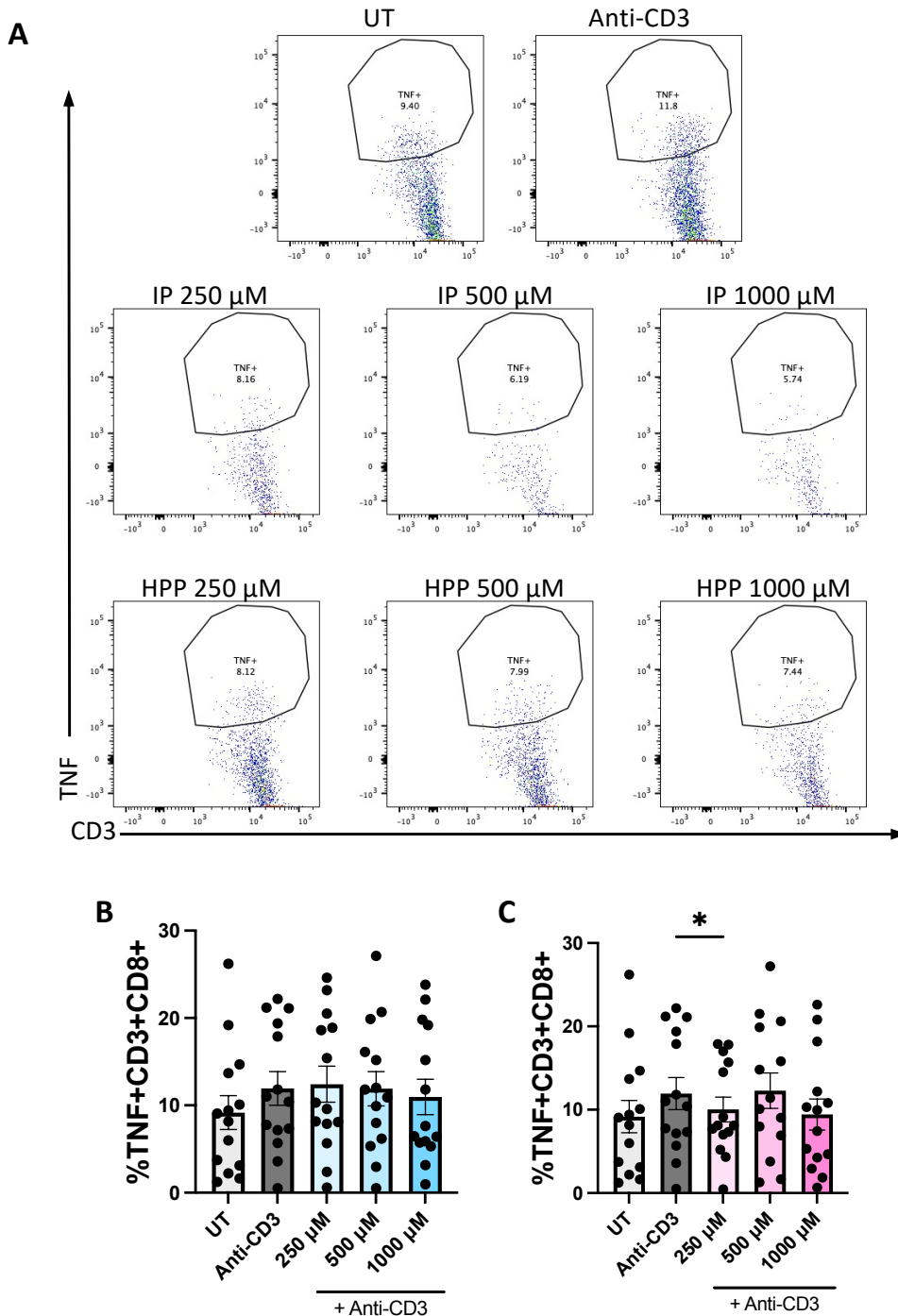


**Figure 4.28 HPP, but not IP, reduces the frequency of TNF<sup>+</sup> CD8<sup>+</sup> T cells in *ex-vivo* stimulated PBMC from patients with IBD.**

PBMC isolated from IBD patients were treated with **(B)** IP or **(C)** HPP (250 μM – 1000 μM) for 6 hours prior to stimulation with anti-CD3 (1 μg/mL) for 12 hours. After 18 hours culture media was replaced with fresh media and cells were incubated for a further 4 days with anti-CD3 (1 μg/mL) stimulation, without ketoacids. **(A)** Dot plots depicting TNF expression by CD3<sup>+</sup>CD8<sup>+</sup> cells from one representative experiment. **(B & C)** Pooled data (n = 14) depicting the mean ± SEM of TNF<sup>+</sup> in CD3<sup>+</sup>CD8<sup>+</sup> T cells. Repeated measures one-way ANOVA, with Dunnett's multiple comparisons post hoc test, was used to determine statistical significance by comparing means of treatment groups against the mean of the control group (\*p < 0.05).

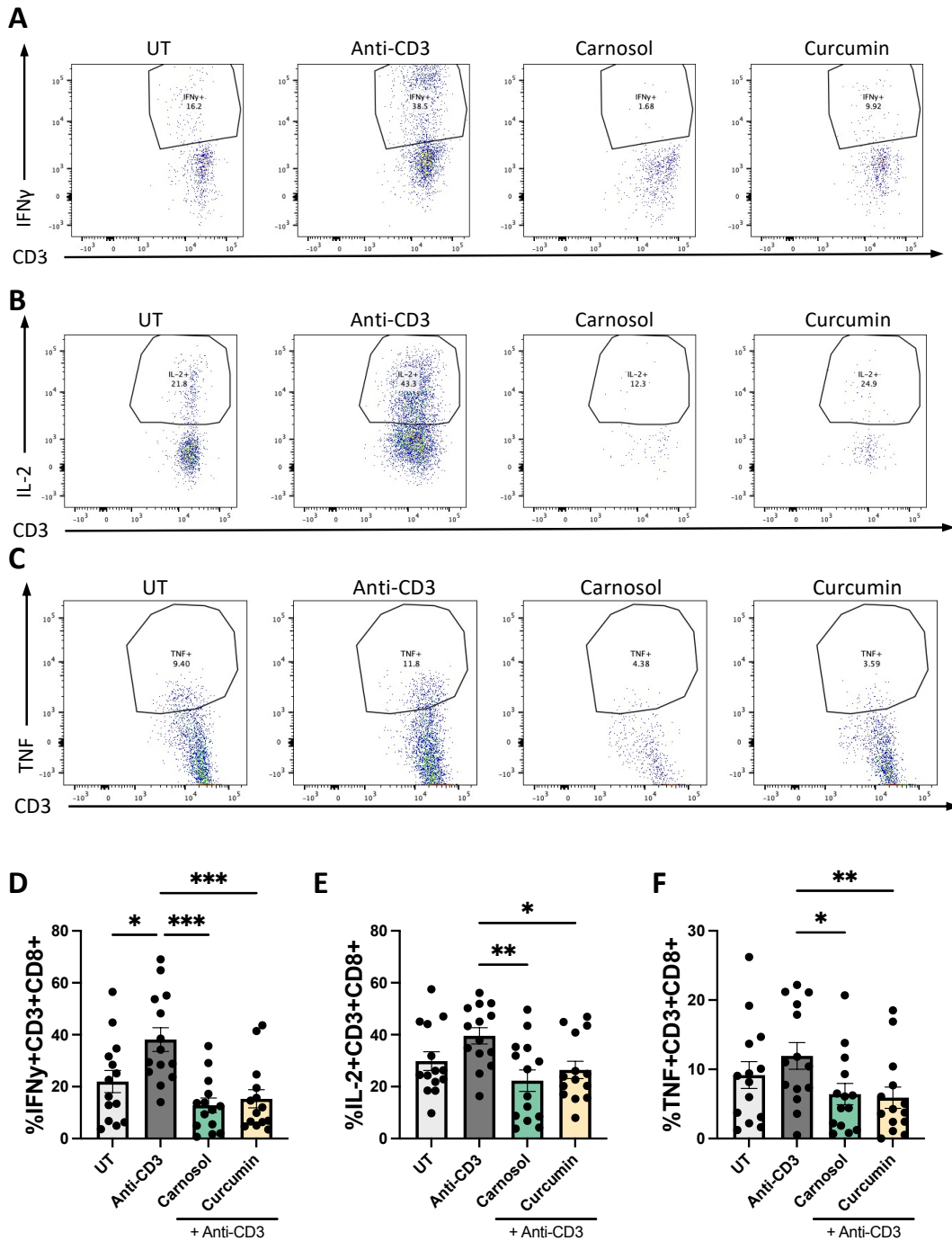


**Figure 4.29 Carnosol and curcumin reduce the frequency of IFN $\gamma$ <sup>+</sup>, IL-2<sup>+</sup> and TNF<sup>+</sup> CD8<sup>+</sup> T cells in *ex-vivo* stimulated PBMC from patients with IBD.**

PBMC isolated from IBD patients were treated with carnosol or curcumin (5  $\mu$ M) for 6 hours prior to stimulation with anti-CD3 (1  $\mu$ g/mL) for 12 hours. After 18 hours culture media was replaced with fresh media and cells were incubated for a further 4 days with anti-CD3 (1  $\mu$ g/mL) stimulation, without ketoacids. Dot plots depicting (A) IFN $\gamma$ , (B) IL-2 and (C) TNF expression by CD3<sup>+</sup>CD8<sup>+</sup> cells from one representative experiment. Pooled data (n = 14) depicting the mean  $\pm$  SEM of (D) IFN $\gamma$ <sup>+</sup>, (E) IL-2<sup>+</sup> and (F) TNF<sup>+</sup> in CD3<sup>+</sup>CD8<sup>+</sup> T cells. Repeated measures one-way ANOVA, with Dunnett's multiple comparisons post hoc test, was used to determine statistical significance by comparing means of treatment groups against the mean of the control group (\*\*\*) p < 0.001, \*\* p < 0.01, \* p < 0.05).

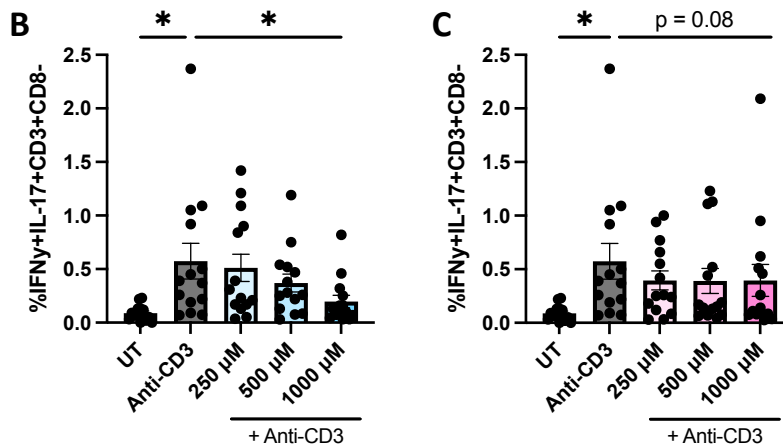
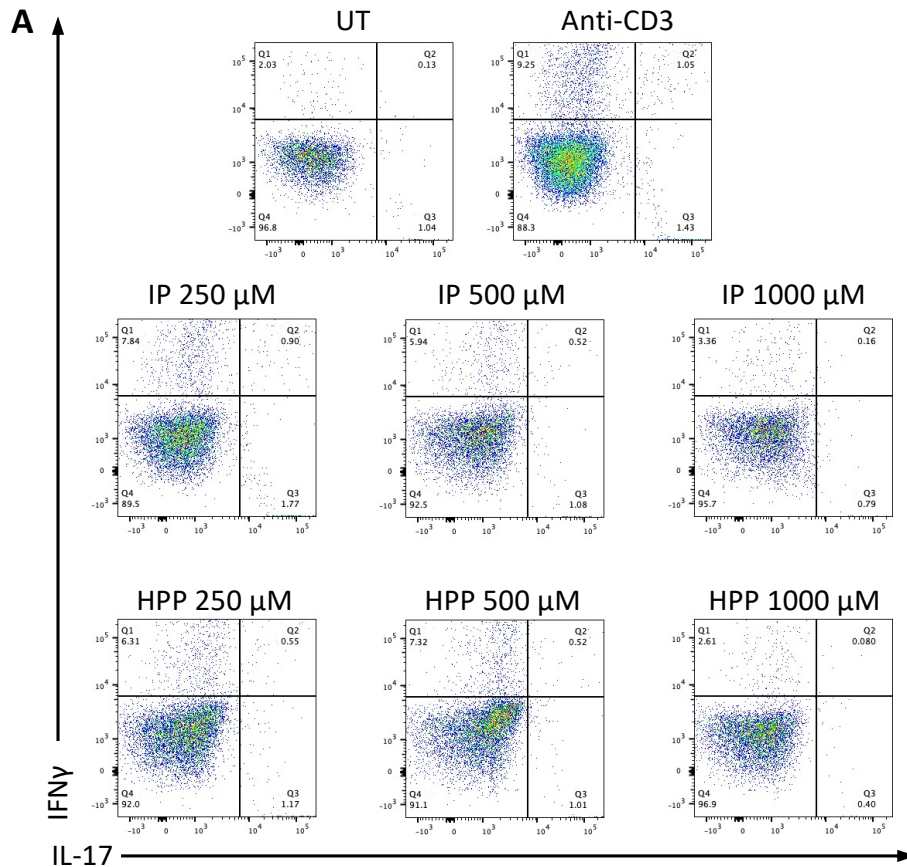


**Figure 4.30 HPP and IP reduce the frequency of IFN $\gamma$ <sup>+</sup>IL-17<sup>+</sup> CD4<sup>+</sup> T cells in *ex-vivo* stimulated PBMC from patients with IBD.**

PBMC isolated from IBD patients were treated with **(B)** IP or **(C)** HPP (250  $\mu$ M – 1000  $\mu$ M) for 6 hours prior to stimulation with anti-CD3 (1  $\mu$ g/mL) for 12 hours. After 18 hours culture media was replaced with fresh media and cells were incubated for a further 4 days with anti-CD3 (1  $\mu$ g/mL) stimulation, without ketoacids. **(A)** Dot plots depicting IFN $\gamma$  and IL-17 expression by CD3<sup>+</sup>CD8<sup>-</sup> cells from one representative experiment. **(B & C)** Pooled data (n = 14) depicting the mean  $\pm$  SEM of IFN $\gamma$ <sup>+</sup>IL-17<sup>+</sup> in CD3<sup>+</sup>CD8<sup>-</sup> T cells. Repeated measures one-way ANOVA, with Dunnett's multiple comparisons post hoc test, was used to determine statistical significance by comparing means of treatment groups against the mean of the control group (\*p < 0.05).

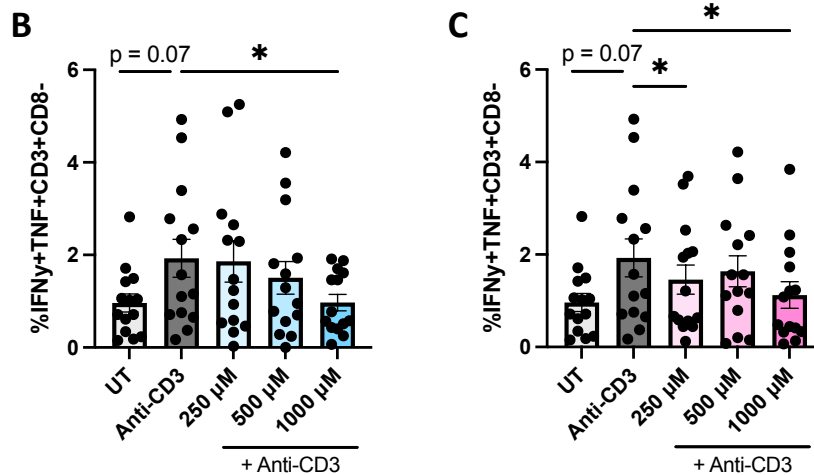
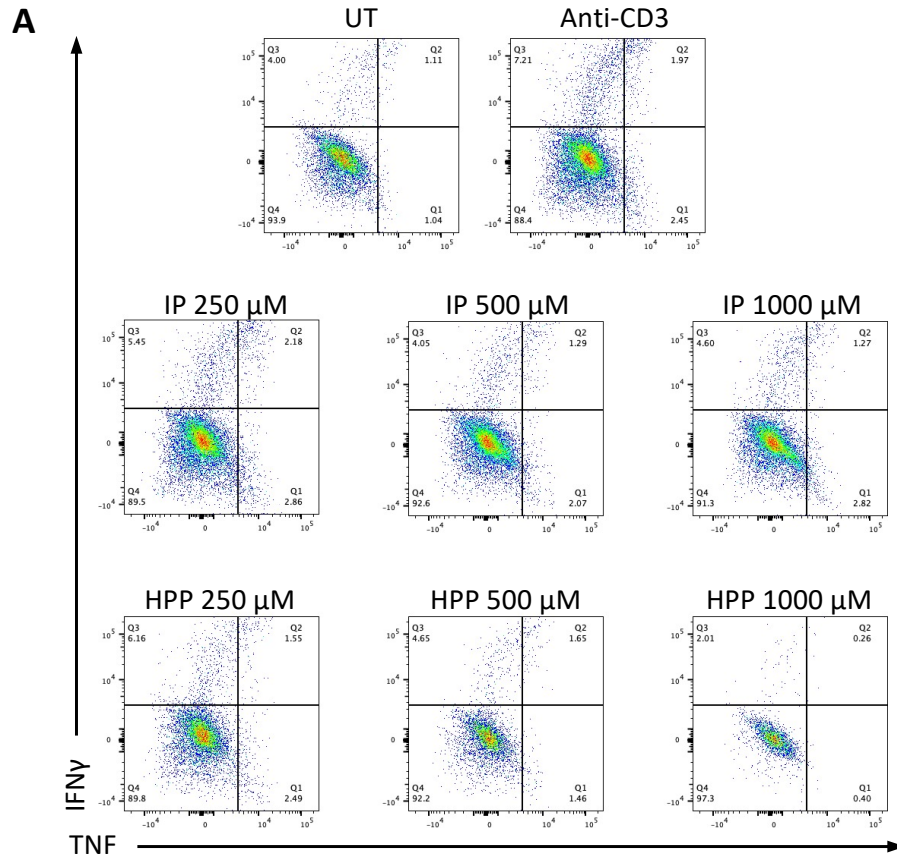


**Figure 4.31 HPP and IP reduce the frequency of IFN $\gamma$ <sup>+</sup>TNF<sup>+</sup> CD4<sup>+</sup> T cells in *ex-vivo* stimulated PBMC from patients with IBD.**

PBMC isolated from IBD patients were treated with (B) IP or (C) HPP (250  $\mu$ M – 1000  $\mu$ M) for 6 hours prior to stimulation with anti-CD3 (1  $\mu$ g/mL) for 12 hours. After 18 hours culture media was replaced with fresh media and cells were incubated for a further 4 days with anti-CD3 (1  $\mu$ g/mL) stimulation, without ketoacids. (A) Dot plots depicting IFN $\gamma$  and TNF expression by CD3<sup>+</sup>CD8<sup>-</sup> cells from one representative experiment. (B & C) Pooled data (n = 14) depicting the mean  $\pm$  SEM of IFN $\gamma$ <sup>+</sup>TNF<sup>+</sup> in CD3<sup>+</sup>CD8<sup>-</sup> T cells. Repeated measures one-way ANOVA, with Dunnett's multiple comparisons post hoc test, was used to determine statistical significance by comparing means of treatment groups against the mean of the control group (\*p < 0.05).

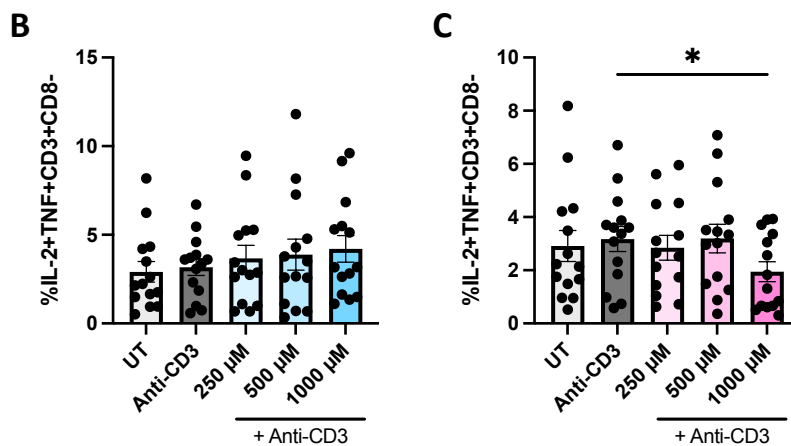
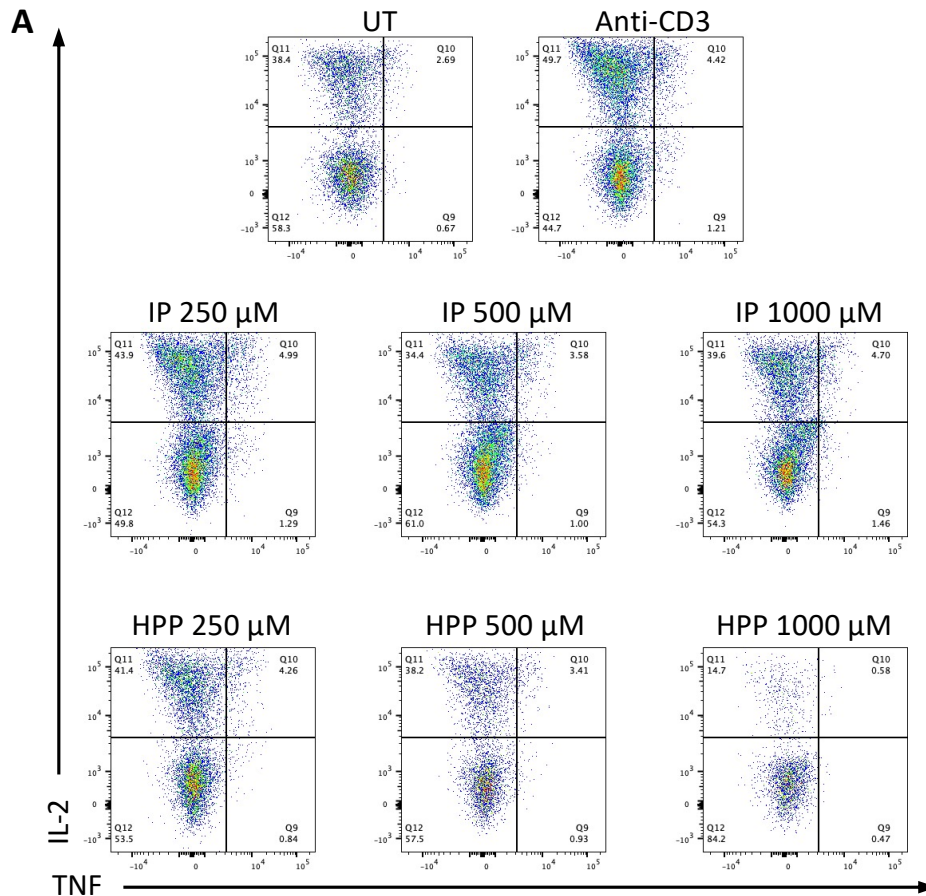


**Figure 4.32 HPP, but not IP, reduces the frequency of IL-2<sup>+</sup>TNF<sup>+</sup> CD4<sup>+</sup> T cells in *ex-vivo* stimulated PBMC from patients with IBD.**

PBMC isolated from IBD patients were treated with **(B)** IP or **(C)** HPP (250 μM – 1000 μM) for 6 hours prior to stimulation with anti-CD3 (1 μg/mL) for 12 hours. After 18 hours culture media was replaced with fresh media and cells were incubated for a further 4 days with anti-CD3 (1 μg/mL) stimulation, without ketoacids. **(A)** Dot plots depicting IL-2 and TNF expression by CD3<sup>+</sup>CD8<sup>-</sup> cells from one representative experiment. **(B & C)** Pooled data (n = 14) depicting the mean ± SEM of IL-2<sup>+</sup>TNF<sup>+</sup> in CD3<sup>+</sup>CD8<sup>-</sup> T cells. Repeated measures one-way ANOVA, with Dunnett's multiple comparisons post hoc test, was used to determine statistical significance by comparing means of treatment groups against the mean of the control group (\*p < 0.05).

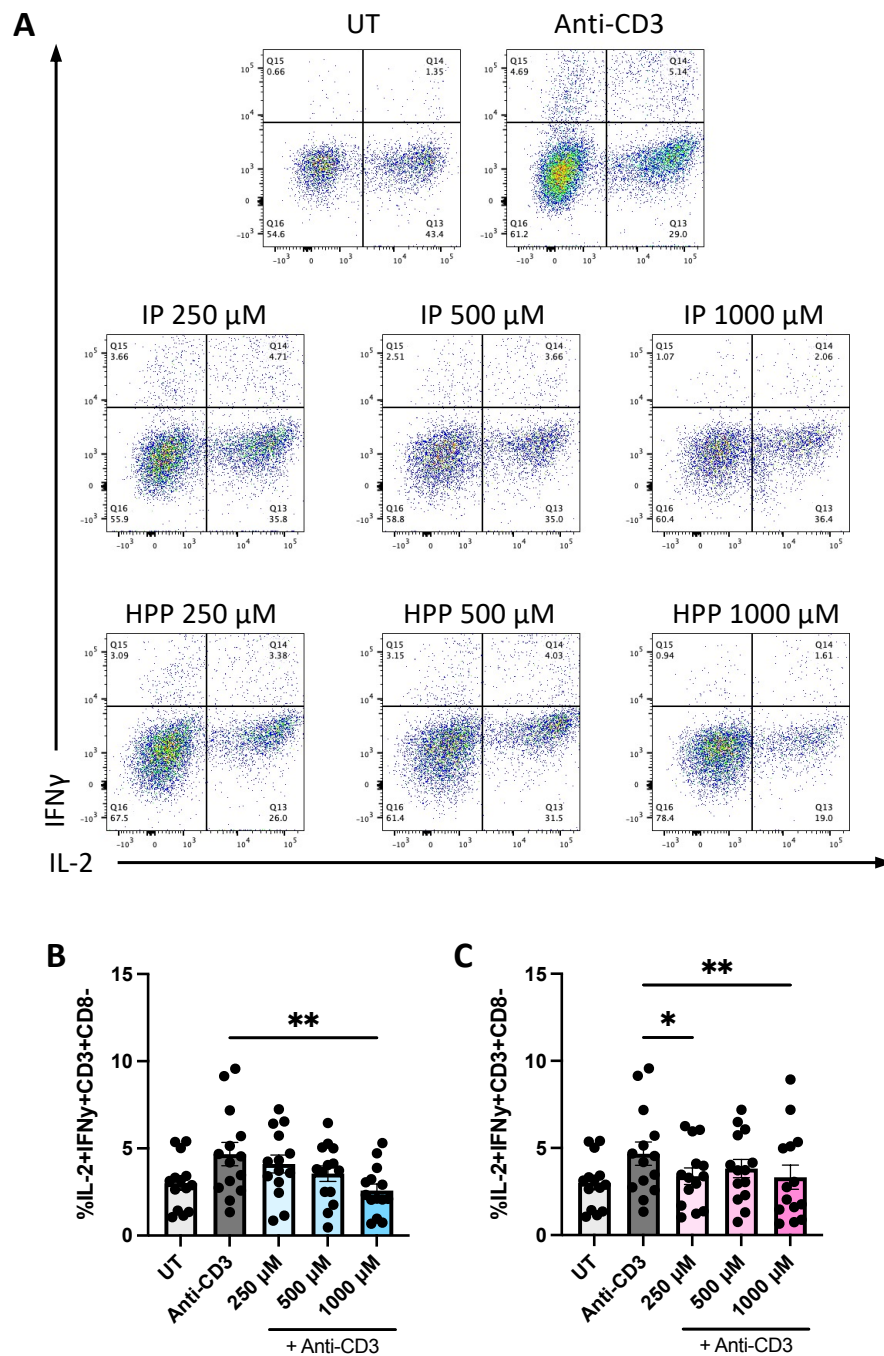


**Figure 4.33 HPP and IP reduce the frequency of IL-2<sup>+</sup>IFN-γ<sup>+</sup> CD4<sup>+</sup> T cells in *ex-vivo* stimulated PBMC from patients with IBD.**

PBMC isolated from IBD patients were treated with **(B)** IP or **(C)** HPP (250 μM – 1000 μM) for 6 hours prior to stimulation with anti-CD3 (1 μg/mL) for 12 hours. After 18 hours culture media was replaced with fresh media and cells were incubated for a further 4 days with anti-CD3 (1 μg/mL) stimulation, without ketoacids. **(A)** Dot plots depicting IL-2 and IFN-γ expression by CD3<sup>+</sup>CD8<sup>-</sup> cells from one representative experiment. **(B & C)** Pooled data (n = 14) depicting the mean ± SEM of IL-2<sup>+</sup>IFN-γ<sup>+</sup> in CD3<sup>+</sup>CD8<sup>-</sup> T cells. Repeated measures one-way ANOVA, with Dunnett's multiple comparisons post hoc test, was used to determine statistical significance by comparing means of treatment groups against the mean of the control group (\*\*p < 0.01, \*p < 0.05).

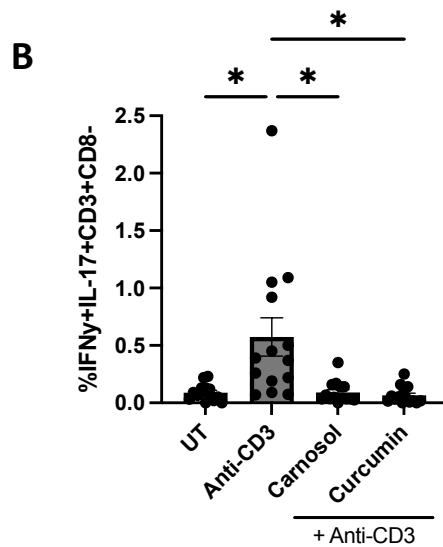
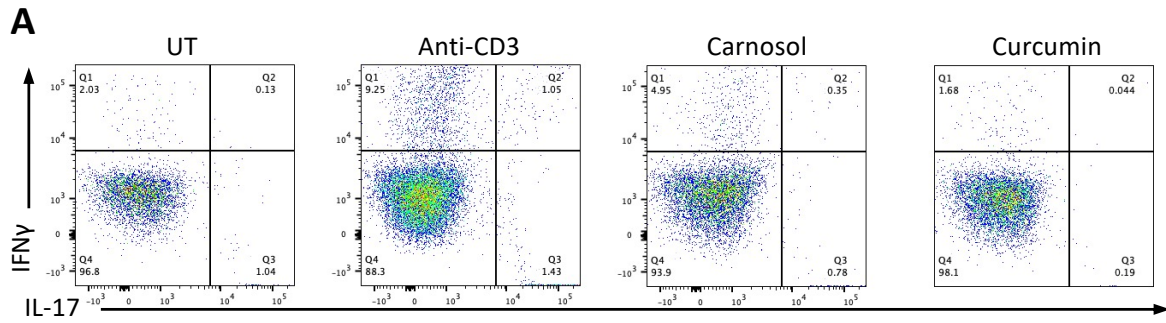


**Figure 4.34 Carnosol and curcumin reduce the frequency of IFN $\gamma$ <sup>+</sup>IL-17<sup>+</sup> CD4<sup>+</sup> T cells in *ex-vivo* stimulated PBMC from patients with IBD.**

PBMC isolated from IBD patients were treated with carnosol or curcumin (5  $\mu$ M) for 6 hours prior to stimulation with anti-CD3 (1  $\mu$ g/mL) for 12 hours. After 18 hours culture media was replaced with fresh media and cells were incubated for a further 4 days with anti-CD3 (1  $\mu$ g/mL) stimulation, without carnosol or curcumin. **(A)** Dot plots depicting IFN $\gamma$  and IL-17 expression by CD3<sup>+</sup>CD8<sup>-</sup> cells from one representative experiment. **(B)** Pooled data (n = 14) depicting the mean  $\pm$  SEM of IFN $\gamma$ <sup>+</sup>IL-17<sup>+</sup> in CD3<sup>+</sup>CD8<sup>-</sup> T cells. Repeated measures one-way ANOVA, with Dunnett's multiple comparisons post hoc test, was used to determine statistical significance by comparing means of treatment groups against the mean of the control group (\*p < 0.05).

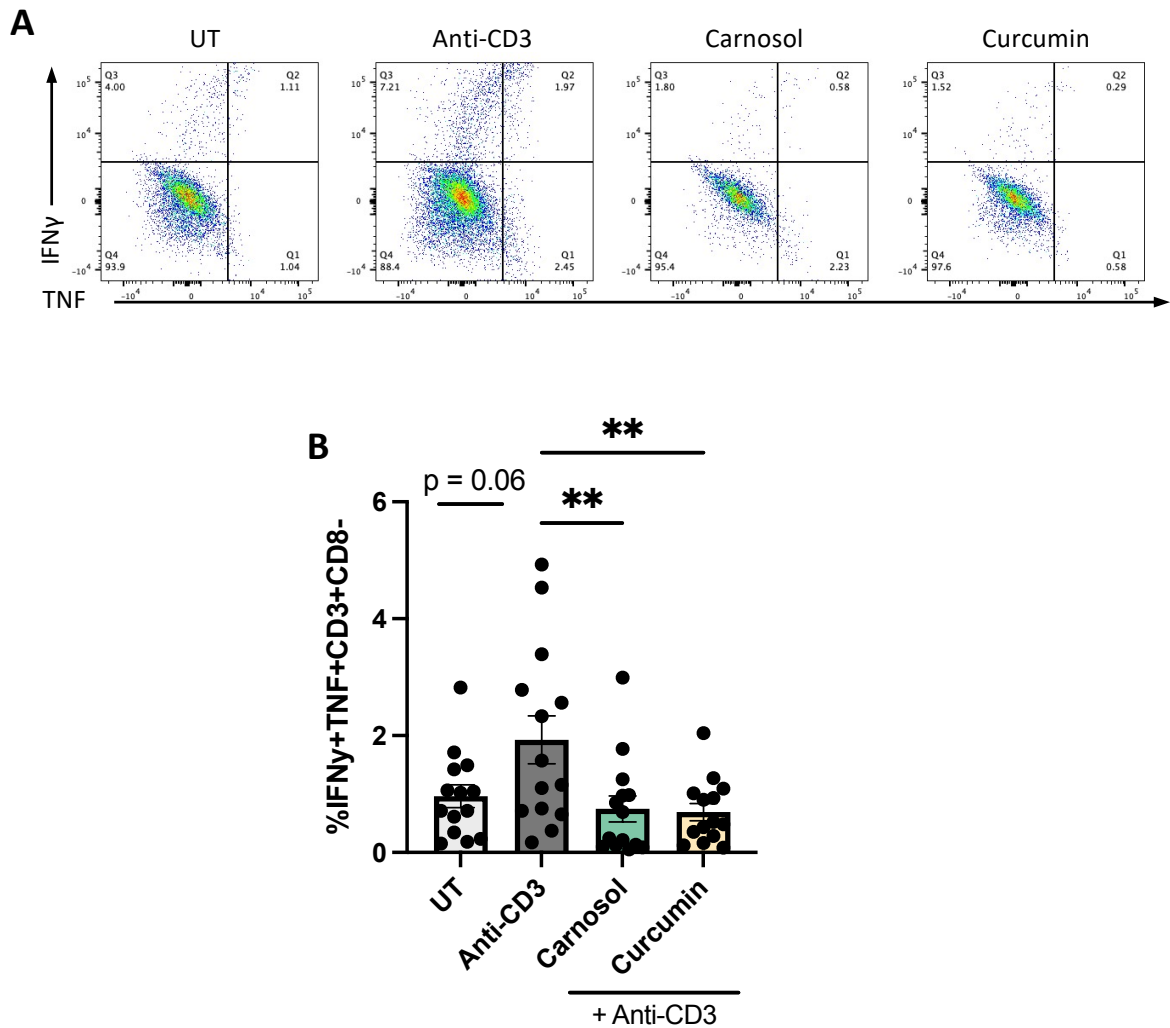


**Figure 4.35 Carnosol and curcumin reduce the frequency of IFN $\gamma$ <sup>+</sup>TNF<sup>+</sup> CD4<sup>+</sup>T cells in *ex-vivo* stimulated PBMC from patients with IBD.**

PBMC isolated from IBD patients were treated with carnosol or curcumin (5  $\mu$ M) for 6 hours prior to stimulation with anti-CD3 (1  $\mu$ g/mL) for 12 hours. After 18 hours culture media was replaced with fresh media and cells were incubated for a further 4 days with anti-CD3 (1  $\mu$ g/mL) stimulation, without carnosol or curcumin. **(A)** Dot plots depicting IFN $\gamma$  and TNF expression by CD3<sup>+</sup>CD8<sup>-</sup> cells from one representative experiment. **(B)** Pooled data (n = 14) depicting the mean  $\pm$  SEM of IFN $\gamma$ <sup>+</sup>TNF<sup>+</sup> in CD3<sup>+</sup>CD8<sup>-</sup> T cells. Repeated measures one-way ANOVA, with Dunnett's multiple comparisons post hoc test, was used to determine statistical significance by comparing means of treatment groups against the mean of the control group (\*\*p < 0.01).



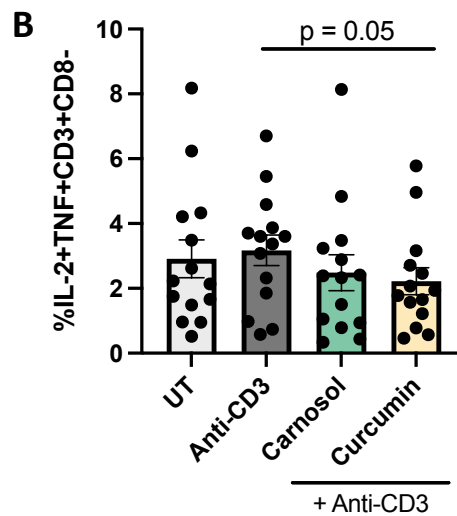
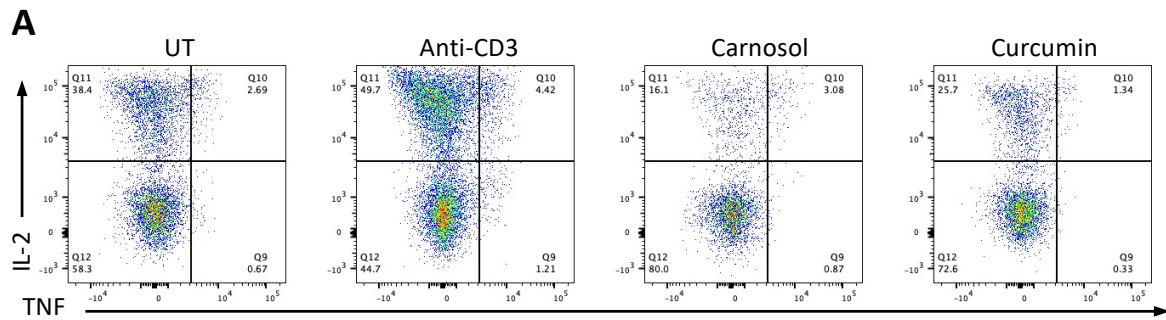


**Figure 4.36 Curcumin, but not carnosol, reduces the frequency of IL-2<sup>+</sup>TNF<sup>+</sup> CD4<sup>+</sup> T cells in *ex-vivo* stimulated PBMC from patients with IBD.**

PBMC isolated from IBD patients were treated with carnosol or curcumin (5  $\mu$ M) for 6 hours prior to stimulation with anti-CD3 (1  $\mu$ g/mL) for 12 hours. After 18 hours culture media was replaced with fresh media and cells were incubated for a further 4 days with anti-CD3 (1  $\mu$ g/mL) stimulation, without carnosol or curcumin. **(A)** Dot plots depicting IL-2 and TNF expression by CD3<sup>+</sup>CD8<sup>-</sup> cells from one representative experiment. **(B)** Pooled data (n = 14) depicting the mean  $\pm$  SEM of IL-2<sup>+</sup>TNF<sup>+</sup> in CD3<sup>+</sup>CD8<sup>-</sup> T cells. Repeated measures one-way ANOVA, with Dunnett's multiple comparisons post hoc test, was used to determine statistical significance by comparing means of treatment groups against the mean of the control group.

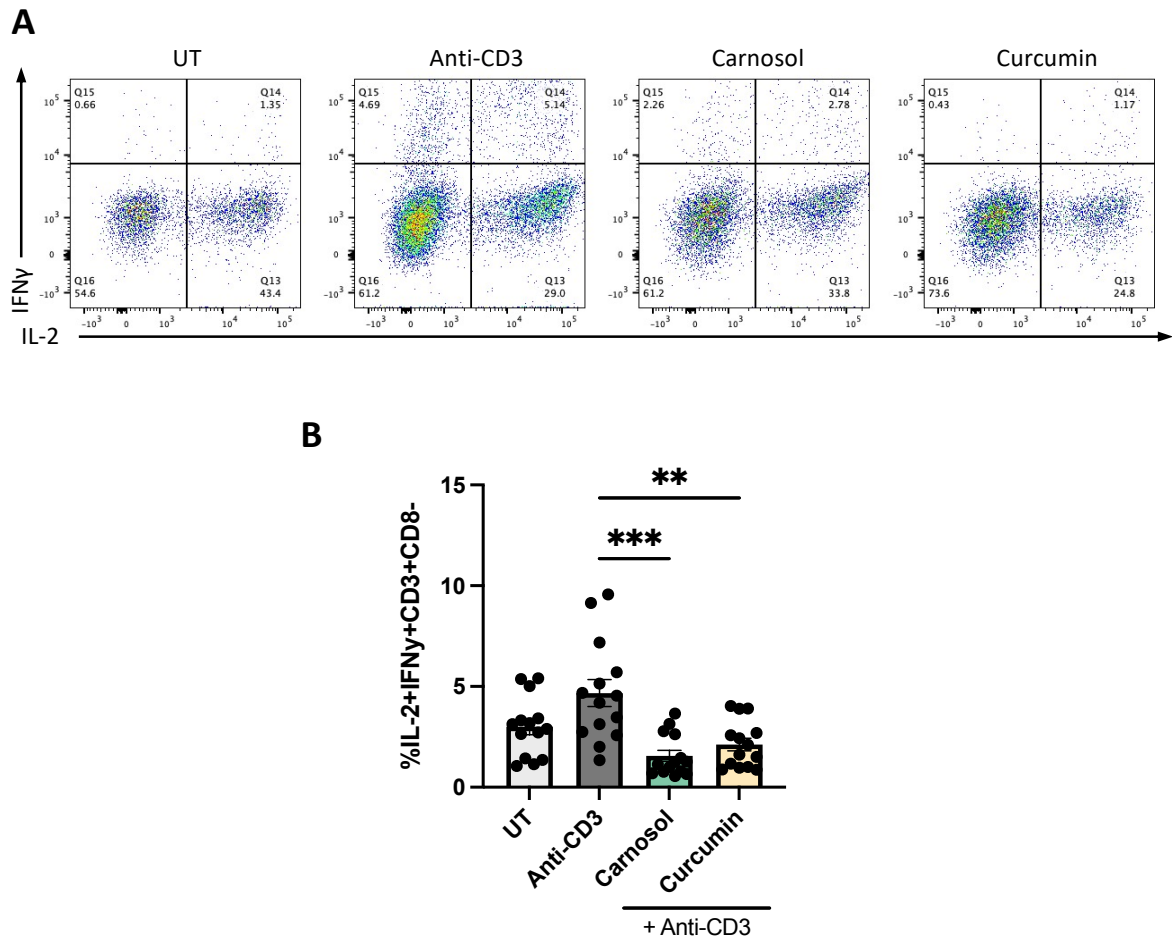


**Figure 4.37 Carnosol and curcumin reduce the frequency of IL-2<sup>+</sup>IFNγ<sup>+</sup> CD4<sup>+</sup> T cells in *ex-vivo* stimulated PBMC from patients with IBD.**

PBMC isolated from IBD patients were treated with carnosol or curcumin (5 μM) for 6 hours prior to stimulation with anti-CD3 (1 μg/mL) for 12 hours. After 18 hours culture media was replaced with fresh media and cells were incubated for a further 4 days with anti-CD3 (1 μg/mL) stimulation, without carnosol or curcumin. **(A)** Dot plots depicting IL-2 and IFNγ expression by CD3<sup>+</sup>CD8<sup>-</sup> cells from one representative experiment. **(B)** Pooled data (n = 14) depicting the mean ± SEM of IL-2<sup>+</sup>IFNγ<sup>+</sup> in CD3<sup>+</sup>CD8<sup>-</sup> T cells. Repeated measures one-way ANOVA, with Dunnett's multiple comparisons post hoc test, was used to determine statistical significance by comparing means of treatment groups against the mean of the control group (\*\*p < 0.01, \*\*\*p < 0.001).

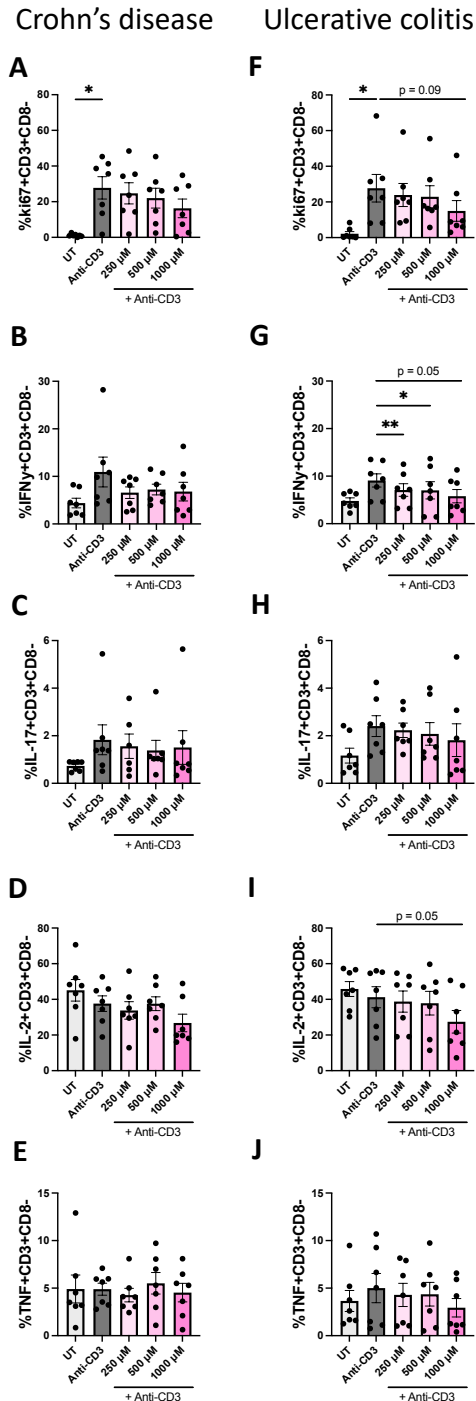


**Figure 4.38 HPP more significantly reduces IFN $\gamma$  expression in CD4<sup>+</sup> T cells in *ex-vivo* stimulated PBMC from patients with ulcerative colitis compared to Crohn's disease.** PBMC isolated from patients with Crohn's disease (A-E) or ulcerative colitis (F-J) were treated with HPP (250  $\mu$ M – 1000  $\mu$ M) for 6 hours prior to stimulation with anti-CD3 (1  $\mu$ g/mL) for 12 hours. After 18 hours culture media was replaced with fresh media and cells were incubated for a further 4 days with anti-CD3 (1  $\mu$ g/mL) stimulation, without HPP. Pooled data (n = 7 for each disease cohort) depicting the mean  $\pm$  SEM of (A & F) ki67<sup>+</sup>, (B & G) IFN $\gamma$ <sup>+</sup>, (C & H) IL-17<sup>+</sup>, (D & I) IL-2<sup>+</sup> and (E & J) TNF<sup>+</sup> in CD3<sup>+</sup>CD8<sup>-</sup> T cells. Repeated measures one-way ANOVA, with Dunnett's multiple comparisons post hoc test, was used to determine statistical significance by comparing means of treatment groups against the mean of the control group (\*\* p < 0.01, \*p < 0.05).

Crohn's disease      Ulcerative colitis

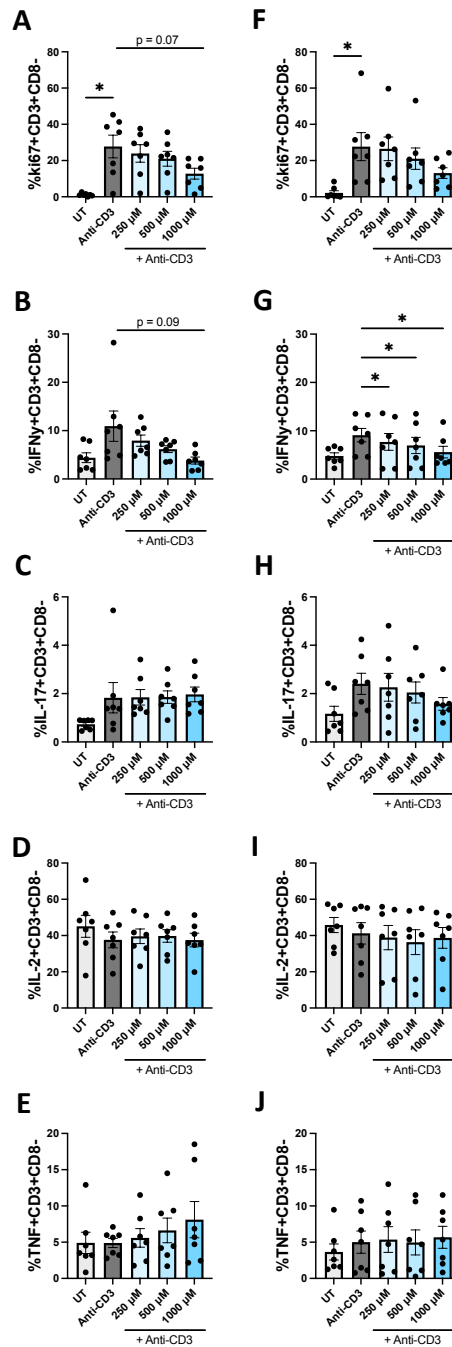


**Figure 4.39 IP more significantly reduces IFN $\gamma$  expression in CD4<sup>+</sup> T cells in *ex-vivo* stimulated PBMC from patients with ulcerative colitis compared to Crohn's disease.**

PBMC isolated from patients with Crohn's disease (A-E) or ulcerative colitis (F-J) were treated with IP (250  $\mu$ M – 1000  $\mu$ M) for 6 hours prior to stimulation with anti-CD3 (1  $\mu$ g/mL) for 12 hours. After 18 hours culture media was replaced with fresh media and cells were incubated for a further 4 days with anti-CD3 (1  $\mu$ g/mL) stimulation, without IP. Pooled data (n = 7 for each disease cohort) depicting the mean  $\pm$  SEM of (A & F) ki67<sup>+</sup>, (B & G) IFN $\gamma$ <sup>+</sup>, (C & H) IL-17<sup>+</sup>, (D & I) IL-2<sup>+</sup> and (E & J) TNF<sup>+</sup> in CD3<sup>+</sup>CD8<sup>-</sup> T cells. Repeated measures one-way ANOVA, with Dunnett's multiple comparisons post hoc test, was used to determine statistical significance by comparing means of treatment groups against the mean of the control group (\*p < 0.05).

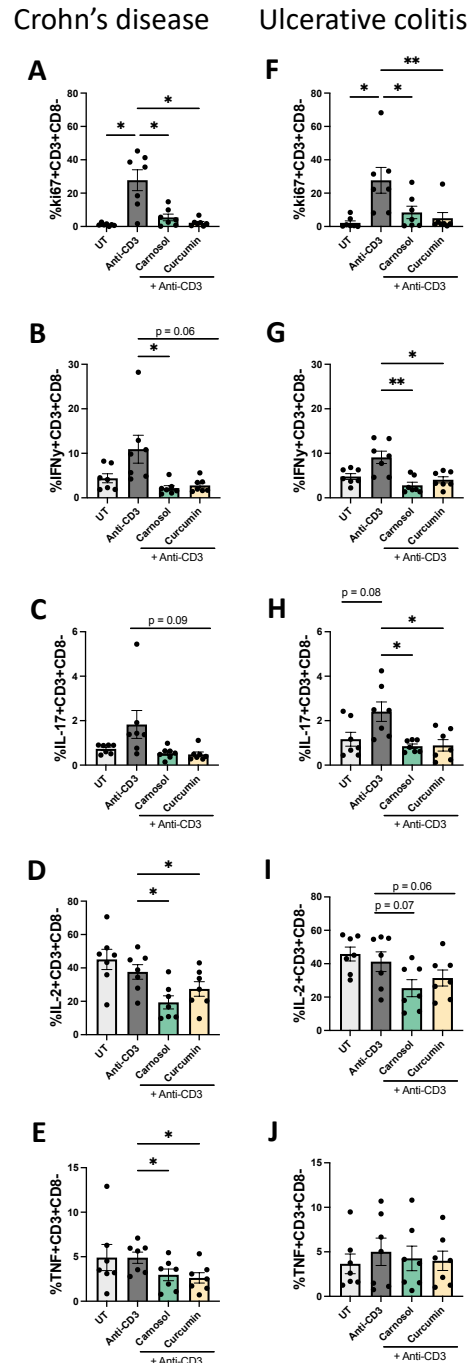


**Figure 4.40 Carnosol and curcumin more significantly reduce TNF expression in CD4<sup>+</sup> T cells in *ex-vivo* stimulated PBMC from patients with Crohn's disease compared to ulcerative colitis.**

PBMC isolated from patients with Crohn's disease (A-E) or ulcerative colitis (F-J) were treated with Carnosol or curcumin (both 5  $\mu$ M) for 6 hours prior to stimulation with anti-CD3 (1  $\mu$ g/mL) for 12 hours. After 18 hours culture media was replaced with fresh media and cells were incubated for a further 4 days with anti-CD3 (1  $\mu$ g/mL) stimulation, without carnosol or curcumin. Pooled data (n = 7 for each disease cohort) depicting the mean  $\pm$  SEM of (A & F) ki67<sup>+</sup>, (B & G) IFN $\gamma$ <sup>+</sup>, (C & H) IL-17<sup>+</sup>, (D & I) IL-2<sup>+</sup> and (E & J) TNF<sup>+</sup> in CD3<sup>+</sup>CD8<sup>-</sup> T cells. Repeated measures one-way ANOVA, with Dunnett's multiple comparisons post hoc test, was used to determine statistical significance by comparing means of treatment groups against the mean of the control group (\*\* p < 0.01, \*p < 0.05).

## 4.4 Discussion

The prevalence of autoimmune and inflammatory diseases has risen significantly in recent years [13]. This is likely due to a combination of environmental factors, along with increased disease awareness and diagnosis. The pathogenesis of autoimmune/inflammatory disease involves many immune cells, with DC and T cells commonly implicated as being key drivers of excessive inflammation. A number of therapeutics have been developed, but they differ in their efficacy depending on the patient and/or disease setting. Furthermore, many individuals can become refractory to therapy, due, for example, to the generation of endogenous neutralising antibodies against biologics [42]. New therapies with increased efficacy and tolerability, as well as fewer side effects, are therefore highly sought after. As mentioned previously, parasite-derived compounds have recently garnered attention as potential therapies for autoimmune/inflammatory diseases due to their ability to dampen excessive inflammation [301–304]. Trypanosome-derived ketoacids represent one such class of potential therapeutics, however, their effects on adaptive immune cells have not been extensively studied. The goal of this chapter was therefore to carry out a detailed analysis of the effects of IP and HPP on human T cell responses from both healthy individuals and those presenting with IBD.

The overactivation of DC can lead to the differentiation and proliferation of T cells in the absence of infection; therefore, dampening the inflammatory response of DC can in turn reduce pathogenic T cell responses. For example, treating DC with agents *ex vivo* which results in the generation of tolerogenic DC, which could then be re-introduced into the host, has been proposed as a potential approach for treating autoimmune disease [17,21,22]. As demonstrated in chapter 3, the ketoacids, IP and HPP, can suppress DC maturation, glycolysis and cytokine production, therefore, it was of interest initially to investigate how these tolerogenic DC impact T cells. In order for T cells to be fully activated, they require three signals from APC: antigen presentation on MHC molecules to the TCR, binding of CD28 on naïve T cells to co-stimulatory molecules (e.g. CD80/86) on APC, and cytokine production by APC to instruct the T cell effector functions further. The distinct

cytokines secreted by the APC will also drive the differentiation of T cells into their specific effector subsets. As demonstrated in chapter 3, DC treated with HPP exhibit decreased expression of co-stimulatory markers, along with reduced pro-inflammatory cytokine production, indicating that they may have a reduced capacity to activate T cells upon co-culture. This was indeed the case, and T cells co-cultured with HPP-treated DC trended towards a reduction in proliferation and expression of the Th1 cytokine, IFN $\gamma$ . Interestingly, despite a trend towards an increase in the secretion of IL-10, there was actually a trend towards a decrease in Treg numbers in the total T cell population. This indicates that the IL-10 being produced may be coming from a different cell type within the co-culture such as a different subset of T cells, or the DC themselves. Surprisingly, T cells co-cultured with IP-treated DC exhibited increased proliferation and IFN $\gamma$  expression; an unexpected result given that IP treatment resulted in a potent decrease in IL-12 secretion from LPS stimulated DC. IP-treated DC did not reduce the levels of Tregs to the same extent as HPP-treated DC, and there was no associated change in IL-10 levels. It was hypothesised that, under co-culture conditions, IP treatment may be increasing the proliferation of Tregs over non-Tregs, however this was not the case. Given the auto-fluorescent nature of IP, it was not possible to assess the effect of this compound on DC maturation (as outlined in chapter 3). Hence, while it may be reducing inflammatory cytokine production by DC, it may not be impacting on antigen presentation and DC maturation which may explain the lack of effect on T cell responses in this particular experimental setting. More promising results were obtained by Aoki *et al.* who reported a reduction in IFN $\gamma$  expression when DC were isolated from the mesenteric lymph nodes of mice administered IP, and co-cultured with murine CD4<sup>+</sup> T cells [258], hence additional factors may be at play *in vivo* to promote the immunosuppressive function of IP. Nonetheless, HPP did exhibit promising results in the *in vitro* model described in this study.

Given the important role played by DC-derived cytokines in polarising T cells towards specific subsets, it was of interest to determine if ketoacid mediated cytokine suppression by DC impacts the phenotypic fate of a T cell. To test this, CD4<sup>+</sup> T cells were isolated from PBMC and stimulated with anti-CD3 and anti-CD28 (to provide two of the three signals necessary for T cell activation) in the presence and absence of supernatants from ketoacid-treated DC. Despite ketoacid autofluorescence causing some interference in these assays,

there did appear to be a reduction in IFN $\gamma$  expression in CD4<sup>+</sup> T cells upon incubation with IP and HPP-treated DC supernatant. This is likely due to the reduction in levels of the Th1 polarising cytokine, IL-12, in the supernatants of ketoacid-treated DC. Notably, IFN $\gamma$  is a highly inflammatory cytokine which has been implicated in the pathogenesis of many autoimmune and inflammatory conditions [339,340].

In order to translate the above findings to a more clinical setting, experiments were carried out using PBMC isolated from patients with IBD. IP and HPP reduced the secretion of IFN $\gamma$ , IL-17, and also the anti-inflammatory cytokine IL-10 from PBMC. Furthermore, IP and HPP reduced the proliferation of CD3<sup>+</sup>CD8<sup>-</sup> cells (assumed to be CD4<sup>+</sup> cells for the purpose of this study), while IFN $\gamma$  expression was also decreased. HPP, but not IP, was also capable of reducing IL-2 expression which is produced in large quantities by activated CD4<sup>+</sup> T cells, and can lead to activation of other effector T cell subsets under inflammatory conditions [341]. Interestingly, neither IP or HPP had any effect on the expression of IL-17 or TNF in CD4<sup>+</sup> cells. However, IP and HPP reduced secretion of IL-17 when examined by ELISA, with IP showing more potent reductions than HPP. IP was effective at even the lowest concentrations tested, and these reductions in secretion of cytokine would unlikely be due to the reduced proliferation caused by IP, as there was no reduction in ki67 expression upon treatment with the lowest concentration. Furthermore, both IP and HPP were capable of reducing the frequency of IFN $\gamma$ <sup>+</sup>IL-17<sup>+</sup>, IFN $\gamma$ <sup>+</sup>TNF<sup>+</sup>, and IL-2<sup>+</sup>IFN $\gamma$ <sup>+</sup> CD4<sup>+</sup> cells, while HPP was also capable of reducing the frequency of IL-2<sup>+</sup>TNF<sup>+</sup> CD4<sup>+</sup> cells. This is more reflective of a clinical disease setting as T cells will express more than one cytokine at a time. This further supports the anti-inflammatory effects of the ketoacids, and also confirms that immune cells from IBD patients are not refractory to these effects, which is an important factor to consider when assessing new therapies.

While the primary T cell subtype examined in IBD has traditionally been CD4<sup>+</sup> T cells, there has recently been interest in the pathogenic role played by CD8<sup>+</sup> T cells [337]. In general, they do appear to contribute to inflammation in this disease [337] and were therefore included in the analysis of patient PBMC. Similar to the effects seen on CD4<sup>+</sup> T cells, IP and HPP were capable of reducing the proliferation of CD8<sup>+</sup> T cells. In terms of cytokine



production, CD8<sup>+</sup> T cells secrete IFN $\gamma$ , IL-2 and TNF, and produce cytotoxins capable of killing infected or compromised cells [342]. The cytotoxic effector functions of CD8<sup>+</sup> T cells were not examined in the course of this study, however, IP treatment was found to significantly reduce IFN $\gamma$  expression, while having no effect on either TNF or IL-2 expression. This is in agreement with the effects observed in IP-treated CD4<sup>+</sup> T cells. On the other hand, HPP significantly reduced IFN $\gamma$  and TNF expression in CD8<sup>+</sup> T cells at the lowest concentration examined, however viability issues at the higher doses of HPP made analysis difficult given the low cell numbers. Further experiments are therefore required to fully elucidate the effects of the ketoacids on CD8<sup>+</sup> T cells, however preliminary results indicate they may suppress pro-inflammatory responses mediated by this cell type.

Carnosol and curcumin are plant-derived polyphenols with documented anti-inflammatory and antioxidant properties. They are potent inducers of HO-1 and have shown efficacy in a number of disease models [269,334–336]. They have also been highlighted as potential therapeutics for IBD [343–347]. These polyphenols have not been assessed in IBD patient samples and were included in this study in order to compare their efficacy to the ketoacids. Both carnosol and curcumin potently reduced the proliferation of CD4<sup>+</sup> and CD8<sup>+</sup> T cells and did so to a greater extent than the ketoacids. Similarly, they decreased the secretion of IFN $\gamma$ , IL-17, and also the anti-inflammatory cytokine IL-10. Investigating this further, it was demonstrated that they potently decreased the expression of all cytokines examined from both CD4<sup>+</sup> and CD8<sup>+</sup> T cells. Furthermore, treatment of cells with the polyphenols resulted in a decrease in the frequency of double positive CD4<sup>+</sup> T cells i.e. IFN $\gamma$ <sup>+</sup>IL-17<sup>+</sup>, IFN $\gamma$ <sup>+</sup>TNF<sup>+</sup>, and IL-2<sup>+</sup> IFN $\gamma$ <sup>+</sup> cells. These results indicate these polyphenols exhibit anti-inflammatory effects in IBD patient PBMC, similar to results reported by our laboratory assessing their effects in samples from psoriasis patients [269]. One of the limitations that has been highlighted regarding the use of polyphenols as therapeutics is their limited bioavailability due to poor absorption from the gut. However, given that the gut is the actual site of inflammation in IBD, this low bioavailability may actually be advantageous.

As previously mentioned, CD is classically described as a Th1 type immune disease with high levels of IFN $\gamma$ , while UC presents with an atypical Th2 type immune response with high

levels of IL-5, IL-4 and IL-13 [331]. Furthermore, IL-17 has been implicated in the pathogenesis of both diseases [331–333]. The cytokines analysed in the IBD patient samples in this study were limited to IFN $\gamma$ , IL-17, TNF, and IL-2, cytokines more typically associated with a Th1 type response, which may be more relevant for CD. However, due to fluorescence issues surrounding the ketoacids, as well as limited cell numbers, the number of cytokines that could be examined were restricted and had to be carefully chosen. Initially it was unclear if there would be access to enough patient samples to stratify them into disease subtypes, therefore they were all treated under the umbrella of ‘IBD samples’, and traditional inflammatory markers were chosen for analysis. Studies have since revealed that is overly simplistic and limiting to define CD as being a Th1 type disease and UC a Th2 type disease; demonstrative of this, not all UC patients express this Th2 type signature [348] and an IL-13 neutralising antibody did not significantly improve clinical responses in UC patients [349]. Therefore, there has been increased interest in moving away from the simplified Th1/Th2 paradigm in characterising CD and UC. There also appears to be a number of emerging T cell subsets implicated in the pathogenesis of both diseases, including Th9 cells and Tfh cells [350,351]. Furthermore, as previously mentioned, polyfunctional T cells, expressing more than one cytokine, have been shown to be more pathogenic in autoimmune and inflammatory conditions [338,352,353], and T cells can also demonstrate considerable phenotypic plasticity [354]. Indeed, studies have discovered a subpopulation of Th17 cells capable of expressing IFN $\gamma$ , with these IFN $\gamma$ <sup>+</sup>IL17<sup>+</sup> cells being considered highly pathogenic in not only IBD, but also other autoimmune and inflammatory conditions [351,355–359]. Based on this it is important to note that the cytokines examined in this study provide a limited insight into the immunomodulatory properties of the ketoacids, and it would be of interest to fully characterise their effect on a wide range of T cell cytokines and inflammatory markers in the future.

In the final part of this study, patient data was stratified based on disease in order to determine if the ketoacids or polyphenols exerted similar effects on UC versus CD. There did not appear to be any major differences in the immunomodulatory effects between diseases. IP and HPP reduced proliferation, IL-17, IL-2 and TNF expression to similar levels in samples from both UC and CD patients. The only statistical difference across the cohorts was observed when examining IFN $\gamma$  expression. IP and HPP both significantly reduced IFN $\gamma$

expression in CD4<sup>+</sup> T cells from patients with UC, however, despite reducing the expression of this cytokine to a similar level in patients with CD, this was not significant. It is likely that a larger spread of data with the CD patients is preventing statistical significance in this case, however, at a biological level, there appeared to be similar effects in both disease cohorts. The polyphenols reduced all markers examined across both disease cohorts to similar levels, with the exception of TNF. Both carnosol and curcumin significantly reduced TNF expression in CD4<sup>+</sup> T cells from patients with CD, while having no effect on the expression of this cytokine in patients with UC. Therefore, for now it appears that all treatments examined would show similar therapeutic efficacy in both UC and CD.

Despite the ketoacids demonstrating promising immunomodulatory effects in the IBD patient samples, this study was limited by a number of factors. The data set investigated in this study was small, 14 patients, as a result of reduced access to samples due to the COVID pandemic. Access to a greater number of samples may have highlighted more interesting results, and may have also strengthened the promising results the ketoacids demonstrated. A greater number of both UC and CD samples may have also led to identification of more pronounced differences between each disease cohort in response to the ketoacids, further identifying their potential as therapeutics for either one of, or both, conditions. Furthermore, the stratification of the disease cohorts in this study was limited in stratifying the patients based only on having either UC or CD; however, there can still be large variations even within these disease subtypes. Therefore, had more information been available, such as patient's disease stage, severity, years since diagnosis, and years in remission, this would have allowed for a deeper stratification and potentially identified more pronounced and clinically translatable results. One of the more important variables that may affect the outcome of this study is the treatment regime of the patients: what treatment they're on and for how long, how responsive they are to it, and what other treatments they have tried and not responded to in the past. The ketoacids may have vastly different effects on a patient who is in remission taking a first line therapy, versus a patient with highly active disease and not responding to many available therapeutics. However, unfortunately this data was not available. As mentioned above, a much larger cohort of patients would be needed to gain valuable insights from a deeper stratification, and it

would greatly expand upon the findings thus far and fully uncover the therapeutic potential of the ketoacids in this way going forward.

In conclusion, the results presented in this chapter demonstrate that, not only do trypanosome-derived ketoacids exert immunomodulatory effects on innate immune cells, but they also impact on adaptive immune cells. HPP-treated DC are capable of reducing the proliferation and pro-inflammatory cytokine production from co-cultured T cells, further supporting the notion that the ketoacids induce a tolerogenic DC phenotype. The ketoacids, along with established HO-1 inducers, carnosol and curcumin, also reduce proliferation and inflammatory cytokine production in immune cells isolated from patients with IBD (Figure 4.41). While further study is required, the results presented here provide further support for their use as potential therapeutics to treat inflammatory disease characterised by excessive and dysregulated immune responses.

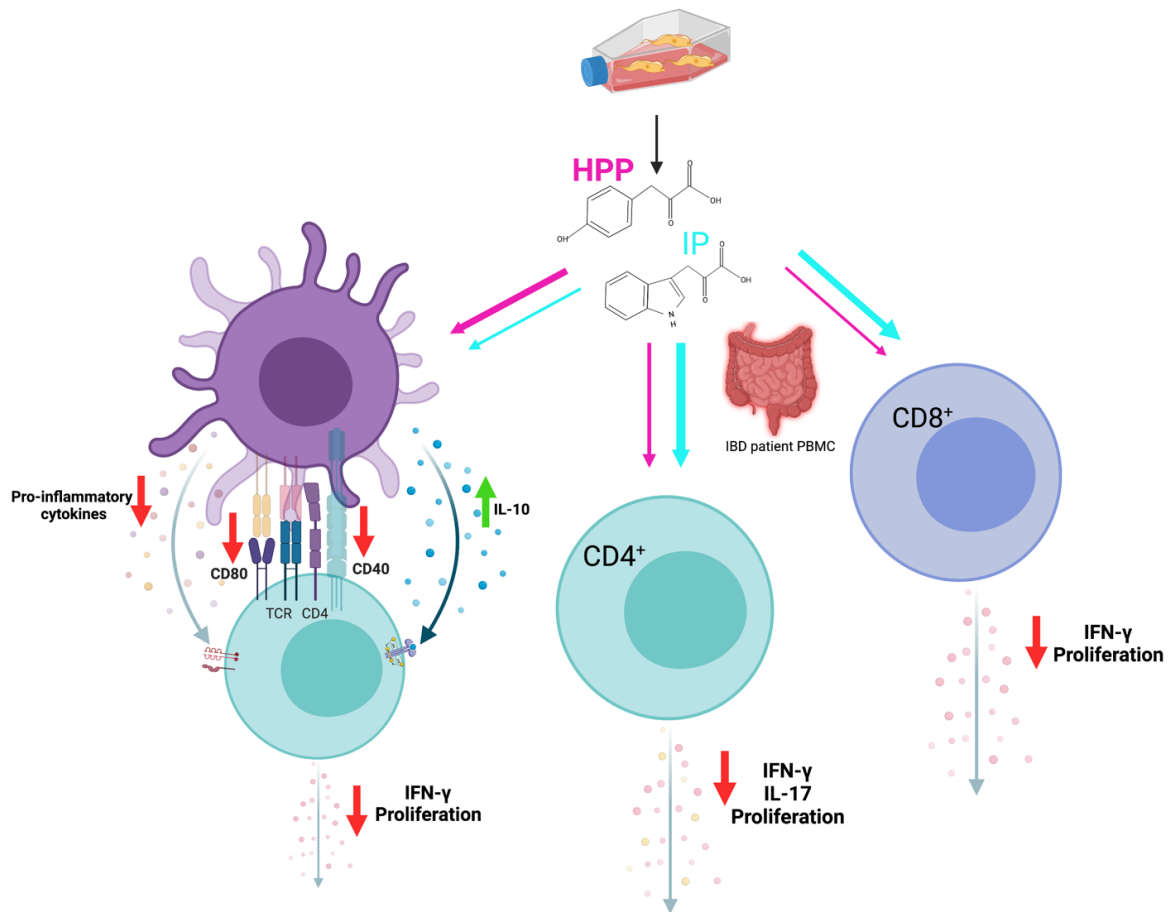


**Figure 4.41 Model of immunomodulatory effects of trypanosome-derived ketoacids in human T cells.**

Trypanosomes secrete the ketoacids IP and HPP. Culturing of human DC with these ketoacids leads to a more tolerogenic phenotype, characterised by reduced maturation marker expression and pro-inflammatory cytokine secretion. Ketoacid-treated DC subsequently reduce the proliferation of CD4<sup>+</sup> T cells and this is accompanied by reduced pathogenic cytokine production. PBMC from IBD patients treated directly with these ketoacids have reduced proliferation and inflammatory cytokine production in both CD4<sup>+</sup> and CD8<sup>+</sup> T cells.

# **Chapter 5:**

## **General Discussion**

## 5.1 General discussion

Autoimmune and inflammatory diseases such as IBD, MS, RA and psoriasis are all characterised by excessive and aberrant inflammation. While each disease has its own distinct pathology, many of the currently available therapeutics target common pathways or mediators, and include, for example, inhibitors of the JAK-STAT pathway or monoclonal antibodies targeting inflammatory cytokines and co-stimulatory molecules [42]. Despite the availability of such therapeutics, most of these diseases are incurable and cause significant morbidity and mortality every year [360,361]. Furthermore, current immunomodulatory therapeutics to treat autoimmune diseases show limited efficacy in many patients, either from initial treatment, or through the patient becoming refractory over time [42]. They are also associated with numerous side effects, and leave patients vulnerable to infections, further adding to disease burden [42]. Therefore, novel therapies that can be used alone, or in combination with existing treatments, are highly sought after.

Parasites are organisms which live in or on a host, eventually causing harm to the host species. Disease severity resulting from parasitic infection differs depending on numerous factors, ranging from the type of parasite, to the health status of the host [362]. Parasites are constantly challenged by the host's immune system and employ numerous mechanisms to dampen these responses in order to ensure both their own and their host's survival [363]. In some ways, this can actually prove beneficial to the host, as the presence of parasites results in reduced allergic, autoimmune, and inflammatory conditions [363]. In support of this notion, the eradication of dangerous parasites in developed countries has coincided with increased incidence of the aforementioned conditions, forming part of the basis of the 'hygiene hypothesis' [364,365]. Indeed, there has recently been increased interest in utilising parasites and their ability to dampen host immune responses to treat autoimmune or inflammatory diseases. Some studies have involved deliberate infection with parasites as one method of treating inflammation, and despite their ability to reduce disease symptoms, these treatments are unsurprisingly accompanied by a number of unwanted side effects [366–369]. Therefore, immunomodulatory products derived from parasites have recently garnered greater interest as potential therapeutics, as they are not

accompanied by infection-associated issues [301–304]. Examples include a peptide derived from the helminth, *Fasciola hepatica*, which was shown to ameliorate disease in murine models of type 1 diabetes and MS, by inhibiting the production of macrophage-derived pro-inflammatory cytokines [302]. Soluble proteins from the blood fluke, *Schistosoma mansoni*, have also been shown to reduce pro-inflammatory cytokine production (IFN $\gamma$  and IL-17), while increasing regulatory cytokines (TGF $\beta$  and IL-10) in a murine model of colitis [370]. Interestingly, the intestinal roundworm, *Heligmosomoides polygyrus*, secretes a TGF $\beta$  mimic, which is capable of binding to the TGF $\beta$  receptor and inducing Tregs, resulting in reduced disease severity in a murine model of MS [371,372]. Many studies investigating parasite-derived compounds are still in the early stages, and have not yet moved to clinical trials, nonetheless there is strong evidence demonstrating their immunomodulatory effects and therapeutic potential.

The *T. brucei*-derived ketoacids investigated in this study may also represent novel immune modulators and, while they have proven efficacy in murine models of disease [255,257,258], there have been no reports examining their effects in human immune cells. Results provided in this thesis confirm that IP and HPP can induce expression of the immune suppressive enzyme, HO-1, and attenuate pro-inflammatory immune responses in human DC. Specifically, HPP reduced the maturation of DC and this was accompanied by a reduction in the secretion of pro-inflammatory cytokines and expression of maturation markers, while at the same time enhancing the phagocytic capacity of the cells. Attempts to investigate maturation marker expression on IP-treated DC were hindered by autofluorescence issues, however, this ketoacid was also found to suppress inflammatory cytokine production. Supernatants from both IP- and HPP-treated DC reduced IFN $\gamma$  expression in CD4<sup>+</sup> T cells, an effect that was recapitulated by HPP in DC:T cell co-culture experiments. However, this was not the case with IP, and it is hypothesised that IP may not impact DC maturation to the same extent as HPP. Further investigation using non-fluorescent based analysis is now required to confirm if this is indeed the case.

Despite both ketoacids exhibiting immunomodulatory properties, other subtle differences were observed during the course of this study. As mentioned, both ketoacids induce HO-1 in human DC, however this occurs more rapidly upon HPP treatment. Similar results were



observed when examining p62 activation, with HPP activating this autophagy-related protein at an earlier time-point compared to IP. This may be due to IP converting to another form over time, and it is possible that the derivative has more potent anti-inflammatory effects than the parent compound. Mass spectrometry and/or NMR will be useful in determining whether such a change occurs in the ketoacid structure. Another notable difference was the ability of IP to induce ROS production and induce expression of CYP1A1 in DC. This may occur via activation of the AHR which is known to be activated by indole based compounds. Of note, AHR activation in murine models of colitis resulted in amelioration of disease, while inhibition or knockout of the AHR increased disease severity [373–377]. Furthermore, AHR expression is lower in the mucosa of patients with IBD, in particular CD, compared to healthy controls [373], further establishing a link between activation of this receptor and gut health. The increase in ROS by IP likely leads to activation of the HO-1/Nrf2 pathway. The pathway leading to induction of HO-1 by HPP may differ, but based on results in this study, likely involves activation of AMPK or p62, both of which have been previously linked to HO-1 activation [131–136,282–284]. Indeed other mechanisms cannot be ruled out and require investigation. For example, the immunomodulatory metabolite, itaconate, activates Nrf2 through alkylation of KEAP1 cysteine residues [312]. This can also be confirmed using mass spectroscopy and may represent yet another mechanism through which the ketoacids activate the HO-1/Nrf2 pathway.

In addition to AMPK and p62, the ketoacids were also found to activate the additional autophagy related protein, LC3. Autophagy functions to eliminate dysfunctional cellular components, e.g. damaged organelles or misfolded proteins, when they are no longer required, may damage the cell, or are needed to generate energy. Autophagy is also important for the elimination of intracellular bacteria [378]. Any defects in autophagy can result in inflammatory conditions and there are strong links between SNPs in autophagy-related genes and CD [85]. It has been hypothesised that defective autophagy leads to reduced killing of pathogens, which may contribute to the dysbiosis found in the gut of patients with IBD [379,380]. While further study is required, it is possible that trypanosome-derived ketoacids may be beneficial as therapies for IBD through activation of autophagy. Indeed, many drugs currently used to treat IBD, including aminosaliclates

and thiopurines, may exert their therapeutic function in part due to activation of this pathway [379,380]. Furthermore, rapamycin, an inhibitor of mTOR which leads to activation of autophagy, has shown therapeutic potential in a number of IBD-related studies [381–383]. However, caution should be exercised with this approach as some pathogens such as *Staphylococcus aureus* have been shown to exploit activation of autophagy to increase survival, which may in turn leave the patient more susceptible to infection [384].

Another key pathway examined in this thesis was DC cellular metabolism. Recently there has been great interest in the metabolic reprogramming of immune cells, since it was shown that they engage different metabolic pathways depending on their activation or maturation state [43]. Indeed, dysregulated immunometabolism has been highlighted as a feature of many autoimmune/inflammatory diseases [44–46], and manipulation of metabolic pathways has been proposed as a potential therapeutic strategy. In this study, IP and HPP were found to downregulate glycolysis, while HPP was shown to enhance oxidative phosphorylation in LPS-stimulated DC. This metabolic profile is associated with immature, tolerogenic DC [51,274]. Due to limited cell numbers it was not possible to examine these effects in PBMC from IBD patients, however, there is some evidence demonstrating an altered immunometabolic phenotype in patients with this disease [385]. Furthermore, the findings here may be intrinsically linked to autophagy, as the pathways share many common activators and inhibitors. Therefore, the abovementioned use of rapamycin to therapeutically treat CD [381–383] may not only be relevant for autophagy activation, but may also impact on metabolic pathways associated with a more tolerogenic DC phenotype. Interestingly, 5-ASA, a first line drug used for the treatment of IBD, can activate AMPK and inhibit mTOR, providing further evidence that altering metabolic pathways may prove efficacious in the treatment of IBD [386,387]. This further supports IP and HPP as potential therapeutics to treat IBD through their effects on metabolic pathways engaged by immune cells.

In this study it is demonstrated that the ketoacids, IP in particular, are capable of not only inhibiting pro-inflammatory cytokines, but also promoting the anti-inflammatory cytokine IL-10. This may be of particular importance for IBD, as IL-10 has been shown to be

protective in murine models of colitis [388,389], while IL-10 deficient mice develop spontaneous colitis [390]. Interestingly, in a study similar to the work presented here, both carnosol and curcumin were shown to significantly inhibit the production of IL-10 from LPS-stimulated DC, indicating they do not promote an anti-inflammatory phenotype in these cells [269]. This may represent an advantage the ketoacids have over the polyphenols examined in this study; the promotion of an anti-inflammatory phenotype is crucial for the resolution of inflammation in IBD and the repair of damaged intestinal walls [391]. The ketoacids have previously been shown to inhibit pro-inflammatory cytokines and iNOS expression in murine macrophages [256], markers more associated with an 'M1-like' macrophage phenotype. Therefore it would be interesting to assess the ability of the ketoacids to induce 'M2-like' macrophages, which are important for promoting wound healing and reducing disease severity in murine models of IBD, through induction of IL-10 [392,393]. M2 macrophages, IL-10, and HO-1 are all intrinsically linked [394], therefore it is likely that the ketoacids would be capable of polarising macrophages towards this anti-inflammatory phenotype, further supporting their therapeutic potential.

One disadvantage for the implementation of already established HO-1 inducers as potential therapies is their limited bioavailability, something that has yet to be established for the ketoacids. However, this problem may be overcome when the target tissue is more easily accessible, in particular in the case of IBD. For example, the HO-1 inducer curcumin has been tested in clinical trials of patients with ulcerative colitis and showed no adverse side effects while demonstrating clear efficacy in inducing and maintaining remission in patients compared to placebo alone [344,395]. Therefore, directly targeting the gut with the ketoacids may also prove beneficial to treat IBD. Furthermore, efforts are underway to produce delivery systems to enhance tissue targeting and curcumin uptake [396–400], another factor which could be utilised with the ketoacids. Interestingly, administration of curcumin along with the first line therapy 5-ASA, which may attribute some of its anti-inflammatory effects to HO-1 induction [179,180], was superior at inducing remission in UC patients, compared to treatment with 5-ASA alone [395]. It would be of interest to determine if the ketoacids are more effective as a standalone therapy, or if, similar to curcumin, they would show increased efficacy in combination with a first-line therapy such as 5-ASA.

Despite the promising results presented in this study, there are a number of limitations that need to be addressed, a major one being the autofluorescence of the ketoacids which restricted the techniques used to analyse samples. The use of flow cytometry in particular, was limited to small panels, or required removal of the compound at an early time-point to prevent it becoming fluorescent. This may have resulted in some of the immunomodulatory effects of IP being missed as it may become more potent over time. HPP was also found to become fluorescent at later time-points, and identification, as well as *in vitro/in vivo* assessment, of IP and HPP breakdown products is now required to move forward with any therapeutic application. Another major limitation faced in the course of this study was reduced access to patient samples as a result of the COVID pandemic. Future experiments involving, for example, *ex vivo* tissue explants and isolated immune cell populations will be of great benefit in determining the true therapeutic potential of these compounds. Finally, assessment of these compounds in a chronic model of colitis, which is more reflective of the clinical condition, will provide further information regarding efficacy, dosing, treatment route and bioavailability.

In conclusion, the data presented in this thesis demonstrates that IP and HPP are capable of modulating DC maturation and cellular metabolism, and suppressing the inflammatory profile of cells isolated from patients with IBD. This study therefore not only provides further evidence of the immune-evasion mechanisms employed by *T. brucei*, but also supports further exploration of this novel class of HO-1 inducers as potential therapeutics for the treatment of inflammatory conditions.

## References

1. Litman, G.W.; Rast, J.P.; Fugmann, S.D. The origins of vertebrate adaptive immunity. *Nat. Rev. Immunol.* **2010**, *10*, 543–553, doi:10.1038/NRI2807.
2. Pancer, Z.; Cooper, M.D. The evolution of adaptive immunity. *Annu. Rev. Immunol.* **2006**, *24*, 497–518, doi:10.1146/ANNUREV.IMMUNOL.24.021605.090542.
3. Buchmann, K. Evolution of innate immunity: Clues from invertebrates via fish to mammals. *Front. Immunol.* **2014**, *5*, 459, doi:10.3389/FIMMU.2014.00459/BIBTEX.
4. Netea, M.G. Training innate immunity: the changing concept of immunological memory in innate host defence. *Eur. J. Clin. Invest.* **2013**, *43*, 881–884, doi:10.1111/eci.12132.
5. Kumar, H.; Kawai, T.; Akira, S. Pathogen recognition by the innate immune system. *Int. Rev. Immunol.* **2011**, *30*, 16–34, doi:10.3109/08830185.2010.529976.
6. Dempsey, P.W.; Vaidya, S.A.; Cheng, G. The art of war: Innate and adaptive immune responses. *Cell. Mol. Life Sci.* **2003**, *60*, 2604–2621, doi:10.1007/S00018-003-3180-Y.
7. Merad, M.; Sathe, P.; Helft, J.; Miller, J.; Mortha, A. The dendritic cell lineage: ontogeny and function of dendritic cells and their subsets in the steady state and the inflamed setting. *Annu. Rev. Immunol.* **2013**, *31*, 563–604, doi:10.1146/annurev-immunol-020711-074950.
8. Banchereau, J.; Briere, F.; Caux, C.; Davoust, J.; Lebecque, S.; Liu, Y.-J.; Pulendran, B.; Palucka, K. Immunobiology of Dendritic Cells. *Annu. Rev. Immunol.* **2000**, *18*, 767–811, doi:10.1146/annurev.immunol.18.1.767.
9. Yoshida, R.; Imai, T.; Hieshima, K.; Kusuda, J.; Baba, M.; Kitaura, M.; Nishimura, M.; Kakizaki, M.; Nomiyama, H.; Yoshie, O. Molecular cloning of a novel human CC chemokine EBI1-ligand chemokine that is a specific functional ligand for EBI1, CCR7. *J. Biol. Chem.* **1997**, *272*, 13803–9, doi:10.1074/jbc.272.21.13803.
10. Kumar, B. V.; Connors, T.J.; Farber, D.L. Human T Cell Development, Localization, and Function throughout Life. *Immunity* **2018**, *48*, 202–213.
11. Godfrey, D.I.; Uldrich, A.P.; McCluskey, J.; Rossjohn, J.; Moody, D.B. The burgeoning family of unconventional T cells. *Nat. Immunol.* **2015**, *16*, 1114–1123.
12. Caza, T.; Landas, S. Functional and Phenotypic Plasticity of CD4(+) T Cell Subsets. *Biomed Res. Int.* **2015**, *2015*, 521957, doi:10.1155/2015/521957.
13. Lerner, A.; Jeremias, P.; Matthias, T. The World Incidence and Prevalence of Autoimmune Diseases is Increasing. *Int. J. Celiac Dis.* **2016**, *3*, 151–155, doi:10.12691/ijcd-3-4-8.
14. Wang, L.; Wang, F.-S.; Gershwin, & M.E.; Wang, A.; Wang, L.; Me, G. Human autoimmune diseases: a comprehensive update. *J. Intern. Med.* **2015**, *278*, 369–395, doi:10.1111/JOIM.12395.

15. Steinman, R.M.; Hawiger, D.; Nussenzweig, M.C. Tolerogenic dendritic cells. *Annu. Rev. Immunol.* 2003, *21*, 685–711.
16. Takenaka, M.C.; Quintana, F.J. Tolerogenic dendritic cells. *Semin. Immunopathol.* 2017, *39*, 113–120.
17. Cools, N.; Ponsaerts, P.; Van Tendeloo, V.F.I.; Berneman, Z.N. Balancing between immunity and tolerance: an interplay between dendritic cells, regulatory T cells, and effector T cells. *J. Leukoc. Biol.* **2007**, *82*, 1365–1374, doi:10.1189/jlb.0307166.
18. Waisman, A.; Lukas, D.; Clausen, B.E.; Yogev, N. Dendritic cells as gatekeepers of tolerance. *Semin. Immunopathol.* 2017, *39*, 153–163.
19. Schwartz, R.H. T cell anergy. *Annu. Rev. Immunol.* 2003, *21*, 305–334.
20. Maldonado, R.A.; Von Andrian, U.H. How tolerogenic dendritic cells induce regulatory T cells., doi:10.1016/B978-0-12-380995-7.00004-5.
21. U Hilkens, C.M.; Isaacs, J.D.; Thomson, A.W. Development of Dendritic Cell-Based Immunotherapy for Autoimmunity. *Int. Rev. Immunol.* **2010**, *29*, 156–183, doi:10.3109/08830180903281193.
22. Lutz, M.B. Therapeutic potential of semi-mature dendritic cells for tolerance induction. *Front. Immunol.* 2012, *3*, 123.
23. Sozzani, S.; Prete, A. Del; Bosisio, D. Dendritic cell recruitment and activation in autoimmunity. **2017**, doi:10.1016/j.jaut.2017.07.012.
24. Merrill, J.E.; Kong, D.H.; Clayton, J.; Ando, D.G.; Hinton, D.R.; Hofman, F.M. Inflammatory leukocytes and cytokines in the peptide-induced disease of experimental allergic encephalomyelitis in SJL and B10.PL mice. *Proc. Natl. Acad. Sci. U. S. A.* **1992**, *89*, 574, doi:10.1073/PNAS.89.2.574.
25. Pettinelli, C.B.; McFarlin, D.E. Adoptive transfer of experimental allergic encephalomyelitis in SJL/J mice after in vitro activation of lymph node cells by myelin basic protein: requirement for Lyt 1+ 2- T lymphocytes. *J. Immunol.* **1981**, *127*.
26. Becher, B.; Durell, B.G.; Noelle, R.J. Experimental autoimmune encephalitis and inflammation in the absence of interleukin-12. *J. Clin. Invest.* **2002**, *110*, 493, doi:10.1172/JCI15751.
27. Damsker, J.M.; Hansen, A.M.; Caspi, R.R. Th1 and Th17 cells: Adversaries and collaborators. *Ann. N. Y. Acad. Sci.* 2010, *1183*, 211–221.
28. Nakae, S.; Nambu, A.; Sudo, K.; Iwakura, Y. Suppression of immune induction of collagen-induced arthritis in IL-17-deficient mice. *J. Immunol.* **2003**, *171*, 6173–6177, doi:10.4049/JIMMUNOL.171.11.6173.
29. Hofstetter, H.H.; Ibrahim, S.M.; Koczan, D.; Kruse, N.; Weishaupt, A.; Toyka, K. V.;

- Gold, R. Therapeutic efficacy of IL-17 neutralization in murine experimental autoimmune encephalomyelitis. *Cell. Immunol.* **2005**, *237*, 123–130, doi:10.1016/J.CELLIMM.2005.11.002.
30. Glatt, S.; Baeten, D.; Baker, T.; Griffiths, M.; Ionescu, L.; Lawson, A.D.G.; Maroof, A.; Oliver, R.; Popa, S.; Strimenopoulou, F.; et al. Dual IL-17A and IL-17F neutralisation by bimekizumab in psoriatic arthritis: evidence from preclinical experiments and a randomised placebo-controlled clinical trial that IL-17F contributes to human chronic tissue inflammation. *Ann. Rheum. Dis.* **2018**, *77*, 523–532, doi:10.1136/ANNRHEUMDIS-2017-212127.
31. Fasching, P.; Stradner, M.; Graninger, W.; Dejaco, C.; Fessler, J. Therapeutic potential of targeting the Th17/Treg axis in autoimmune disorders. *Molecules* **2017**, *22*.
32. Li, S.; Wu, Z.; Li, L.; Liu, X. Interleukin-6 (IL-6) Receptor Antagonist Protects Against Rheumatoid Arthritis. *Med. Sci. Monit.* **2016**, *22*, 2113–8, doi:10.12659/MSM.896355.
33. Samson, M.; Audia, S.; Janikashvili, N.; Ciudad, M.; Trad, M.; Fraszczak, J.; Ornetti, P.; Maillefert, J.-F.; Miossec, P.; Bonnotte, B. Brief Report: Inhibition of interleukin-6 function corrects Th17/Treg cell imbalance in patients with rheumatoid arthritis. *Arthritis Rheum.* **2012**, *64*, 2499–2503, doi:10.1002/art.34477.
34. Kikuchi, J.; Hashizume, M.; Kaneko, Y.; Yoshimoto, K.; Nishina, N.; Takeuchi, T. Peripheral blood CD4+CD25+CD127low regulatory T cells are significantly increased by tocilizumab treatment in patients with rheumatoid arthritis: increase in regulatory T cells correlates with clinical response. *Arthritis Res. Ther.* **2015**, *17*, 10, doi:10.1186/s13075-015-0526-4.
35. Mease, P.J.; McInnes, I.B.; Kirkham, B.; Kavanaugh, A.; Rahman, P.; van der Heijde, D.; Landewé, R.; Nash, P.; Pricop, L.; Yuan, J.; et al. Secukinumab Inhibition of Interleukin-17A in Patients with Psoriatic Arthritis. *N. Engl. J. Med.* **2015**, *373*, 1329–1339, doi:10.1056/NEJMoa1412679.
36. McInnes, I.B.; Mease, P.J.; Kirkham, B.; Kavanaugh, A.; Ritchlin, C.T.; Rahman, P.; van der Heijde, D.; Landewé, R.; Conaghan, P.G.; Gottlieb, A.B.; et al. Secukinumab, a human anti-interleukin-17A monoclonal antibody, in patients with psoriatic arthritis (FUTURE 2): a randomised, double-blind, placebo-controlled, phase 3 trial. *Lancet* **2015**, *386*, 1137–1146, doi:10.1016/S0140-6736(15)61134-5.
37. Hueber, W.; Sands, B.E.; Lewitzky, S.; Vandemeulebroecke, M.; Reinisch, W.; Higgins, P.D.R.; Wehkamp, J.; Feagan, B.G.; Yao, M.D.; Karczewski, M.; et al. Secukinumab, a human anti-IL-17A monoclonal antibody, for moderate to severe Crohn's disease: unexpected results of a randomised, double-blind placebo-controlled trial. *Gut* **2012**, *61*, 1693–700, doi:10.1136/gutjnl-2011-301668.
38. Maloy, K.J.; Kullberg, M.C. IL-23 and Th17 cytokines in intestinal homeostasis. *Mucosal Immunol.* **2008**, *1*, 339–349, doi:10.1038/mi.2008.28.



39. Pavelka, K.; Chon, Y.; Newmark, R.; Lin, S.-L.; Baumgartner, S.; Erondy, N. A Study to Evaluate the Safety, Tolerability, and Efficacy of Brodalumab in Subjects with Rheumatoid Arthritis and an Inadequate Response to Methotrexate. *J. Rheumatol.* **2015**, *42*, 912–919, doi:10.3899/jrheum.141271.
40. Papp, K.A.; Langley, R.G.; Lebwohl, M.; Krueger, G.G.; Szapary, P.; Yeilding, N.; Guzzo, C.; Hsu, M.-C.; Wang, Y.; Li, S.; et al. Efficacy and safety of ustekinumab, a human interleukin-12/23 monoclonal antibody, in patients with psoriasis: 52-week results from a randomised, double-blind, placebo-controlled trial (PHOENIX 2). *Lancet* **2008**, *371*, 1675–1684, doi:10.1016/S0140-6736(08)60726-6.
41. Segal, B.M.; Constantinescu, C.S.; Raychaudhuri, A.; Kim, L.; Fidelus-Gort, R.; Kasper, L.H. Repeated subcutaneous injections of IL12/23 p40 neutralising antibody, ustekinumab, in patients with relapsing-remitting multiple sclerosis: a phase II, double-blind, placebo-controlled, randomised, dose-ranging study. *Lancet Neurol.* **2008**, *7*, 796–804, doi:10.1016/S1474-4422(08)70173-X.
42. Fugger, L.; Jensen, L.T.; Rossjohn, J. Challenges, Progress, and Prospects of Developing Therapies to Treat Autoimmune Diseases. *Cell* **2020**, *181*, 63–80, doi:10.1016/J.CELL.2020.03.007.
43. O’Neill, L.A.J.; Kishton, R.J.; Rathmell, J. A guide to immunometabolism for immunologists. *Nat. Rev. Immunol.* **2016**, *16*, 553–565, doi:10.1038/nri.2016.70.
44. Buerger, C.; Malisiewicz, B.; Eiser, A.; Hardt, K.; Boehncke, W.H. Mammalian target of rapamycin and its downstream signalling components are activated in psoriatic skin. *Br. J. Dermatol.* **2013**, *169*, 156–159, doi:10.1111/bjd.12271.
45. Weyand, C.M.; Goronzy, J.J. Immunometabolism in early and late stages of rheumatoid arthritis. *Nat. Rev. Rheumatol.* **2017**, *13*, 291–301, doi:10.1038/nrrheum.2017.49.
46. Perl, A. Review: Metabolic Control of Immune System Activation in Rheumatic Diseases. *Arthritis Rheumatol.* **2017**, *69*, 2259–2270, doi:10.1002/art.40223.
47. Düvel, K.; Yecies, J.L.; Menon, S.; Raman, P.; Lipovsky, A.I.; Souza, A.L.; Triantafellow, E.; Ma, Q.; Gorski, R.; Cleaver, S.; et al. Activation of a metabolic gene regulatory network downstream of mTOR complex 1. *Mol. Cell* **2010**, *39*, 171–183, doi:10.1016/j.molcel.2010.06.022.
48. de Carvalho, C.; Caramujo, M. The Various Roles of Fatty Acids. *Molecules* **2018**, *23*, 2583, doi:10.3390/molecules23102583.
49. Ma, E.H.; Poffenberger, M.C.; Wong, A.H.-T.; Jones, R.G. The role of AMPK in T cell metabolism and function. *Curr. Opin. Immunol.* **2017**, *46*, 45–52, doi:10.1016/J.COI.2017.04.004.
50. Warburg, O. On the origin of cancer cells. *Science* **1956**, *123*, 309–14.

51. O'Neill, L.A.J.; Pearce, E.J. Immunometabolism governs dendritic cell and macrophage function. *J. Exp. Med.* **2016**, *213*, 15–23, doi:10.1084/jem.20151570.
52. Pearce, E.J.; Everts, B. Dendritic cell metabolism. *Nat. Rev. Immunol.* **2015**, *15*, 18–29, doi:10.1038/nri3771.
53. Almeida, L.; Lochner, M.; Berod, L.; Sparwasser, T. Metabolic pathways in T cell activation and lineage differentiation. *Semin. Immunol.* **2016**, *28*, 514–524, doi:10.1016/J.SMIM.2016.10.009.
54. Jha, A.K.; Huang, S.C.-C.; Sergushichev, A.; Lampropoulou, V.; Ivanova, Y.; Loginicheva, E.; Chmielewski, K.; Stewart, K.M.; Ashall, J.; Everts, B.; et al. Network Integration of Parallel Metabolic and Transcriptional Data Reveals Metabolic Modules that Regulate Macrophage Polarization. *Immunity* **2015**, *42*, 419–430, doi:10.1016/j.immuni.2015.02.005.
55. Tannahill, G.M.; Curtis, A.M.; Adamik, J.; Palsson-McDermott, E.M.; McGettrick, A.F.; Goel, G.; Frezza, C.; Bernard, N.J.; Kelly, B.; Foley, N.H.; et al. Succinate is an inflammatory signal that induces IL-1 $\beta$  through HIF-1 $\alpha$ . *Nature* **2013**, *496*, 238–242, doi:10.1038/nature11986.
56. Everts, B.; Amiel, E.; Huang, S.C.-C.; Smith, A.M.; Chang, C.-H.; Lam, W.Y.; Redmann, V.; Freitas, T.C.; Blagih, J.; van der Windt, G.J.W.; et al. TLR-driven early glycolytic reprogramming via the kinases TBK1-IKK $\epsilon$  supports the anabolic demands of dendritic cell activation. *Nat. Immunol.* **2014**, *15*, 323–332, doi:10.1038/ni.2833.
57. Ecker, J.; Liebisch, G.; Englmaier, M.; Grandl, M.; Robenek, H.; Schmitz, G. Induction of fatty acid synthesis is a key requirement for phagocytic differentiation of human monocytes. *Proc. Natl. Acad. Sci. U. S. A.* **2010**, *107*, 7817–22, doi:10.1073/pnas.0912059107.
58. Vats, D.; Mukundan, L.; Odegaard, J.I.; Zhang, L.; Smith, K.L.; Morel, C.R.; Wagner, R.A.; Greaves, D.R.; Murray, P.J.; Chawla, A. Oxidative metabolism and PGC-1 $\beta$  attenuate macrophage-mediated inflammation. *Cell Metab.* **2006**, *4*, 13–24, doi:10.1016/j.cmet.2006.05.011.
59. Malandrino, M.I.; Fucho, R.; Weber, M.; Calderon-Dominguez, M.; Mir, J.F.; Valcarcel, L.; Escoté, X.; Gómez-Serrano, M.; Peral, B.; Salvadó, L.; et al. Enhanced fatty acid oxidation in adipocytes and macrophages reduces lipid-induced triglyceride accumulation and inflammation. *Am. J. Physiol. Metab.* **2015**, *308*, E756–E769, doi:10.1152/ajpendo.00362.2014.
60. Wang, R.; Dillon, C.P.; Shi, L.Z.; Milasta, S.; Carter, R.; Finkelstein, D.; McCormick, L.L.; Fitzgerald, P.; Chi, H.; Munger, J.; et al. The transcription factor Myc controls metabolic reprogramming upon T lymphocyte activation. *Immunity* **2011**, *35*, 871–82, doi:10.1016/j.immuni.2011.09.021.
61. Gerriets, V.A.; Kishton, R.J.; Nichols, A.G.; Macintyre, A.N.; Inoue, M.; Ilkayeva, O.; Winter, P.S.; Liu, X.; Priyadharshini, B.; Slawinska, M.E.; et al. Metabolic

- programming and PDHK1 control CD4<sup>+</sup> T cell subsets and inflammation. *J. Clin. Invest.* **2015**, *125*, 194–207, doi:10.1172/JCI76012.
62. Berod, L.; Friedrich, C.; Nandan, A.; Freitag, J.; Hagemann, S.; Harmrolfs, K.; Sandouk, A.; Hesse, C.; Castro, C.N.; Bähre, H.; et al. De novo fatty acid synthesis controls the fate between regulatory T and T helper 17 cells. *Nat. Med.* **2014**, *20*, 1327–1333, doi:10.1038/nm.3704.
  63. Gergely, P.; Grossman, C.; Niland, B.; Puskas, F.; Neupane, H.; Allam, F.; Banki, K.; Phillips, P.E.; Perl, A. Mitochondrial hyperpolarization and ATP depletion in patients with systemic lupus erythematosus. *Arthritis Rheum.* **2002**, *46*, 175–190, doi:10.1002/1529-0131(200201)46:1<175::AID-ART10015>3.0.CO;2-H.
  64. La Rocca, C.; Carbone, F.; De Rosa, V.; Colamatteo, A.; Galgani, M.; Perna, F.; Lanzillo, R.; Brescia Morra, V.; Orefice, G.; Cerillo, I.; et al. Immunometabolic profiling of T cells from patients with relapsing-remitting multiple sclerosis reveals an impairment in glycolysis and mitochondrial respiration. *Metabolism* **2017**, *77*, 39–46, doi:10.1016/j.metabol.2017.08.011.
  65. Procaccini, C.; De Rosa, V.; Galgani, M.; Abanni, L.; Calì, G.; Porcellini, A.; Carbone, F.; Fontana, S.; Horvath, T.L.; La Cava, A.; et al. An oscillatory switch in mTOR kinase activity sets regulatory T cell responsiveness. *Immunity* **2010**, *33*, 929–41, doi:10.1016/j.immuni.2010.11.024.
  66. Lai, Z.-W.; Borsuk, R.; Shadakshari, A.; Yu, J.; Dawood, M.; Garcia, R.; Francis, L.; Tily, H.; Bartos, A.; Faraone, S. V.; et al. Mechanistic target of rapamycin activation triggers IL-4 production and necrotic death of double-negative T cells in patients with systemic lupus erythematosus. *J. Immunol.* **2013**, *191*, 2236–46, doi:10.4049/jimmunol.1301005.
  67. Rena, G.; Hardie, D.G.; Pearson, E.R. The mechanisms of action of metformin. *Diabetologia* **2017**, *60*, 1577, doi:10.1007/S00125-017-4342-Z.
  68. Dowling, R.J.O.; Zakikhani, M.; Fantus, I.G.; Pollak, M.; Sonenberg, N. Metformin Inhibits Mammalian Target of Rapamycin–Dependent Translation Initiation in Breast Cancer Cells. *Cancer Res.* **2007**, *67*, 10804–10812, doi:10.1158/0008-5472.CAN-07-2310.
  69. Nath, N.; Khan, M.; Paintlia, M.K.; Singh, I.; Hoda, M.N.; Giri, S. Metformin attenuated the autoimmune disease of the central nervous system in animal models of multiple sclerosis. *J. Immunol.* **2009**, *182*, 8005–14, doi:10.4049/jimmunol.0803563.
  70. Lee, S.-Y.; Lee, S.H.; Yang, E.-J.; Kim, E.-K.; Kim, J.-K.; Shin, D.-Y.; Cho, M.-L. Metformin Ameliorates Inflammatory Bowel Disease by Suppression of the STAT3 Signaling Pathway and Regulation of the between Th17/Treg Balance. *PLoS One* **2015**, *10*, e0135858, doi:10.1371/journal.pone.0135858.
  71. Son, H.-J.; Lee, J.; Lee, S.-Y.; Kim, E.-K.; Park, M.-J.; Kim, K.-W.; Park, S.-H.; Cho, M.-

- L. Metformin attenuates experimental autoimmune arthritis through reciprocal regulation of Th17/Treg balance and osteoclastogenesis. *Mediators Inflamm.* **2014**, *2014*, 973986, doi:10.1155/2014/973986.
72. Parzych, K.R.; Klionsky, D.J. An Overview of Autophagy: Morphology, Mechanism, and Regulation. *Antioxid. Redox Signal.* **2014**, *20*, 460, doi:10.1089/ARS.2013.5371.
73. Levine, B.; Mizushima, N.; Virgin, H.W. Autophagy in immunity and inflammation. *Nature* **2011**, *469*, 323–35, doi:10.1038/nature09782.
74. Glick, D.; Barth, S.; Macleod, K.F. Autophagy: Cellular and molecular mechanisms. *J. Pathol.* **2010**, *221*, 3–12, doi:10.1002/path.2697.
75. Yang, Z.; Klionsky, D.J. Mammalian autophagy: Core molecular machinery and signaling regulation. *Curr. Opin. Cell Biol.* **2010**, *22*, 124–131, doi:10.1016/j.ceb.2009.11.014.
76. Pankiv, S.; Clausen, T.H.; Lamark, T.; Brech, A.; Bruun, J.A.; Outzen, H.; Øvervatn, A.; Bjørkøy, G.; Johansen, T. p62/SQSTM1 binds directly to Atg8/LC3 to facilitate degradation of ubiquitinated protein aggregates by autophagy\*[S]. *J. Biol. Chem.* **2007**, *282*, 24131–24145, doi:10.1074/jbc.M702824200.
77. Kinsella, R.L.; Nehls, E.M.; Stallings, C.L. Roles for Autophagy Proteins in Immunity and Host Defense. *Vet. Pathol.* **2018**, *55*, 366–373, doi:10.1177/0300985818754967.
78. Chandra, P.; Ghanwat, S.; Matta, S.K.; Yadav, S.S.; Mehta, M.; Siddiqui, Z.; Singh, A.; Kumar, D. Mycobacterium tuberculosis Inhibits RAB7 Recruitment to Selectively Modulate Autophagy Flux in Macrophages. *Sci. Rep.* **2015**, *5*, doi:10.1038/srep16320.
79. Seto, S.; Tsujimura, K.; Koide, Y. Coronin-1a inhibits autophagosome formation around Mycobacterium tuberculosis-containing phagosomes and assists mycobacterial survival in macrophages. *Cell. Microbiol.* **2012**, *14*, 710–727, doi:10.1111/j.1462-5822.2012.01754.x.
80. Ghislat, G.; Lawrence, T. Autophagy in dendritic cells. *Cell. Mol. Immunol.* **2018**, *15*, 944–952, doi:10.1038/cmi.2018.2.
81. Harris, J.; Hartman, M.; Roche, C.; Zeng, S.G.; O’Shea, A.; Sharp, F.A.; Lambe, E.M.; Creagh, E.M.; Golenbock, D.T.; Tschopp, J.; et al. Autophagy controls IL-1 $\beta$  secretion by targeting Pro-IL-1 $\beta$  for degradation. *J. Biol. Chem.* **2011**, *286*, 9587–9597, doi:10.1074/jbc.M110.202911.
82. Abdel Fattah, E.; Bhattacharya, A.; Herron, A.; Safdar, Z.; Eissa, N.T. Critical Role for IL-18 in Spontaneous Lung Inflammation Caused by Autophagy Deficiency. *J. Immunol.* **2015**, *194*, 5407–5416, doi:10.4049/jimmunol.1402277.
83. Saitoh, T.; Fujita, N.; Jang, M.H.; Uematsu, S.; Yang, B.G.; Satoh, T.; Omori, H.;

- Noda, T.; Yamamoto, N.; Komatsu, M.; et al. Loss of the autophagy protein Atg16L1 enhances endotoxin-induced IL-1 $\beta$  production. *Nature* **2008**, *456*, 264–268, doi:10.1038/nature07383.
84. Peral de Castro, C.; Jones, S.A.; Ní Cheallaigh, C.; Hearnden, C.A.; Williams, L.; Winter, J.; Lavelle, E.C.; Mills, K.H.G.; Harris, J. Autophagy regulates IL-23 secretion and innate T cell responses through effects on IL-1 secretion. *J. Immunol.* **2012**, *189*, 4144–53, doi:10.4049/jimmunol.1201946.
85. Iida, T.; Onodera, K.; Nakase, H. Role of autophagy in the pathogenesis of inflammatory bowel disease. *World J. Gastroenterol.* **2017**, *23*, 1944–1953, doi:10.3748/wjg.v23.i11.1944.
86. Hampe, J.; Franke, A.; Rosenstiel, P.; Till, A.; Teuber, M.; Huse, K.; Albrecht, M.; Mayr, G.; De, F.M.; Vega, L.; et al. A genome-wide association scan of nonsynonymous SNPs identifies a susceptibility variant for Crohn disease in ATG16L1. **2007**, doi:10.1038/ng1954.
87. Lassen, K.G.; Kuballa, P.; Conway, K.L.; Patel, K.K.; Becker, C.E.; Peloquin, J.M.; Villablanca, E.J.; Norman, J.M.; Liu, T.C.; Heath, R.J.; et al. Atg16L1 T300A variant decreases selective autophagy resulting in altered cytokine signaling and decreased antibacterial defense. *Proc. Natl. Acad. Sci. U. S. A.* **2014**, *111*, 7741–7746, doi:10.1073/pnas.1407001111.
88. Cadwell, K. Crosstalk between autophagy and inflammatory signalling pathways: balancing defence and homeostasis. *Nat. Rev. Immunol.* **2016**, *16*, 661–675, doi:10.1038/nri.2016.100.
89. Murthy, A.; Li, Y.; Peng, I.; Reichelt, M.; Katakam, A.K.; Noubade, R.; Roose-Girma, M.; Devoss, J.; Diehl, L.; Graham, R.R.; et al. A Crohn's disease variant in Atg16l1 enhances its degradation by caspase 3. **2014**, doi:10.1038/nature13044.
90. Gateva, V.; Sandling, J.K.; Hom, G.; Taylor, K.E.; Chung, S.A.; Sun, X.; Ortmann, W.; Kosoy, R.; Ferreira, R.C.; Nordmark, G.; et al. A large-scale replication study identifies TNIP1, PRDM1, JAZF1, UHRF1BP1 and IL10 as risk loci for systemic lupus erythematosus. *Nat. Genet.* **2009**, *41*, 1228–1233, doi:10.1038/ng.468.
91. Harley, J.B.; Alarcón-Riquelme, M.E.; Criswell, L.A.; Jacob, C.O.; Kimberly, R.P.; Moser, K.L.; Tsao, B.P.; Vyse, T.J.; Langefeld, C.D.; Nath, S.K.; et al. Genome-wide association scan in women with systemic lupus erythematosus identifies susceptibility variants in ITGAM, PXX, KIAA1542 and other loci. *Nat. Genet.* **2008**, *40*, 204–210, doi:10.1038/ng.81.
92. Yang, Z.; Goronzy, J.J.; Weyand, C.M. Autophagy in autoimmune disease. *J. Mol. Med.* **2015**, *93*, 707–717.
93. Paoli, M.; Marles-Wright, J.; Smith, A. Structure-function relationships in heme-proteins. *DNA Cell Biol.* **2002**, *21*, 271–280, doi:10.1089/104454902753759690.

94. Kumar, S.; Bandyopadhyay, U. Free heme toxicity and its detoxification systems in human. *Toxicol. Lett.* **2005**, *157*, 175–188, doi:10.1016/j.toxlet.2005.03.004.
95. Gozzelino, R.; Jeney, V.; Soares, M.P. Mechanisms of cell protection by heme oxygenase-1. *Annu. Rev. Pharmacol. Toxicol.* **2010**, *50*, 323–54, doi:10.1146/annurev.pharmtox.010909.105600.
96. Tenhunen, R.; Marver, H.S.; Schmid, R. The enzymatic conversion of heme to bilirubin by microsomal heme oxygenase. *Proc. Natl. Acad. Sci. U. S. A.* **1968**, *61*, 748–755, doi:10.1073/pnas.61.2.748.
97. Singleton, J.W.; Laster, L. Biliverdin reductase of guinea pig liver. *J. Biol. Chem.* **1965**, *240*, 4780–4789, doi:10.1016/s0021-9258(18)97023-7.
98. Yamaguchi, T.; Komoda, Y.; Nakajima, H. Biliverdin-IX alpha reductase and biliverdin-IX beta reductase from human liver. Purification and characterization. *J. Biol. Chem.* **1994**, *269*, 24343–8.
99. Trakshel, G.M.; Kutty, R.K.; Maines, M.D. Purification and characterization of the major constitutive form of testicular heme oxygenase. The noninducible isoform. *J. Biol. Chem.* **1986**, *261*, 11131–11137.
100. Maines, M.D.; Trakshel, G.M.; Kutty, R.K. Characterization of two constitutive forms of rat liver microsomal heme oxygenase. Only one molecular species of the enzyme is inducible. *J. Biol. Chem.* **1986**, *261*, 411–419.
101. Maines, M.D. The Heme Oxygenase System: A Regulator of Second Messenger Gases. *Annu. Rev. Pharmacol. Toxicol.* **1997**, *37*, 517–54, doi:10.1146/annurev.pharmtox.37.1.517.
102. Verma, A.; Hirsch, D.; Glatt, C.; Ronnett, G.; Snyder, S. Carbon monoxide: a putative neural messenger. *Science (80-. )*. **1993**, *259*, 381–384, doi:10.1126/science.7678352.
103. Maines, M.D.; Kappas, A. Cobalt induction of hepatic heme oxygenase; with evidence that cytochrome P 450 is not essential for this enzyme activity. *Proc. Natl. Acad. Sci. U. S. A.* **1974**, *71*, 4293–4297, doi:10.1073/pnas.71.11.4293.
104. Campbell, N.K.; Fitzgerald, H.K.; Dunne, A. Regulation of inflammation by the antioxidant haem oxygenase 1. *Nat. Rev. Immunol.* **2021**, *21*, 411–425, doi:10.1038/s41577-020-00491-x.
105. Immenschuh, S.; Ramadori, G. Gene regulation of heme oxygenase-1 as a therapeutic target. *Biochem. Pharmacol.* **2000**, *60*, 1121–1128, doi:10.1016/S0006-2952(00)00443-3.
106. Devesa, M.L.F. and I. Inducers of Heme Oxygenase-1. *Curr. Pharm. Des.* 2008, *14*, 473–486.
107. Applegate, L.A.; Luscher, P.; Tyrrell, R.M. Induction of heme oxygenase: a general

- response to oxidant stress in cultured mammalian cells. *Cancer Res.* **1991**, *51*, 974–8.
108. Ma, Q. Role of Nrf2 in Oxidative Stress and Toxicity. *Annu. Rev. Pharmacol. Toxicol.* **2013**, *53*, 401–26, doi:10.1146/annurev-pharmtox-011112-140320.
  109. Kansanen, E.; Kuosmanen, S.M.; Leinonen, H.; Levonen, A.-L. The Keap1-Nrf2 pathway: Mechanisms of activation and dysregulation in cancer. *Redox Biol.* **2013**, *1*, 45–49, doi:10.1016/j.redox.2012.10.001.
  110. Taguchi, K.; Motohashi, H.; Yamamoto, M. Molecular mechanisms of the Keap1-Nrf2 pathway in stress response and cancer evolution. *Genes to Cells* **2011**, *16*, 123–140, doi:10.1111/j.1365-2443.2010.01473.x.
  111. Sun, J.; Hoshino, H.; Takaku, K.; Nakajima, O.; Muto, A.; Suzuki, H.; Tashiro, S.; Takahashi, S.; Shibahara, S.; Alam, J.; et al. Hemoprotein Bach1 regulates enhancer availability of heme oxygenase-1 gene. *EMBO J.* **2002**, *21*, 5216–5224, doi:10.1093/emboj/cdf516.
  112. Zenke-Kawasaki, Y.; Dohi, Y.; Katoh, Y.; Ikura, T.; Ikura, M.; Asahara, T.; Tokunaga, F.; Iwai, K.; Igarashi, K. Heme Induces Ubiquitination and Degradation of the Transcription Factor Bach1. *Mol. Cell. Biol.* **2007**, *27*, 6962–6971, doi:10.1128/MCB.02415-06.
  113. Suzuki, H.; Tashiro, S.; Hira, S.; Sun, J.; Yamazaki, C.; Zenke, Y.; Ikeda-Saito, M.; Yoshida, M.; Igarashi, K. Heme regulates gene expression by triggering Crm1-dependent nuclear export of Bach1. *EMBO J.* **2004**, *23*, 2544–2553, doi:10.1038/sj.emboj.7600248.
  114. Liao, R.; Zheng, Y.; Liu, X.; Zhang, Y.; Seim, G.; Tanimura, N.; Wilson, G.M.; Hematti, P.; Coon, J.J.; Fan, J.; et al. Discovering How Heme Controls Genome Function Through Heme-omics. *Cell Rep.* **2020**, *31*, 107832, doi:https://doi.org/10.1016/j.celrep.2020.107832.
  115. Mense, S.M.; Zhang, L. Heme: a versatile signaling molecule controlling the activities of diverse regulators ranging from transcription factors to MAP kinases. *Cell Res.* **2006**, *16*, 681–692, doi:10.1038/sj.cr.7310086.
  116. Zhang, X.; Guo, J.; Wei, X.; Niu, C.; Jia, M.; Li, Q.; Meng, D. Bach1: Function, Regulation, and Involvement in Disease. *Oxid. Med. Cell. Longev.* **2018**, *2018*, 1347969, doi:10.1155/2018/1347969.
  117. Kataoka, K.; Igarashi, K.; Itoh, K.; Fujiwara, K.T.; Noda, M.; Yamamoto, M.; Nishizawa, M. Small Maf proteins heterodimerize with Fos and may act as competitive repressors of the NF-E2 transcription factor. *Mol. Cell. Biol.* **1995**, *15*, 2180 LP – 2190, doi:10.1128/MCB.15.4.2180.
  118. Lee, P.J.; Jiang, B.-H.; Chin, B.Y.; Iyer, N. V.; Alam, J.; Semenza, G.L.; Choi, A.M.K. Hypoxia-inducible Factor-1 Mediates Transcriptional Activation of the Heme

- Oxygenase-1 Gene in Response to Hypoxia. *J. Biol. Chem.* **1997**, *272*, 5375–5381, doi:10.1074/jbc.272.9.5375.
119. Lavrovsky, Y.; Schwartzman, M.L.; Levere, R.D.; Kappas, A.; Abraham, N.G. Identification of binding sites for transcription factors NF-kappa B and AP-2 in the promoter region of the human heme oxygenase 1 gene. *Proc. Natl. Acad. Sci. U. S. A.* **1994**, *91*, 5987–91.
  120. Alam, J.; Cook, J.L. How Many Transcription Factors Does It Take to Turn On the Heme Oxygenase-1 Gene? *Am. J. Respir. Cell Mol. Biol.* **2007**, *36*, 166–174, doi:10.1165/rcmb.2006-0340TR.
  121. Zhang, Z.; Guo, Z.; Zhan, Y.; Li, H.; Wu, S. Role of histone acetylation in activation of nuclear factor erythroid 2-related factor 2/heme oxygenase 1 pathway by manganese chloride. *Toxicol. Appl. Pharmacol.* **2017**, *336*, 94–100, doi:https://doi.org/10.1016/j.taap.2017.10.011.
  122. Magalhães, M.; Rivals, I.; Claustres, M.; Varilh, J.; Thomasset, M.; Bergougnoux, A.; Mely, L.; Leroy, S.; Corvol, H.; Guillot, L.; et al. DNA methylation at modifier genes of lung disease severity is altered in cystic fibrosis. *Clin. Epigenetics* **2017**, *9*, 19, doi:10.1186/s13148-016-0300-8.
  123. Ray, P.D.; Huang, B.-W.; Tsuji, Y. Coordinated regulation of Nrf2 and histone H3 serine 10 phosphorylation in arsenite-activated transcription of the human heme oxygenase-1 gene. *Biochim. Biophys. Acta - Gene Regul. Mech.* **2015**, *1849*, 1277–1288, doi:https://doi.org/10.1016/j.bbarm.2015.08.004.
  124. Medina, M.V.; Sapochnik, D.; Garcia Solá, M.; Coso, O. Regulation of the Expression of Heme Oxygenase-1: Signal Transduction, Gene Promoter Activation, and Beyond. *Antioxid. Redox Signal.* **2019**, *32*, 1033–1044, doi:10.1089/ars.2019.7991.
  125. Cheng, X.; Ku, C.-H.; Siow, R.C.M. Regulation of the Nrf2 antioxidant pathway by microRNAs: New players in micromanaging redox homeostasis. *Free Radic. Biol. Med.* **2013**, *64*, 4–11, doi:https://doi.org/10.1016/j.freeradbiomed.2013.07.025.
  126. Lin, C.-C.C.-H.; Chiang, L.-L.; Lin, C.-C.C.-H.; Shih, C.-H.; Liao, Y.-T.; Hsu, M.-J.; Chen, B.-C. Transforming growth factor- $\beta$ 1 stimulates heme oxygenase-1 expression via the PI3K/Akt and NF- $\kappa$ B pathways in human lung epithelial cells. *Eur. J. Pharmacol.* **2007**, *560*, 101–109, doi:10.1016/j.ejphar.2007.01.025.
  127. Martin, D.; Rojo, A.I.; Salinas, M.; Diaz, R.; Gallardo, G.; Alam, J.; De Galarreta, C.M.R.; Cuadrado, A. Regulation of heme oxygenase-1 expression through the phosphatidylinositol 3-kinase/Akt pathway and the Nrf2 transcription factor in response to the antioxidant phytochemical carnosol. *J. Biol. Chem.* **2004**, *279*, 8919–29, doi:10.1074/jbc.M309660200.
  128. Seo, S.H.; Jeong, G.S. Fisetin inhibits TNF-alpha-induced inflammatory action and hydrogen peroxide-induced oxidative damage in human keratinocyte HaCaT cells through PI3K/AKT/Nrf-2-mediated heme oxygenase-1 expression. *Int.*



- Immunopharmacol.* **2015**, *29*, 246–253, doi:10.1016/j.intimp.2015.11.014.
129. Ricchetti, G.A.; Williams, L.M.; Foxwell, B.M.J. Heme oxygenase 1 expression induced by IL-10 requires STAT-3 and phosphoinositol-3 kinase and is inhibited by lipopolysaccharide. *J. Leukoc. Biol.* **2004**, *76*, 719–26, doi:10.1189/jlb.0104046.
  130. Lee, T.-S.; Chau, L.-Y. Heme oxygenase-1 mediates the anti-inflammatory effect of interleukin-10 in mice. *Nat. Med.* **2002**, *8*, 240–6, doi:10.1038/nm0302-240.
  131. Cho, R.-L.; Lin, W.-N.; Wang, C.-Y.; Yang, C.-C.; Hsiao, L.-D.; Lin, C.-C.; Yang, C.-M. Heme oxygenase-1 induction by rosiglitazone via PKC $\alpha$ /AMPK $\alpha$ /p38 MAPK $\alpha$ /SIRT1/PPAR $\gamma$  pathway suppresses lipopolysaccharide-mediated pulmonary inflammation. *Biochem. Pharmacol.* **2018**, *148*, 222–237, doi:10.1016/j.bcp.2017.12.024.
  132. Liu, X.; Peyton, K.J.; Shebib, A.R.; Wang, H.; Korthuis, R.J.; Durante, W. Activation of AMPK stimulates heme oxygenase-1 gene expression and human endothelial cell survival. *Am. J. Physiol. Circ. Physiol.* **2011**, *300*, H84–H93, doi:10.1152/ajpheart.00749.2010.
  133. Mo, C.; Wang, L.; Zhang, J.; Numazawa, S.; Tang, H.; Tang, X.; Han, X.; Li, J.; Yang, M.; Wang, Z.; et al. The Crosstalk Between Nrf2 and AMPK Signal Pathways Is Important for the Anti-Inflammatory Effect of Berberine in LPS-Stimulated Macrophages and Endotoxin-Shocked Mice. *Antioxid. Redox Signal.* **2014**, *20*, 574–588, doi:10.1089/ars.2012.5116.
  134. Campbell, N.K.; Fitzgerald, H.K.; Fletcher, J.M.; Dunne, A. Plant-Derived Polyphenols Modulate Human Dendritic Cell Metabolism and Immune Function via AMPK-Dependent Induction of Heme Oxygenase-1. *Front. Immunol.* **2019**, *10*, 345, doi:10.3389/fimmu.2019.00345.
  135. Zimmermann, K.; Baldinger, J.; Mayerhofer, B.; Atanasov, A.G.; Dirsch, V.M.; Heiss, E.H. Activated AMPK boosts the Nrf2/HO-1 signaling axis - A role for the unfolded protein response. *Free Radic. Biol. Med.* **2015**, *88*, 417–426, doi:10.1016/j.freeradbiomed.2015.03.030.
  136. Joo, M.S.; Kim, W.D.; Lee, K.Y.; Kim, J.H.; Koo, J.H.; Kim, S.G. AMPK Facilitates Nuclear Accumulation of Nrf2 by Phosphorylating at Serine 550. *Mol. Cell. Biol.* **2016**, *36*, 1931–1942, doi:10.1128/MCB.00118-16.
  137. Baldelli, S.; Aquilano, K.; Ciriolo, M.R. Punctum on two different transcription factors regulated by PGC-1 $\alpha$ : Nuclear factor erythroid-derived 2-like 2 and nuclear respiratory factor 2. *Biochim. Biophys. Acta - Gen. Subj.* **2013**, *1830*, 4137–4146, doi:10.1016/j.bbagen.2013.04.006.
  138. Otterbein, L.; Sylvester, S.L.; Choi, A.M. Hemoglobin provides protection against lethal endotoxemia in rats: the role of heme oxygenase-1. *Am. J. Respir. Cell Mol. Biol.* **1995**, *13*, 595–601, doi:10.1165/ajrcmb.13.5.7576696.

139. Otterbein, L.E.; Kolls, J.K.; Mantell, L.L.; Cook, J.L.; Alam, J.; Choi, A.M.K. Exogenous administration of heme oxygenase-1 by gene transfer provides protection against hyperoxia-induced lung injury. *J. Clin. Invest.* **1999**, *103*, 1047–1054, doi:10.1172/JCI5342.
140. Poss, K.D.; Tonegawa, S. Reduced stress defense in heme oxygenase 1-deficient cells. *Proc. Natl. Acad. Sci. U. S. A.* **1997**, *94*, 10925–10930, doi:10.1073/pnas.94.20.10925.
141. Radhakrishnan, N.; Yadav, S.P.; Sachdeva, A.; Pruthi, P.K.; Sawhney, S.; Piplani, T.; Wada, T.; Yachie, A. Human Heme Oxygenase-1 Deficiency Presenting With Hemolysis, Nephritis, and Asplenia. *J. Pediatr. Hematol. Oncol.* **2011**, *33*, 74–78, doi:10.1097/MPH.0b013e3181fd2aae.
142. Kapturczak, M.H.; Wasserfall, C.; Brusko, T.; Campbell-Thompson, M.; Ellis, T.M.; Atkinson, M.A.; Agarwal, A. Heme oxygenase-1 modulates early inflammatory responses: Evidence from the heme oxygenase-1-deficient mouse. *Am. J. Pathol.* **2004**, *165*, 1045–1053, doi:10.1016/S0002-9440(10)63365-2.
143. Kawashima, A.; Oda, Y.; Yachie, A.; Koizumi, S.; Nakanishi, I. Heme oxygenase–1 deficiency: The first autopsy case. *Hum. Pathol.* **2002**, *33*, 125–130, doi:10.1053/HUPA.2002.30217.
144. Sarady, J.K.; Otterbein, S.L.; Liu, F.; Otterbein, L.E.; Choi, A.M.K. Carbon Monoxide Modulates Endotoxin-Induced Production of Granulocyte Macrophage Colony-Stimulating Factor in Macrophages. *Am. J. Respir. Cell Mol. Biol.* **2002**, *27*, 739–745, doi:10.1165/rcmb.4816.
145. Otterbein, L.E.; Bach, F.H.; Alam, J.; Soares, M.; Tao Lu, H.; Wysk, M.; Davis, R.J.; Flavell, R.A.; Choi, A.M.K. Carbon monoxide has anti-inflammatory effects involving the mitogen-activated protein kinase pathway. *Nat. Med.* **2000**, *6*, 422–428, doi:10.1038/74680.
146. Sawle, P.; Foresti, R.; Mann, B.E.; Johnson, T.R.; Green, C.J.; Motterlini, R. Carbon monoxide-releasing molecules (CO-RMs) attenuate the inflammatory response elicited by lipopolysaccharide in RAW264.7 murine macrophages. *Br. J. Pharmacol.* **2005**, *145*, 800–810, doi:10.1038/sj.bjp.0706241.
147. Tardif, V.; Riquelme, S.A.; Remy, S.; Carreño, L.J.; Cortés, C.M.; Simon, T.; Hill, M.; Louvet, C.; Riedel, C.A.; Blancou, P.; et al. Carbon monoxide decreases endosome-lysosome fusion and inhibits soluble antigen presentation by dendritic cells to T cells. *Eur. J. Immunol.* **2013**, *43*, 2832–2844, doi:10.1002/eji.201343600.
148. Rémy, S.; Blancou, P.; Tesson, L.; Tardif, V.; Brion, R.; Royer, P.J.; Motterlini, R.; Foresti, R.; Painchaut, M.; Pogu, S.; et al. Carbon monoxide inhibits TLR-induced dendritic cell immunogenicity. *J. Immunol.* **2009**, *182*, 1877–84, doi:10.4049/jimmunol.0802436.
149. Riquelme, S.A.; Pogu, J.; Anegón, I.; Bueno, S.M.; Kalergis, A.M. Carbon monoxide

- impairs mitochondria-dependent endosomal maturation and antigen presentation in dendritic cells. *Eur. J. Immunol.* **2015**, *45*, 3269–3288, doi:10.1002/eji.201545671.
150. Chora, A.A.; Fontoura, P.; Cunha, A.; Pais, T.F.; Cardoso, S.; Ho, P.P.; Lee, L.Y.; Sobel, R.A.; Steinman, L.; Soares, M.P. Heme oxygenase-1 and carbon monoxide suppress autoimmune neuroinflammation. *J. Clin. Invest.* **2007**, *117*, 438–47, doi:10.1172/JCI28844.
  151. Uddin, M.J.; Jeong, S.; Zheng, M.; Chen, Y.; Cho, G.J.; Chung, H.T.; Joe, Y. Carbon monoxide attenuates dextran sulfate sodium-induced colitis via inhibition of GSK-3 $\beta$  signaling. *Oxid. Med. Cell. Longev.* **2013**, *2013*, 210563, doi:10.1155/2013/210563.
  152. Hegazi, R.A.F.; Rao, K.N.; Mayle, A.; Sepulveda, A.R.; Otterbein, L.E.; Plevy, S.E. Carbon monoxide ameliorates chronic murine colitis through a heme oxygenase 1-dependent pathway. *J. Exp. Med.* **2005**, *202*, 1703–1713, doi:10.1084/jem.20051047.
  153. Sheikh, S.Z.; Hegazi, R.A.; Kobayashi, T.; Onyiah, J.C.; Russo, S.M.; Matsuoka, K.; Sepulveda, A.R.; Li, F.; Otterbein, L.E.; Plevy, S.E. An Anti-Inflammatory Role for Carbon Monoxide and Heme Oxygenase-1 in Chronic Th2-Mediated Murine Colitis. *J. Immunol.* **2011**, *186*, 5506–5513, doi:10.4049/jimmunol.1002433.
  154. Yang, Y.-C.; Huang, Y.-T.; Hsieh, C.-W.; Yang, P.-M.; Wung, B.-S. Carbon Monoxide Induces Heme Oxygenase-1 to Modulate STAT3 Activation in Endothelial Cells via S-Glutathionylation. *PLoS One* **2014**, *9*, e100677, doi:10.1371/journal.pone.0100677.
  155. Kim, K.M.; Pae, H.-O.; Zheng, M.; Park, R.; Kim, Y.-M.; Chung, H.-T. Carbon Monoxide Induces Heme Oxygenase-1 via Activation of Protein Kinase R-Like Endoplasmic Reticulum Kinase and Inhibits Endothelial Cell Apoptosis Triggered by Endoplasmic Reticulum Stress. *Circ. Res.* **2007**, *101*, 919–927, doi:10.1161/CIRCRESAHA.107.154781.
  156. Lin, C.C.; Yang, C.C.; Hsiao, L. Der; Chen, S.Y.; Yang, C.M. Heme oxygenase-1 induction by carbon monoxide releasing molecule-3 suppresses interleukin-1 $\beta$ -mediated neuroinflammation. *Front. Mol. Neurosci.* **2017**, *10*, 387, doi:10.3389/fnmol.2017.00387.
  157. Chiang, N.; Shinohara, M.; Dalli, J.; Mirakaj, V.; Kibi, M.; Choi, A.M.K.; Serhan, C.N. Inhaled Carbon Monoxide Accelerates Resolution of Inflammation via Unique Proresolving Mediator-Heme Oxygenase-1 Circuits. *J. Immunol.* **2013**, *190*, 6378–6388, doi:10.4049/jimmunol.1202969.
  158. Kawade, N.; Onishi, S. The prenatal and postnatal development of UDP-glucuronyltransferase activity towards bilirubin and the effect of premature birth on this activity in the human liver. *Biochem. J.* **1981**, *196*, 257–60.

159. Wang, W.W.; Smith, D.L.H.; Zucker, S.D. Bilirubin inhibits iNOS expression and NO production in response to endotoxin in rats. *Hepatology* **2004**, *40*, 424–433, doi:10.1002/hep.20334.
160. Idelman, G.; Smith, D.L.H.; Zucker, S.D. Bilirubin inhibits the up-regulation of inducible nitric oxide synthase by scavenging reactive oxygen species generated by the toll-like receptor 4-dependent activation of NADPH oxidase. *Redox Biol.* **2015**, *5*, 398–408, doi:10.1016/j.redox.2015.06.008.
161. Vogel, M.E.; Zucker, S.D. Bilirubin acts as an endogenous regulator of inflammation by disrupting adhesion molecule-mediated leukocyte migration. *Inflamm. Cell Signal.* **2016**, *3*, doi:10.14800/ics.1178.
162. Bellner, L.; Wolstein, J.; Patil, K.A.; Dunn, M.W.; Laniado-Schwartzman, M. Biliverdin Rescues the HO-2 Null Mouse Phenotype of Unresolved Chronic Inflammation Following Corneal Epithelial Injury. *Investig. Ophthalmology Vis. Sci.* **2011**, *52*, 3246, doi:10.1167/iovs.10-6219.
163. Bellner, L.; Vitto, M.; Patil, K.A.; Dunn, M.W.; Regan, R.; Laniado-Schwartzman, M. Exacerbated corneal inflammation and neovascularization in the HO-2 null mice is ameliorated by biliverdin. *Exp. Eye Res.* **2008**, *87*, 268–78, doi:10.1016/j.exer.2008.06.007.
164. Sarady-Andrews, J.K.; Liu, F.; Gallo, D.; Nakao, A.; Overhaus, M.; Öllinger, R.; Choi, A.M.; Otterbein, L.E. Biliverdin administration protects against endotoxin-induced acute lung injury in rats. *Am. J. Physiol. Cell. Mol. Physiol.* **2005**, *289*, L1131–L1137, doi:10.1152/ajplung.00458.2004.
165. Li, J.-J.; Zou, Z.-Y.; Liu, J.; Xiong, L.-L.; Jiang, H.-Y.; Wang, T.-H.; Shao, J.-L. Biliverdin administration ameliorates cerebral ischemia reperfusion injury in rats and is associated with proinflammatory factor downregulation. *Exp. Ther. Med.* **2017**, *14*, 671–679, doi:10.3892/etm.2017.4549.
166. ISCC Gut Decisions- Leading change to improve the lives of people with Crohn's and colitis. **2015**.
167. Halling, M.L.; Kjeldsen, J.; Knudsen, T.; Nielsen, J.; Hansen, L.K. Patients with inflammatory bowel disease have increased risk of autoimmune and inflammatory diseases. *World J. Gastroenterol.* **2017**, *23*, 6137–6146, doi:10.3748/wjg.v23.i33.6137.
168. Zhang, Y.-Z.; Li, Y.-Y. Inflammatory bowel disease: pathogenesis. *World J. Gastroenterol.* **2014**, *20*, 91–9, doi:10.3748/wjg.v20.i1.91.
169. Mowat, C.; Cole, A.; Windsor, A.; Ahmad, T.; Arnott, I.; Driscoll, R.; Mitton, S.; Orchard, T.; Rutter, M.; Younge, L.; et al. Guidelines for the management of inflammatory bowel disease in adults. *Gut* **2011**, *60*, 571–607, doi:10.1136/gut.2010.224154.

170. Takagi, T.; Naito, Y.; Mizushima, K.; Nukigi, Y.; Okada, H.; Suzuki, T.; Hirata, I.; Omatsu, T.; Okayama, T.; Handa, O.; et al. Increased intestinal expression of heme oxygenase-1 and its localization in patients with ulcerative colitis. *J. Gastroenterol. Hepatol.* **2008**, *23*, S229–S233, doi:10.1111/j.1440-1746.2008.05443.x.
171. Paul, G.; Bataille, F.; Obermeier, F.; Bock, J.; Klebl, F.; Strauch, U.; Lochbaum, D.; Rummele, P.; Farkas, S.; Scholmerich, J.; et al. Analysis of intestinal haem-oxygenase-1 (HO-1) in clinical and experimental colitis. *Clin. Exp. Immunol.* **2005**, *140*, 547–555, doi:10.1111/j.1365-2249.2005.02775.x.
172. Takagi, T.; Naito, Y.; Uchiyama, K.; Yoshikawa, T. The role of heme oxygenase and carbon monoxide in inflammatory bowel disease. *Redox Rep.* **2010**, *15*, 193–201, doi:10.1179/174329210X12650506623889.
173. Wang, W.P.; Guo, X.; Koo, M.W.L.; Wong, B.C.Y.; Lam, S.K.; Ye, Y.N.; Cho, C.H. Protective role of heme oxygenase-1 on trinitrobenzene sulfonic acid-induced colitis in rats. *Am. J. Physiol. Liver Physiol.* **2001**, *281*, G586–G594, doi:10.1152/ajpgi.2001.281.2.G586.
174. Takagi, T.; Naito, Y.; Mizushima, K.; Hirai, Y.; Harusato, A.; Okayama, T.; Katada, K.; Kamada, K.; Uchiyama, K.; Handa, O.; et al. Heme oxygenase-1 prevents murine intestinal inflammation. *J. Clin. Biochem. Nutr.* **2018**, *63*, 169–174, doi:10.3164/jcbrn.17-133.
175. Zheng, J.-D.; He, Y.; Yu, H.-Y.; Liu, Y.-L.; Ge, Y.-X.; Li, X.-T.; Li, X.; Wang, Y.; Guo, M.-R.; Qu, Y.-L.; et al. Unconjugated bilirubin alleviates experimental ulcerative colitis by regulating intestinal barrier function and immune inflammation. *World J Gastroenterol* **2019**, *25*, 1865–1878, doi:10.3748/wjg.v25.i15.1865.
176. Longhi, M.S.; Vuerich, M.; Kalbasi, A.; Kenison, J.E.; Yeste, A.; Csizmadia, E.; Vaughn, B.; Feldbrugge, L.; Mitsushashi, S.; Wegiel, B.; et al. Bilirubin suppresses Th17 immunity in colitis by upregulating CD39. *JCI insight* **2017**, *2*, doi:10.1172/jci.insight.92791.
177. Zhang, L.; Zhang, Y.; Zhong, W.; Di, C.; Lin, X.; Xia, Z. Heme oxygenase-1 ameliorates dextran sulfate sodium-induced acute murine colitis by regulating Th17/Treg cell balance. *J. Biol. Chem.* **2014**, *289*, 26847–26858, doi:10.1074/jbc.M114.590554.
178. Wu, Y.; Wu, B.; Zhang, Z.; Lu, H.; Fan, C.; Qi, Q.; Gao, Y.; Li, H.; Feng, C.; Zuo, J.; et al. Heme protects intestinal mucosal barrier in DSS-induced colitis through regulating macrophage polarization in both HO-1-dependent and HO-1-independent way. *FASEB J.* **2020**, *34*, 8028–8043, doi:10.1096/fj.202000313RR.
179. Horváth, K.; Varga, C.; Berkó, A.; Pósa, A.; László, F.; Whittle, B.J.R. The involvement of heme oxygenase-1 activity in the therapeutic actions of 5-aminosalicylic acid in rat colitis. *Eur. J. Pharmacol.* **2008**, *581*, 315–323, doi:10.1016/j.ejphar.2007.12.004.

180. Kang, S.; Kim, W.; Jeong, S.; Lee, Y.; Nam, J.; Lee, S.; Jung, Y. Oxidized 5-aminosalicylic acid activates Nrf2-HO-1 pathway by covalently binding to Keap1: Implication in anti-inflammatory actions of 5-aminosalicylic acid. *Free Radic. Biol. Med.* **2017**, *108*, 715–724, doi:10.1016/j.freeradbiomed.2017.04.366.
181. Wu, J.J.; Nguyen, T.U.; Poon, K.-Y.T.; Herrinton, L.J. The association of psoriasis with autoimmune diseases. *J. Am. Acad. Dermatol.* **2012**, *67*, 924–930, doi:10.1016/j.jaad.2012.04.039.
182. Hsu, L.N.; Armstrong, A.W. Psoriasis and autoimmune disorders: A review of the literature. *J. Am. Acad. Dermatol.* **2012**, *67*, 1076–1079, doi:10.1016/j.jaad.2012.01.029.
183. Elder, J.T. Genome-wide association scan yields new insights into the immunopathogenesis of psoriasis. *Genes Immun.* **2009**, *10*, 201–9, doi:10.1038/gene.2009.11.
184. Boehncke, W.-H.; Schön, M.P. Psoriasis. *Lancet (London, England)* **2015**, *386*, 983–94, doi:10.1016/S0140-6736(14)61909-7.
185. Lowes, M.A.; Bowcock, A.M.; Krueger, J.G. Pathogenesis and therapy of psoriasis. *Nature* **2007**, *445*, 866–873, doi:10.1038/nature05663.
186. Johnson-Huang, L.M.; Lowes, M.A.; Krueger, J.G. Putting together the psoriasis puzzle: an update on developing targeted therapies. *Dis. Model. Mech.* **2012**, *5*, 423–33, doi:10.1242/dmm.009092.
187. Tyrrell, R.M.; Reeve, V.E. Potential protection of skin by acute UVA irradiation—From cellular to animal models. *Prog. Biophys. Mol. Biol.* **2006**, *92*, 86–91, doi:https://doi.org/10.1016/j.pbiomolbio.2006.02.002.
188. Hanselmann, C.; Mauch, C.; Werner, S. Haem oxygenase-1: a novel player in cutaneous wound repair and psoriasis? *Biochem. J.* **2001**, *353*, 459–66.
189. El-Rifaie, A.-A.A.; Sabry, D.; Doss, R.W.; Kamal, M.A.; Abd El Hassib, D.M. Heme oxygenase and iron status in exosomes of psoriasis patients. *Arch. Dermatol. Res.* **2018**, *310*, 651–656, doi:10.1007/s00403-018-1852-6.
190. Ma, L.J.; You, Y.; Bai, B.X.; Li, Y.-Z. Therapeutic effects of heme oxygenase-1 on psoriasiform skin lesions in guinea pigs. *Arch. Dermatol. Res.* **2009**, *301*, 459–66, doi:10.1007/s00403-009-0956-4.
191. Listopad, J.; Asadullah, K.; Sievers, C.; Ritter, T.; Meisel, C.; Sabat, R.; Döcke, W.-D. Heme oxygenase-1 inhibits T cell-dependent skin inflammation and differentiation and function of antigen-presenting cells. *Exp. Dermatol.* **2007**, *16*, 661–70, doi:10.1111/j.1600-0625.2007.00581.x.
192. Zhang, B.; Xie, S.; Su, Z.; Song, S.; Xu, H.; Chen, G.; Cao, W.; Yin, S.; Gao, Q.; Wang, H. Heme oxygenase-1 induction attenuates imiquimod-induced psoriasiform

- inflammation by negative regulation of Stat3 signaling. *Sci. Rep.* **2016**, *6*, 21132, doi:10.1038/srep21132.
193. Nisar, M.F.; Parsons, K.S.G.; Bian, C.X.; Zhong, J.L. UVA irradiation induced heme oxygenase-1: A novel phototherapy for morphea. *Photochem. Photobiol.* **2015**, *91*, 210–220, doi:10.1111/php.12342.
194. Lehmann, J.C.U.; Listopad, J.J.; Rentzsch, C.U.; Igney, F.H.; von Bonin, A.; Hennekes, H.H.; Asadullah, K.; Docke, W.-D.F. Dimethylfumarate induces immunosuppression via glutathione depletion and subsequent induction of heme oxygenase 1. *J. Invest. Dermatol.* **2007**, *127*, 835–45, doi:10.1038/sj.jid.5700686.
195. Kasarełto, K.; Jesion, A.; Tyszkowska, K.; Matusik, K.; Czarzasta, K.; Wrzesień, R.; Cudnoch-Jedrzejewska, A.; Kasarello, K.; Jesion, A.; Tyszkowska, K.; et al. Effect of dimethyl fumarate on heme oxygenase-1 expression in experimental allergic encephalomyelitis in rats. *Folia Neuropathol.* **2017**, *55*, 325–332, doi:10.5114/fn.2017.72394.
196. Foresti, R.; Bains, S.K.; Pitchumony, T.S.; de Castro Brás, L.E.; Drago, F.; Dubois-Randé, J.-L.; Bucolo, C.; Motterlini, R. Small molecule activators of the Nrf2-HO-1 antioxidant axis modulate heme metabolism and inflammation in BV2 microglia cells. *Pharmacol. Res.* **2013**, *76*, 132–48, doi:10.1016/j.phrs.2013.07.010.
197. Ghoreschi, K.; Brück, J.; Kellerer, C.; Deng, C.; Peng, H.; Rothfuss, O.; Hussain, R.Z.; Gocke, A.R.; Respa, A.; Glocova, I.; et al. Fumarates improve psoriasis and multiple sclerosis by inducing type II dendritic cells. *J. Exp. Med.* **2011**, *208*, 2291–303, doi:10.1084/jem.20100977.
198. Ogawa, T.; Ishitsuka, Y.; Inoue, S.; Nakamura, Y.; Saito, A.; Okiyama, N.; Fujisawa, Y.; Furuta, J.; Watanabe, R.; Fujimoto, M. Nuclear Factor Erythroid 2-Related Factor 2 (Nrf2) Regulates Epidermal Keratinization under Psoriatic Skin Inflammation. *Am. J. Pathol.* **2020**, *190*, 577–585, doi:10.1016/j.ajpath.2019.10.022.
199. Ghasemi, N.; Razavi, S.; Nikzad, E. Multiple Sclerosis: Pathogenesis, Symptoms, Diagnoses and Cell-Based Therapy. *Cell J.* **2017**, *19*, 1–10, doi:10.22074/CELLJ.2016.4867.
200. Hart, F.M.; Bainbridge, J. Current and emerging treatment of multiple sclerosis. *Am. J. Manag. Care* **2016**, *22*, s159–70.
201. Liu, Y.; Zhu, B.; Luo, L.; Li, P.; Paty, D.W.; Cynader, M.S. Heme oxygenase-1 plays an important protective role in experimental autoimmune encephalomyelitis. *Neuroreport* **2001**, *12*, 1841–5.
202. Chora, Â.A.; Fontoura, P.; Cunha, A.; Pais, T.F.; Cardoso, S.; Ho, P.P.; Lee, L.Y.; Sobel, R.A.; Steinman, L.; Soares, M.P. Heme oxygenase–1 and carbon monoxide suppress autoimmune neuroinflammation. *J. Clin. Invest.* **2007**, *117*, 438–447, doi:10.1172/JCI28844.

203. Fagone, P.; Patti, F.; Mangano, K.; Mammana, S.; Coco, M.; Touil-Boukoffa, C.; Chikovani, T.; Di Marco, R.; Nicoletti, F. Heme oxygenase-1 expression in peripheral blood mononuclear cells correlates with disease activity in multiple sclerosis. *J. Neuroimmunol.* **2013**, *261*, 82–6, doi:10.1016/j.jneuroim.2013.04.013.
204. Schipper, H.M. Heme oxygenase expression in human central nervous system disorders. *Free Radic. Biol. Med.* 2004, *37*, 1995–2011.
205. Chen, S.-J.; Wang, Y.-L.; Lo, W.-T.; Wu, C.-C.; Hsieh, C.-W.; Huang, C.-F.; Lan, Y.-H.; Wang, C.-C.; Chang, D.-M.; Sytwu, H.-K. Erythropoietin enhances endogenous haem oxygenase-1 and represses immune responses to ameliorate experimental autoimmune encephalomyelitis. *Clin. Exp. Immunol.* **2010**, *162*, 210–23, doi:10.1111/J.1365-2249.2010.04238.X.
206. Fagone, P.; Mangano, K.; Quattrocchi, C.; Motterlini, R.; Di Marco, R.; Magro, G.; Penacho, N.; Romao, C.C.; Nicoletti, F. Prevention of clinical and histological signs of proteolipid protein (PLP)-induced experimental allergic encephalomyelitis (EAE) in mice by the water-soluble carbon monoxide-releasing molecule (CORM)-A1. *Clin. Exp. Immunol.* **2011**, *163*, 368–374, doi:10.1111/j.1365-2249.2010.04303.x.
207. Liu, Y.; Zhu, B.; Wang, X.; Luo, L.; Li, P.; Paty, D.W.; Cynader, M.S. Bilirubin as a potent antioxidant suppresses experimental autoimmune encephalomyelitis: implications for the role of oxidative stress in the development of multiple sclerosis. *J. Neuroimmunol.* **2003**, *139*, 27–35, doi:10.1016/s0165-5728(03)00132-2.
208. Liu, Y.; Liu, J.; Tetzlaff, W.; Paty, D.W.; Cynader, M.S. Biliverdin reductase, a major physiologic cytoprotectant, suppresses experimental autoimmune encephalomyelitis. *Free Radic. Biol. Med.* **2006**, *40*, 960–967, doi:10.1016/j.freeradbiomed.2005.07.021.
209. De Vries, D.K.; Kortekaas, K.A.; Tsikas, D.; Wijermars, L.G.M.; Van Noorden, C.J.F.; Suchy, M.T.; Cobbaert, C.M.; Klautz, R.J.M.; Schaapherder, A.F.M.; Lindeman, J.H.N. Oxidative Damage in Clinical Ischemia/Reperfusion Injury: A Reappraisal. *Antioxid. Redox Signal.* **2013**, *19*, 535, doi:10.1089/ARS.2012.4580.
210. Ingulli, E. Mechanism of cellular rejection in transplantation. *Pediatr. Nephrol.* **2010**, *25*, 61, doi:10.1007/S00467-008-1020-X.
211. Nakao, A.; Otterbein, L.E.; Overhaus, M.; Sarady, J.K.; Tsung, A.; Kimizuka, K.; Nalesnik, M.A.; Kaizu, T.; Uchiyama, T.; Liu, F.; et al. Biliverdin protects the functional integrity of a transplanted syngeneic small bowel. *Gastroenterology* **2004**, *127*, 595–606, doi:10.1053/j.gastro.2004.05.059.
212. Tang, L.M.; Wang, Y.P.; Wang, K.; Pu, L.Y.; Zhang, F.; Li, X.C.; Kong, L.B.; Sun, B.C.; Li, G.Q.; Wang, X.H. Exogenous Biliverdin Ameliorates Ischemia-Reperfusion Injury in Small-for-Size Rat Liver Grafts. *Transplant. Proc.* **2007**, *39*, 1338–1344, doi:10.1016/j.transproceed.2006.11.032.



213. Sugimoto, R.; Tanaka, Y.; Noda, K.; Kawamura, T.; Toyoda, Y.; Billiar, T.R.; McCurry, K.R.; Nakao, A. Preservation solution supplemented with biliverdin prevents lung cold ischaemia/reperfusion injury. *Eur. J. Cardiothorac. Surg.* **2012**, *42*, 1035–41, doi:10.1093/ejcts/ezs298.
214. Yamashita, K.; McDaid, J.; Ollinger, R.; Tsui, T.Y.; Berberat, P.O.; Usheva, A.; Csizmadia, E.; Smith, R.N.; Soares, M.P.; Bach, F.H. Biliverdin, a natural product of heme catabolism, induces tolerance to cardiac allografts.
215. Ozaki, K.S.; Kimura, S.; Murase, N. Use of carbon monoxide in minimizing ischemia/reperfusion injury in transplantation. *Transplant. Rev.* **2012**, *26*, 125–139.
216. Zhou, H.; Qian, H.; Liu, J.; Zhu, D.; Ding, W.; Pan, P.; Jin, D.; Wang, J.; Li, W. Protection against lung graft injury from brain-dead donors with carbon monoxide, biliverdin, or both. *J. Hear. Lung Transplant.* **2011**, *30*, 460–466, doi:10.1016/j.healun.2010.11.020.
217. Nakao, A.; Neto, J.S.; Kanno, S.; Stolz, D.B.; Kimizuka, K.; Liu, F.; Bach, F.H.; Billiar, T.R.; Choi, A.M.; Otterbein, L.E.; et al. Protection Against Ischemia/Reperfusion Injury in Cardiac and Renal Transplantation with Carbon Monoxide, Biliverdin and Both. *Am. J. Transplant.* **2005**, *5*, 282–291, doi:10.1111/j.1600-6143.2004.00695.x.
218. Pileggi, A.; Damaris Molano, R.; Berney, T.; Cattan, P.; Vizzardelli, C.; Oliver, R.; Fraker, C.; Ricordi, C.; Pastori, R.L.; Bach, F.H.; et al. Heme Oxygenase-1 Induction in Islet Cells Results in Protection from Apoptosis and Improved in Vivo Function after Transplantation. *Diabetes* **2001**, *50*, 1983–1991, doi:10.2337/diabetes.50.9.1983.
219. Wang, H.; Lee, S.S.; Gao, W.; Czismadia, E.; McDaid, J.; Öllinger, R.; Soares, M.P.; Yamashita, K.; Bach, F.H. Donor treatment with carbon monoxide can yield islet allograft survival and tolerance. *Diabetes* **2005**, *54*, 1400–1406, doi:10.2337/diabetes.54.5.1400.
220. Yi, T.; Li, X.; Wang, E.; Zhang, Y.; Fu, Y.; Li, J.; Jiang, T. Activation of the nuclear erythroid 2-related factor 2 antioxidant responsive element (Nrf2-ARE) signaling pathway alleviates acute graft-versus-host disease by reducing oxidative stress and inhibiting infiltration of inflammatory cells in an allogeneic s. *Med. Sci. Monit.* **2018**, *24*, 5973–5979, doi:10.12659/MSM.908130.
221. Bedard, E.L.R.; Jiang, J.; Parry, N.; Wang, H.; Liu, W.; Garcia, B.; Kim, P.; Chakrabarti, S.; Buelow, R.; Zhong, R. Peritransplant treatment with cobalt protoporphyrin attenuates chronic renal allograft rejection. *Transpl. Int.* **2005**, *18*, 341–349, doi:10.1111/j.1432-2277.2004.00062.x.
222. Tsui, T.Y.; Wu, X.; Lau, C.K.; Ho, D.W.Y.; Xu, T.; Siu, Y.T.; Fan, S.T. Prevention of chronic deterioration of heart allograft by recombinant adeno-associated virus-mediated heme oxygenase-1 gene transfer. *Circulation* **2003**, *107*, 2623–2629, doi:10.1161/01.cir.0000066911.03770.8d.

223. Chauveau, C.; Bouchet, D.; Roussel, J.C.; Mathieu, P.; Braudeau, C.; Renaudin, K.; Tesson, L.; Soullillou, J.P.; Iyer, S.; Buelow, R.; et al. Gene transfer of heme oxygenase-1 and carbon monoxide delivery inhibit chronic rejection. *Am. J. Transplant.* **2002**, *2*, 581–592, doi:10.1034/j.1600-6143.2002.20702.x.
224. Horio, T.; Morishita, E.; Mizuno, S.; Uchino, K.; Hanamura, I.; Espinoza, J.L.; Morishima, Y.; Kodera, Y.; Onizuka, M.; Kashiwase, K.; et al. Donor heme oxygenase-1 promoter gene polymorphism predicts survival after unrelated bone marrow transplantation for high-risk patients. *Cancers (Basel)*. **2020**, *12*, doi:10.3390/cancers12020424.
225. Schulz, S.; Wong, R.J.; Vreman, H.J.; Stevenson, D.K. Metalloporphyrins - An update. *Front. Pharmacol.* **2012**, *3 APR*, 68, doi:10.3389/fphar.2012.00068.
226. Mucha, O.; Podkalicka, P.; Czarnek, M.; Biela, A.; Mieczkowski, M.; Kachamakova-Trojanowska, N.; Stepniewski, J.; Jozkowicz, A.; Dulak, J.; Loboda, A. Pharmacological versus genetic inhibition of heme oxygenase-1 - The comparison of metalloporphyrins, shRNA and CRISPR/Cas9 system. *Acta Biochim. Pol.* **2018**, *65*, 277–286, doi:10.18388/abp.2017\_2542.
227. Cory, H.; Passarelli, S.; Szeto, J.; Tamez, M.; Mattei, J. The Role of Polyphenols in Human Health and Food Systems: A Mini-Review. *Front. Nutr.* **2018**, *5*, 87.
228. Motterlini, R.; Foresti, R.; Bassi, R.; Green, C.J. Curcumin, an antioxidant and anti-inflammatory agent, induces heme oxygenase-1 and protects endothelial cells against oxidative stress. *Free Radic. Biol. Med.* **2000**, *28*, 1303–1312, doi:10.1016/S0891-5849(00)00294-X.
229. Chen, C.Y.; Jang, J.H.; Li, M.H.; Surh, Y.J. Resveratrol upregulates heme oxygenase-1 expression via activation of NF-E2-related factor 2 in PC12 cells. *Biochem. Biophys. Res. Commun.* **2005**, *331*, 993–1000, doi:10.1016/j.bbrc.2005.03.237.
230. Kim, Y.; Kim, C.-S.; Joe, Y.; Chung, H.T.; Ha, T.Y.; Yu, R. Quercetin Reduces Tumor Necrosis Factor Alpha-Induced Muscle Atrophy by Upregulation of Heme Oxygenase-1. *J. Med. Food* **2018**, *21*, 551–559, doi:10.1089/jmf.2017.4108.
231. Funes, S.C.; Rios, M.; Fernández-Fierro, A.; Covián, C.; Bueno, S.M.; Riedel, C.A.; Mackern-Oberti, J.P.; Kalergis, A.M. Naturally Derived Heme-Oxygenase 1 Inducers and Their Therapeutic Application to Immune-Mediated Diseases. *Front. Immunol.* **2020**, *11*, 1467, doi:10.3389/fimmu.2020.01467.
232. Williamson, G.; Clifford, M.N. Role of the small intestine, colon and microbiota in determining the metabolic fate of polyphenols. *Biochem. Pharmacol.* **2017**, *139*, 24–39, doi:10.1016/j.bcp.2017.03.012.
233. Del Rio, D.; Rodriguez-Mateos, A.; Spencer, J.P.E.; Tognolini, M.; Borges, G.; Crozier, A. Dietary (poly)phenolics in human health: Structures, bioavailability, and evidence of protective effects against chronic diseases. *Antioxidants Redox Signal.* **2013**, *18*, 1818–1892, doi:10.1089/ars.2012.4581.

234. Liu, X.; Zhou, W.; Zhang, X.; Lu, P.; Du, Q.; Tao, L.; Ding, Y.; Wang, Y.; Hu, R. Dimethyl fumarate ameliorates dextran sulfate sodium-induced murine experimental colitis by activating Nrf2 and suppressing NLRP3 inflammasome activation. *Biochem. Pharmacol.* **2016**, *112*, 37–49, doi:10.1016/j.bcp.2016.05.002.
235. Nakayama, T.; Kobayashi, T.; Shimpei, O.; Fukuhara, H.; Namikawa, T.; Inoue, K.; Hanazaki, K.; Takahashi, K.; Nakajima, M.; Tanaka, T.; et al. Photoirradiation after aminolevulinic acid treatment suppresses cancer cell proliferation through the HO-1/p21 pathway. *Photodiagnosis Photodyn. Ther.* **2019**, *28*, 10–17, doi:10.1016/j.pdpdt.2019.07.021.
236. Hou, J.; Zhang, Q.; Fujino, M.; Cai, S.; Ito, H.; Takahashi, K.; Abe, F.; Nakajima, M.; Tanaka, T.; Xu, J.; et al. 5-Aminolevulinic acid with ferrous iron induces permanent cardiac allograft acceptance in mice via induction of regulatory cells. *J. Hear. Lung Transplant.* **2015**, *34*, 254–263, doi:10.1016/j.healun.2014.09.037.
237. Narimiya, T.; Kanzaki, H.; Yamaguchi, Y.; Wada, S.; Katsumata, Y.; Tanaka, K.; Tomonari, H. Nrf2 activation in osteoblasts suppresses osteoclastogenesis via inhibiting IL-6 expression. *Bone Reports* **2019**, *11*, doi:10.1016/j.bonr.2019.100228.
238. Yan, S.C.; Wang, Y.J.; Li, Y.J.; Cai, W.Y.; Weng, X.G.; Li, Q.; Chen, Y.; Yang, Q.; Zhu, X.X. Dihydroartemisinin regulates the Th/Treg balance by inducing activated CD4+ T cell apoptosis via heme oxygenase-1 induction in mouse models of inflammatory bowel disease. *Molecules* **2019**, *24*, doi:10.3390/molecules24132475.
239. Lin, C.-C.C.; Yang, C.-C.C.C.-M.M.; Hsiao, L.-D. Der; Chen, S.-Y.Y.; Yang, C.-C.C.C.-M.M. Heme Oxygenase-1 Induction by Carbon Monoxide Releasing Molecule-3 Suppresses Interleukin-1 $\beta$ -Mediated Neuroinflammation. *Front. Mol. Neurosci.* **2017**, *10*, 387, doi:10.3389/fnmol.2017.00387.
240. Song, L.; Li, J.Y.; Yuan, X.; Liu, W.; Chen, Z.; Guo, D.; Yang, F.; Guo, Q.Y.; Song, H. Carbon monoxide-releasing molecule suppresses inflammatory and osteoclastogenic cytokines in nicotine- and lipopolysaccharide-stimulated human periodontal ligament cells via the heme oxygenase-1 pathway. *Int. J. Mol. Med.* **2017**, *40*, 1591–1601, doi:10.3892/ijmm.2017.3129.
241. Mangano, K.; Cavalli, E.; Mammana, S.; Basile, M.S.; Caltabiano, R.; Pesce, A.; Puleo, S.; Atanasov, A.G.; Magro, G.; Nicoletti, F.; et al. Involvement of the Nrf2/HO-1/CO axis and therapeutic intervention with the CO-releasing molecule CORM-A1, in a murine model of autoimmune hepatitis. *J. Cell. Physiol.* **2018**, *233*, 4156–4165, doi:10.1002/jcp.26223.
242. Takagi, T.; Naito, Y.; Tanaka, M.; Mizushima, K.; Ushiroda, C.; Toyokawa, Y.; Uchiyama, K.; Hamaguchi, M.; Handa, O.; Itoh, Y. Carbon monoxide ameliorates murine T-cell-dependent colitis through the inhibition of Th17 differentiation. *Free Radic. Res.* **2018**, *52*, 1328–1335, doi:10.1080/10715762.2018.1470327.
243. Ji, X.; Damera, K.; Zheng, Y.; Yu, B.; Otterbein, L.E.; Wang, B. Toward Carbon Monoxide-Based Therapeutics: Critical Drug Delivery and Developability Issues. *J.*

- Pharm. Sci.* 2016, 105, 406–416.
244. Motterlini, R.; Otterbein, L.E. The therapeutic potential of carbon monoxide. *Nat. Rev. Drug Discov.* **2010**, 9, 728–743, doi:10.1038/nrd3228.
245. El Ali, Z.; Ollivier, A.; Manin, S.; Rivard, M.; Motterlini, R.; Foresti, R. Therapeutic effects of CO-releaser/Nrf2 activator hybrids (HYCOs) in the treatment of skin wound, psoriasis and multiple sclerosis. *Redox Biol.* **2020**, 34, 101521, doi:10.1016/j.redox.2020.101521.
246. Motterlini, R.; Nikam, A.; Manin, S.; Ollivier, A.; Wilson, J.L.; Djouadi, S.; Muchova, L.; Martens, T.; Rivard, M.; Foresti, R. HYCO-3, a dual CO-releaser/Nrf2 activator, reduces tissue inflammation in mice challenged with lipopolysaccharide. *Redox Biol.* **2019**, 20, 334–348, doi:10.1016/j.redox.2018.10.020.
247. Mills, E.L.; Ryan, D.G.; Prag, H.A.; Dikovskaya, D.; Menon, D.; Zaslona, Z.; Jedrychowski, M.P.; H Costa, ana S.; Higgins, M.; Hams, E.; et al. Itaconate is an anti-inflammatory metabolite that activates Nrf2 via alkylation of KEAP1. *Nature* **2018**, 556, 113–117, doi:10.1038/nature25986.
248. Bambouskova, M.; Gorvel, L.; Lampropoulou, V.; Sergushichev, A.; Loginicheva, E.; Johnson, K.; Korenfeld, D.; elizabeth Mathyer, M.; Kim, H.; Huang, L.-H.H.; et al. Electrophilic properties of itaconate and derivatives regulate the I $\kappa$ B $\zeta$ -ATF3 inflammatory axis. *Nature* **2018**, 556, 501–504, doi:10.1038/s41586-018-0052-z.
249. Tang, C.; Wang, X.; Xie, Y.; Cai, X.; Yu, N.; Hu, Y.; Zheng, Z. 4-Octyl itaconate activates Nrf2 signaling to inhibit pro-inflammatory cytokine production in peripheral blood mononuclear cells of systemic lupus erythematosus patients. *Cell. Physiol. Biochem.* **2018**, 51, 979–990, doi:10.1159/000495400.
250. Davies, T.G.; Wixted, W.E.; Coyle, J.E.; Griffiths-Jones, C.; Hearn, K.; McMenamin, R.; Norton, D.; Rich, S.J.; Richardson, C.; Saxty, G.; et al. Monoacidic Inhibitors of the Kelch-like ECH-Associated Protein 1: Nuclear Factor Erythroid 2-Related Factor 2 (KEAP1:NRF2) Protein-Protein Interaction with High Cell Potency Identified by Fragment-Based Discovery. *J. Med. Chem.* **2016**, 59, 3991–4006, doi:10.1021/acs.jmedchem.6b00228.
251. Bewley, M.A.; Budd, R.C.; Ryan, E.; Cole, J.; Collini, P.; Marshall, J.; Kolsum, U.; Beech, G.; Emes, R.D.; Tcherniaeva, I.; et al. Opsonic phagocytosis in chronic obstructive pulmonary disease is enhanced by Nrf2 agonists. *Am. J. Respir. Crit. Care Med.* **2018**, 198, 739–750, doi:10.1164/rccm.201705-0903OC.
252. Stijlemans, B.; Caljon, G.; Van Den Abbeele, J.; Van Ginderachter, J.A.; Magez, S.; De Trez, C. Immune Evasion Strategies of *Trypanosoma brucei* within the Mammalian Host: Progression to Pathogenicity. *Front. Immunol.* **2016**, 7, 233, doi:10.3389/fimmu.2016.00233.
253. Berger, B.J.; Dai, W.W.; Wang, H.; Stark, R.E.; Cerami, A. Aromatic amino acid transamination and methionine recycling in trypanosomatids. *Proc. Natl. Acad. Sci.*

- U. S. A. **1996**, *93*, 4126–4130, doi:10.1073/pnas.93.9.4126.
254. Marciano, D.; Llorente, C.; Maugeri, D.A.; de la Fuente, C.; Opperdoes, F.; Cazzulo, J.J.; Nowicki, C. Biochemical characterization of stage-specific isoforms of aspartate aminotransferases from *Trypanosoma cruzi* and *Trypanosoma brucei*. *Mol. Biochem. Parasitol.* **2008**, *161*, 12–20, doi:10.1016/j.molbiopara.2008.05.005.
255. McGettrick, A.F.; Corcoran, S.E.; Barry, P.J.G.; McFarland, J.; Crès, C.; Curtis, A.M.; Franklin, E.; Corr, S.C.; Mok, K.H.; Cummins, E.P.; et al. *Trypanosoma brucei* metabolite indolepyruvate decreases HIF-1 $\alpha$  and glycolysis in macrophages as a mechanism of innate immune evasion. *Proc. Natl. Acad. Sci.* **2016**, *113*, E7778–E7787, doi:10.1073/pnas.1608221113.
256. Campbell, N.K.; Williams, D.G.; Fitzgerald, H.K.; Barry, P.J.; Cunningham, C.C.; Nolan, D.P.; Dunne, A. *Trypanosoma brucei* Secreted Aromatic Ketoacids Activate the Nrf2/HO-1 Pathway and Suppress Pro-inflammatory Responses in Primary Murine Glia and Macrophages. *Front. Immunol.* **2019**, *10*, 2137, doi:10.3389/fimmu.2019.02137.
257. Aoki, R.; Aoki-Yoshida, A.; Suzuki, C.; Takayama, Y. Protective Effect of Indole-3-Pyruvate against Ultraviolet B-Induced Damage to Cultured HaCaT Keratinocytes and the Skin of Hairless Mice. *PLoS One* **2014**, *9*, e96804, doi:10.1371/journal.pone.0096804.
258. Aoki, R.; Aoki-Yoshida, A.; Suzuki, C.; Takayama, Y. Indole-3-Pyruvic Acid, an Aryl Hydrocarbon Receptor Activator, Suppresses Experimental Colitis in Mice. *J. Immunol.* **2018**, *201*, 3683–3693, doi:10.4049/jimmunol.1701734.
259. Diskin, C.; Corcoran, S.E.; Tyrrell, V.J.; McGettrick, A.F.; Zaslona, Z.; O'Donnell, V.B.; Nolan, D.P.; O'Neill, L.A.J. The Trypanosome-Derived Metabolite Indole-3-Pyruvate Inhibits Prostaglandin Production in Macrophages by Targeting COX2. *J. Immunol.* **2021**, *207*, 2551–2560, doi:10.4049/jimmunol.2100402.
260. Loboda, A.; Jozkowicz, A.; Dulak, J. *HO-1/CO system in tumor growth, angiogenesis and metabolism - Targeting HO-1 as an anti-tumor therapy*; Elsevier B.V., 2015; Vol. 74; ISBN 4812664691.
261. Kimura, S.; Aung, N.Y.; Ohe, R.; Yano, M.; Hashimoto, T.; Fujishima, T.; Kimura, W.; Yamakawa, M. Increasing Heme Oxygenase-1-Expressing Macrophages Indicates a Tendency of Poor Prognosis in Advanced Colorectal Cancer. *Digestion* **2020**, *101*, 401–410, doi:10.1159/000500225.
262. Chung, S.W.; Hall, S.R.; Perrella, M.A. Role of heme oxygenase-1 in microbial host defense. *Cell. Microbiol.* **2009**, *11*, 199, doi:10.1111/J.1462-5822.2008.01261.X.
263. Dauchy, F.A.; Contin-Bordes, C.; Nzoumbou-Boko, R.; Bonhivers, M.; Landrein, N.; Robinson, D.R.; Rambert, J.; Courtois, P.; Daulouède, S.; Vincendeau, P. *Trypanosoma brucei gambiense* excreted/secreted factors impair lipopolysaccharide-induced maturation and activation of human monocyte-derived

- dendritic cells. *Parasite Immunol.* **2019**, *41*, e12632, doi:10.1111/PIM.12632.
264. Garzón, E.; Holzmüller, P.; Bras-Gonçalves, R.; Vincendeau, P.; Cuny, G.; Lemesre, J.L.; Geiger, A. The *Trypanosoma brucei gambiense* Secretome Impairs Lipopolysaccharide-Induced Maturation, Cytokine Production, and Allostimulatory Capacity of Dendritic Cells. *Infect. Immun.* **2013**, *81*, 3300, doi:10.1128/IAI.00125-13.
265. Moreau, A.; Hill, M.; Thébault, P.; Deschamps, J.Y.; Chiffolleau, E.; Chauveau, C.; Moullier, P.; Anegon, I.; Alliot-Licht, B.; Cuturi, M.C. Tolerogenic dendritic cells actively inhibit T cells through heme oxygenase-1 in rodents and in nonhuman primates. *FASEB J.* **2009**, *23*, 3070–7, doi:10.1096/fj.08-128173.
266. Chauveau, C.; Rémy, S.; Royer, P.J.; Hill, M.; Tanguy-Royer, S.S.; Hubert, F.-X.F.X.; Tesson, L.; Brion, R.R.; Beriou, G.G.; Gregoire, M.; et al. Heme oxygenase-1 expression inhibits dendritic cell maturation and proinflammatory function but conserves IL-10 expression. *Blood* **2005**, *106*, 1694–1702, doi:10.1182/blood-2005-02-0494.
267. George, J.F.; Braun, A.; Brusko, T.M.; Joseph, R.; Bolisetty, S.; Wasserfall, C.H.; Atkinson, M.A.; Agarwal, A.; Kapturczak, M.H. Suppression by CD4+CD25+ regulatory T cells is dependent on expression of heme oxygenase-1 in antigen-presenting cells. *Am. J. Pathol.* **2008**, *173*, 154–60, doi:10.2353/ajpath.2008.070963.
268. Schumacher, A.; Wafula, P.O.; Teles, A.; El-Mousleh, T.; Linzke, N.; Zenclussen, M.L.; Langwisch, S.; Heinze, K.; Wollenberg, I.; Casalis, P.A.; et al. Blockage of heme oxygenase-1 abrogates the protective effect of regulatory T cells on murine pregnancy and promotes the maturation of dendritic cells. *PLoS One* **2012**, *7*, e42301, doi:10.1371/journal.pone.0042301.
269. Campbell, N.K.; Fitzgerald, H.K.; Malara, A.; Hambly, R.; Sweeney, C.M.; Kirby, B.; Fletcher, J.M.; Dunne, A. Naturally derived Heme-Oxygenase 1 inducers attenuate inflammatory responses in human dendritic cells and T cells: relevance for psoriasis treatment. *Sci. Rep.* **2018**, *8*, 10287, doi:10.1038/s41598-018-28488-6.
270. Al-Huseini, L.M.A.; Aw Yeang, H.X.; Hamdam, J.M.; Sethu, S.; Alhumeed, N.; Wong, W.; Sathish, J.G. Heme oxygenase-1 regulates dendritic cell function through modulation of p38 MAPK-CREB/ATF1 signaling. *J. Biol. Chem.* **2014**, *289*, 16442–51, doi:10.1074/jbc.M113.532069.
271. Wong, T.-H.; Chen, H.-A.; Gau, R.-J.; Yen, J.-H.; Suen, J.-L. Heme Oxygenase-1-Expressing Dendritic Cells Promote Foxp3 + Regulatory T Cell Differentiation and Induce Less Severe Airway Inflammation in Murine Models. *PLoS One* **2016**, *11*, 1–14, doi:10.1371/journal.pone.0168919.
272. Brück, J.; Holstein, J.; Glocova, I.; Seidel, U.; Geisel, J.; Kanno, T.; Kumagai, J.; Mato, N.; Sudowe, S.; Widmaier, K.; et al. Nutritional control of IL-23/Th17-mediated autoimmune disease through HO-1/STAT3 activation. *Sci. Rep.* **2017**, *7*, 44482,

doi:10.1038/srep44482.

273. Simon, T.; Pogu, J.; Rémy, S.; Brau, F.; Pogu, S.; Maquigneau, M.; Fonteneau, J.-F.; Poirier, N.; Vanhove, B.; Blancho, G.; et al. Inhibition of effector antigen-specific T cells by intradermal administration of heme oxygenase-1 inducers. *J. Autoimmun.* **2017**, *81*, 44–55, doi:10.1016/j.jaut.2017.03.005.
274. Wculek, S.K.; Khouili, S.C.; Priego, E.; Heras-Murillo, I.; Sancho, D. Metabolic Control of Dendritic Cell Functions: Digesting Information. *Front. Immunol.* **2019**, *10*, 775, doi:10.3389/FIMMU.2019.00775/BIBTEX.
275. Figueiredo-Pereira, C.; Dias-Pedroso, D.; Soares, N.L.; Vieira, H.L.A. CO-mediated cytoprotection is dependent on cell metabolism modulation. *Redox Biol.* **2020**, *32*, 101470, doi:10.1016/j.redox.2020.101470.
276. Park, J.; Joe, Y.; Ryter, S.W.; Surh, Y.J.; Chung, H.T. Similarities and Distinctions in the Effects of Metformin and Carbon Monoxide in Immunometabolism. *Mol. Cells* **2019**, *42*, 292–300, doi:10.14348/molcells.2019.0016.
277. Vítek, L. The role of bilirubin in diabetes, metabolic syndrome, and cardiovascular diseases. *Front. Pharmacol.* **2012**, *3 APR*, doi:10.3389/fphar.2012.00055.
278. Dennery, P.A. Evaluating the Beneficial and Detrimental Effects of Bile Pigments in Early and Later Life. *Front. Pharmacol.* **2012**, *3*, 115, doi:10.3389/fphar.2012.00115.
279. Carroll, K.C.; Viollet, B.; Suttles, J. AMPK $\alpha$ 1 deficiency amplifies proinflammatory myeloid APC activity and CD40 signaling. *J. Leukoc. Biol.* **2013**, *94*, 1113–21, doi:10.1189/jlb.0313157.
280. Michalek, R.D.; Gerriets, V.A.; Jacobs, S.R.; Macintyre, A.N.; MacIver, N.J.; Mason, E.F.; Sullivan, S.A.; Nichols, A.G.; Rathmell, J.C. Cutting Edge: Distinct Glycolytic and Lipid Oxidative Metabolic Programs Are Essential for Effector and Regulatory CD4+ T Cell Subsets. *J. Immunol.* **2011**, *186*, 3299–3303, doi:10.4049/jimmunol.1003613.
281. Krawczyk, C.M.; Holowka, T.; Sun, J.; Blagih, J.; Amiel, E.; DeBerardinis, R.J.; Cross, J.R.; Jung, E.; Thompson, C.B.; Jones, R.G.; et al. Toll-like receptor-induced changes in glycolytic metabolism regulate dendritic cell activation. *Blood* **2010**, *115*, 4742–9, doi:10.1182/blood-2009-10-249540.
282. Komatsu, M.; Kurokawa, H.; Waguri, S.; Taguchi, K.; Kobayashi, A.; Ichimura, Y.; Sou, Y.S.; Ueno, I.; Sakamoto, A.; Tong, K.I.; et al. The selective autophagy substrate p62 activates the stress responsive transcription factor Nrf2 through inactivation of Keap1. *Nat. Cell Biol.* **2010**, *12*, 213–223, doi:10.1038/ncb2021.
283. Katsuragi, Y.; Ichimura, Y.; Komatsu, M. Regulation of the Keap1–Nrf2 pathway by p62/SQSTM1. *Curr. Opin. Toxicol.* **2016**, *1*, 54–61, doi:10.1016/J.COTOX.2016.09.005.

284. Jiang, T.; Harder, B.; Rojo De La Vega, M.; Wong, P.K.; Chapman, E.; Zhang, D.D. p62 links autophagy and Nrf2 signaling. *Free Radic. Biol. Med.* **2015**, *88*, 199, doi:10.1016/J.FREERADBIOMED.2015.06.014.
285. El Sawalhy, A.; Seed, J.R.; Hall, J.E.; El Attar, H. Increased excretion of aromatic amino acid catabolites in animals infected with *Trypanosoma brucei evansi*. *J. Parasitol.* **1998**, *84*, 469–473, doi:10.2307/3284707.
286. Epiphanio, S.; Mikolajczak, S.A.; Gonçalves, L.A.; Pamplona, A.; Portugal, S.; Albuquerque, S.; Goldberg, M.; Rebelo, S.; Anderson, D.G.; Akinc, A.; et al. Heme Oxygenase-1 Is an Anti-Inflammatory Host Factor that Promotes Murine Plasmodium Liver Infection. *Cell Host Microbe* **2008**, *3*, 331–338, doi:10.1016/j.chom.2008.04.003.
287. Carasi, P.; Rodríguez, E.; da Costa, V.; Frigerio, S.; Brossard, N.; Noya, V.; Robello, C.; Anegón, I.; Freire, T. Heme-Oxygenase-1 Expression Contributes to the Immunoregulation Induced by *Fasciola hepatica* and Promotes Infection. *Front. Immunol.* **2017**, *8*, 883, doi:10.3389/fimmu.2017.00883.
288. Luz, N.F.; Andrade, B.B.; Feijó, D.F.; Araújo-Santos, T.; Carvalho, G.Q.; Andrade, D.; Abánades, D.R.; Melo, E. V.; Silva, A.M.; Brodskyn, C.I.; et al. Heme oxygenase-1 promotes the persistence of *Leishmania chagasi* infection. *J. Immunol.* **2012**, *188*, 4460–7, doi:10.4049/jimmunol.1103072.
289. Hull, T.D.; Agarwal, A.; George, J.F. The mononuclear phagocyte system in homeostasis and disease: a role for heme oxygenase-1. *Antioxid. Redox Signal.* **2014**, *20*, 1770–88, doi:10.1089/ars.2013.5673.
290. Chowdhury, G.; Dostalek, M.; Hsu, E.L.; Nguyen, L.P.; Stec, D.F.; Bradfield, C.A.; Guengerich, F.P. Structural Identification of Diindole Agonists of the Aryl Hydrocarbon Receptor Derived from Degradation of Indole-3-pyruvic Acid. *Chem. Res. Toxicol.* **2009**, *22*, 1905, doi:10.1021/TX9000418.
291. Tivendale, N.D.; Davies, N.W.; Horne, J.; Ross, J.J.; Smith, J.A. Analysis of the Enol-Keto Tautomers of Indole-3-pyruvic Acid. *Aust. J. Chem.* **2015**, *68*, 345–348, doi:10.1071/CH14343.
292. Chauveau, C.; Rémy, S.; Royer, P.J.; Hill, M.; Tanguy-Royer, S.; Hubert, F.X.; Tesson, L.; Brion, R.; Beriou, G.; Gregoire, M.; et al. Heme oxygenase-1 expression inhibits dendritic cell maturation and proinflammatory function but conserves IL-10 expression. *Blood* **2005**, *106*, 1694–1702, doi:10.1182/blood-2005-02-0494.
293. Cramer, T.; Yamanishi, Y.; Clausen, B.E.; Förster, I.; Pawlinski, R.; Mackman, N.; Haase, V.H.; Jaenisch, R.; Corr, M.; Nizet, V.; et al. HIF-1 $\alpha$  Is Essential for Myeloid Cell-Mediated Inflammation. *Cell* **2003**, *112*, 645–657, doi:10.1016/S0092-8674(03)00154-5.
294. Byles, V.; Covarrubias, A.J.; Ben-Sahra, I.; Lamming, D.W.; Sabatini, D.M.; Manning, B.D.; Horng, T. The TSC-mTOR pathway regulates macrophage polarization. *Nat.*



- Commun.* **2013**, *4*, 2834, doi:10.1038/ncomms3834.
295. Hyams, C.; Camberlein, E.; Cohen, J.M.; Bax, K.; Brown, J.S. The *Streptococcus pneumoniae* capsule inhibits complement activity and neutrophil phagocytosis by multiple mechanisms. *Infect. Immun.* **2010**, *78*, 704–15, doi:10.1128/IAI.00881-09.
  296. Russell, D.G. *Mycobacterium tuberculosis*: here today, and here tomorrow. *Nat. Rev. Mol. Cell Biol.* **2001**, *2*, 569–578, doi:10.1038/35085034.
  297. Gebert, B.; Fischer, W.; Weiss, E.; Hoffmann, R.; Haas, R. *Helicobacter pylori* vacuolating cytotoxin inhibits T lymphocyte activation. *Science (80-. ).* **2003**, *301*, 1099–1102, doi:10.1126/science.1086871.
  298. Finney, C.A.M.; Taylor, M.D.; Wilson, M.S.; Maizels, R.M. Expansion and activation of CD4+CD25+ regulatory T cells in *Heligmosomoides polygyrus* infection. *Eur. J. Immunol.* **2007**, *37*, 1874–1886, doi:10.1002/eji.200636751.
  299. Satoguina, J.; Mempel, M.; Larbi, J.; Badusche, M.; Lölliger, C.; Adjei, O.; Gachelin, G.; Fleischer, B.; Hoerauf, A. Antigen-specific T regulatory-1 cells are associated with immunosuppression in a chronic helminth infection (onchocerciasis). *Microbes Infect.* **2002**, *4*, 1291–300.
  300. Nash, T.E. Antigenic variation in *Giardia lamblia* and the host's immune response. *Philos. Trans. R. Soc. B Biol. Sci.* **1997**, *352*, 1369, doi:10.1098/RSTB.1997.0122.
  301. Ryan, S.M.; Eichenberger, R.M.; Ruscher, R.; Giacomin, P.R.; Loukas, A. Harnessing helminth-driven immunoregulation in the search for novel therapeutic modalities. *PLoS Pathog.* **2020**, *16*, e1008508, doi:10.1371/JOURNAL.PPAT.1008508.
  302. Lund, M.E.; Greer, J.; Dixit, A.; Alvarado, R.; McCauley-Winter, P.; To, J.; Tanaka, A.; Hutchinson, A.T.; Robinson, M.W.; Simpson, A.M.; et al. A parasite-derived 68-mer peptide ameliorates autoimmune disease in murine models of Type 1 diabetes and multiple sclerosis. *Sci. Reports 2016 61* **2016**, *6*, 1–11, doi:10.1038/srep37789.
  303. Smallwood, T.B.; Giacomin, P.R.; Loukas, A.; Mulvenna, J.P.; Clark, R.J.; Miles, J.J. Helminth Immunomodulation in Autoimmune Disease. *Front. Immunol.* **2017**, *8*, 1, doi:10.3389/FIMMU.2017.00453.
  304. Wu, Z.; Wang, L.; Tang, Y.; Sun, X. Parasite-derived proteins for the treatment of allergies and autoimmune diseases. *Front. Microbiol.* **2017**, *8*, 2164, doi:10.3389/FMICB.2017.02164/BIBTEX.
  305. Borst, P. Antigenic variation and allelic exclusion. *Cell* **2002**, *109*, 5–8, doi:10.1016/S0092-8674(02)00711-0.
  306. De Muylder, G.; Daulouède, S.; Lecordier, L.; Uzureau, P.; Morias, Y.; Van Den Abbeele, J.; Caljon, G.; Hérin, M.; Holzmüller, P.; Semballa, S.; et al. A *Trypanosoma brucei* kinesin heavy chain promotes parasite growth by triggering host arginase activity. *PLoS Pathog.* **2013**, *9*, e1003731, doi:10.1371/journal.ppat.1003731.

307. Rücker, H.; Amslinger, S. Identification of heme oxygenase-1 stimulators by a convenient ELISA-based bilirubin quantification assay. *Free Radic. Biol. Med.* **2015**, *78*, 135–146, doi:10.1016/J.FREERADBIOMED.2014.10.506.
308. Martin, D.; Rojo, A.I.; Salinas, M.; Diaz, R.; Gallardo, G.; Alam, J.; Ruiz De Galarreta, C.M.; Cuadrado, A. Regulation of Heme Oxygenase-1 Expression through the Phosphatidylinositol 3-Kinase/Akt Pathway and the Nrf2 Transcription Factor in Response to the Antioxidant Phytochemical Carnosol. *J. Biol. Chem.* **2004**, *279*, 8919–8929, doi:10.1074/jbc.M309660200.
309. Gu, T.; Wang, N.; Wu, T.; Ge, Q.; Chen, L. Antioxidative Stress Mechanisms behind Resveratrol: A Multidimensional Analysis. *J. Food Qual.* **2021**, *2021*, doi:10.1155/2021/5571733.
310. Li, Z.; Moalin, M.; Zhang, M.; Vervoort, L.; Hursel, E.; Mommers, A.; Haenen, G.R.M.M. The Flow of the Redox Energy in Quercetin during Its Antioxidant Activity in Water. *Int. J. Mol. Sci.* **2020**, *21*, 1–16, doi:10.3390/IJMS21176015.
311. Kaspar, J.W.; Niture, S.K.; Jaiswal, A.K. Nrf2:INrf2(Keap1) Signaling in Oxidative Stress. *Free Radic. Biol. Med.* **2009**, *47*, 1304, doi:10.1016/J.FREERADBIOMED.2009.07.035.
312. Mills, E.L.; Ryan, D.G.; Prag, H.A.; Dikovskaya, D.; Menon, D.; Zaslona, Z.; Jedrychowski, M.P.; Costa, A.S.H.; Higgins, M.; Hams, E.; et al. Itaconate is an anti-inflammatory metabolite that activates Nrf2 via alkylation of KEAP1. *Nature* **2018**, *556*, 113–117, doi:10.1038/nature25986.
313. Rothhammer, V.; Quintana, F.J. The aryl hydrocarbon receptor: an environmental sensor integrating immune responses in health and disease. *Nat. Rev. Immunol.* **2019**, *19*, 184–197, doi:10.1038/s41577-019-0125-8.
314. Gilardi, G.; Di Nardo, G. Heme iron centers in cytochrome P450: structure and catalytic activity. *Rend. Lincei* **2016**, *28*, 159–167, doi:10.1007/S12210-016-0565-Z.
315. Dietrich, C. Antioxidant Functions of the Aryl Hydrocarbon Receptor. *Stem Cells Int.* **2016**, *2016*, doi:10.1155/2016/7943495.
316. Kelly, B.; O'Neill, L.A.J. Metabolic reprogramming in macrophages and dendritic cells in innate immunity. *Cell Res.* **2015**, *25*, 771–784.
317. Krawczyk, C.M.; Holowka, T.; Sun, J.; Blagih, J.; Amiel, E.; DeBerardinis, R.J.; Cross, J.R.; Jung, E.; Thompson, C.B.; Jones, R.G.; et al. Toll-like receptor-induced changes in glycolytic metabolism regulate dendritic cell activation. *Blood* **2010**, *115*, 4742–9, doi:10.1182/blood-2009-10-249540.
318. Jantsch, J.; Chakravorty, D.; Turza, N.; Prechtel, A.T.; Buchholz, B.; Gerlach, R.G.; Volke, M.; Gläsner, J.; Warnecke, C.; Wiesener, M.S.; et al. Hypoxia and hypoxia-inducible factor-1 alpha modulate lipopolysaccharide-induced dendritic cell

- activation and function. *J. Immunol.* **2008**, *180*, 4697–4705, doi:10.4049/JIMMUNOL.180.7.4697.
319. Malinarich, F.; Duan, K.; Hamid, R.A.; Bijin, A.; Lin, W.X.; Poidinger, M.; Fairhurst, A.-M.; Connolly, J.E. High Mitochondrial Respiration and Glycolytic Capacity Represent a Metabolic Phenotype of Human Tolerogenic Dendritic Cells. *J. Immunol.* **2015**, *194*, 5174–5186, doi:10.4049/jimmunol.1303316.
320. Scrima, R.; Menga, M.; Pacelli, C.; Agriesti, F.; Cela, O.; Piccoli, C.; Cotoia, A.; De Gregorio, A.; Geftter, J. V.; Cinnella, G.; et al. Para-hydroxyphenylpyruvate inhibits the pro-inflammatory stimulation of macrophage preventing LPS-mediated nitro-oxidative unbalance and immunometabolic shift. *PLoS One* **2017**, *12*, e0188683, doi:10.1371/journal.pone.0188683.
321. Kim, D.-H.; Sarbassov, D.D.; Ali, S.M.; King, J.E.; Latek, R.R.; Erdjument-Bromage, H.; Tempst, P.; Sabatini, D.M. mTOR interacts with raptor to form a nutrient-sensitive complex that signals to the cell growth machinery. *Cell* **2002**, *110*, 163–75.
322. Linke, M.; Fritsch, S.D.; Sukhbaatar, N.; Hengstschläger, M.; Weichhart, T. mTORC1 and mTORC2 as regulators of cell metabolism in immunity. *FEBS Lett.* **2017**, *591*, 3089–3103, doi:10.1002/1873-3468.12711.
323. Mihaylova, M.M.; Shaw, R.J. The AMP-activated protein kinase (AMPK) signaling pathway coordinates cell growth, autophagy, & metabolism. *Nat. Cell Biol.* **2011**, *13*, 1016, doi:10.1038/NCB2329.
324. Deodhar, A.; Gottlieb, A.B.; Boehncke, W.H.; Dong, B.; Wang, Y.; Zhuang, Y.; Barchuk, W.; Xu, X.L.; Hsia, E.C.; AELION, J.; et al. Efficacy and safety of guselkumab in patients with active psoriatic arthritis: a randomised, double-blind, placebo-controlled, phase 2 study. *Lancet* **2018**, *391*, 2213–2224, doi:10.1016/S0140-6736(18)30952-8.
325. Blauvelt, A.; Papp, K.A.; Griffiths, C.E.M.; Randazzo, B.; Wasfi, Y.; Shen, Y.K.; Li, S.; Kimball, A.B. Efficacy and safety of guselkumab, an anti-interleukin-23 monoclonal antibody, compared with adalimumab for the continuous treatment of patients with moderate to severe psoriasis: Results from the phase III, double-blinded, placebo- and active comparator–controlled VOYAGE 1 trial. *J. Am. Acad. Dermatol.* **2017**, *76*, 405–417, doi:10.1016/J.JAAD.2016.11.041.
326. Wasan, S.K.; Kane, S. V. Adalimumab for the treatment of inflammatory bowel disease. *Expert Rev. Gastroenterol. Hepatol.* **2011**, *5*, 679–684, doi:10.1586/EGH.11.81.
327. Zhao, S.; Chadwick, L.; Mysler, E.; Moots, R.J. Review of Biosimilar Trials and Data on Adalimumab in Rheumatoid Arthritis. *Curr. Rheumatol. Rep.* **2018**, *20*, doi:10.1007/S11926-018-0769-6.
328. Alwawi, E.A.; Mehlis, S.L.; Gordon, K.B. Treating psoriasis with adalimumab. *Ther. Clin. Risk Manag.* **2008**, *4*, 345, doi:10.2147/TCRM.S1265.

329. Mohammadi, P.; Hesari, M.; Chalabi, M.; Salari, F.; Khademi, F. An overview of immune checkpoint therapy in autoimmune diseases. *Int. Immunopharmacol.* **2022**, *107*, 108647, doi:10.1016/J.INTIMP.2022.108647.
330. Wallace, K.L.; Zheng, L.-B.; Kanazawa, Y.; Shih, D.Q. Immunopathology of inflammatory bowel disease. *World J. Gastroenterol.* **2014**, *20*, 6–21, doi:10.3748/wjg.v20.i1.6.
331. Neurath, M.F. Cytokines in inflammatory bowel disease. *Nat. Rev. Immunol.* **2014**, *14*, 329–342.
332. Geremia, A.; Biancheri, P.; Allan, P.; Corazza, G.R.; Di Sabatino, A. Innate and adaptive immunity in inflammatory bowel disease. *Autoimmun. Rev.* **2014**, *13*, 3–10.
333. Tang, C.; Kakuta, S.; Shimizu, K.; Kadoki, M.; Kamiya, T.; Shimazu, T.; Kubo, S.; Saijo, S.; Ishigame, H.; Nakae, S.; et al. Suppression of IL-17F, but not of IL-17A, provides protection against colitis by inducing Treg cells through modification of the intestinal microbiota., doi:10.1038/s41590-018-0134-y.
334. Brück, J.; Holstein, J.; Glocova, I.; Seidel, U.; Geisel, J.; Kanno, T.; Kumagai, J.; Mato, N.; Sudowe, S.; Widmaier, K.; et al. Nutritional control of IL-23/Th17-mediated autoimmune disease through HO-1/STAT3 activation. *Sci. Rep.* **2017**, *7*, 44482, doi:10.1038/srep44482.
335. Dai, Q.; Zhou, D.; Xu, L.; Song, X. Curcumin alleviates rheumatoid arthritis-induced inflammation and synovial hyperplasia by targeting mTOR pathway in rats. *Drug Des. Devel. Ther.* **2018**, *12*, 4095–4105, doi:10.2147/DDDT.S175763.
336. Li, X.; Zhao, L.; Han, J.J.; Zhang, F.; Liu, S.; Zhu, L.; Wang, Z.Z.; Zhang, G.X.; Zhang, Y. Carnosol modulates Th17 cell differentiation and microglial switch in experimental autoimmune encephalomyelitis. *Front. Immunol.* **2018**, *9*, 1807, doi:10.3389/FIMMU.2018.01807/FULL.
337. Casalegno Garduño, R.; Däbritz, J. New Insights on CD8+ T Cells in Inflammatory Bowel Disease and Therapeutic Approaches. *Front. Immunol.* **2021**, *12*, 4100, doi:10.3389/FIMMU.2021.738762/BIBTEX.
338. Basdeo, S.A.; Moran, B.; Cluxton, D.; Canavan, M.; McCormick, J.; Connolly, M.; Orr, C.; Mills, K.H.G.; Veale, D.J.; Fearon, U.; et al. Polyfunctional, Pathogenic CD161 + Th17 Lineage Cells Are Resistant to Regulatory T Cell-Mediated Suppression in the Context of Autoimmunity . *J. Immunol.* **2015**, *195*, 528–540, doi:10.4049/JIMMUNOL.1402990/-/DCSUPPLEMENTAL.
339. Andreou, N.P.; Legaki, E.; Gazouli, M. Inflammatory bowel disease pathobiology: the role of the interferon signature. *Ann. Gastroenterol.* **2020**, *33*, 125, doi:10.20524/AOG.2020.0457.
340. Pollard, K.M.; Cauvi, D.M.; Toomey, C.B.; Morris, K. V.; Kono, D.H. Interferon- $\gamma$  and

- Systemic Autoimmunity. *Discov. Med.* **2013**, *16*, 123.
341. Boyman, O.; Sprent, J. The role of interleukin-2 during homeostasis and activation of the immune system. *Nat. Rev. Immunol.* *2012* **12**, 180–190, doi:10.1038/nri3156.
342. Seder, R.A.; Ahmed, R. Similarities and differences in CD4+ and CD8+ effector and memory T cell generation. *Nat. Immunol.* *2003* **4**, 835–842, doi:10.1038/ni969.
343. Zhao, H.M.; Xu, R.; Huang, X.Y.; Cheng, S.M.; Huang, M.F.; Yue, H.Y.; Wang, X.; Zou, Y.; Lu, A.P.; Liu, D.Y. Curcumin suppressed activation of dendritic cells via jak/stat/socs signal in mice with experimental colitis. *Front. Pharmacol.* **2016**, *7*, 1–1, doi:10.3389/fphar.2016.00455.
344. Hanai, H.; Iida, T.; Takeuchi, K.; Watanabe, F.; Maruyama, Y.; Andoh, A.; Tsujikawa, T.; Fujiyama, Y.; Mitsuyama, K.; Sata, M.; et al. Curcumin Maintenance Therapy for Ulcerative Colitis: Randomized, Multicenter, Double-Blind, Placebo-Controlled Trial. *Clin. Gastroenterol. Hepatol.* **2006**, *4*, 1502–1506, doi:10.1016/j.cgh.2006.08.008.
345. Liu, L.; Liu, Y.L.; Liu, G.X.; Chen, X.; Yang, K.; Yang, Y.X.; Xie, Q.; Gan, H.K.; Huang, X.L.; Gan, H.T. Curcumin ameliorates dextran sulfate sodium-induced experimental colitis by blocking STAT3 signaling pathway. *Int. Immunopharmacol.* **2013**, *17*, 314–320, doi:10.1016/j.intimp.2013.06.020.
346. Zhao, H.-M.; Xu, R.; Huang, X.-Y.; Cheng, S.-M.; Huang, M.-F.; Yue, H.-Y.; Wang, X.; Zou, Y.; Lu, A.-P.; Liu, D.-Y. Curcumin improves regulatory T cells in gut-associated lymphoid tissue of colitis mice. *World J. Gastroenterol.* **2016**, *22*, 5374, doi:10.3748/wjg.v22.i23.5374.
347. Veenstra, J.P.; Vemu, B.; Tocmo, R.; Nauman, M.C.; Johnson, J.J. Pharmacokinetic Analysis of Carnosic Acid and Carnosol in Standardized Rosemary Extract and the Effect on the Disease Activity Index of DSS-Induced Colitis. *Nutrients* **2021**, *13*, 1–16, doi:10.3390/NU13030773.
348. Biancheri, P.; Di Sabatino, A.; Ammoscato, F.; Facciotti, F.; Caprioli, F.; Curciarello, R.; Hoque, S.S.; Ghanbari, A.; Joe-Njoku, I.; Giuffrida, P.; et al. Absence of a role for interleukin-13 in inflammatory bowel disease. *Eur. J. Immunol.* **2014**, *44*, 370–385, doi:10.1002/EJL.201343524.
349. Danese, S.; Rudziński, J.; Brandt, W.; Dupas, J.L.; Peyrin-Biroulet, L.; Bouhnik, Y.; Kleczkowski, D.; Uebel, P.; Lukas, M.; Knutsson, M.; et al. Tralokinumab for moderate-to-severe UC: a randomised, double-blind, placebo-controlled, phase IIa study. *Gut* **2015**, *64*, 243–249, doi:10.1136/GUTJNL-2014-308004.
350. Chen, M.L.; Sundrud, M.S. Cytokine networks and T-cell subsets in inflammatory bowel diseases. *Inflamm. Bowel Dis.* *2016*, *22*, 1157–1167.

351. Tindemans, I.; Joosse, M.E.; Samsom, J.N. Dissecting the Heterogeneity in T-Cell Mediated Inflammation in IBD. *Cells* **2020**, *9*, doi:10.3390/CELLS9010110.
352. Jandus, C.; Bioley, G.; Rivals, J.P.; Dudler, J.; Speiser, D.; Romero, P. Increased numbers of circulating polyfunctional Th17 memory cells in patients with seronegative spondylarthritides. *Arthritis Rheum.* **2008**, *58*, 2307–2317, doi:10.1002/ART.23655.
353. Wade, S.M.; Canavan, M.; Mccgarry, T.; Low, C.; Wade, S.C.; Mullan, H.; Veale, D.J.; Fearon, U. Association of synovial tissue polyfunctional T-cells with DAPSA in psoriatic arthritis. *Ann Rheum Dis* **2019**, *0*, 1–5, doi:10.1136/annrheumdis-2018-214138.
354. Geginat, J.; Paroni, M.; Maglie, S.; Alfen, J.S.; Kastirr, I.; Gruarin, P.; de Simone, M.; Pagani, M.; Abrignani, S. Plasticity of human CD4 T cell subsets. *Front. Immunol.* **2014**, *5*, 630, doi:10.3389/FIMMU.2014.00630/BIBTEX.
355. Chen, Y.; Chauhan, S.K.; Shao, C.; Omoto, M.; Inomata, T.; Dana, R. IFN- $\gamma$ -Expressing Th17 Cells Are Required for Development of Severe Ocular Surface Autoimmunity. *J. Immunol.* **2017**, *199*, 1163–1169, doi:10.4049/JIMMUNOL.1602144/-/DCSUPPLEMENTAL.
356. Duhon, R.; Glatigny, S.; Arbelaez, C.A.; Blair, T.C.; Oukka, M.; Bettelli, E. Pathogenicity of IFN- $\gamma$ -producing Th17 cells is independent of T-bet. *J. Immunol.* **2013**, *190*, 4478, doi:10.4049/JIMMUNOL.1203172.
357. Boniface, K.; Blumenschein, W.M.; Brovont-Porth, K.; McGeachy, M.J.; Basham, B.; Desai, B.; Pierce, R.; McClanahan, T.K.; Sadekova, S.; de Waal Malefyt, R. Human Th17 cells comprise heterogeneous subsets including IFN-gamma-producing cells with distinct properties from the Th1 lineage. *J. Immunol.* **2010**, *185*, 679–687, doi:10.4049/JIMMUNOL.1000366.
358. Shao, H.; Kaplan, H.J.; Sun, D. Bidirectional Effect of IFN- $\gamma$  on Th17 Responses in Experimental Autoimmune Uveitis. *Front. Ophthalmol.* **2022**, *0*, 3, doi:10.3389/FOPHT.2022.831084.
359. Harbour, S.N.; Maynard, C.L.; Zindl, C.L.; Schoeb, T.R.; Weaver, C.T. Th17 cells give rise to Th1 cells that are required for the pathogenesis of colitis., doi:10.1073/pnas.1415675112.
360. Thomas, S.L.; Griffiths, C.; Smeeth, L.; Rooney, C.; Hall, A.J. Burden of Mortality Associated With Autoimmune Diseases Among Females in the United Kingdom. *Am. J. Public Health* **2010**, *100*, 2279, doi:10.2105/AJPH.2009.180273.
361. Scherlinger, M.; Mertz, P.; Sagez, F.; Meyer, A.; Felten, R.; Chatelus, E.; Javier, R.M.; Sordet, C.; Martin, T.; Korganow, A.S.; et al. Worldwide trends in all-cause mortality of auto-immune systemic diseases between 2001 and 2014. *Autoimmun. Rev.* **2020**, *19*, 102531, doi:10.1016/J.AUTREV.2020.102531.

362. Näreaho, A. Parasites. *Saf. Anal. Foods Anim. Orig.* **2016**, 59–75, doi:10.1128/MICROBIOLSPEC.DMIH2-0013-2015/ASSET/66927D1D-11C6-4C0C-8DDF-BF200355D28E/ASSETS/GRAPHIC/DMIH2-0013-2015-FIG11B.GIF.
363. Maizels, R.M.; McSorley, H.J. Regulation of the host immune system by helminth parasites. *J. Allergy Clin. Immunol.* **2016**, *138*, 666–675, doi:10.1016/J.JACI.2016.07.007.
364. Smallwood, T.B.; Giacomini, P.R.; Loukas, A.; Mulvenna, J.P.; Clark, R.J.; Miles, J.J. Helminth Immunomodulation in Autoimmune Disease. *Front. Immunol.* **2017**, *8*, 1, doi:10.3389/FIMMU.2017.00453.
365. Okada, H.; Kuhn, C.; Feillet, H.; Bach, J.F. The ‘hygiene hypothesis’ for autoimmune and allergic diseases: an update. *Clin. Exp. Immunol.* **2010**, *160*, 1, doi:10.1111/J.1365-2249.2010.04139.X.
366. Van Kruiningen, H.J.; West, A.B. Potential danger in the medical use of *Trichuris suis* for the treatment of inflammatory bowel disease. *Inflamm. Bowel Dis.* **2005**, *11*, 515, doi:10.1097/01.MIB.0000160369.47671.A2.
367. Bager, P.; Kapel, C.; Roepstorff, A.; Thamsborg, S.; Arved, J.; Rønborg, S.; Kristensen, B.; Poulsen, L.K.; Wohlfahrt, J.; Melbye, M. Symptoms after Ingestion of Pig Whipworm *Trichuris suis* Eggs in a Randomized Placebo-Controlled Double-Blind Clinical Trial. *PLoS One* **2011**, *6*, doi:10.1371/JOURNAL.PONE.0022346.
368. Maruszewska-Cheruiyot, M.; Donskow-Lysoniewska, K.; Doligalska, M. Helminth Therapy: Advances in the use of Parasitic Worms Against Inflammatory Bowel Diseases and its Challenges. *Helminthologia* **2018**, *55*, 1, doi:10.1515/HELM-2017-0048.
369. Croese, J.; O’Neil, J.; Masson, J.; Cooke, S.; Melrose, W.; Pritchard, D.; Speare, R. A proof of concept study establishing *Necator americanus* in Crohn’s patients and reservoir donors. *Gut* **2006**, *55*, 136–137, doi:10.1136/GUT.2005.079129.
370. Ruysers, N.E.; De Winter, B.Y.; De Man, J.G.; Loukas, A.; Pearson, M.S.; Weinstock, J. V.; Van den Bossche, R.M.; Martinet, W.; Pelckmans, P.A.; Moreels, T.G. Therapeutic potential of helminth soluble proteins in TNBS-induced colitis in mice. *Inflamm. Bowel Dis.* **2009**, *15*, 491–500, doi:10.1002/IBD.20787.
371. Johnston, C.J.C.; Smyth, D.J.; Kodali, R.B.; White, M.P.J.; Harcus, Y.; Filbey, K.J.; Hewitson, J.P.; Hinck, C.S.; Ivens, A.; Kemter, A.M.; et al. A structurally distinct TGF- $\beta$  mimic from an intestinal helminth parasite potently induces regulatory T cells. *Nat. Commun.* **2017**, *8*, doi:10.1038/S41467-017-01886-6.
372. White, M.P.J.; Smyth, D.J.; Cook, L.; Ziegler, S.F.; Levings, M.K.; Maizels, R.M. The parasite cytokine mimic Hp-TGM potently replicates the regulatory effects of TGF- $\beta$  on murine CD4<sup>+</sup> T cells. *Immunol. Cell Biol.* **2021**, *99*, 848–864, doi:10.1111/IMCB.12479.

373. Monteleone, I.; Rizzo, A.; Sarra, M.; Sica, G.; Sileri, P.; Biancone, L.; MacDonald, T.T.; Pallone, F.; Monteleone, G. Aryl Hydrocarbon Receptor-Induced Signals Up-regulate IL-22 Production and Inhibit Inflammation in the Gastrointestinal Tract. *Gastroenterology* **2011**, *141*, 237–248.e1, doi:10.1053/J.GASTRO.2011.04.007.
374. Wang, Q.; Yang, K.; Han, B.; Sheng, B.; Yin, J.; Pu, A.; Li, L.; Sun, L.; Yu, M.; Qiu, Y.; et al. Aryl hydrocarbon receptor inhibits inflammation in DSS-induced colitis via the MK2/p-MK2/TTP pathway. *Int. J. Mol. Med.* **2018**, *41*, 868–876, doi:10.3892/IJMM.2017.3262.
375. Furumatsu, K.; Nishiumi, S.; Kawano, Y.; Ooi, M.; Yoshie, T.; Shiomi, Y.; Kutsumi, H.; Ashida, H.; Fujii-Kuriyama, Y.; Azuma, T.; et al. A Role of the Aryl Hydrocarbon Receptor in Attenuation of Colitis. *Dig. Dis. Sci. 2011 569* **2011**, *56*, 2532–2544, doi:10.1007/S10620-011-1643-9.
376. Lv, Q.; Wang, K.; Qiao, S.; Yang, L.; Xin, Y.; Dai, Y.; Wei, Z. Norisoboldine, a natural AhR agonist, promotes Treg differentiation and attenuates colitis via targeting glycolysis and subsequent NAD<sup>+</sup>/SIRT1/SUV39H1/H3K9me3 signaling pathway. *Cell Death Dis.* **2018**, *9*, doi:10.1038/S41419-018-0297-3.
377. Goettel, J.A.; Gandhi, R.; Kenison, J.E.; Yeste, A.; Murugaiyan, G.; Sambanthamoorthy, S.; Griffith, A.E.; Patel, B.; Shouval, D.S.; Weiner, H.L.; et al. AHR Activation Is Protective against Colitis Driven by T Cells in Humanized Mice. *Cell Rep.* **2016**, *17*, 1318–1329, doi:10.1016/j.celrep.2016.09.082.
378. Yuk, J.M.; Yoshimori, T.; Jo, E.K. Autophagy and bacterial infectious diseases. *Exp. Mol. Med.* **2012**, *44*, 99–108, doi:10.3858/emmm.2012.44.2.032.
379. Hooper, K.M.; Barlow, P.G.; Stevens, C.; Henderson, P. Inflammatory Bowel Disease Drugs: A Focus on Autophagy. *J. Crohns. Colitis* **2017**, *11*, 118, doi:10.1093/ECCO-JCC/JJW127.
380. Azzman, N. Crohn's Disease: Potential Drugs for Modulation of Autophagy. *Medicina (B. Aires).* **2019**, *55*, doi:10.3390/MEDICINA55060224.
381. Zhong, M.; Cui, B.; Xiang, J.; Wu, X.; Wen, Q.; Li, Q.; Zhang, F. Rapamycin is Effective for Upper but not for Lower Gastrointestinal Crohn's Disease-Related Stricture: A Pilot Study. *Front. Pharmacol.* **2021**, *11*, 2451, doi:10.3389/FPHAR.2020.617535/BIBTEX.
382. Mutalib, M.; Borrelli, O.; Blackstock, S.; Kiparissi, F.; Elawad, M.; Shah, N.; Lindley, K. The use of sirolimus (rapamycin) in the management of refractory inflammatory bowel disease in children. *J. Crohns. Colitis* **2014**, *8*, 1730–1734, doi:10.1016/J.CROHNS.2014.08.014.
383. Massey, D.C.O.; Bredin, F.; Parkes, M. Use of sirolimus (rapamycin) to treat refractory Crohn's disease. *Gut* **2008**, *57*, 1294–1296, doi:10.1136/GUT.2008.157297.



384. Mulcahy, M.E.; O'Brien, E.C.; O'Keefe, K.M.; Voza, E.G.; Leddy, N.; McLoughlin, R.M. Manipulation of Autophagy and Apoptosis Facilitates Intracellular Survival of *Staphylococcus aureus* in Human Neutrophils. *Front. Immunol.* **2020**, *11*, doi:10.3389/FIMMU.2020.565545.
385. Zaiatz Bittencourt, V.; Jones, F.; Doherty, G.; Ryan, E.J. Targeting Immune Cell Metabolism in the Treatment of Inflammatory Bowel Disease. *Inflamm. Bowel Dis.* **2021**, *27*, 1684–1693, doi:10.1093/ibd/izab024.
386. Baan, B.; Dihal, A.A.; Hoff, E.; Voorneveld, P.W.; Koelink, P.J.; Verspaget, H.W.; Richel, D.J.; Hardwick, J.C.; Hommes, D.W.; Peppelenbosch, M.P.; et al. 5-ASA Inhibits Phospholipase D-Dependent Mammalian Target of Rapamycin Signaling in Colorectal Cancer. *Gastroenterology* **2011**, *140*, S-351, doi:10.1016/S0016-5085(11)61430-3.
387. Park, H.; Kim, W.; Kim, D.; Jeong, S.; Jung, Y. Mesalazine activates adenosine monophosphate-activated protein kinase: Implication in the anti-inflammatory activity of this anti-colitic drug. *Curr. Mol. Pharmacol.* **2019**, *12*, doi:10.2174/1874467212666190308103448.
388. Wei, H.X.; Wang, B.; Li, B. IL-10 and IL-22 in Mucosal Immunity: Driving Protection and Pathology. *Front. Immunol.* **2020**, *11*, 1315, doi:10.3389/FIMMU.2020.01315/BIBTEX.
389. Tomoyose, M.; Mitsuyama, K.; Ishida, H.; Toyonaga, A.; Tanikawa, K. Role of Interleukin-10 in a Murine Model of Dextran Sulfate Sodium-Induced Colitis. <http://dx.doi.org/10.1080/00365529850171080> **2009**, *33*, 435–440, doi:10.1080/00365529850171080.
390. Kühn, R.; Löhler, J.; Rennick, D.; Rajewsky, K.; Müller, W. Interleukin-10-deficient mice develop chronic enterocolitis. *Cell* **1993**, *75*, 263–274, doi:10.1016/0092-8674(93)80068-P.
391. Ho, G.T.; Cartwright, J.A.; Thompson, E.J.; Bain, C.C.; Rossi, A.G. Resolution of Inflammation and Gut Repair in IBD: Translational Steps Towards Complete Mucosal Healing. *Inflamm. Bowel Dis.* **2020**, *26*, 1131, doi:10.1093/IBD/IZAA045.
392. Isidro, R.A.; Appleyard, C.B. Colonic macrophage polarization in homeostasis, inflammation, and cancer. *Am. J. Physiol. - Gastrointest. Liver Physiol.* **2016**, *311*, G59, doi:10.1152/AJPGI.00123.2016.
393. Zhu, W.; Yu, J.; Nie, Y.; Shi, X.; Liu, Y.; Li, F.; Zhang, X.L. Disequilibrium of M1 and M2 macrophages correlates with the development of experimental inflammatory bowel diseases. *Immunol. Invest.* **2014**, *43*, 638–652, doi:10.3109/08820139.2014.909456.
394. Naito, Y.; Takagi, T.; Higashimura, Y. Heme oxygenase-1 and anti-inflammatory M2 macrophages. *Arch. Biochem. Biophys.* **2014**, *564*, 83–88, doi:10.1016/J.ABB.2014.09.005.

395. Lang, A.; Salomon, N.; Wu, J.C.Y.; Kopylov, U.; Lahat, A.; Har-Noy, O.; Ching, J.Y.L.; Cheong, P.K.; Avidan, B.; Gamus, D.; et al. Curcumin in Combination With Mesalamine Induces Remission in Patients With Mild-to-Moderate Ulcerative Colitis in a Randomized Controlled Trial. *Clin. Gastroenterol. Hepatol.* **2015**, *13*, 1444-1449.e1, doi:10.1016/j.cgh.2015.02.019.
396. Ipar, V.S.; Dsouza, A.; Devarajan, P. V. Enhancing Curcumin Oral Bioavailability Through Nanoformulations. *Eur. J. Drug Metab. Pharmacokinet.* **2019**, 1–22, doi:10.1007/s13318-019-00545-z.
397. Sareen, R.; Nath, K.; Jain, N.; Dhar, K.L. Curcumin Loaded Microsponges for Colon Targeting in Inflammatory Bowel Disease: Fabrication, Optimization, and In Vitro and Pharmacodynamic Evaluation. *Biomed Res. Int.* **2014**, *2014*, doi:10.1155/2014/340701.
398. Ohno, M.; Nishida, A.; Sugitani, Y.; Nishino, K.; Inatomi, O.; Sugimoto, M.; Kawahara, M.; Andoh, A. Nanoparticle curcumin ameliorates experimental colitis via modulation of gut microbiota and induction of regulatory T cells. *PLoS One* **2017**, *12*, e0185999, doi:10.1371/JOURNAL.PONE.0185999.
399. Chen, Q.; Gou, S.; Huang, Y.; Zhou, X.; Li, Q.; Han, M.K.; Kang, Y.; Xiao, B. Facile fabrication of bowl-shaped microparticles for oral curcumin delivery to ulcerative colitis tissue. *Colloids Surf. B. Biointerfaces* **2018**, *169*, 92–98, doi:10.1016/J.COLSURFB.2018.05.012.
400. Huang, Y.; Canup, B.S.B.; Gou, S.; Chen, N.; Dai, F.; Xiao, B.; Li, C. Oral nanotherapeutics with enhanced mucus penetration and ROS-responsive drug release capacities for delivery of curcumin to colitis tissues. *J. Mater. Chem. B* **2021**, *9*, 1604–1615, doi:10.1039/D0TB02092C.



# Regulation of inflammation by the antioxidant haem oxygenase 1

Nicole K. Campbell<sup>1,2,3</sup>✉, Hannah K. Fitzgerald<sup>1</sup> and Aisling Dunne<sup>1,4</sup>

**Abstract** | Haem oxygenase 1 (HO-1), an inducible enzyme responsible for the breakdown of haem, is primarily considered an antioxidant, and has long been overlooked by immunologists. However, research over the past two decades in particular has demonstrated that HO-1 also exhibits numerous anti-inflammatory properties. These emerging immunomodulatory functions have made HO-1 an appealing target for treatment of diseases characterized by high levels of chronic inflammation. In this Review, we present an introduction to HO-1 for immunologists, including an overview of its roles in iron metabolism and antioxidant defence, and the factors which regulate its expression. We discuss the impact of HO-1 induction in specific immune cell populations and provide new insights into the immunomodulation that accompanies haem catabolism, including its relationship to immunometabolism. Furthermore, we highlight the therapeutic potential of HO-1 induction to treat chronic inflammatory and autoimmune diseases, and the issues faced when trying to translate such therapies to the clinic. Finally, we examine a number of alternative, safer strategies that are under investigation to harness the therapeutic potential of HO-1, including the use of phytochemicals, novel HO-1 inducers and carbon monoxide-based therapies.

## Porphyrin

An organic molecule comprising four pyrrole rings connected to form a larger ring structure, which readily binds metal ions. Iron-containing porphyrins are known as 'haems'.

<sup>1</sup>School of Biochemistry and Immunology, Trinity Biomedical Sciences Institute, Trinity College Dublin, Dublin, Ireland.

<sup>2</sup>Centre for Innate Immunity and Infectious Diseases, Hudson Institute of Medical Research, Clayton, Victoria, Australia.

<sup>3</sup>Department of Molecular and Translational Sciences, Monash University, Clayton, Victoria, Australia.

<sup>4</sup>School of Medicine, Trinity College Dublin, Dublin, Ireland.

✉e-mail: nicole.campbell@hudson.org.au

<https://doi.org/10.1038/s41577-020-00491-x>

Haem oxygenases are diverse, multifunctional enzymes that catalyse the breakdown of haem. Haem is an iron-containing porphyrin that is a component of many biologically important proteins. These include haemoglobin and myoglobin, which are used to carry oxygen in red blood cells and muscle cells, respectively; cytochromes, which facilitate electron transport during oxidative respiration, redox and drug metabolism; and enzymes such as catalases and haem peroxidases, which are involved in a range of critical cellular functions<sup>1</sup>. However, despite its ubiquitous nature within cellular proteins, free haem is highly cytotoxic and must be rapidly metabolized to avoid cell damage through oxidative stress<sup>2,3</sup>. Haem oxygenases catalyse the first, rate-limiting, step of haem degradation, using NADPH-cytochrome P450 reductase and oxygen, to generate equimolar amounts of the linear tetrapyrrole biliverdin, ferrous iron (Fe<sup>2+</sup>) and carbon monoxide (CO)<sup>4</sup>. Biliverdin can be subsequently converted into the linear tetrapyrrole bilirubin by the enzyme biliverdin reductase<sup>5,6</sup> (FIG. 1).

Two functional isoforms of haem oxygenase exist in mammalian cells: haem oxygenase 1 (HO-1) and HO-2. HO-2 is constitutively expressed within certain tissues, including the brain, testis, cardiovascular and liver, where it contributes to homeostatic iron and redox metabolism and cellular messaging (via CO)<sup>7–10</sup>.

By contrast, HO-1 is a stress-inducible isozyme encoded by the gene *HMOX1* in humans<sup>11</sup>. Under homeostatic conditions, HO-1 expression is low or absent in most cells and tissues, with some exceptions, including iron-recycling macrophages in the spleen and liver (BOX 1), and certain tolerogenic immune cells, which display constitutive expression of HO-1 and are discussed later in this Review. However, HO-1 is highly upregulated by most cells in response to a vast number of pro-oxidant stimuli and provides protection against oxidative damage (BOX 2).

The HO-1 system also has important anti-inflammatory properties<sup>12–15</sup>. These are exemplified by the rare HO-1 deficiencies seen in humans and by HO-1-deficient animal models, which in addition to showing increased sensitivity to oxidative stress are characterized by high levels of chronic inflammation<sup>16–19</sup>. Research over the past 20 years has highlighted the promising immunomodulatory functions of the HO-1 system, establishing it as a target of interest for a broad range of inflammatory diseases. In this Review, we discuss the consequences of HO-1 induction in immune cell populations and the potential of the HO-1 system for treatment of diseases characterized by chronic inflammation. We also highlight a number of therapeutic strategies currently under investigation as potential modulators of the HO-1 system.

**Regulation of HO-1 expression.** HO-1 can be upregulated in response to numerous different stress stimuli, including various pro-oxidants and pro-inflammatory mediators<sup>20–22</sup>. Given its protective antioxidant and anti-inflammatory properties, understanding how HO-1 expression is controlled under different circumstances and in different cell types has been the subject of considerable research. The multifactorial regulation of HO-1 provides important context to its functions in immune cells and in inflammatory disease, and several therapies under investigation target factors regulating the HO-1 system. Below, we summarize the major regulatory mechanisms that control HO-1 expression both generally and in immune cells (FIG. 2).

Expression of HO-1 is largely under the control of the redox-sensitive transcription factor nuclear factor erythroid 2-related factor 2 (NRF2; encoded by *NFE2L2*), which binds to the antioxidant response element (ARE) in the promoter region of many antioxidant genes, including *HMOX1* (REF.<sup>23</sup>). Under steady-state conditions, NRF2 is bound to Kelch-like ECH-associated protein 1 (KEAP1) in the cytoplasm; this suppresses NRF2 activity by facilitating the ubiquitylation and subsequent degradation of NRF2 by the proteasome<sup>23</sup>. However, in the presence of oxidants, reactive oxygen species and other NRF2 activators, cysteine residues within KEAP1 are modified, resulting in the release, and consequent stabilization, of NRF2 (REFS<sup>24,25</sup>). NRF2 can then migrate to the nucleus, where it forms heterodimers with small MAF proteins to bind AREs and promote expression of antioxidant genes<sup>23</sup>. BACH1, a transcriptional repressor and haem sensor, also forms heterodimers with small MAF proteins and regulates HO-1 expression by competing with NRF2 for the ARE-binding site on the *HMOX1* promoter<sup>26</sup>. Binding of free haem to BACH1 causes it

to dissociate from the ARE, after which it is exported from the nucleus, ubiquitylated and degraded, allowing *HMOX1* transcription to occur<sup>27,28</sup>. Together, NRF2, KEAP1 and BACH1 constitute an intricate feedback system that enables cells to respond to oxidative stress and increased levels of cytotoxic haem through upregulation of HO-1. However, it is important to note that other genes involved in antioxidant and anti-inflammatory responses that are independent of HO-1 are also regulated by NRF2 and haem (via both BACH1-dependent and BACH1-independent mechanisms)<sup>29–31</sup>. Therefore, care must be taken when one is interpreting the role of HO-1 in situations where the presence or activity of these transcriptional regulators is altered.

Although NRF2 and BACH1 are the primary regulators of HO-1, other transcription factors have also been described to modulate HO-1 expression, such as hypoxia-inducible factor 1 $\alpha$  (HIF1 $\alpha$ ) and various small MAF protein dimers<sup>23,32,33</sup>. With particular relevance to immune cells, binding sites for the pro-inflammatory transcription factors NF- $\kappa$ B and AP-1 have been identified within the *HMOX1* promoter<sup>34</sup>. Furthermore, some instances of HO-1 upregulation in vitro have been shown to be dependent on or correlated with NF- $\kappa$ B or AP-1 expression (reviewed in REF.<sup>35</sup>). HO-1 may therefore be upregulated during inflammation to protect against potential deleterious effects of reactive oxygen species and pro-inflammatory cytokines, and to provide negative feedback during induction of inflammatory responses. In addition to direct regulation by transcription factors, emerging evidence suggests a role for epigenetic regulation of HO-1 expression<sup>36–38</sup>, as well as post-transcriptional regulation by alternative splicing and microRNAs<sup>39,40</sup>, while poorly understood at present, these indirect regulatory mechanisms are interesting avenues to explore when one is considering targeting HO-1 expression.

While there appear to be multiple transcriptional regulators of HO-1 expression, many HO-1 inducers do not interact with transcription factors directly, but instead activate them via intermediate signalling pathways. Protein kinase pathways associated with responses to cellular stress have been implicated in the regulation of HO-1 expression. For example, the mitogen-activated protein kinases (MAPKs) extracellular signal-regulated kinase (ERK), JUN amino-terminal kinase (JNK) and p38 have all been reported to regulate HO-1 expression in different cell types and conditions; however, p38 appears to be the most common MAPK involved in HO-1 upregulation<sup>35</sup>. The phosphatidylinositol 3-kinase (PI3K)–AKT pathway can also regulate HO-1 expression in response to cytokines and prostaglandins as well as some alternative HO-1 inducers<sup>41–43</sup>. For example, the upregulation of HO-1 by the cytokine IL-10 is thought to be achieved via activation of PI3K and STAT3 (REFS<sup>14,44</sup>). Finally, the cellular energy sensor AMP-activated protein kinase (AMPK) has recently been identified as a modulator of HO-1 expression and is responsible for the upregulation of HO-1 by many metabolic regulators and HO-1 inducers<sup>45–48</sup>. The mechanism by which AMPK upregulates HO-1 appears to involve crosstalk between AMPK, its downstream effectors and NRF2

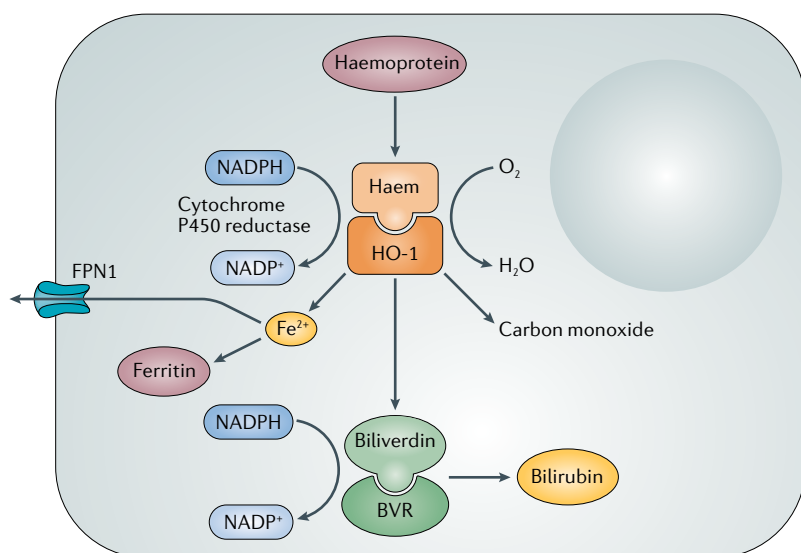
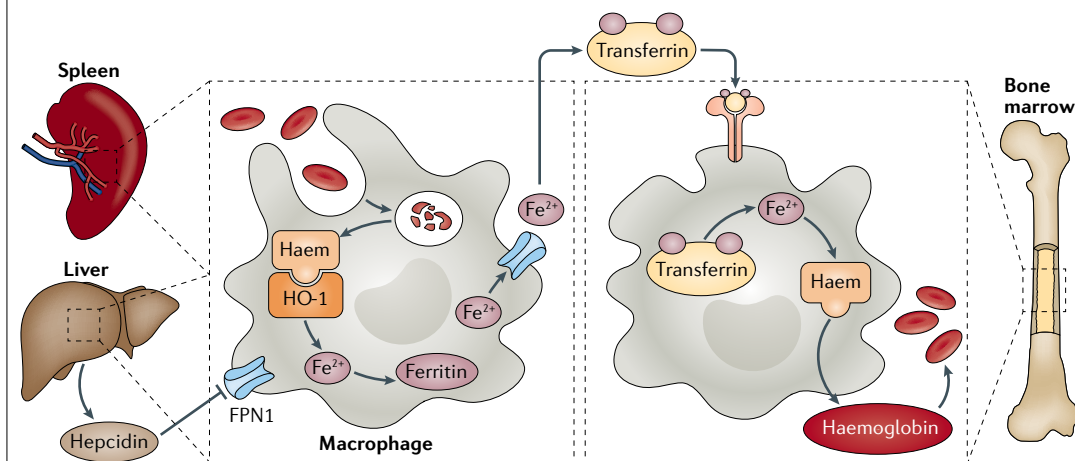


**Fig. 1 | HO-1 and haem catabolism.** Haem degradation occurs in the cytosol of the cell, where haem is catabolized by the enzyme haem oxygenase 1 (HO-1). This reaction requires cytochrome P450 reductase as a cofactor to metabolize NADPH and O<sub>2</sub>, leading to the production of NADP<sup>+</sup> and H<sub>2</sub>O. Breakdown of haem results in the generation of equimolar amounts of biliverdin, carbon monoxide and ferrous iron (Fe<sup>2+</sup>), which is rapidly exported from the cell via ferroportin 1 (FPN1) or sequestered into ferritin for storage. Biliverdin can be subsequently converted into bilirubin by the enzyme biliverdin reductase (BVR).

## Box 1 | HO-1 and iron homeostasis

Iron is a trace element fundamental to life. Owing to its limited dietary bioavailability, mammalian iron stores are carefully controlled to ensure that iron released from spent haemoproteins is either recycled or stored. The most prevalent haemoprotein in mammals is haemoglobin, which facilitates oxygen transport in red blood cells (RBCs) and contains more than half of the total iron content in humans<sup>218</sup>. Given the short lifespan of RBCs (approximately 120 days), haemoglobin turnover is responsible for the vast majority of iron flux and must be tightly regulated to avoid uncontrolled release of cytotoxic free haem or ferrous iron ( $\text{Fe}^{2+}$ )<sup>3,218,219</sup>. This is achieved through the activity of iron-recycling erythrophagocytic macrophages, which detect and phagocytose senescent RBCs<sup>218</sup>.

Erythrophagocytic macrophages, located as red-pulp macrophages in the spleen and as Kupffer cells or monocyte-derived macrophages in the liver, highly express haem oxygenase 1 (HO-1) to break down haem released from ingested haemoglobin<sup>220,221</sup> (see the figure). The importance of HO-1 expression in these macrophage populations is evident in cases of human HO-1 deficiencies and in *Hmox1*<sup>-/-</sup> mice, which are characterized by depletion of erythrophagocytic macrophages (due to the cytotoxic effects of haem accumulation), low serum iron levels and increased deposition of iron in hepatic and renal tissues, resulting in tissue injury and chronic inflammation<sup>19,222,223</sup>. Iron released from haem catabolism by HO-1 can be either exported from macrophages via the iron transporter ferroportin 1 (FPN1) or stored intracellularly by ferritin<sup>68</sup>. Exported iron is loaded onto plasma transferrin for systemic circulation and is used by specialized bone marrow 'nurse' macrophages and developing erythrocytes for haemoglobin synthesis during erythropoiesis<sup>68,224</sup>. Iron homeostasis is largely controlled by the hepatic hormone hepcidin, which is induced in response to iron and binds FPN1, causing its degradation and, consequently, inhibition of iron export<sup>224</sup>. Hepcidin can also be induced during infection to limit the availability of iron to invading pathogens<sup>68</sup>.



(REFS<sup>46,47,49-51</sup>). In summary, induction of HO-1 is a general adaptive mechanism of cells to protect against damage under stress conditions, and HO-1 upregulation can be achieved through activation of multiple different regulatory mechanisms. While this adaption is most clearly indicated during oxidative stress (see BOX 2), it has also evolved as a component of metabolic and immune signalling, with particular relevance for immunomodulation of certain immune cells; this will be explored in the next section.

### Regulation of immune responses by HO-1

Although HO-1 can be upregulated by most cell types during stress conditions<sup>22</sup>, it plays a significant role in the regulation of immune cells. HO-1 has demonstrable anti-inflammatory properties, and its expression is often upregulated during inflammation<sup>12-14,52-54</sup>. In this section, the regulation of key immune cell subsets by HO-1 will be reviewed, as well as recent evidence of cross-regulation between the HO-1 system and immunometabolism (FIG. 3).

**Regulation of macrophages by HO-1.** HO-1 is of particular importance to iron-recycling macrophages, which highly express HO-1 under homeostasis to catabolize

haem (see BOX 1). However, HO-1 also acts as an important immunoregulator in other macrophage populations. HO-1-derived CO promotes the differentiation of macrophages from myeloid progenitor cells, both in vitro and in vivo<sup>55</sup>. Furthermore, numerous reports have suggested that HO-1 expression promotes macrophage polarization towards an anti-inflammatory 'M2-like' macrophage phenotype (reviewed in REF.<sup>56</sup>). HO-1 expression by M2-like macrophages serves multiple purposes; first, it allows tissue-resident macrophages to regulate local iron homeostasis and respond to tissue injury by metabolizing cytotoxic haem released from damaged cells, in line with the traditional role of these macrophages in wound repair<sup>57-59</sup>. Second, HO-1 and its products promote the resolution of inflammation by macrophages, by increasing phagocytosis, inhibiting pro-inflammatory responses and inducing the anti-inflammatory cytokine IL-10 (reviewed in REF.<sup>60</sup>). Third, the HO-1 system permits macrophages to protect tissues against oxidative damage (see BOX 2), a role that appears to have particular relevance in certain disease contexts such as atherosclerosis and ischaemic injury<sup>61-63</sup>.

Although HO-1 is associated with M2-like macrophage polarization, its expression has also been described in M1-like or pro-inflammatory macrophage

### 'M2-like' macrophage

'M1' and 'M2' are classifications historically used to define macrophages activated in vitro as pro-inflammatory (when 'classically' activated with interferon- $\gamma$  and lipopolysaccharide) or anti-inflammatory (when 'alternatively' activated with IL-4 or IL-10), respectively. However, in vivo macrophages are highly specialized, transcriptomically dynamic and extremely heterogeneous with regard to their phenotypes and functions, which are continuously shaped by their tissue microenvironment. Therefore, the M1 or M2 classification is too simplistic to explain the true nature of in vivo macrophages, although these terms are still often used to indicate whether the macrophages in question are more pro-inflammatory or anti-inflammatory.

## Box 2 | Antioxidant activity of HO-1

Haem oxygenases have long been recognized as cytoprotective enzymes, owing to their ability to catabolize cytotoxic free haem and generate antioxidants. Haem oxygenase 1 (HO-1) is the most important haem oxygenase isozyme in providing protection against oxidative stress, as it is highly inducible by free haem and numerous other pro-oxidant stimuli<sup>3,21,22</sup>. The significance of HO-1 as a general cytoprotective mechanism is highlighted in studies of HO-1-deficient cells and animals, as well as patients with HO-1 deficiencies or impairments, which display increased susceptibility to oxidative stress and associated diseases<sup>16,19,225,226</sup>.

Although free haem is highly cytotoxic, it is unclear why haem catabolism is upregulated in response to oxidative stress; one suggestion is that release of labile haem from haemoproteins might be a generalized feature of cell stress<sup>3</sup>. It has also been reported that HO-1 can translocate to the nucleus and upregulate antioxidant genes independently of its enzymatic function<sup>227,228</sup>. However, it is believed that most of its cytoprotective effects result from the activity of its reaction products: carbon monoxide (CO), biliverdin and bilirubin. Bilirubin is one of the most potent antioxidants found in mammalian cells and is particularly important in protection against lipid peroxidation<sup>229–231</sup>. Although not as potent as bilirubin, biliverdin also displays antioxidant activity and can be tolerated at higher concentrations than bilirubin<sup>232</sup>. Additionally, biliverdin reductase, which is induced by biliverdin to catalyse its conversion into bilirubin, exerts broad antioxidant and anti-inflammatory effects, both dependent on and independently of its enzymatic activity<sup>232,233</sup>. Meanwhile, CO, although not an antioxidant itself, mediates a significant portion of the cytoprotective effects ascribed to HO-1; this is largely achieved through its interactions with metalloproteins, which generate reactive oxygen species and activate various antioxidant and anti-inflammatory pathways<sup>3,121,226</sup>. The antioxidant response initiated by CO includes upregulation of HO-1 itself<sup>34–236</sup>, allowing the HO-1 system to exert positive feedback over its own activity.

subsets. HO-1 expression is strongly upregulated by macrophages exposed to pro-inflammatory stimuli such as lipopolysaccharide and poly(I:C)<sup>64–66</sup> and is required for the downstream activation of interferon regulatory factor 3 (IRF3) and consequent induction of interferon- $\beta$  (IFN $\beta$ )<sup>66</sup>. HO-1-derived CO can also promote the microbicidal activity of macrophages<sup>67</sup>, and it has been suggested that regulation of intracellular haem-iron stores by HO-1 can limit availability of these essential nutrients to intracellular pathogens, thus promoting microbial clearance by macrophages<sup>68</sup>. However, upregulation of HO-1 also provides negative feedback to M1-like macrophages by limiting their pro-inflammatory activity<sup>69,70</sup>. Therefore, while broadly anti-inflammatory in nature, the functions of the HO-1 system in macrophages appear to be as varied as the macrophages themselves and are likely dependent on the integration of other context-specific and tissue-specific signals. It should be mentioned, however, that expression of HO-1 by macrophages is not always beneficial and is associated with detrimental outcomes in diseases such as cancer, obesity and chronic infection<sup>71–76</sup>. Thus, either induction or inhibition of HO-1 in macrophages may be of therapeutic benefit depending on the disease context.

**Regulation of dendritic cells by HO-1.** Unlike macrophages, which typically upregulate HO-1 in response to pro-inflammatory signals and cellular stress, HO-1 is constitutively expressed by immature dendritic cells (DCs) both in vitro and in vivo and is downregulated on DC maturation<sup>77,78</sup>. Inhibition of HO-1 in DCs reduces their phagocytic capacity, enhances their expression of co-stimulatory molecules and increases their production

of pro-inflammatory cytokines such as IL-12 and IL-23, resulting in greater activation and polarization of T cells towards inflammatory subsets such as T helper 1 cells (T<sub>H</sub>1 cells) and T<sub>H</sub>17 cells<sup>77–82</sup>. Conversely, HO-1 induction promotes tolerogenic DCs by inhibiting these pro-inflammatory functions and maintaining DCs in an immature-like phenotype, with a consequent reduction in effector T cell responses and promotion of regulatory T cell (T<sub>reg</sub> cell) responses<sup>77,78,81–83</sup>. These observations are supported by multiple in vivo models of inflammatory or autoimmune disease, where upregulation of HO-1 in DCs was responsible for the suppression of pro-inflammatory T cells, promotion of T<sub>reg</sub> cell differentiation and amelioration of harmful inflammation<sup>84–87</sup>. Both CO and biliverdin have been reported to exert similar immunomodulatory effects in DCs in vitro<sup>88–91</sup>, suggesting that there are multiple mechanisms downstream of haem catabolism by HO-1 that contribute to its activity in DCs. For example, inhibition of MAPK signalling has been reported as a potential mechanism underlying the suppression of DC maturation and pro-inflammatory functions by HO-1 (REFS<sup>82,83</sup>). However, further research is required to elucidate the contributions of HO-1 reaction products and their mechanism of action in DCs, particularly in relevant in vivo settings. Nonetheless, it is evident that the HO-1 system is of particular importance in DCs, and given the central immunoregulatory role played by these cells in the generation of both innate and adaptive immune responses, they are an attractive target for the development of novel anti-inflammatory therapies.

**Regulation of T cells by HO-1.** While HO-1 is strongly associated with immunoregulation in myeloid cells, less is known of its role in T cell biology. A number of studies using in vitro T cell models in the absence of DCs or other antigen-presenting cells have reported that HO-1 expression by T cells promotes T<sub>reg</sub> cells and inhibits T<sub>H</sub>17 cell differentiation and T cell proliferation<sup>92–95</sup>. Furthermore, it has been reported that HO-1 can inhibit T<sub>H</sub>17 cell differentiation through direct binding of STAT3, both in vitro and in an in vivo airway inflammation model<sup>96</sup>. However, other reports of HO-1-mediated anti-inflammatory effects in T cells appear to be dependent on HO-1 expression in DCs rather than in T cells themselves<sup>97</sup>. For example, T<sub>reg</sub> cells from *Hmox1*<sup>-/-</sup> mice were found to be non-impaired and functionally suppressive, and the reduced suppression by T<sub>reg</sub> cells observed under HO-1 inhibition was shown to be controlled by HO-1 activity in DCs<sup>80,81,98</sup>. Therefore, current evidence suggests that HO-1 modulates T cell activity primarily indirectly through its expression in DCs; HO-1 maintains DCs in an immature state, which promotes T<sub>reg</sub> cell differentiation and inhibits the generation of pro-inflammatory T cell responses. However, direct action of HO-1 may contribute to some of its observed effects in T cells, such as inhibition of proliferation and regulation of differentiation. HO-1 has been reported to ameliorate T<sub>H</sub>17 cell–T<sub>reg</sub> cell imbalances in various in vivo models of T cell-mediated disease<sup>96,99–101</sup>. Whether this is achieved via HO-1 activity in DCs or other antigen-presenting

cells or in T cells remains unclear, however, there clearly exists a solid rationale for targeting the HO-1 system to regulate T cell responses.

**Regulation of immunometabolism by HO-1.** Finally, emerging evidence suggests that crosstalk between the HO-1 system and cellular metabolism may contribute to the regulation of immune cells by HO-1. It is now appreciated that the metabolic activity of immune cells underpins their differentiation and function, with different bioenergetic pathways supporting different modes of immune programming that are both cell specific and context specific<sup>102</sup>. Although HO-1 is known to modulate cellular bioenergetics via its role in haem/iron metabolism and redox homeostasis (reviewed in REF.<sup>103</sup>), its relationship to the metabolism of immune cells has only recently begun to be explored. Many of the effects of HO-1 on cellular and systemic metabolism have been attributed to the activity of its reaction products. For example, CO has been described to inhibit glycolysis and promote mitochondrial metabolism (reviewed in REF.<sup>104</sup>), and numerous similarities between the activities of CO and the antidiabetes drug metformin have been observed in immunometabolism and metabolic disease<sup>105</sup>. Meanwhile, Gilbert syndrome (adult hyperbilirubinaemia) is believed to be protective against metabolic syndrome, diabetes and obesity<sup>106,107</sup>, and

an iron-rich diet has been reported to improve glucose tolerance in mice via activation of AMPK<sup>108</sup>.

Metabolic signalling has also been described to regulate HO-1 expression. For example, blockade of fumarate (the tricarboxylic acid (TCA) cycle enzyme that converts fumarate into malate) has been reported to upregulate HO-1 (REF.<sup>109</sup>), as has itaconate, another TCA cycle-derived metabolite produced by activated macrophages<sup>110</sup>. The transcription factor HIF1 $\alpha$  — now identified as one of the major drivers of enhanced glycolysis in activated macrophages, DCs and certain T cell subsets<sup>111–113</sup> — is also a known promoter of HO-1 expression<sup>33</sup>. Additionally, HO-1 has been reported to downregulate the expression and activity of nitric oxide synthases<sup>114</sup>, which generate NO required for the inhibition of oxidative phosphorylation during the switch to glycolytic metabolism in pro-inflammatory macrophages<sup>111</sup>. Moreover, NO itself can also promote expression of HO-1 (REF.<sup>114</sup>). It is therefore plausible that HO-1 is upregulated during metabolic reprogramming in activated immune cells as a negative-feedback mechanism to counteract associated increases in reactive oxygen species generation and inflammation<sup>102,115</sup>. Furthermore, AMPK appears to be a central regulator of immunometabolism, linking activation of catabolic metabolism, such as oxidative phosphorylation and fatty acid oxidation, with anti-inflammatory immune

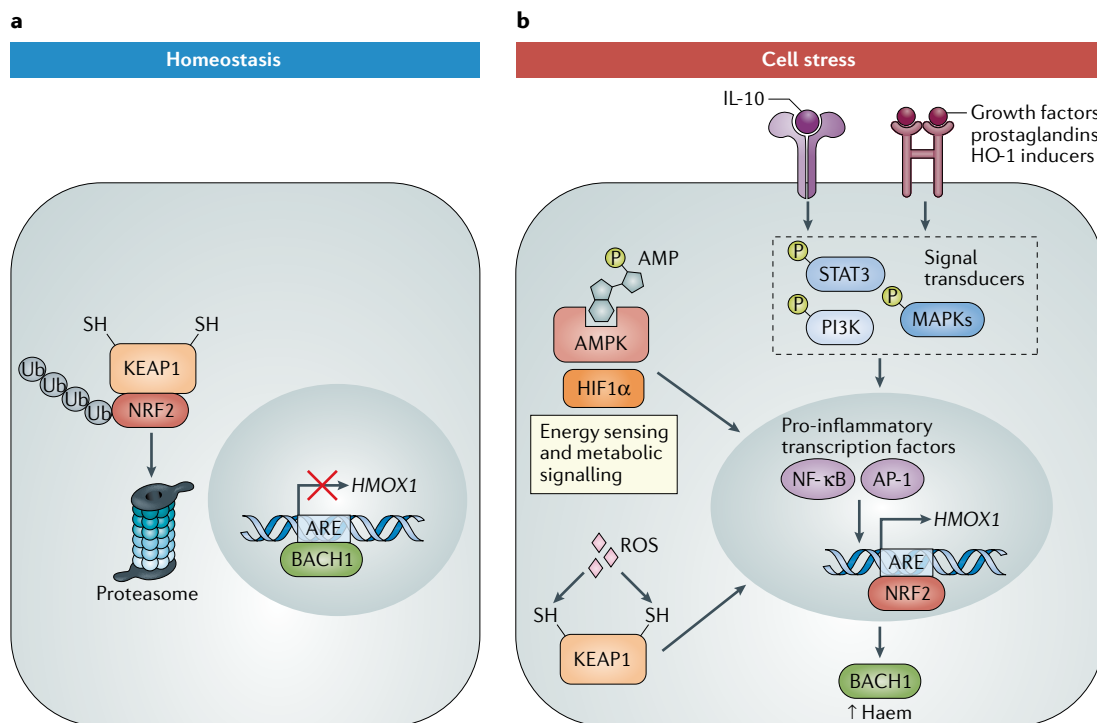


**Fig. 2 | Regulation of HO-1 expression.** **a** | Under homeostatic conditions, nuclear factor erythroid 2-related factor 2 (NRF2) is bound to Kelch-like ECH-associated protein 1 (KEAP1), ubiquitylated and targeted by the proteasome for degradation. BACH1 binds to the antioxidant response element (ARE) on the *HMOX1* promoter and inhibits gene transcription. **b** | During cell stress, increased intracellular levels of haem cause BACH1 to dissociate from the ARE, and reactive oxygen species (ROS) interact with cysteine residues on KEAP1, causing it to dissociate from NRF2. This allows NRF2 to migrate to the nucleus and bind the ARE to promote transcription of *HMOX1*. The transcription factors NF- $\kappa$ B, AP-1 and hypoxia-inducible factor 1 $\alpha$  (HIF-1 $\alpha$ ) can also bind the *HMOX1* promoter to upregulate haem oxygenase 1 (HO-1). Finally, signalling through AMP-activated protein kinase (AMPK), mitogen-activated protein kinases (MAPKs), phosphatidylinositol 3-kinase (PI3K) and IL-10 has also been reported to regulate HO-1 expression in certain cell types.

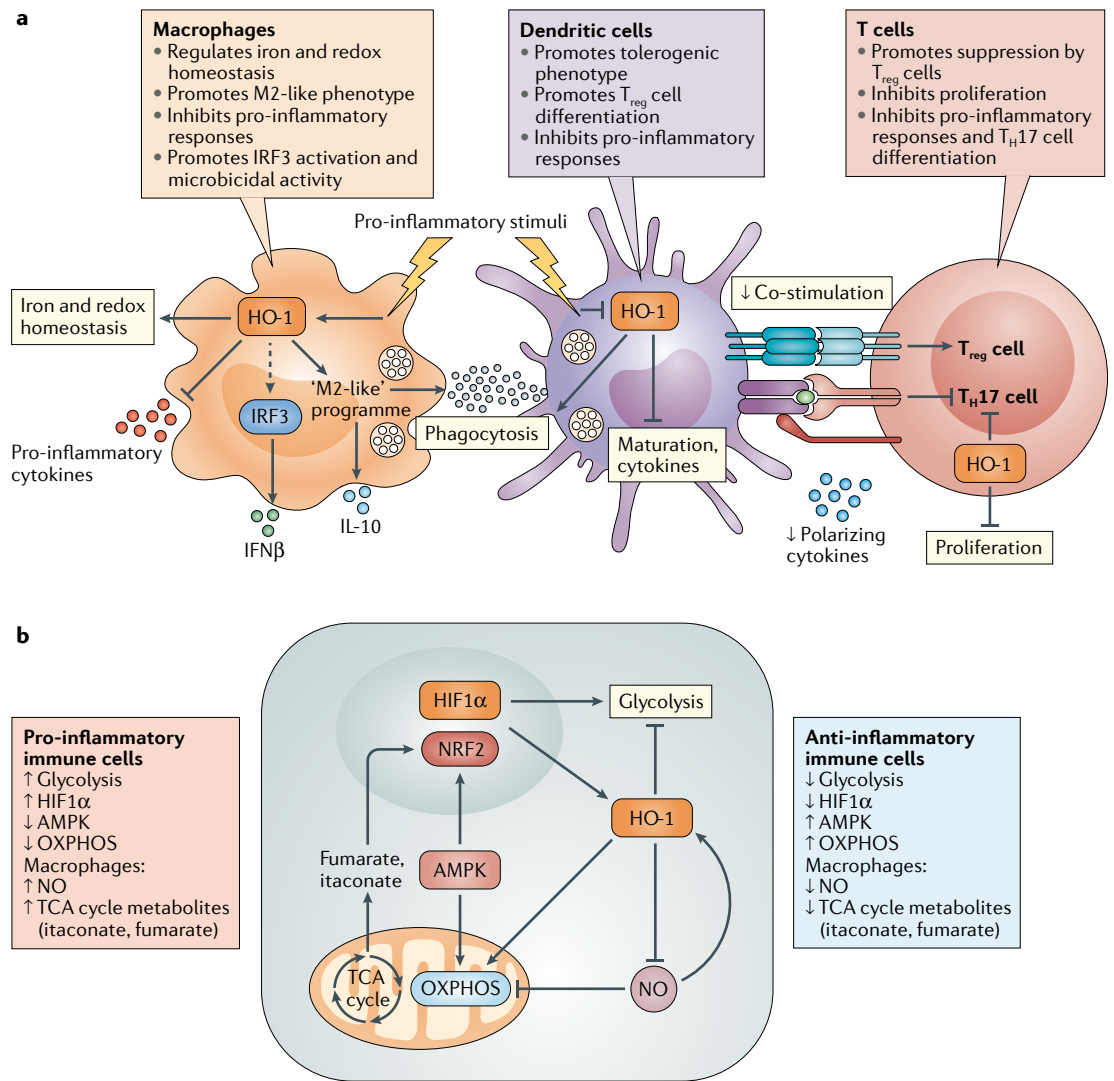


**Fig. 3 | Immunoregulation by the HO-1 system. a** | Immunomodulatory activity of haem oxygenase 1 (HO-1) in macrophages, dendritic cells and T cells. HO-1 is stress-inducible by macrophages and promotes differentiation into an ‘M2-like’ phenotype, with associated anti-inflammatory activities. HO-1 expression by macrophages also facilitates interferon regulatory factor 3 (IRF3) activation in response to pro-inflammatory stimuli and permits macrophages to regulate local iron and redox homeostasis. Immature dendritic cells constitutively express HO-1, which is downregulated during maturation in response to pro-inflammatory stimuli. Expression of HO-1 by dendritic cells promotes their anti-inflammatory activities and limits their expression of co-stimulatory molecules and pro-inflammatory or polarizing cytokines. This results in the promotion of regulatory T cell ( $T_{reg}$  cell) differentiation over differentiation of pro-inflammatory T cell subsets such as T helper 17 cells ( $T_H17$  cells). HO-1 expression by T cells can additionally inhibit  $T_H17$  cell differentiation, as well as limit proliferation. **b** | Relationship between HO-1 and immunometabolism. HO-1 expression by immune cells is regulated by metabolic signalling: hypoxia-inducible factor 1 $\alpha$  (HIF1 $\alpha$ ) and NO promote glycolytic metabolism, are upregulated during activation of pro-inflammatory immune cells and induce HO-1 expression. Metabolites derived from the tricarboxylic acid (TCA) cycle such as fumarate and itaconate have been reported to upregulate HO-1 expression via activation of nuclear factor erythroid 2-related factor 2 (NRF2). The cellular energy sensor AMPK-activated protein kinase (AMPK) promotes oxidative phosphorylation (OXPHOS) in anti-inflammatory immune cells and has been reported to induce HO-1 expression via NRF2. Finally, HO-1 or its products can also regulate immunometabolism, through inhibition of glycolysis and NO and promotion of OXPHOS. IFN $\beta$ , interferon- $\beta$ .

programmes, in part through upregulation of HO-1. Increased activation of AMPK has been reported in anti-inflammatory immune cells such as  $T_{reg}$  cells, alternatively activated/M2-like macrophages and tolerogenic DCs<sup>116–118</sup>, and signalling through AMPK can activate NRF2 and upregulate HO-1 in multiple cell types<sup>45–47,49,50</sup>. We have recently demonstrated that certain

phytochemicals (discussed later in this Review) modulate human DC metabolism and immune function via AMPK-dependent induction of HO-1 (REF.<sup>48</sup>). As the field of immunometabolism continues to evolve, it will be interesting to further explore the role of HO-1 as an immunomodulator and cytoprotectant during metabolic reprogramming in immune cells, and as a potential target



for therapeutic modulation of immunometabolism in inflammatory disease<sup>119,120</sup>.

### HO-1 in disease

Given their extensive antioxidant and anti-inflammatory properties, it is unsurprising that HO-1 and its products have been associated with beneficial outcomes in inflammatory diseases. It has been suggested that *HMOX1* polymorphisms resulting in greater expression of HO-1 are protective against harmful inflammation, while those resulting in impaired *HMOX1* transcription have been associated with an increased risk of diseases such as atherosclerosis<sup>121–123</sup>. For example, the presence of the long allele of a (GT)<sub>n</sub> microsatellite polymorphism in the *HMOX1* gene promoter results in decreased HO-1 expression, conferring susceptibility to diseases including rheumatoid arthritis and chronic obstructive pulmonary disease (COPD)<sup>124,125</sup>. However, the short allele, which results in increased HO-1 expression, confers protection in these diseases. Furthermore, modulation of the HO-1 system has been widely investigated as a novel treatment strategy in various preclinical disease models; a selection of inflammatory and autoimmune diseases for which HO-1 and its products have shown the most promise are discussed in the following subsections.

**Inflammatory bowel disease.** Under homeostatic conditions, HO-1 is weakly expressed in the gastrointestinal tract. However, increased HO-1 expression has been observed in both inflammatory cells and intestinal epithelial cells from patients with inflammatory bowel disease (IBD)<sup>52,53</sup>. In murine models of colitis, increased levels of HO-1 have been observed in inflamed colonic tissue, particularly in endothelial cells, macrophages and neutrophils, and it has been proposed that these cells may increase HO-1 expression to control inflammation and oxidative stress<sup>126–128</sup>. In support of this hypothesis, inhibition of haem oxygenase activity results in increased damage to the colon in the 2,4,6-trinitrobenzenesulfonic acid (TNBS)-induced colitis model<sup>127</sup> and elevated levels of pro-inflammatory cytokines in the dextran sodium sulfate (DSS)-induced colitis model<sup>128</sup>. Furthermore, administration of low concentrations of CO alleviates colitis symptoms in mouse models through upregulation of HO-1 expression<sup>129,130</sup>. Bilirubin has also been reported to attenuate symptoms of colitis in multiple models, through limiting leukocyte trafficking and pro-inflammatory cytokine production, and promoting IL-10 signalling<sup>131–133</sup>. HO-1 induction via haemin in the DSS-induced colitis model was correlated with an inhibition of T<sub>H</sub>17 cell responses, and promotion of T<sub>reg</sub> cell numbers and function<sup>100</sup>. Haemin administration has also recently been reported to attenuate colitis symptoms by reducing the number of pro-inflammatory myeloid-derived cells, such as M1 macrophages, and increasing the number of anti-inflammatory M2 macrophages in colon tissue<sup>134</sup>. Furthermore, administration of the HO-1 inducer cobalt protoporphyrin IX before initiation of DSS-induced colitis has been reported to reduce apoptosis of colonic epithelial cells and decrease colonic inflammation<sup>53</sup>. The mechanism of action of 5-aminosalicylic acid (5-ASA), an anti-inflammatory

drug used as a first-line treatment for IBD, may be attributed, in part, to upregulation of HO-1 (REFS<sup>135,136</sup>). Together, this evidence provides a strong basis for HO-1 induction as a potential therapy for IBD; however, further clinical investigation is necessary.

**Psoriasis.** The skin is constantly exposed to environmental stressors such as UV radiation, requiring it to have access to a robust suite of antioxidant and anti-inflammatory mediators, including both HO-1 and HO-2, to protect itself from cellular damage<sup>137</sup>. In psoriasis, HO-1 appears to play a central role in the protection of skin from chronic inflammation: upregulation of HO-1 has been observed in psoriatic plaques, and increased levels of HO-1 have been detected in serum of patients compared with controls<sup>138,139</sup>. Furthermore, upregulation of HO-1 has been demonstrated to inhibit skin inflammation and keratinocyte proliferation in preclinical models of psoriasis. In two different rodent models, upregulation of HO-1 via cobalt protoporphyrin IX was associated with amelioration of skin lesions and reduced inflammation; Listopad et al. reported a decrease in T cell-mediated skin inflammation, which was accompanied by increased HO-1 activity in antigen-presenting cells, while Ma et al. observed a reduction in tumour necrosis factor (TNF) expression and an increase in IL-10 expression, which were reversible with HO-1 inhibition<sup>79,140</sup>. Similarly, topical application of haemin in the imiquimod-induced psoriasis model resulted in increased expression of HO-1 and a concomitant decrease in the severity of psoriatic lesions, which was attributed to negative regulation of STAT3 signalling by HO-1 (REF.<sup>141</sup>). Induction of HO-1 is also associated with existing treatments for psoriasis. For example, phototherapy involving exposure to UVA radiation upregulates HO-1 expression in skin<sup>137,142</sup>. Dimethyl fumarate (DMF), an immunosuppressant used to treat both psoriasis and multiple sclerosis, has also been reported to act in part through HO-1 induction<sup>143–147</sup>. Whether HO-1 activity is required for the efficacy of these therapies remains unclear; however, these studies provide further support for the modulation of HO-1 expression as a potential treatment for psoriasis.

**Multiple sclerosis.** HO-1 and its products have been shown to have protective effects in multiple sclerosis and its mouse model, experimental autoimmune encephalomyelitis (EAE)<sup>87,148</sup>. HO-1 expression is reduced in peripheral blood mononuclear cells of patients with multiple sclerosis compared with controls and is further downregulated in patients experiencing disease relapse compared with those with stable disease or receiving corticosteroid treatment<sup>54</sup>. Furthermore, HO-1 upregulation has been observed in glial cells within multiple sclerosis plaques, likely as a local response to neuroinflammation<sup>149</sup>. In an EAE model, HO-1-deficient mice exhibited a severer disease phenotype than wild-type mice, and induction of HO-1 resulted in reduced disease scores and a reduction in inflammatory T cell infiltration into the central nervous system<sup>87</sup>. Induction of HO-1 during EAE has also been reported to reduce production of pro-inflammatory cytokines and to

#### Haemin

An endogenously produced haem molecule containing a chloride ion. Haemin is also available as a purified product from mammalian red blood cells, which is used both in research as an inducer of haem oxygenase 1 (HO-1) and in medicine as a treatment for porphyria.

increase production of IL-10 (REF.<sup>150</sup>). Furthermore, CO has been demonstrated to improve disease outcomes in EAE, while biliverdin reductase and bilirubin suppressed EAE onset and progression<sup>87,151–153</sup>. While research in this area is still in the early stages, these studies indicate that therapies modulating the HO-1 system may be beneficial as a novel treatment strategy for multiple sclerosis.

**Inflammatory lung diseases.** HO-1 and its products have shown therapeutic potential for a number of diseases characterized by lung inflammation. For example, biliverdin administration protected rats from endotoxic shock, reduced serum levels of IL-6 and promoted IL-10 expression in a model of acute lung injury<sup>154</sup>. Moreover, inhaled CO has been extensively investigated as a potential therapy for lung inflammation<sup>155,156</sup>. However, despite being well tolerated, it showed no therapeutic efficacy in a recent phase II clinical trial for idiopathic pulmonary fibrosis<sup>157</sup>. Low-dose CO inhalation appears to specifically upregulate genes associated with oxidative phosphorylation in peripheral blood mononuclear cells from patients with idiopathic pulmonary fibrosis<sup>158</sup>, indicating that this therapy may promote metabolic phenotypes associated with anti-inflammatory immune cells. However, further studies are required to fully elucidate these effects and determine whether CO administration is beneficial in idiopathic pulmonary fibrosis.

Meanwhile, the chronic inflammation associated with COPD has been identified as a promising target for treatment with HO-1 and/or CO. As previously mentioned, polymorphisms resulting in reduced HO-1 expression lead to increased susceptibility to COPD<sup>125,159</sup>. It has also been suggested that a decrease in NRF2 and HO-1 expression is associated with COPD progression, and therefore their induction could potentially be therapeutic<sup>160</sup>. NRF2 activation can reverse defects typically seen in the alveolar macrophages of patients with COPD by increasing their phagocytic capacity<sup>161,162</sup>. NRF2 activation, downstream of AMPK and WNT signalling, also resulted in decreased expression of pro-inflammatory markers in normal human bronchial epithelial cells and murine models of COPD<sup>163</sup>. Overexpression of HO-1 in a murine model of COPD also results in decreased expression of pro-inflammatory markers and increased expression of IL-10 (REF.<sup>164</sup>). The leading cause of COPD is smoking, and patients with COPD who smoke display higher levels of exhaled CO than non-smoking controls<sup>165</sup>. Higher levels of CO-bound haemoglobin have been observed in patients with COPD than in controls, with increased levels correlating with increased disease severity<sup>166</sup>. Despite this, CO inhalation has also shown therapeutic potential for treatment of COPD; a clinical trial involving patients with COPD reported a reduction in sputum eosinophil numbers and improved responsiveness to methacholine as a measure of airway sensitivity with CO treatment<sup>167</sup>.

**Organ transplantation.** Oxidative damage and ischaemic stress are of major concern during organ transplantation, as they can negatively impact the health and survival of grafted tissue. Furthermore, ongoing suppression of the host immune response is necessary to prevent graft

rejection. HO-1 and its products are under investigation as protective agents during transplantation, due to their recognized antioxidant and anti-inflammatory properties. Biliverdin administration has been found to be particularly efficacious against ischaemia–reperfusion injury in animal models of small bowel<sup>168</sup>, liver<sup>169</sup>, lung<sup>170</sup> and heart<sup>171</sup> transplant. Furthermore, CO administration in models of organ transplantation has been shown to limit ischaemia–reperfusion injury to donor organs and suppress graft rejection (reviewed in REF.<sup>172</sup>). Dual treatment with both biliverdin and CO displayed increased efficacy compared with either treatment alone in animal models of lung transplant<sup>173</sup>, or heart and kidney transplant<sup>174</sup>. Furthermore, HO-1 induction displayed protection during transplantation of pancreatic islets for treatment of type 1 diabetes, increasing the survival, improving the function and increasing the number of effectively transplanted islets<sup>175,176</sup>. As well as providing graft protection during transplantation, NRF2 activation and/or HO-1 induction has been reported to increase long-term host survival in a murine model of graft-versus-host disease<sup>177</sup> and to attenuate chronic rejection following transplantation<sup>178–180</sup>. Furthermore, an *HMOX1* polymorphism resulting in higher HO-1 expression results in greater survival for patients undergoing bone marrow transplants<sup>122</sup>.

In summary, HO-1 and its products have been demonstrated to protect against harmful inflammation in numerous preclinical disease models. This compelling evidence supports HO-1 as a viable therapeutic target for the treatment of chronic inflammation. However, clinical implementation of this treatment strategy faces further challenges, as discussed in the next section.

### Therapeutic modulation of HO-1

Despite the body of evidence supporting modulation of the HO-1 system as a treatment for diseases characterized by damaging inflammation or oxidative stress, clinical implementation of HO-1-based therapies faces numerous challenges. Traditional HO-1 inducers are primarily metalloporphyrins, which strongly upregulate HO-1 expression but are also associated with significant toxicity concerns and thus are unsuitable for clinical use. Furthermore, clinical administration of HO-1 reaction products — such as CO or linear tetrapyrroles — is also limited by toxicity and bioavailability issues. Therefore, there is a great need to identify safer and better-tolerated alternatives to currently available sources of HO-1 inducers and reaction products. We highlight some of the most promising candidates in the following discussion (TABLE 1).

**Phytochemicals.** Many plant-derived compounds (phytochemicals) are commonly used as dietary and health supplements and have been extensively studied as antioxidant and anti-inflammatory agents<sup>181</sup>. Owing to their natural occurrence and regular consumption, indicating low toxicity, many are being explored as potential disease-modifying drugs, and a number have been reported to upregulate HO-1 (REFS<sup>42,182–184</sup>). The ability of phytochemicals to induce HO-1, along with their therapeutic potential for inflammatory diseases, has

Table 1 | Therapeutic potential of HO-1 inducers

Type of HO-1 inducer	Specific chemical or drug	Cell type or disease model	Effects of treatment	Disease relevance	Effect dependent on HO-1?	Ref.
Phytochemicals	Curcumin	Human DCs	Reduced DC maturation and pro-inflammatory cytokine production	Psoriasis	Yes — the HO-1 inhibitor SnPP and the CO scavenger haemoglobin reversed effects	82
		Human PBMCs	Reduced T cell proliferation and cytokine production	Psoriasis	Unknown — not examined	82
		EAE, murine DCs	Reduced EAE disease scores, increased STAT3 activation and inhibited <i>Il12b</i> and <i>Il23a</i> expression in DCs	Multiple sclerosis	Unknown — inferred from data as overexpression of HO-1 results in increased STAT3 phosphorylation	85
	Carnosol	Human DCs	Reduced DC maturation and pro-inflammatory cytokine production	Psoriasis	Yes — the HO-1 inhibitor SnPP and the CO scavenger haemoglobin reversed effects	82
		Endothelial cells	Inhibited NF-κB nuclear translocation and inhibited ICAM1 expression	Atherosclerosis	Yes — <i>HMOX1</i> siRNA reversed effects	209
	Resveratrol	HT-29 intestinal cells	Increased nuclear accumulation of PPARγ	IBD	Unknown — not examined	210
		Synoviocytes, adjuvant-induced arthritis	Decreased arthritis scores and inhibited NF-κB activation and promoted miR-29a and miR-23a expression	Rheumatoid arthritis	Potentially — <i>Nfe2l2</i> siRNA, and miR-29a and miR-23a inhibition, prevented HO-1 induction and promoted proliferation	211
	Quercetin	T cell-dependent colitis model	Reduced disease symptoms and pro-inflammatory cytokine production	IBD	Yes — effects reversed with <i>Hmox1</i> siRNA	212
		Zymosan-induced arthritis	Reduced pro-inflammatory cytokine production, NF-κB activation and disease symptoms	Rheumatoid arthritis	Unknown — not examined	213
		Collagen-induced arthritis	Reduced disease scores, increased T <sub>reg</sub> cell numbers and decreased production of pro-inflammatory cytokines	Rheumatoid arthritis	Yes — decrease in production of pro-inflammatory markers inhibited by <i>Hmox1</i> siRNA	214
	Sulforaphane	DSS-induced colitis	Reduced disease scores and decreased levels of pro-inflammatory markers	IBD	Unknown — not examined	215
		EAE	Reduced disease scores, inhibited IL-17, IFNγ, IL-12 and IL-23	Multiple sclerosis	Unknown — not examined	216
Murine DCs		Inhibited IL-12, IL-23 and NF-κB	Multiple sclerosis	Yes — HO-1 binds to p65, reducing binding to <i>Il12b</i> and <i>Il23a</i> promoter sites	217	
Existing drugs	DMF	PBMCs	Reduced pro-inflammatory cytokine production	Psoriasis	Partially — reduction in IL-12 and IFNγ production reversed by <i>HMOX1</i> siRNA and SnPP	143
		Human DCs, CD4 <sup>+</sup> T cells, EAE	Inhibited pro-inflammatory cytokines and promoted anti-inflammatory cytokines, ameliorating disease	Multiple sclerosis, psoriasis	Partially — IL-23 inhibition reversed by <i>HMOX1</i> siRNA	146
		DSS-induced colitis	Attenuated disease and reduced production of pro-inflammatory markers	IBD	Potentially — reduction in pro-inflammatory marker production and HO-1 induction abolished in <i>Nrf2</i> <sup>-/-</sup> mice	190
	5-ASA	TNBS-induced colitis	Reduced disease severity, lesion area and MPO activity	IBD	Yes — effects reversed with the HO-1 inhibitor ZnPP	135
		TNBS-induced colitis	Ameliorated disease and reduced production of inflammatory markers	IBD	Unknown — not examined	136
	5-ALA	Cardiac allograft	Increased graft acceptance and T <sub>reg</sub> cell numbers, and decreased numbers of CD8 <sup>+</sup> T cells	Transplantation	Partially — ZnPP, an HO-1 inhibitor, decreased survival in 5-ALA-treated mice	192
		Osteoclasts, osteoblasts	Inhibited IL-6 and RANKL expression	Rheumatoid arthritis	Unknown — not examined	193
	DHA	TNBS-induced and OXA-induced colitis	Ameliorated symptoms and decreased numbers of T <sub>H</sub> 1 cells and T <sub>H</sub> 17 cells and increased numbers of T <sub>reg</sub> cells	IBD	Yes — effects reversed on inhibition of HO-1 with SnPP	194

Table 1 (cont.) | Therapeutic potential of HO-1 inducers

Type of HO-1 inducer	Specific chemical or drug	Cell type or disease model	Effects of treatment	Disease relevance	Effect dependent on HO-1?	Ref.
Carbon monoxide-based therapies	CORMs	Rat brain astrocytes	Inhibited <i>Mmp9</i> mRNA expression and cell migration	Neuroinflammation	Yes — reversed with <i>Hmox1</i> siRNA	195
		ConA-induced hepatitis	Reduced disease scores and reduced production of pro-inflammatory markers	Autoimmune hepatitis	Unknown — not examined	197
		T cell transfer colitis model	Attenuated disease symptoms and reduced IL-17 secretion	IBD	Unknown — not examined	198
	Hybrid carbon monoxide-releasing molecules	LPS-challenged mice	Reduced production of pro-inflammatory and increased production of anti-inflammatory markers	Inflammatory diseases	Potentially — reversal of effects in <i>Nrf2</i> <sup>-/-</sup> mice was partially observed and organ specific	201
		EAE, imiquimod-induced psoriasis	Reduced disease scores and symptoms	Multiple sclerosis, psoriasis	Unknown — not examined	200
Novel inducers	Itaconate	Murine BMDMs, human PBMCs	Reduced pro-inflammatory cytokine production	Inflammatory diseases	Potentially — inhibition of IL-1β reversed with <i>Nrf2</i> <sup>-/-</sup> mice and <i>Nfe2l2</i> siRNA	110
		Murine BMDMs, imiquimod-induced psoriasis	Reduced pro-inflammatory cytokine production and ameliorated disease	Psoriasis	No — reduction in pro-inflammatory cytokine production not reversed in <i>Nrf2</i> <sup>-/-</sup> BMDMs, but not examined in the in vivo model	202
		Patient-derived PBMCs	Reduced NF-κB activation and TNF production	SLE	Potentially — reduction reversed with <i>NFE2L2</i> shRNA	203
	KI-696	Ozone-exposed rats	Reduced numbers of inflammatory cells in bronchoalveolar lavage fluid, and increased antioxidant levels	Lung inflammation/ COPD	Potentially — inferred from data due to specificity of agonist and induction of HO-1, however not definitively proven	204
		Macrophages (from patients with COPD)	Increased phagocytosis of the bacterium <i>Streptococcus pneumoniae</i>	COPD	Potentially — inferred from data due to specificity of agonist and induction of HO-1, however not definitively proven	162
	Aromatic ketoacids	Murine BMDMs, glial cells	Inhibited pro-IL-1β, iNOS and IL-6	Inflammatory diseases	Unknown — not examined	205
		Murine BMDMs, LPS-challenged mice	Inhibited LPS-induced glycolytic shift, pro-IL-1β and HIF1α	Inflammatory diseases	Unknown — not examined	206

5-ALA, 5-aminolevulinic acid; 5-ASA, 5-aminosalicylic acid; BMDM, bone marrow-derived macrophage; ConA, concanavalin A; COPD, chronic obstructive pulmonary disease; CORM, carbon monoxide-releasing molecule; DC, dendritic cell; DHA, dihydroartemisinin; DMF, dimethyl fumarate; DSS, dextran sulfate sodium; EAE, experimental autoimmune encephalomyelitis; HIF1α, hypoxia-inducible factor 1 α; HO-1, haem oxygenase 1; IBD, inflammatory bowel disease; IFNγ, interferon-γ; iNOS, inducible nitric oxide synthase; LPS, lipopolysaccharide; MPO, myeloperoxidase; OXA, oxazolone; PPARγ, peroxisome proliferator-activated receptor-γ; PBMC, peripheral blood mononuclear cell; shRNA, small hairpin RNA; siRNA, small interfering RNA; SLE, systemic lupus erythematosus; SnPP, tin protoporphyrin IX; T<sub>H</sub>1 cell, T helper 1 cell; T<sub>H</sub>17 cell, T helper 17 cell; TNBS, 2,4,6-trinitrobenzenesulfonic acid; TNF, tumour necrosis factor; T<sub>reg</sub> cell, regulatory T cell; ZnPP, zinc protoporphyrin IX.

recently been reviewed in detail elsewhere<sup>185</sup>; therefore, we have provided only a brief overview of some of the leading candidates in TABLE 1. Despite the considerable number of preclinical studies that support the use of phytochemicals as anti-inflammatory agents and alternative HO-1 inducers, much of this research is limited in its applicability to human disease. For example, many phytochemicals have low oral bioavailability and/or are digested and metabolized into different conjugates before reaching the systemic circulation<sup>186</sup>. Moreover, they are frequently studied at supraphysiological concentrations far in excess of those achievable by dietary consumption<sup>186,187</sup>. However, two small patient trials investigating the polyphenol and HO-1 inducer curcumin as a treatment for psoriasis both reported reduced

disease scores using oral formulations with increased bioavailability<sup>188,189</sup>. Therefore, it is clear that consideration of the bioavailability, route of administration and effective dosages, as well as further human studies, are necessary before phytochemical HO-1 inducers can be translated to the clinic.

**Existing drugs.** Certain existing drugs used to treat inflammation have been reported to activate NRF2 and/or upregulate HO-1. As previously mentioned, the efficacy of DMF, a drug licensed for treatment of psoriasis and multiple sclerosis, may be partially attributed to activation of NRF2 and induction of HO-1 (REFS<sup>143–147</sup>). DMF treatment has also shown promise in a colitis model, in which it attenuated disease symptoms and

reduced levels of pro-inflammatory markers through NRF2 activation<sup>190</sup>. Similarly, 5-ASA, the aforementioned first-line therapy for IBD, may also count HO-1 upregulation as part of its mechanism of action<sup>135,136</sup>. Administration of 5-ASA in the TNBS-induced model increased colonic haem oxygenase activity and HO-1 expression and reduced colonic inflammation, while inhibition of HO-1 abolished its anticolitic effect<sup>135</sup>. 5-ASA, and its prodrug sulfasalazine, activated NRF2 and HO-1 only when gut inflammation was present, which was attributed to the oxidation requirement of the drug<sup>136</sup>. 5-Aminolevulinic acid is a haem precursor typically used in the diagnosis and treatment of cancer, and a recent study reported that HO-1 induction may partially contribute to its therapeutic mechanism<sup>191</sup>. NRF2 activation and HO-1 upregulation by 5-aminolevulinic acid have also shown therapeutic potential for prolonging graft survival and treatment of rheumatoid arthritis<sup>192,193</sup>. In a murine model of IBD, dihydroartemisinin, a drug typically used to treat malaria, ameliorated disease symptoms by decreasing the number of inflammatory CD4<sup>+</sup> T cells through HO-1 induction<sup>194</sup>. These drugs could therefore be suitable for use as HO-1 inducers owing to their existing regulatory approval and safety data.

**CO-based therapies.** CO-releasing molecules (CORMs) are CO-carrier compounds designed to deliver controlled release of CO to target tissues as an alternative to CO gas inhalation. Two CORM candidates, CORM-A1 and CORM3, have been reported to upregulate HO-1 and provide protection in various models of inflammation<sup>195–198</sup>. This method of CO administration may therefore allow safer therapeutic use of CO, particularly as CORMs do not alter levels of CO-bound haemoglobin, overcoming the risk of CO poisoning associated with gas inhalation<sup>199</sup>. However, further research is required before the use of CORMs is extended to clinical settings, particularly regarding the toxicity associated with the backbone carrier moiety of these compounds, which typically contains a heavy metal, as well as determination of a safe dose that will produce an effective concentration in specific tissues<sup>121</sup>. Hybrid CO-releasing molecules are an interesting class of novel CO-based therapies and are synthesized by conjugation

of a CORM with an NRF2-inducing factor, for example CORM-401 combined with analogues of DMF. These compounds have the dual benefit of releasing CO for initial, rapid action, followed by longer-lasting protection produced by activation of NRF2 (REFS<sup>200,201</sup>). Examples of these compounds have been confirmed to activate NRF2 and upregulate HO-1 in different cells and tissues, and to reduce inflammation in lipopolysaccharide-challenged mice and in models of psoriasis and multiple sclerosis<sup>200,201</sup>. However, similarly to their parent compounds, hybrid CO-releasing molecules face challenges regarding their toxicity owing to the presence of metals in their structures.

**Novel inducers.** Recently, there has been interest in identifying novel HO-1 inducers that may show potential as anti-inflammatory therapies. Itaconate, an endogenous metabolite, has been reported to activate NRF2 through modification of cysteine residues on KEAP1, inducing downstream HO-1 expression and reducing inflammation in both murine and human immune cells<sup>110</sup>. Itaconate also ameliorated disease severity in a murine model of psoriasis and limited pro-inflammatory cytokine production via NRF2 activation in samples from patients with systemic lupus erythematosus<sup>202,203</sup>. Another novel NRF2 activator, KI-696, has shown therapeutic potential for COPD. This compound specifically inhibits the KEAP1–NRF2 interaction, leading to activation of NRF2 and upregulation of NRF2-regulated genes, including *HMOX1* (REF<sup>204</sup>). KI-696 has shown therapeutic potential to treat COPD by reducing the number of inflammatory cells in the bronchoalveolar lavage fluid of ozone-exposed mice, used as a model of respiratory disease, as well as increasing the phagocytic capacity of lung macrophages in patients with COPD<sup>162</sup>. Finally, aromatic ketoacids secreted by the parasite *Trypanosoma brucei* have recently been reported to induce HO-1 via NRF2 activation and to downregulate inflammation in murine immune cells<sup>205,206</sup>. These ketoacids require further study to fully elucidate their mechanism of action; however, they may be novel therapeutic candidates for inflammatory diseases through their upregulation of HO-1.

**Limitations of HO-1-based therapies.** Despite the large amount of evidence presented in this Review in support of HO-1 as a promising candidate to treat inflammatory diseases, there remain many limitations to its application that need to be overcome. Most of the studies examining the role of HO-1 in disease have used metalloporphyrins, *Hmox1*<sup>-/-</sup> animals or gene silencing to modify HO-1 expression and determine HO-1-specific efficacy. However, these methods are not suitable for use in humans, making the findings of these studies difficult to translate to the clinic. These methods can also produce off-target effects: for example, metalloporphyrins can inhibit other important signalling molecules, and simultaneously increase HO-1 expression while inhibiting its enzymatic activity<sup>207,208</sup>. The immunomodulatory effects of some HO-1 inducers may not appear to be attributed to HO-1 (TABLE 1). However, these associations can be difficult to test experimentally; for example, the weak enzymatic inhibitors available for HO-1

### Box 3 | Outstanding questions

1. To what extent is haem oxygenase 1 (HO-1) expression regulated by epigenetic or post-transcriptional mechanisms? Are these mechanisms relevant to immune cells and can they be targeted to modulate HO-1 in clinical settings?
2. Does HO-1 play a significant role in immune cells other than myeloid-lineage cells such as monocytes, macrophages and dendritic cells?
3. What are the mechanisms that contribute to the immunomodulatory activity of HO-1 in immune cells, and to what extent are these relevant *in vivo*?
4. How does expression of HO-1 regulate immunometabolism, and vice versa?
5. What alternative models are available to study the therapeutic potential of HO-1 that are more relevant to human disease (for example, organoids or humanized mice)?
6. How can the issues surrounding HO-1 inducers and inhibitors (such as toxicity, specificity and bioavailability) be overcome in order to use these in the clinic?
7. Can existing drugs that have been reported to upregulate HO-1 be repurposed to exploit their HO-1-inducing capacity for the treatment of diseases where HO-1 has shown therapeutic potential?

may be overwhelmed by particularly strong inducers, while use of *Hmox1*<sup>-/-</sup> mice is often limited by breeding difficulties associated with this particular strain<sup>208</sup>. Many studies have therefore turned to NRF2 inhibitors or knockout mice as an alternative, but it is then difficult to parse HO-1-specific effects given the wide range of antioxidant and cytoprotective genes regulated by NRF2. Finally, as mentioned earlier, many HO-1-based therapeutics under investigation have associated toxicity or bioavailability concerns, while HO-1 induction itself can prove detrimental in situations where inflammation is beneficial, potentially putting patients at increased risk of infection or cancer. All of these factors must be considered for successful translation of potential HO-1-based therapeutics to the clinic.

**Concluding remarks**

The haem oxygenase system, an ancient arm of iron metabolism common to bacteria, plants and animals, has long been ignored by immunologists as a routine biochemical pathway of little clinical consequence.

However, research over the last two decades has renewed interest in haem catabolism as its diverse roles in regulating oxidative stress, immune function and cellular metabolism have become apparent. The stress-inducible isozyme HO-1 is protective in numerous models of autoimmune disease and inflammation and is a viable clinical target. Harnessing the therapeutic potential of HO-1 remains limited by a lack of clinically suitable HO-1 inducers and reaction products. Therefore, further study of novel or alternative HO-1 modulators, as well as the potential to repurpose existing drugs as HO-1 inducers, should be pursued. Furthermore, a number of outstanding questions surrounding the immunomodulatory role of HO-1 and its application require exploration (BOX 3). Future research will no doubt uncover additional links between this polyfunctional enzyme and the complex networks of redox, immune and metabolic signalling and further enhance its reputation as an important immunomodulator.

Published online 29 January 2021

1. Paoli, M., Marles-Wright, J. & Smith, A. Structure-function relationships in heme-proteins. *DNA Cell Biol.* **21**, 271–280 (2002).
2. Kumar, S. & Bandyopadhyay, U. Free heme toxicity and its detoxification systems in human. *Toxicol. Lett.* **157**, 175–188 (2005).
3. Gozzelino, R., Jeney, V. & Soares, M. P. Mechanisms of cell protection by heme oxygenase-1. *Annu. Rev. Pharmacol. Toxicol.* **50**, 323–354 (2010).
4. Tenhunen, R., Marver, H. S. & Schmid, R. The enzymatic conversion of heme to bilirubin by microsomal heme oxygenase. *Proc. Natl Acad. Sci. USA* **61**, 748–755 (1968).
5. Singleton, J. W. & Laster, L. Biliverdin reductase of guinea pig liver. *J. Biol. Chem.* **240**, 4780–4789 (1965).
6. Yamaguchi, T., Komoda, Y. & Nakajima, H. Biliverdin-IX alpha reductase and biliverdin-IX beta reductase from human liver. Purification and characterization. *J. Biol. Chem.* **269**, 24343–24348 (1994).
7. Trakshel, G. M., Kutty, R. K. & Maines, M. D. Purification and characterization of the major constitutive form of testicular heme oxygenase. The noninducible isoform. *J. Biol. Chem.* **261**, 11131–11137 (1986).
8. Maines, M. D., Trakshel, G. M. & Kutty, R. K. Characterization of two constitutive forms of rat liver microsomal heme oxygenase. Only one molecular species of the enzyme is inducible. *J. Biol. Chem.* **261**, 411–419 (1986).
9. Maines, M. D. The heme oxygenase system: a regulator of second messenger gases. *Annu. Rev. Pharmacol. Toxicol.* **37**, 517–554 (1997).
10. Verma, A., Hirsch, D., Glatt, C., Ronnett, G. & Snyder, S. Carbon monoxide: a putative neural messenger. *Science* **259**, 381–384 (1993).
11. Maines, M. D. & Kappas, A. Cobalt induction of hepatic heme oxygenase; with evidence that cytochrome P-450 is not essential for this enzyme activity. *Proc. Natl Acad. Sci. USA* **71**, 4293–4297 (1974).
12. Otterbein, L., Sylvester, S. L. & Choi, A. M. Hemoglobin provides protection against lethal endotoxemia in rats: the role of heme oxygenase-1. *Am. J. Respir. Cell Mol. Biol.* **13**, 595–601 (1995).
13. Otterbein, L. E. et al. Exogenous administration of heme oxygenase-1 by gene transfer provides protection against hyperoxia-induced lung injury. *J. Clin. Invest.* **103**, 1047–1054 (1999).
14. Lee, T.-S. & Chau, L.-Y. Heme oxygenase-1 mediates the anti-inflammatory effect of interleukin-10 in mice. *Nat. Med.* **8**, 240–246 (2002).  
**One of the earliest studies to establish an anti-inflammatory role for HO-1, this article reports that IL-10 upregulates HO-1 in murine macrophages and mediates the protective effects of IL-10 in an in vivo model of lipopolysaccharide-induced septic shock.**
15. Otterbein, L. E. et al. Carbon monoxide has anti-inflammatory effects involving the mitogen-activated protein kinase pathway. *Nat. Med.* **6**, 422–428 (2000).  
**This is an important early study demonstrating the anti-inflammatory effects of carbon monoxide in an in vivo model of lipopolysaccharide-induced septic shock.**
16. Poss, K. D. & Tonegawa, S. Reduced stress defense in heme oxygenase 1-deficient cells. *Proc. Natl Acad. Sci. USA* **94**, 10925–10930 (1997).
17. Radhakrishnan, N. et al. Human heme oxygenase-1 deficiency presenting with hemolysis, nephritis, and asplenia. *J. Pediatr. Hematol. Oncol.* **33**, 74–78 (2011).
18. Kapturczak, M. H. et al. Heme oxygenase-1 modulates early inflammatory responses: evidence from the heme oxygenase-1-deficient mouse. *Am. J. Pathol.* **165**, 1045–1053 (2004).  
**This landmark article is the first to describe the pro-inflammatory phenotype observed in *Hmox1*<sup>-/-</sup> mice.**
19. Yachie, A. et al. Oxidative stress causes enhanced endothelial cell injury in human heme oxygenase-1 deficiency. *J. Clin. Invest.* **103**, 129–135 (1999).  
**This is the first study to identify HO-1 deficiency in humans, exhibiting an increased inflammatory response.**
20. Immenschuh, S. & Ramadori, G. Gene regulation of heme oxygenase-1 as a therapeutic target. *Biochem. Pharmacol.* **60**, 1121–1128 (2000).
21. Ferrandiz, M. L. & Devesa, I. Inducers of heme oxygenase-1. *Curr. Pharm. Des.* **14**, 473–486 (2008).
22. Applegate, L. A., Luscher, P. & Tyrrell, R. M. Induction of heme oxygenase: a general response to oxidant stress in cultured mammalian cells. *Cancer Res.* **51**, 974–978 (1991).
23. Ma, Q. Role of Nrf2 in oxidative stress and toxicity. *Annu. Rev. Pharmacol. Toxicol.* **53**, 401–426 (2013).
24. Kansanen, E., Kuosmanen, S. M., Leinonen, H. & Levonen, A.-L. The Keap1-Nrf2 pathway: mechanisms of activation and dysregulation in cancer. *Redox Biol.* **1**, 45–49 (2013).
25. Taguchi, K., Motohashi, H. & Yamamoto, M. Molecular mechanisms of the Keap1-Nrf2 pathway in stress response and cancer evolution. *Genes Cell* **16**, 123–140 (2011).
26. Sun, J. et al. Hemoprotein Bach1 regulates enhancer availability of heme oxygenase-1 gene. *EMBO J.* **21**, 5216–5224 (2002).
27. Zenke-Kawasaki, Y. et al. Heme induces ubiquitination and degradation of the transcription factor Bach1. *Mol. Cell Biol.* **27**, 6962–6971 (2007).
28. Suzuki, H. et al. Heme regulates gene expression by triggering Crm1-dependent nuclear export of Bach1. *EMBO J.* **23**, 2544–2553 (2004).
29. Liao, R. et al. Discovering how heme controls genome function through heme-omics. *Cell Rep.* **31**, 107832 (2020).
30. Mense, S. M. & Zhang, L. Heme: a versatile signaling molecule controlling the activities of diverse regulators ranging from transcription factors to MAP kinases. *Cell Res.* **16**, 681–692 (2006).
31. Zhang, X. et al. Bach1: function, regulation, and involvement in disease. *Oxid. Med. Cell. Longev.* **2018**, 1347969 (2018).
32. Kataoka, K. et al. Small Maf proteins heterodimerize with Fos and may act as competitive repressors of the NF-E2 transcription factor. *Mol. Cell Biol.* **15**, 2180–2190 (1995).
33. Lee, P. J. et al. Hypoxia-inducible factor-1 mediates transcriptional activation of the heme oxygenase-1 gene in response to hypoxia. *J. Biol. Chem.* **272**, 5375–5381 (1997).
34. Lavrovsky, Y., Schwartzman, M. L., Levere, R. D., Kappas, A. & Abraham, N. G. Identification of binding sites for transcription factors NF-kappa B and AP-2 in the promoter region of the human heme oxygenase 1 gene. *Proc. Natl Acad. Sci. USA* **91**, 5987–5991 (1994).
35. Alam, J. & Cook, J. L. How many transcription factors does it take to turn on the heme oxygenase-1 gene? *Am. J. Respir. Cell Mol. Biol.* **36**, 166–174 (2007).
36. Zhang, Z., Guo, Z., Zhan, Y., Li, H. & Wu, S. Role of histone acetylation in activation of nuclear factor erythroid 2-related factor 2/heme oxygenase 1 pathway by manganese chloride. *Toxicol. Appl. Pharmacol.* **336**, 94–100 (2017).
37. Magalhães, M. et al. DNA methylation at modifier genes of lung disease severity is altered in cystic fibrosis. *Clin. Epigenetics* **9**, 19 (2017).
38. Ray, P. D., Huang, B. W. & Tsuiji, Y. Coordinated regulation of Nrf2 and histone H3 serine 10 phosphorylation in arsenite-activated transcription of the human heme oxygenase-1 gene. *Biochim. Biophys. Acta Gene Regul. Mech.* **1849**, 1277–1288 (2015).
39. Medina, M. V., Sapochnik, D., Garcia Solá, M. & Coso, O. Regulation of the expression of heme oxygenase-1: signal transduction, gene promoter activation, and beyond. *Antioxid. Redox Signal.* **32**, 1033–1044 (2019).
40. Cheng, X., Ku, C.-H. & Siow, R. C. M. Regulation of the Nrf2 antioxidant pathway by microRNAs: new players in micromanaging redox homeostasis. *Free Radic. Biol. Med.* **64**, 4–11 (2013).
41. Lin, C.-C. et al. Transforming growth factor-β1 stimulates heme oxygenase-1 expression via the PI3K/Akt and NF-κB pathways in human lung epithelial cells. *Eur. J. Pharmacol.* **560**, 101–109 (2007).
42. Martin, D. et al. Regulation of heme oxygenase-1 expression through the phosphatidylinositol 3-kinase/Akt pathway and the Nrf2 transcription factor in response to the antioxidant phytochemical carnosol. *J. Biol. Chem.* **279**, 8919–8929 (2004).
43. Seo, S. H. & Jeong, G. S. Fisetin inhibits TNF-alpha-induced inflammatory action and hydrogen peroxide-induced oxidative damage in human keratinocyte

- HaCaT cells through PI3K/AKT/Nrf-2-mediated heme oxygenase-1 expression. *Int. Immunopharmacol.* **29**, 246–253 (2015).
44. Ricchetti, G. A., Williams, L. M. & Foxwell, B. M. J. Heme oxygenase 1 expression induced by IL-10 requires STAT3 and phosphoinositid-3 kinase and is inhibited by lipopolysaccharide. *J. Leukoc. Biol.* **76**, 719–726 (2004).
45. Cho, R.-L. et al. Heme oxygenase-1 induction by rosiglitazone via PKC $\alpha$ /AMPK $\alpha$ /p38 MAPK $\alpha$ /SIRT1/PPAR $\gamma$  pathway suppresses lipopolysaccharide-mediated pulmonary inflammation. *Biochem. Pharmacol.* **148**, 222–237 (2018).
46. Liu, X. et al. Activation of AMPK stimulates heme oxygenase-1 gene expression and human endothelial cell survival. *Am. J. Physiol. Circ. Physiol.* **300**, H84–H93 (2011).
47. Mo, C. et al. The crosstalk between Nrf2 and AMPK signal pathways is important for the anti-inflammatory effect of berberine in LPS-stimulated macrophages and endotoxin-shocked mice. *Antioxid. Redox Signal.* **20**, 574–588 (2014).
48. Campbell, N. K., Fitzgerald, H. K., Fletcher, J. M. & Dunne, A. Plant-derived polyphenols modulate human dendritic cell metabolism and immune function via AMPK-dependent induction of heme oxygenase-1. *Front. Immunol.* **10**, 345 (2019).  
**This article identifies an important link between a central regulator of immunometabolism, AMPK, and HO-1.**
49. Zimmermann, K. et al. Activated AMPK boosts the Nrf2/HO-1 signaling axis - a role for the unfolded protein response. *Free Radic. Biol. Med.* **88**, 417–426 (2015).
50. Joo, M. S. et al. AMPK facilitates nuclear accumulation of Nrf2 by phosphorylating at serine 550. *Mol. Cell. Biol.* **36**, 1931–1942 (2016).
51. Baldelli, S., Aquilano, K. & Ciriolo, M. R. Punctum on two different transcription factors regulated by PGC-1 $\alpha$ : Nuclear factor erythroid-derived 2-like 2 and nuclear respiratory factor 2. *Biochim. Biophys. Acta Gen. Subj.* **1830**, 4137–4146 (2013).
52. Takagi, T. et al. Increased intestinal expression of heme oxygenase-1 and its localization in patients with ulcerative colitis. *J. Gastroenterol. Hepatol.* **23**, S229–S233 (2008).
53. Paul, G. et al. Analysis of intestinal haem-oxygenase-1 (HO-1) in clinical and experimental colitis. *Clin. Exp. Immunol.* **140**, 547–555 (2005).
54. Fagone, P. et al. Heme oxygenase-1 expression in peripheral blood mononuclear cells correlates with disease activity in multiple sclerosis. *J. Neuroimmunol.* **261**, 82–86 (2013).  
**This study demonstrates a link between HO-1 expression and disease severity in patients with multiple sclerosis.**
55. Wegiel, B. et al. Heme oxygenase-1 derived carbon monoxide permits maturation of myeloid cells. *Cell Death Dis.* **5**, e1139 (2014).
56. Naito, Y., Takagi, T. & Higashimura, Y. Heme oxygenase-1 and anti-inflammatory M2 macrophages. *Arch. Biochem. Biophys.* **564C**, 83–88 (2014).
57. Recalcati, S. et al. Differential regulation of iron homeostasis during human macrophage polarized activation. *Eur. J. Immunol.* **40**, 824–835 (2010).
58. Cairo, G., Recalcati, S., Mantovani, A. & Locati, M. Iron trafficking and metabolism in macrophages: contribution to the polarized phenotype. *Trends Immunol.* **32**, 241–247 (2011).
59. Winn, N. C., Volk, K. M. & Hasty, A. H. Regulation of tissue iron homeostasis: the macrophage “ferrostat”. *JCI Insight* **5**, e132964 (2020).
60. Vijayan, V., Wagener, F. A. D. T. G. & Immenschuh, S. The macrophage heme-heme oxygenase-1 system and its role in inflammation. *Biochem. Pharmacol.* **153**, 159–167 (2018).
61. Boyle, J. J. et al. Activating transcription factor 1 directs Mhem atheroprotective macrophages through coordinated iron handling and foam cell protection. *Circ. Res.* **110**, 20–33 (2012).
62. Orozco, L. D. et al. Heme oxygenase-1 expression in macrophages plays a beneficial role in atherosclerosis. *Circ. Res.* **100**, 1703–1711 (2007).
63. Zhang, M. et al. Myeloid HO-1 modulates macrophage polarization and protects against ischemia-reperfusion injury. *JCI insight* **3**, e120596 (2018).
64. Camhi, S. L., Alam, J., Wiegand, G. W., Chin, B. Y. & Choi, A. M. K. Transcriptional activation of the HO-1 gene by lipopolysaccharide is mediated by 5' distal enhancers: role of reactive oxygen intermediates and AP-1. *Am. J. Respir. Cell Mol. Biol.* **18**, 226–234 (1998).
65. Immenschuh, S., Stritzke, J., Iwahara, S. I. & Ramadori, G. Up-regulation of heme-binding protein 23 (HBP23) gene expression by lipopolysaccharide is mediated via a nitric oxide-dependent signaling pathway in rat Kupffer cells. *Hepatology* **30**, 118–127 (1999).
66. Tzima, S., Victoratos, P., Kranidioti, K., Alexiou, M. & Kollias, G. Myeloid heme oxygenase-1 regulates innate immunity and autoimmunity by modulating IFN- $\beta$  production. *J. Exp. Med.* **206**, 1167–1179 (2009).
67. Onyiah, J. C. et al. Carbon monoxide and heme oxygenase-1 prevent intestinal inflammation in mice by promoting bacterial clearance. *Gastroenterology* **144**, 789–798 (2013).
68. Soares, M. P. & Hamza, I. Macrophages and iron metabolism. *Immunity* **44**, 492–504 (2016).
69. Hull, T. D., Agarwal, A. & George, J. F. The mononuclear phagocyte system in homeostasis and disease: a role for heme oxygenase-1. *Antioxid. Redox Signal.* **20**, 1770–1788 (2014).
70. Waltz, P. et al. Lipopolysaccharide induces autophagic signaling in macrophages via a TLR4, heme oxygenase-1 dependent pathway. *Autophagy* **7**, 315–320 (2011).
71. Jais, A. et al. Heme oxygenase-1 drives metaflammation and insulin resistance in mouse and man. *Cell* **158**, 25–40 (2014).
72. Kimura, S. et al. Increasing heme oxygenase-1-expressing macrophages indicates a tendency of poor prognosis in advanced colorectal cancer. *Digestion* **101**, 401–410 (2020).
73. Chau, L. Y. Heme oxygenase-1: emerging target of cancer therapy. *J. Biomed. Sci.* **22**, 22 (2015).
74. Mitterstiller, A. M. et al. Heme oxygenase-1 controls early innate immune response of macrophages to Salmonella Typhimurium infection. *Cell. Microbiol.* **18**, 1374–1389 (2016).
75. Scharr, C. R. et al. Heme oxygenase-1 regulates inflammation and mycobacterial survival in human macrophages during mycobacterium tuberculosis infection. *J. Immunol.* **196**, 4641–4649 (2016).
76. Carasi, P. et al. Heme-oxygenase-1 expression contributes to the immunoregulation induced by fasciola hepatica and promotes infection. *Front. Immunol.* **8**, 883 (2017).
77. Moreau, A. et al. Tolerogenic dendritic cells actively inhibit T cells through heme oxygenase-1 in rodents and in nonhuman primates. *FASEB J.* **23**, 3070–3077 (2009).
78. Chauveau, C. et al. Heme oxygenase-1 expression inhibits dendritic cell maturation and proinflammatory function but conserves IL-10 expression. *Blood* **106**, 1694–1702 (2005).  
**This important study is the first to describe the constitutive expression of HO-1 by immature DCs and its downregulation during DC maturation.**
79. Listopad, J. et al. Heme oxygenase-1 inhibits T cell-dependent skin inflammation and differentiation and function of antigen-presenting cells. *Exp. Dermatol.* **16**, 661–670 (2007).
80. George, J. F. et al. Suppression by CD4+CD25+ regulatory T cells is dependent on expression of heme oxygenase-1 in antigen-presenting cells. *Am. J. Pathol.* **173**, 154–160 (2008).
81. Schumacher, A. et al. Blockage of heme oxygenase-1 abrogates the protective effect of regulatory T cells on murine pregnancy and promotes the maturation of dendritic cells. *PLoS ONE* **7**, e42301 (2012).
82. Campbell, N. K. et al. Naturally derived heme-oxygenase-1 inducers attenuate inflammatory responses in human dendritic cells and T cells: relevance for psoriasis treatment. *Sci. Rep.* **8**, 10287 (2018).
83. Al-Huseini, L. M. A. et al. Heme oxygenase-1 regulates dendritic cell function through modulation of p38 MAPK-CREB/ATF1 signaling. *J. Biol. Chem.* **289**, 16442–16451 (2014).
84. Wong, T.-H., Chen, H.-A., Gau, R.-J., Yen, J.-H. & Suen, J.-L. Heme oxygenase-1-expressing dendritic cells promote Foxp3+regulatory T cell differentiation and induce less severe airway inflammation in murine models. *PLoS ONE* **1**, 1–14 (2016).  
**This study reports that murine DCs conditioned to express HO-1 promote antigen-specific T<sub>reg</sub> cell differentiation both in vitro and in vivo and induce less inflammation in a model of asthma.**
85. Brück, J. et al. Nutritional control of IL-23/Th17-mediated autoimmune disease through HO-1/STAT3 activation. *Sci. Rep.* **7**, 44482 (2017).
86. Simon, T. et al. Inhibition of effector antigen-specific T cells by intradermal administration of heme oxygenase-1 inducers. *J. Autoimmun.* **81**, 44–55 (2017).
87. Chora, Á. A. et al. Heme oxygenase-1 and carbon monoxide suppress autoimmune neuroinflammation. *J. Clin. Invest.* **117**, 438–447 (2007).
88. Tardif, V. et al. Carbon monoxide decreases endosome-lysosome fusion and inhibits soluble antigen presentation by dendritic cells to T cells. *Eur. J. Immunol.* **43**, 2832–2844 (2013).
89. Rémy, S. et al. Carbon monoxide inhibits TLR-induced dendritic cell immunogenicity. *J. Immunol.* **182**, 1877–1884 (2009).
90. Riquelme, S. A., Pogu, J., Anegón, I., Bueno, S. M. & Kalergis, A. M. Carbon monoxide impairs mitochondria-dependent endosomal maturation and antigen presentation in dendritic cells. *Eur. J. Immunol.* **45**, 3269–3288 (2015).
91. Basdeo, S. A. et al. Suppression of human alloreactive T cells by linear tetrapyrroles; relevance for transplantation. *Transl. Res.* **178**, 81–94.e2 (2016).
92. Pae, H.-O., Oh, G.-S., Choi, B.-M., Chae, S.-C. & Chung, H.-T. Differential expressions of heme oxygenase-1 gene in CD25<sup>-</sup> and CD25<sup>+</sup> subsets of human CD4<sup>+</sup> T cells. *Biochem. Biophys. Res. Commun.* **306**, 701–705 (2003).
93. Choi, B. M., Pae, H. O., Jeong, Y. R., Kim, Y. M. & Chung, H. T. Critical role of heme oxygenase-1 in Foxp3-mediated immune suppression. *Biochem. Biophys. Res. Commun.* **327**, 1066–1071 (2005).
94. Xia, Z.-W. et al. Heme oxygenase-1 attenuates ovalbumin-induced airway inflammation by up-regulation of Foxp3<sup>+</sup> regulatory cells, interleukin-10, and membrane-bound transforming growth factor- $\beta$ 1. *Am. J. Pathol.* **171**, 1904–1914 (2007).
95. Zhang, Y., Zhang, L., Wu, J., Di, C. & Xia, Z. Heme oxygenase-1 exerts a protective role in ovalbumin-induced neutrophilic airway inflammation by inhibiting Th17 cell-mediated immune response. *J. Biol. Chem.* **288**, 34612–34626 (2013).
96. Lin, X. L. et al. Heme oxygenase-1 directly binds STAT3 to control the generation of pathogenic Th17 cells during neutrophilic airway inflammation. *Eur. J. Allergy Clin. Immunol.* **72**, 1972–1987 (2017).
97. Burt, T. D., Seu, L., Mold, J. E., Kappas, A. & McCune, J. M. Naive human T cells are activated and proliferate in response to the heme oxygenase-1 inhibitor tin mesoporphyrin. *J. Immunol.* **185**, 5279–5288 (2010).
98. Zelenay, S., Chora, A., Soares, M. P. & Demengeot, J. Heme oxygenase-1 is not required for mouse regulatory T cell development and function. *Int. Immunol.* **19**, 11–18 (2007).
99. Chen, X. et al. Sodium butyrate regulates Th17/Treg cell balance to ameliorate uveitis via the Nrf2/HO-1 pathway. *Biochem. Pharmacol.* **142**, 111–119 (2017).
100. Zhang, L. et al. Heme oxygenase-1 ameliorates dextran sulfate sodium-induced acute murine colitis by regulating Th17/Treg cell balance. *J. Biol. Chem.* **289**, 26847–26858 (2014).
101. Yu, M. et al. High expression of heme oxygenase-1 in target organs may attenuate acute graft-versus-host disease through regulation of immune balance of TH17/Treg. *Transpl. Immunol.* **37**, 10–17 (2016).
102. O'Neill, L. A. J., Kishton, R. J. & Rathmell, J. A guide to immunometabolism for immunologists. *Nat. Rev. Immunol.* **16**, 553–565 (2016).
103. Wegiel, B., Nemeth, Z., Correa-Costa, M., Bulmer, A. C. & Otterbein, L. E. Heme oxygenase-1: a metabolic nuke. *Antioxid. Redox Signal.* **20**, 1709–1722 (2014).
104. Figueiredo-Pereira, C., Dias-Pedroso, D., Soares, N. L. & Vieira, H. L. A. CO-mediated cytoprotection is dependent on cell metabolism modulation. *Redox Biol.* **32**, 101470 (2020).
105. Park, J., Joe, Y., Rytter, S. W., Surh, Y. J. & Chung, H. T. Similarities and distinctions in the effects of metformin and carbon monoxide in immunometabolism. *Mol. Cell* **42**, 292–300 (2019).
106. Vitek, L. The role of bilirubin in diabetes, metabolic syndrome, and cardiovascular diseases. *Front. Pharmacol.* **3**, 55 (2012).
107. Dennerly, P. A. Evaluating the beneficial and detrimental effects of bile pigments in early and later life. *Front. Pharmacol.* **3**, 1–5 (2012).
108. Huang, J. et al. Iron regulates glucose homeostasis in liver and muscle via AMP-activated protein kinase in mice. *FASEB J.* **27**, 2845–2854 (2013).
109. Frezza, C. et al. Haem oxygenase is synthetically lethal with the tumour suppressor fumarate hydratase. *Nature* **477**, 225–228 (2011).

110. Mills, E. L. et al. Itaconate is an anti-inflammatory metabolite that activates Nrf2 via alkylation of KEAP1. *Nature* **556**, 113–117 (2018). **This study identifies the metabolite itaconate as an NRF2 activator and HO-1 inducer, with immunomodulatory effects.**
111. Kelly, B. & O'Neill, L. A. J. Metabolic reprogramming in macrophages and dendritic cells in innate immunity. *Cell Res.* **25**, 771–784 (2015).
112. Shi, L. Z. et al. HIF1 $\alpha$ -dependent glycolytic pathway orchestrates a metabolic checkpoint for the differentiation of TH17 and Treg cells. *J. Exp. Med.* **208**, 1367–1376 (2011).
113. Finlay, D. K. et al. PDK1 regulation of mTOR and hypoxia-inducible factor 1 integrate metabolism and migration of CD8 $^{+}$  T cells. *J. Exp. Med.* **209**, 2441–2453 (2012).
114. Foresti, R. & Motterlini, R. The heme oxygenase pathway and its interaction with nitric oxide in the control of cellular homeostasis. *Free Radic. Res.* **31**, 459–475 (1999).
115. Franchina, D. G., Dostert, C. & Brenner, D. Reactive oxygen species: involvement in T cell signaling and metabolism. *Trends Immunol.* **39**, 489–502 (2018).
116. Carroll, K. C., Viollet, B. & Suttles, J. AMPK $\alpha$ 1 deficiency amplifies proinflammatory myeloid APC activity and CD40 signaling. *J. Leukoc. Biol.* **94**, 1113–1121 (2013).
117. Michalek, R. D. et al. Cutting edge: distinct glycolytic and lipid oxidative metabolic programs are essential for effector and regulatory CD4 $^{+}$  T cell subsets. *J. Immunol.* **186**, 3299–3303 (2011).
118. Krawczyk, C. M. et al. Toll-like receptor-induced changes in glycolytic metabolism regulate dendritic cell activation. *Blood* **115**, 4742–4749 (2010).
119. Pålsson-McDermott, E. M. & O'Neill, L. A. J. Targeting immunometabolism as an anti-inflammatory strategy. *Cell Res.* **30**, 300–314 (2020).
120. Makowski, L., Chaib, M. & Rathmell, J. C. Immunometabolism: from basic mechanisms to translation. *Immunol. Rev.* **295**, 5–14 (2020).
121. Motterlini, R. & Otterbein, L. E. The therapeutic potential of carbon monoxide. *Nat. Rev. Drug Discov.* **9**, 728–743 (2010).
122. Horio, T. et al. Donor heme oxygenase-1 promoter gene polymorphism predicts survival after unrelated bone marrow transplantation for high-risk patients. *Cancers* **12**, 424 (2020). **This study shows a polymorphism resulting in increased HO-1 expression leads to increased survival in patients undergoing bone marrow transplantations.**
123. Ryter, S. W. & Choi, A. M. K. Targeting heme oxygenase-1 and carbon monoxide for therapeutic modulation of inflammation. *Transl. Res.* **167**, 7–34 (2016).
124. Rueda, B. et al. HO-1 promoter polymorphism associated with rheumatoid arthritis. *Arthritis Rheum.* **56**, 3953–3958 (2007).
125. Yamada, N. et al. Microsatellite polymorphism in the heme oxygenase-1 gene promoter is associated with susceptibility to emphysema. *Am. J. Hum. Genet.* **66**, 187–195 (2000).
126. Takagi, T., Naito, Y., Uchiyama, K. & Yoshikawa, T. The role of heme oxygenase and carbon monoxide in inflammatory bowel disease. *Redox Rep.* **15**, 193–201 (2010).
127. Wang, W. P. et al. Protective role of heme oxygenase-1 on trinitrobenzene sulfonic acid-induced colitis in rats. *Am. J. Physiol. Liver Physiol.* **281**, G586–G594 (2001).
128. Takagi, T. et al. Heme oxygenase-1 prevents murine intestinal inflammation. *J. Clin. Biochem. Nutr.* **63**, 169–174 (2018).
129. Hegazi, R. A. F. et al. Carbon monoxide ameliorates chronic murine colitis through a heme oxygenase 1-dependent pathway. *J. Exp. Med.* **202**, 1703–1713 (2005).
130. Sheikh, S. Z. et al. An anti-inflammatory role for carbon monoxide and heme oxygenase-1 in chronic Th2-mediated murine colitis. *J. Immunol.* **186**, 5506–5513 (2011).
131. Vogel, M. E. & Zucker, S. D. Bilirubin acts as an endogenous regulator of inflammation by disrupting adhesion molecule-mediated leukocyte migration. *Inflamm. Cell Signal.* **3**, e1178 (2016).
132. Zheng, J.-D. et al. Unconjugated bilirubin alleviates experimental ulcerative colitis by regulating intestinal barrier function and immune inflammation. *World J. Gastroenterol.* **25**, 1865–1878 (2019).
133. Longhi, M. S. et al. Bilirubin suppresses Th17 immunity in colitis by upregulating CD39. *JCI Insight* **2**, e92791 (2017).
134. Wu, Y. et al. Heme protects intestinal mucosal barrier in DSS-induced colitis through regulating macrophage polarization in both HO-1-dependent and HO-1-independent way. *FASEB J.* **34**, 8028–8043 (2020).
135. Horváth, K. et al. The involvement of heme oxygenase-1 activity in the therapeutic actions of 5-aminosalicylic acid in rat colitis. *Eur. J. Pharmacol.* **581**, 315–323 (2008).
136. Kang, S. et al. Oxidized 5-aminosalicylic acid activates Nrf2-HO-1 pathway by covalently binding to Keap1: implication in anti-inflammatory actions of 5-aminosalicylic acid. *Free Radic. Biol. Med.* **108**, 715–724 (2017).
137. Tyrrell, R. M. & Reeve, V. E. Potential protection of skin by acute UVA irradiation — from cellular to animal models. *Prog. Biophys. Mol. Biol.* **92**, 86–91 (2006).
138. Hanselmann, C., Mauch, C. & Werner, S. Haem oxygenase-1: a novel player in cutaneous wound repair and psoriasis? *Biochem. J.* **353**, 459–466 (2001).
139. El-Rifaie, A.-A. A., Sabry, D., Doss, R. W., Kamal, M. A. & Abd El Hassib, D. M. Heme oxygenase and iron status in exosomes of psoriasis patients. *Arch. Dermatol. Res.* **310**, 651–656 (2018).
140. Ma, L. J., You, Y., Bai, B. X. & Li, Y.-Z. Therapeutic effects of heme oxygenase-1 on psoriasisform skin lesions in guinea pigs. *Arch. Dermatol. Res.* **301**, 459–466 (2009).
141. Zhang, B. et al. Heme oxygenase-1 induction attenuates imiquimod-induced psoriasisform inflammation by negative regulation of Stat3 signaling. *Sci. Rep.* **6**, 21132 (2016).
142. Nisar, M. F., Parsons, K. S. G., Bian, C. X. & Zhong, J. L. UVA irradiation induced heme oxygenase-1: a novel phototherapy for morphea. *Photochem. Photobiol.* **91**, 210–220 (2015).
143. Lehmann, J. C. U. et al. Dimethylfumarate induces immunosuppression via glutathione depletion and subsequent induction of heme oxygenase 1. *J. Invest. Dermatol.* **127**, 835–845 (2007).
144. Kasareho, K. et al. Effect of dimethyl fumarate on heme oxygenase-1 expression in experimental allergic encephalomyelitis in rats. *Folia Neuropathol.* **55**, 325–332 (2017).
145. Foresti, R. et al. Small molecule activators of the Nrf2-HO-1 antioxidant axis modulate heme metabolism and inflammation in BV2 microglia cells. *Pharmacol. Res.* **76**, 132–148 (2013).
146. Ghoreschi, K. et al. Fumarates improve psoriasis and multiple sclerosis by inducing type II dendritic cells. *J. Exp. Med.* **208**, 2291–2303 (2011).
147. Ogawa, T. et al. Nuclear factor erythroid 2-related factor 2 (Nrf2) regulates epidermal keratinization under psoriatic skin inflammation. *Am. J. Pathol.* **190**, 577–585 (2020).
148. Liu, Y. et al. Heme oxygenase-1 plays an important protective role in experimental autoimmune encephalomyelitis. *Neuroreport* **12**, 1841–1845 (2001).
149. Schipper, H. M. Heme oxygenase expression in human central nervous system disorders. *Free Radic. Biol. Med.* **37**, 1995–2011 (2004).
150. Chen, S.-J. et al. Erythropoietin enhances endogenous haem oxygenase-1 and represses immune responses to ameliorate experimental autoimmune encephalomyelitis. *Clin. Exp. Immunol.* **162**, 210–223 (2010).
151. Fagone, P. et al. Prevention of clinical and histological signs of proteolipid protein (PLP)-induced experimental allergic encephalomyelitis (EAE) in mice by the water-soluble carbon monoxide-releasing molecule (CORM)-A1. *Clin. Exp. Immunol.* **163**, 368–374 (2011).
152. Liu, Y. et al. Bilirubin as a potent antioxidant suppresses experimental autoimmune encephalomyelitis: implications for the role of oxidative stress in the development of multiple sclerosis. *J. Neuroimmunol.* **139**, 27–35 (2003).
153. Liu, Y., Liu, J., Tetzlaff, W., Paty, D. W. & Cynader, M. S. Biliverdin reductase, a major physiologic cytoprotectant, suppresses experimental autoimmune encephalomyelitis. *Free Radic. Biol. Med.* **40**, 960–967 (2006).
154. Sarady-Andrews, J. K. et al. Biliverdin administration protects against endotoxin-induced acute lung injury in rats. *Am. J. Physiol. Cell. Mol. Physiol.* **289**, L1131–L1137 (2005).
155. Di Pietro, C., Öz, H. H., Murray, T. S. & Bruscia, E. M. Targeting the heme oxygenase 1/carbon monoxide pathway to resolve lung hyper-inflammation and restore a regulated immune response in cystic fibrosis. *Front. Pharmacol.* **11**, 1059 (2020).
156. Ryter, S. W., Ma, K. C. & Choi, A. M. K. Carbon monoxide in lung cell physiology and disease. *Am. J. Physiol. Physiol.* **314**, C211–C227 (2018).
157. Rosas, I. O. et al. A phase II clinical trial of low-dose inhaled carbon monoxide in idiopathic pulmonary fibrosis. *Chest* **153**, 94–104 (2018).
158. Casanova, N. et al. Low Dose carbon monoxide exposure in idiopathic pulmonary fibrosis produces a CO signature comprised of oxidative phosphorylation genes. *Sci. Rep.* **9**, 1–8 (2019).
159. Du, Y. et al. Association among genetic polymorphisms of GSTP1, HO-1, and SOD-3 and chronic obstructive pulmonary disease susceptibility. *Int. J. Chron. Obstruct. Pulmon. Dis.* **14**, 2081–2088 (2019).
160. Fratta Pasini, A. M. et al. Oxidative stress and Nrf2 expression in peripheral blood mononuclear cells derived from COPD patients: an observational longitudinal study. *Respir. Res.* **21**, 37 (2020).
161. Harvey, C. J. et al. Targeting Nrf2 signaling improves bacterial clearance by alveolar macrophages in patients with COPD and in a mouse model. *Sci. Transl. Med.* **3**, 78ra32 (2011).
162. Bewley, M. A. et al. Opsonic phagocytosis in chronic obstructive pulmonary disease is enhanced by Nrf2 agonists. *Am. J. Respir. Crit. Care Med.* **198**, 739–750 (2018).
163. Cui, W. et al. Nrf2 attenuates inflammatory response in COPD/emphysema: crosstalk with Wnt3 $\alpha$ / $\beta$ -catenin and AMPK pathways. *J. Cell. Mol. Med.* **22**, 3514–3525 (2018).
164. Shinohara, T. et al. Adenovirus-mediated transfer and overexpression of heme oxygenase 1 cDNA in lungs attenuates elastase-induced pulmonary emphysema in mice. *Hum. Gene Ther.* **16**, 318–327 (2005).
165. Montuschi, P., Kharitonov, S. A. & Barnes, P. J. Exhaled carbon monoxide and nitric oxide in COPD. *Chest* **120**, 496–501 (2001).
166. Yasuda, H. et al. Increased arterial carboxyhemoglobin concentrations in chronic obstructive pulmonary disease. *Am. J. Respir. Crit. Care Med.* **171**, 1246–1251 (2005).
167. Bathoorn, E. et al. Anti-inflammatory effects of inhaled carbon monoxide in patients with COPD: a pilot study. *Eur. Respir. J.* **30**, 1131–1137 (2007). **This article reports a key clinical trial highlighting the therapeutic potential of inhaled CO to treat inflammatory lung diseases.**
168. Nakao, A. et al. Biliverdin protects the functional integrity of a transplanted synthetic small bowel. *Gastroenterology* **127**, 595–606 (2004).
169. Tang, L.-M. M. et al. Exogenous biliverdin ameliorates ischemia-reperfusion injury in small-for-size rat liver grafts. *Transplant. Proc.* **39**, 1338–1344 (2007).
170. Sugimoto, R. et al. Preservation solution supplemented with biliverdin prevents lung cold ischaemia/reperfusion injury. *Eur. J. Cardiothorac. Surg.* **42**, 1035–1041 (2012).
171. Yamashita, K. et al. Biliverdin, a natural product of heme catabolism, induces tolerance to cardiac allografts. *FASEB J.* **18**, 765–767 (2004).
172. Ozaki, K. S., Kimura, S. & Murase, N. Use of carbon monoxide in minimizing ischemia/reperfusion injury in transplantation. *Transplant. Rev.* **26**, 125–139 (2012).
173. Zhou, H. et al. Protection against lung graft injury from brain-dead donors with carbon monoxide, biliverdin, or both. *J. Heart Lung Transpl.* **30**, 460–466 (2011).
174. Nakao, A. et al. Protection against ischemia/reperfusion injury in cardiac and renal transplantation with carbon monoxide, biliverdin and both. *Am. J. Transplant.* **5**, 282–291 (2005).
175. Pileggi, A. et al. Heme oxygenase-1 induction in islet cells results in protection from apoptosis and improved in vivo function after transplantation. *Diabetes* **50**, 1983–1991 (2001).
176. Wang, H. et al. Donor treatment with carbon monoxide can yield islet allograft survival and tolerance. *Diabetes* **54**, 1400–1406 (2005).
177. Yi, T. et al. Activation of the nuclear erythroid 2-related factor 2 antioxidant responsive element (Nrf2-ARE) signaling pathway alleviates acute graft-versus-host disease by reducing oxidative stress and inhibiting infiltration of inflammatory cells in an allogeneic stem cell transplantation mouse model. *Med. Sci. Monit.* **24**, 5973–5979 (2018).
178. Bedard, E. L. R. et al. Peritransplant treatment with cobalt protoporphyrin attenuates chronic renal allograft rejection. *Transpl. Int.* **18**, 341–349 (2005).
179. Tsui, T. Y. et al. Prevention of chronic deterioration of heart allograft by recombinant adeno-associated



- virus-mediated heme oxygenase-1 gene transfer. *Circulation* **107**, 2623–2629 (2003).
180. Chauveau, C. et al. Gene transfer of heme oxygenase-1 and carbon monoxide delivery inhibit chronic rejection. *Am. J. Transpl.* **2**, 581–592 (2002).
181. Cory, H., Passarelli, S., Szeto, J., Tamez, M. & Mattei, J. The role of polyphenols in human health and food systems: a mini-review. *Front. Nutr.* **5**, 87 (2018).
182. Motterlini, R., Foresti, R., Bassi, R. & Green, C. J. Curcumin, an antioxidant and anti-inflammatory agent, induces heme oxygenase-1 and protects endothelial cells against oxidative stress. *Free Radic. Biol. Med.* **28**, 1303–1312 (2000).
183. Chen, C. Y., Jang, J. H., Li, M. H. & Surh, Y. J. Resveratrol upregulates heme oxygenase-1 expression via activation of NF-E2-related factor 2 in PC12 cells. *Biochem. Biophys. Res. Commun.* **331**, 993–1000 (2005).
184. Kim, Y. et al. Quercetin reduces tumor necrosis factor alpha-induced muscle atrophy by upregulation of heme oxygenase-1. *J. Med. Food* **21**, 551–559 (2018).
185. Funes, S. C. et al. Naturally derived heme-oxygenase 1 inducers and their therapeutic application to immune-mediated diseases. *Front. Immunol.* **11**, 1467 (2020). **This review provides a comprehensive overview of the therapeutic potential of naturally derived HO-1 inducers.**
186. Williamson, G. & Clifford, M. N. Role of the small intestine, colon and microbiota in determining the metabolic fate of polyphenols. *Biochem. Pharmacol.* **139**, 24–39 (2017).
187. Del Rio, D. et al. Dietary (poly)phenolics in human health: structures, bioavailability, and evidence of protective effects against chronic diseases. *Antioxid. Redox Signal.* **18**, 1818–1892 (2013).
188. Antiga, E. et al. Oral curcumin (Neriva) is effective as an adjuvant treatment and is able to reduce IL-22 serum levels in patients with Psoriasis vulgaris. *Biomed. Res. Int.* **2015**, 283634 (2015).
189. Kurd, S. K. et al. Oral curcumin in the treatment of moderate to severe psoriasis vulgaris: a prospective clinical trial. *J. Am. Acad. Dermatol.* **58**, 625–631 (2008).
190. Liu, X. et al. Dimethyl fumarate ameliorates dextran sulfate sodium-induced murine experimental colitis by activating Nrf2 and suppressing NLRP3 inflammasome activation. *Biochem. Pharmacol.* **112**, 37–49 (2016).
191. Nakayama, T. et al. Photoirradiation after aminolevulinic acid treatment suppresses cancer cell proliferation through the HO-1/p21 pathway. *Photodiagnosis Photodyn. Ther.* **28**, 10–17 (2019).
192. Hou, J. et al. 5-Aminolevulinic acid with ferrous iron induces permanent cardiac allograft acceptance in mice via induction of regulatory cells. *J. Heart Lung Transpl.* **34**, 254–263 (2015).
193. Narimiya, T. et al. Nrf2 activation in osteoblasts suppresses osteoclastogenesis via inhibiting IL-6 expression. *Bone Rep.* **11**, 100228 (2019).
194. Yan, S. C. et al. Dihydroartemisinin regulates the Th/Treg balance by inducing activated CD4+ T cell apoptosis via heme oxygenase-1 induction in mouse models of inflammatory bowel disease. *Molecules* **24**, 2475 (2019).
195. Lin, C.-C., Yang, C.-C., Hsiao, L.-D., Chen, S.-Y. & Yang, C.-M. Heme oxygenase-1 induction by carbon monoxide releasing molecule-3 suppresses interleukin-1 $\beta$ -mediated neuroinflammation. *Front. Mol. Neurosci.* **10**, 387 (2017).
196. Song, L. et al. Carbon monoxide-releasing molecule suppresses inflammatory and osteoclastogenic cytokines in nicotine- and lipopolysaccharide-stimulated human periodontal ligament cells via the heme oxygenase-1 pathway. *Int. J. Mol. Med.* **40**, 1591–1601 (2017).
197. Mangano, K. et al. Involvement of the Nrf2/HO-1/CO axis and therapeutic intervention with the CO-releasing molecule CORM-A1, in a murine model of autoimmune hepatitis. *J. Cell. Physiol.* **233**, 4156–4165 (2018).
198. Takagi, T. et al. Carbon monoxide ameliorates murine T-cell-dependent colitis through the inhibition of Th17 differentiation. *Free Radic. Res.* **52**, 1328–1335 (2018).
199. Ji, X. et al. Toward carbon monoxide-based therapeutics: critical drug delivery and developability issues. *J. Pharm. Sci.* **105**, 406–416 (2016).
200. El Ali, Z. et al. Therapeutic effects of CO-releaser/Nrf2 activator hybrids (HYCOs) in the treatment of skin wound, psoriasis and multiple sclerosis. *Redox Biol.* **34**, 101521 (2020). **This is an important study examining the therapeutic potential of hybrid CO-releasing molecules for a number of inflammatory diseases.**
201. Motterlini, R. et al. HYCO-3, a dual CO-releaser/Nrf2 activator, reduces tissue inflammation in mice challenged with lipopolysaccharide. *Redox Biol.* **20**, 334–348 (2019).
202. Bambouskova, M. et al. Electrophilic properties of itaconate and derivatives regulate the I $\kappa$ B/NF- $\kappa$ B inflammatory axis. *Nature* **556**, 501–504 (2018).
203. Tang, C. et al. 4-Octyl itaconate activates Nrf2 signaling to inhibit pro-inflammatory cytokine production in peripheral blood mononuclear cells of systemic lupus erythematosus patients. *Cell. Physiol. Biochem.* **51**, 979–990 (2018).
204. Davies, T. G. et al. Monoacidic inhibitors of the Kelch-like ECH-associated protein 1: nuclear factor erythroid 2-related factor 2 (KEAP1:NRF2) protein-protein interaction with high cell potency identified by fragment-based discovery. *J. Med. Chem.* **59**, 3991–4006 (2016).
205. Campbell, N. K. et al. Trypanosoma brucei secreted aromatic ketoacids activate the Nrf2/HO-1 pathway and suppress pro-inflammatory responses in primary murine glia and macrophages. *Front. Immunol.* **10**, 2137 (2019).
206. McGettrick, A. F. et al. Trypanosoma brucei metabolite indolepyruvate decreases HIF-1 $\alpha$  and glycolysis in macrophages as a mechanism of innate immune evasion. *Proc. Natl Acad. Sci. USA* **113**, E7778–E7787 (2016).
207. Schulz, S., Wong, R. J., Vreman, H. J. & Stevenson, D. K. Metalloporphyrins - an update. *Front. Pharmacol.* **3**, 68 (2012).
208. Mucha, O. et al. Pharmacological versus genetic inhibition of heme oxygenase-1 - the comparison of metalloporphyrins, shRNA and CRISPR/Cas9 system. *Acta Biochim. Pol.* **65**, 277–286 (2018). **This article compares a number of methods to inhibit HO-1, with relevance to experimental modulation of HO-1 and development of therapeutic HO-1 inhibitors.**
209. Lian, K.-C. et al. Dual mechanisms of NF- $\kappa$ B inhibition in carnosol-treated endothelial cells. *Toxicol. Appl. Pharmacol.* **245**, 21–35 (2010).
210. Serra, D., Almeida, L. M. & Dinis, T. C. P. Anti-inflammatory protection afforded by cyanidin-3-glucoside and resveratrol in human intestinal cells via Nrf2 and PPAR- $\gamma$ : comparison with 5-aminosalicylic acid. *Chem. Biol. Interact.* **260**, 102–109 (2016).
211. Wang, G. et al. Resveratrol ameliorates rheumatoid arthritis via activation of SIRT1-Nrf2 signaling pathway. *Biofactors* **46**, 441–453 (2020).
212. Ju, S. et al. Dietary quercetin ameliorates experimental colitis in mouse by remodeling the function of colonic macrophages via a heme oxygenase-1-dependent pathway. *Cell Cycle* **17**, 53–63 (2018).
213. Guazelli, C. F. S. et al. Quercetin attenuates zymosan-induced arthritis in mice. *Biomed. Pharmacother.* **102**, 175–184 (2018).
214. Yang, Y. et al. Quercetin attenuates collagen-induced arthritis by restoration of Th17/Treg balance and activation of heme oxygenase 1-mediated anti-inflammatory effect. *Int. Immunopharmacol.* **54**, 153–162 (2018).
215. Wagner, A. E. et al. DSS-induced acute colitis in C57BL/6 mice is mitigated by sulfuraphane pre-treatment. *J. Nutr. Biochem.* **24**, 2085–2091 (2013).
216. Li, B. et al. Sulfuraphane ameliorates the development of experimental autoimmune encephalomyelitis by antagonizing oxidative stress and Th17-related inflammation in mice. *Exp. Neurol.* **250**, 239–249 (2013).
217. Geisel, J. et al. Sulfuraphane protects from T cell-mediated autoimmune disease by inhibition of IL-23 and IL-12 in dendritic cells. *J. Immunol.* **192**, 3530–3539 (2014).
218. Ganz, T. Macrophages and systemic iron homeostasis. *J. Innate Immun.* **4**, 446–453 (2012).
219. Dixon, S. J. et al. Ferroptosis: an iron-dependent form of nonapoptotic cell death. *Cell* **149**, 1060–1072 (2012).
220. Korolnek, T. & Hamza, I. Macrophages and iron trafficking at the birth and death of red cells. *Blood* **125**, 2893–2897 (2015).
221. Theurl, I. et al. On-demand erythrocyte disposal and iron recycling requires transient macrophages in the liver. *Nat. Med.* **22**, 945–951 (2016).
222. Kovtunovich, G., Eckhaus, M. A., Ghosh, M. C., Ollivierre-Wilson, H. & Rouault, T. A. Dysfunction of the heme recycling system in heme oxygenase 1-deficient mice: effects on macrophage oxygenase and tissue iron distribution. *Blood* **116**, 6054–6062 (2010).
223. Poss, K. D. & Tonegawa, S. Heme oxygenase 1 is required for mammalian iron reutilization. *Proc. Natl Acad. Sci. USA* **94**, 10919–10924 (1997).
224. Sukhbaatar, N. & Weichhart, T. Iron regulation: macrophages in control. *Pharmaceuticals* **11**, 137 (2018).
225. Exner, M., Minar, E., Wagner, O. & Schillinger, M. The role of heme oxygenase-1 promoter polymorphisms in human disease. *Free Radic. Biol. Med.* **37**, 1097–1104 (2004).
226. Soares, M. P. & Bach, F. H. Heme oxygenase-1: from biology to therapeutic potential. *Trends Mol. Med.* **15**, 50–58 (2009).
227. Lin, Q. et al. Heme oxygenase-1 protein localizes to the nucleus and activates transcription factors important in oxidative stress. *J. Biol. Chem.* **282**, 20621–20633 (2007).
228. Biswas, C. et al. Nuclear heme oxygenase-1 (HO-1) modulates subcellular distribution and activation of Nrf2, impacting metabolic and anti-oxidant defenses. *J. Biol. Chem.* **289**, 26882–26894 (2014).
229. Stocker, R., Yamamoto, Y., McDonagh, A. F., Glazer, A. N. & Ames, B. N. Bilirubin is an antioxidant of possible physiological importance. *Science* **235**, 1043–1046 (1987).
230. Barañano, D. E. et al. Biliverdin reductase: a major physiologic cytoprotectant. *Proc. Natl Acad. Sci. USA* **99**, 16093–16098 (2002).
231. Sedlak, T. W. et al. Bilirubin and glutathione have complementary antioxidant and cytoprotective roles. *Proc. Natl Acad. Sci. USA* **106**, 5171–5176 (2009).
232. Jansen, T. & Daiber, A. Direct antioxidant properties of bilirubin and biliverdin. Is there a role for biliverdin reductase? *Front. Pharmacol.* **3**, 30 (2012).
233. Canesin, G., Hejazi, S. M., Swanson, K. D. & Wegiel, B. Heme-derived metabolic signals dictate immune responses. *Front. Immunol.* **11**, 66 (2020).
234. Kim, K. M. et al. Carbon monoxide induces heme oxygenase-1 via activation of protein kinase R-like endoplasmic reticulum kinase and inhibits endothelial cell apoptosis triggered by endoplasmic reticulum stress. *Circ. Res.* **101**, 919–927 (2007).
235. Yang, Y.-C. C., Huang, Y.-T. T., Hsieh, C.-W. W., Yang, P.-M. M. & Wung, B.-S. S. Carbon monoxide induces heme oxygenase-1 to modulate STAT3 activation in endothelial cells via S-glutathionylation. *PLoS ONE* **9**, e100677 (2014).
236. Chiang, N. et al. Inhaled carbon monoxide accelerates resolution of inflammation via unique proresolving mediator-heme oxygenase-1 circuits. *J. Immunol.* **190**, 6378–6388 (2013).

**Acknowledgements**

The authors acknowledge support from the Health Research Board (ILP-POR-2017-041), Ireland.

**Author contributions**

N.K.C, H.K.F and A.D conceptualized the article. N.K.C and H.K.F prepared the manuscript and figures together. All authors contributed equally to the revision and editing of the submitted article.

**Competing interests**

The authors declare no competing interests.

**Peer review information**

*Nature Reviews Immunology* thanks E. Bruscia, C. Di Pietro, J. S. Lee and the other, anonymous, reviewer(s) for their contribution to the peer review of this work.

**Publisher's note**

Springer Nature remains neutral with regard to jurisdictional claims in published maps and institutional affiliations.

© Springer Nature Limited 2021



## Article

# The *Trypanosoma brucei*-Derived Ketoacids, Indole Pyruvate and Hydroxyphenylpyruvate, Induce HO-1 Expression and Suppress Inflammatory Responses in Human Dendritic Cells

Hannah K. Fitzgerald <sup>1</sup>, Sinead A. O'Rourke <sup>1,2</sup>, Eva Desmond <sup>1</sup>, Nuno G. B. Neto <sup>2</sup>, Michael G. Monaghan <sup>2</sup>, Miriam Tosetto <sup>3</sup>, Jayne Doherty <sup>3</sup>, Elizabeth J. Ryan <sup>4</sup>, Glen A. Doherty <sup>3</sup>, Derek P. Nolan <sup>1</sup>, Jean M. Fletcher <sup>1,5,†</sup> and Aisling Dunne <sup>1,5,\*,†</sup>

<sup>1</sup> School of Biochemistry and Immunology, Trinity Biomedical Sciences Institute, Trinity College Dublin, D02 R590 Dublin, Ireland; hfitzge@tcd.ie (H.K.F.); siorourk@tcd.ie (S.A.O.); evadesmond@gmail.com (E.D.); DENOLAN@tcd.ie (D.P.N.); Fletchj@tcd.ie (J.M.F.)

<sup>2</sup> Trinity Centre for Biomedical Engineering, Trinity Biomedical Sciences Institute, Trinity College Dublin, D02 R590 Dublin, Ireland; neton@tcd.ie (N.G.B.N.); monaghmi@tcd.ie (M.G.M.)

<sup>3</sup> Centre for Colorectal Disease, St. Vincent's University Hospital, School of Medicine, University College Dublin, D04 YN26 Dublin, Ireland; mtosetto@ucd.ie (M.T.); Jayne.Doherty@svph.ie (J.D.); gdoherty@svhg.ie (G.A.D.)

<sup>4</sup> Department of Biological Sciences, Health Research Institute, University of Limerick, V94 T9PX Limerick, Ireland; Elizabeth.Ryan@ul.ie

<sup>5</sup> School of Medicine, Trinity Biomedical Sciences Institute, Trinity College Dublin, D02 R590 Dublin, Ireland

\* Correspondence: aidunne@tcd.ie

† These authors contributed equally to this work.



**Citation:** Fitzgerald, H.K.; O'Rourke, S.A.; Desmond, E.; Neto, N.G.B.; Monaghan, M.G.; Tosetto, M.; Doherty, J.; Ryan, E.J.; Doherty, G.A.; Nolan, D.P.; et al. The *Trypanosoma brucei*-Derived Ketoacids, Indole Pyruvate and Hydroxyphenylpyruvate, Induce HO-1 Expression and Suppress Inflammatory Responses in Human Dendritic Cells. *Antioxidants* **2022**, *11*, 164. <https://doi.org/10.3390/antiox11010164>

Academic Editors: Elias Lianos and Maria G. Detsika

Received: 20 December 2021

Accepted: 12 January 2022

Published: 15 January 2022

**Publisher's Note:** MDPI stays neutral with regard to jurisdictional claims in published maps and institutional affiliations.



**Copyright:** © 2022 by the authors. Licensee MDPI, Basel, Switzerland. This article is an open access article distributed under the terms and conditions of the Creative Commons Attribution (CC BY) license (<https://creativecommons.org/licenses/by/4.0/>).

**Abstract:** The extracellular parasite and causative agent of African sleeping sickness *Trypanosoma brucei* (*T. brucei*) has evolved a number of strategies to avoid immune detection in the host. One recently described mechanism involves the conversion of host-derived amino acids to aromatic ketoacids, which are detected at relatively high concentrations in the bloodstream of infected individuals. These ketoacids have been shown to directly suppress inflammatory responses in murine immune cells, as well as acting as potent inducers of the stress response enzyme, heme oxygenase 1 (HO-1), which has proven anti-inflammatory properties. The aim of this study was to investigate the immunomodulatory properties of the *T. brucei*-derived ketoacids in primary human immune cells and further examine their potential as a therapy for inflammatory diseases. We report that the *T. brucei*-derived ketoacids, indole pyruvate (IP) and hydroxyphenylpyruvate (HPP), induce HO-1 expression through Nrf2 activation in human dendritic cells (DC). They also limit DC maturation and suppress the production of pro-inflammatory cytokines, which, in turn, leads to a reduced capacity to differentiate adaptive CD4<sup>+</sup> T cells. Furthermore, the ketoacids are capable of modulating DC cellular metabolism and suppressing the inflammatory profile of cells isolated from patients with inflammatory bowel disease. This study therefore not only provides further evidence of the immune-evasion mechanisms employed by *T. brucei*, but also supports further exploration of this new class of HO-1 inducers as potential therapeutics for the treatment of inflammatory conditions.

**Keywords:** heme oxygenase 1; *Trypanosoma brucei*; inflammatory bowel disease; aromatic ketoacids; dendritic cells; immunomodulation; anti-inflammatory therapies

## 1. Introduction

Infection of the mammalian vasculature and central nervous system (CNS) with the extracellular protozoan parasite *Trypanosoma brucei* (*T. brucei*) can lead to fatal human sleeping sickness, also known as African trypanosomiasis. Like most parasites, trypanosomes are continuously challenged by the host-immune system, however, they have evolved very effective evasion strategies in order to maintain infection and prolong the host's survival [1].

An infection with *T. brucei* is accompanied by the excretion of high levels of ketoacids into the host's bloodstream [2,3], a phenomenon that was, until recently, largely unexplained. The ketoacids are derived from the conversion of aromatic amino acids (tryptophan, tyrosine, and phenylalanine) to indole pyruvate (IP), hydroxyphenylpyruvate (HPP), and phenyl pyruvate (PP), through the action of a cytoplasmic aspartate aminotransferase (TbcASAT), which is expressed by the parasite.

In recent years, we, and others, have demonstrated that these molecules have potent immunomodulatory properties, which likely contribute to the suppression of host immune responses, but that may also be exploited for potential therapeutic benefit [4–8]. For example, IP and HPP are potent inducers of the immunosuppressive enzyme heme oxygenase-1 (HO-1) in murine glia and macrophages [5]. This occurs in a nuclear factor (erythroid-derived 2)-like 2 (Nrf2) dependent manner and leads to a reduction in LPS-induced pro-inflammatory cytokines and innate immune cell maturation. Indeed, HO-1 has well established anti-inflammatory properties and is induced by a vast number of stimuli during oxidative stress and inflammation. It catalyses the conversion of heme to biliverdin with the liberation of free iron and carbon monoxide (CO). Biliverdin is then converted to bilirubin by biliverdin reductase [9,10] and both biliverdin and bilirubin are considered powerful antioxidants, while many of the anti-inflammatory effects of HO-1 are attributed to CO. The potent anti-inflammatory properties of HO-1 are underlined by rare HO-deficiencies in humans and HO-1 knockout mice, which, along with the expected sensitivity to oxidative stress, show high levels of chronic inflammation [11–13]. Unsurprisingly, induction of HO-1 with known and novel HO-1 inducers is now being explored as a therapy for a number of autoimmune and inflammatory diseases and we have recently reviewed this in detail elsewhere [14].

In addition to HO-1 induction, *T. brucei*-derived ketoacids are also capable of inhibiting HIF-1 $\alpha$ -induced pro-IL-1 $\beta$  expression, as well as prostaglandin production, an effect which was shown to be dependent on the activation of the aryl hydrocarbon receptor [4,5,8]. The immunomodulatory effects of IP and HPP have also been confirmed in animal models of disease. In a murine model of skin damage caused by exposure to ultraviolet B radiation, administration of IP resulted in a reduction in damage lesions and expression of the pro-inflammatory cytokines, IL-1 $\beta$  and IL-6 [6]. Furthermore, IP administration reduced disease severity in the DSS colitis model, and this was accompanied by a decrease in the expression of pro-inflammatory cytokines IL-12, TNF, IFN $\gamma$ , and IL-1 $\beta$ , and an increase in the expression of the anti-inflammatory cytokine IL-10 [7]. A reduction in Th1 cells, as well as a reduced capacity for dendritic cells (DC) to activate T cells, was also observed [7].

Despite the recent interest in these ketoacids as immunomodulators, to date, they have been primarily studied in murine immune cells with very little evidence to support their mechanism of action in human immune cells. In this study, we investigate the immunomodulatory properties of the *T. brucei*-derived ketoacids, IP and HPP, in primary human immune cells and further examine their potential as a therapy for inflammatory diseases.

## 2. Materials and Methods

### 2.1. Reagents and Chemicals

4-hydroxyphenylpyruvic acid (HPP) and indole-3-pyruvic acid (IP) were purchased from Merck (Darmstadt, Germany) and dissolved in RPMI to a final concentration of 2 mM before use. Ultrapure lipopolysaccharide (LPS) from *E. Coli* O111:B4 was purchased from Enzo Life Sciences (Bruxelles, Belgium). Complete RPMI or complete IMDM were prepared by supplementing with 10% foetal bovine serum (FBS), 2 mM L-glutamine, 100 U/mL penicillin, and 100  $\mu$ g/mL streptomycin, which were all purchased from Merck (Darmstadt, Germany). Lymphoprep is manufactured by Axis-Shield poC (Dundee, Scotland). GM-CSF and IL-4 were purchased from Miltenyi Biotec (Bergisch Gladbach, Germany). The protease inhibitor cocktail and High-Pure RNA Isolation Kit were purchased from Roche (Basel, Switzerland). The western blot antibodies for Nrf2, HK2, p-AMPK, t-AMPK, p62 and LC3 were all purchased from Cell Signalling Technology (Danvers, MA, USA), while

the antibody for HO-1 was purchased from Enzo Life Sciences (Bruxelles, Belgium), and the  $\beta$ -actin antibody and secondary anti-rabbit were purchased from Merck (Darmstadt, Germany). The Fixable Viability Dye, antibodies for CD40, CD80, CD83, and CD86, and Annexin V & PI staining kit were all purchased from eBioscience (San Diego, CA, USA). The DQ-Ovalbumin, CD3 and IL-17 flow antibodies, FIX & PERM™ Cell Permeabilization Kit, anti-CD3, and all ELISA kits used were purchased from Invitrogen (Waltham, MA, USA). The High-Capacity cDNA reverse transcription kit was purchased from Applied Biosystems (Beverly, MA, USA) and the iTaq Universal SYBR Green mastermix from Bio-Rad (Hercules, CA, USA). The MagniSort Human CD14 Positive Selection kit and MagniSort Human CD4 T cell Positive Selection kit were purchased from Thermo Fisher Scientific (Waltham, MA, USA). The Zombie NIR™ Fixable Viability kit was purchased from BioLegend (San Diego, CA, USA). The antibodies for CD8, ki67 and IFN $\gamma$  were purchased from BD biosciences (East Rutherford, NJ, USA). The Complete XF assay medium was purchased from Agilent (Santa Clara, CA, USA). The Corning™ Cell-Tak Cell and Tissue Adhesive was purchased from Fisher Scientific (Waltham, MA, USA). Oligomycin was purchased from Cayman Chemicals (Ann Arbor, MI, USA) and carbonyl cyanide-p trifluoromethoxyphenylhydrazone (FCCP) from Santa Cruz biotechnology (Dallas, TX, USA). The HEK-Blue™ hTLR4 assay system was purchased from InvivoGen (San Diego, CA, USA). Dulbecco's phosphate buffered saline (PBS), enhanced chemiluminescent substrate, phosphatase inhibitor cocktail, Antioxidant assay kit, Phorbol 12-myristate 13-acetate (PMA), ionomycin, brefeldin A, rotenone, antimycin A, and 2-deoxy-D-glucose (2-DG) were all purchased from Merck (Darmstadt, Germany).

## 2.2. Human Blood Samples

The Irish Blood Transfusion Service (IBTS) at St. James's Hospital in Dublin supplied leukocyte-enriched buffy coats for these studies, from donors who provided informed written consent. Ethical approval was obtained from the research ethics committee of the School of Biochemistry and Immunology at Trinity College Dublin, and all experiments were carried out in accordance with the Declaration of Helsinki. Peripheral blood mononuclear cells (PBMC) were isolated by a density gradient centrifugation. The cells were cultured in complete RPMI medium and maintained in humidified incubators at 37 °C with 5% CO<sub>2</sub>.

## 2.3. Dendritic Cell Culture

The MagniSort Human CD14 Positive Selection kit was used according to the manufacturer's protocol to positively select for CD14<sup>+</sup> monocytes from PBMC. CD14<sup>+</sup> monocytes were then cultured at  $1 \times 10^6$  cells/mL in complete RPMI and supplemented with GM-CSF (50 ng/mL) and IL-4 (40 ng/mL) to generate monocyte-derived DC. On day three of culture, half of the media was replaced with fresh media supplemented with cytokines at the same starting concentration. On day six, non-adherent and loosely adherent cells were gently removed for use. The purity of CD14<sup>lo</sup>DC-SIGN<sup>+</sup> DC was confirmed by flow cytometry and was routinely >95%. DC were cultured at  $1 \times 10^6$  cells/mL for all further assays.

## 2.4. Western Blot Experiments

For detection of HO-1 expression, DC were cultured in the presence of HPP or IP (250–1000  $\mu$ M) for 3, 6, and 24 h, or treated with the Nrf2 inhibitor ML385 (10  $\mu$ M) for 1 h prior to treatment with HPP or IP at 1000  $\mu$ M for 24 h. Cell lysates were prepared by washing cells in PBS prior to lysis in RIPA buffer (Tris 50 mM; NaCl 150 mM; SDS 0.1%; Na.Deoxycholate 0.5%; Triton X 100). For detection of Nrf2 expression, DC were cultured in the presence of HPP (1000  $\mu$ M) or IP (1000  $\mu$ M) for 6 or 24 h, then washed in PBS and lysed in Laemmli loading buffer. For detection of hexokinase 2 (HK2) expression, DC were cultured in the presence of HPP or IP at 1000  $\mu$ M for 6 h prior to stimulation with LPS (100 ng/mL) for 12 h, then washed in PBS and lysed in Laemmli loading buffer. For detection of p-AMPK and t-AMPK expression, DC were cultured in the presence of

HPP or IP (both 1000  $\mu\text{M}$ ) for 15 min, then washed in PBS and lysed in Laemmli loading buffer. For the detection of p62 and LC3, DC were cultured in the presence of HPP or IP (both 1000  $\mu\text{M}$ ) for 6, 12, or 24 h, then washed in PBS, lysed in Laemmli loading buffer, and sonicated. All samples were lysed in the presence of a protease inhibitor cocktail and phosphatase inhibitor cocktail set. Samples were electrophoresed and transferred to PVDF. The membranes were incubated overnight at 4 °C with monoclonal antibodies specific for HO-1, Nrf2, HK2, p-AMPK, t-AMPK, p62, and LC3. The membranes were washed in TBS–Tween prior to incubation with an anti-rabbit streptavidin-conjugated secondary antibody for 2 h at room temperature. A Bio-Rad ChemiDoc MP system was used for developing the blots. The membranes were subsequently re-probed with a loading control,  $\beta$ -actin, in order to normalise the protein of interest to the loading control for densitometric analysis.

### 2.5. Antioxidant Assay

DC were cultured in the presence of IP or HPP (both 1000  $\mu\text{M}$ ) for 1 h. The cells were lysed by sonication in ice-cold PBS and centrifuged at 14,000 rpm for 10 min to pellet any debris. The total antioxidant capacity of the cells was analysed using an Antioxidant assay kit according to the manufacturer’s protocol. The assay measures the reduction of  $\text{Cu}^{2+}$  by an antioxidant to  $\text{Cu}^+$ , which can subsequently form a coloured complex with a dye reagent in the kit. The absorbances of the samples were read at 570 nm and compared to the absorbances of a range of known concentrations of Trolox standards. The data is displayed as the total antioxidant capacity of the cells expressed as an equivalent concentration of Trolox ( $\mu\text{M}$ ).

### 2.6. DC Flow Cytometry Experiments

DC were collected upon completion of the experiment, washed in PBS, and stained accordingly. DC were stained using an Annexin V & PI staining kit according to the manufacturer’s protocol for viability assays. For the maturation marker assay, DC were initially stained with Fixable Viability Dye, for dead cells, and subsequently with fluorochrome-conjugated antibodies for CD40, CD80, CD83, and CD86. In order to measure the phagocytic capacity, DC were incubated with RPMI-containing DQ-Ovalbumin (500 ng/mL) for 20 min at 37 °C, before transferring to 4 °C for a further 10 min incubation to stop the uptake of the model antigen. DC were then washed in PBS and immediately acquired. All of the above experiments were acquired on a BD FACS Canto II, and the analysis was performed using FlowJo v.10 software (Tree Star Inc., Ashland, OR, USA).

### 2.7. Quantitative Real-Time PCR

DC were cultured in the presence of HPP or IP (both 1000  $\mu\text{M}$ ) for 6 or 24 h. Detection of NAD(P)H dehydrogenase (quinone 1) (NQO1, accession number P15559) expression and glutathione reductase (GSR, accession number P00390) expression were measured using quantitative real-time PCR. RNA was first extracted using the High-Pure RNA Isolation Kit, followed by cDNA synthesis using the High-Capacity cDNA reverse transcription kit. iTaq Universal SYBR Green mastermix was used in the reaction along with relevant primers—the sequences are listed in Table 1. A Bio-Rad CFX96 Real-Time System was used to carry out the reaction. mRNA expression levels for genes of interest were quantified and normalized to the housekeeping ( $\beta$ -actin) mRNA levels.

**Table 1.** Primer sequences. Table containing the forward and reverse primer sequences for NQO1, GSR, and  $\beta$ -actin.

Gene	Forward Primer	Reverse Primer
NQO1	5' TGAAGAAGAAAGGATGGGAG 3'	5' TTTACCTGTGATGTCCTTTC 3'
GSR	5' GACCTATTCAACGAGCTTTAC 3'	5' CAACCACCTTTTCTTCCTTG 3'
$\beta$ -actin	5' GGACTTCGAGCAAGAGATGG 3'	5' AGCACTGTGTTGGCGTACAG 3'

### 2.8. DC ELISA Experiments

For detection of cytokines, DC were cultured in the presence of HPP or IP (500–1000  $\mu\text{M}$ ) for 6 h prior to stimulation with LPS (100 ng/mL) for 24 h. Concentrations of IL-12p70, IL-23, TNF, IL-6, and IL-10 were quantified from supernatants by ELISA as per the manufacturers' protocols.

### 2.9. DC-CD4<sup>+</sup> T Cell Co-Cultures

The MagniSort Human CD4 T cell Positive Selection kit was used according to the manufacturer's protocol to isolate CD4<sup>+</sup> T cells from PBMC. CD4<sup>+</sup> T cells were co-cultured with allogeneic DC that had been pre-treated with IP or HPP and stimulated with LPS as before. The cells were co-cultured at a ratio of 10:1 T cells to DC for five days with no ketoacid present. The supernatants were removed for analysis of IL-10 by ELISA prior to restimulation of the cells in complete RPMI in the presence of 50 ng/mL PMA, 500 ng/mL ionomycin, and 5  $\mu\text{g}/\text{mL}$  brefeldin A for 4 h. The cells were washed in PBS and stained for viability (Zombie NIR<sup>TM</sup> Fixable Viability kit) for 15 min at room temperature. The cells were then washed again in PBS and stained with fluorochrome-conjugated antibodies for surface markers CD3 and CD8 for 15 min at room temperature. The cells were then washed and fixed (FIX & PERM<sup>TM</sup> Cell Permeabilization Kit) for 15 min at room temperature. Finally, the cells were washed and stained for intracellular markers Ki67 and IFN $\gamma$  in permeabilization buffer for 15 min at room temperature. A BD LSRFortessa flow cytometer was used to acquire samples, and analysis was performed using FlowJo v.10 software.

### 2.10. Two-Photon Fluorescence Lifetime Imaging Microscopy (FLIM)

DC were cultured in the presence of HPP (1000  $\mu\text{M}$ ) for 6 h prior to stimulation with LPS (100 ng/mL) for 12 h. Two-photon excited NAD(P)H- Fluorescence Lifetime Imaging Microscopy (FLIM) was used to measure the levels of free and protein-bound NADH within these cells, and was performed on a custom multiphoton system (further details regarding experimental setup can be found at the following [15,16]). At least three images for each model were acquired. Afterwards, regions of interest (ROI) were selected, and the NAD(P)H fluorescence decay was analysed.

For the NAD(P)H fluorescence decay analysis, an overall decay curve was generated by the contribution of all pixels in the ROI area. Afterwards, it was fitted with a double exponential decay curve (Equation (1)):

$$I(t) = \alpha_1 e^{-\frac{t}{\tau_1}} + \alpha_2 e^{-\frac{t}{\tau_2}} + c \quad (1)$$

$I(t)$  represents the fluorescence intensity at time ( $t$ ) after laser excitation.  $\alpha_1$  and  $\alpha_2$  represent the fraction of the overall signal comprised of a short and long lifetime component, respectively.  $\tau_1$  and  $\tau_2$  are the long and short lifetime components, respectively.  $C$  corresponds to background light.  $\chi^2$  is calculated to evaluate the goodness of multi-exponential fit to the raw fluorescence decay data—the lowest  $\chi^2$  values were considered in this study.

For NAD(P)H, a two-component fit was used to differentiate between the free ( $\tau_1$ ) and protein-bound ( $\tau_2$ ) NAD(P)H. The average lifetime ( $\tau_{avg}$ ) of NAD(P)H for each pixel is calculated by a weighted average of both the free and bound lifetime contributions (Equation (2)):

$$\tau_{avg} = \frac{(\alpha_1 \times \tau_1) + (\alpha_2 \times \tau_2)}{(\alpha_1 + \alpha_2)} \quad (2)$$

### 2.11. Metabolic Profiling Using Seahorse Analysis

DC were cultured in the presence of IP or HPP (both 1000  $\mu\text{M}$ ) for 6 h prior to stimulation with LPS (100 ng/mL) for 12 h. The cell culture medium was replaced with complete XF assay medium (pH of 7.4, supplemented with 10 mM glucose, 1 mM sodium pyruvate, 2 mM L-glutamine) and DC were then transferred at a density of  $2 \times 10^5$

cells/well to a Seahorse 96-well microplate, which was coated with Corning™ Cell-Tak Cell and Tissue Adhesive and incubated in a non-CO<sub>2</sub> incubator. Blank wells were prepared containing XF assay medium only to subtract the background oxygen consumption rate (OCR) and extracellular acidification rate (ECAR) during analysis. Oligomycin (1 mM), FCCP (1 mM), rotenone (500 nM), antimycin A (500 nM), and 2-DG (25 mM) were prepared in XF assay medium. Inhibitors were loaded into the appropriate injection ports on the cartridge plate and incubated for 10 min in a non-CO<sub>2</sub> incubator at 37 °C. Oligomycin, FCCP, rotenone and antimycin A, and 2-DG were sequentially injected while the OCR and ECAR readings were simultaneously measured. Wave software (Agilent Technologies, Santa Clara, CA, USA) was used to analyse the results. The rates of basal glycolysis, max glycolysis, glycolytic reserve, basal respiration, max respiration, and respiratory reserve were calculated as detailed in the manufacturer's protocol and as supplied in Supplementary Table S1.

### 2.12. IBD Patient PBMC Experiments

This study received ethical approval from St Vincent's University Hospital Ethics and Medical Research Committee to take blood samples from consenting patients ( $N = 14$ ) attending a specialist outpatient clinic for inflammatory bowel disease (IBD). PBMC were isolated as above and frozen at  $-80$  °C. PBMC were thawed and treated with either IP or HPP (250–1000  $\mu$ M) for 6 h prior to stimulation with anti-CD3 (1  $\mu$ g/mL) for 12 h. The media was then removed and replaced with fresh media to circumvent issues that occur as the compounds become fluorescent after incubations over long periods of time, and cells were maintained in the presence of anti-CD3 for a further four days. The supernatants were then removed for analysis of IL-10, IFN $\gamma$ , and IL-17A by ELISA. PBMC were restimulated in complete IMDM medium in the presence of 50 ng/mL PMA, 500 ng/mL ionomycin, and 5  $\mu$ g/mL brefeldin A for 4 h. The cells were washed in PBS and stained for viability (Zombie NIR™ Fixable Viability kit) for 15 min at room temperature. The cells were then washed in PBS and stained with fluorochrome-conjugated antibodies for surface markers CD3 and CD8 for 15 min at room temperature. After this, the cells were then washed and fixed (FIX & PERM™ Cell Permeabilization Kit) for 15 min at room temperature. Finally, the cells were washed and stained for intracellular markers Ki67, IFN $\gamma$  and IL-17 in permeabilization buffer for 15 min at room temperature. The cells were then washed and acquired on a BD LSRFortessa flow cytometer. The analysis was performed with FlowJo v.10. All antibodies used in this experiment were chosen carefully to avoid channels which still had some fluorescence issues, despite the steps taken to overcome this.

### 2.13. Assessment of Endotoxin Contamination

The HEK-Blue™ hTLR4 assay system was used to test IP and HPP for LPS contamination. HEK-blue cells ( $5 \times 10^5$  cells/mL) expressing TLR4 were stimulated with LPS (0.1–100 ng/mL; positive control), or HPP or IP (both 1000  $\mu$ M) for 24 h. Supernatants from the HEK-blue cells were incubated with HEK-blue detection medium, to measure SEAP expression, for 30 min at 37 °C and absorbance was read at 650 nm.

### 2.14. Statistical Analysis

Prism 9 software (GraphPad Software Inc., San Diego, CA, USA) was used to perform the statistical analysis on all datasets. A repeated measures one-way ANOVA, with either Dunnett's or Šidák's post hoc test, as appropriate, was used for analysis of three or more datasets. A Paired Student's *t*-test was used for the analysis of only two datasets. The analysis of datasets with more than one variable were performed using a two-way ANOVA with Šidák's multiple comparisons post hoc test. Asterisks are used in the figures to denote *p* values  $< 0.05$ , which were considered significant.

### 3. Results

#### 3.1. HPP and IP Upregulate HO-1 in Primary Human DC

We have previously shown that HPP and IP are capable of inducing HO-1, as well as having immunomodulatory effects, in murine macrophages and glia [5]. Therefore, we sought to investigate if *T. brucei*-derived ketoacids have similar effects in primary human DC, as these are crucial immune cells linking the innate and adaptive immune system. DC were treated with HPP or IP (500–1000  $\mu\text{M}$ ) for 24 h (these concentrations are similar to the levels of aromatic ketoacids in circulation close to the peak of parasitaemia during trypanosomiasis and have been used in previously published studies [4,5,8,17]). Both HPP and IP were found to be non-toxic to human DC, having no effect on cell viability at these concentrations, and were confirmed to be endotoxin free (Supplementary Figures S1 and S2). HO-1 expression in HPP- and IP-treated DC was next examined by western blot at a range of timepoints (3, 6, and 24 h) and concentrations (250–1000  $\mu\text{M}$ ). Immature DC constitutively expressed HO-1 in line with previous reports [18–20], however, treatment with either HPP or IP resulted in a trend towards increased expression of HO-1 at all concentrations tested with a significance observed at 1000  $\mu\text{M}$  in each case (Figure 1A). At this concentration, significant upregulation of HO-1 occurred within 3 h of HPP treatment, while significant induction of HO-1 occurred following 24 h treatment with IP (Figure 1B). Both IP and HPP also increased the total antioxidant capacity of DC and this was observed within 1 h of incubation with either compound (Figure 1C). The ketoacids also appear to be more potent antioxidants than the established HO-1 inducers, carnosol and curcumin (Figure 1C). These results indicate that IP and HPP rapidly enhance the total antioxidant capacity of human DC, while also upregulating the stress-response protein, HO-1.

#### 3.2. HPP and IP Induce HO-1 through Nrf2 Activation

We have previously reported that HPP and IP activate Nrf2 in murine immune cells, and this is likely the mechanism through which they upregulate HO-1 [5]. We therefore sought to investigate if they have a similar mechanism of action in human DC. To test this, DC were treated with HPP or IP (1000  $\mu\text{M}$ ) for 6 and 24 h, and Nrf2 protein expression was measured by western blot. An increase in Nrf2 protein was observed in HPP-treated DC at 6 h (Figure 2A), while IP-treated DC showed increased Nrf2 protein expression (and therefore accumulation) at 24 h (Figure 2A). Both HPP and IP were also found to drive mRNA expression of the additional Nrf2-regulated genes, NQO1 and GSR, further confirming their ability to activate this transcription factor (Figure 2B). Finally, treatment of DC with the Nrf2 inhibitor ML385 (10  $\mu\text{M}$ , a non-toxic dose, Supplementary Figure S3) for 1 h, prior to treatment with either HPP or IP (1000  $\mu\text{M}$ ) for 24 h, resulted in a significant decrease in the expression of HO-1 (Figure 2C), further confirming that ketoacid driven HO-1 expression is regulated by Nrf2.



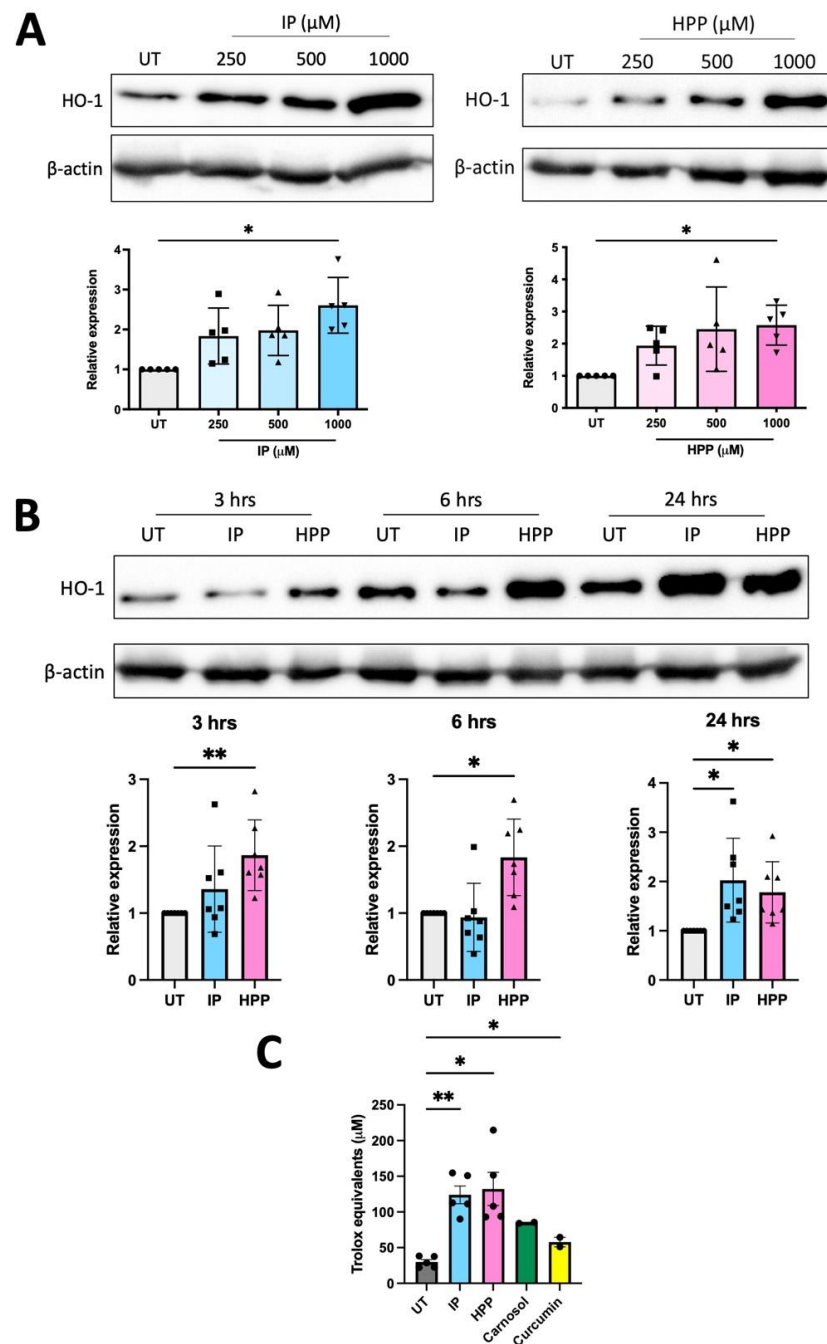


**Figure 1.** Hydroxyphenylpyruvate (HPP) and indole pyruvate (IP) upregulate HO-1 in primary human dendritic cells (DC). **(A)** Primary human DC were left untreated (UT) or incubated with HPP or IP (250–1000 μM) for 24 h. HO-1 expression was detected by western blot. Densitometry results shown are mean ± SEM of the relative expression of HO-1: β-actin from five healthy donors. **(B)** DC were left UT or incubated with HPP or IP at 1000 μM for 3, 6, or 24 h. HO-1 expression was detected by western blot. Densitometry results shown are mean ± SEM of the relative expression of HO-1: β-actin from seven healthy donors. **(C)** Primary human DC were left UT or incubated with HPP or IP at 1000 μM, or carnosol or curcumin (both 10 μM), for 1 h. Total antioxidant capacity of the cells was determined and expressed as an equivalent concentration of Trolox (μM). Pooled data showing the mean (±SEM) from five healthy donors. Repeated measures one-way ANOVA, with Dunnett’s multiple comparisons post hoc test, was used to determine statistical significance by comparing means of treatment groups against the mean of the control group (\*\*  $p < 0.01$ , \*  $p < 0.05$ ). ImageLab (Bio-Rad) software was used to perform densitometric analysis.

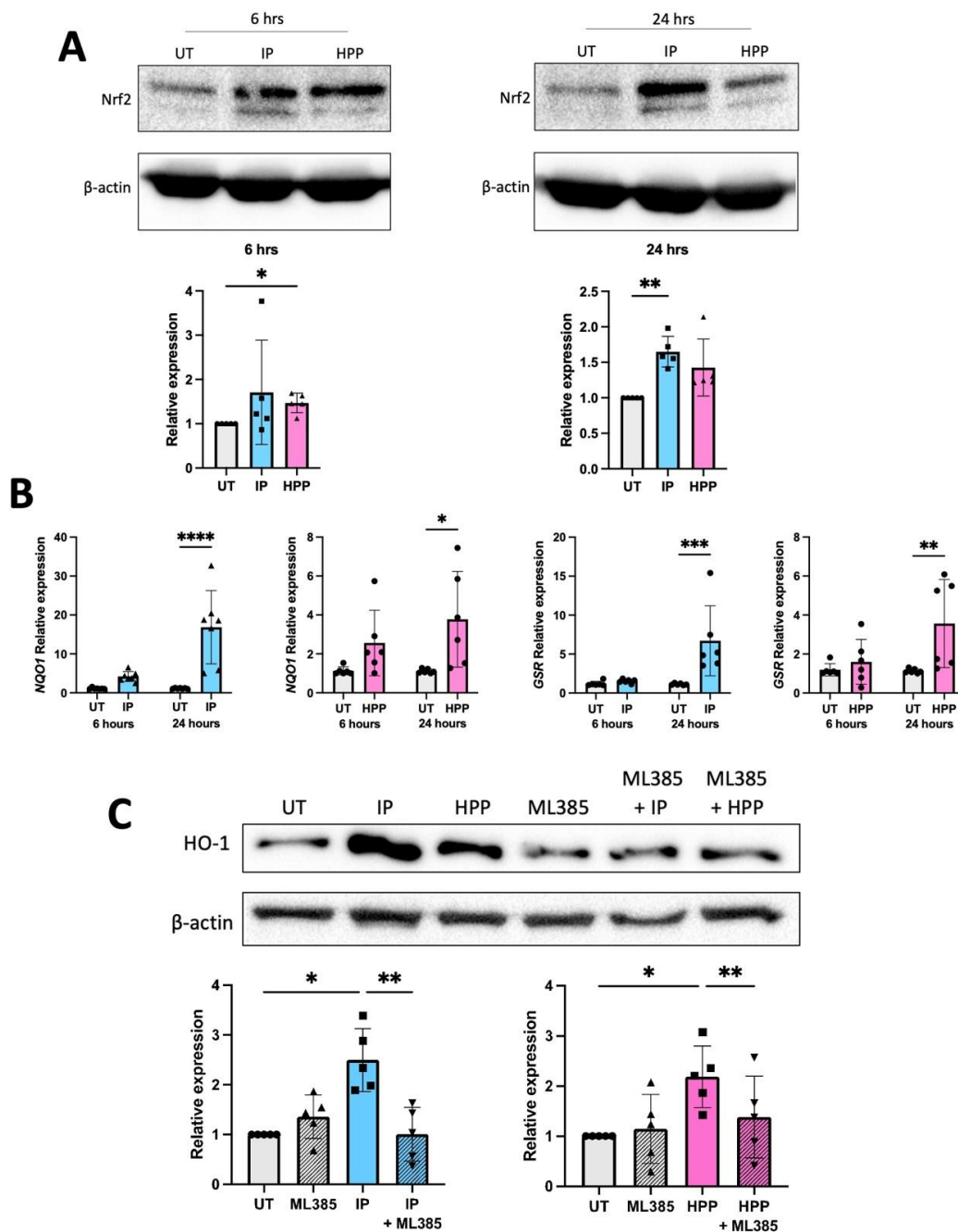


**Figure 2.** HPP and IP induce HO-1 through Nrf2 activation. (A) Primary human DC were left untreated (UT) or incubated with HPP or IP at 1000  $\mu$ M for 6 or 24 h. Nrf2 expression was measured by western blot. Densitometry results shown are mean  $\pm$  SEM of the relative expression of Nrf2:  $\beta$ -actin from five healthy donors. (B) Primary human DC were left UT or incubated with HPP or IP at 1000  $\mu$ M for 24 h. mRNA expression of the Nrf2-dependent genes, NQO-1 and GSR, were measured by RT-PCR. Results show mean ( $\pm$ SEM) for six healthy donors. (C) Primary human DC were pre-treated either with or without the Nrf2 inhibitor ML385 (10  $\mu$ M) for 1 h, prior to incubation with HPP or IP at 1000  $\mu$ M for 24 h. HO-1 expression was measured by western blot. Densitometry results shown are mean  $\pm$  SEM of the relative expression of HO-1:  $\beta$ -actin from five healthy donors. (A) One-way ANOVA, with Dunnett’s multiple comparisons post hoc test, was used to determine statistical significance. (B) Two-way ANOVA, with Šidák’s multiple comparisons post hoc test, was used to determine statistical significance. (C) One-way ANOVA, with Šidák’s multiple comparisons post hoc test, was used to determine statistical significance (\*\*\*\*  $p < 0.0001$ , \*\*\*  $p < 0.001$ , \*\*  $p < 0.01$ , \*  $p < 0.05$ ). ImageLab (Bio-Rad) software was used to perform densitometric analysis.

### 3.3. HPP and IP Reduce the Production of Pro-Inflammatory Cytokines in LPS-Stimulated Human DC

We recently demonstrated that HPP and IP are capable of reducing the production of pro-inflammatory cytokines in murine glia and macrophages [5]. We next sought to determine if they have similar immune modulating activity in human DC. To test this, DC were treated with either HPP or IP (500–1000  $\mu$ M) for 6 h prior to stimulation with LPS (100 ng/mL) for 24 h. Cytokine concentrations were measured in cell supernatants by ELISA. Both HPP and IP treatment dose-dependently reduced production of the pro-inflammatory cytokines TNF, IL-6, IL-12p70, and IL-23, and this effect was most potent at the 1000  $\mu$ M concentration (Figure 3A–H). As well as driving the production of pro-inflammatory cytokines, LPS treatment over time is usually accompanied by production of the anti-inflammatory cytokine IL-10 as a means of regulating inflammatory responses. Interestingly, IP treatment resulted in a significant enhancement of IL-10, while HPP treatment showed a similar, albeit non-significant, trend (Figure 3I,J). These results suggest that both IP and HPP are capable of reducing the production of pro-inflammatory cytokines in LPS-stimulated DC, whilst also promoting a more anti-inflammatory phenotype.

### 3.4. HPP Treatment Inhibits the Maturation of LPS-Stimulated Human DC, Resulting in Reduced Activation of CD4<sup>+</sup> T Cells

In order to determine if the ketoacids impact DC maturation (and in turn T cell activation), human DC were treated with HPP (500–1000  $\mu$ M) for 6 h prior to stimulation with LPS (100 ng/mL) for 24 h. Surface expression of maturation and co-stimulatory markers (CD40, CD80, CD83 and CD86) were measured by flow cytometry (due to the fluorescent nature of IP it is unsuitable for this flow cytometric analysis and hence was not included in these experiments). As expected, the expression of co-stimulatory markers was increased in LPS-stimulated DC. The average Median Fluorescent Intensity (MFI) of these cells was set to 100% and used as a control for comparison to the HPP-treated cells. There was a significant decrease in MFI at both HPP concentrations when compared to the LPS-stimulated control (Figure 4A). The phagocytic capacity of DC was next measured upon incubation of DC with FITC-conjugated DQ-Ovalbumin (DQ-Ova; 500 ng/mL) and uptake of the model antigen was assessed by flow cytometry. Compared to untreated cells, the ability of LPS-treated DC to phagocytose DQ-OVA was significantly impaired, signifying a heightened maturation status, however, pre-incubation with HPP prior to LPS treatment attenuated this effect and maintained the DC in an immature state (Figure 4B). Finally, and in order to determine if the reduced DC activation status that occurs in the presence of HPP has an impact on T cell activation, DC were treated with HPP (1000  $\mu$ M) for 6 h prior to stimulation with LPS (100 ng/mL) for 24 h. The cells were then incubated with CD4<sup>+</sup> T cells at a ratio of 10:1 (CD4<sup>+</sup> T cells:DC) for five days. The supernatants were removed for cytokine analysis by ELISA and cells were stimulated with PMA (50 ng/mL), ionomycin (500 ng/mL) and brefeldin A (5  $\mu$ g/mL) for 4 h. Expression of ki67, which is a measure of cell proliferation, was assessed by flow cytometry in CD3<sup>+</sup>CD8<sup>-</sup> cells (gating strategy shown in Supplementary Figure S4), as was production of the pathogenic Th1 cytokine, IFN $\gamma$ . T cells co-cultured with HPP-treated, LPS-stimulated DC showed a trend towards reduced ki67 and IFN $\gamma$  expression when compared to T cells co-cultured with LPS-stimulated DC alone (Figure 4C). Interestingly, the T cells exhibited a trend towards enhanced production of the anti-inflammatory cytokine IL-10, when compared to T cells co-cultured with LPS-stimulated DC alone (Figure 4D). Overall, these results indicate that HPP reduces the maturation of innate DC, which in turn impacts adaptive T cell responses and may skew them towards a more anti-inflammatory phenotype.

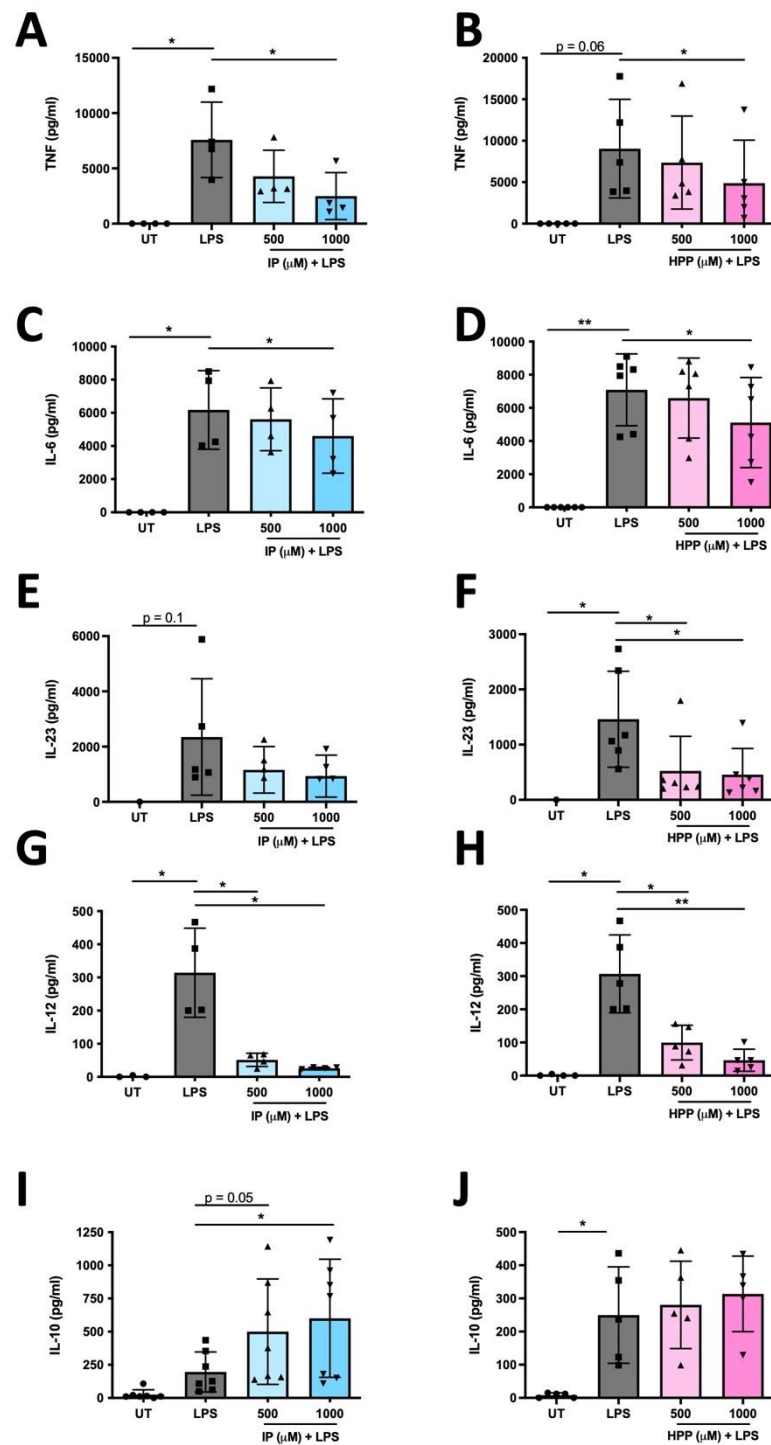


**Figure 3.** HPP and IP reduce the production of pro-inflammatory cytokines in LPS-stimulated human DC. Primary human DC were left untreated (UT) or incubated with IP (A,C,E,G,I) or HPP (B,D,F,H,J) (500–1000  $\mu$ M) for 6 h prior to stimulation with LPS (100 ng/mL) for 24 h. Cell supernatants were assessed for TNF, IL-6, IL-23, IL-12p70, and IL-10 secretion by ELISA. Pooled data depict mean ( $\pm$ SEM) cytokine concentrations for four to seven healthy donors (means of three technical replicates per donor). Repeated measures one-way ANOVA, with Dunnett's multiple comparisons post hoc test, was used to determine statistical significance, by comparing means of treatment groups against the mean of the control group (\*\*  $p < 0.01$ , \*  $p < 0.05$ ).

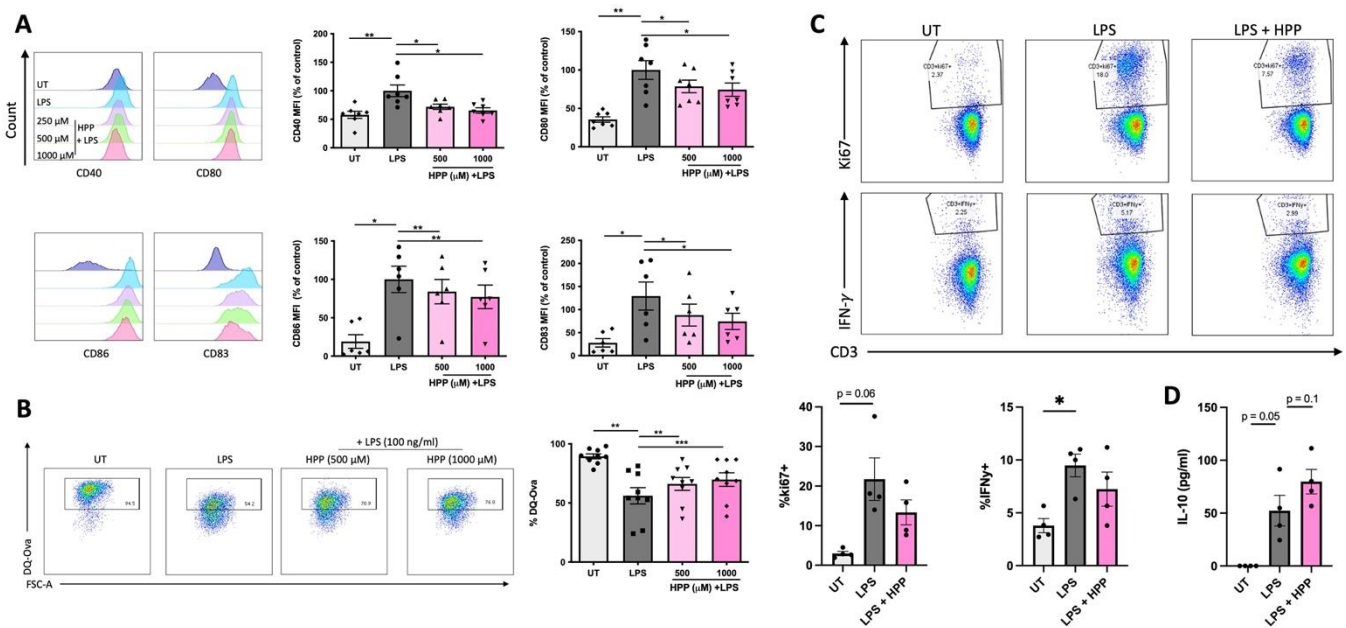


**Figure 4.** HPP treatment reduces DC maturation and subsequent CD4<sup>+</sup> T cell activation. Primary human DC were left untreated (UT) or incubated with HPP (500–1000  $\mu$ M) for 6 h prior to stimulation with LPS (100 ng/mL) for 24 h. (A) Cells were stained for CD40, CD80, CD86, and CD83 and analysed by flow cytometry. Histograms showing the expression of maturation markers for HPP-treated, LPS-stimulated DC compared to unstimulated cells or LPS stimulation alone from one representative experiment. Pooled data showing the mean ( $\pm$ SEM) MFI for each marker expressed as a percentage of control (LPS stimulation alone) from six to seven healthy donors. (B) DC were incubated with FITC-conjugated DQ-Ovalbumin (DQ-Ova; 500 ng/mL) for 20 min and were immediately acquired by flow cytometry. Dot plots depicting DQ-Ova uptake from one representative experiment. Pooled data showing the mean ( $\pm$ SEM) DQ-Ova uptake as a percentage of total cells from nine healthy donors. (C) DC were pre-treated with HPP prior to stimulation with LPS, and subsequently cultured with CD4<sup>+</sup> T cells for five days. Dot plots depicting ki67 expression (as a measure of proliferation) and IFN $\gamma$  expression from one representative experiment. Pooled data showing the mean ( $\pm$ SEM) of ki67<sup>+</sup> and IFN $\gamma$ <sup>+</sup> cells as a percentage of CD3<sup>+</sup>CD8<sup>-</sup> cells from four healthy donors. (D) Cell supernatants were assessed for IL-10 secretion by ELISA. Pooled data depict mean ( $\pm$ SEM) cytokine concentrations for four healthy donors (means of three technical replicates per donor). Repeated measures one-way ANOVA, with Dunnett's multiple comparisons post hoc test, was used to determine statistical significance by comparing means of treatment groups against the mean of the control group (\*\* $p < 0.001$ , \*\*  $p < 0.01$ , \*  $p < 0.05$ ).

### 3.5. HPP and IP Modulate Metabolic Reprogramming in LPS-Stimulated Human DC

Metabolic reprogramming has been observed in immune cells and numerous recent studies have demonstrated that their activation/maturation is accompanied by a metabolic switch favouring glycolysis over oxidative phosphorylation [21]. In order to determine if *T. brucei*-derived ketoacids have an effect on immune cell metabolism, DC were pre-treated with IP or HPP (1000  $\mu$ M) for 6 h prior to stimulation with LPS (100 ng/mL) for 12 h. These cells were then analysed in a Seahorse XFe96 analyser following the addition of oligomycin (1 mM), an inhibitor of mitochondrial complex V, FCCP (1 mM), a mitochondrial uncoupler, rotenone (500 nM) and antimycin A (500 nM), which are inhibitors of the mitochondrial complexes I & III, respectively, and 2-DG (25 mM), an inhibitor of glycolysis. The metabolic activity of the cells was then determined by measuring the ECAR, which is a measure of glycolysis, and the OCR, which is a measure of oxidative phosphorylation. IP- and HPP-treated DC showed no change in basal glycolysis when compared to LPS stimulation alone (Figure 5B). LPS-treated cells showed a trend towards increased max glycolysis, and this was significantly decreased in the presence of either HPP or IP (Figure 5C). Both IP and

HPP were also capable of significantly decreasing the glycolytic reserve in LPS-stimulated cells (Figure 5C). There were no significant changes in the basal respiration (Figure 5F), max respiration (Figure 5G), and respiratory reserve (Figure 5H) in IP- or HPP-treated DC when compared to LPS stimulation alone, suggesting that they have no impact on oxidative phosphorylation.

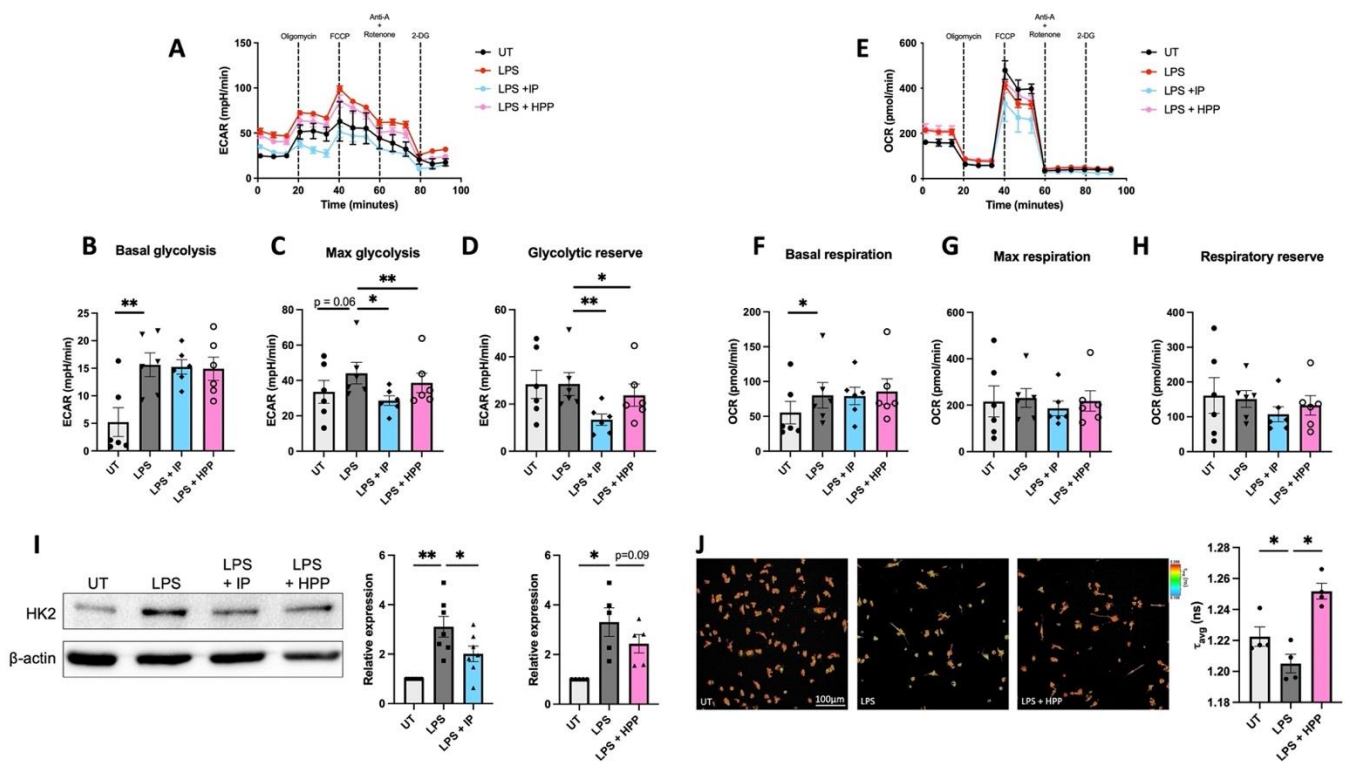


**Figure 5.** HPP and IP modulate metabolic reprogramming in LPS-stimulated DC. Primary human DC were pre-treated with either HPP or IP at 1000  $\mu$ M for 6 h before stimulation with LPS (100 ng/mL) for 12 h. The extracellular acidification rate (ECAR) and the oxygen consumption rate (OCR) were measured using a Seahorse XFe96 analyser before and after the injections of oligomycin (1 mM), FCCP (1 mM), antimycin A (500 nM) and rotenone (500 nM), and 2-DG (25 mM). Bioenergetic profiles from one representative experiment depicting (A) ECAR and (E) OCR measurements over time. Pooled data ( $N = 6$ ) depicts the calculated mean ( $\pm$ SEM) of (B) basal glycolytic rate, (C) max glycolytic rate, (D) glycolytic reserve, (F) basal respiratory rate, (G) max respiratory rate, and (H) respiratory reserve for each treatment group. (I) HK2 expression was measured by western blot. Densitometry results shown are mean  $\pm$  SEM of the relative expression of HK2:  $\beta$ -actin from five to seven healthy donors. (J) FLIM images of DC measuring intracellular NADH. Pooled data ( $N = 4$ ) depicts the mean ( $\pm$ SEM) of the ratio of bound:free NADH, represented by the  $\tau$  average. Repeated measures one-way ANOVA, with Dunnett's multiple comparisons post hoc test, was used to determine statistical significance by comparing means of treatment groups against the mean of the control group (\*\*  $p < 0.01$ , \*  $p < 0.05$ ). ImageLab (Bio-Rad) software was used to perform densitometric analysis.

Expression of HK2, the rate limiting enzyme in the glycolytic pathway, was next assessed by western blotting. HK2 is known to be induced by inflammatory stimuli and, as expected, LPS stimulation induced the upregulation of HK2 in DC. However, there was reduced expression of the enzyme in IP-treated DC, and a trend towards reduced expression (albeit not significant) in HPP-treated DC when compared to LPS-stimulated DC (Figure 5I). The effects of HPP treatment on the metabolism of DC was further investigated using FLIM, which measures the intracellular levels of NADH. Bound NADH, which is associated with oxidative phosphorylation, or free NADH, which is associated with glycolysis, can be distinguished based on their distinct lifetimes upon fluorescence excitation. The ratio of

bound to free NADH can be used to measure whether a cell is favouring the engagement of glycolysis (a decrease in the ratio due to increased free NADH) or oxidative phosphorylation (an increase in the ratio due to increased bound NADH). Similar to the Seahorse results reported above, LPS-stimulated DC ramped up glycolysis, as represented by a decrease in the  $\tau$  average compared to untreated DC (Figure 5J). Cells pre-treated with HPP exhibited a significant increase in the  $\tau$  average compared to the LPS-stimulated controls, indicating they are favouring oxidative phosphorylation to generate their energy (Figure 5J). Overall, these results indicate that *T. brucei*-derived ketoacids modulate DC metabolism, reducing engagement of glycolysis, which is associated with rapid inflammatory responses.

### 3.6. HPP and IP Activate Autophagy-Related Proteins

We have previously demonstrated that the HO-1 inducers carnosol and curcumin activate the autophagy regulator AMPK, which incidentally is also known to downmodulate glycolysis in immune activated cells [22]. Furthermore, the key autophagy-related protein, p62, is linked to Nrf2 activation [23–25]. In order to determine if *T. brucei*-derived ketoacids have any impact on autophagy-related proteins, DC were treated with IP or HPP (both 1000  $\mu$ M) for 15 min and phosphorylation (and therefore activation) of AMPK was assessed by western blotting. IP treatment resulted in a significant increase in AMPK phosphorylation while there was a trend towards increased activation with HPP (Figure 6A). DC treated with IP also showed an increase in both p62 and LC3-II (which is converted from LC3-I during autophagy) over time, and this was most potent after 24 h (Figure 6B,C). HPP treatment significantly increased p62 expression after 6 h and significantly increased LC3-II expression after 24 h (Figure 6B,C). These results indicate both ketoacids are activating autophagy-related proteins in human DC.

### 3.7. HPP and IP Reduce Proliferation and Cytokine Expression in PBMC Isolated from IBD Patients

It has previously been reported that IP has powerful immune suppressive effects in a murine experimental colitis model [7]. In order to determine if these results translate to a more clinical setting, PBMC were isolated from IBD patients and treated with IP or HPP (250–1000  $\mu$ M) for 6 h prior to stimulation with anti-CD3 (1  $\mu$ g/mL) for a further four days. Furthermore, the culture media was replaced with fresh media after 18 h of incubation with the compounds to circumvent issues surrounding the fluorescence of IP over long periods of time. The supernatants were removed for cytokine analysis by ELISA and cells were stimulated with PMA (50 ng/mL), ionomycin (500 ng/mL), and brefeldin A (5  $\mu$ g/mL) for 4 h. Expression of ki67, and the cytokines IFN $\gamma$  and IL-17 (both of which are known to play a pathogenic role in IBD), were measured by flow cytometry in CD3<sup>+</sup>CD8<sup>-</sup> cells (gating strategy shown in Supplementary Figure S5). IP was non-toxic to PBMC at all concentrations tested, however there was some toxicity seen when using the higher concentrations of HPP (Supplementary Figure S6). Despite this being significant, it is unlikely to account for the effects seen, as flow markers were examined in live cells only. Both IP- and HPP-treated cells were capable of dose-dependently reducing the proliferation and expression of IFN $\gamma$  when compared to anti-CD3 stimulation alone (Figure 7A,B), while having no effect on the intracellular levels of IL-17. However, when cell supernatants were assessed by ELISA, there was a significant reduction in both IFN $\gamma$  and IL-17 production in IP- and HPP-treated cells (Figure 7C,D). Unlike purified DC, the ketoacids did not enhance the production of IL-10 from PBMC, suggesting a cell-type specific effect (Figure 7C,D).

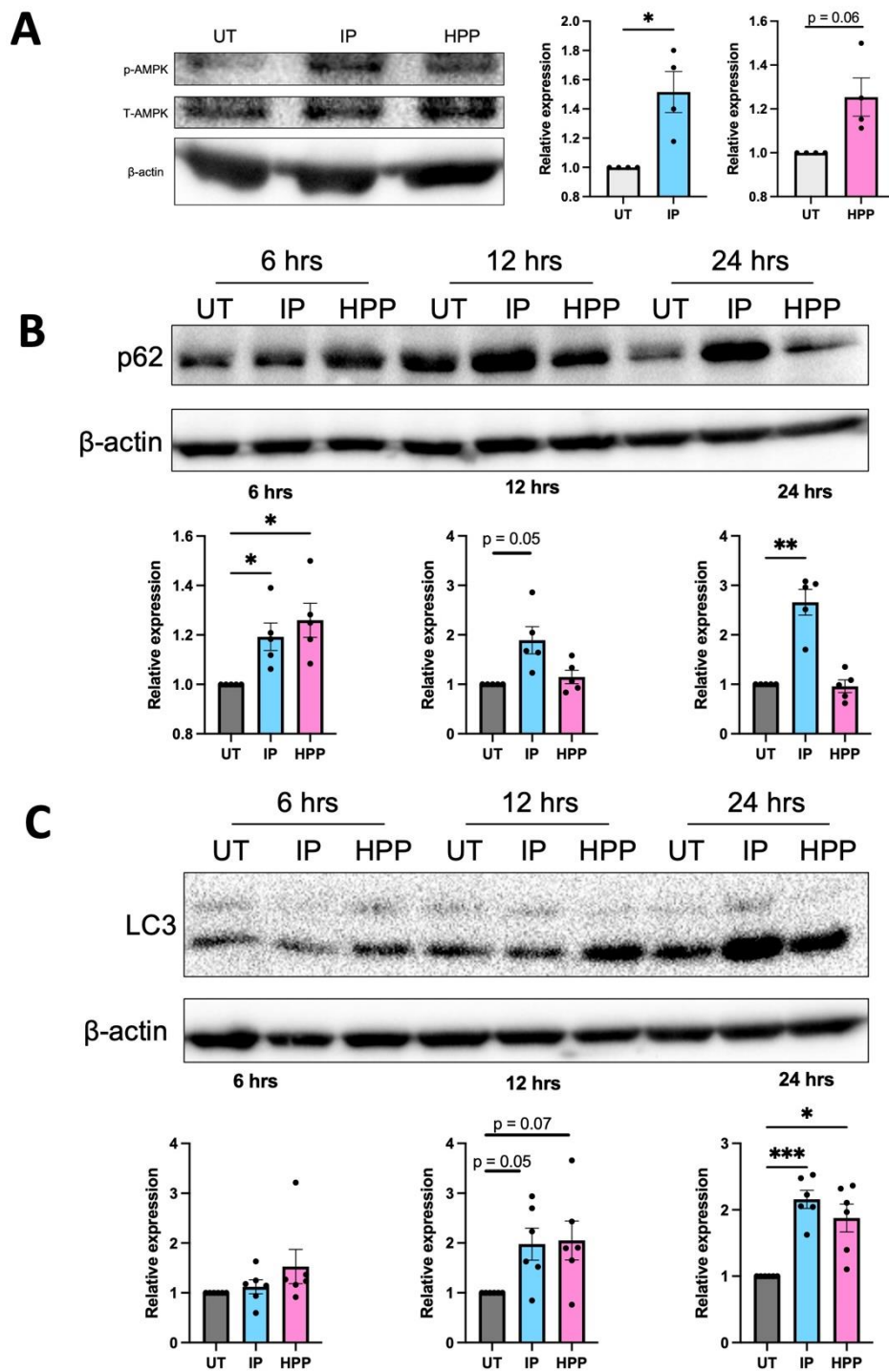


**Figure 6.** HPP and IP modulate autophagy-related proteins. (A) Primary human DC were left untreated (UT) or incubated with IP or HPP at 1000 μM for 15 min. Phosphorylation of AMPK was measured by western blot. Densitometry results shown are mean ± SEM of the relative expression of p-AMPK: β-actin from four healthy donors. (B,C) Primary human DC were left UT or incubated with IP or HPP at 1000 μM for 6, 12, or 24 h. Expression of (B) p62 and (C) LC3 were measured by western blot. Densitometry results shown are mean ± SEM of the relative expression of (B) p62: β-actin from five healthy donors and (C) LC3 II: β-actin from six healthy donors. (A) Statistical significance was determined using a Paired *t*-test. (B,C) Statistical significance was determined by repeated measures one-way ANOVA with Dunnett’s multiple comparisons post hoc test to compare means of treatment groups to the control group (\*\**p* < 0.001, \*\**p* < 0.01, \**p* < 0.05). ImageLab (Bio-Rad) software was used to perform densitometric analysis.



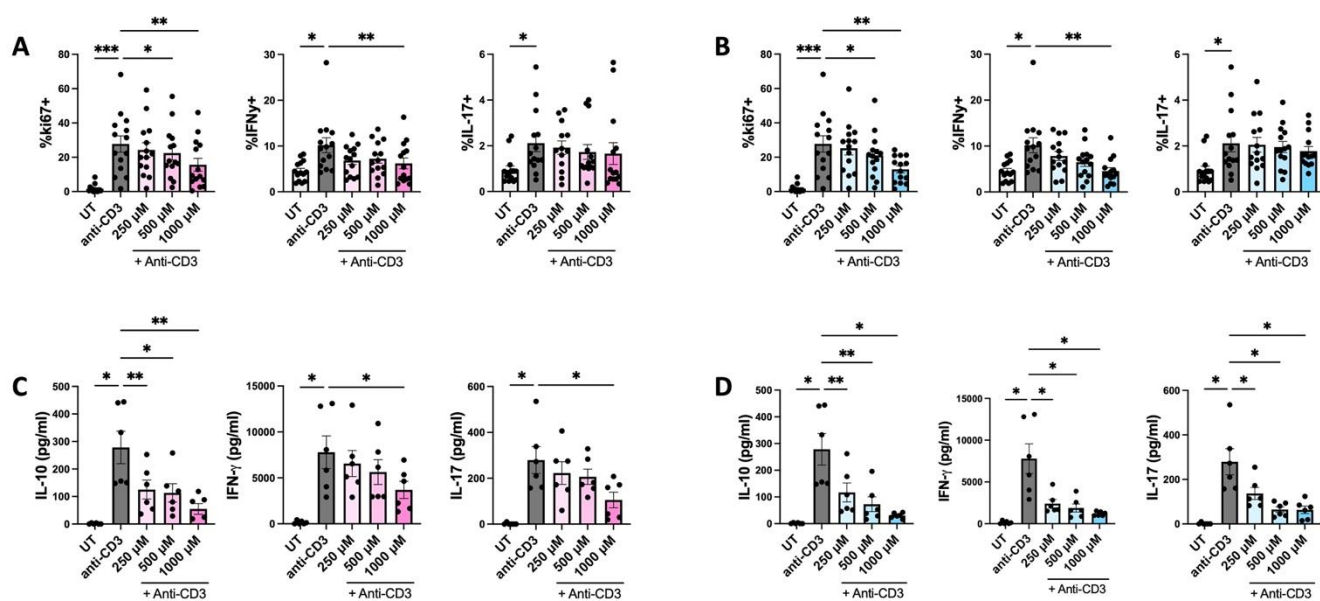


**Figure 7.** HPP and IP reduce proliferation and cytokine expression in ex vivo stimulated PBMC from patients with Inflammatory Bowel Disease. PBMC isolated from IBD patients were treated with (A,C) HPP or (B,D) IP (250  $\mu\text{M}$ –1000  $\mu\text{M}$ ) for 6 h prior to stimulation with anti-CD3 for 12 h. After 18 h, culture media was replaced with fresh media and cells were incubated for a further 4 days with anti-CD3 stimulation. Supernatants were removed for analysis of cytokine concentration by ELISA. (A,B) Proliferation and cytokine production by  $\text{CD3}^+\text{CD8}^-$  cells was analysed by flow cytometry. Pooled data ( $N = 14$ ) depicting the mean  $\pm$  SEM of ki67 (as a measure of proliferation),  $\text{IFN}\gamma$ , and IL-17 in  $\text{CD3}^+\text{CD8}^-$  T cells. (C,D) Cell supernatants were assessed for concentrations of IL-10,  $\text{IFN}\gamma$ , and IL-17 by ELISA. Pooled data depicts mean ( $\pm$ SEM) cytokine concentrations for six IBD patients (means of three technical replicates per donor). Statistical significance was determined by repeated measures one-way ANOVA with Dunnett’s multiple comparisons post hoc test to compare means of treatment groups to the control group (\*\* $p < 0.001$ , \*\* $p < 0.01$ , \* $p < 0.05$ ).

#### 4. Discussion

The production of large amounts of immunomodulatory aromatic ketoacids during *T. brucei* infection likely serves to benefit the parasite by prolonging infection, proliferation, and, ultimately, survival in the host. While the secretome of *T. brucei* has been shown to reduce the secretion of IL-12, IL-10, IL-6, and TNF in both murine and human DC [26,27], the ketoacids, IP and HPP, have been shown to directly ameliorate inflammatory cytokine production in murine macrophages and glia [4,5]. This is further supported by studies demonstrating their therapeutic efficacy in murine models of disease [4,6,7]. Given the key role played by DC in shaping both innate and adaptive immune cell responses, we sought to determine if these effects translate to this vital human immune cell population, which not only serves to present antigens during infection, but also plays a key role in determining pathogenic T cell responses during disease. We demonstrate that both IP and HPP are capable of significantly reducing the secretion of a number of pro-inflammatory cytokines, including TNF, IL-6, IL-12, and IL-23 in LPS-stimulated DC. Furthermore, the ketoacids upregulate HO-1 in an Nrf2 dependant manner, which is in line with studies demonstrating that HO-1 induction can promote a more tolerogenic DC phenotype [18,19,28]. In support of this, we also demonstrate that ketoacid-treated DC have a reduced capacity to activate T cells, which in turn limits the production of the pathogenic T cell cytokine  $\text{IFN}\gamma$ , which is known to play a deleterious role in a number of inflammatory/autoimmune conditions including IBD [29].

In comparison to the previous data from murine macrophages and glia, a larger repertoire of cytokines is inhibited by the ketoacids in human DC. For example, IP and HPP had no effect on TNF secretion in murine glia and no effect on either TNF or IL-6 secretion

in bone marrow derived macrophages [4,5], however, these cytokines were significantly reduced in LPS-activated human DC. Furthermore, IP directly induced the production of the anti-inflammatory cytokine IL-10 in DC. The maturation status of DC is also impacted by ketoacid treatment, with the HPP-treated cells exhibiting a reduction in co-stimulatory and maturation markers, which, in turn, prevents their ability to participate in T cell activation. The upregulation of HO-1 was also accompanied by the expression of additional Nrf2-regulated genes and both IP and HPP appeared to exhibit direct antioxidant activity, which may explain their ability to activate Nrf2, given its well documented capacity to rapidly respond to oxidative stress.

Further analysis of these novel HO-1 inducers also revealed that they can modulate immune cell metabolism. Indeed, recent studies have highlighted an important link between immune cell activation and metabolism. It is now well recognised that, not only do different immune cells engage different metabolic pathways, but that the activation/maturation state of the immune cells is accompanied by metabolic switches. For example, innate immune cells, including macrophages and DC, ramp up glycolysis in order to rapidly generate sufficient energy and the building blocks required to fight infection [21]. This phenomenon is also a feature of pathogenic immune cells, and a significant effort is underway to determine if controlling/preventing dysregulated metabolic reprogramming can serve to ameliorate detrimental immune cell activation during disease. Here we demonstrate that both IP and HPP can decrease the max glycolysis observed in LPS-treated DC while also downregulating the expression of hexokinase 2, the rate-limiting enzyme in glycolysis. These results are similar to our recent observations with the HO-1 inducers, carnosol and curcumin, suggesting that HO-1 may be an important regulator of immune cell metabolism [30]. Further study is required to determine if additional features of metabolism are affected by ketoacids and whether metabolic reprogramming occurs during *T. brucei* infection, but these in vitro results are in line with the notion that metabolism is intricately linked with immune cell activation, and that the downmodulation of glycolysis in immune cells promotes a more tolerogenic phenotype.

From a therapeutic stance, IP in particular has shown potential in a murine model of colitis where administration of the ketoacid not only improved disease outcome, but also decreased expression of pro-inflammatory cytokines, including IL-12, IFN $\gamma$ , and TNF [7]. We observed similar results in PBMC from IBD patients where both HPP and IP reduced the proliferation of anti-CD3 stimulated T cells, as well as the secretion of both IL-17 and IFN $\gamma$ . Indeed, induction of HO-1 is being explored as a therapy for IBD and has shown promise in a number of murine models of disease [31–35]. Patients are currently treated largely with anti-inflammatories including 5-aminosalicylic acid (5-ASA), corticosteroids, methotrexate, and anti-TNF therapies [36]. However, many patients are/become refractory to these treatments and will require surgery in their lifetime. While further in vivo study is required to fully elucidate their efficacy and provide further information regarding treatment route, dosing, and long-term effects, these findings provide further impetus to explore aromatic ketoacids as a treatment for IBD (and indeed other inflammatory diseases), either alone or in combination with existing therapies.

Finally, a particularly interesting finding of this study is the observation that IP and HPP can activate key autophagic proteins. Autophagy itself is carried out by a number of autophagy-related (Atg) proteins and initiation is under the control of the protein kinases mTOR and AMPK, which are both intrinsically linked to immune cell metabolism (AMPK inhibits glycolysis while mTOR activation is linked to induction of glycolysis). The autophagic process is complicated and involves many different proteins and has been reviewed in detail elsewhere [37–39]. Briefly, a complex of Atg proteins lipidates LC3-I converting it to LC3-II [37,38]. LC3-II binds to the autophagosome membrane and facilitates the docking of cargos and proteins for degradation through their binding to p62 [40]. Following maturation, the autophagosome fuses with the lysosome to form the autolysosome, the contents of which are then degraded and recycled. In this study, we show that IP and HPP activate AMPK and increase expression of p62 and LC3-II.

Autophagy is of particular importance for DC, as many of their key functions, including antigen uptake and presentation, are strongly associated with autophagy [41]. Despite some conflicting reports, generally it appears that activation of autophagy gives rise to a more tolerogenic DC phenotype, exhibiting reduced antigen presentation and maturation [41], which is similar to the results seen in this study. Furthermore, AMPK activation has been shown to attenuate pro-inflammatory cytokine production and DC maturation [22,42]. Therefore, ketoacid-induced AMPK and subsequent autophagy activation may serve to downmodulate DC maturation, antigen presentation, and glycolysis.

Notably, p62 is not only an important autophagy-related protein, it also plays a crucial role in the activation of Nrf2 [23–25]. Nrf2 is activated upon release from KEAP1, which can occur when p62 sequesters KEAP1, targeting it for degradation and allowing Nrf2 to translocate to the nucleus [23–25]. Therefore, the activation of p62 by both ketoacids, but in particular IP, may be responsible for the subsequent activation of Nrf2, and therefore HO-1, by these ketoacids. While HPP induces HO-1 at an earlier time than IP, the latter appears to have more potent effects overall. In most cases, the *in vitro* effects of IP are most apparent at 24 h, and we cannot rule out the possibility that it is converting to another form over time. Further study is undoubtedly required to delineate the true impact of aromatic ketoacids (and their potential derivatives) and HO-1 induction on autophagy-related processes, in addition to the noted effects on DC metabolic reprogramming.

## 5. Conclusions

In conclusion, the data presented here expands our understanding of the mechanism of action of *T. brucei*-derived ketoacids in human immune cells and suggests that HO-1 induction may be useful to regulate the metabolism and, therefore, function of immune cells in inflammatory disease. We firmly believe that these compounds represent novel and exciting HO-1 inducers worthy of further exploration.

**Supplementary Materials:** The following supporting information can be downloaded at: <https://www.mdpi.com/article/10.3390/antiox11010164/s1>, Figure S1: HPP and IP are non-toxic to human DC; Figure S2: IP and HPP are not contaminated with endotoxin; Figure S3: ML385 is non-toxic to human DC; Figure S4: Gating strategy used to generate data shown in Figure 4; Figure S5: Gating strategy used to generate data shown in Figure 6; Figure S6: IP is non-toxic to PBMC, while higher concentrations of HPP shows significant, albeit mild, reductions in viability; Table S1: Seahorse calculations.

**Author Contributions:** H.K.F., J.M.F. and A.D. conceptualized and designed experiments. H.K.F. performed all experiments with laboratory assistance and intellectual input from S.A.O. and E.D. N.G.B.N. performed the FLIM experiments. N.G.B.N. and M.G.M. contributed to the interpretation of the FLIM data. D.P.N. contributed to the interpretation of data. M.T., J.D., E.J.R. and G.A.D. provided access to IBD patient samples. H.K.F., J.M.F. and A.D. wrote, reviewed, and edited the manuscript. All authors have read and agreed to the published version of the manuscript.

**Funding:** This research was funded by Health Research Board, Ireland, grant number ILP-POR-2017-041.

**Institutional Review Board Statement:** The study was conducted in accordance with the Declaration of Helsinki, and approved by the Research Ethics Committee of the School of Biochemistry and Immunology, Trinity College, Dublin (BI-HF-300921, approved 18 October 2018).

**Informed Consent Statement:** Informed consent was obtained from all subjects involved in the study.

**Data Availability Statement:** The data is contained within the article or supplementary material.

**Conflicts of Interest:** The authors declare no conflict of interest.

## References

1. Stijlemans, B.; Caljon, G.; Van Den Abbeele, J.; Van Ginderachter, J.A.; Magez, S.; De Trez, C. Immune Evasion Strategies of *Trypanosoma brucei* within the Mammalian Host: Progression to Pathogenicity. *Front. Immunol.* **2016**, *7*, 233. [[CrossRef](#)] [[PubMed](#)]
2. Berger, B.J.; Dai, W.W.; Wang, H.; Stark, R.E.; Cerami, A. Aromatic amino acid transamination and methionine recycling in trypanosomatids. *Proc. Natl. Acad. Sci. USA* **1996**, *93*, 4126–4130. [[CrossRef](#)]
3. Marciano, D.; Llorente, C.; Maugeri, D.A.; de la Fuente, C.; Opperdoes, F.; Cazzulo, J.J.; Nowicki, C. Biochemical characterization of stage-specific isoforms of aspartate aminotransferases from *Trypanosoma cruzi* and *Trypanosoma brucei*. *Mol. Biochem. Parasitol.* **2008**, *161*, 12–20. [[CrossRef](#)] [[PubMed](#)]
4. McGettrick, A.F.; Corcoran, S.E.; Barry, P.J.G.; McFarland, J.; Crès, C.; Curtis, A.M.; Franklin, E.; Corr, S.C.; Mok, K.H.; Cummins, E.P.; et al. *Trypanosoma brucei* metabolite indolepyruvate decreases HIF-1 $\alpha$  and glycolysis in macrophages as a mechanism of innate immune evasion. *Proc. Natl. Acad. Sci. USA* **2016**, *113*, E7778–E7787. [[CrossRef](#)] [[PubMed](#)]
5. Campbell, N.K.; Williams, D.G.; Fitzgerald, H.K.; Barry, P.J.; Cunningham, C.C.; Nolan, D.P.; Dunne, A. *Trypanosoma brucei* Secreted Aromatic Ketoacids Activate the Nrf2/HO-1 Pathway and Suppress Pro-inflammatory Responses in Primary Murine Glia and Macrophages. *Front. Immunol.* **2019**, *10*, 2137. [[CrossRef](#)]
6. Aoki, R.; Aoki-Yoshida, A.; Suzuki, C.; Takayama, Y. Protective Effect of Indole-3-Pyruvate against Ultraviolet B-Induced Damage to Cultured HaCaT Keratinocytes and the Skin of Hairless Mice. *PLoS ONE* **2014**, *9*, e96804. [[CrossRef](#)]
7. Aoki, R.; Aoki-Yoshida, A.; Suzuki, C.; Takayama, Y. Indole-3-Pyruvic Acid, an Aryl Hydrocarbon Receptor Activator, Suppresses Experimental Colitis in Mice. *J. Immunol.* **2018**, *201*, 3683–3693. [[CrossRef](#)]
8. Diskin, C.; Corcoran, S.E.; Tyrrell, V.J.; McGettrick, A.F.; Zaslona, Z.; O'Donnell, V.B.; Nolan, D.P.; O'Neill, L.A.J. The *Trypanosoma*-Derived Metabolite Indole-3-Pyruvate Inhibits Prostaglandin Production in Macrophages by Targeting COX2. *J. Immunol.* **2021**, *207*, 2551–2560. [[CrossRef](#)]
9. Yamaguchi, T.; Komoda, Y.; Nakajima, H. Biliverdin-IX $\alpha$  reductase and biliverdin-IX $\beta$  reductase from human liver. Purification and characterization. *J. Biol. Chem.* **1994**, *269*, 24343–24348. [[CrossRef](#)]
10. Singleton, J.W.; Laster, L. Biliverdin reductase of guinea pig liver. *J. Biol. Chem.* **1965**, *240*, 4780–4789. [[CrossRef](#)]
11. Radhakrishnan, N.; Yadav, S.P.; Sachdeva, A.; Pruthi, P.K.; Sawhney, S.; Piplani, T.; Wada, T.; Yachie, A. Human heme oxygenase-1 deficiency presenting with hemolysis, nephritis, and asplenia. *J. Pediatr. Hematol. Oncol.* **2011**, *33*, 74–78. [[CrossRef](#)] [[PubMed](#)]
12. Kapturczak, M.H.; Wasserfall, C.; Brusko, T.; Campbell-Thompson, M.; Ellis, T.M.; Atkinson, M.A.; Agarwal, A. Heme oxygenase-1 modulates early inflammatory responses: Evidence from the heme oxygenase-1-deficient mouse. *Am. J. Pathol.* **2004**, *165*, 1045–1053. [[CrossRef](#)]
13. Poss, K.D.; Tonegawa, S. Reduced stress defense in heme oxygenase 1-deficient cells. *Proc. Natl. Acad. Sci. USA* **1997**, *94*, 10925–10930. [[CrossRef](#)] [[PubMed](#)]
14. Campbell, N.K.; Fitzgerald, H.K.; Dunne, A. Regulation of inflammation by the antioxidant haem oxygenase 1. *Nat. Rev. Immunol.* **2021**, *21*, 411–425. [[CrossRef](#)] [[PubMed](#)]
15. Neto, N.; Dmitriev, R.I.; Monaghan, M.G. Seeing Is Believing: Noninvasive Microscopic Imaging Modalities for Tissue Engineering and Regenerative Medicine. In *Cell Engineering and Regeneration*; Springer: Cham, Switzerland, 2020; pp. 599–638.
16. Floudas, A.; Neto, N.; Marzaioli, V.; Murray, K.; Moran, B.; Monaghan, M.G.; Low, C.; Mullan, R.H.; Rao, N.; Krishna, V.; et al. Pathogenic, glycolytic PD-1+ B cells accumulate in the hypoxic RA joint. *JCI Insight* **2020**, *5*, e139032. [[CrossRef](#)]
17. El Sawalhy, A.; Seed, J.R.; Hall, J.E.; El Attar, H. Increased excretion of aromatic amino acid catabolites in animals infected with *Trypanosoma brucei evansi*. *J. Parasitol.* **1998**, *84*, 469–473. [[CrossRef](#)]
18. Campbell, N.K.; Fitzgerald, H.K.; Malara, A.; Hambly, R.; Sweeney, C.M.; Kirby, B.; Fletcher, J.M.; Dunne, A. Naturally derived Heme-Oxygenase 1 inducers attenuate inflammatory responses in human dendritic cells and T cells: Relevance for psoriasis treatment. *Sci. Rep.* **2018**, *8*, 10287. [[CrossRef](#)]
19. Chauveau, C.; Rémy, S.; Royer, P.J.; Hill, M.; Tanguy-Royer, S.S.; Hubert, F.-X.F.X.; Tesson, L.; Brion, R.R.; Berioui, G.G.; Gregoire, M.; et al. Heme oxygenase-1 expression inhibits dendritic cell maturation and proinflammatory function but conserves IL-10 expression. *Blood* **2005**, *106*, 1694–1702. [[CrossRef](#)]
20. Hull, T.D.; Agarwal, A.; George, J.F. The mononuclear phagocyte system in homeostasis and disease: A role for heme oxygenase-1. *Antioxid. Redox Signal.* **2014**, *20*, 1770–1788. [[CrossRef](#)]
21. O'Neill, L.A.J.; Kishton, R.J.; Rathmell, J. A guide to immunometabolism for immunologists. *Nat. Rev. Immunol.* **2016**, *16*, 553–565. [[CrossRef](#)]
22. Krawczyk, C.M.; Holowka, T.; Sun, J.; Blagih, J.; Amiel, E.; DeBerardinis, R.J.; Cross, J.R.; Jung, E.; Thompson, C.B.; Jones, R.G.; et al. Toll-like receptor-induced changes in glycolytic metabolism regulate dendritic cell activation. *Blood* **2010**, *115*, 4742–4749. [[CrossRef](#)] [[PubMed](#)]
23. Komatsu, M.; Kurokawa, H.; Waguri, S.; Taguchi, K.; Kobayashi, A.; Ichimura, Y.; Sou, Y.S.; Ueno, I.; Sakamoto, A.; Tong, K.I.; et al. The selective autophagy substrate p62 activates the stress responsive transcription factor Nrf2 through inactivation of Keap1. *Nat. Cell Biol.* **2010**, *12*, 213–223. [[CrossRef](#)] [[PubMed](#)]
24. Katsuragi, Y.; Ichimura, Y.; Komatsu, M. Regulation of the Keap1–Nrf2 pathway by p62/SQSTM1. *Curr. Opin. Toxicol.* **2016**, *1*, 54–61. [[CrossRef](#)]

25. Jiang, T.; Harder, B.; Rojo De La Vega, M.; Wong, P.K.; Chapman, E.; Zhang, D.D. p62 links autophagy and Nrf2 signaling. *Free Radic. Biol. Med.* **2015**, *88*, 199. [[CrossRef](#)]
26. Dauchy, F.A.; Contin-Bordes, C.; Nzoumbou-Boko, R.; Bonhivers, M.; Landrein, N.; Robinson, D.R.; Rambert, J.; Courtois, P.; Daulouède, S.; Vincendeau, P. Trypanosoma brucei gambiense excreted/secreted factors impair lipopolysaccharide-induced maturation and activation of human monocyte-derived dendritic cells. *Parasite Immunol.* **2019**, *41*, e12632. [[CrossRef](#)] [[PubMed](#)]
27. Garzón, E.; Holzmüller, P.; Bras-Gonçalves, R.; Vincendeau, P.; Cuny, G.; Lemesre, J.L.; Geiger, A. The Trypanosoma brucei gambiense Secretome Impairs Lipopolysaccharide-Induced Maturation, Cytokine Production, and Allostimulatory Capacity of Dendritic Cells. *Infect. Immun.* **2013**, *81*, 3300. [[CrossRef](#)] [[PubMed](#)]
28. Moreau, A.; Hill, M.; Thébault, P.; Deschamps, J.Y.; Chiffolleau, E.; Chauveau, C.; Moullier, P.; Anegon, I.; Alliot-Licht, B.; Cuturi, M.C. Tolerogenic dendritic cells actively inhibit T cells through heme oxygenase-1 in rodents and in nonhuman primates. *FASEB J.* **2009**, *23*, 3070–3077. [[CrossRef](#)] [[PubMed](#)]
29. Andreou, N.P.; Legaki, E.; Gazouli, M. Inflammatory bowel disease pathobiology: The role of the interferon signature. *Ann. Gastroenterol.* **2020**, *33*, 125. [[CrossRef](#)] [[PubMed](#)]
30. Campbell, N.K.; Fitzgerald, H.K.; Fletcher, J.M.; Dunne, A. Plant-derived polyphenols modulate human dendritic cell metabolism and immune function via AMPK-dependent induction of heme oxygenase-1. *Front. Immunol.* **2019**, *10*, 345. [[CrossRef](#)]
31. Sheikh, S.Z.; Hegazi, R.A.; Kobayashi, T.; Onyiah, J.C.; Russo, S.M.; Matsuoka, K.; Sepulveda, A.R.; Li, F.; Otterbein, L.E.; Plevy, S.E. An Anti-Inflammatory Role for Carbon Monoxide and Heme Oxygenase-1 in Chronic Th2-Mediated Murine Colitis. *J. Immunol.* **2011**, *186*, 5506–5513. [[CrossRef](#)]
32. Hegazi, R.A.F.; Rao, K.N.; Mayle, A.; Sepulveda, A.R.; Otterbein, L.E.; Plevy, S.E. Carbon monoxide ameliorates chronic murine colitis through a heme oxygenase 1-dependent pathway. *J. Exp. Med.* **2005**, *202*, 1703–1713. [[CrossRef](#)] [[PubMed](#)]
33. Zhang, L.; Zhang, Y.; Zhong, W.; Di, C.; Lin, X.; Xia, Z. Heme oxygenase-1 ameliorates dextran sulfate sodium-induced acute murine colitis by regulating Th17/Treg cell balance. *J. Biol. Chem.* **2014**, *289*, 26847–26858. [[CrossRef](#)]
34. Paul, G.; Bataille, F.; Obermeier, F.; Bock, J.; Klebl, F.; Strauch, U.; Lochbaum, D.; Rümmele, P.; Farkas, S.; Schölmerich, J.; et al. Analysis of intestinal haem-oxygenase-1 (HO-1) in clinical and experimental colitis. *Clin. Exp. Immunol.* **2005**, *140*, 547–555. [[CrossRef](#)] [[PubMed](#)]
35. Longhi, M.S.; Vuerich, M.; Kalbasi, A.; Kenison, J.E.; Yeste, A.; Csizmadia, E.; Vaughn, B.; Feldbrugge, L.; Mitsuhashi, S.; Wegiel, B.; et al. Bilirubin suppresses Th17 immunity in colitis by upregulating CD39. *JCI Insight* **2017**, *2*, e92791. [[CrossRef](#)] [[PubMed](#)]
36. Mowat, C.; Cole, A.; Windsor, A.; Ahmad, T.; Arnott, I.; Driscoll, R.; Mitton, S.; Orchard, T.; Rutter, M.; Younge, L.; et al. Guidelines for the management of inflammatory bowel disease in adults. *Gut* **2011**, *60*, 571–607. [[CrossRef](#)] [[PubMed](#)]
37. Yang, Z.; Klionsky, D.J. Mammalian autophagy: Core molecular machinery and signaling regulation. *Curr. Opin. Cell Biol.* **2010**, *22*, 124–131. [[CrossRef](#)]
38. Glick, D.; Barth, S.; Macleod, K.F. Autophagy: Cellular and molecular mechanisms. *J. Pathol.* **2010**, *221*, 3–12. [[CrossRef](#)] [[PubMed](#)]
39. Feng, Y.; He, D.; Yao, Z.; Klionsky, D.J. The machinery of macroautophagy. *Cell Res.* **2014**, *24*, 24–41. [[CrossRef](#)]
40. Pankiv, S.; Clausen, T.H.; Lamark, T.; Brech, A.; Bruun, J.A.; Outzen, H.; Øvervatn, A.; Bjørkøy, G.; Johansen, T. p62/SQSTM1 binds directly to Atg8/LC3 to facilitate degradation of ubiquitinated protein aggregates by autophagy. *J. Biol. Chem.* **2007**, *282*, 24131–24145. [[CrossRef](#)] [[PubMed](#)]
41. Ghislat, G.; Lawrence, T. Autophagy in dendritic cells. *Cell. Mol. Immunol.* **2018**, *15*, 944–952. [[CrossRef](#)] [[PubMed](#)]
42. Carroll, K.C.; Viollet, B.; Suttles, J. AMPK $\alpha$ 1 deficiency amplifies proinflammatory myeloid APC activity and CD40 signaling. *J. Leukoc. Biol.* **2013**, *94*, 1113–1121. [[CrossRef](#)] [[PubMed](#)]